

**Biodiversity of marine-derived fungi
and identification of their metabolites**

**Biodiversität von Pilzen mariner Herkunft und
Identifizierung ihrer Sekundärstoffe**

Inaugural-Dissertation
zur Erlangung des Doktorgrades
der Mathematisch-Naturwissenschaftlichen Fakultät
der Heinrich-Heine-Universität Düsseldorf

vorgelegt von
Ine Dewi Indriani
aus Bandung

Düsseldorf, 2007

Aus dem Institut für Pharmazeutische Biologie und Biotechnologie
der Heinrich-Heine-Universität Düsseldorf

Gedruckt mit der Genehmigung der
Mathematisch-Naturwissenschaftlichen Fakultät der
Heinrich-Heine-Universität Düsseldorf

Gedruckt mit Unterstützung des
Deutschen Akademischen Austauschdienstes (DAAD)

Referent : Prof. Dr. Peter Proksch
Koreferent : Dr. Rainer Ebel, Juniorprofessor

Tag der mündlichen Prüfung: 11.12.2007

Erklärung

Hiermit erkläre ich ehrenwörtlich, dass ich die vorliegende Dissertation mit dem Titel "Biodiversität von Pilzen mariner Herkunft und Identifizierung ihrer Sekundärstoffe" selbständig angefertigt und keine anderen als die angegebenen Quellen und Hilfsmittel benutzt habe. Ich habe diese Dissertation in gleicher oder ähnlicher Form in keinem anderen Prüfungsverfahren vorgelegt. Außerdem erkläre ich, dass ich bisher noch keine weiteren akademischen Grade erworben oder zu erwerben versucht habe.

Düsseldorf, den 30.10.2007

Ine Dewi Indriani

Acknowledgements

I would like to express my deep gratitude and sincere appreciation to Juniorprofessor Dr. Rainer Ebel for his excellent supervision, guidance, continuous support, fruitful discussions and deep encouragement during my doctoral study until the very end.

I wish to thank Prof Dr. Peter Proksch for giving me the chance and opportunity to conduct my doctoral research at his institute, also for his support and excellent guidance.

I would like to show my deep gratitude and thanks to Dr. RuAngelie Edrada-Ebel for sharing her deep expertise especially in NMR interpretation and also for her help elucidating the spectra.

I am indebted to Prof. Dr. W.E.G Müller and his team (Institut für Physiologische Chemie und Pathobiochemie, Universität Mainz) for conducting the cytotoxicity assays, and Dr. Michael Kubbutat and his co-workers (ProQinase GmbH, Freiburg) for the protein kinase inhibition assay. I would like to acknowledge Dr. Yudi Rusman, Mrs. Clécia Freitas-Richard, and Mr. Abdessamad Debbab (Institut für Pharmazeutische Biologie und Biotechnologie, Heinrich-Heine Universität Düsseldorf) for conducting antimicrobial assay.

I wish to thank Dr. W. Peters and his co-workers (Institut für Anorganische und Strukturchemie, Heinrich-Heine-Universität Düsseldorf) for NMR measurements and Dr. Victor Wray (Helmholtz Center for Infection Research, Braunschweig) for NMR measurements and discussion for spectra elucidation. My deep acknowledgement is headed to Dr. H. Keck and Dr. P. Tommes (Institut für Anorganische und Strukturchemie, Heinrich-Heine-Universität Düsseldorf) for conducting EI experiments.

I am indebted to Prof. Dr. Franz Brümmer (Biologisches Institut, Universität Stuttgart) and Prof. Dr. R. Batel (Center for Marine Research Rudjer Boskovic Institute, Rovinj, Croatia) for giving me the chance to collect the sponge samples in Limski Kanal, Croatia.

I would like to thank Mr. Reinhard Ueberschär (Underwater No.1, Düsseldorf) for equipping the field trip to Croatia with scuba gear and breathing gases.

I would like to show my deep thankfulness to Dr. Chaidir (Agency for the Assessment and Application of Technology BPPT, Indonesia) and Dr. Yasman (Biology Department, University of Indonesia) for giving me the possibility to collect algae samples in Seribu Island, Indonesia.

I would like to thank Prof. Dr. Sangkot Marzuki and Dr. Nurjati Chaerani Siregar at Eijkman institute for molecular biology, Jakarta, Indonesia who allowed and put trust on me to pursue my doctor research in this 'new field'.

I would like to express my deep thanks to Ms. Mareike Thiel for great help and friendly assistance during my doctoral study, Mrs. Katrin Rohde, Mrs. Waltraud Schlag, Mrs. Eva Müller, Mrs. Sabine Borstel, Ms. Katja Rätke and Mr. Klaus-Dieter Jansen for providing me help, laboratorium equipment and material during the work.

I wish to thank my colleagues Mrs. Julia Kjer, Ms. Annika Putz, Mrs. Katrin Rohde, Ms. Mareike Thiel, Dr. Sofia Ortlepp, and Dr. Nadine Weber ('the shopping team') for their kindly help, support, discussions, many nice conversations during the working time, the lunch time, the coffee time, even in the shopping time.

I am deeply indebted to Dr. Amal Hassan for her help, support and her friendship especially in the beginning of my study time.

I wish also to express my thankfulness to Prof. Dr. Shu-Ming Li, Prof. Dr. Claus Passreiter, Dr. Jandirk Sendker, Mrs. Anke Suckow-Schnitker, Mr. Sven Ruhl, Mr. Ehab Moustafa, Mr. Ashraf Hamed, Mr. Mirko Bayer, Mr. Frank Riebe, Mr. Edi Sri Mulyono, Mr. Yao Wang, Mr. Sabri Younes, Ms. Nicola Steffan, Mr. Alexander Grundmann, Ms. Anika Kremer, Mr. Wenbing Yin for the nice friendship, as well as the nice working atmosphere.

I would like to thank the former colleagues, Drs. Hefni Effendi, Gernot Brauers, Gero Eck, Carsten Thoms, Yudi Rusman, Yosi Bayu Murti, Bärbel and Jan Hiort, Ziyad Baker and Mohamed Ashour for their help, friendship and encouragement in the first beginning of my study time, and especially Dr. Franka Teuscher for also providing me mangrove samples.

I would like to thank my best friends Dr. Triana Hadna, Mrs. Sophi Damayanti, Mrs. Metta Yuniati, Ms. Indrawati Yudhasmara, and Dr. Neni Nuraeni for their friendship, encouragements, supports and help that I can always count on.

I would like to express my deep appreciation for my husband, as well as my beloved colleague, Arnulf Diesel for his everlasting love, continuous support, great patience, long discussion and also for his guidance in the beginning of my doctoral study. I am indebted to my father and my mother who always give me love, support and prayers even from afar, also to the Diesel family, Mama Doris, “Vadder” Ingolf, Roland and Suzan for all the love, support and encouragement.

Financial support by the DAAD through a PhD fellowship is gratefully acknowledged.

Zusammenfassung

Insgesamt wurden 31 Verbindungen aus Pilzen isoliert, die aus 12 verschiedenen marinen Organismen stammen, darunter Vertreter unterschiedlicher Substanzklassen wie Alkaloide, Polyketide und Terpene. Eine Verbindung, ein Pyranacetal, erwies sich dabei als neuer Naturstoff. Die Strukturen der Verbindungen wurden durch massenspektrometrische Verfahren sowie ein- und zweidimensionale NMR-Spektroskopie aufgeklärt.

1. Pilze aus der Klasse Eurotiomycetes

Sechs stickstoffhaltige Verbindungen wurden aus *Penicillium polonicum*, isoliert aus dem marinen Schwamm *Tethya* sp., erhalten. Fünf davon, Cyclophenin, Cyclophenol, Viridicatol, Viridicatin sowie 3-Methylviridicatin waren biogenetisch verwandt.

Meleagrin, Roquefortin, Citrinin, Citrininhydrat und die Diastereomere Quinolactacin A1 und A2 wurden aus *Penicillium citrinum* erhalten, welcher aus der marinen Alge *Sargassum* sp. isoliert wurde. Meleagrin, Roquefortin und Citrininhydrat zeigten eine beachtliche zytotoxische Wirkung gegen die murine Lymphomazelllinie L5178Y, wohingegen Citrinin nicht aktiv war.

Das Anthrachinon Skyrin und die Preanthrachinone Atrovirin B1 und B2 wurden aus einem Extrakt des aus dem Schwamm *Aplysina aerophoba* isolierten *Talaromyces wortmanii* erhalten.

Zwei bekannte Verbindungen, Tenuazonsäure und Alternariol, wurden aus dem Pilz *Alternaria compacta* erhalten, der aus dem marinen Schwamm *Suberites domuncula* isoliert wurde.

2. Pilze aus der Klasse Sordariomycetes

Drei verwandte Alkaloide, Chaetomin, Cochliodinol und Semicochliodinol wurden vom aus dem marinen Schwamm *Tethya* sp. isolierten Pilz *Chaetomium* sp. erhalten. Alle zeigten starke zytotoxische Aktivität gegenüber L5178Y-Zellen und zeigten inhibitorische Aktivität gegenüber Proteinkinasen.

Ein neues, mit der Familie der Cholesterolsynthesehemmstoffe Agistatine verwandtes Pyranacetal wurde vom Pilz *Xylaria* sp. erhalten, der aus der marinen

Alge *Padina australis* isoliert wurde. Diese Verbindung wurde 3-Methylmethoxyagistatin D genannt, basierend auf der Methylmethoxygruppe in Position C-3.

Daldinia escholzii aus der marinen Alge *Halimeda berneoensis* produzierte die bekannte Verbindung 4,4',5,5'-tetrahydroxy-1,1'-binaphthyl. Diese Verbindung zeigte eine beträchtliche zytotoxische Aktivität gegenüber L5178Y-Zellen und erwies darüber hinaus als Inhibitor von Proteinkinasen auf; beide Eigenschaften wurden bisher noch nicht in der Literatur beschrieben.

Das Makrolid Zearalenon wurde von dem aus *Sargassum* sp. isolierten Pilz *Fusarium equiseti* erhalten.

Indol-3-carbonsäure und das Diterpen Myrocin A wurden aus *Arthrinium* sp. gewonnen, der aus *Tethya* sp. isoliert wurde. Myrocin A bewies zytotoxische Wirkung und Aktivität als Inhibitor von Proteinkinasen. Die chemotaxonomische Markersubstanz 5-Carboxymellein wurde aus dem Pilzstamm PV 1.1 erhalten. Aufgrund dieser chemischen Befunde ist anzunehmen, dass dieser Pilz aus der Familie der Xylariaceae stammt.

3. Pilze aus der Klasse Dothideomycetes

Die antimykotische Verbindung Griseofulvin wurde vom aus dem marinen Schwamm *Suberites domuncula* isolierten Pilz *Botryosphaeria stevensii* erhalten; damit erwies sich dieser Pilz als einer der wenigen bekannten Griseofulvin-Produzenten außerhalb der Gattung *Penicillium*. Der aus dem marinen Schwamm *Petrosia ficiformis* isolierte Pilz *Paraphaeosphaera michotii* produzierte die Substanzen Cyclopenin, Cyclophenol, Viridicatol, Viridicatin und 3,4,8-Trihydroxy-1-tetralon.

Die Bestimmung der Diversität der Pilze in marinen Organismen wurde mithilfe der Polymerasekettenreaktion (PCR) unter Verwendung von Primern, die auf konservierte, taxonomisch signifikante Gene gerichtet waren, durchgeführt, gefolgt von denaturierender Gradientengelelektrophorese (DGGE). Das universelle Pilzprimerpaar ITS1 und ITS4 erzeugte DNA-Amplifikate, die sich per DGGE trennen ließen und eine Identifizierung der zugrunde liegenden Pilzstämme auf breiter Basis erlaubten. Es konnte gezeigt werden, dass die DGGE unter Verwendung dieses Primerpaares eine zuverlässige und aussagekräftige Methode zur Erfassung der Diversität von Pilzen in komplexen biologischen Proben darstellt, insbesondere, was Mangrovenpflanzen betrifft.

Pilz-Sequenzen konnten aus den DGGE-Experimenten mit Mangrovenpflanzen erhalten werden, wobei zweifelsfrei nachgewiesen wurde, dass eine Bande jeweils auf einen Pilzstamm zurückzuführen ist. Zwei Banden mit vergleichbarer Laufstrecke in Proben der Rinde und Blätter von *Avicennia marina* wurden sequenziert und mittels BLAST-Suche jeweils dem Pilz *Alternaria* sp. zugeordnet. Eine weitere, aus den Blättern von *Avicennia marina* stammende Bande wurde nach Sequenzierung als *Fusarium* sp. identifiziert.

Im Rahmen dieser Arbeit wurde erstmalig der erfolgreiche Nachweis von Pilz-DNA im Gesamt-DNA-Extrakt von marinen Schwämmen auf der Basis von PCR und DGGE geführt. Dabei zeigte sich, dass neben den Banden, welche Pilze repräsentieren, auch solche auftraten, die auf DNA des Schwammes zurückgehen. Allerdings ließen sich Banden von Schwamm-DNA von denen der Pilze durch ihre unterschiedlichen Laufstrecken in den DGGE-Gelen sicher unterscheiden.

Anhand der Sequenzen aller im Rahmen dieser Arbeit untersuchten Pilzstämmen, die auf Amplifikation mit dem Primerpaar ITS1 und ITS4 zurückgehen, wurde eine phylogenetische Analyse durchgeführt. Der aus diesen Sequenzen konstruierte phylogenetische Baum wurde mithilfe bioinformatischer Methoden validiert, und es konnte gezeigt werden, dass er die Evolutionsgeschichte und Verwandtschaft innerhalb des Reichs der Pilze bis herunter zur Gattungsebene wider gibt.

Table of Contents

1. Introduction

1.1 Natural Products	1
1.1.1 Natural Products Drug Discovery	1
1.1.2 Natural products as drugs in the past	2
1.1.3 Natural products today	4
1.2 Fungi as Natural Products Sources	5
1.3 Marine-derived fungi	7
1.4 Endophytic fungi	11
1.5 Identification of fungi	14
1.6 Estimation of fungal diversity in the host of marine derived fungi by DGGE method	17
1.7. Aim and scope of the study	19

2. Materials and Methods

	20
2.1 Field trip and sample collecting	
2.2 Cultivation and screening of fungi	21
2.3 Fungi collection	21
2.4 Identification of fungi	23
2.4.1 DNA isolation	23
2.4.2. DNA amplification	24
2.4.3. DNA electrophoresis	26
2.4.4. Purification of PCR products	26
2.4.5. DNA sequencing	27
2.5 Denaturing gradient gel electrophoresis (DGGE)	27
2.5.1 Amplification of ITS region with addition of GC Clamp	28
2.5.2 Preparation of DGGE gel	29
2.5.3 DGGE	30
2.5.4 Purification of bands	31
2.6 Cultivation of fungi	31
2.7 Extraction of fungal culture	32
2.8 Chemical substances and equipment	46
2.8.1 Equipments and machine	46
2.8.2 Chemicals	47
2.8.3 Software	47
2.9 Screening and bioassay	48
2.9.1 Antimicrobial assay	48
2.9.1.1 Antibacterial assay	49
2.9.1.2 Antifungal assay	50
2.9.2 Cytotoxicity assay	50
2.9.3 Prokinase assay	52

2.10 Chromatographic methods	56
2.10.1 Thin layer chromatography (TLC)	56
2.10.2 Vacuum liquid Chromatography	57
2.10.3 Column chromatography	57
2.10.4 Analytical high performance liquid chromatography (HPLC)	58
2.10.5 Preparative HPLC	60
2.11 Structure elucidation of secondary metabolites	61
2.11.1 Mass spectroscopy	61
2.11.1.1 Electron impact mass spectrometry (EI-MS)	62
2.11.1.2 Electron spray ionization (ESI-MS)	63
2.11.1.3 Fast atom bombardment mass spectrometry (FAB-MS)	63
2.11.2 Nuclear magnetic resonance (NMR)	64
2.11.2 Optical rotation	65

3. RESULT OF ISOLATED METABOLITES

3.1 Isolated compounds of fungus <i>Chaetomium</i>.	68
3.1.1 Compound 1 (chetomin)	69
3.1.2 Compound 2 (cochliodinol)	75
3.1.3 Compound 3 (Semicochliodinol A)	79
3.1.4 Compound 5 (cycloalanyl tryptophan)	83
3.2 Isolated compounds of fungus <i>Penicillium citrinum</i>.	87
3.2.1 Compound 6 (meleagrins)	88
3.2.2 Compound 7 (roquefortine C)	93
3.2.3 Compound 8 (quinolactacin A1) and compound 9 (quinolactacin A2)	97
3.2.4 Compound 10 (Citrinin)	102
3.2.5 Compound 11 (Citrinin hydrate)	106
3.3 Isolated secondary metabolites of fungus <i>Xylaria</i> sp.	111
3.3.1 Compound 12 (3-methyl-methoxy agistatine D), NEW	112
3.4 Isolated secondary metabolites of fungus <i>Fusarium equiseti</i>	121
3.4.1 Compound 13 (zearalenone)	122
3.5 Secondary metabolites of fungus <i>Penicillium polonicum</i>	127
2.10.2 Compound 15 (fructigenin A)	128
2.10.3 Compound 16 (cyclophenol)	132
3.5.3 Compound 17 (cyclophenin)	136
3.5.4 Compound 18 (viridicatol)	141
3.5.5 Compound 19 (viridicatin)	145
3.5.6 Compound 20 (<i>O</i> -methyl viridicatin)	149
3.6 Secondary metabolites of fungus <i>Arthrimum</i> sp.	154
3.6.1 Compound 21 (indol-3-carboxylic acid)	154
3.6.2 Compound 22 (Myrocin A)	158
3.7 Secondary metabolites of fungus <i>Botryosphaeria stevensii</i>	165
3.7.1 Compound 23 (griseofulvin)	166
3.8 Secondary metabolites of fungus PV1.1 (unidentified fungus)	167
3.8.1 Compound 24 (5-carboxy mellein)	168
3.9 Secondary metabolites of fungus <i>Alternaria alternata</i>	172
3.9.1 Compound 25 (tenuazonic acid).	173
3.9.2 Compound 26 (alternariol)	179
3.10 Secondary metabolites of fungus <i>Paraphaeosphaeria michotii</i>	181

3.10.1 Compound 27 (3,4,8-trihydroxy 1-tetralone)	182
3.11 Isolated secondary metabolites of fungus <i>Daldinia escholszii</i>	189
3.11.1 Compound 28 (4,4',5,5' tetrahydroxy 1,1' binaphthyl)	190
3.11 Isolated secondary metabolites of fungus <i>Talaromyces wortmanii</i>.	194
3.11.1 Compound 29 (atrovirin B1) and compound 30 (atrovirin B2)	195
3.11.2 .Compound 31 (Skyrin)	201

4. RESULT OF BIODIVERSITY DETERMINATION

4.1 Identification of fungi	208
4.1.1 Optimization of fungal identification	208
4.1.2 Optimization of fungal DNA isolation	208
4.1.3 Evaluating the primers	208
4.1.4 Optimization of PCR conditions	212
4.1.5 Identification of fungi	219
4.1.6 BLAST search for fungal identification	223
4.1.6 Constructing of Phylogenetic Tree	227
4.1.6.1 Multiple sequence alignment	234
3.12.3.2 Phylogenetic analysis	238
3.13 Assessing fungal diversity by DGGE methods using the DNA sequences of ITS region	241
3.13.1 Optimization of DGGE methods	241
3.13.2 Estimating fungal diversity in marine sponges by DGGE	244
3.13.3 Estimating fungal diversity in mangrove plants by DGGE	251

5. DISCUSSION OF ISOLATED SECONDARY METABOLITES

5.1 Alkaloids	257
5.1.1 Alkaloids from <i>Penicillium citrinum</i>	257
5.1.1.1 Meleagrine and Roquefortine	257
5.1.1.2 Quinolactacin A1 and A2	260
5.1.2 Alkaloids isolated from <i>Penicillium polonicum</i>	262
5.1.2.1 Cyclophenol, cyclophenin, viridicatol and viridicatin	262
5.1.2.2 Fructigenin A	264
5.1.3 Alkaloids isolated from <i>Chaetomium</i> sp.	265
5.1.3.1 Chetomin	265
5.1.3.2 Cochliodinol and semicochliodinol A	268
5.1.4 Alkaloid isolated from <i>Alternaria alternata</i>	269
5.1.4.1 Tenuazonic acid	269
5.2 Polyketides	270
5.2.1 Polyketide isolated from <i>Penicillium citrinum</i> (Citrinin and citrinin hydrate)	271
5.2.2 Polyketide isolated from <i>Botryosphaeria stevensii</i>	272
5.2.2.1 Griseofulvin	272
5.2.3 Polyketide isolated from <i>Alternaria alternata</i>	274
5.2.3.1 Alternariol	274
5.2.4 Polyketide from unidentified fungus	275
5.2.4.1 5-carboxymellein	275
5.2.5 Macrolide isolated from <i>Fusarium equiseti</i> (zearalenone)	276

5.2.6 Polyketide from fungus <i>Paraphaeosphaeria michotii</i>	277
5.2.6.1 3,4,8-trihydroxy 1-tetralone	277
5.2.7 Pre-anthraquinones and anthraquinones from <i>Talaromyces wotmanii</i>	278
5.2.7.1 Atrovirin B1 and B2	279
5.2.7.2 S kyrin	280
5.2.8 Pyranacetal compound isolated from <i>Xylaria</i> sp.	283
5.2.8.1 Methyl methoxy agistatine D (new compound)	283
5.3 Diterpene	284
5.3.1 Diterpene isolated from <i>Arthrinium</i> sp. (myrocin A)	284

6. DISCUSSION OF BIODIVERSITY DETERMINATION

6.1 Fungal identification	287
4.7 Phylogenetic tree	291
4.8 The assessment of fungal diversity in marine organisms and mangrove plants	300

7. SUMMARY

308

8. REFERENCES

311

9. ABBREVIATIONS

336

10. ATTACHMENTS

338

1. Introduction

1.1 Natural Products

1.1.1 Natural Products Drug Discovery

Natural products are chemical compounds derived from living organisms throughout the six kingdoms Eubacteria, Archaeobacteria, Protista, Fungi, Plantae and Animalia (Woese *et al.*, 1977). As diverse as their sources, so are the compounds themselves and their biological functions that are often highly specific. Since ancient times until today natural products have been used to cure human diseases. With rapidly increasing knowledge in science, especially structure elucidation and synthetic chemistry, natural products became a major source for new synthetic drugs. Many successful drugs in the market today were originally synthesized to mimic the action of molecules found in nature (Fehler and Schmidt, 2003).

Natural product derived drugs are usually secondary metabolites and their derivatives. In contradiction to the compounds of the basic metabolism such as amino acids, sugars and fatty acids which are – beside some exceptions - very similar in organisms even in different kingdoms, secondary metabolites are not essential for normal growth, development or reproduction of an organism. Instead, their functions may be as diverse as: competitive weapons used against other bacteria, fungi, amoebae, plants, insects and large animals; metal transporting agents; agents of symbiosis between microbes and plants, nematodes, insects, and higher animals; sexual hormones; differentiation effectors (Demain and Fang, 2000).

1.1.2 Natural products as drugs in the past

Ever since being expelled from paradise as believed by the members of the Abrahamic religions, human suffered from various kinds of diseases seeking cure and easement not only in prayer, but increasingly by application of drugs usually derived from plants, but also from animals and other sources. Knowledge was acquired by trial and error and observation of effects and side effects. Probably the most known written evidence of the early use of drugs is the Ebers papyrus (about 1550 BC), a 110-page scroll, among the other important ancient Egyptian medical papyri, such as Edwin Smith papyrus (about 1600 BC). It contained chapters on treatment of many mental and physical diseases and their remedies (Taylor, 2001).

A new era of pharmacotherapy begun with the first pharmacopeia by the Greek physician Galen (AD 129 – 200) describing the appearance, properties and the use of many plants in this time (Patwardhan *et al.*,2004). More famous is certainly the destiny of the Greek philosopher Socrates (470 – 399 BC) who was sentenced to death by drinking a lethal cocktail containing the poison hemlock *Conium maculatum* (Taylor, 2001).

With Christianity in Europe, a sophisticated system of recording and spreading knowledge was established. Monasteries have been the first institutions operating libraries and exchanging documents. Following the Christian values, nuns and monks provided help for the sick, but this was mostly limited to nursing. Active treatment by drugs was considered as an intrusion in Gods will, and a doctor's work rejected as sinful or at least useless (Keil, 1989).

This drastically changed by the Lorsch Pharmacopeia, written in a monastery near Worms, Germany in the late 8th century. The book contained numerous medical compositions as well as an index allowing the reader to quickly find the right remedy.

In the introduction, the big gap between religion and scientific was closed and the medicine was legally put in the service for mankind not as a right, but as a duty (Keil, 1989). Since this time, monasteries cultured medical plants in their gardens.

Eventhough the industrial drugs displaced them already for a long time, the spirit is still found today in the name of the pharmaceutical company “Klosterfrau”, which is specialized on natural remedies.

In Asia, traditional medicine was and is still widely used. Ayurveda, the traditional medicine in India has been used for more than three thousand years. As well as in China, the traditional system of medicine has been used also for several thousand years. The Chinese herbal medicine was first recorded in the Emperor Shennung’s classic herbals, about 2700 BC (Patwardhan *et al.*, 2004).

Indonesia has a long tradition in the use of natural remedies that are called Jamu, an originally Javanese word. Jamu holds an important share of the today Indonesian health expenses (Proksch *et al.*, 1997). The ingredients are usually of plant origin like leaves, bark, roots or flowers, but may also contain others such as powderized egg shell or charcoal prepared from the nest of mice (Sidik, 1994).

In the past, Jamu was prepared within the family or by a healer from ingredients cultured by themselves or purchased on the market. Nowadays, Jamu is industrially produced mostly in form of powders or tablets. The formerly adhering spiritual component was thereby totally lost. Even though the Indonesian scientific medicine does not admit Jamu, 70 – 80 % of the Indonesians trust in and regularly use Jamu (Soedigyo, 1990; Afdhal and Welsch, 1991), since the chemical drugs are too expensive for a major part of them.

1.1.3 Natural products today

The average patient might assume that most – if not all – of the drugs sold in the pharmacy are not of natural origin. This is only partially true. In fact, the progress of science opens new ways for natural products into the pharmacy, so that we can differentiate four major classes.

Herbal drugs are the most traditional form of natural product remedies and sold as dried parts of plants for preparation of medical teas (aqueous extract). Easier in applications are capsules, tablets or syrups made from whole extracts obtained using a certain solvent or a combination of solvents which will be stated on the package. Preparations of *Ginkgo biloba* are successfully used in the treatment of dementia, vertigo and arterial obstruction (Napryeyenko and Borzenko, 2007; Liu *et al.*, 2007).

Exact dosage of pure single compounds is required for highly effective drugs, but the content of the effective compound in a plant may strongly fluctuate within a day and also depend on environmental factors like rain, sunshine and geographical position making its direct use risky. The discovery of pure natural compounds as active principles was first described at the beginning of the 19th century. In 1806, the German pharmacist Sertürner isolated the alkaloid morphine *Papaver somniferum*, one among the first isolated active compounds (Newman *et al.*, 2000). Today morphine is applied in very different ways from oral to intrathecal as a strong analgesic.

Partial synthesis resembles a modification of a natural product by chemical methods, resulting in different effects of the new compound compared to the original one. Naloxone is derived from thebaine, an alkaloid related to morphine. The introduction of an N-allyl group instead of methyl created a potent μ -opioid receptor competitive antagonist. Its substantial first-pass effect makes it very useful to prevent abusive injection of oral opioid painkillers (van Dorp *et al.*, 2007).

Providing a greater structural diversity than standard combinatorial chemistry, natural products offer major opportunities for finding novel molecules. Beginning with the structure of a natural product, molecular modelling studies ligand-receptor interactions and suggests optimized structures for agonists or antagonists. The angiotensin-converting enzyme inhibitor captopril and its successors have been developed from a peptide in the pit viper (*Bothrops jararaca*) via QSAR-based modification (Nemec and Schubert-Zsilavec, 2003; Cushman and Ondetti, 1999).

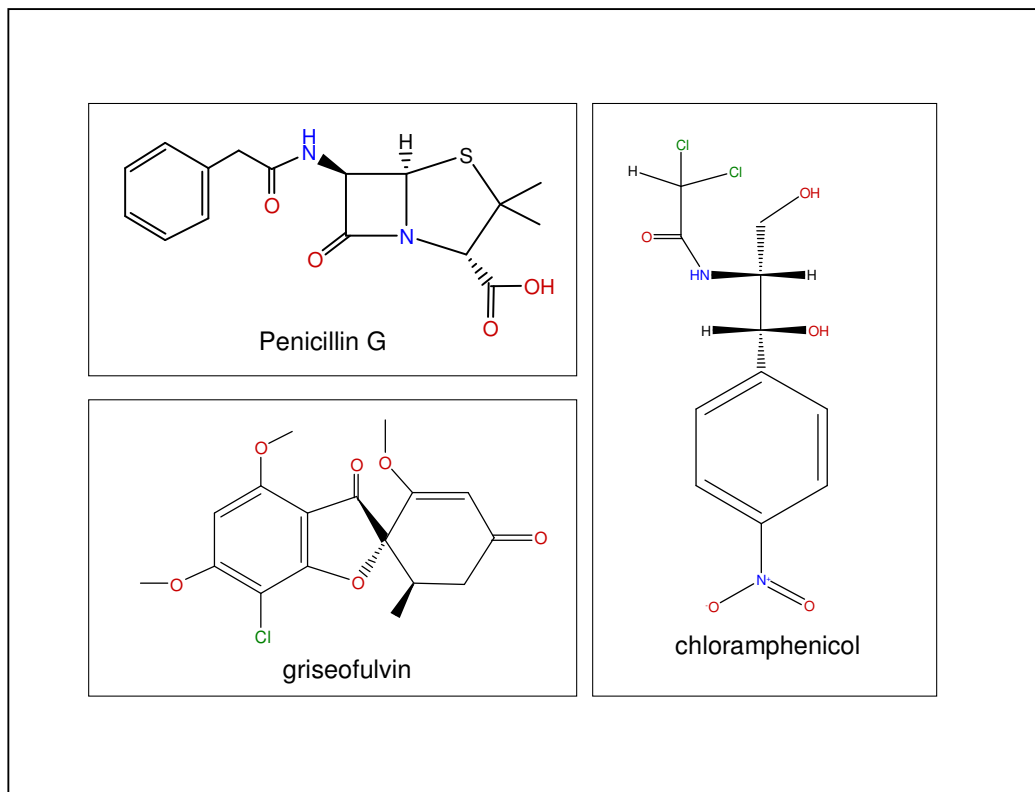
1.2 Fungi as Natural Products Sources

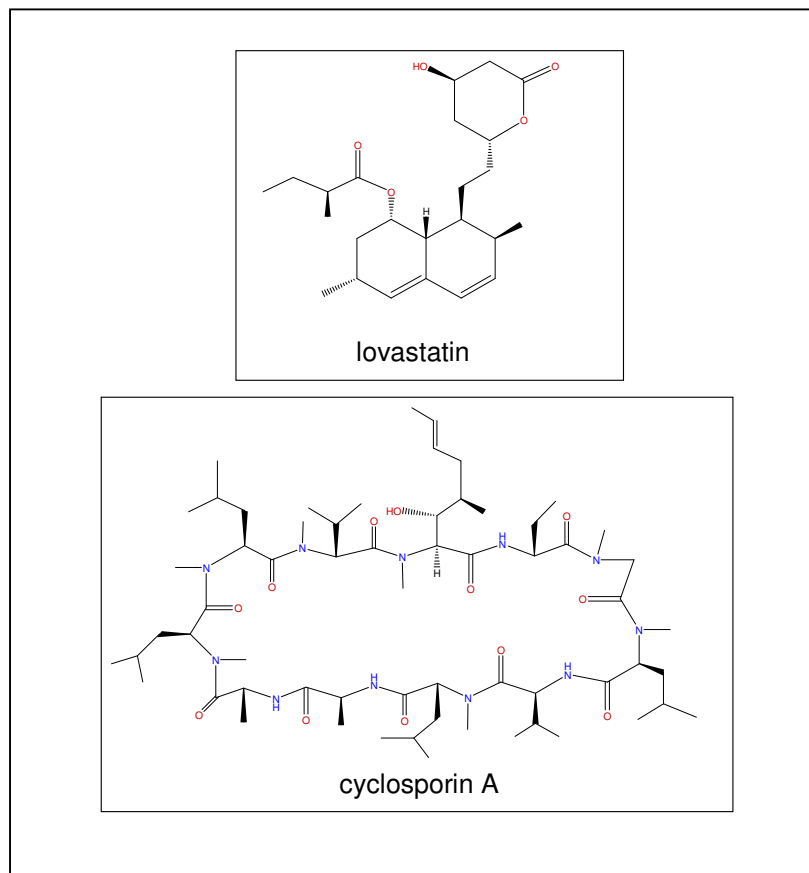
Fungi are heterotrophic eukaryotes that lack chlorophyll. On one hand, they depend on nutrients from external sources; on the other hand they are independent of light and can inhabit also dark places (de Hoog *et al.*, 2000). Fungi currently are classified into five phyla or divisions which are Basidiomycota, Ascomycota, Chytridiomycota, Zygomycota and Glomeromycota (Alexopoulos *et al.*, 2004).

Fungi produce a broad range of secondary metabolites. Some of them have antibacterial or antifungal activities, so we can conclude that these compounds serve as a chemical weapon against competitors of a fungus. In many cases, the benefit these compounds confer to the fungus is unknown.

The first recorded medical use of fungi is the treatment of infected wounds in ancient Egypt by applying moldy bread (Sipos *et al.*, 2004). Thousands of years later, in 1929 fungi had been discovered having bio-active properties when Sir Alexander Fleming described the effect of *Penicillium notatum* and penicillin on bacteria. Unfortunately, the importance of his study and result was not completely realized until the early of 1940 when a research group in Oxford started investigating the potential of penicillin as antibiotic agent in human (Bugni and Ireland, 2004; Butler, 2004).

Two decades after the discovery of penicillin, several other antimicrobial compounds such as chloramphenicol (Long and Troutman, 1949) and griseofulvin (Grove *et al.*, 1952) had been isolated from fungi. Cyclosporine (Traber *et al.*, 1982; Traber *et al.*, 1987) is an immunosuppressant used for organ and bone marrow transplantation, psoriasis and atopic skin disease. Economically most important are lovastatin which was first isolated from *Aspergillus terreus* (Endo *et al.*, 1979) and its successors, which reduce cholesterol biosynthesis by inhibition of 5-HMG-CoA reductase and have an annual revenue of 26 billion US\$.





1.3 Marine-derived fungi

Giuseppe Brotzu in the late 1940s isolated and cultivated the fungus *Cephalosporium acremonium* from sea water samples near a sewage outlet in Sardinia (Kelecom, 2001; Bugni and Ireland, 2004). It took almost ten years until Newton and Abraham at Oxford University discovered cephalosporin C which is responsible for the antibacterial activity of this fungus (Newton and Abraham, 1955).

Fungi isolated from marine organisms or marine environment have shown enormous potential as suggested by the diversity of secondary metabolites (Bugni and Ireland, 2004). Most recently, marine derived fungi have also come into one of the focus of marine drug prospection (Proksch *et al.*, 2006). The ocean once again began to become a new scientifically attractive field.

Overall, research on marine derived fungi has led to the discovery of more than 300 new natural products including many that have novel carbon skeletons providing evidence that marine derived fungi have enormous potential and represent a rich source of pharmaceutical lead structures [figure 1.1](Bugni and Ireland, 2004).

A major problem is that many promising bioactive marine compounds often can only be isolated in extreme low yields. Fungi in general can be cultured to overcome this problem of short supply. Unfortunately, culture of many marine fungi cannot always be performed using standard procedures of fermentation. Even if the fungus may grow, the metabolite patterns might already change in the first culture, or in a later upscale fermentation. A possible reason might be that some of these compounds perhaps are only produced as a result of symbiosis between source (marine organisms) and fungus (Proksch *et al.*, 2006).

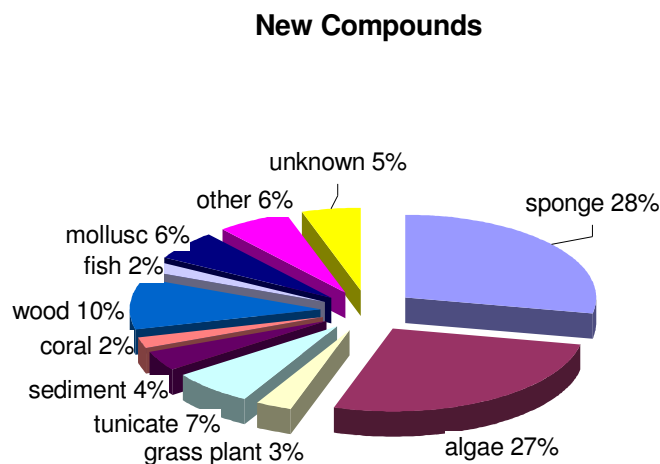


Figure 1.1 The distribution of new compounds reported from marine derived fungi [Bugni and Ireland, 2004]

Kohlmeyer and Kohlmeyer (1979) stated that marine fungi can be divided into two groups, obligate and facultative marine fungi. Obligate marine fungi are those that grow and sporulate exclusively in a marine or estuarine habitat, while facultative marine fungi are those from freshwater or terrestrial milieus able to grow and possibly also to sporulate in the marine environment (Kohlmeyer and Kohlmeyer, 1979). That definition is problematic because terrestrial strains washed into the marine environment, so that many marine taxa are already known for the terrestrial habitat, only a few are specifically from marine. Thus, marine fungi are certainly not systematically and taxonomically, but rather physiologically and ecologically defined groups of fungi, (Miller, 2000).

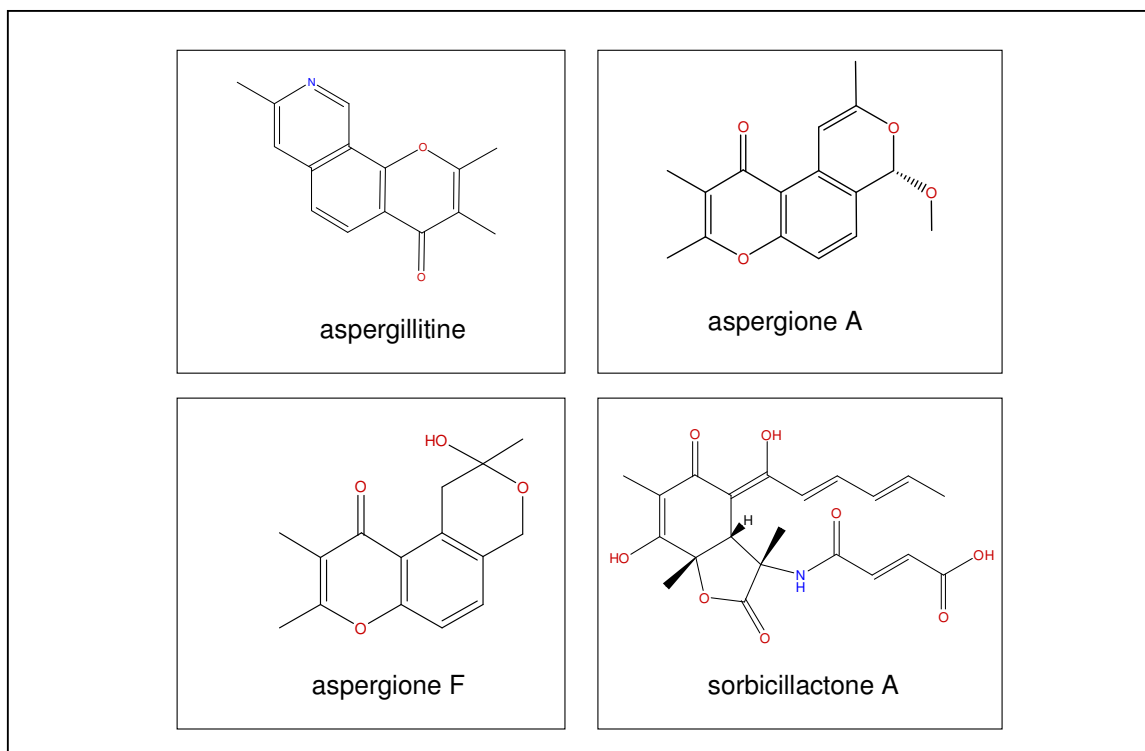
Marine derived fungi can be isolated from inorganic matters such as sea water, soil, sediments, and sandy habitats. Successful isolation from such sources will usually require concentration processes, which may be filtering of large volumes of seawater through microbiological filter disks or suspending the solid material in saline and perform fractionated centrifugation (Fieseler *et al.*, 2004). Samples from marine sponges and marine invertebrates such as coral, abscidians, bivalves, crustaceans, as well as marine algae, sea grasses, other higher plants including mangrove plants in contrary will need appropriate surface sterilization to ensure that no adhering fungi are isolated (Ebel, 2006).

Regardless of the fact that many marine derived fungi can probably not be considered as being obligate marine fungi, they continue to yield new bioactive constituents unknown from any previously isolated terrestrial strains of the same taxa (Proksch *et al.*, 2006), for example *Penicillium* spp., *Aspergillus* spp., and *Fusarium* spp which are isolated from marine algae and sponge. Ebel *et al.* (2002) found several new metabolites such as aspergillitine and aspergione A – F from *Aspergillus niger*

isolated from sponge *Ircinia* sp. which have not been found in *Aspergillus niger* isolated from terrestrial environment (Ebel *et al.*, 2002; Lin *et al.*, 2001). Another example is a marine derived fungus *Penicillium chrysogenum* derived from marine sponge *Ircinia fasciculata* which produces the new cytotoxic alkaloid sorbicillactone A (Bringmann *et al.*, 2003). Sorbicillactone A was not found in *Penicillium chrysogenum* or other *Penicillium* sp. isolated from terrestrial plants.

It was not really proven that terrestrial fungal spores will be enriched and the fungus will live inside the sponge cells. It is also possible that terrestrial fungal spores can stay there in dormant state which is later isolated and will grow under the laboratory condition (Proksch *et al.*, 2003).

itine



Fungi derived from marine algae, sea grasses and mangroves are marine fungi due to their habitats, but may also be categorized as endophytic fungi because their hosts belong to the kingdom plantae.

1.4 Endophytic fungi

Endophytic fungi represent a huge diversity of fungal adaptations that have developed in special and sequestered environments and their diversity and specialized habituation make them as an exciting source of study in the search of new medicines (Owen and Hundley, 2004).

Endophytic fungi are fungi that live throughout their entire life cycle within stems or leaves of their host plants without causing apparent symptoms of infection (Moore-Landecker, 1996; Faeth, 2002). Almost all vascular plants species examined to date were found to harbor endophytic fungi (Tan and Zhou, 2001). Moreover, the colonization of endophytes in marine algae, mosses and fern has also been recorded in many publications (Bugni and Ireland, 2004; Strobel *et al.*, 2002)

The relationship between endophytic fungi and their host plant may range from latent phytopathogenesis to mutualistic symbiosis (Owen and Hudley, 2004). Some phytopathogenic fungi originated from endophytic fungi. Many endophytic fungi are quiescent phytopathogens which may cause infectious symptoms when the host plant is old or having stress condition (Tan and Zhou, 2001).

Endophytic fungi derived from grasses represent one example of microbial symbionts which are estimated to occur in 20 – 30% of grass species. These endophytes can play important roles in plant communities and contribute substantially to the structure and function of terrestrial community (Rudgers *et al.*, 2004). By producing mycotoxins including several classes of alkaloids, endophytic fungi derived

from grasses can enhance the resistance of the host plant against herbivores. Beside this purpose, some publications reported that endophytic fungi derived from grasses can also increase drought resistance (Elmi and West, 1995), and enhance nutrient uptake of the host plant (Malinowsky and Belesky, 2000).

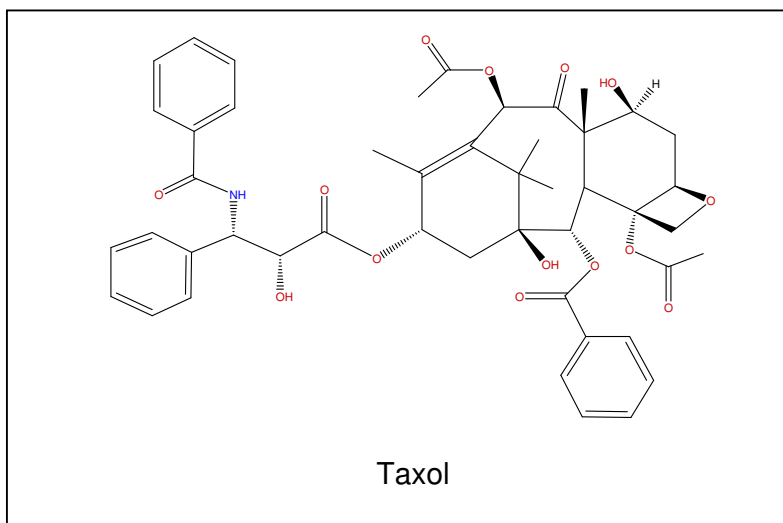
One example of the special relationship between endophytic fungi and host plant was shown in the case of pacific yew tree *Taxus brevifolia*. Paclitaxel (taxol®), a highly functionalized diterpenoid was first isolated from the inner bark of *Taxus brevifolia* in 1969. Taxol is used as a cytostatic agent since 1992 against several tumors such as breast cancer and ovarian carcinoma; and also to treat some of other human tissue proliferating diseases as well (Wani *et al.*, 1971; Strobel *et al.*, 2004).

Taxol treatment to battle several cancer diseases unfortunately was facing the problem of short supply, since the geographical abundance of the pacific yew is limited to the Pacific coast of North America and harvesting the inner bark means death of the whole tree. Even though taxol became accessible by partial synthesis starting from Acetyl-Baccatin III, that can be isolated from the much more abundant *Taxus baccata*, this anticancer drug is still extremely expensive. The price of a single dosage is approaching 1.000 US\$ (Rote Liste, 2007).

This problem then prompted the study of endophytic fungi derived from the yew species which can produce taxol. After several years of effort, Strobel *et al.* in 1993 reported a finding of a novel taxol-producing endophytic fungus which isolated from *Taxus brevifolia*, *Taxomyces andreanae*. The evidence of taxol presence has been proven by electrospray mass spectrum of the putative taxol in culture fluid of this fungus (Strobel *et al.*, 1993).

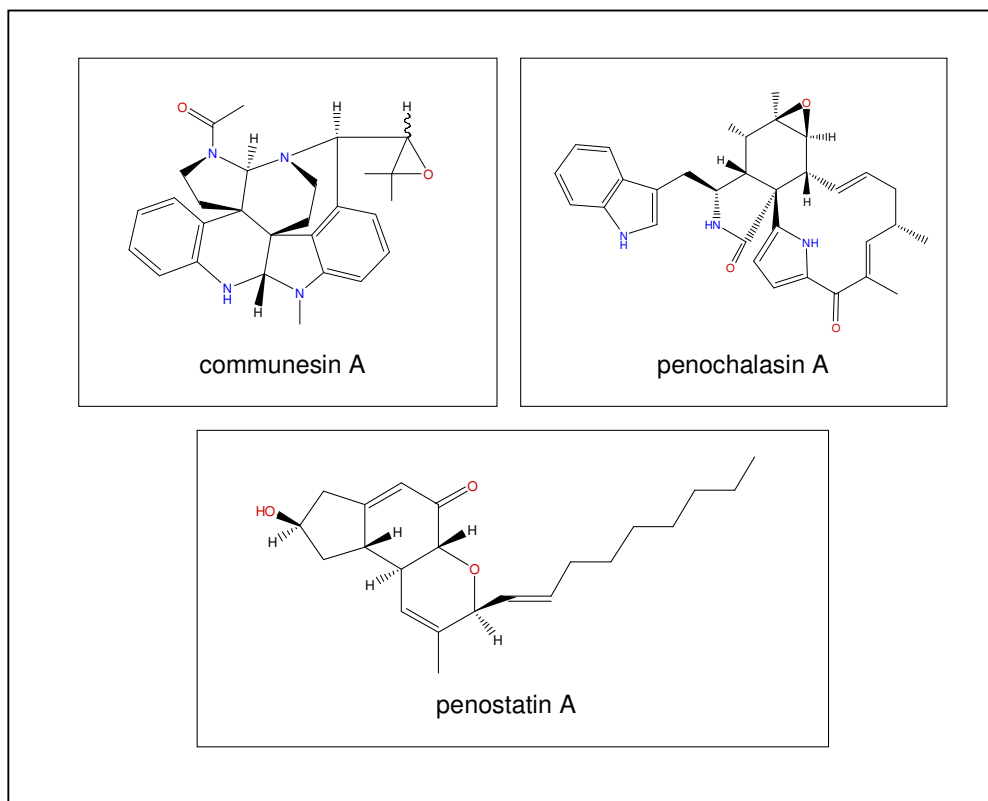
Further researches also found several other taxol-producing endophytic fungi which derived not only from yews but also from other trees such as cypress tree and

Wollemi pine (Strobel *et al.*, 2003). Endophyte *Pestalotiopsis microspora* was obtained from a bald cypress tree in South Carolina and also were shown to produce taxol. This was the first indication that endophytes residing in plants other than *Taxus* spp. were producing taxol (Li *et al.*, 1998).



The ecological and physiological explanation for the wide distribution of taxol-producing endophytes seems to be related to the fact that taxol is an antifungal agent to protect the plant and also the fungus from other pathogenic fungi (Strobel *et al.*, 2003; Owen and Hudley, 2004).

One scientifically fascinating example of endophytic fungus derived from marine algae is *Penicillium* sp. which was isolated from *Enteromorpha intestinalis*. This fungus produced several cytotoxic compounds such as communesin A and B; penochalasin A, B, C and D; and penostatin A, B, C and D (Numata *et al.*, 1996; Takahasi *et al.*, 1996). Communesin A and B, penostatin A, B and C exhibited significant cytotoxic activity in the P388 lymphocytic leukemia test system in cell culture (Numata *et al.*, 1993; Takahasi *et al.*, 1996).



1.5 Identification of fungi

Proper and suitable identification and classification of fungi is critical to the study of natural products produced by marine derived fungi. Without proper identification, chemical investigations of fungi become more difficult to reproduce (Bugni and Ireland, 2004).

The systematic biological study of fungi entered a new era with the introduction of molecular biological techniques. This new approach to fungal systematics has been accelerated by the relative simplicity of these techniques and the use of particular regions of the relatively small fungal genomes. Fungal molecular systematics has increased our understanding of taxonomic groupings and evolutionary histories within

different groups of fungi. An evolutionary approach to define fungal taxa is preferred because it is more objective and provides outstanding predictive value (Geiser, 2004).

On the contrary, traditional morphological approaches to fungal systematics are problematic because they owe a lack of characters useful for grouping and they frequently fail to provide a solid evolutionary framework, particularly at the species level (Geiser, 2004; Guarro *et al.*, 1999).

The use of nuclear ribosomal DNA sequences (rDNA) has become one of the most useful and important techniques for identifying the fungi and studying the phylogenetics. Comparative studies of the nucleotide sequences of ribosomal DNA (rDNA) genes provide a means for analyzing phylogenetic relationships over a wide range of taxonomic levels (White *et al.*, 1990; Woese and Olsen, 1986).

For example, the nuclear small subunit rDNA sequences (18S) evolve relatively slow and are useful for studying distantly related organisms whereas the mitochondrial rDNA genes evolve more rapidly and can be useful at the ordinal or family level (White *et al.*, 1990).

The ribosomal RNA genes (rDNA) possess characteristics that are suitable for identification of fungi at many levels. These genes are relatively small, highly stable and exhibit a mosaic of conserved and diverse regions within the genome. They also occur in multiple copies with up to 200 copies per haploid genome arranged in tandem repeat or clusters (Karp *et al.*, 1999; Hibbet, 1992).

The ribosomal gene cluster is comprised of three regions coding for the small subunit ribosomal genes (18S) and large subunit ribosomal genes (28S) which are separated by intergenic transcribed spacer (ITS) region or 5.8S [figure 1.4]. Each cluster is separated from the next cluster by intergenic spacer (IGS) region which comprises two spacers, non transcribed spacer (NTS) and external transcribed spacer

(ETS) that serves to separate the repeats or clusters from one another on the chromosomes (Guarro *et al.*, 1999). The NTS region evolves more rapidly and less conservative than other regions (Dixon and Hillis, 1991). Although these rDNA genes are presents as tandem repeats, they evolve as a single unit even though the rate of evolution may vary within individual regions of the ribosomal DNA cluster and therefore can be used to compare organisms at several levels [figure 1.2].

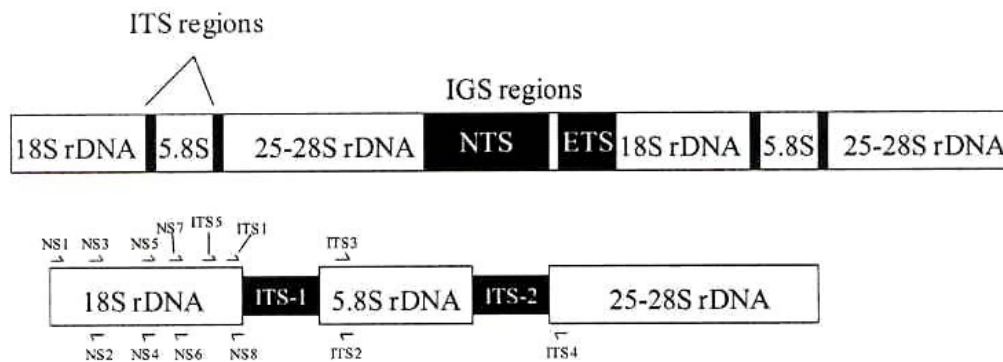


Figure 1.2 Fungal rDNA gene cluster with an expansion showing common primer binding sites (Bugni and Ireland, 2004)

Internal transcribed spacer (ITS) region of ribosomal DNA is defined as a unit containing the ITS 1 spacer, 5.8 rRNA genes and ITS 2 spacer (Jobes and Thien, 1997). The ITS region is now perhaps the most widely sequenced DNA region using in fungal identification at species level because they are the most divergent and variable compared to the other regions, but the sequences still can be aligned and allow amplification using universal primers. These regions may also demonstrate patterns of microevolution (Guarro *et al.*, 1999).

By using ITS 1 and ITS 4 primers, the ITS1-5.8S-ITS2 region (approximately 550 base pairs) can be amplified by polymerase chain reaction (PCR) method and subsequently sequenced (White *et al.*, 1980; Abd-Elsalam *et al.*, 2003). PCR method is used for amplifying one region of DNA that lies between two primers. This method

was first invented by Kary Mullis in 1985 (Newton and Graham, 1997). After amplifying, PCR products were then subjected to direct sequencing to get the sequences in ITS region. ITS sequences (about 550 basepairs) are very well represented in the sequence databases, so one can identify a fungus quite accurately simply by sequencing the ITS region, performing a BLAST (basic local alignment search tool) search of public databases, and finding an exact match so that in the final end taxonomic information could be obtained (Geiser, 2004).

Not in all cases that identification using ITS sequences can define taxonomy of fungi until species level. Furthermore in some genera such as *Aspergillus* and, *Penicillium*, identification using ITS region can define the taxonomy only until genus level. In the case of genus *Penicillium*, large subunit region (28S) is useful for identifying closely related species that have almost identical ITS sequence by using primers ITS 1 and D2R which are covering some part of 28S region and a whole of 5.8S (about 1200 basepairs) for obtaining the taxonomical information until species level (Peterson, 2000).

1.6 Estimation of fungal diversity in the host of marine derived fungi by DGGE method

The use of this highly variable region as a molecular indicator for complex microbial populations, based on total DNA extracts of environmental samples was developed by Muyzer (Muyzer *et al.*, 1993). While originally, individual PCR products (which share a similar size for each individual of the microbial population) were isolated by cloning prior to sequencing, separation can nowadays also be achieved by electrophoretic techniques such as denaturing gradient gel electrophoresis (DGGE) method (O'Callaghan *et al.*, 2003).

DGGE is a technique that allows the comparison and analysis of total microbial populations coupling with polymerase chain reaction (PCR) using primers that target conserved, taxonomically significant genes. It was originally used in the fields of medicine and diagnostic research to detect point mutations (O'Callaghan *et al.*, 2003).

The application of DGGE to estimate fungal biodiversity is a multi step procedure which relies on several other methods. DNA must be extracted first from the environmental sample. Second, DNA has to be amplified by PCR using taxonomically significant primers. In an additional PCR step, a so called GC-clamp is added by using a modified primer. The PCR products obtained from the previous step then last would be subjected to DGGE. The DGGE technique enables PCR products which have the same size of nucleotides, but with different internal sequence composition to be separated in gradient gel according to the melting behavior of the DNA (Koschinsky *et al.*, 1999; O' Calaghan *et al.*, 2003).

In DGGE method, samples are loaded vertically onto the gel which has characteristic of increasing denaturing chemical gradient. In a denaturing gradient, double-stranded DNA is subjected to an increasing denaturant environment and will melt in discrete segments called "melting domains". The melting temperature (T_m) of these domains is sequence-specific. When the T_m of the lowest domain is reached, DNA will become partially melted, creating branched Y-shaped molecules. Partial melting of DNA reduces its mobility in a polyacrylamide gel. Addition of GC clamp is necessary to ensure that they do not melt completely during electrophoresis (Koschinsky *et al.*, 1999).

Vainio and Hantula (1999) reported the estimation of fungal biodiversity in some woody plants by DGGE technique which was achieved by amplifying total DNA with fungal small subunit rDNA using primers FR1 and FF700 (about 390 base pairs).

Other example of estimating fungal biodiversity by DGGE technique was reported by the research group of Dr. Schultz in Braunschweig who investigated ascomycetes associated with marine algae *Fucus seratus*. In this research, total DNA isolated from *Fucus seratus* was amplified in small subunit rDNA (18S) region using primers NS1-EF3 and NS1-EF3 and also in large subunit rDNA (28 S) region (Zuccaro *et al.*, 2003).

1.7. Aim and scope of the study

The aims of this study were to investigate bioactive compounds of fungi derived from marine organisms collected from Java Sea and Mediterranean Sea, and to estimate the real biodiversity of endophytic fungi in marine organisms using molecular biology approaches.

Some pure fungi isolated from marine algae collected from Java Sea and those isolated from sponges collected from Mediterranean Sea, were grown in Wickerham medium (added with artificial sea salt). After growing them for 3-4 weeks, the fungi were harvested and extracted with various organic solvents. The extracts then have been subjected to a diverse array of chromatographic methods (VLC, column chromatography, semi preparative HPLC, preparative HPLC etc) in order to get pure compounds. The structures of isolated compounds were then elucidated with the aid of NMR and mass spectroscopic methods.

The isolated pure compounds were subjected to various bioassays such as cytotoxicity assay using L5178Y mouse lymphoma T cancer cells and to protein-kinases assays.

Estimation of fungal biodiversity within marine organisms was performed using denaturing gradient gel electrophoresis (DGGE).

2. MATERIALS AND METHODS

2.1 Field trip and sample collecting

The source for marine-organism derived fungi in this study originated from Pulau Seribu, Java Sea, Indonesia, collected in 2004 and from Limski Kanal, Mediterranean Sea, Croatia, collected in 2005. In Java Sea, the samples of marine algae were taken by SCUBA diving and snorkeling. In the Mediterranean Sea, samples of sponges and anemone were taken by SCUBA diving.

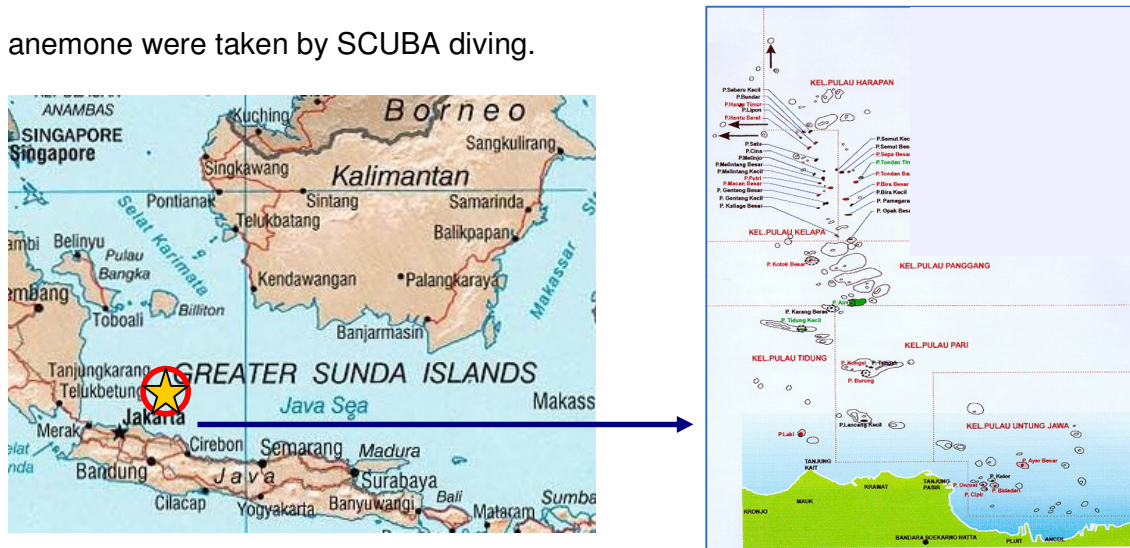


Figure 2.1 Map of collection site in Pulau Seribu, Java Sea, Indonesia



Figure 2.2 Map of collection site in Limski Kanal, Mediterranean Sea, Croatia

2.2 Cultivation and screening of fungi

A piece of the inner part of the source (marine algae or sponge) was immersed in ethanol 70% for 60 - 120 seconds and sliced under sterile condition. The pieces then were positioned on the surface of malt agar dish. Chloramphenicol 0.2 g/l had been added to the malt agar medium in order to avoid bacterial contamination. Negative control is absolutely necessary in order to see whether there is contamination from external parts of the slices. The fungi started growing from the pieces after 3 days until 14 days. Some steps of purification might be needed in order to get pure fungi strains [figure 2.5].

Malt Agar Medium:

Substances	Amounts
Malt extract (Merck)	15.0 g
Bacto Agar (Merck)	15.0 g
Distilled water	1 l
Sea salt	24.4 g

2.3 Fungi collection

Table 2.1 Marine-algae derived fungi from Seribu Island, Indonesia

Code	Fungi	Source Organisms
1t1	<i>Xylaria</i> sp.	<i>Padina australis</i>
2h1	<i>Daldinia escholzii</i>	<i>Halimeda bornealis</i>
4h1	<i>Penicillium chrysogenum</i>	<i>Sargassum</i> sp.
4h2b	<i>Penicillium citrinum</i>	<i>Sargassum</i> sp.
7h	<i>Aspergillus</i> sp.	<i>Turbinaria ornata</i>
8t	<i>Aspergillus</i> sp.	<i>Caulerpa sertularoides</i>
10h1	<i>Diaporthe phaseolorum</i>	<i>Gracilaria arcuata</i>
15t1	<i>Fusarium equiseti</i>	<i>Sargassum</i> sp.
15t2	<i>Nodulisporium</i> sp.	<i>Sargassum</i> sp.
16h1	<i>Penicillium citrinum</i>	<i>Sargassum</i> sp.

18h	<i>Eutypella scoparia</i>	<i>Turbinaria ducerens</i>
-----	---------------------------	----------------------------

Table 2.2 Marine-sponges derived fungi from Mediterranean Sea, Croatia

Code	Fungi Species	Source Organisms
AA1.1	NN	<i>Aplysina aerophoba</i>
AA2.2	<i>Trichoderma citrinoviride</i>	<i>Aplysina aerophoba</i>
AA3.4	NN	<i>Aplysina aerophoba</i>
AA3.5	<i>Didymella cucurbitacearum</i>	<i>Aplysina aerophoba</i>
AA3.6	<i>Cladosporium sphaerospermum</i>	<i>Aplysina aerophoba</i>
AA4.7	<i>Nectria haematococca</i>	<i>Aplysina aerophoba</i>
AA4.8	NN	<i>Aplysina aerophoba</i>
AA5.9	<i>Lewia infectoria</i>	<i>Aplysina aerophoba</i>
AA9.23	<i>Talaromyces wortmanii</i>	<i>Aplysina aerophoba</i>
CN1.1	<i>Tritirachium</i> sp.	<i>Chondrilla nucula</i>
CN4.10	<i>Cladosporium cladosporioides</i>	<i>Chondrilla nucula</i>
CN5.5	<i>Penicillium chrysogenum</i>	<i>Chondrilla nucula</i>
CN5.6	NN	<i>Chondrilla nucula</i>
CN5.7	NN	<i>Chondrilla nucula</i>
CN9.1	<i>Paraphaeosphaeria michotii</i>	<i>Chondrilla nucula</i>
DA1.1	unidentified	<i>Dysidea avara</i>
PV1.1	unidentified	<i>Petrosia figiformis</i>
PV2.2	<i>Diatrype stigma</i>	<i>Petrosia figiformis</i>
PV3.3	NN	<i>Petrosia figiformis</i>
PV4.8	<i>Paraphaeosphaeria michotii</i>	<i>Petrosia figiformis</i>
PV5.4	NN	<i>Petrosia figiformis</i>
PV6.6	<i>Paraphaeosphaeria</i> sp.	<i>Petrosia figiformis</i>
SD1.1	<i>Botryosphaeria stevensii</i>	<i>Suberites domuncula</i>
SD1.2	<i>Penicillium chrysogenum</i>	<i>Suberites domuncula</i>
SD1.3	<i>Cladosporium herbarum</i>	<i>Suberites domuncula</i>
SD2.4	<i>Alternaria compacta</i>	<i>Suberites domuncula</i>
SD3.6	<i>Pestalotiopsis funereoidea</i>	<i>Suberites domuncula</i>
SD4.9	<i>Penicillium chrysogenum</i>	<i>Suberites domuncula</i>

SD4.12	<i>Myrothecium</i> sp.	<i>Suberites domuncula</i>
Te1.1	<i>Arthrimum</i> sp.	<i>Tethya</i> sp.
Te1.2	<i>Chaetomium</i> sp.	<i>Tethya</i> sp.
Te1.3	<i>Biscogniauxia mediterranea</i>	<i>Tethya</i> sp.
Te1.4	<i>Penicillium polonicum</i>	<i>Tethya</i> sp.
Te3.6	<i>Arthrimum</i> sp.	<i>Tethya</i> sp.
Te3.7	<i>Chaetomium globosum</i>	<i>Tethya</i> sp.
Te4.8	<i>Sclerotinia sclerotiorum</i>	<i>Tethya</i> sp.
Te6.13	<i>Peniophora cinerea</i>	<i>Tethya</i> sp.

NN : not identified

Table 2.3 Marine-anemone derived fungi from Mediterranean Sea, Croatia

Code	Fungi Species	Source Organism
AE1.1	unidentified	<i>Actinia equinia</i>
AE1.2	NN	<i>Actinia equinia</i>
AE1.3	unidentified	<i>Actinia equinia</i>
AE1.4	NN	<i>Actinia equinia</i>
AE1.5	unidentified	<i>Actinia equinia</i>
AE2.6	<i>Cordyceps bassiana</i>	<i>Actinia equinia</i>
AE3.8	<i>Lewia infectoria</i>	<i>Actinia equinia</i>
AE4.13	<i>Verticillium luteoalbum</i>	<i>Actinia equinia</i>
AE4.17	NN	<i>Actinia equinia</i>
AE6.23	<i>Beauveria bassiana</i>	<i>Actinia equinia</i>

NN : not identified

2.4 Identification of fungi

The most common technique for obtaining DNA involves cultivation of fungi in agar medium, harvesting a piece of mycelium, lysing the cell wall and separation of DNA from debris (DNA isolation).

2.4.1 DNA isolation

The fungus was grown on a malt agar dish. Following growth of the mycelium for one week, a piece (0.5 cm²) of fungal culture was cut from the agar dish and lyophilized in a sample tube (2 mL) closed with a hydrophobic membrane in the freezedrier. The sample was powderized in a MixerMill MM300 (Retsch, Haan, Germany) for 8 minutes after adding a tungsten carbide bead (Qiagen, Hilden, Germany).

DNA isolation from fungi was performed using the DNeasy Plant Mini Kit from Qiagen according to the manufacturer's protocol. The procedure includes cell lysis, digestion of RNA by RNase A, removing of precipitates and cell debris, DNA shearing, DNA precipitation and purification.

400 µl of AP1 buffer (lysis buffer) and 4 µl of RNase were added to the powderized tissue in the eppendorf tube and the mixture was incubated in the water bath at 60° C for ten minutes. RNase was added for destructing unwanted RNA from the cell. For separating DNA from protein, detergent and polysaccharides, 130 µl of AP2 buffer (precipitation buffer) were added to the lysate and incubated for 5 minutes on ice. The lysate was then put into the Qiasredder spin column and centrifuged for 2 minutes at 13.000 rpm. 1.5 volumes of buffer AP3/E (binding buffer) were then added to the filtrate. The mixture of them then was loaded onto the column and centrifuged at 8000 rpm for 1 minute. The DNA was trapped in the column material, then washed with 500 µl of AW buffer (washing buffer containing ethanol) twice and centrifuged until the column was free of washing buffer. The DNA was eluted by adding 50 µL of elution buffer onto the column and centrifuged at 8000 rpm for 1 minute. DNA quantification was carried out by spectrophotometry (Nanodrop ND1000).

2.4.2. DNA amplification

DNA amplification by PCR was then performed using Hot StarTaq Master Mix Taq polymerase (Qiagen) and the primer pair ITS1 and ITS4 from Invitrogen (White *et al.*, 1990) in an iCycler thermocycler. PCR is an essential DNA amplification technique that eventually leads to amplification of various parts of the genome. This process is in fact an *in vitro* DNA replication reaction by means of a thermostable DNA polymerase that polymerizes DNA chains, which results in the synthesis of large quantities of a defined sequence. The polymerase will generally recognize single-stranded DNA as an appropriate template. Usually the genomic DNA is denatured at 95° C to produce single-stranded DNA. The *in vivo* DNA replication is achieved artificially by creating a replication startpoint at the position of the gene to be amplified by making use of short oligonucleotides with complementary base sequences to the template DNA, commonly known as primers.

The primers facilitate the polymerization of this region. The enzyme will then move to the new end of the new strand and finally only replicate the gene of interest. The whole process takes only minutes and can be repeated many times specifically replicating and thereby amplifying the selected region. The amplification can be controlled by monitoring the number of cycles repeated in the reaction. PCR takes place in the automated thermocycler which will control the different temperatures during the whole PCR reaction. The thermocycler is programmed to cycle at certain temperatures, which consists of a high temperature at 95°C for denaturing DNA, a relatively low temperature that depends on the base composition of the primers to allow the annealing of the primers to the DNA template and finally followed by an intermediate temperature (usually 72°C) for extension.

PCR was carried out according to the following protocol:

- 1) Initial denaturation 95,0 °C 15:00 min.
- 2) Denaturation 95,0 °C 1:00 min.
- 3) Annealing 56,0 °C 0:30 min.
- 4) Extension 72,0 °C 1:00 min.
- 5) Final extension 72,0 °C 10:00 min.

Steps 2) – 4) have been repeated 35 times.

Each sample consisted of 25 µL Taq polymerase master mix, 3 µL primer mix (10 pmol / µL each), 3 µL template DNA and 19 µL RNA-free water.

Primer sequences

ITS1 : TCCGTAGGTGAACCTGCGG

ITS4: TCCTCCGCTTATTGATATGC

2.4.3. DNA electrophoresis

PCR products and DNA ladders were loaded into the wells of an agarose gel after addition of loading buffer containing glycerol and bromophenol blue. The addition of this buffer is aimed to visualize the migration of PCR product (DNA) in the gel and to increase the weight of the PCR products so that they would sink into the gel wells. Electrophoresis was conducted at 70 volts for 80 min. The gel consisted of 2% agarose (Sigma) in 100 mL TBE buffer. 10 µl of Sybr Safe stain (Invitrogen) had been added before casting.

2.4.4. Purification of PCR products

After electrophoresis, the gel was transferred into the UV-transluminator to confirm that the PCR has been successfully carried out and the PCR products had the

right size of about 550 bp by comparing them with the DNA ladder. The DNA would appear as yellow bands under UV light.

The band was precisely excised from the gel and placed into an Eppendorf tube. The PCR product was isolated from the gel slice using the PerfectPrep Gel Cleanup Kit (Eppendorf).

Three volumes of binding buffer were added to the gel slices and incubated in a water bath at 50° C for 10 minutes in order to dissolve the gel matrix. After the gel slices were completely dissolved, one volume of isopropanol was added to precipitate the DNA. The lysate was then placed into a spin column in a 2 mL collection tube and centrifuged at 8.000 rpm for 1 minute to adsorb the PCR product to the spin column material. The spin column was transferred to a new collection tube and then washed with washing buffer containing ethanol by centrifugation at 8.000 rpm for 1 minute. After that step, elution buffer was added to the spin column in a collection tube in order to elute PCR products from the spin column by centrifugation at 8.000 rpm for 1 minute. The purified PCR products were stored at -20 °C before sequencing.

2.4.5. DNA sequencing

The PCR products were submitted for direct sequencing to SeqLab GmbH, Goettingen, Germany and BMBF, Heinrich Heine Universität Düsseldorf with the primer ITS1.

The next step consisted of the alignment of these sequences. BLAST search of the FASTA sequence was performed with the option “nr”, including GenBank, RefSeq Nucleotides, EMBL, DDBJ and PDB sequences on the BLAST homepage, NCBI, Bethesda, USA.

2.5 Denaturing gradient gel electrophoresis (DGGE)

The use of a highly variable region as molecular indicator for microbial populations in environmental samples in an electrophoretic approach was developed by Muyzer *et al.*, 1993. The electrophoretic technique used most often has been denaturing gradient gel electrophoresis (DGGE).

Denaturing gradient gel electrophoresis (DGGE) is an electrophoretic method to identify single base changes in a segment of DNA. In a denaturing gradient acrylamide gel, double-stranded DNA is subjected to an increasing denaturant environment and will melt in discrete segments called “melting domains”. The melting temperature of these domains is sequence-specific. When the T_m of the lowest domain is reached, DNA will become partially melted, creating branched molecules. Partial melting of DNA reduces its mobility in a polyacrylamide gel [figure 2.3].

PCR product with addition of GC Clamp

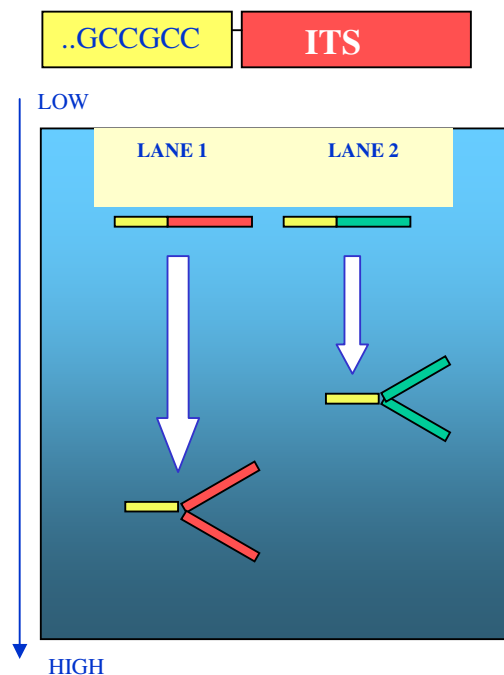


Figure 2.3 The migration of PCR products with addition of GC clamp in DGGE Gel

In DGGE, the denaturing environment is created by a combination of uniform temperature (60° C) and a linear denaturing gradient formed with urea and formamide. The denaturing gradient may be formed perpendicular or parallel to the direction of electrophoresis.

2.5.1 Amplification of ITS region with addition of GC Clamp

The ITS region with addition of GC clamp in upstream position could be amplified by two steps of PCR. The first PCR was conducted using primers ITS 1 and ITS 4 without addition of GC clamp. PCR products then were purified using the Perfectprep Gel Cleanup Kit (Eppendorf) and used as templates for the next PCR.

Re-amplification was conducted using primers ITS 1 with addition of GC Clamp and ITS 4. Both amplifications were using 1 unit of Platinum[®] PCR Super Mix (Invitrogen) for each reaction. Amplifications were carried out with the following conditions: 35 cycles of 94° C for 2 minutes, 50° C for 25 seconds, and 65° C for 2 minutes, followed by one cycle of 65° C for 10 minutes.

The addition of a 30-40 base pair GC clamp to one of the PCR primers ensured that the region screened was in the lower melting domain and that the DNA would remain partly double-stranded.

2.5.2 Preparation of DGGE gel

Denaturing gel solutions 40% and 70% were prepared by mixing of the denaturing gel solutions 0% and 100% until they reached appropriate concentrations. Ammonium persulfate and TEMED (final concentration of each was 0.09%) in order to polymerase the polyacrylamide gel. Both solutions had been mixed by the gradient delivery system (Biorad) and delivered into the assembled vertical gel form (gel

sandwich) in order to cast the gel vertically and parallel gradually from 40% (upper position of the gel) to 70% (lower position of the gel) [figure 2.4].

40% Acrylamide/Bis (filtered and stored at 4° C)

Reagent	Amount
Acrylamide	38.93 g
Bis-acrylamid	1.07 g
Distilled water	Up to 100 mL

Denaturing Solution

Reagent	Denaturing Solution 0%	Denaturing Solution 100%
40% Acrylamide/Bis	25 mL	25 mL
50 x TAE Buffer	2 mL	2 mL
Formamide (deionized)	-	40 mL
Urea	-	42 g
Distilled water	Up to 100 mL	Up to 100 mL

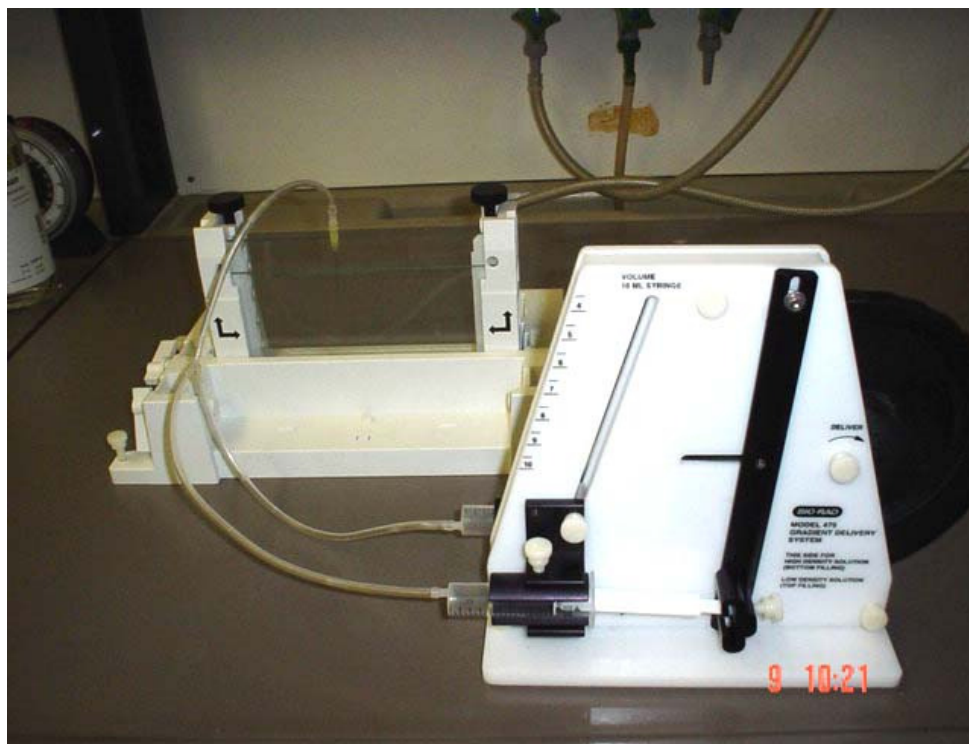


Figure 2.4 DGGE Gel sandwich and gradient delivery system

2.5.3 DGGE

The gel in the vertical sandwich form was placed into the DGGE electrophoresis tank containing 7 l of preheated TAE buffer. The purified PCR products were loaded and run at 110 Volts for 6 hours. After completing electrophoresis, the gel was removed from the tank and stained using 50 µg/mL of Sybr Gold in TAE buffer for 10 minutes in the dark and destained using 1x TAE buffer for 15 minutes. Bands which appeared in UV light revealed the real diversity of the fungal community in the sample.

2.5.4 Purification of bands

These bands were excised from the polyacrylamide gel and purified by PerfectPrep Gel Cleanup Kit from Eppendorf according to the modified manufacturer's protocol and amplified by PCR using primers ITS 1 and ITS 4 (step 2.4.2). PCR products were then purified (step 2.4.4) and submitted for direct sequencing to BMBF, Heinrich Heine Universität Düsseldorf with the primer ITS1.

These sequences were subsequently compared with the genbank using BLAST search (www.ncbi.nlm.nih.gov/blast) to identify each fungus which was represented by each single band.

2.6 Cultivation of fungi

The pure fungus was inoculated in sterilized 300 mL Wickerham Medium with addition of 24.4 g/l sea salt in a 500 mL Erlenmeyer flask under sterile conditions and incubated for 21 – 28 days at room temperature (20°C). Termination of the fermentation was performed by adding 250 mL ethyl acetate to the culture flask for at least 24 hours before extraction could be performed [figure 2.5].

Wickerham Medium:

Substances	Amounts
Malt extract (Merck)	3.0 g
Yeast extract (Sigma)	3.0 g
Pepton (Merck)	5.0 g
Glucose monohydrate	10.0 g
Bacto Agar (Merck)	15.0 g
Sea salt	24.4 g
Distilled water	1 l

2.7 Extraction of fungal culture

The content of the culture flask including the ethyl acetate was thoroughly mixed with an ultraturrax for 10 minutes and filtrated with a Büchner funnel under vacuum. The filtrate was then extracted three times with ethyl acetate in a separating funnel. The aqueous phase was again extracted three times with 250 mL of water-saturated *n*-butanol. The dried ethyl acetate extract was then fractionated with 150 mL of 90% methanol and 150 mL of hexane to separate the fatty acids. After evaporating the solvent, the crude extract was submitted to bioassay tests including antimicrobial assay and cytotoxicity assay, and also subjected to analytic HPLC in order to observe the UV patterns and retention times of the compounds present in the extract [figure 2.5].

Isolation of natural products was carried out from 12 marine-organisms derived fungi, which were *Penicillium citrinum* (4h2b), *Xylaria* sp. (1t1), *Fusarium equiseti* (15t1) and *Daldinia escholzii* (2h1) derived from marine algae; and *Chaetomium* sp. (Te3.7), *P. polonicum* (Te1.4), *Botryosphaeria stevensii* (SD1.1), unidentified fungus PV1.1, *Paraphaeosphaeria michotii* (PV6.6), *Alternaria compacta* (SD2.4), *Arthrinium* sp. (Te1.1) and *Talaromyces wortmanii* (AA9.23) derived from marine sponges. These

fungi were chosen based on their bioactivity and chemical patterns of their extracts in HPLC chromatograms. Isolating procedures of natural products from these fungi were described in the figure 2.6 until figure 2.17.

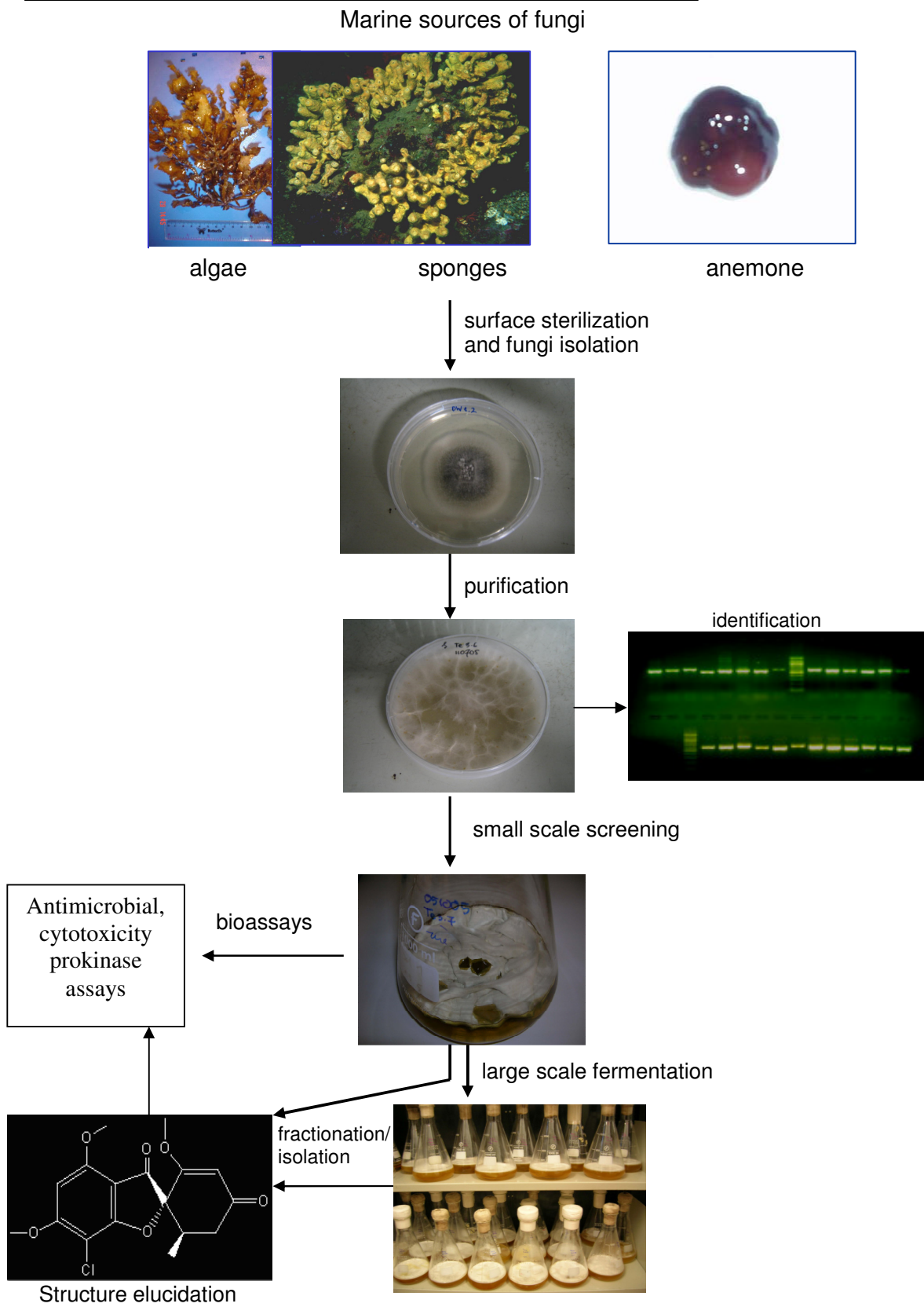


Figure 2.5 Methods of fungi isolation from marine organisms and compounds isolation from marine-organisms derived fungi

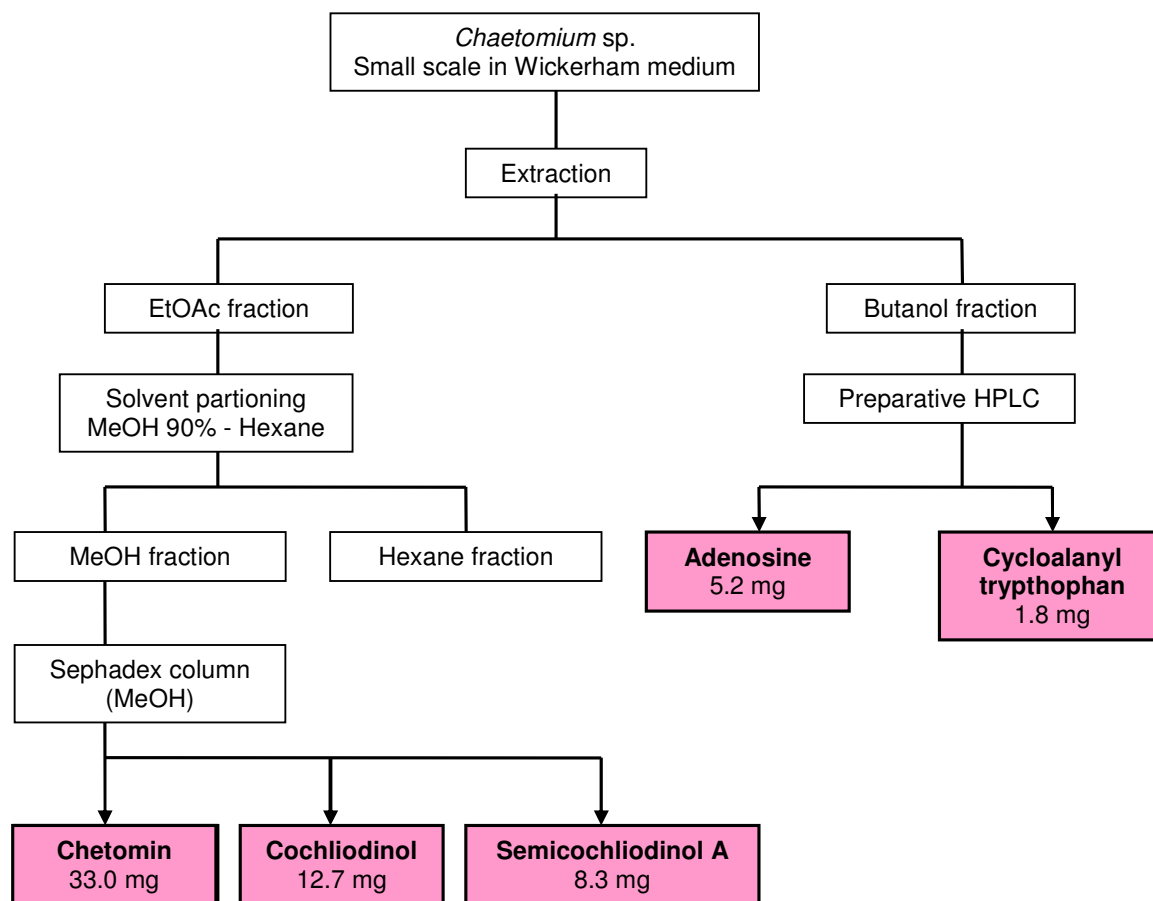
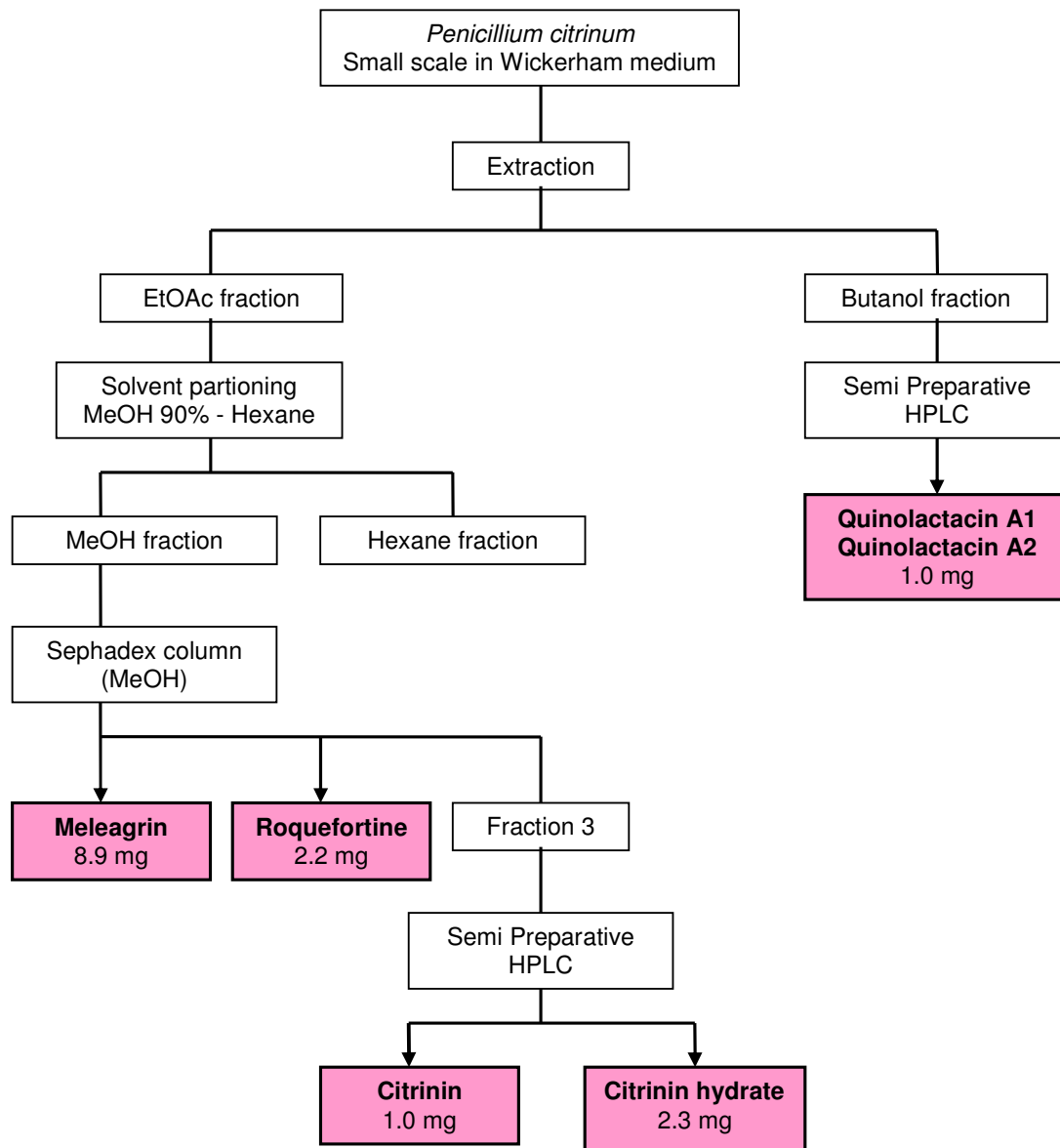


Figure 2.6 Isolation scheme of metabolites from *Chaetomium* sp.

Figure 2.7 Isolation scheme of metabolites from *Penicillium citrinum*

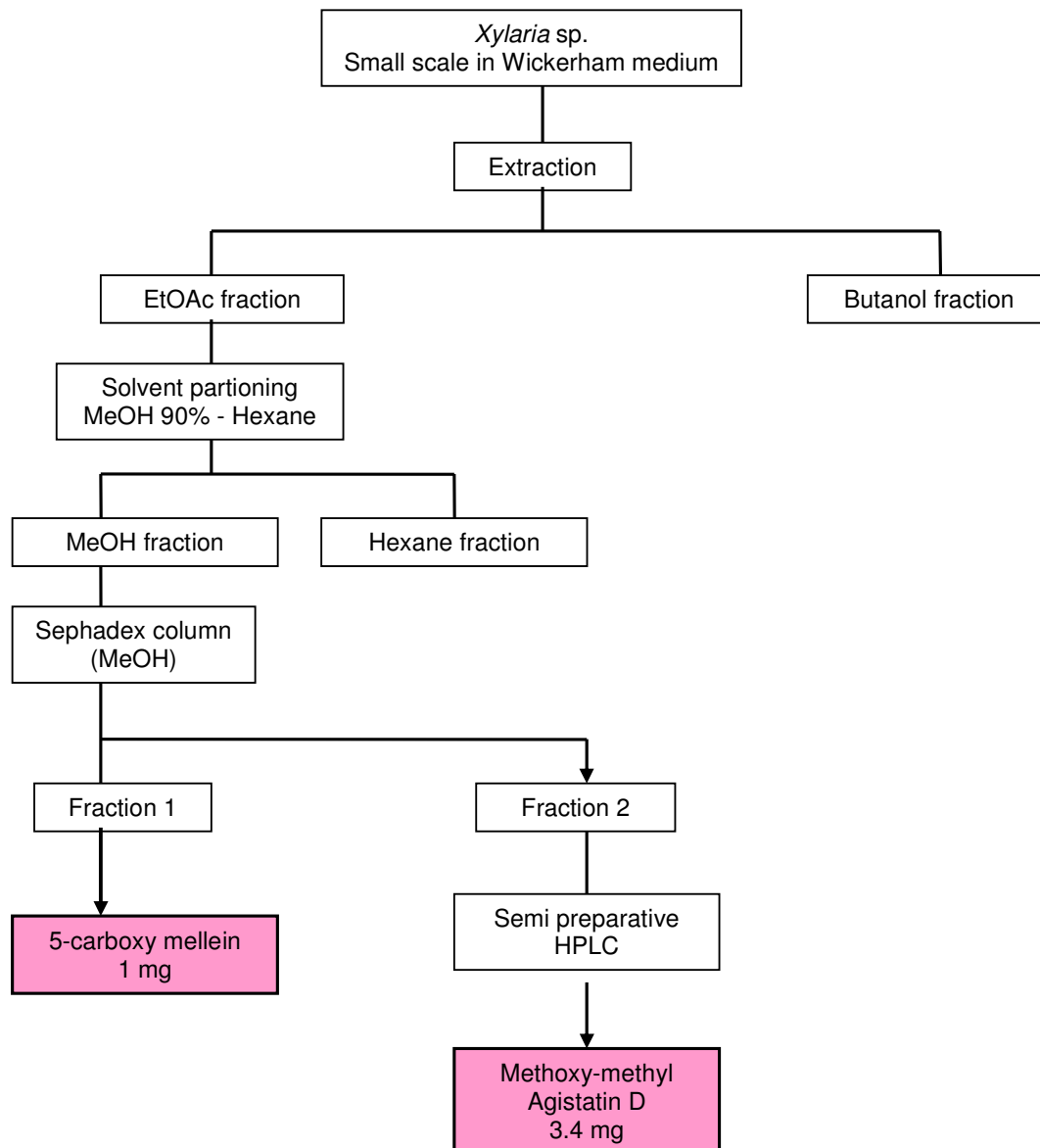


Figure 2.8 Isolation scheme of metabolites from *Xylaria* sp.

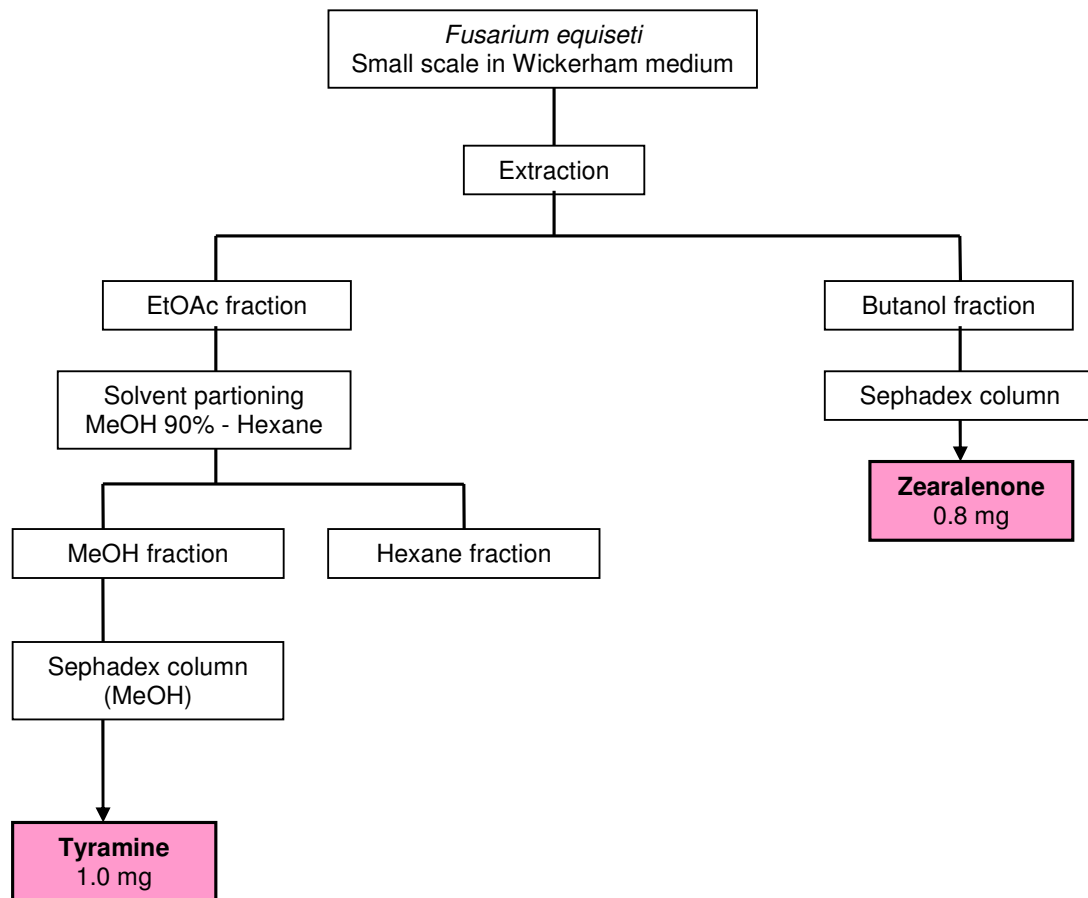
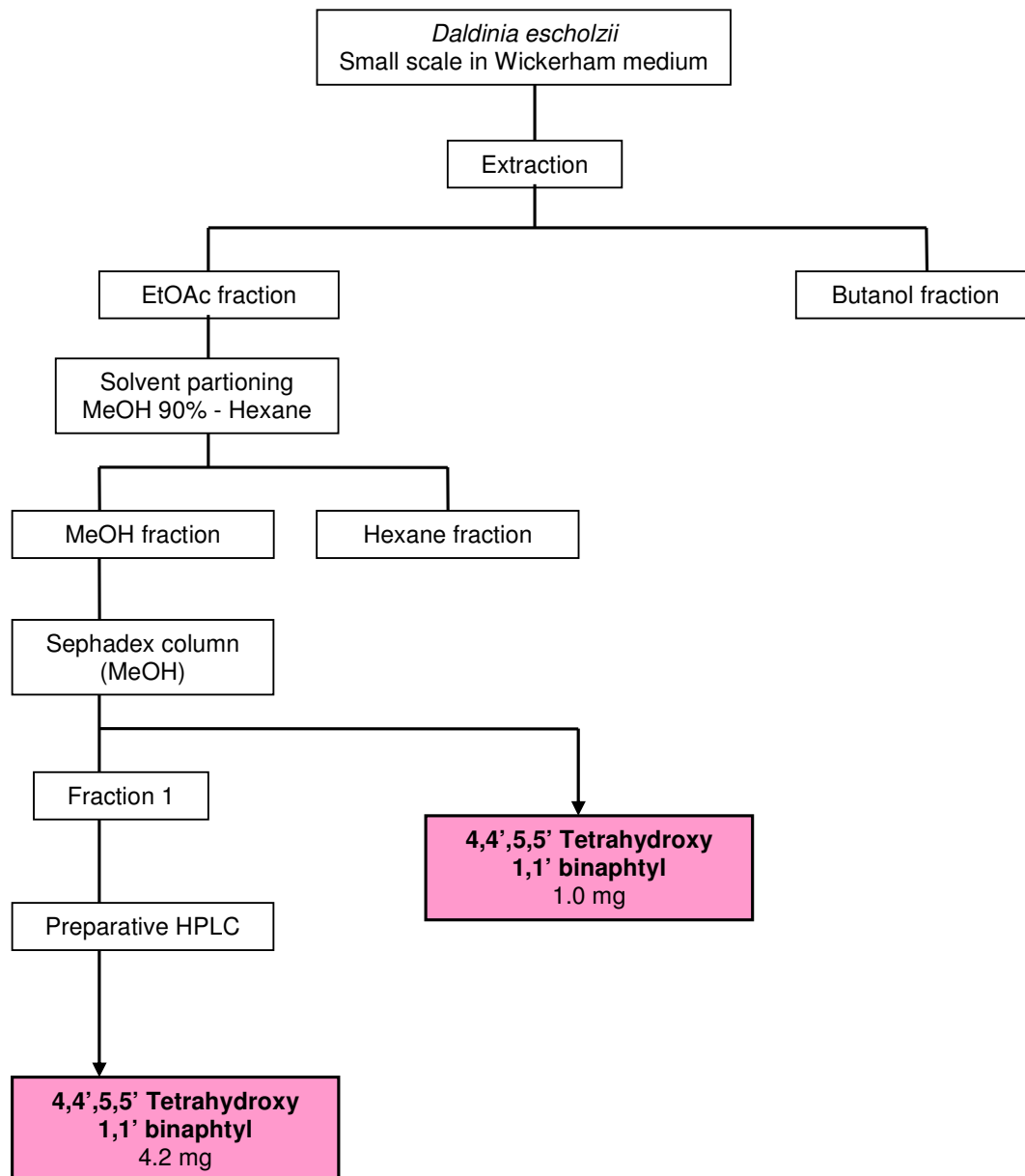
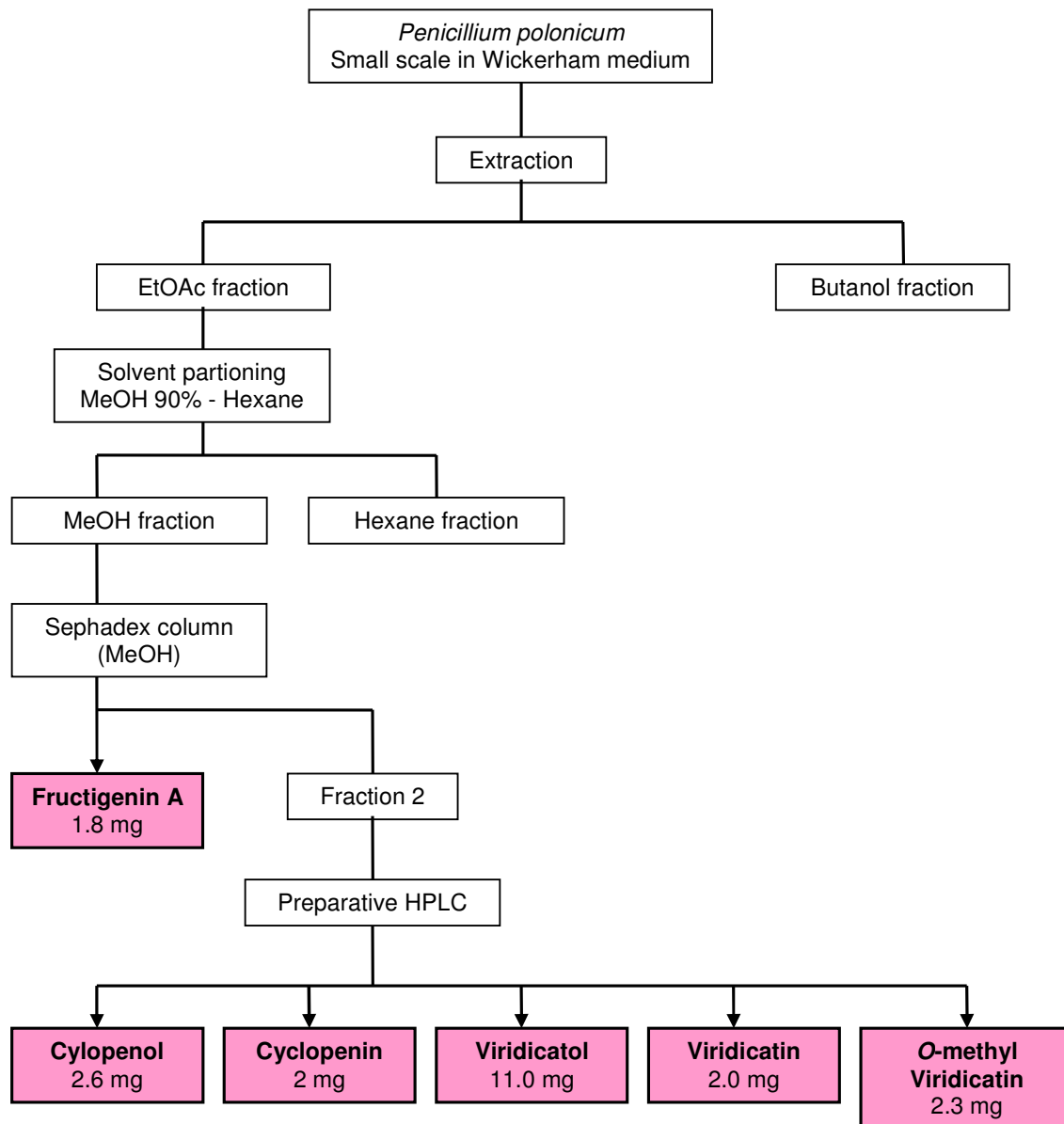


Figure 2.9 Isolation scheme of metabolites from *Fusarium equiseti*

Figure 2.10 Isolation scheme of metabolites from *Daldinia escholzii*

Figure 2.11 Isolation scheme of metabolites from *Penicillium polonicum*

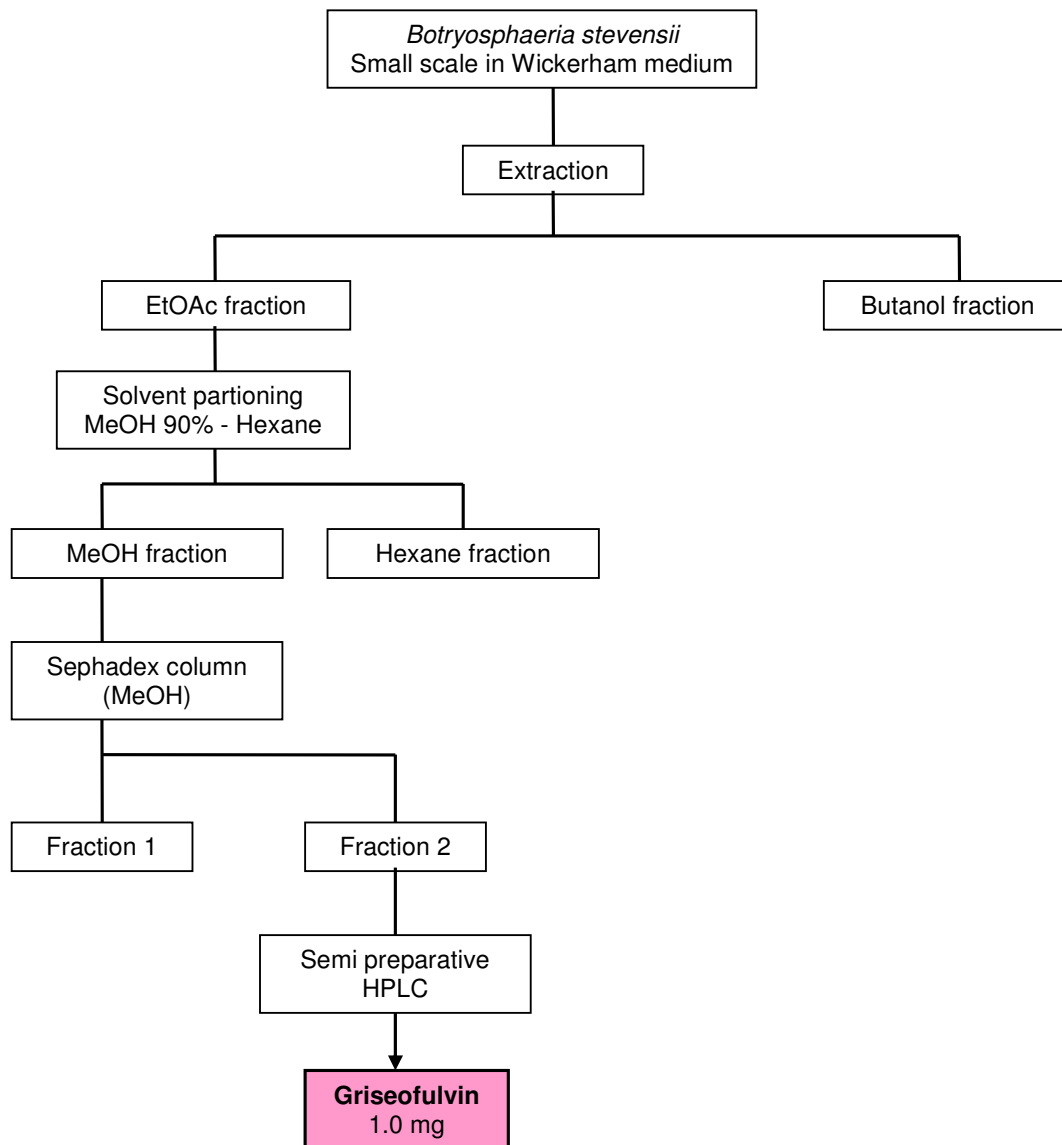


Figure 2.12 Isolation scheme of metabolites from *Botryosphaeria stevensii*

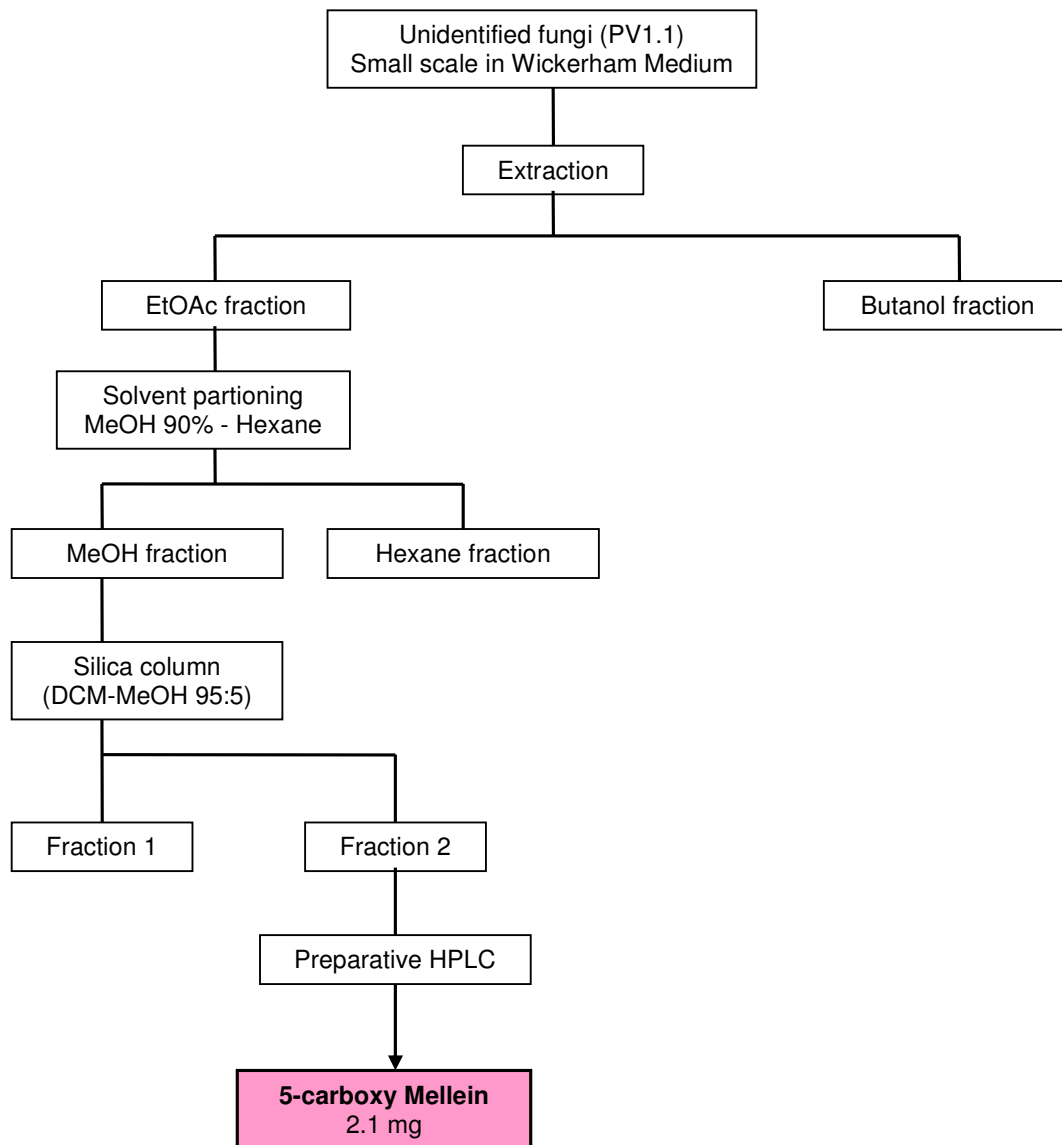


Figure 2.13 Isolation scheme of metabolites from unidentified fungus PV1.1 isolated from marine sponge *Petrosia ficiformis*

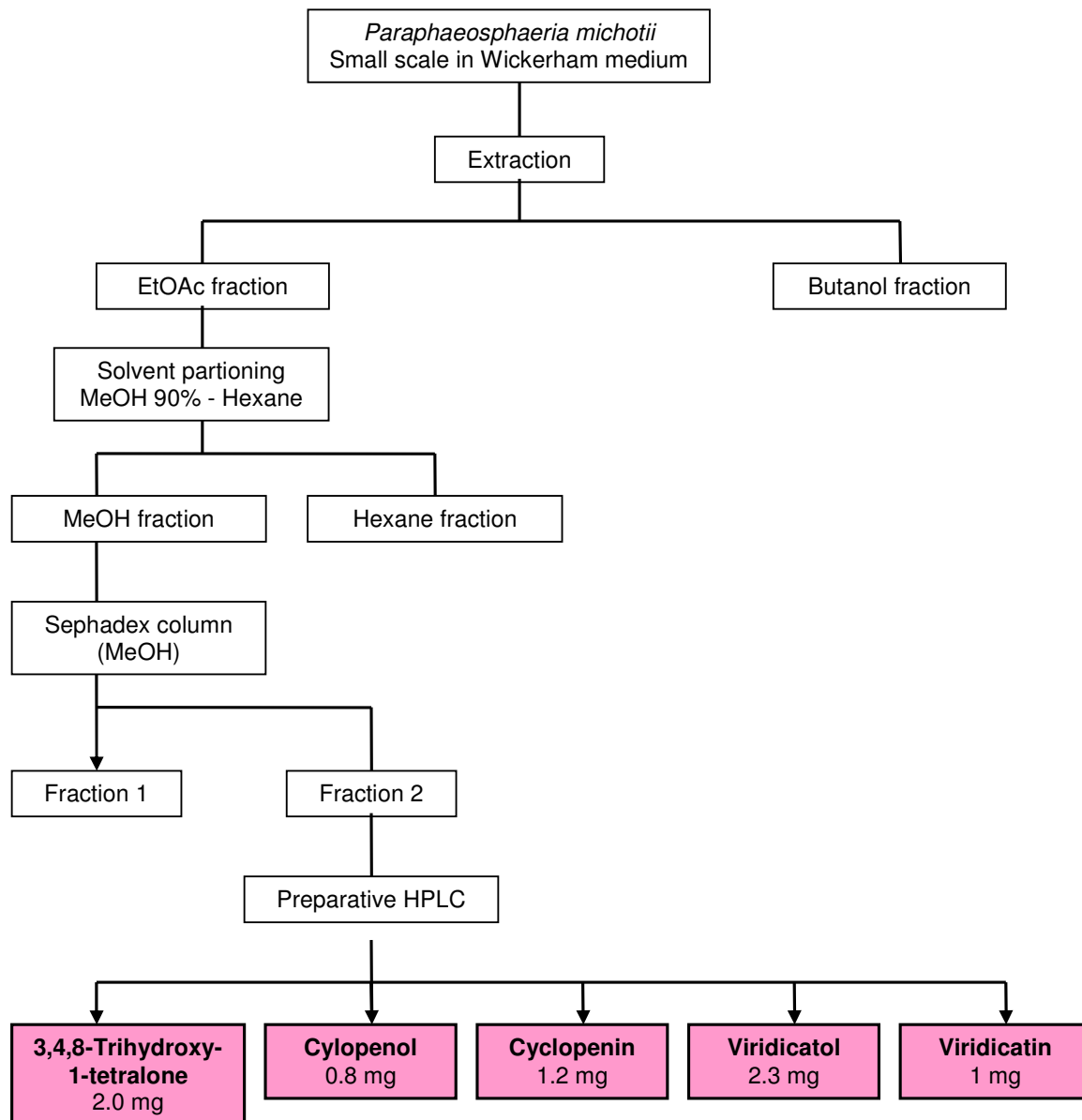
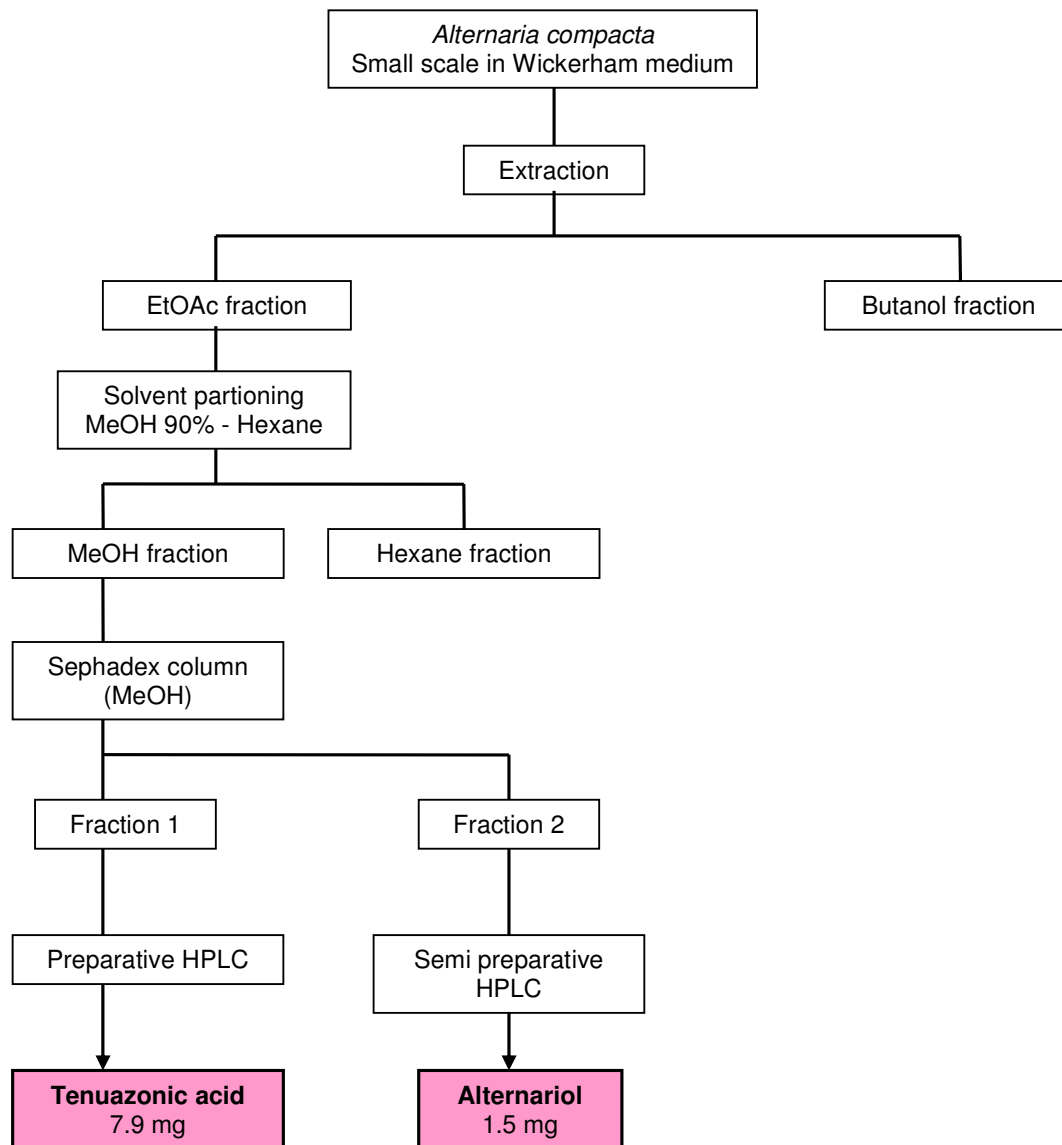


Figure 2.14 Isolation scheme of metabolites from *Paraphaeosphaeria michotii*

Figure 2.15 Isolation scheme of metabolites from *Alternaria compacta*

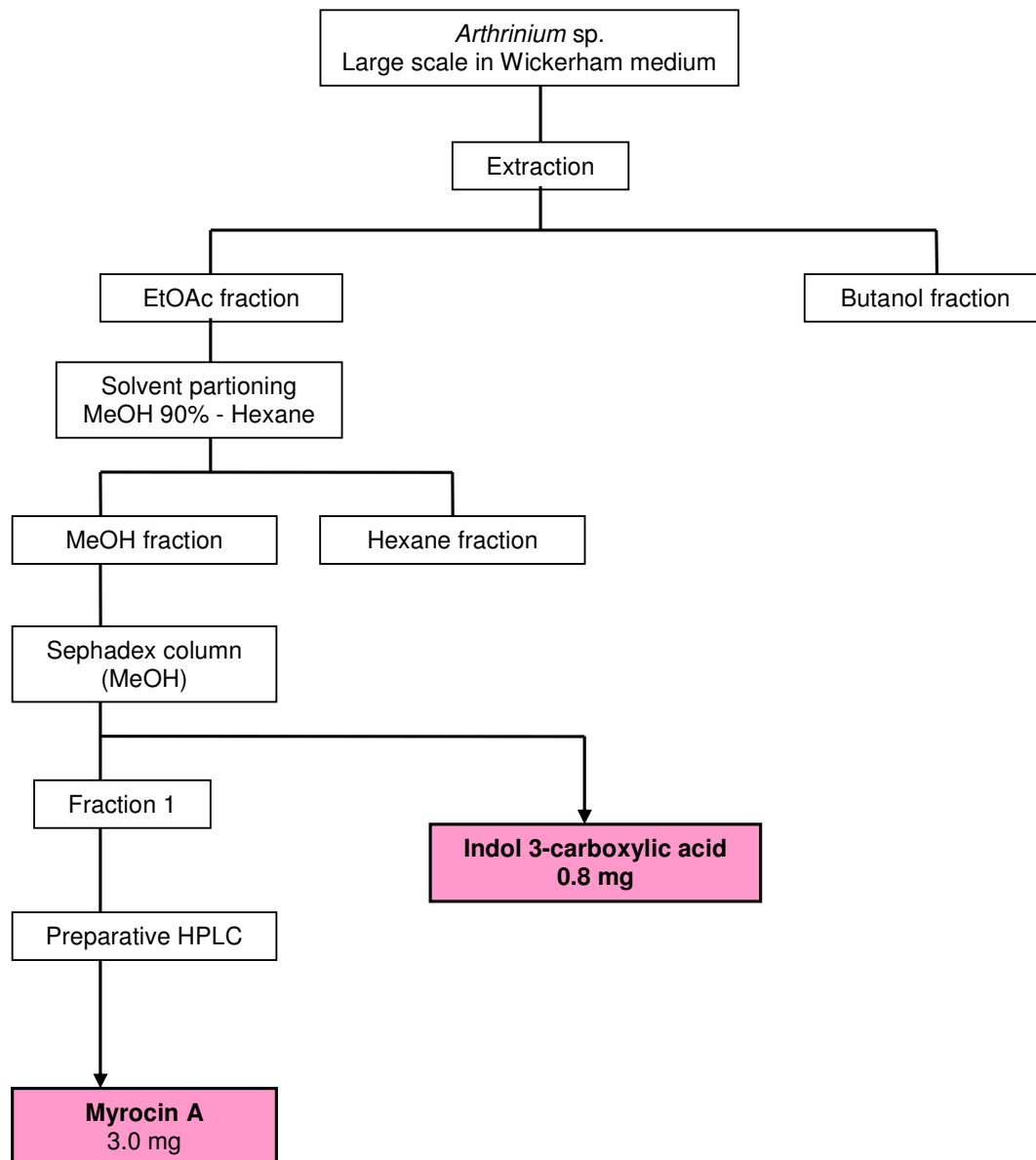


Figure 2.16 Isolation scheme of metabolites from *Arthrinium* sp.

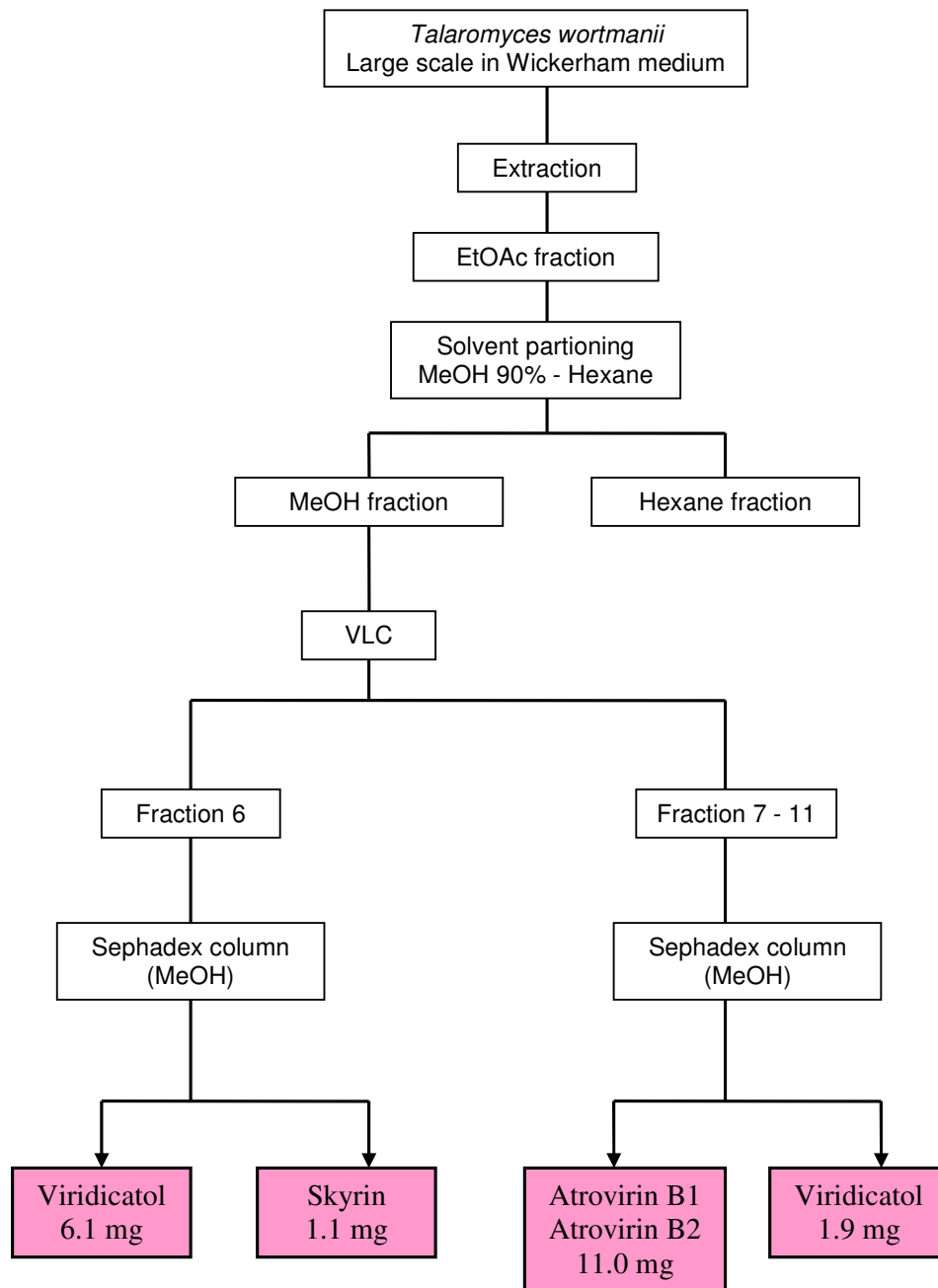


Figure 2.17 Isolation scheme of metabolites from *Talaromyces wortmanii*

2.8 Chemical substances and equipment

2.8.1 Equipments and machines

Nr.	Equipments/machines	Brand
1.	Micropipette 1-10, 10–100, 100-1000 μ l	Eppendorf
2.	Autoclave	Varioklav, H&P
3.	Laminar air flow	HERAsafe, Heraeus
4.	Digital pH meter	420Aplus, Orion
5.	Ultra Turrax	T18 basic, IKA
6.	Balance	Sartorius RC210P
7.	Microcentrifuge	Biofuge pico, Heraeus
8.	Freezedryer	Lyovac GT2 Pump Trivac D10E, Steris
9.	Hot plate	Camag
10.	Magnetic stirrer	Combimag Ika
11.	Rotary-evaporator	Büchi Rotavap RE 111
12.	Vacuum desiccator	SpeedVac SPD 111V, Savant
13.	Oven	Heraeus T5050
14.	PCR Machine	iCycler, Bio-Rad
15.	UV transilluminator	Syngene GVM 20
16.	Mixer mill	MixerMill MM300 (Retsch, Haan, Germany)
17.	Camera	Canon
18.	Water bath	IKA TE 2
19.	Vacuum filtration	Vacuuband (Supelco)
20.	Vacuum desiccator	Savant speedvac SPD111V Savant refrigerator vapour trap RVT400 Pump Savant VLP80
21.	Fraction collector	ISCO Sygnet
22.	Sonicator	Bandelin Sonorek RK 102
23.	Syringe	Hamilton 1701 RSN
24.	UV lamp	Camag (wave length 254 and 366 nm)
25.	NMR	DRX-500 Bruker
26.	Analytic HPLC	Dionex
27.	LCMS	HP1100, Agilent Finnigan LCQ ^{DecaXP} Thermoquest
28.	Semipreparative HPLC	Merck

29.	Polarimeter	Polarimeter 241 MC, Perkin Elmer
30.	Freezer -80° C	Forma Scientific, 86-Freezer

2.8.2 Chemicals

Nr.	Chemical substances	Company
1.	Sephadex LH 20	Sigma
2.	Silica gel 60 diameter 0.2 – 0.5 mm	Merck
3.	Hotstart Taq Mastermix	Qiagen
4.	Primer	Invitrogen
5.	DNA ladder	NEB
6.	TBE Buffer	Merck
7.	Ethidium bromide	Serva
8.	SYBR Safe	Invitrogen
9.	Agarose gel	Serva
10.	DNeasy plant kit	Qiagen
11.	Perfectprep Gel Cleanup Kit	Eppendorf
12.	Anisaldehyde	Sigma
13.	Glacial acetic acid	Sigma
14.	Methanol	LiChroSolv HPLC Grade, Merck
15.	Acetonitril	LiChroSolv HPLC Grade, Merck
16.	Deuterated chloroform (CDCl ₃)	Euriso-top
17.	Deuterated methanol (MeOD)	Euriso-top
18.	Deuterated dimetyl sulfoxide (DMSO- <i>d</i> 6)	Euriso-top
19.	Chloramphenicol	Sigma
20.	Sodium chloride	Sigma

2.8.3 Software

Nr.	Analytical program	Software
1.	HPLC chromatogram	ChromeleonV6.3, Dionex
2.	LCMS	Xcalibur, version 1.3
2.	NMR	NMR Suite Bruker
3.	Sequence alignment	Bioedit
4.	Phylogenetic tree	Mega 21

2.9 Screening and bioassay

2.9.1 Antimicrobial assay

Antimicrobial assays were conducted at the Institut für Pharmazeutische Biologie und Biotechnologie, Heinrich-Heine-Universität Düsseldorf. *Bacillus subtilis* (gram positive bacterium), *Escherichia coli* (gram negative bacterium), and the yeast *Saccharomyces cerevisiae* were employed as test organisms. Luria Bertoni medium was used for the assays against *B. subtilis* and *E. coli* and yeast universal medium was used for assays against *S. cerevisiae*.

Besides antibacterial and anti yeast assays, the antifungal assay was also carried out against the phytopathogenic fungi *Cladosporium cucumerinum* and *C. herbarum* using Potato Dextrose Agar (PDA) medium.

1. Luria-Bertoni Medium for bacteria *Escherichia coli* and *Bacillus subtilis*

Substances	Amounts
Trypton (Sigma)	10.0 g
Yeast extract (Sigma)	5.0 g
Sodium chloride (Aldrich)	10.0 g
Bacto agar (Galke)	15.0 g
Distilled water	up to 1 l
pH	7.0

2. Yeast universal medium for *Saccharomyces cerevisiae*

Substances	Amounts
Yeast extract (Sigma)	3.0 g
Malt extract (Merck)	3.0 g
Pepton (BD)	5.0 g
Glucose (Caelo)	10.0 g
Bacto agar (Galke)	15.0 g
Distilled water	up to 1 l

3. Potato dextrose agar (PDA) medium for *Cladosporium cucumerinum* and *C. herbarum*

Substances	Amounts
Glucose (Caelo)	20.0 g
Bacto agar (Galke)	15.0 g
Potato extract	1 l

2.9.1.1 Antibacterial assay

The antimicrobial assay was performed as an agar diffusion assay according to the Bauer Kirby Test (Bauer *et al.*, 1966). A few colonies (about 3 to 10) of each test microorganism were subcultured in 4 mL of Tryptose-soy broth medium and incubated for 2 until 5 hours allowing producing microbial suspension of moderate cloudiness.

The suspension was then diluted with sterile saline solution to reach the density which was equivalent to that of the barium sulphate (BaSO₄) standard solution. The standard was prepared by mixing 0.5 mL of 1% BaCl₂ and 99.5 mL 1% H₂SO₄ (0.36 N). The prepared bacterial broth was inoculated onto Müller-Hinton-Agar plates and dispersed by means of sterile beads.

Aliquots of the test solution were applied to sterile filter-paper discs (5 mm diameter, Oxid Ltd.) using a final disc loading concentration of 500 µg for the crude extract and two different concentrations of 50 and 100 µg for pure compounds. The substance-impregnated discs were allowed to dry for some time and then subsequently placed on the surface of the test dishes, along with the discs containing solvent blanks as negative control and those containing penicillin G, streptomycin and gentamycin, respectively. The plates were incubated at 37° C for one or two days. Anti-microbial activity was recorded as the clear zones of inhibition surrounding the

discs (measured in mm diameter). The wider the inhibition zone, the greater the antimicrobiological activity of the test substance or crude extracts.

2.9.1.2 Antifungal assay

After growing the test fungi *Cladosporium herbarum*, and *C. cucumerinum* for about a month, mycelium of those were put into fresh fungal medium and homogenized by an ultraturrax mixer. The mycelium was removed by vacuum filtration and the filtrate containing fungal spores was then used for the next step.

100 μ l of the fungal spore preparation was spread onto the surface of potato dextrose agar (PDA) dish. Immediately after that, five sample discs were put onto the surface of the PDA medium, in each dish with a concentration of 500 μ g for the crude extract and two different concentrations of 50 or 100 μ g for pure compounds. The dishes were then incubated at room temperature for 5 days and the growth inhibition zone was measured around the disc. Nystatin was used as positive control.

Table 2.4 Inhibition zone of positive control

Positive control	<i>B. subtilis</i> 10 – 20 μ l	<i>S. cerevisiae</i> 10 – 20 μ l	<i>C. herbarum</i> 10 μ l	<i>C. cucumerinum</i> 10 μ l
Streptomycin	14 - 15			
Penicillin	27 - 35			
Gentamycin	15 - 10			
Nystatin	7 - 9	20 - 8	19	39

2.9.2 Cytotoxicity assay

Cytotoxicity assays were carried out by Prof. Dr. W.E.G. Müller and his co-workers at the Institute of Physiological Chemistry, University of Mainz, Germany. The cytotoxicity against L5178Y mouse T-cell lymphoma cells was determined using the

microculture tetrazolium (MTT) assay and compared to that of untreated controls (Carmichael *et al.*, 1987). Stock solutions of test samples were prepared in ethanol 96% (v/v).

Exponentially growing cells were harvested, counted and diluted appropriately. 50 μ L of cell suspension containing 3750 cells were pipetted into 96-well microtiter plates. Subsequently, 50 μ L of the test sample solution containing the appropriate concentration were added to each well. The concentration range was 3 – 10 μ g/mL. The small amount of ethanol present in the wells did not affect the experiments. The test plates were incubated at 37° C with 5% CO₂ for 72 h. A solution of 3-(4,5-dimethylthiazol-2-yl)-2,5-diphenyltetrazolium bromide (MTT) was prepared at 5 mg/mL in phosphate-buffered saline (PBS: 1,5 mM KH₂PO₄ 6.5 mM Na₂HPO₄, 137 mM NaCl, 2.7 mM KCl; pH 7,4), and 20 μ L from this solution were pipetted into each well.

The yellow MTT penetrates the healthy living cells. MTT is transformed to its blue formazan complex in the presence of mitochondrial dehydrogenases. After an incubation period of 3 h 45 min at 37° C in a humidified incubator with 5% CO₂, the medium was centrifuged (15 min, 20°C, 210 g) and 200 μ L of DMSO were added. The cells were lysed to liberate the formazan product. After thorough mixing, the absorbance was measured at 520 nm using a scanning microtiter-well-spectrometer. The color intensity is correlated with the number of healthy living cells. The ED₅₀ was estimated by logit regression (Sach, 1984).

Cell survival was calculated using the formula:

$$\text{Survival (\%)} = \frac{100 \times (Abs_{tc} - Abs_{cm})}{(Abs_{uc} - Abs_{cm})}$$

Where Abs_{tc} : Absorbance of treated cells;

Abs_{cm} : Absorbance of culture medium;

Abs_{utc} : Absorbance of untreated cells.

All experiments were carried out in triplicate and repeated three times. As controls, media with 0.1% EGMME/DMSO were included in the experiments.

2.9.3 Prokinase assay

Protein kinase screening assay was carried out by Dr. Michael Kubbutat and his coworkers at ProQinase, Freiburg, Germany, for screening the inhibition on protein kinases. The samples were subjected to protein kinase screening assays to provide further information on their mechanism of action particularly in the alteration of cell cycle pathways in a tumour cell (Karp, 1999).

As cancer cells proliferate, secondary mutations are developed which normally also include the genes responsible for DNA repair mechanism, thus enhancing their mutability and plasticity. Protein kinases are involved in the cell cycle pathways and can be a potential cancer therapeutic target.

The inhibitory profile of the samples tested was determined using 24 protein kinases by measuring the kinase activity. The samples were tested at two concentrations (1×10^{-06} g/mL and 1×10^{-05} g/mL).

Stock solutions were dissolved in DMSO (1×10^{-03} g/mL) in column 3 – 12 of a 96-well micronic box. Columns 1 and 2 were filled with micronic tubes containing 100 % DMSO. The box is in the following referred to as “master box”, stored at -20°C for later use. Prior to testing, 10 μ L of each tube of the micronic box were transferred into a 96 well microtiter plate and diluted with 90 μ L of 100 % DMSO, resulting in a “dilution plate” with 1×10^{-4} g/mL in 100% DMSO stock solutions. From each well of the dilution plate, 7 x 5 μ L was aliquoted into 7 identical “copy plates”.

Assays were carried out by using a separate copy plate for each set of 4 protein kinases. Upon thawing of the stock solutions, 45 μL of water was added to each well of the copy plate only a few minutes before the transfer of the compound solutions into the assay plates in order to minimize precipitation. The plate was shaken thoroughly, resulting in a “compound dilution plate” with a concentration of 1×10^{-05} g/mL in 10% DMSO. This plate was used for the transfer of 5 μL compound solution into the assay plates. The final volume of the assay was 50 μL . All compounds were tested at a final assay concentration of 1×10^{-06} g/mL in 1% DMSO in singlicate.

All protein kinases were expressed in Sf9 insect cells as human recombinant GST-fusion proteins of His-tagged proteins by means of the baculovirus expression system. Protein kinases were purified by affinity chromatography using either GSH-agarose (Sigma) or Ni-NTH-agarose (Qiagen). The purity of each kinase was checked by SDS-PAGE/silver staining and the identity of each protein kinase was verified by western blot analyses with kinase specific antibodies or by mass spectroscopy.

A proprietary protein kinase assay ($^{33}\text{PanQinase}^{\text{®}}$ Activity Assay) was used for measuring the kinase activity of the 24 protein kinases. All kinase assays were performed in 96-well FlashPlatesTM from Perkin Elmer/NEN (Boston, MA, USA) in a 50 μL reaction volume. The reaction cocktail was pipetted in 4 steps in the following order: 20 μL of assay buffer; 5 μL of ATP solution (in H_2O); 5 μL of test compound (in 10% DMSO); 10 μL of substrate/10 μL of enzyme solution (premixed). Table 2.1 shows the kinases and the substrate used in the assays.

The protein kinases employed for determination of inhibitory profiles as well as the amounts of enzyme and substrate used per well are as described in table 2.1.

The assay for all enzymes contained 60mM HEPES-NaOH, pH 7.5, 3 mM Magnesium dichloride (MgCl₂), 3 mM MnCl₂, 3 μM Na-orthovanadate, 1.2 mM DTT, 50 μg/mL PEG₂₀₀₀₀, 1 μM [γ -³³P]-ATP (approx. 5 x 10⁰⁵ cpm per well).

The reaction cocktails were incubated at 30° C for 80 minutes. The reaction was stopped with addition of 50 μL of 2% (v/v) phosphoric acid (H₃PO₄). Plates were then aspirated and washed two times with 200 μL of 0.9% (w/v) sodium chloride (NaCl). The incorporation of ³³P was determined with a microplate scintillation counter (Microbeta Trilux, Wallac). All assays were performed with a BeckmanCoulter/Sagian robotic system.

Table 2.1 List of protein kinases and their substrates

Family	Kinases	Substrate	Oncologically relevant mechanisms	Diseases
Ser/Thr kinase	AKT1/PKB alpha	GCS3 (14-27)	Apoptosis	Gastric cancer (Staal, 1987)
	ARK5	Autophos.	Apoptosis	Colorectal cancer (Kusakai <i>et al</i> , 2004)
	Aurora-A	Tetra(LRRWSLG)	Proliferation	Pancreatic cancer (Li <i>et al</i> , 2003)
	Aurora-B	Tetra(LRRWSLG)	Proliferation	Breast cancer (Keen and Taylor, 2004)
	CDK2/CycA	Histone H1	Proliferation	Pancreatic cancer (Iseki <i>et al</i> , 1998)
	CDK4/CycD1	Rb-CTF	Proliferation	Breast cancer (Yu <i>et al</i> , 2006)
	CK2-alpha1	P53-CTM	Proliferation	Rhabdomyosarcoma (Izeradjene <i>et al</i> , 2004)
	COT	Autophos	Proliferation	Breast cancer (Sourvinos, 1999)
	PLK-1	Casein	Proliferation	Prostate cancer (Weichert <i>et al</i> , 2004)
	B-RAF-VE	MEK1-KM	Proliferation	Thyroid cancer

				(Ouyang <i>et al</i> , 2006)
	SAK	Autophos	Proliferation	Colorectal cancer (Macmillan <i>et al</i> , 2001)
Receptor tyr kinase	EGFR	Poly (glu,tyr) _{4:1}	Angiogenesis	Glioblastoma multiforme (National cancer Institute, 2005)
	EPHB4	Poly (glu,tyr) _{4:1}	Proliferation	Prostate cancer (Xia <i>et al</i> , 2005)
	ERBB2	Poly (glu,tyr) _{4:1}	Proliferation	Gastric carcinomas (Lee <i>et al</i> , 2005)
	FLT3	Poly(ala,glu,lys,tyr) 6:2:4:	Apoptosis	Leukemia (Menezes <i>et al</i> , 2005)
	IGF1-R	Poly (glu,tyr) _{4:1}	Counter kinase	Breast cancer (Zhang and Yee, 2000)
	INS-R	Poly(ala,glu,lys,tyr) 6:2:4:1	Metastasis	Ovarian cancer (Kalli <i>et al</i> , 2002)
	MET	Poly(ala,glu,lys,tyr) 6:2:4:1	Proliferation	Lung cancer (Qiao, 2002)
	PDGFR-beta	Poly(ala,glu,lys,tyr) 6:2:4:1	Proliferation	Prostate cancer (Hofer <i>et al</i> , 2004)
	TIE-2	Poly (glu,tyr) _{4:1}	Angiogenesis	Rheumatoid arthritis (DeBusk <i>et al</i> , 2003)
	VEGF-R2	Poly (glu,tyr) _{4:1}	Angiogenesis	Pancreatic cancer (Li <i>et al</i> , 2003)
	VEGF-R3	Poly (glu,tyr) _{4:1}	Angiogenesis	Breast cancer (Gareces <i>et al</i> , 2006)
Soluble tyr kinase	FAK	Poly (glu,tyr) _{4:1}	Metastasis	Breast cancer (Schmit <i>et al</i> , 2005)
	SRC	Poly (glu,tyr) _{4:1}	Metastasis	Colon cancer (Dehm <i>et al</i> , 2001)

The residual activity (in %) for each well of a particular plate was calculated by using the following formula:

$$\text{Res. Activity (\%)} = 100 \times [(\text{cpm of compound-low control}) / (\text{high control-low control})]$$

Low control reflected the unspecific binding of radioactivity to the plate in the absence of a protein kinase but in the presence of the substrate, while high control reflects full activity in the absence of any inhibitor. The difference between high and low control was taken as 100% activity.

2.10 Chromatographic methods

Chromatography was first introduced by Tswett in 1906. It refers to any separation methods in which components are distributed between stationary phase and a mobile phase (William and Fleming, 1995).

2.10.1 Thin layer chromatography (TLC)

TLC consists of stationary phase immobilized on a glass, metal or plastic plate, and a solvent mixture as the mobile phase. The sample is deposited as a spot on the stationary phase. The bottom edge of the plate is placed in a solvent reservoir, and the solvent moves up the plate by the capillary force. When the solvent front reaches the edge at the other side of the stationary phase, the plate is removed from the solvent chamber. The separated spots are visualized with ultraviolet light at the wavelengths of 254 nm and 366 nm. The different compounds in the mixture move up the plate at different migration rates due to their partitioning behaviour.

The bands were detected at 254 nm and 266 nm, followed by spraying with anisaldehyde reagent and subsequent heating at 110° C. Anisaldehyde reagent was a mixture of anisaldehyde (5 parts), glacial acetic acid (100 parts), methanol (85 parts) and concentrated sulphuric acid (5 parts).

2.10.2 Vacuum liquid Chromatography

VLC is a normal phase column chromatography using silica gel as stationary phase. The prepared VLC column was loaded with the extract. Elution was performed with a series of non-polar to polar solvents. The solvent flow is forced by vacuum, which is an advantage for fast processing of bigger extract quantities.

2.10.3 Column chromatography

The mobile phase of the column chromatography is a solvent and the stationary phase is a liquid on a solid support, a solid or an ion exchange resin. Liquid chromatography can be distinguished into four general classes:

1. Normal phase chromatography was the first chromatography setup used and retains analytes based on their polarity. This method uses a polar stationary phase typically silica gel in conjunction with a nonpolar mobile phase (*n*-hexane, chloroform, dichloromethane, etc). Thus hydrophobic compounds elute more quickly than hydrophilic compounds. Normal phase chromatography which has been used in this study employed silica gel 60 with diameter 0.2 – 0.5 mm.
2. Reverse Phase (RP) chromatography consists of a non polar stationary phase and a polar mobile phase, and was developed due to the increasing interest in large non polar biomolecules. One common stationary phase is silica which has been treated with RMe_2SiCl , where R is a straight chain alkyl group such as $\text{C}_{18}\text{H}_{37}$ or C_8H_{17} . The retention time is therefore longer for molecules which are more non-polar in nature, allowing polar molecules to elute more readily. Reversed phase columns are quite difficult to damage compared with normal silica columns; however, they should never be used with aqueous bases as these will destroy the silica.

3. Ion exchange chromatography

Ion-exchange chromatography allows the separation of ions and polar molecules based on the charge properties of the molecules. It can separate proteins based on their isoelectric points and is often used as a first step in protein purification. Both positively-charged and negatively-charged molecules can be separated based on their charge, meaning that this process is not just restricted to proteins. The mobile phase supports ionization to ensure solubility of ionic solutes. The stationary phase must be partially ionic to promote some retention. Consequently, the interactions with the stationary phase are strong which is usually reflected in longer analysis times and broader peaks

4. Size exclusion chromatography also known as gel permeation chromatography or gel filtration chromatography, separates molecules on the basis of size. It is generally a low resolution chromatography and thus it is often reserved for the final, polishing step of purification. It is also useful for determining the tertiary structure and quaternary of purified proteins, and is the primary technique for determining the average molecular weight of natural and synthetic polymers. The stationary phase consists of porous beads. The larger compounds will be excluded from the interior of the bead and thus will elute first. The smaller compounds will be allowed to enter the beads and elute according to their ability to exit the same size pores they were internalized through. In this study, Sephadex LH-20 was used for this purpose.

2.10.4 Analytical high performance liquid chromatography (HPLC)

High performance liquid chromatography (HPLC) was developed in the middle of 1970's and improved quickly with the development of column packing materials and the additional on-line detector. In the late 1970's, new methods including reverse

phase liquid chromatography allowed for improved separation of very similar compounds.

HPLC utilizes high pressure pumps to increase the efficiency of the separation. The use of analytical HPLC was meant to identify the distribution of peaks from the samples, either raw extracts or fractions as well as to evaluate the purity of isolated compounds obtained from a column or semi preparative HPLC. Compounds are separated by injecting some sample mixture into the system. The different components in the mixture pass through the column at different rates due to differences in their partitioning behaviour between the mobile liquid phase and the stationary phase.

The solvent gradient applied started with 10:90 (methanol : nanopure water pH 2) to 100% methanol in 35 minutes. The samples were injected by the autosampler at a volume of 20 μ L. All peaks pointing out the compounds that have UV absorption in wavelength 235, 254, 280 and 340 nm were detected by UV-VIS diode array detector. The HPLC instrument consists of the reservoirs of mobile phases, the gradient pump, the autosampler, the separating column, and the detector as listed below.

Table 2.5 Standard gradient of analytic HPLC

Time (min)	Methanol (%)	Water pH 2 (%)
0	10	90
5	10	90
35	100	0
45	100	0
60	10	90

System component	Specification
Pump	P580 LPG Dionex
Software	Chromeleon V6.3
Autosampler	ASI-100T, Dionex
Column oven	STH 585, Dionex
Column	Eurospher 100-C18, Knauer
Detector	Photoarray detector UVD 340 S, Dionex

2.10.5 Preparative HPLC

Chemical separation can be accomplished by using preparative HPLC in order to isolate and purify compounds. Preparative HPLC is different to analytic HPLC, which focused on obtaining information about compounds such as identification, quantification and resolution.

After pre-separation by column chromatography, the (semi) preparative HPLC machine was used for final purification respectively of the pure compounds from fractions. Solvent systems or eluent systems should be optimized by using an analytical column to find the best mobile phase combination of either methanol and nano pure water, or acetonitrile and water and optimal pH value which could be adjusted by addition of 0.1% TFA. The proportion of the eluent combination depends mainly on the retention time of the compound.

After setting up the systems, the separation run can be started. Every injection contains about 1 – 2 mg of the fraction dissolved in 500 μ l of the solvent system. This solution was pumped through the column at a rate of 5 mL/min. The eluted compound would be detected by UV detector and collected manually in separate tubes.

For proper purification of bigger amount, the Varian preparative HPLC system was used. The set up consists of two separate solvent pumps to form the gradient,

injector block, column and detector. The system is controlled and monitored by the Varian Prepstar software. Since analytical and preparative column are only different in diameter, the method optimized on the analytical column may directly be applied on the bigger one. Upscaling is simply performed by changing the column and increasing the flow by a certain upscaling factor to 20 mL per minute. The compounds were collected manually in separate tubes.

The analytical column (250 x 4.6 mm, i.d.) was prefilled with Microsorb 60-8 C18 (Varian) and the big preparative column (250 x 21.4 mm, i.d.) was also prefilled with Microsorb 60-8 C18 (Varian). Each injection onto the big column may contain a maximum amount of 70 – 80 mg/mL of sample.

Semi preparative HPLC Merck :

System component	Specification
Pump	LaChrom L-7100, Merck/Hitachi
Detector	LaChrom L-7400, Merck/Hitachi
Printer	Chromato-Integrator D-2000, Merck/Hitachi
Column	Eurospher 100-C18, Knauer
Pre-column	Eurospher 100-C18, Knauer

Preparative HPLC Varian:

System component	Specification
Pump	Varian Prepstar 218
Detector	Varian Prepstar 320
Injection block	Rheodyne 7725i

2.11 Structure elucidation of secondary metabolites

2.11.1 Mass spectroscopy

The mass spectrometer, in its simplest form, is designed to perform three basic functions: to vaporize compounds of widely varying volatility; to produce ions from the

resulting gas-phase molecules; and to separate ions according to their mass-to-charge ratios (m/z), and subsequently detect and record them.

Since multiple charged ions are produced only rarely relative to single charged ions, z can normally be presumed as one; and since e is a constant (the charge of one electron), m/z then gives the mass of ions. Thus, the mass spectrometer is a device for the production and weighing of ions.

The most intense peak in the spectrum is termed the base peak and all others are reported relative to its intensity. The highest molecular weight peak observed in the spectrum will typically represent the molecular weight of the measured compound. Its appearance depends on the compound stability. Structures with double bonds, aliphatic and aromatic rings stabilize the molecular ion.

Molecules have distinctive fragmentation patterns which provide structural information of the compound. The fragmentation process usually follows the chemical pathway. ESI-LCMS measurement was conducted at the Institut für Pharmazeutische Biologie und Biotechnologie, Heinrich-Heine-Universität Düsseldorf. EI and FAB-MS measurement was performed in the Institut für Anorganische Chemie and Strukturchemie, Heinrich-Heine-Universität Düsseldorf.

2.11.1.1 Electron impact mass spectrometry (EI-MS)

The vaporized sample which is produced from thermally volatile materials is bombarded with a beam of electrons (10-100eV). These electrons have sufficient energy not only to ionize an organic molecule but also to cause extensive fragmentation. The electron deposits typically all its energy into a molecule with which it interacts. If it causes ionization, it will then deposit only 0-6eV of internal energy in the resulting ions. The advantage is that the extensive fragmentations as result of the

bombardment give a pattern of fragment ions which can help to characterize the compound.

2.11.1.2 Electron spray ionization (ESI-MS)

Electron spray ionization is most commonly used on quadrupole and FT/ICR mass spectrometers. The former combination has been encouraged by the ease of coupling these methods of ion production and analysis, and the latter by the advantage of coupling a method for production of ions from large biomolecules with a method for the detection of these ions with high sensitivity and high resolution. An enormous advantage of ESI is that it generates a distribution of molecular ion charged states

ESI is an excellent technique for the production of molecular ions from large polar molecules and it will be seen subsequently that it frequently produces multiply charged ions. This method can be conveniently used to analyze the effluent from the HPLC column directly.

The electron spray system produces highly charged droplets which may be positively or negatively charged depending on the polarity of the voltage applied. When the droplets contain dissolved sample molecules, then molecular ions of these sample molecules can be obtained by evaporation of the solvent. As the solvent evaporates under reduced pressure, the droplets disappear leaving highly charged molecules.

2.11.1.3 Fast atom bombardment mass spectrometry (FAB-MS)

In FAB desorption, the energy is provided by a beam of ions or atoms, respectively, of large translational energies. The sample may be bombarded typically

with xenon (Xe) or argon (Ar) in its solid state, but more commonly is to first dissolve it in a matrix of low volatility. Salts (A+B⁻) and highly polar molecules of molecular weights up to ca. 3000 Dalton give good results when analyzed by this technique.

In general, FAB mass spectrometry results in relatively little fragmentation and usually gives a large molecular peak, making it useful for determination of the molecular weight. The atomic beam is produced by accelerating ions from an ion source through a charge-exchange cell. The ions pick up an electron in collisions with neutral atoms to form a beam of high energy atoms.

2.11.2 Nuclear magnetic resonance (NMR)

The phenomenon of nuclear magnetic resonance was first observed in 1946 and it has been routinely applied in organic chemistry since about 1961. NMR data for protons and carbons determine chemical shift, coupling constant, multiplicity and peak areas or integrals.

Some atomic nuclei have a nuclear spin (I), and the presence of a spin makes these nuclei behave rather like bar magnets. In the presence of an applied magnetic field, the nuclear magnets can orient themselves in $2I + 1$ ways. Those nuclei with an odd mass number have nuclear spin of $\frac{1}{2}$, or $\frac{3}{2}$ or $\frac{5}{2}$,... etc. In the application of NMR spectroscopy, ^1H and ^{13}C are the most important and both have spins of $\frac{1}{2}$. These nuclei therefore can take up one of only two orientations, a low energy orientation aligned with the applied field and a high energy orientation opposed to the applied magnetic field. The nuclei then are irradiated with electromagnetic radiation which is absorbed and places the parallel nuclei into a higher energy state; consequently, they are now in resonance with the radiation. Each C and H will produce different spectra depending on their location and adjacent molecules, or

elements in the compound, because all nuclei in molecules are surrounded by electron clouds which change the encompassing magnetic field and thereby alter the absorption frequency.

NMR measurement was carried out by Dr. W. Peters at the NMR service, Institut für Anorganische Chemie, Heinrich-Heine-Universität Düsseldorf, Germany and Dr. Victor Wray at the Institute for Biotechnology (Gesellschaft für Biotechnologische Forschung/GBF), Braunschweig, Germany.

Several deuterated solvents such as MeOD, DMSO-d₆, CDCl₃ were used to dissolve samples for NMR measurement. The selection of the NMR solvents was dependent on the solubility of the sample and the consideration to obtain signals of hydroxyl and amine groups. One and two dimensional NMR spectra then were processed and analyzed using the NMR software 1D WIN-NMR and 2D WIN-NMR Bruker NMR Suite.

The NMR spectra were calibrated using solvent signals of their protons (¹H: MeOH 3.30 ppm, DMSO-d₆ 2.49 ppm, CDCl₃ 7.26 ppm) and carbons (¹³C: MeOH 49.00 ppm, DMSO-d₆ 39.70 ppm, CDCl₃ 77.00 ppm). The observed chemical shift values (δ) were given in ppm and the coupling constants (J) in Hertz (Hz).

2.11.3 Optical rotation

The rotation of the orientation of linearly polarized light was first observed in the 1811 in quartz by the French physicist Dominique F.J. Arago. Around this same time, Jean Baptiste Biot also observed the effect in liquids and gases of organic substances. In 1822, the English astronomer Sir John F.W. Herschel discovered that different crystal forms of quartz rotated the linear polarization in different directions.

Compounds which can be categorized as optically active should at least contain one chiral centre.

Optical activity is a macroscopic property of a collection of these molecules that arises from the way they interact with light. The instrument for measuring optical rotation in optically active compounds is polarimeter. This equipment consists of a light source, two polarising filters and a cell that contains a solution of the analyzed compound.

A method of differentiating enantiomers is based on the following differences: the *d* or (+) optical isomer rotates the light plane clockwise (*dextro*-rotary) and the *l* or (-) optical isomers rotates the light plane counter-clockwise (*levo*-rotary)

Optical rotation was carried out on a Perkin Elmer-241 MC Polarimeter by measuring the angle of rotation at the wavelength of 546 and 579 nm of a mercury vapour lamp at room temperature (25°C) in a 0.5 mL cuvette with 0.1 diameter length. The calculation of specific optical rotation is calculated using this formula:

$$[\alpha]_D^{20} = \frac{3.199 \times [\alpha]_{579}}{4.199 - \frac{[\alpha]_{579}}{[\alpha]_{546}}}$$

Where $[\alpha]_D^{20}$ = the specific rotation at sodium D-line (589 nm) at a temperature of 20° C.

$[\alpha]_{579}$ and $[\alpha]_{546}$ = the optical rotation at wavelength 579 and 546 nm, calculated by the following formula.

$$[\alpha]_\lambda = \frac{100 \times \alpha}{l \times c}$$

Where: α = the angle of rotation (°),

l = the length of polarimeter tube (dm),

c = the concentration of the substance (g/100 mL of the solution).

3. RESULT OF ISOLATED METABOLITES

3.1 Isolated compounds of fungus *Chaetomium* sp.

Chaetomium sp. was isolated from marine sponge *Tethya* sp. collected from the Mediterranean Sea. Five metabolites were isolated from the ethyl acetate and *n*-butanol extracts of this fungus which was grown first in Wickerham Medium. They were chetomin (compound **1**), cochliodinol (compound **2**), semicochliodinol A (compound **3**), adenosine (compound **4**) and cyclo alanyl tryptophan (compound **5**).

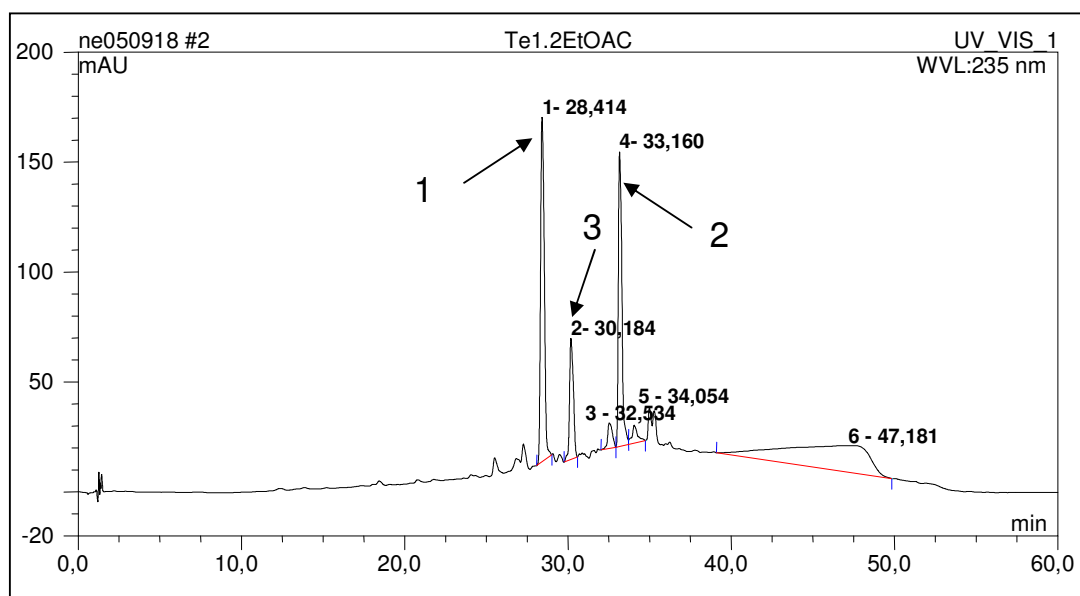


Figure 3.1 HPLC chromatogram of the ethyl acetate extract of *Chaetomium* sp.

Table 3.1 Biological test result of *Chaetomium* sp. and its metabolites

Sample	L5178Y growth (%) Conc. 10 µg/mL	EC ₅₀ (µg/mL)
Ethyl acetate extract of <i>Chaetomium</i> sp.	2.5	
Chetomin	0.4	< 0.1
Cochliodinol	0.4	0.33
Semicochliodinol A	0.7	0.52
Adenosine	104.6	
Cycloalanyl tryptophan	95.9	

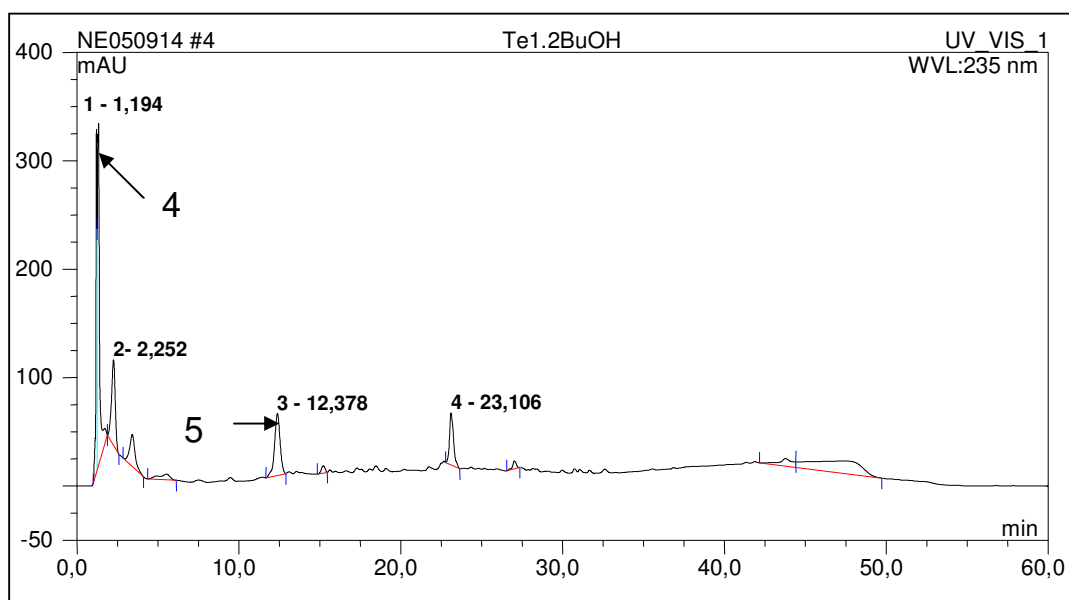


Figure 3.2 HPLC chromatogram of *n*-butanol extract of *Chaetomium* sp.

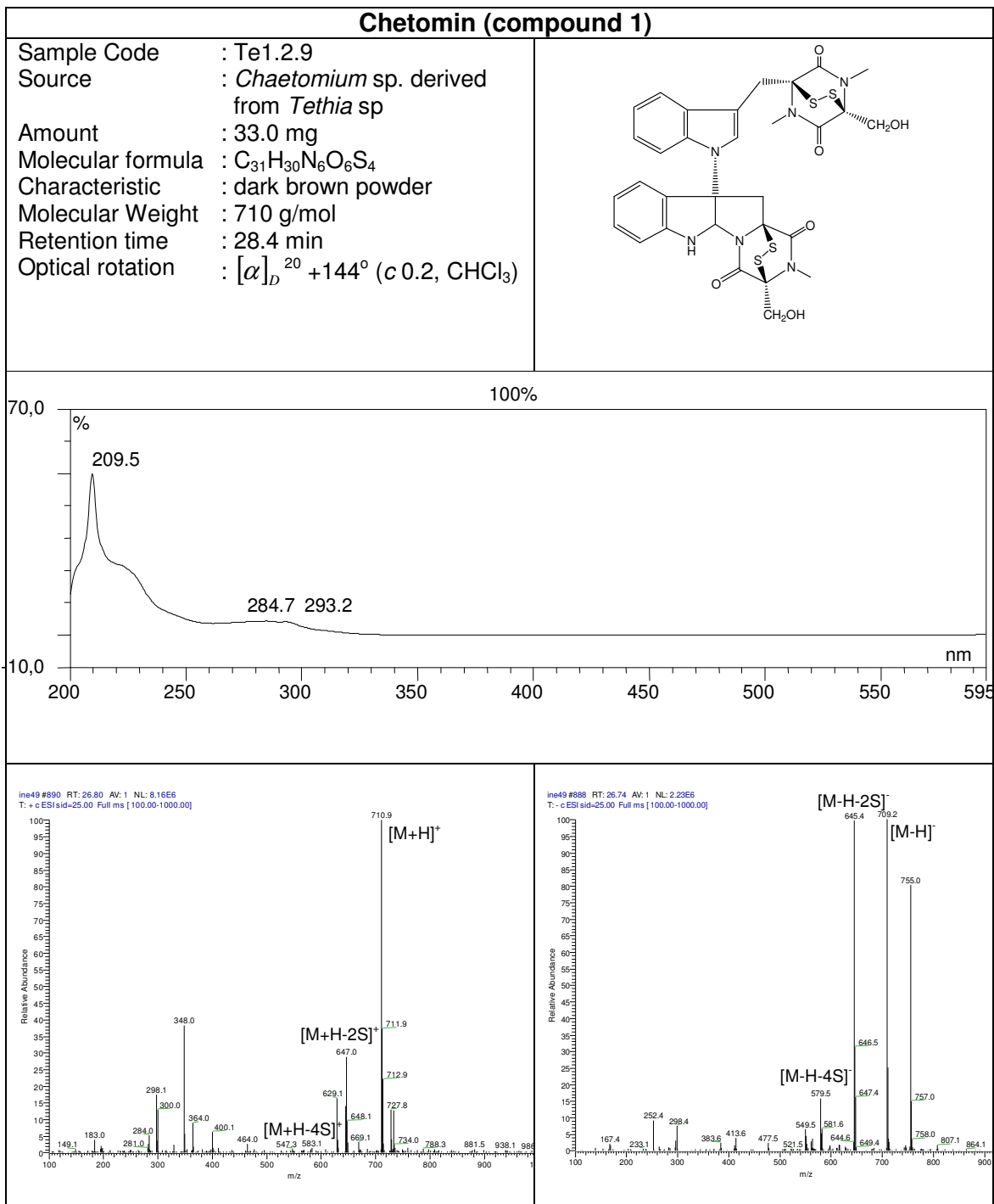
3.1.1 Compound 1 (chetomin)

Compound 1 (chetomin) was a major compound isolated from the ethyl acetate extract of *Chaetomium* sp. through Sephadex LH-20 column chromatography with 100% methanol. The UV spectrum of compound 1 showed maxima λ_{\max} (MeOH) at 209.5, 284.7 and 293.2 nm. Its ESI-MS showed the most intense peaks at m/z 711 $[M+H]^+$ and m/z 709 $[M-H]^-$ in accordance with a molecular weight of 710 g/mol. Together with the careful inspection of the ^1H NMR and ^{13}C NMR data, a molecular formula $\text{C}_{31}\text{H}_{30}\text{N}_6\text{O}_6\text{S}_4$ was derived.

In the ^{13}C NMR and DEPT spectra [figure 3.4], 31 carbon atoms were observed, consisting of four methylene groups and 13 signals from methyl and methine groups. Although chetomin possessed 31 carbons, the ^{13}C spectrum contained only 30 distinct resonances because carbon C-1 and carbon C-1' overlapped.

In the ^1H NMR spectrum [figure 3.3], eight protons resonating between δ 6.74 and 7.71 ppm were detected. The COSY spectrum [figure 3.5A] and the data of

splitting patterns and coupling constants proved that those protons assembled into two individual ABCD spin systems characteristic of two 1,2-disubstituted aromatic systems.



Both of these systems were annealed to a pyrrole ring each, forming two indole skeletons. The protons in the two pyrrole rings were detected at the chemical shifts of 6.17 (H-5) and 7.21 ppm (H-9'). H-9' was located more downfield because of the deshielding effect of the electron-withdrawing carbonyl group C-1'.

The carbon types were revealed by the ^{13}C spectrum and the HMQC spectrum [figure 3.6], including three methyl groups which were linked to nitrogen atoms (NCH_3) characterized by signals appearing upfield at δ 28.0 (C-13), 28.1 (C-16') and 28.3 ppm (C-17'), four methylene groups (C-7', C-15', C-11, C-12), 10 methine groups (C-9', C-11', C-12', C-13', C-14', C-5, C-7, C-8, C-9, C-10), 14 quaternary carbon atom groups, four of which showing chemical shifts typical for carbonyl groups at δ 167.3 (C-1 and C-1'), δ 163.3 (C-4) and δ 167.4 ppm (C-4').

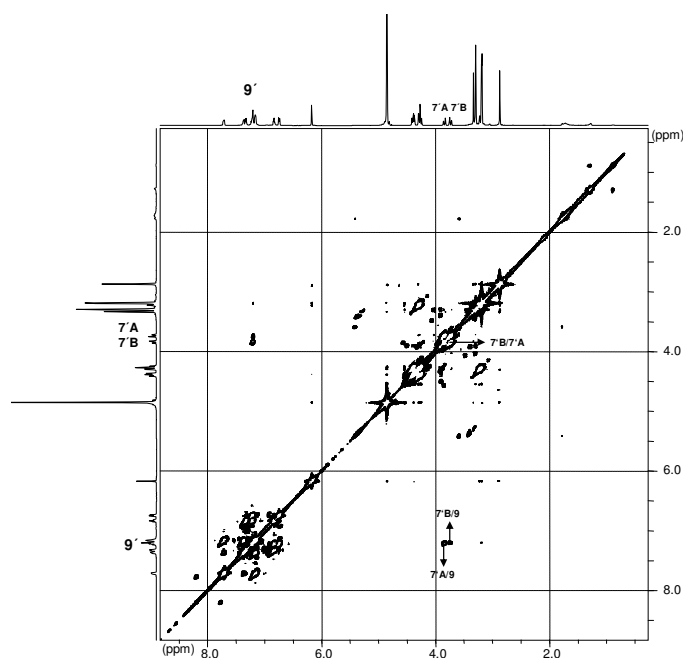
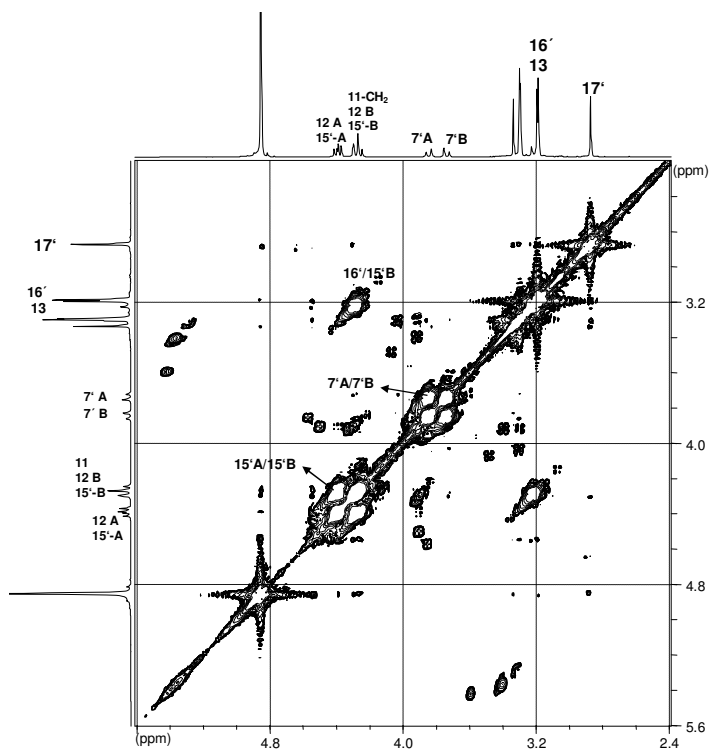
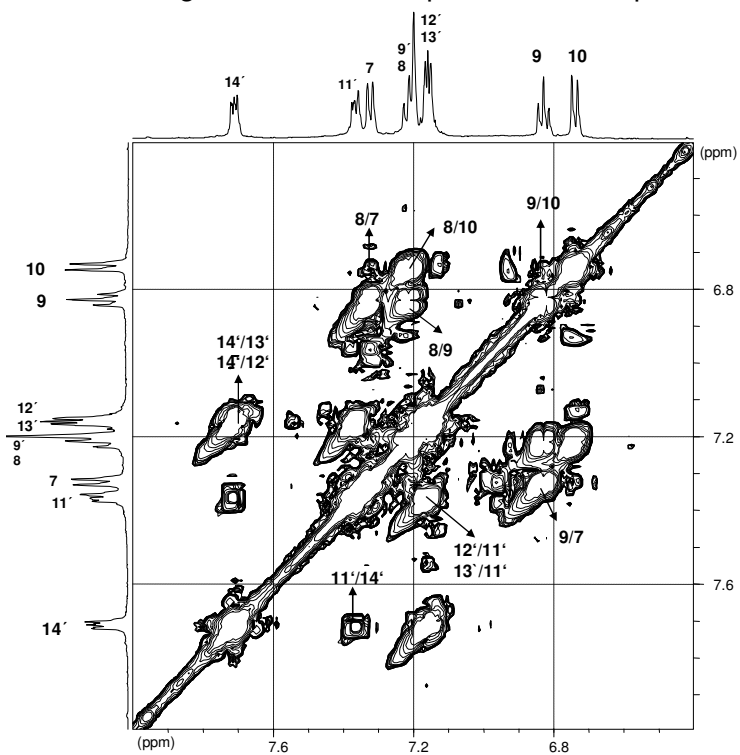


Figure 3.5A COSY spectrum of compound 1 (CD_3OD , 500 MHz)

Figure 3.5B COSY spectrum of compound **1** (CD₃OD, 500 MHz)Figure 3.5C COSY spectrum of compound **1** (CD₃OD, 500 MHz)

Long range correlation between proton H-7' and H-9' could be observed in the COSY spectrum [figure 3.5B] and it was proven by HMBC [figure 3.8] that H-7' was connecting the indole ring to a piperazine-2,5-dione ring. Other spin systems observed in the COSY spectrum consisted of H-15' and methyl group H₃-16', and H-12 and methyl H₃-13, respectively.

In the HMBC spectrum [figure 3.8], a long range correlation between H-9' and C-10a proved that two substructures were connected through C-10b and N-10' [figure 3.7 and 3.8].

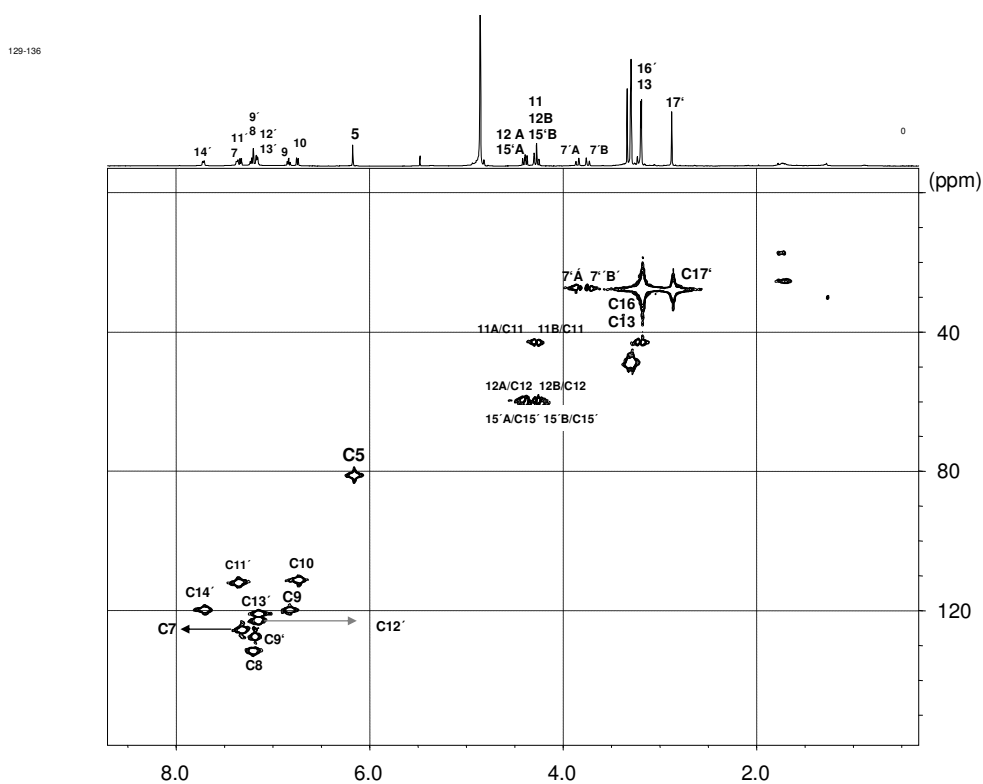
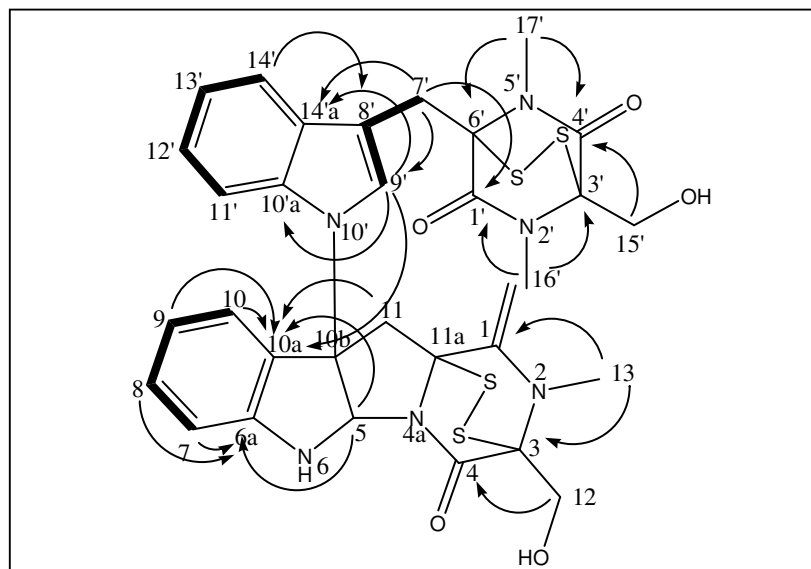
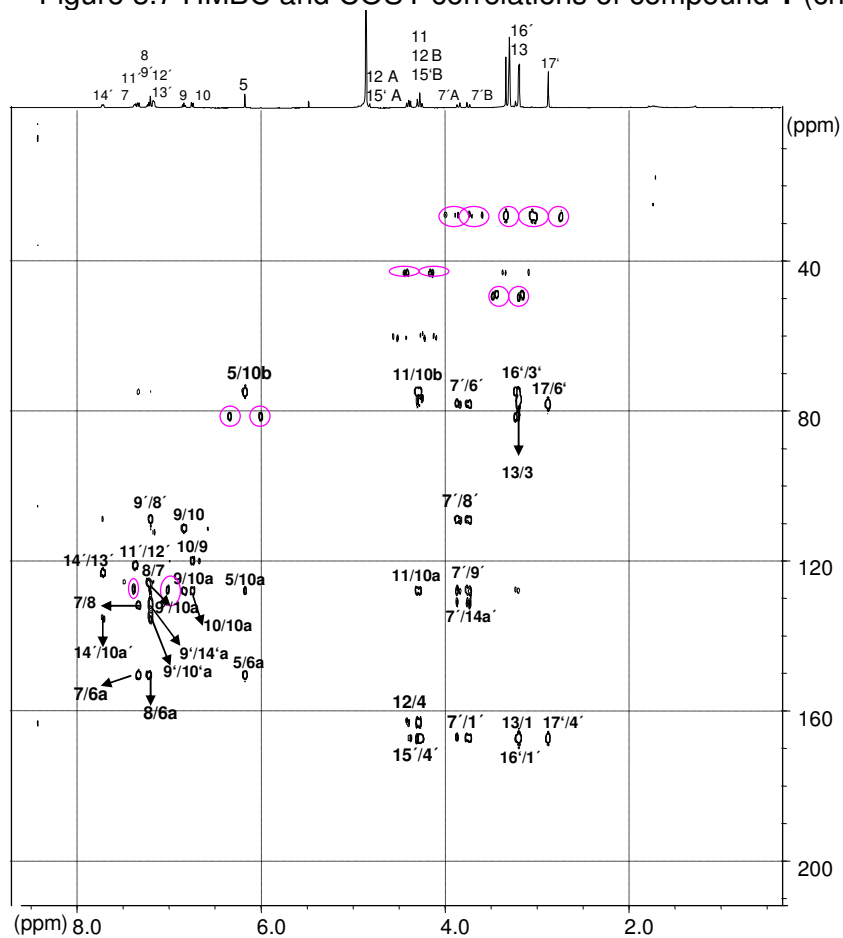


Figure 3.6 HMQC spectrum of compound **1** (CD₃OD, 500 MHz)

Figure 3.7 HMBC and COSY correlations of compound **1** (chetomin)Figure 3.8 HMBC spectrum of compound **1** (CD₃OD, 500 MHz)

Compound **1** was identified as chetomin which was substantiated by comparing its NMR data with that of chetomin isolated from *Chaetomium cochliodes* reported in the literature (Fujimoto *et al.*, 2004).

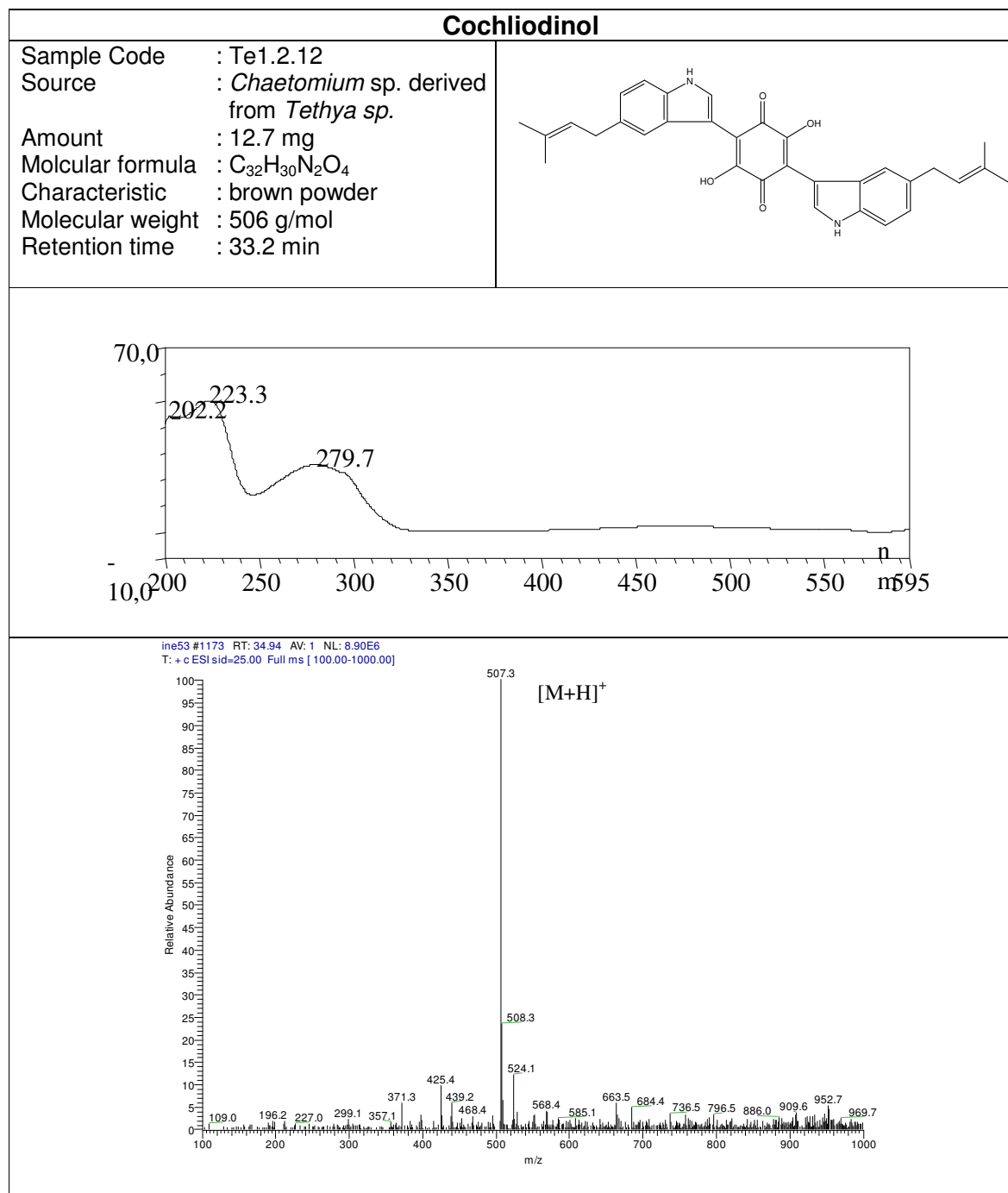
The optical rotation of compound **1** was $[\alpha]_D^{20} +144^\circ$ (*c* 0.2, CHCl₃), whereas the one previously reported for chetomin in the literature was $[\alpha]_D^{20} +257^\circ$ (*c* 0.1, CHCl₃) (McInnes *et al.*, 1976) suggesting both compounds to have the same stereochemistry.

Tabel 3.2 NMR data of compound **1** (chetomin)

Position	δ H (ppm) multiplicity (<i>J</i> in Hz)(in CD ₃ OD)	δ H (ppm) multiplicity (<i>J</i> in Hz) (Fujimoto <i>et al.</i> , 2004 in CDCl ₃)	δ C (ppm) (in CD ₃ OD)	δ C (ppm) (Fujimoto <i>et al.</i> , 2004 in CDCl ₃)	HMBC (in CD ₃ OD)
1			167.3	165.6	
3			74.5	74.8	
4			163.3	163.2	
5	6.17 (1H,s)	6.21 (1H,s)	81.5	80.1	6a,10a,10b
6-NH	-	5.35 (1H,s)			
6a			150.5	148.4	
7	7.33 (1H,d,7.6)	7.34 (1H,d,7.6)	125.9	125.0	6a,8
8	7.21 (1H,t,7.6)*	7.31 (1H,t,7.6)	131.9	131.4	6a,7
9	6.83 (1H,t,7.6)	6.95 (1H,t,7.6)	120.1	120.4	10,10a
10	6.74 (1H,d,7.9)	6.80 (1H,d,7.6)	111.5	111.2	9,10a
10a			128.0	126.6	
10b			76.9	73.8	
11	4.27 (2H,m)	4.42 (1H,d,15.4) 3.10 (1H,d,15.4)	43.3	42.7	10a,10b
11a			75.0	73.6	
12	4.39 (1H) 4.27 (1H,m)	4.35 (1H,d,12.6) 4.29 (1H,d,12.6)	60.1	60.6	4
13	3.19 (3H,s)	3.20 (3H,s)	28.1	27.5	1,3
1'			167.3	165.6	
3'			78.2	76.1	
4'			167.4	166.9	
6'			78.1	76.5	
7'	3.85 (1H,d,15.8) 3.74 (1H,d,15.5)	3.89 (1H,d,15.6) 3.74 (1H,d,15.6)	27.8	27.1	1',6',8',9',14'a
8'			109.1	107.7	
9'	7.21 (1H,s)*	7.19 (1H,s)	127.8	127.3	8',10'a,14'a,10a
10a'			135.3	134.1	
11'	7.37 (1H,dd,6.9,1.9)	7.31 (1H,1H,bd,6.7)	112.3	111.4	12'
12'	7.16 (1H,m)	7.23 (1H,m)	123.3	120.6	
13'	7.16 (1H,m)	7.23 (1H,m)	121.2	122.8	
14'	7.71 (1H,dd,6.9,1.9)	7.66 (1H,d,6.7)	120.2	119.2	
14a'			131.5	130.4	
15'	4.39 (1H,m) 4.27 (1H,m)	4.32 (1H, d, 12.6) 4.27 (1H, d, 12.6)	60.6	61.2	4'
16'	3.19 (3H,s)	3.17 (3H,s)	28.0	27.4	1',3'
17'	2.88 (3H,s)	2.96 (3H,s)	28.3	28.2	4',6'

* : overlapping signals

3.1.2 Compound 2 (cochliodinol)



Compound **2** (cochlodinol) was a dimer compound isolated from *Chaetomium* sp. through Sephadex LH-20 column chromatography with 100% methanol. It showed a UV maximum at 223.3 nm, with shoulders at 202.2 and 279.7 nm. The ESI-MS of compound **2** showed a prominent $[M-H]^+$ pseudomolecular ion at 507, indicating a molecular weight of 506 g/mol. In conjunction with the analysis of ^1H and ^{13}C NMR data, a molecular formula of $\text{C}_{32}\text{H}_{30}\text{N}_2\text{O}_4$ was assumed.

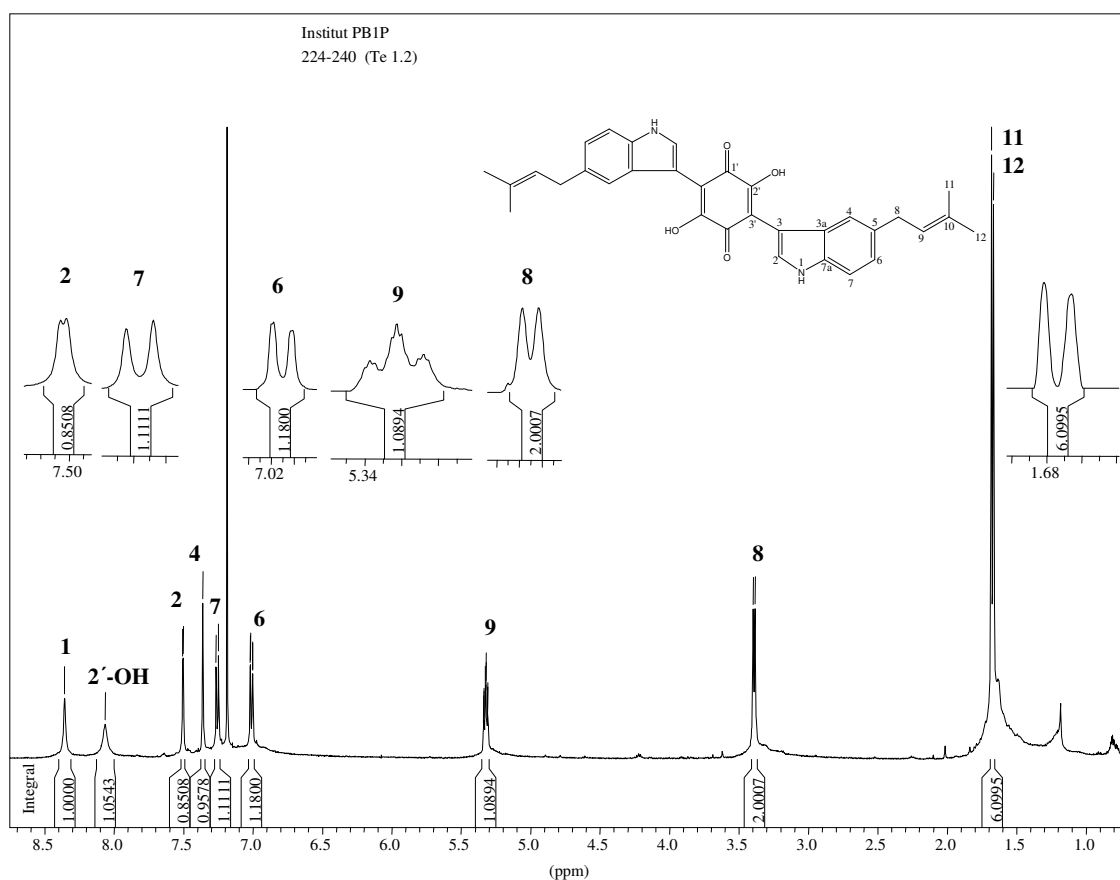


Figure 3.9 ^1H NMR spectrum of compound **2** (CDCl_3 , 500 MHz)

Since the estimated number of proton signals in the ^1H spectrum did not match with the number of signals observed [figure 3.9] but rather with the double number, it was concluded that compound **2** was a symmetrical dimer.

Three aromatic protons H-4, H-6 and H-7 were observed constituting one ABC spin system characteristic of one 1,2,4-trisubstituted aromatic system, which was confirmed by coupling constants derived from the ^1H NMR spectrum [figure 3.9].

Both hydroxyl groups of the central ring appeared as a broad singlet at the chemical shift δ_{H} of 8.12 ppm. Due to tautomerism, the hydrogen atom is shared by the oxygen atoms adjacent to C-1' and C-2'.

Three more signals confirmed the presence of one dimethylallyl side chain. Due to the presence of the double bond, the geminal methyl groups H₃-11 and H₃-12 were shifted downfield and appeared as a doublet coupling to the olefinic proton H-9. The methylene group H₂-8 was located vicinally to H-9.

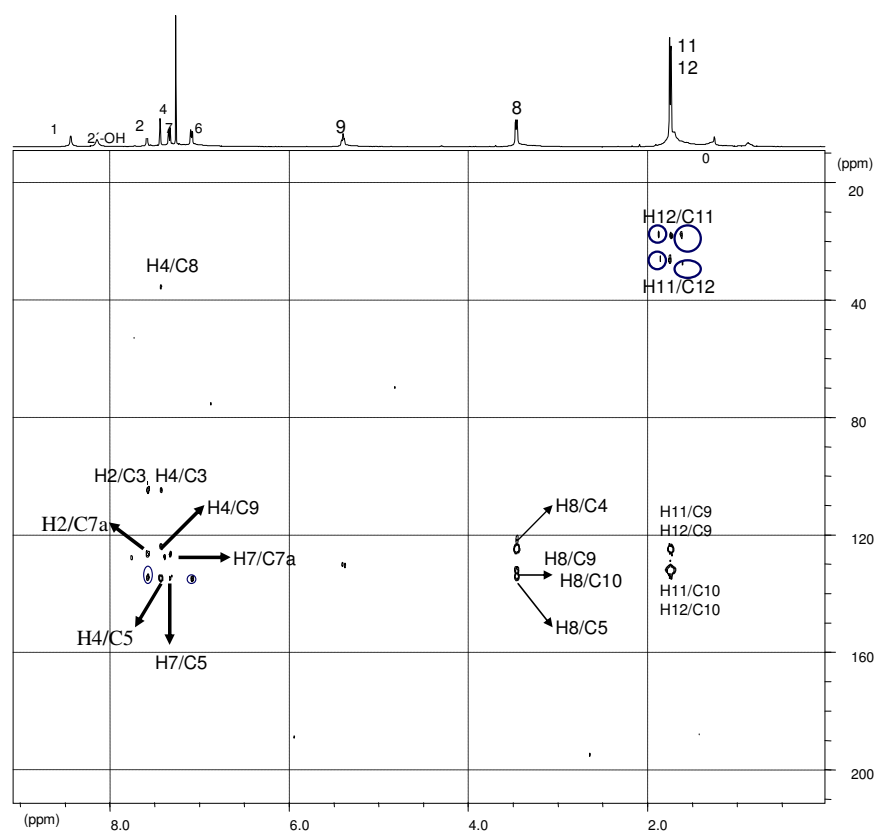


Figure 3.10 HMBC spectrum of compound 2 (CDCl_3 , 500 MHz)

In the HMBC spectrum [figure 3.10], observation of the long range correlations between H₂-8 and C-4, H-4 and C-9, H-4 and C-3 allowed to determine the position of the dimethylallyl substituent at the indole ring. The correlations between H-2 and C-7a and also between H-7 and C-7a showed the presence of another substituent in position 3 of the indole moiety, revealing the link of the monomers.

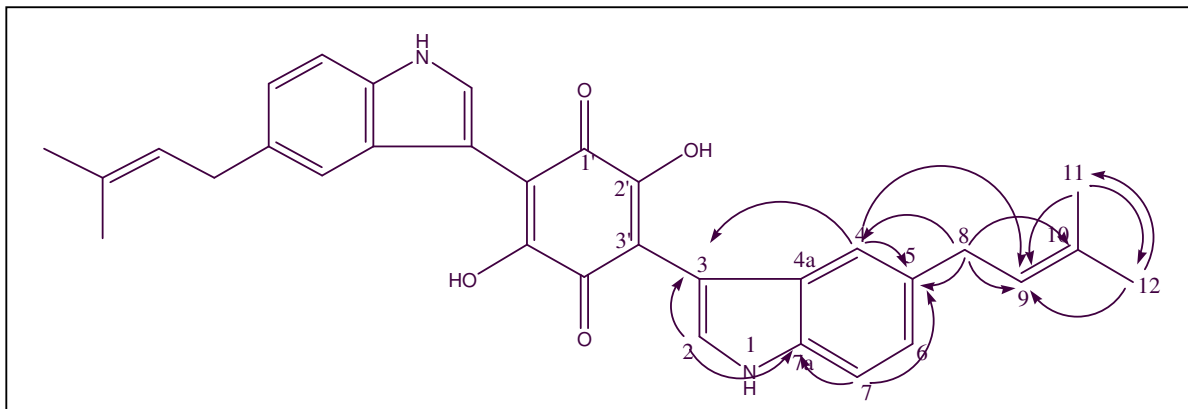


Figure 3.11 HMBC correlations in compound **2** (cochlodinol)

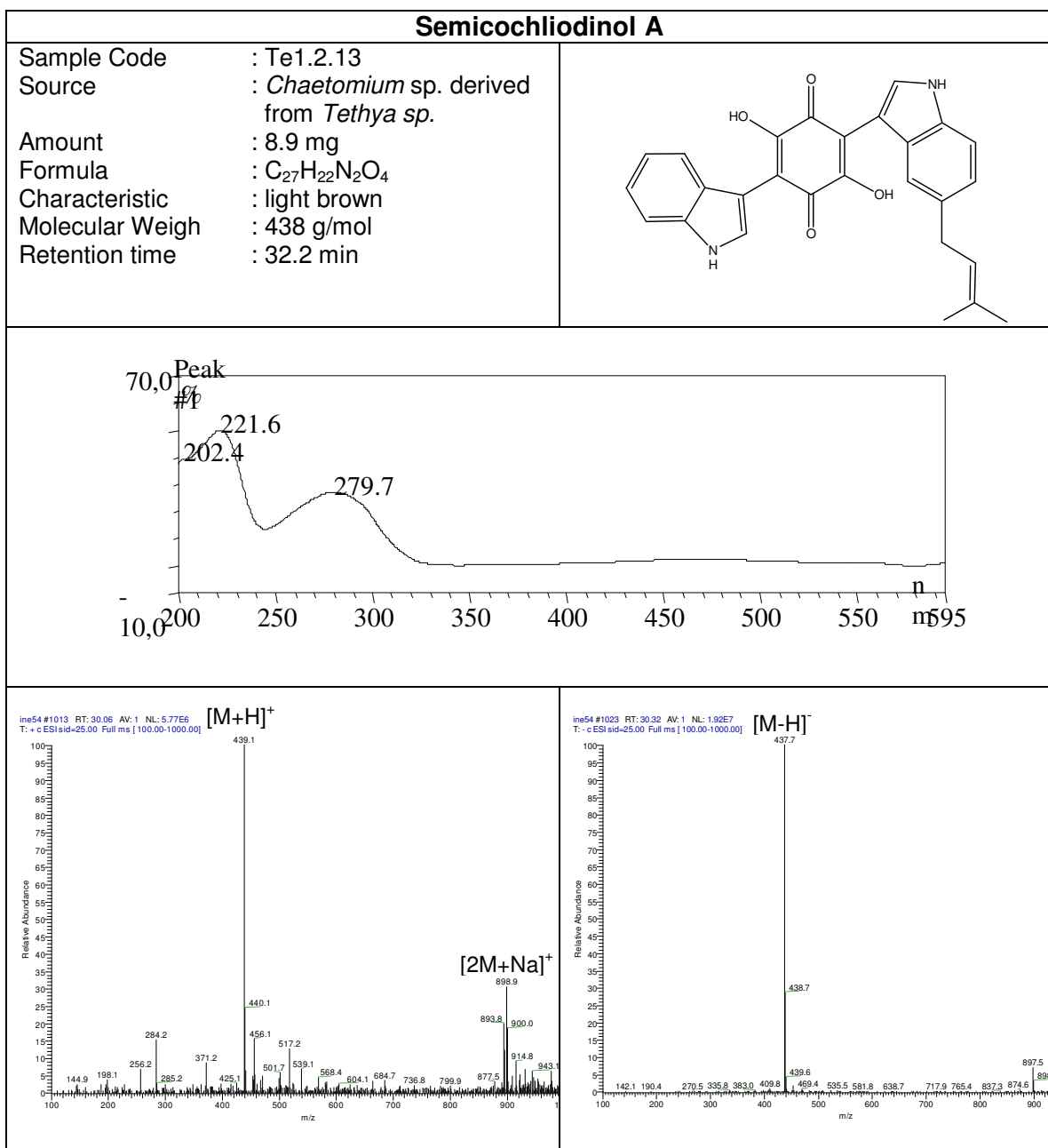
Compound **2** was identified as cochliodinol based on the comparison of its NMR data with that of cochliodinol described in the literature (Sekita *et al.*, 1983). Cochliodinol was first isolated in 1975 from the fungus *Chaetomium cochliodes* (Jerram *et al.*, 1975).

Table 3.3 NMR data of compound **2** (cochlodinol)

Position	δ H (ppm) multiplicity (<i>J</i> in Hz)(in CD ₃ OD)	δ H (ppm) multiplicity (<i>J</i> in Hz) (in CDCl ₃)	δ H (ppm) multiplicity (<i>J</i> in Hz) (Sekita <i>et al.</i> , 1983 in THF- <i>d</i> 8)	δ C (ppm) (in CD ₃ OD)	HMBC (in CD ₃ OD)
1'/2'-OH		8.12 (2H,bs)	9.72 (2H,s)		
1-NH		8.41 (2H,s)	10.3 (2H,bs)		
2	7.49 (2H,bd)	7.56 (2H,d,2.2)	7.51 (2H,d,2.4)	127.9	3,7a
3				106.3	
4	7.32 (2H,bs)	7.41 (2H,bs)	7.39 (2H,bs)	122.8	3,5,8,9
4a					
5				136.0	
6	6.94 (2H,dd,8.5,1.6)	7.06 (2H,dd,8.5,1.3)	6.90 (2H,dd,8.3,1.5)		
7	7.29 (2H,d,8.5)	7.31 (2H,d,8.5)	7.19 (2H,d,8.3)		5,7a

8	3.40 (4H,d,7.3)	3.44 (4H,d,7.3)	3.40 (4H,6.8)	37.1	4,5,9,10
9	5.37 (2H,dd,7.3,1.6)	5.37 (2H,dd,7.3,1.3)	5.36 (2H,tqq,6.8,1.5)	125.4	
10				131.3	
11	1.73 (6H,bd,9.5)	1.73 (6H,bd,7.9)	1.72 (6H,bs)	19.6	9,10,12
12	1.73 (6H,bd,9.5)	1.73 (6H,bd,7.9)	1.72 (6H,bs)	27.7	9,10,11

3.1.3 Compound 3 (Semicochliodinol A)



Semicochliodinol A was isolated together with chetomin and cochliodinol from the ethyl acetate extract of *Chaetomium* sp. through Sephadex LH-20 column chromatography. Its ESI-MS showed an intense pseudomolecular ion at m/z 439 $[M+H]^+$ together with m/z 437 $[M-H]^-$ indicating a molecular weight of 438 g/mol. In conjunction with the NMR spectral data, a molecular formula of $C_{27}H_{22}N_2O_4$ was derived.

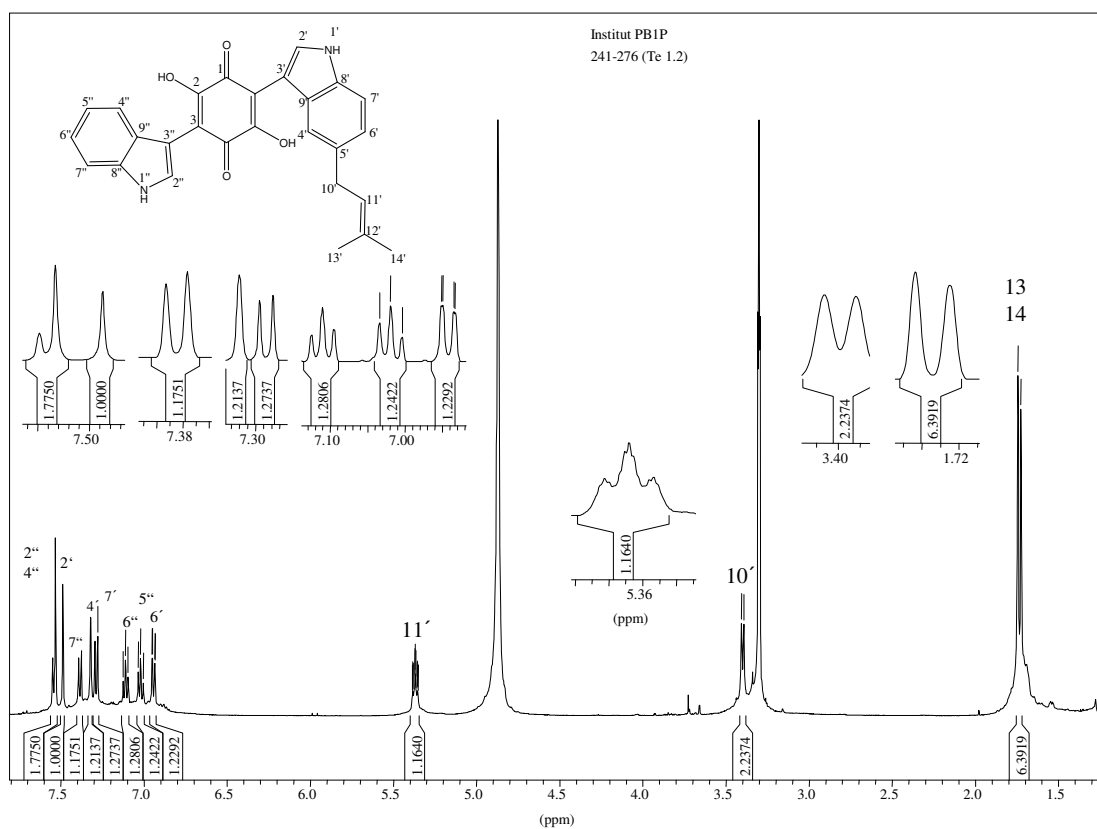


Figure 3.12 ^1H NMR spectrum of compound **3** (semicochliodinol A)

In the ^1H NMR spectrum [figure 3.12], the compound showed seven aromatic protons which appeared at chemical shifts between δ 6.94 ppm and δ 7.54 ppm. The COSY spectrum [figure 3.13] and analysis of the coupling constants suggested the conclusion that those seven protons represented an ABC spin system and an ABCD

spin system, respectively. The ABC system revealed one 1,2,4-trisubstituted aromatic ring consisting of H-4', H-6' and H-7', based on coupling constants and splitting patterns. The ABCD system was formed by H-4'', H-5'', H-6'' and H-7'' of one 1,2-disubstituted aromatic ring showing ABCD multiplicity signals, doublet-triplet-triplet-doublet.

Three more signals confirmed the presence of one dimethylallyl side chain. Due to the presence of the double bond, the geminal methyl groups H-13' and H-14' were shifted downfield and appeared as a doublet coupling to the olefinic proton H-11'. The doublet at δ 3.40 was assigned to the methylene group H₂-10'.

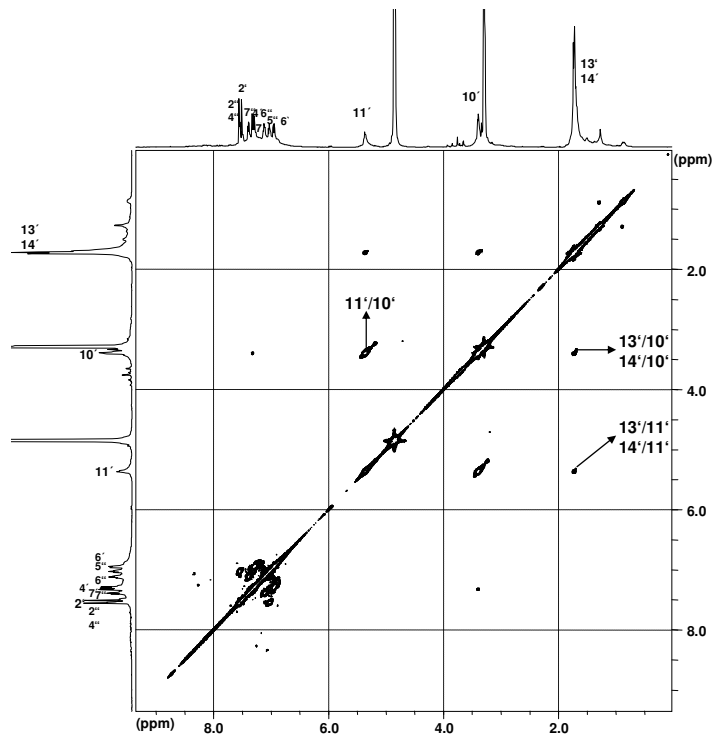


Figure 3.13A COSY spectrum of compound **3** (semicochliodinol A)

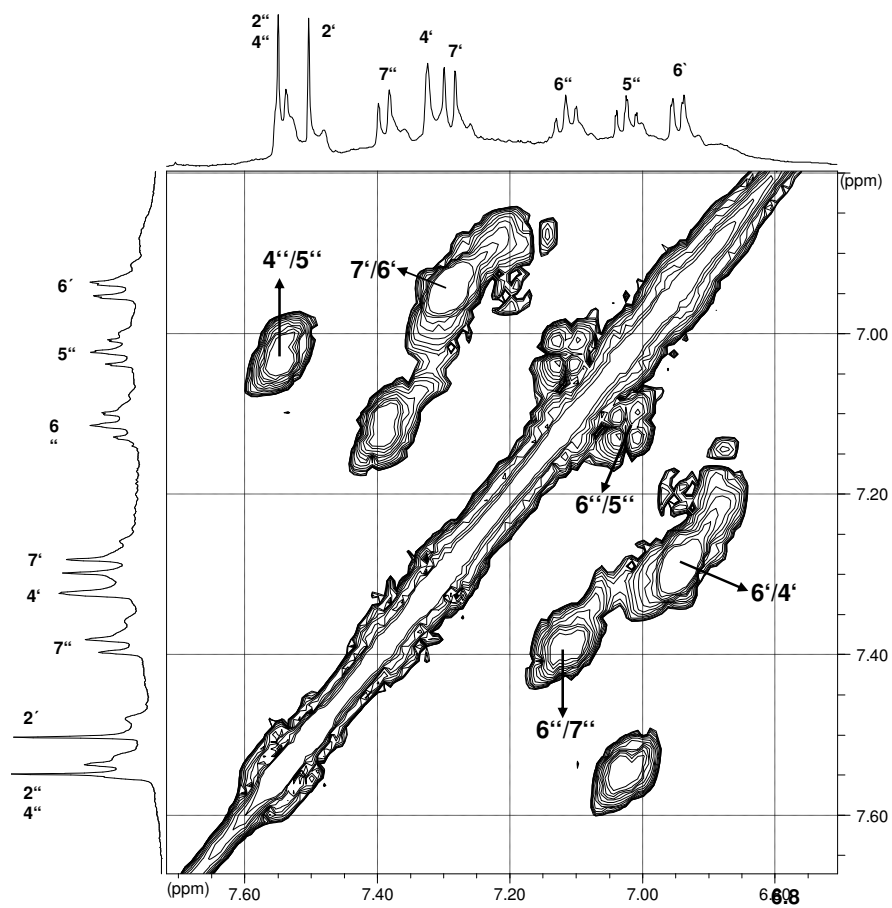


Figure 3.13B COSY spectrum of compound **3** (semicochliodinol A)

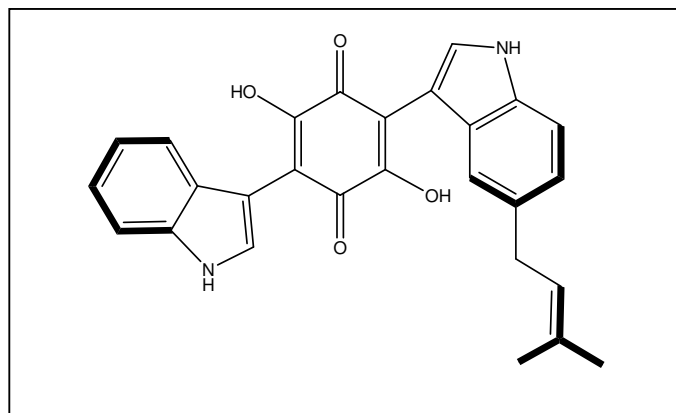


Figure 3.14 COSY correlations of compound **3** (semicochliodinol A)

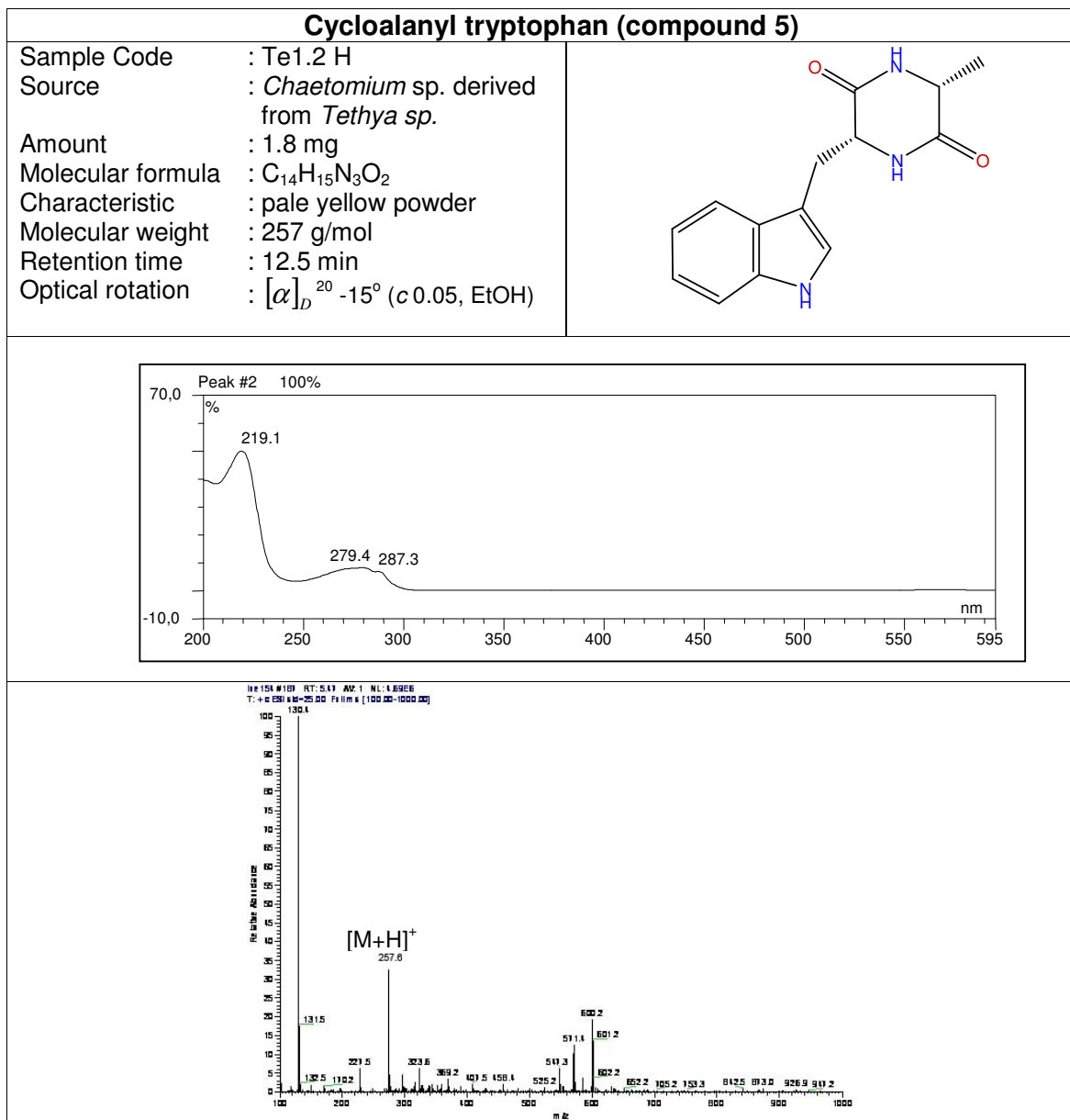
Comparison of the observed NMR spectra [table 3.4] with published data in the literature allowed to identifying compound **3** as semicochliodinol A, first isolated from *Chrysosporium merdarium* (Fredenhagen *et al.*, 1997).

Table 3.4 NMR data of compound **3** (semicochliodinol A)

Position	δ H (ppm), multiplicity (J in Hz) (in MeOD)	δ H (ppm) multiplicity (J in Hz) (Fredenhagen <i>et al.</i> , 1997 in DMSO)
1'		10.55 (bs)
1''		10.61 (bs)
2'	7.49 (1H,s)	7.63 (m)
2''	7.54 (1H,s)*	7.68 (d)
4'	7.32 (1H,s)	7.45 (s)
4''	7.54 (1H,d,9.14)*	7.64 (s)
5''	7.02 (1H,t,7.3)	7.06 (t)
6'	6.94 (1H,dd,6.9,1.0)	6.98 (d)
6''	7.11 (1H,t,7.3)	7.14 (t)
7'	7.29 (1H,d,8.2)	7.37 (d)
7''	7.38 (1H,d,8.2)	7.46 (d)
10'	3.40 (2H,d,7.3)	3.42 (d)
11'	5.37 (1H,dt,7.3,1.5)	5.38 (t)
13'	1.73 (3H,d,9.14)	1.72 (s)
14'	1.73 (3H, d, 9.14)	1.75 (s)

3.1.4 Compound **5** (cycloalanyl tryptophan)

Compound **5** (cycloalanyl tryptophan) was isolated from the *n*-butanol extract of *Chaetomium* sp. using semi-preparative HPLC. The UV maximum of compound **5** was 219.1 nm with shoulders at 279.4 and 287.3 nm. Its ESI mass spectrum showed the most intense pseudomolecular peak at 258 [M+H]⁺ upon positive ionization indicating molecular weight of 257 g/mol. The ESI mass spectrum of compound **5** showed another peak at 130 upon positive ionization revealing the loss of the diketopiperazine (C₃H₅ON) ring as much as 228 *amu*.



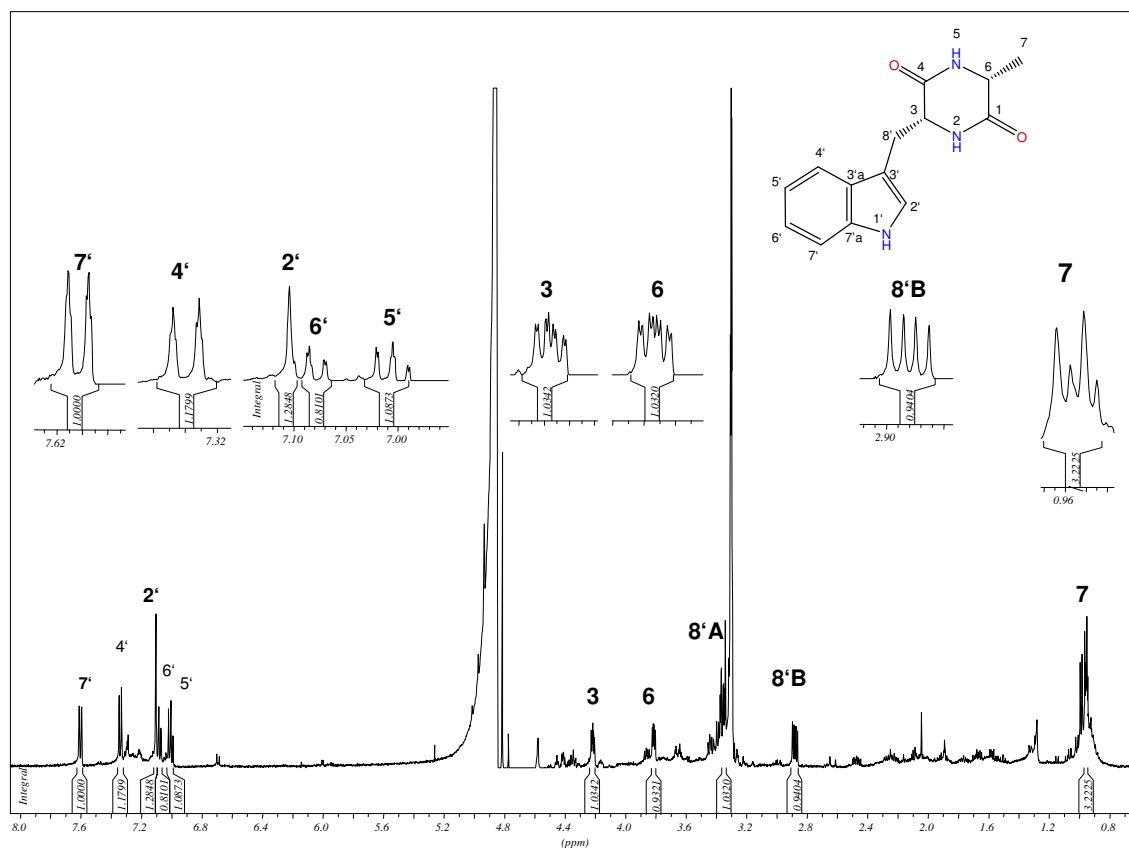
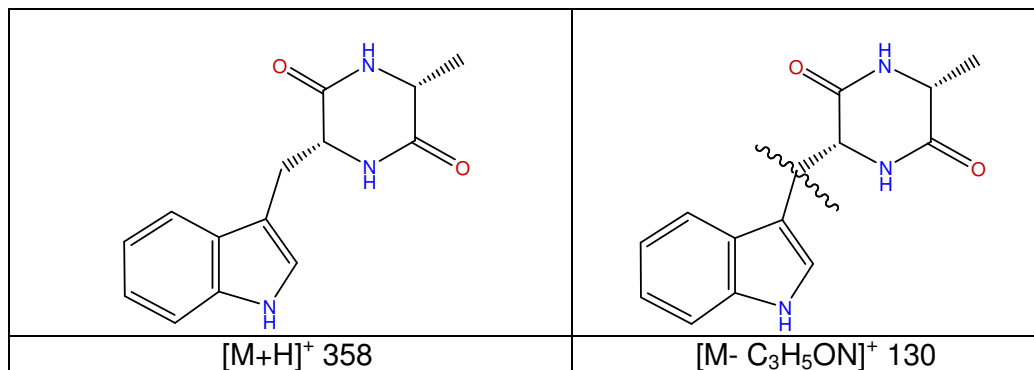


Figure 3.15 ^1H NMR spectrum of compound **5** (CD_3OD , 500 MHz)

From the ^1H NMR spectrum [figure 3.15], signals of aromatic protons typical for an indole ring were observed in the downfield area. H-2' appeared at the chemical shift of 7.09 ppm. Four aromatic protons were detected resonating at the chemical shifts δ_{H} 7.34 ppm (H-4', dd, 8.2/*ortho*, and 1.0 Hz/*meta*), 7.00 ppm (H-5', dt, 8.2/*ortho*

and 1.0 Hz/*meta*), 7.08 ppm (H-6', dd, 8.2/*ortho* and 1.0 Hz/*meta*), and 7.60 ppm (H-7', dd, 7.3/*ortho* and 1.0 Hz/*meta*). Those aromatic protons were part of an ABCD spin system characteristic of an *ortho*-disubstituted phenyl ring which was also confirmed and verified by the multiplicity and coupling constant of aromatic protons.

Besides the indole ring system, compound **5** also contained a diketopiperazine moiety. One methyl group in position 6 and one methylene group – linking to the indole – in position 3 allowed the conclusion that the diketopiperazine ring was formed by condensation of one alanine and one tryptophane residue.

Table 3.5 NMR data of compound **5** (cycloalanyl tryptophan)

Position	δ H (ppm), multiplicity (J in Hz) (in CD ₃ OD)	δ H (ppm) multiplicity (J in Hz) (Effendi, 2004 in MeOD)
3	4.22 (1H, ddd, 6.9, 4.1, 1.0)	4.31 (1H, m)
6	3.81 (1H, ddd, 6.3, 3.5, 1.0)	3.74 (1H, q, 7.0)
7	0.95 (3H, d, 6.3)	0.42 (3H, d, 7.0)
2'	7.09 (1H, bs)	7.05 (1H, m)
4'	7.34 (1H, dd, 8.2, 1.0)	7.35 (1H, ddd, 7.2, 1.9, 0.9)
5'	7.00 (1H, dt, 8.2, 1.0)	7.03 (1H, m)
6'	7.08 (1H, dd, 8.2, 1.0)	7.11 (1H, m)
7'	7.60 (1H, dd, 7.3, 1.0)	7.64 (1H, ddd, 7.2, 1.9, 0.9)
8'	3.40 (1H, m) 2.88 (1H, dd, 11.4, 5.7)	3.49 (1H, dd, 14.1, 4.0) 3.19 (1H, dd, 14.1, 4.0)

Compound **5** was identified as cycloalanyl tryptophan which was substantiated by comparison with NMR data of cycloalanyl tryptophan isolated from *Fusarium graminearum* (Effendi, 2004). The optical rotation of compound **5** $[\alpha]_D^{20} -15^\circ$ allowed to conclude that this compound had the same stereochemistry with cycloalanyl tryptophan described in the literature (Nakashima and Slater, 1969) which had an optical rotation of $[\alpha]_D^{20} -10.2^\circ$.

3.2 Isolated secondary metabolites of fungus *Penicillium citrinum*.

Penicillium citrinum was isolated from marine alga *Sargassum* sp. collected from the Java Sea. Six metabolites were isolated from this fungus. They were melegrine (compound **6**), roquefortine C (compound **7**), quinolactacin A1 (compound **8**), quinolactacin A2 (compound **9**), citrinin (compound **10**) and citrinin hydrate (compound **11**).

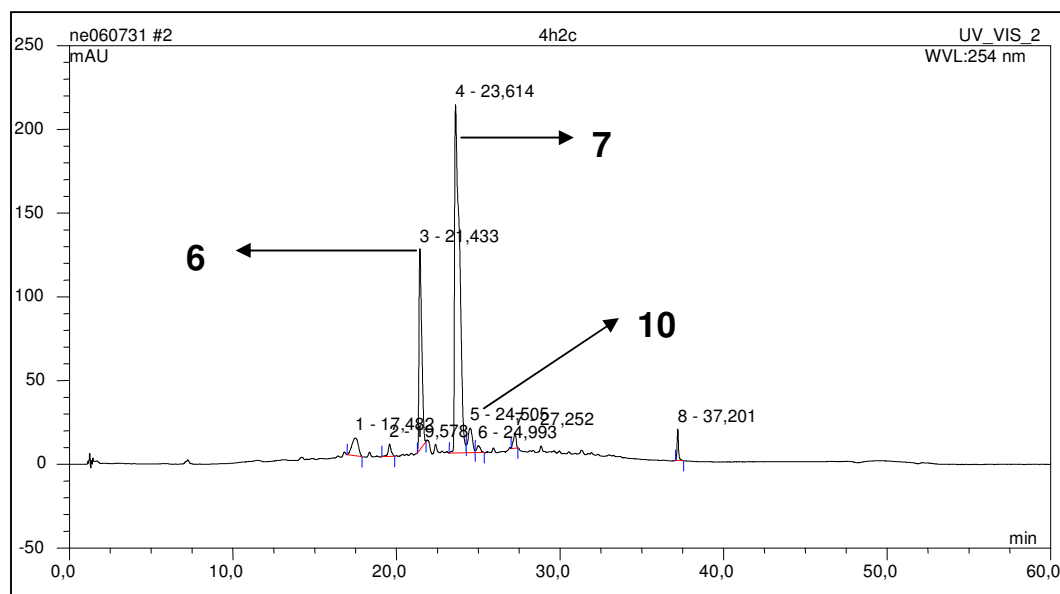


Figure 3.16 HPLC chromatogram of the ethyl acetate extract of *P. citrinum*

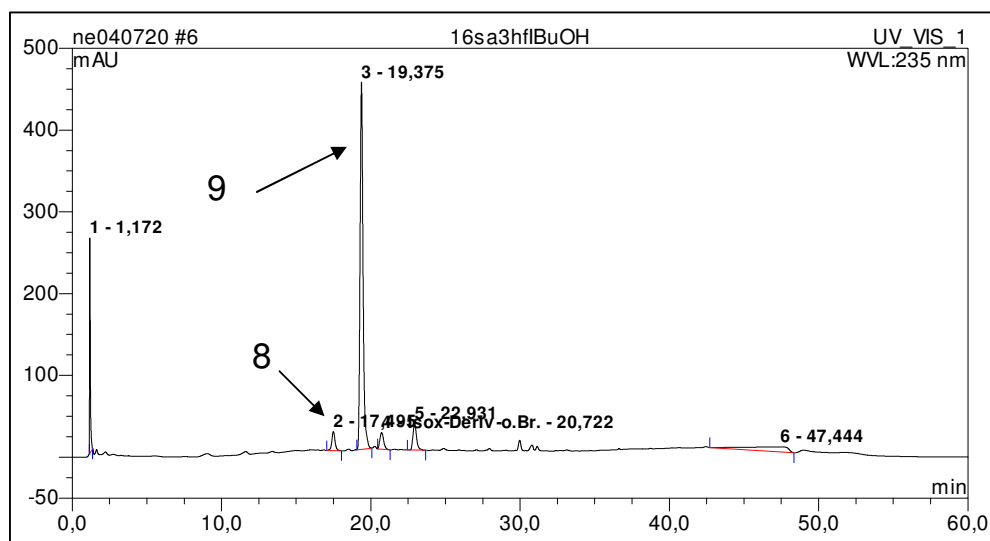


Figure 3.17 HPLC chromatogram of the *n*-butanol extract of *P. citrinum*

Table 3.6 Biological test results of *P. citrinum* and its metabolites

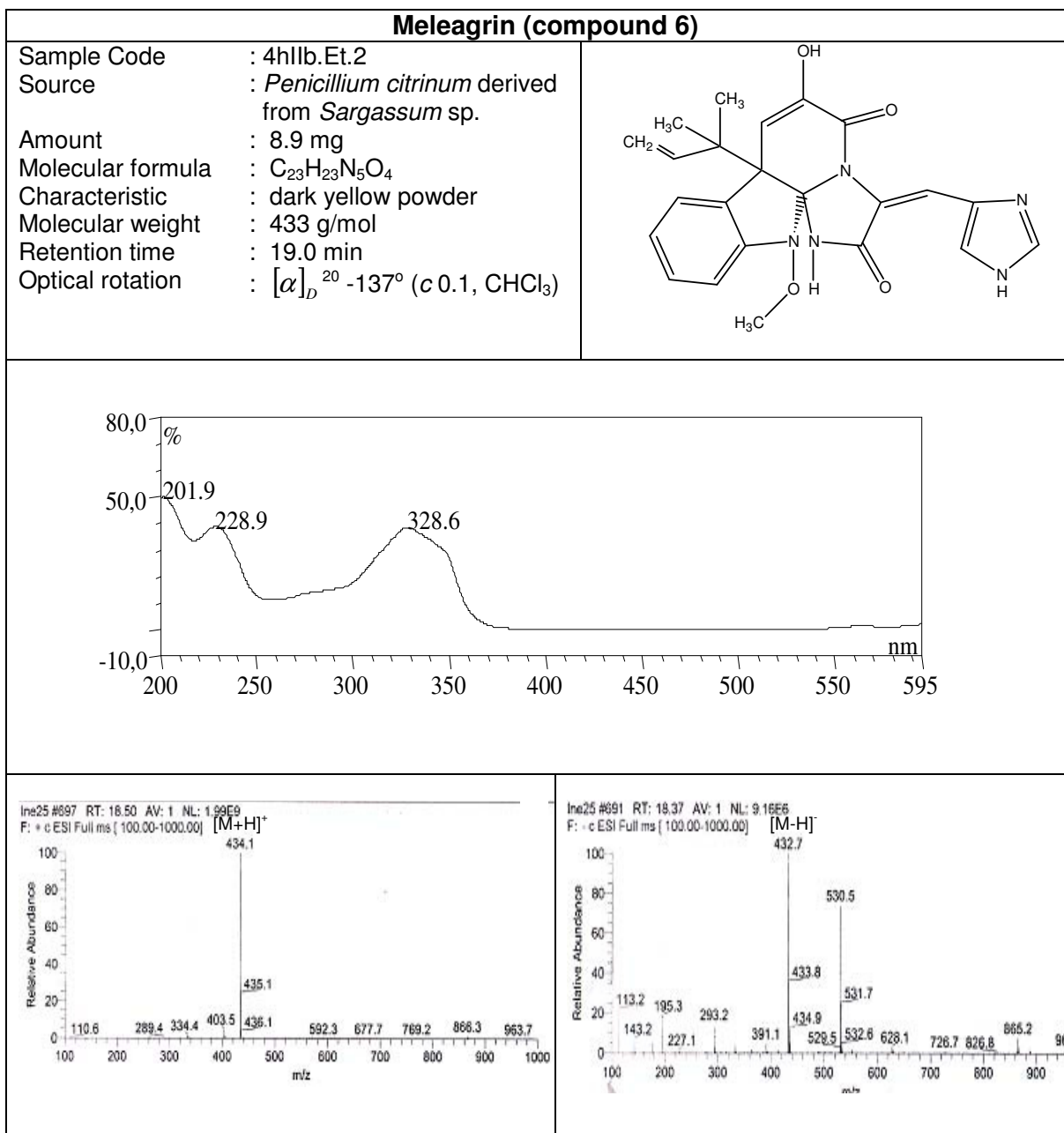
Sample	Antimicrobial assay				L5178Y growth (%)	EC ₅₀
	BS	SC	CC	CH	Conc.10 µg/mL	(µg/mL)
Ethyl acetate extract of <i>Penicillium citrinum</i>	-	-	-	-	107.0	
Meleagrins					1.6	4.2
Roquefortine C					82.6	
Citrinin					109.3	
Citrinin hydrate					5.5	5.1
Quinolactacin A					86.1	

BS = *Bacillus subtilis*, SC = *Saccharomyces cerevisiae*, CC = *Cladosporium cucumerinum* and CH = *C. herbarum*

3.2.1 Compound 6 (meleagrins)

Compound 6 (meleagrins) was isolated from the ethyl acetate extract of *Penicillium citrinum* through Sephadex LH-20 column chromatography with 100% methanol. The UV spectrum exhibited maximum absorptions at 201.9, 228.8 and 328.6 nm. In the ESI mass spectrum, a prominent $[M+H]^+$ pseudomolecular ion was observed at m/z 434 upon positive ionization together with an intense $[M-H]^-$ at m/z 432 upon negative ionization which indicated a molecular weight of 433 g/mol. Together with analysis of the 1H NMR spectrum, the molecular formula of $C_{23}H_{23}N_5O_4$ was derived.

In 1H NMR spectrum [figure 3.18], four aromatic protons were observed at 7.51 (H-7), 7.22 (H-6), 7.02 (H-5) and 6.91 ppm (H-4). Those protons constituted a classical ABCD spin system characteristic of one 1,2-bisubstituted phenyl ring which was confirmed by the COSY spectrum [figure 3.20B].



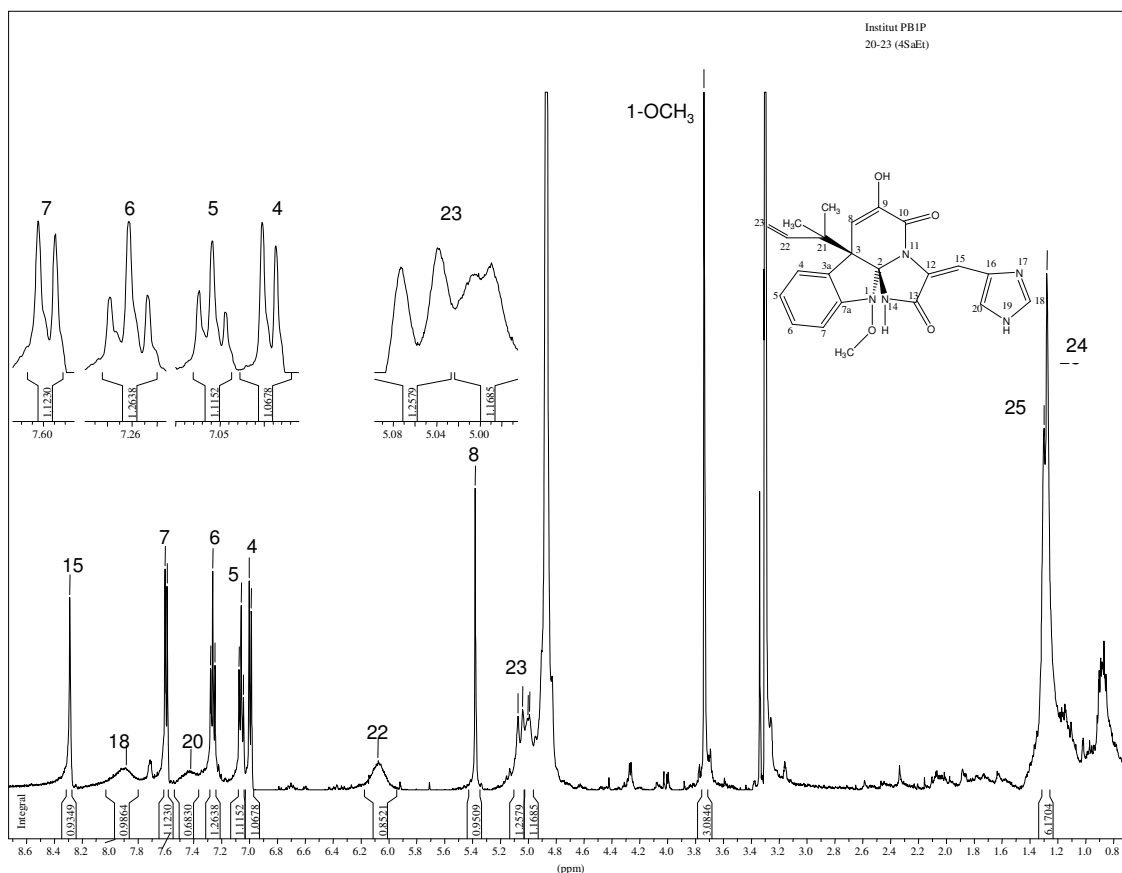
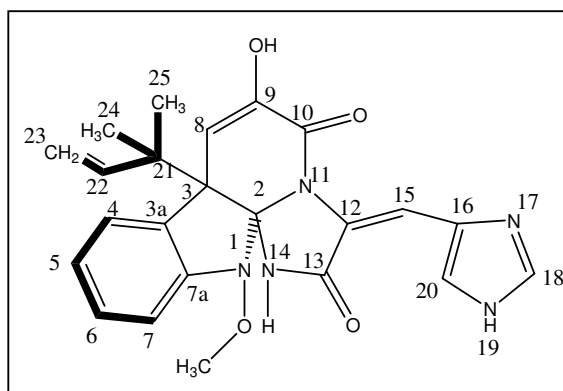
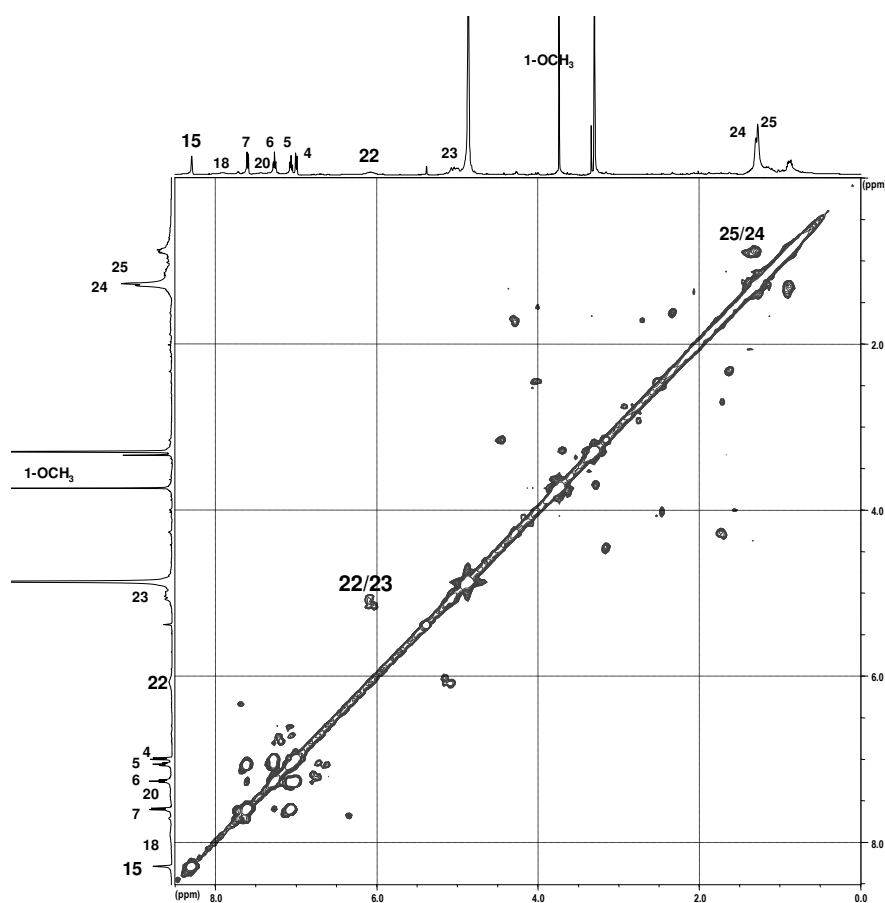


Figure 3.18 ^1H NMR spectrum of compound **6** (CD_3OD , 500 MHz)

Signals of olefinic protons were detected as singlets at δ 5.38 (H-8) and 8.29 ppm (H-15). Geminal methyl groups appeared as singlets at δ 1.28 (H_3 -24) and 1.30 (H_3 -25). Together with the olefinic protons H-22, H-23A and H-23B this suggested the presence of one dimethylallyl moiety in the compound. The correlations between the protons H-22 and H-23A/B, and the methyl groups 24 and 25 were observed in the COSY spectrum [figure 3.20A] and suggested the link to the main skeleton to be located at H-21.

The signal of the methoxy group was detected in the ^1H NMR spectrum at 3.74 ppm as a singlet.

Figure 3.19 COSY correlations of compound **6** (meleagrin)Figure 3.20A COSY spectrum of compound **6** (CD₃OD, 500 MHz)

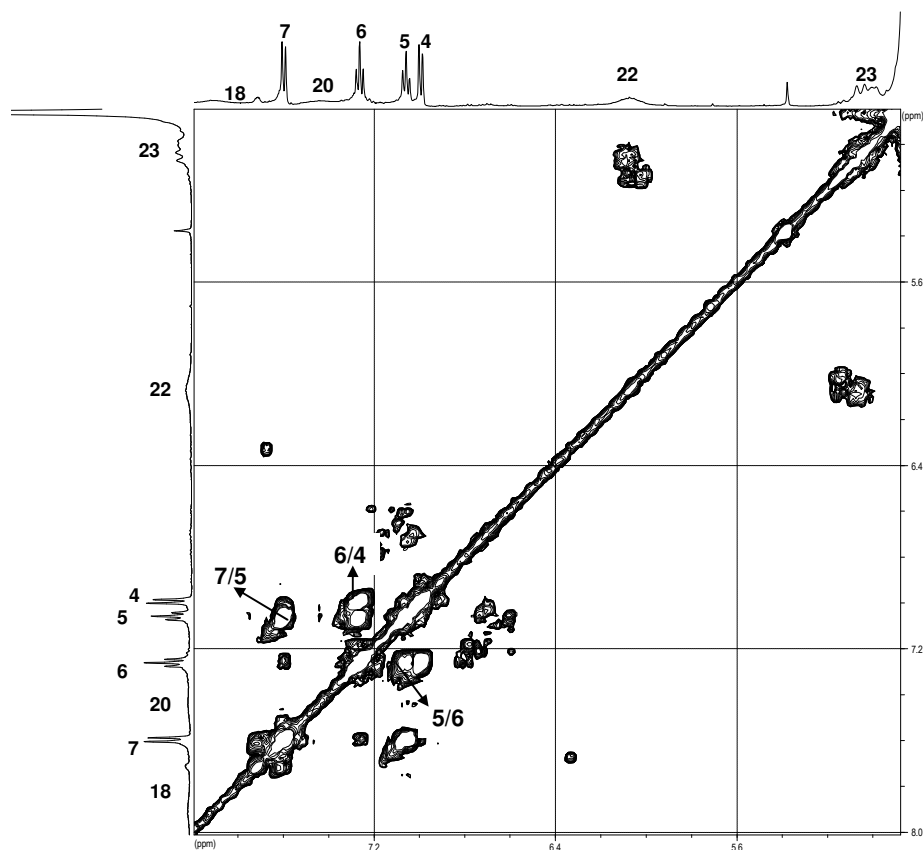


Figure 3.20B COSY spectrum of compound **6** (CD₃OD, 500 MHz)

Compound **6** was identified as meleagrins which was fundamentally based on the comparison with published NMR data of meleagrins isolated from *Penicillium meleagrinum* by Kawai *et al.* (1984). The optical rotation of compound **6** was $[\alpha]_D^{20} -137^\circ$, whereas optical rotation of meleagrins previously described in literature was $[\alpha]_D^{20} -116^\circ$ (Kawai *et al.*, 1984) suggesting both compounds to have the same stereochemistry.

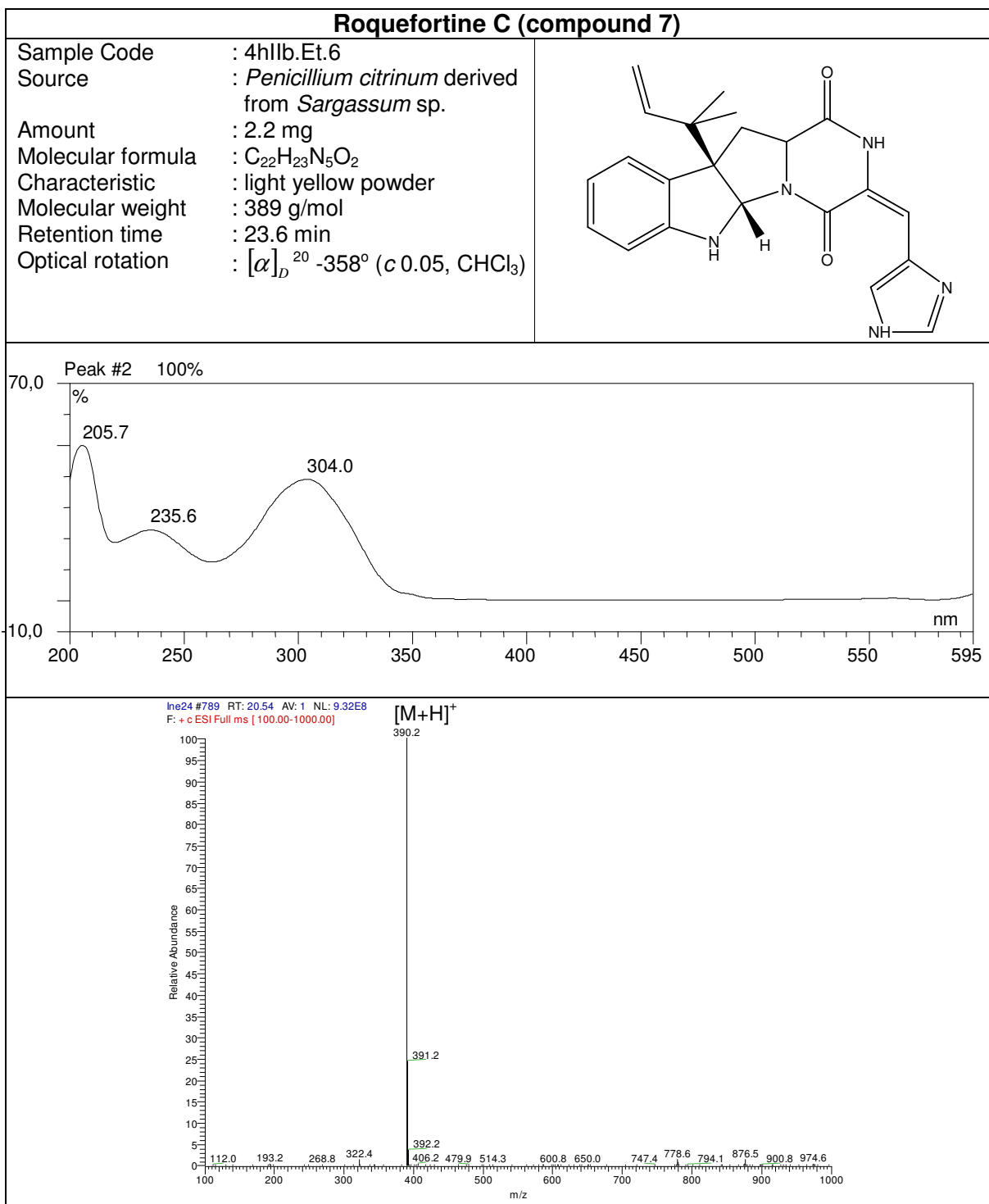
Table 3.7 NMR data of compound **6** (meleagrin)

Position	δ H (ppm), multiplicity (<i>J</i> in Hz) (in CD ₃ OD)	δ H (ppm), multiplicity (<i>J</i> in Hz) (in CDCl ₃)	δ H (ppm) multiplicity (<i>J</i> in Hz) (Kawai <i>et al.</i> , 1984 in CDCl ₃)
1-OCH ₃	3.74 (3H,s)	3.67 (3H,s)	3.73 (3H,s)
1		12.80 (1H,br)	12.72 (1H,br)
4	6.99 (1H,bd,7.9)	6.91 (1H,brd,7.9)	6.96 (1H,bd,7.5)
5	7.06(1H,bt,7.5)	7.02 (1H,brt,7.8)	7.06 (1H,bt,7.5)
6	7.26 (1H,bt,7.5)	7.22 (2H,brt,7.8)	7.07 (1H,bt,7.5)
7	7.60 (1H,bd,7.9)	7.51 (1H,brd,7.6)	7.58 (1H,bd,7.5)
8	5.38 (1H,s)	5.50 (1H,s)	5.50 (1H,s)
15	8.29 (1H,s)	8.21 (1H,s)	8,27 (1H,s)
18	7.88 (1H,s)	7.65 (1H,s)	7.61 (1H,s)
20	7.42 (1H,s)	7.32 (1H,s)	7.25 (1H,s)
22	6.08 (1H,br)	6.08 (1H,br)	6.12 (1H,dd,17.0,10.6)
23	5.06 (1H,d,16.7) 5.00 (1H,d,6.0)	5.05 (1H,d,17.3) 4.98 (1H,d,9.4)	5.10 (1H,d,17.2) 5.06 (1H,d,10.6)
24	1.28 (3H,s)	1.20 (3H,s)	1.24 (3H,s)
25	1.30 (3H,s)	1,28 (3H,s)	1.35 (3H,s)

3.2.2 Compound **7** (roquefortine C)

Compound **7** (roquefortine C) was isolated from the ethyl acetate extract of *Penicillium citrinum* through Sephadex LH-20 column chromatography with 100% methanol. The UV spectrum showed λ_{\max} (MeOH) at 205.7, 235.6 and 304.0 nm. In the ESI MS compound **7** showed the most intense $[M+H]^+$ pseudomolecular peak at m/z 390 indicating a molecular weight of 389 g/mol. After analyzing the ¹H NMR, it was deduced that the molecular formula was C₂₃H₂₃N₅O₂.

In the ¹H NMR spectrum [figure 3.21], signals of aromatic protons were detected at the chemical shifts δ 6.60 (H-7), δ 6.72 (H-8), δ 7.06 (H-9) and δ 7.21 (H-10) with a splitting pattern of doublet-triplet-triplet-doublet. By inspection the data of multiplicity and coupling constants as well as the COSY spectrum [figure 3.22 and figure 3.23], those aromatic protons were proven assembling a classical ABCD spin system, characteristic of one 1,2-disubstituted aromatic system.



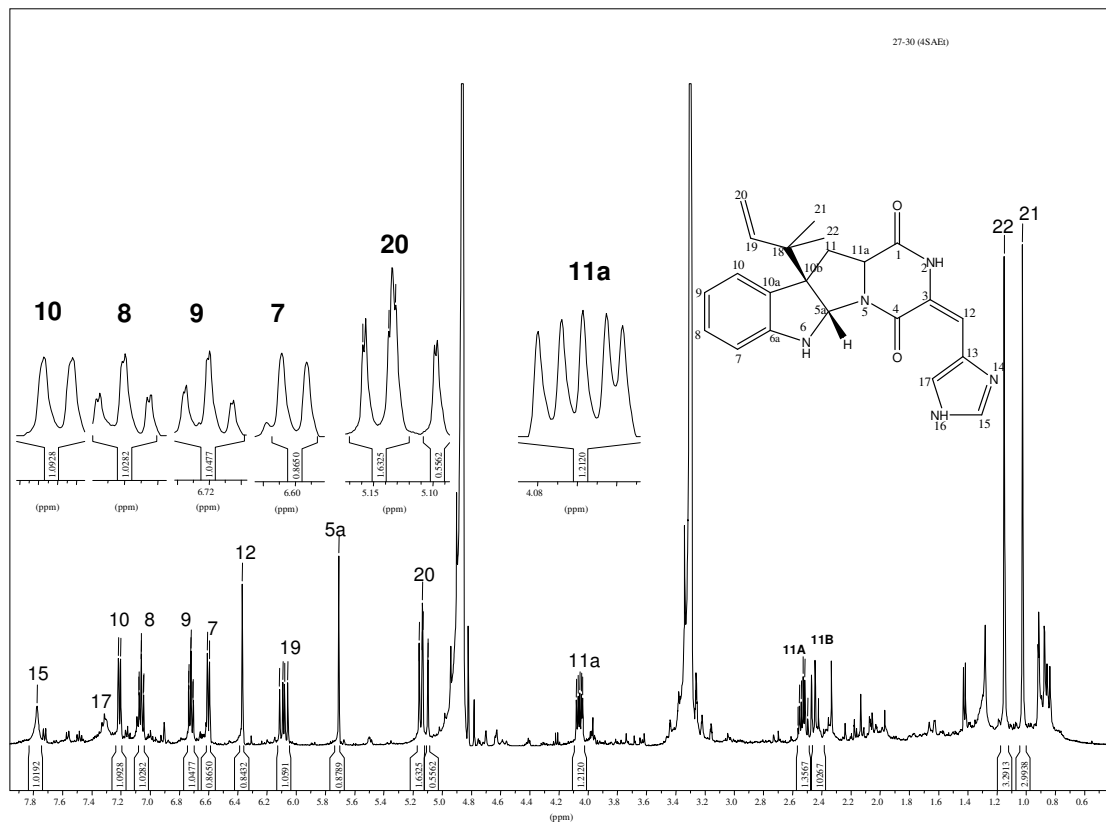


Figure 3.21 ^1H NMR spectrum of compound **7** (CD_3OD , 500 MHz)

Two methyl proton signals were detected in the ^1H NMR spectrum as singlets at the chemical shifts δ 1.01 (H-21) and 1.15 ppm (H-22). One methylene group was observed as two doublets at 5.15 (H-20A) and 5.10 ppm (H-20B), showing a correlation to the olefinic proton H-19 at 6.08 ppm in the COSY spectrum [figure 3.22]. In conjunction with the two geminal methyl groups, these three olefinic protons assembled a dimethylallyl moiety.

It was detected as well that compound **7** possessed another isolated olefinic proton appearing as a singlet at 6.39 ppm (H-12) and two more aromatic protons located in the imidazole ring appeared as broad singlets at 7.31 (H-17) and δ 7.70 ppm (H-15). The methylene group and its α -proton located in the pyrrolidine ring were

observed in the ^1H NMR spectrum as a multiplet at the 2.50 ppm ($\text{H}_2\text{-11}$) and at 4.06 ppm as doublet of doublet (H-11a). The COSY spectrum [figure 3.22] showed the correlation between $\text{H}_2\text{-11}$ and H-11a .

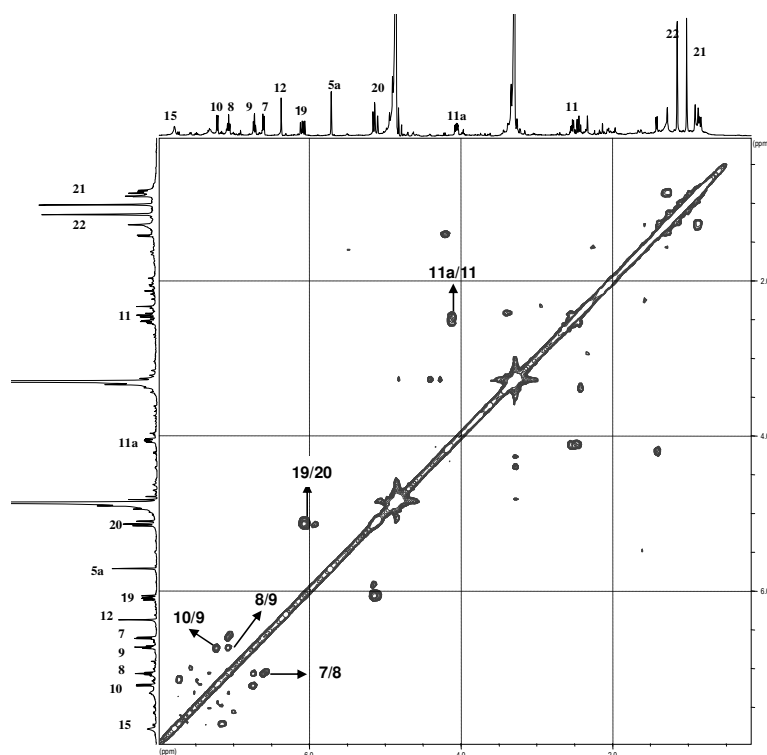


Figure 3.22 COSY spectrum of compound **7** (CD_3OD , 500 MHz)

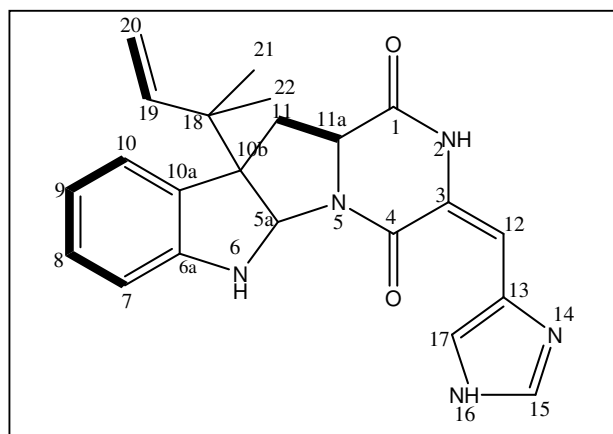


Figure 3.23 COSY correlations of compound **7** (roquefortine C)

Compound **7** was identified as roquefortine C by comparison of its NMR data with that of roquefortine C isolated from *Penicillium corymbiferum* published by Scott *et al.* (1976). Optical rotation of compound **1** was $[\alpha]_D^{20} -358^\circ$, whereas optical rotation of roquefortine C previously described in literature was $[\alpha]_D^{20} -703^\circ$ (Scott *et al.*, 1976) leading the conclusion that both compounds have the same stereochemistry.

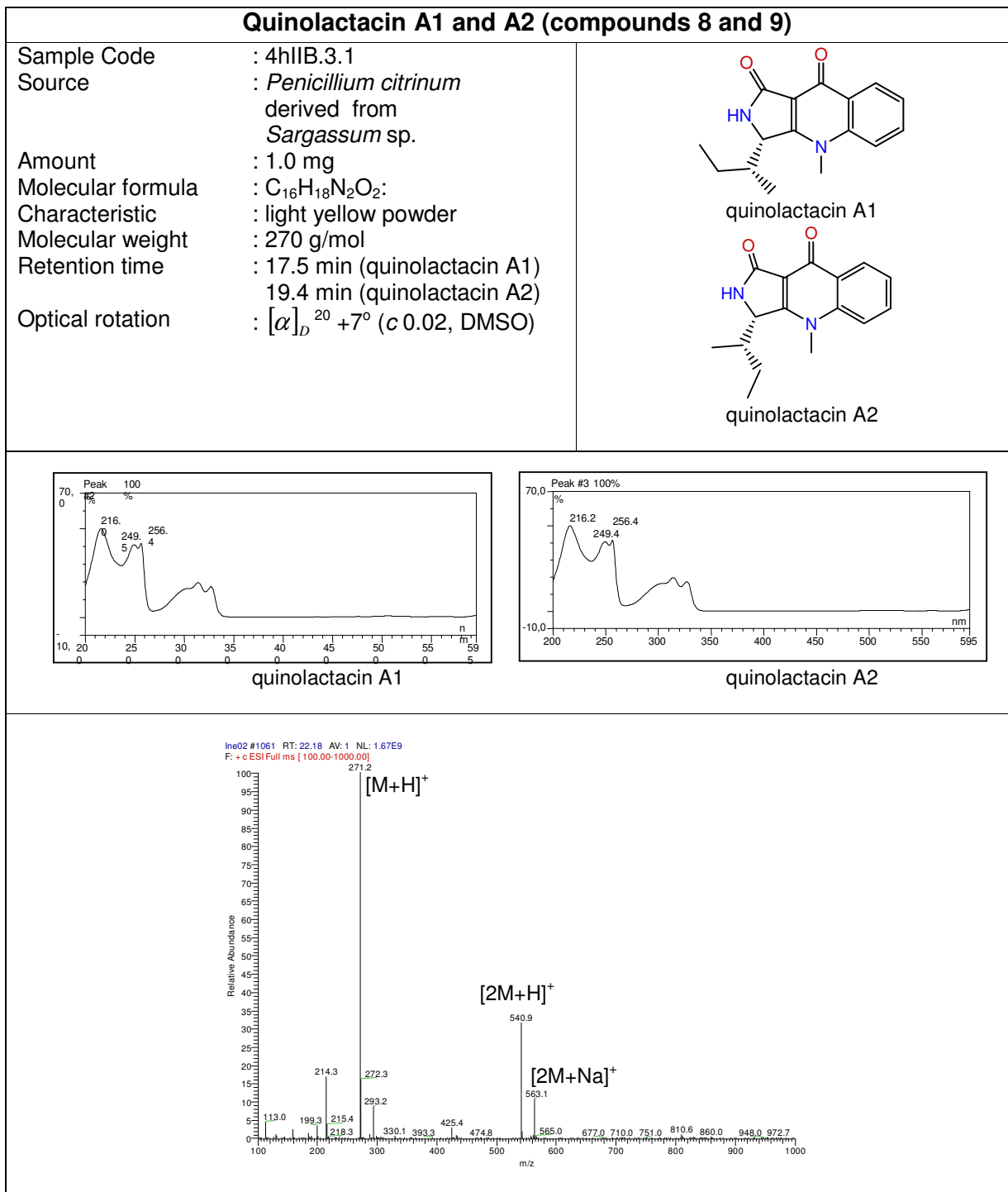
Table 3.8 NMR data of compound 5 (roquefortine C)

Position	δ H (ppm), multiplicity (<i>J</i> in Hz) (in CD ₃ OD)	δ H (ppm) multiplicity (<i>J</i> in Hz) (Scott <i>et al.</i> , 1976 in CDCl ₃)
5a	5.71 (1H,s)	5.70 (1H,s)
7	6.60 (1H,d,7.6)	6.58 – 7.30 (5H)
8	7.06 (1H,t,7.6)	
9	6.72 (1H,t,7.6)	
10	7.21 (1H,d,7.6)	
17	7.31 (1H,s)	
11	2.50 (2H,m)	2.58 (2H,m)
11a	4.06 (1H,dd,11.4,6.0)	4.12 (1H,dd)
12	6.39 (1H,s)	6.40 (1H,s)
15	7.70 (1H,s)	7.73 (1H,s)
19	6.08 (1H,m)	6.07 (1H,m)
20	5.15 (2H,dd,11.0,1.3) 5.10 (1H,dd,17.7,1.3)	5.28 (1H,m) 5.04 (1H,m)
21	1.02 (3H,s)	1.06 (3H,s)
22	1.15 (3H,s)	1.17 (3H,s)

3.2.3 Compound **8** (quinolactacin A1) and compound **9** (quinolactacin A2)

Compound **8** (quinolactacin A1) and **9** (quinolactacin A2) were isolated together as an inseparable mixture from the *n*-butanol extract of *Penicillium citrinum* through Sephadex LH-20 column chromatography using 100% methanol, followed by semipreparative HPLC in the form of light yellow powder. The UV spectrum of quinolactacin A1 showed UV maxima at $\lambda_{\max}(\text{MeOH})$ 216.0, 249.5 and 256.4 nm, whereas that of quinolactacin A2 had $\lambda_{\max}(\text{MeOH})$ at 216.2, 249.4 and 256.4 nm. Their ESI mass spectra showed a pseudomolecular ion peak at m/z 271 $[\text{M}+\text{H}]^+$ upon

positive ionization, indicating the molecular weight of 270 g/mol. The ratio of quinolactacin A1 and quinolactacin A2 in the mixture was almost 1:1 based on the integration in the NMR spectrum [figure 3.24].



Quinolactacin A1 is actually the C-1' diastereomer of quinolactacin A2. Both quinolactacins A1 and A2 had a molecular weight of 270 g/mol. In the ^1H NMR spectrum [figure 3.24], the complete signals of both diastereomers appeared. The aliphatic signals of both diastereomers were observed at different chemical shifts in the upfield region, while the aromatic protons of both compounds were detected overlapping in the downfield region which was proven by the integrations.

The signals of the aromatic protons were observed resonating between the chemical shifts δ 7.80 and 8.25, H-5 at δ 7.82 (2H,bd), H-6 at δ 7.81 (2H,m), H-7 at δ 7.48 (2H,m) and H-8 at δ 8.25 (2H,bd,7.6). H-8 was shifted to the downfield area due to deshielding of the carbonyl group in β -position. These aromatic protons represented an ABCD spin system typical of a 1,2-bisubstituted phenyl ring which was proven by the COSY spectrum [figure 3.25].

In the ^1H NMR spectrum [figure 3.24], the protons of one N-methyl group and one NH group of compound **8** (quinolactacin A1) were observed as singulets at the chemical shift δ 8.07 (2-NH) and 3.81 (4-NCH₃) and those of compound **9** (quinolactacin A2) appeared as singulets at δ 8.15 (2-NH) and 3.84 (4-NCH₃). Both methyl groups were shifted downfield due to the influence of nitrogen atoms at α -positions.

In the ^1H NMR spectrum [figure 3.24], the signals of the isobutyl moiety of compound **8** (quinolactacin A1) appeared at 4.82 ppm (H-3,1H,bs), 2.16 ppm (H-1',1H,m), 0.48 ppm (1'-CH₃,3H,d,6.6 Hz), 1.58 (H-2'A,1H,m), 1.39 ppm (H-2'B,1H,m) and 0.98 ppm (H₃-3,3H,t,7.6), whereas those of compound **9** (quinolactacin A2) were detected at 4.84 ppm (H-3,1H,bs), 2.16 ppm (H-1',1H,m), 1.13 ppm (1'-CH₃,3H,d,6.9 Hz), 0.94 (H-2'A,1H,m), 0.84 ppm (H-2'B,1H,m) and 0.65 ppm (H₃-3,3H,t,7.4 Hz). In

the COSY spectrum [figure 3.25], these two spin systems of both diastereomers were observed and could be clearly distinguished.

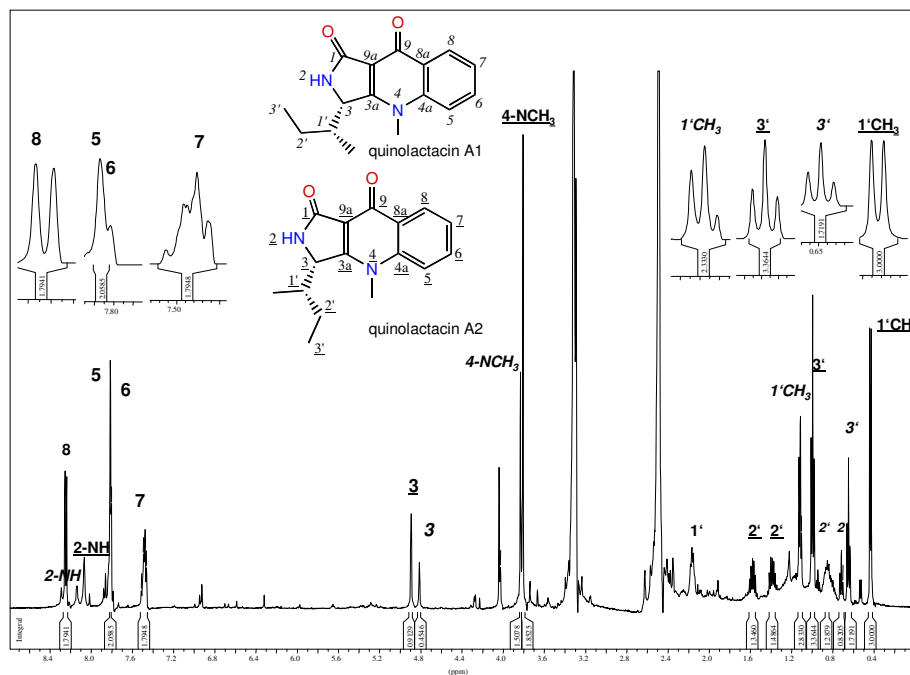


Figure 3.24 ^1H NMR spectrum of compounds **8** and **9** (DMSO, 500MHz)

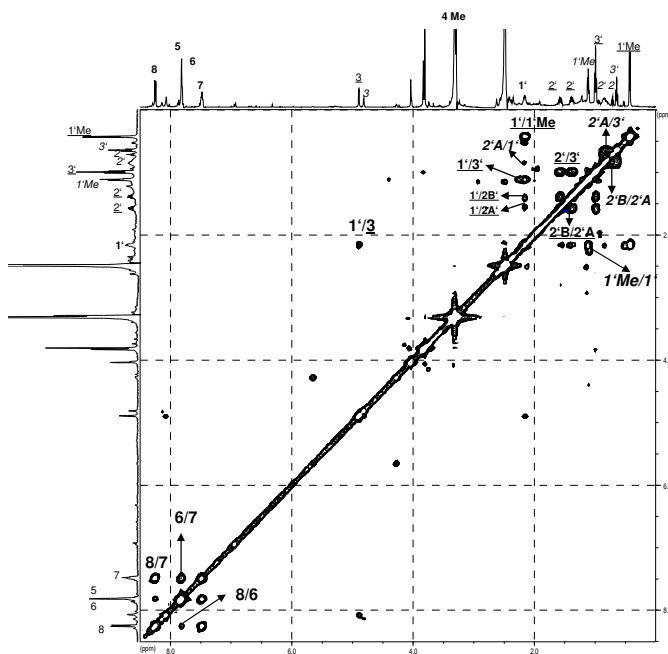


Figure 3.25 COSY spectrum of compounds **8** and **9** (DMSO, 500 MHz)

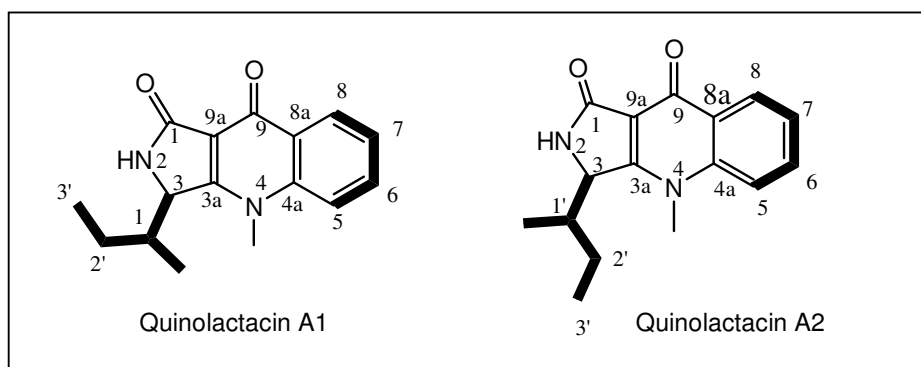


Figure 3.26 COSY correlations of compounds **8** and **9** (quinolactacin A1 and A2)

The ^1H NMR spectrum of compounds **8** and **9** in comparison with that of quinolactacin A1 and A2 reported by Kim *et al.* (2001) and Takahashi *et al.* (2000) indicated similar chemical shifts which led to the conclusion that both pairs of compounds were the same.

Compound **8** and **9** had been isolated together in one fraction and could not be separated either by Sephadex column chromatography or by semipreparative HPLC. Due to the fact that quinolactacin A1 and A2 were diastereomers but not enantiomers, they should have shown different physical properties, e.g. retention times. Kim *et al.* in 2001 reported that they successfully separated both compounds by chiral HPLC. These quinolone antibiotics were first isolated from the culture broth of *Penicillium* sp., which was derived from the larvae of mulberry pyralid (*Margaronia pyloalis* Welker).

Table 3.9 NMR data of compound **8** (quinolactacin A1)

Position	δH (ppm), multiplicity (J in Hz (in DMSO)	δH (ppm) multiplicity (J in Hz) (Kim <i>et al.</i> , 2001 in CDCl_3)
2-NH	8.07 (1H,s)	7.37 (1H, bs)
3	4.82 (1H,bs)	4.80(1H,d,2.5)
4-CH3	3.81 (3H,s)	3.80 (3H,s)
5	7.82 (1H,bd)*	7.47(1H,d,8.2)
6	7.82 (1H,m)	7.66 (1H,ddd,8.2,7.5,1.4)
7	7.48 (1H,m)	7.29 (1H,dd,7.6,1.4)
8	8.25 (1H,bd,7.6)	8.23 (1H,dd,7.6,1.4)

1'	2.16(1H,m)	2.13 (1H, m)
1'-CH3	0.43 (3H,d,6.6)	0.51 (3H,d,6.7)
2'	1.58 (1H,m) 1.39 (1H,m)	1.62 (1H,m) 1.48 (1H,m)
3'	0.98 (3H,t,7.6)	1.09 (3H,t,7.4)

* : overlapping signals

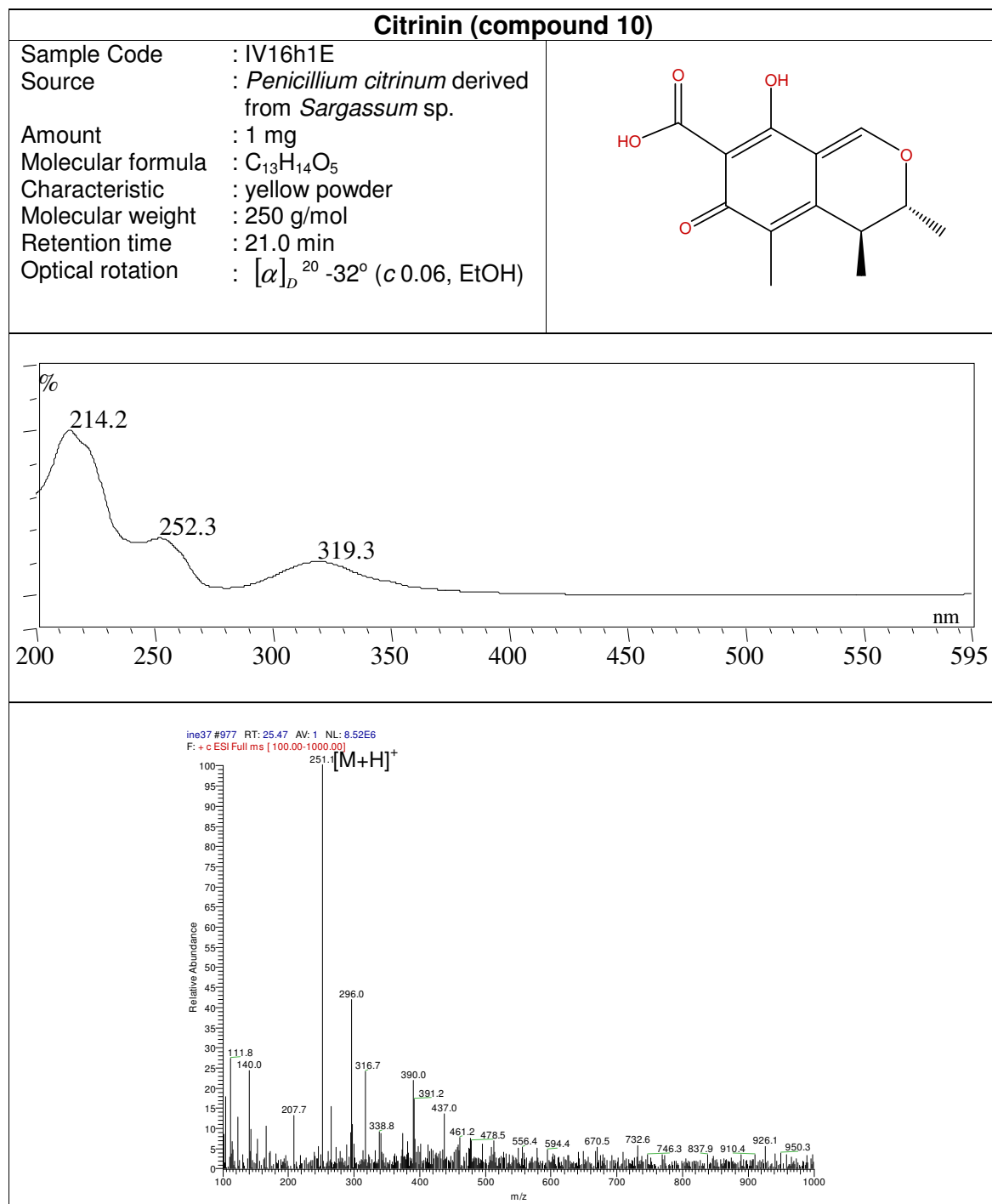
Table 3.10 NMR data of compound **9** (quinolactacin A2)

Position	δ H (ppm), multiplicity (<i>J</i> in Hz) (in DMSO)	δ H (ppm) multiplicity (<i>J</i> in Hz) (Takahashi, <i>et al.</i> , 2000 in DMSO)
2-NH	8.15 (1H,s)	8.17 (1H,s)
3	4.84 (1H,s)	4.84 (1H,s)
4-CH3	3.84 (3H,s)	3.86 (3H,s)
5	7.82 (1H,bd)*	7.83 (1H, d,8.4)
6	7.82 (1H,m)*	7.81(1H,dd,8.4,6.8)
7	7.48 (1H,m)	7.48 (1H,dd,7.2,6.8)
8	8.25 (1H,bd,6.6)	8.26 (1H,d,7.2)
1'	2.16 (1H,m)	2.19(1H,m)
1'-CH3	1.13 (3H,d,6.9)	1.14(3H,d,6.8)
2'	0.94 (1H,m) 0.84 (1H,m)	0.88 (1H,m) 0.83 (1H,m)
3'	0.65 (3H,t,7.4)	0.65 (3H,t,7.4)

* : overlapping signals

3.2.4 Compound **10** (citrinin)

Compound **10** (citrinin) was isolated as yellow powder from the ethyl acetate extract of *Penicillium citrinum* through Sephadex LH-20 column chromatography with 100% methanol followed by semipreparative HPLC .It showed UV absorbances at λ_{\max} (MeOH) 214.2, 252.3 and 319.3 nm. The ESI-MS of this compound exhibited an intense pseudomolecular peak at m/z 251 $[M+H]^+$ upon positive ionization, revealing the molecular weight of 250 g/mol



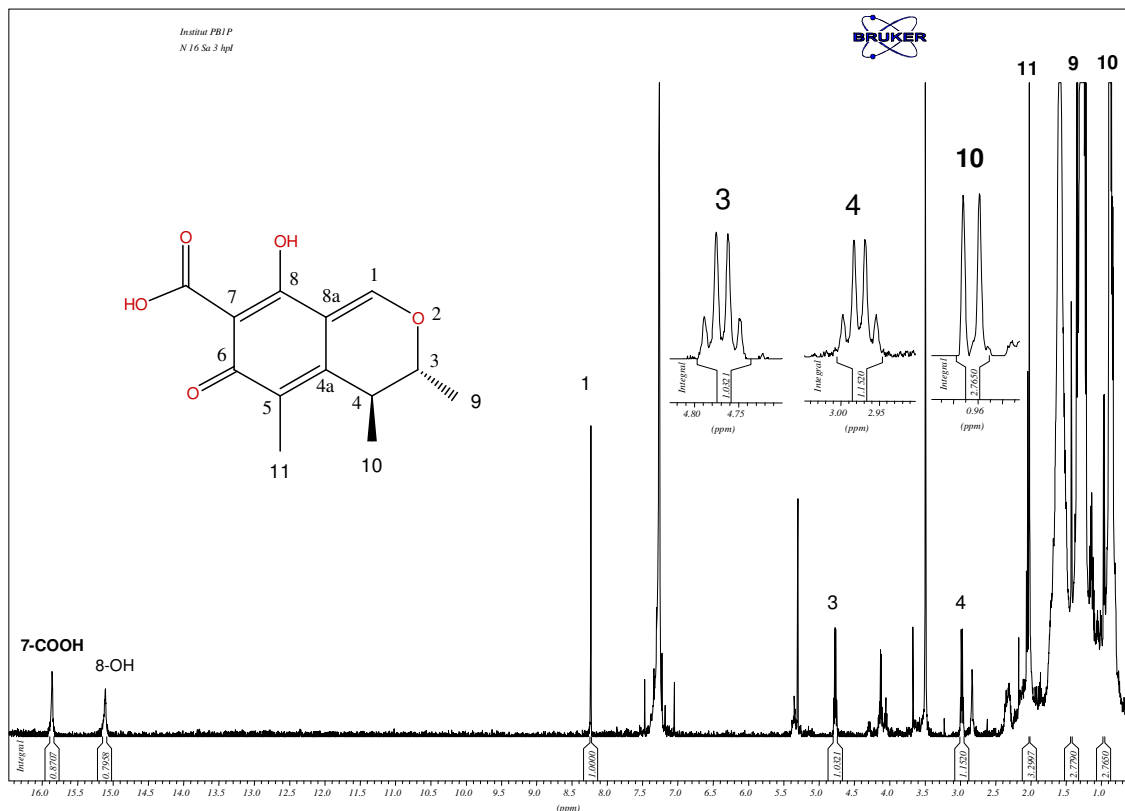


Figure 3.27 ^1H NMR spectrum of compound **10** (CDCl_3 , 500 MHz)

In the ^1H NMR spectrum [figure 3.27], three methyl groups, two more aliphatic protons, one aromatic OH proton, and two protons originating from hydroxyl groups were observed. One aliphatic methyl group was detected at 0.97 ppm ($\text{H}_3\text{-10}$) as a doublet, coupled to H-4 at δ 2.98 ppm (dd, $J = 14.5, 7.3$ Hz), the other aliphatic methyl group appeared as a doublet at δ 0.97 ppm ($\text{H}_3\text{-9}$) coupled with H-3 at δ 4.77 ppm (dd, $J = 13.6, 6.6$ Hz), while the third methyl group ($\text{H}_3\text{-11}$) appeared as a singlet at 2.02 ppm.

The hydroxyl protons were observed in the downfield area as broad singlets at δ 15.87 (7-COOH) and 15.11 (8-OH) due to the fact that they were part of a carboxylic acid and a vinylogous carboxylic acid, respectively. An aromatic proton appeared at δ

8.23 (H-1) as a singlet, shifted considerably downfield due to the electron-withdrawing influence of the oxygen atom in α -position.

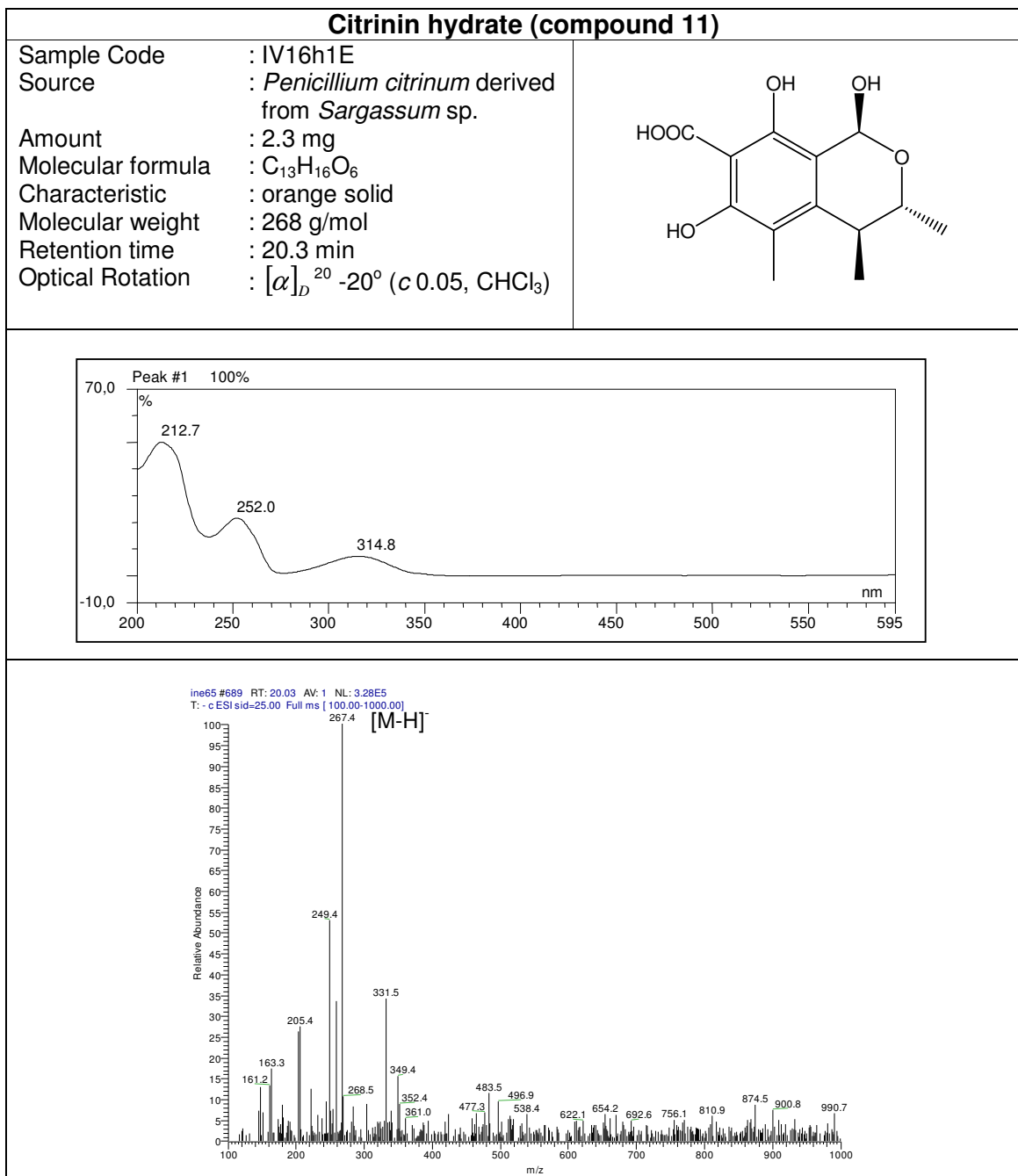
Compound **10** was substantially identified as citrinin based on the comparison with NMR data of citrinin reported by Barber *et al.* (1981). Citrinin was first isolated in 1964 from *Penicillium citrinum* and later also reported from several different species of *Penicillium*, *Aspergillus*, *Candida* and *Monascus* (Wyllie *et al.*, 1964).

Table 3.11 NMR data of compound **10** (citrinin)

Position	δ H (ppm), multiplicity (<i>J</i> in Hz) (in CDCl ₃)	δ H (ppm) multiplicity (<i>J</i> in Hz) (Barber <i>et al.</i> , 1981 in CDCl ₃)
1	8.23 (1H, s)	8.24 (1H, s)
3	4.77 (1H,q, 6.9)	4.78 (1H, q, 6.8)
4	2.98 (1H,q, 7.3)	2.99 (1H, q, 7.3)
7 - COOH	15.87 (1H, s)	15.86 (1H, s)
8 - OH	15.11 (1H, s)	15.09 (1H, s)
9	1.43 (3H, d, 6.6)	1.35 (3H, d, 6.8)
10	0.97 (3H,d,7.3)	1.23 (3H, d, 7.3)
11	2.02 (3H, s)	2.02 (3H, s)

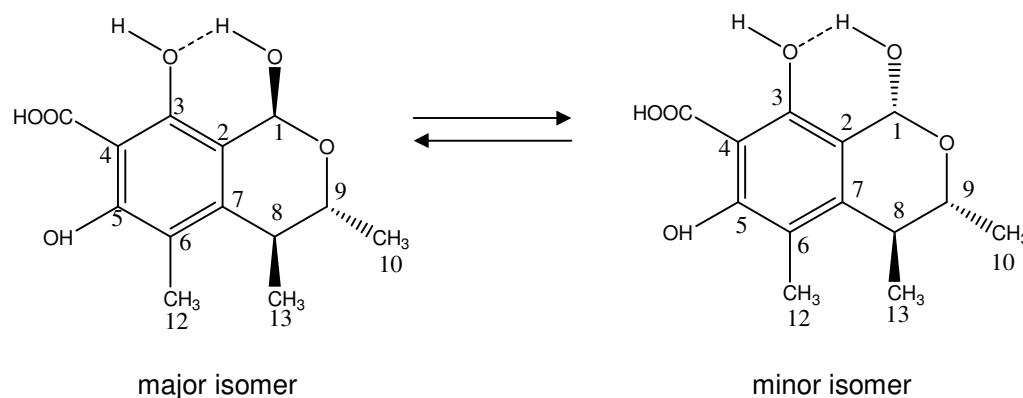
The measured optical rotation of compound **10** was $[\alpha]_D^{20}$ -32° whereas the optical rotation previously reported in literature was $[\alpha]_D^{20}$ -43.1° (Barber *et al.*, 1981) suggesting both compounds to have the same stereochemistry.

3.2.5 Compound 11 (Citrinin hydrate)



Compound **11** (citrinin hydrate) was isolated from the ethyl acetate extract of *Penicillium citrinum* through Sephadex LH-20 column chromatography with 100% methanol followed by semipreparative HPLC. The ESI mass spectrum of this compound showed a pseudomolecular ion at m/z 267 $[M-H]^-$ under negative ionization indicating a molecular weight of 268 g/mol. UV maxima were at λ_{\max} (MeOH) 212.7, 252.0, 314.8 nm.

The ^1H NMR [figure 3.28] and COSY spectra [figure 3.29] revealed that the substance was a mixture of citrinin hydrate isomers. Kadam *et al.* (1994) discovered that the isomers appeared as an equilibrium mixture because their ratio varied with solvent.



The ^1H NMR spectrum [figure 3.28] showed that there were two sets of signals from two isomers which had a ratio of approximately 2:1. Each consisted of three methyl groups, and three more aliphatic protons. One methyl group of the major isomer was detected at 1.31 ppm (H_3 -10) and of the minor isomer at 1.23 ppm as doublets, coupled to H-9. The other methyl doublet (H_3 -13) resonated at 1.19 ppm for the major isomer and at 1.14 ppm for the minor isomer, coupled to H-8. The third

methyl group (H₃-12) appeared as singlet at 2.09 ppm (major isomer) and 2.03 ppm (minor isomer), respectively.

One aliphatic proton was detected at 5.54 ppm (major isomer) and 5.42 ppm (minor isomer) as singlets (H-1). The other two aliphatic protons appeared at 2.64 ppm (major isomer) and 2.73 ppm (minor isomer) with multiplicities of doublets (H-8), and at 3.93 ppm (major isomer) and 4.06 ppm (minor isomer) with multiplicities of doublets of doublets (H-9).

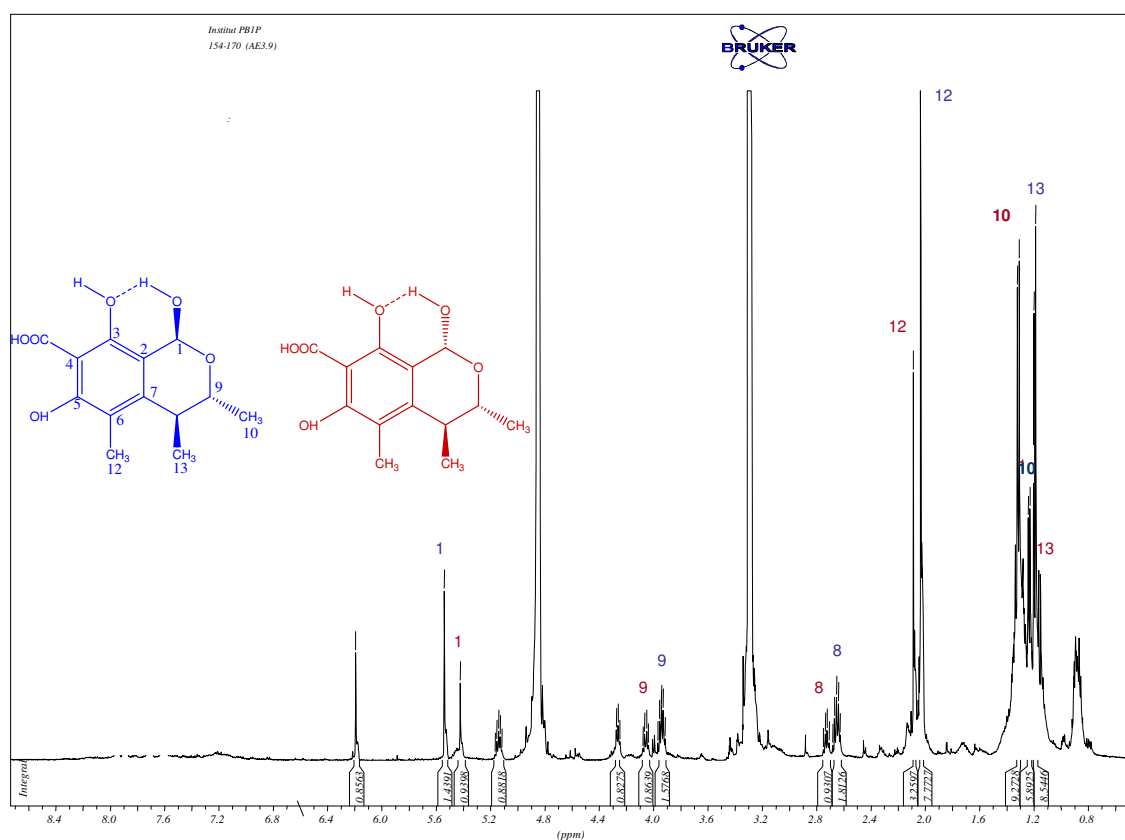


Figure 3.28 ¹H NMR spectrum of compound 11 (CD₃OD, 500 MHz)

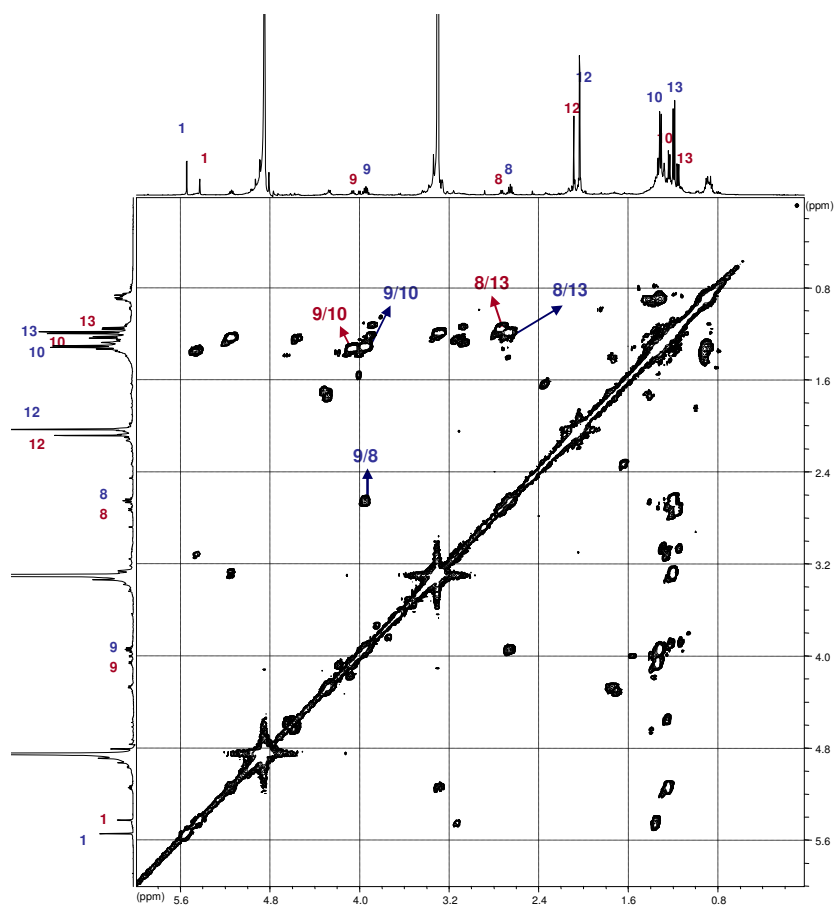


Figure 3.29 COSY spectrum of compound **11** (CD_3OD , 500 MHz)

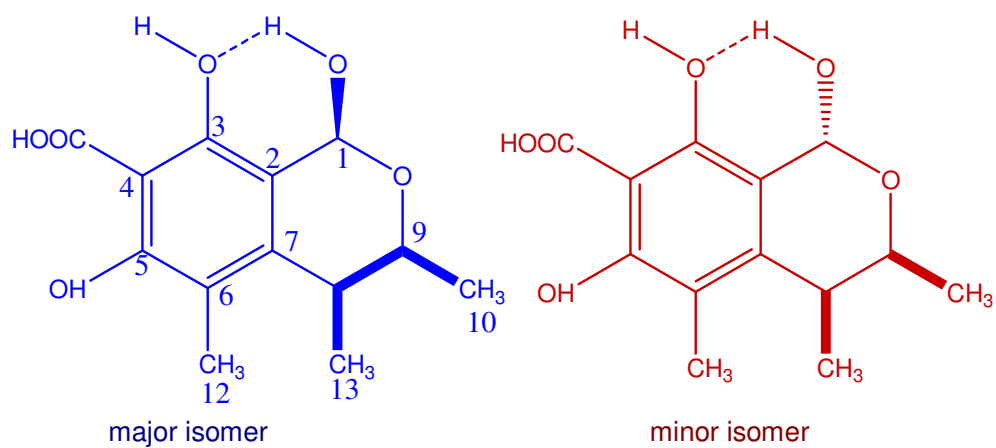


Figure 3.30 COSY correlations of compound **11** (citrinin hydrate)

Table 3.12 showed the comparison of NMR data of compound **11** with literature data which led to the conclusion that both compounds were identical. Citrinin hydrate was first isolated in 1994 from *Penicillium* sp. (Kadam *et al.*,1994).

Table 3.12 NMR data of compound **11** (citrinin hydrate, major and minor isomers)

Position	δ H (ppm), multiplicity (<i>J</i> in Hz) (in CD ₃ OD) major isomer	δ H (ppm) multiplicity (<i>J</i> in Hz) (Kadam <i>et al.</i> , 1994 in CD ₃ OD) major isomer
1	5.54 (1H, s)	5.55 (1H,s)
8	2.64 (1H,dd,13.6,6.6)	2.65 (1H,qd,6.8,6.6)
9	3.93 (1H,dd,13.5,6.7)	3.94 (1H,dq,6.6,6.2)
10	1.31 (3H,d,6.3)	1.31 (3H,d,6.2)
12	2.09 (3H, s)	2.03 (3H, s)
13	1.19 (3H,d,6.6)	1.19 (3H,d,6.8)

Position	δ H (ppm), multiplicity (<i>J</i> in Hz) (in CD ₃ OD) minor isomer	δ H (ppm) multiplicity (<i>J</i> in Hz) (Kadam <i>et al.</i> , 1994 in in CD ₃ OD) minor isomer
1	5.42 (1H, s)	5.43 (1H,s)
8	2.73 (1H,dd,13.9,6.6)	2.72 (1H,qd,7.0,0.9)
9	4.06 (1H,dd,13.6,6.7)	4.05 (1H,dq,7.0,0.9)
10	1.23 (3H,d,6.3)	1.33 (3H,d,7.0)
12	2.03 (3H, s)	2.03 (3H, s)
13	1.16 (3H,d,6.9)	1.15 (3H,d,7.0)

3.3 Isolated secondary metabolites of the fungus *Xylaria* sp.

Xylaria sp. was isolated from the marine alga *Padina australis* collected from the Java Sea. One new compound, 3-methoxymethyl-agistatine D (compound **12**) and 5-carboxy mellein were isolated from this fungus. 5 carboxy mellein (compound **24**) was also isolated from fungus PV1.1 derived from marine sponge *Petrosia ficiformis*.

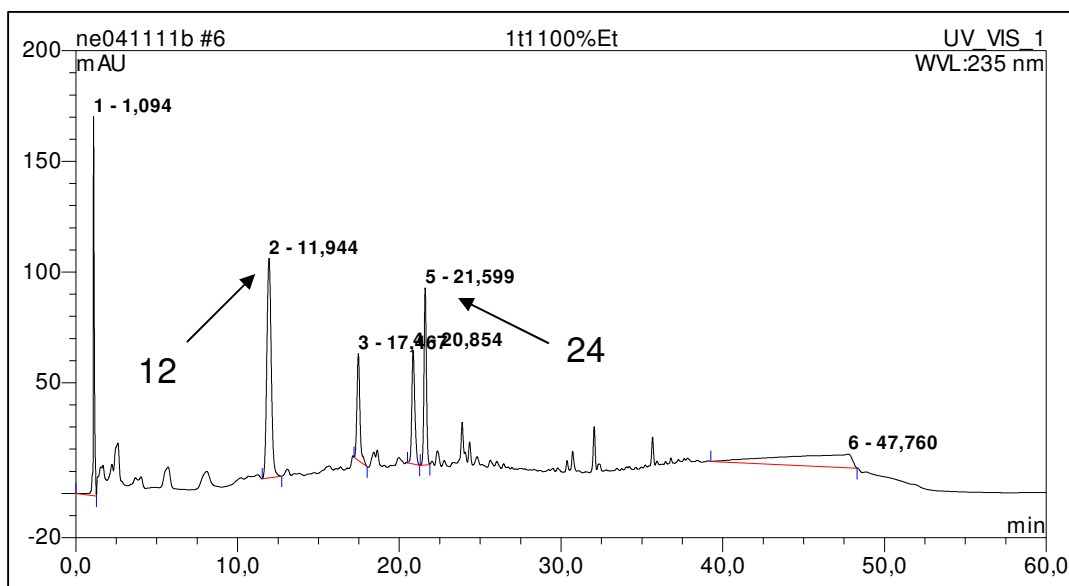
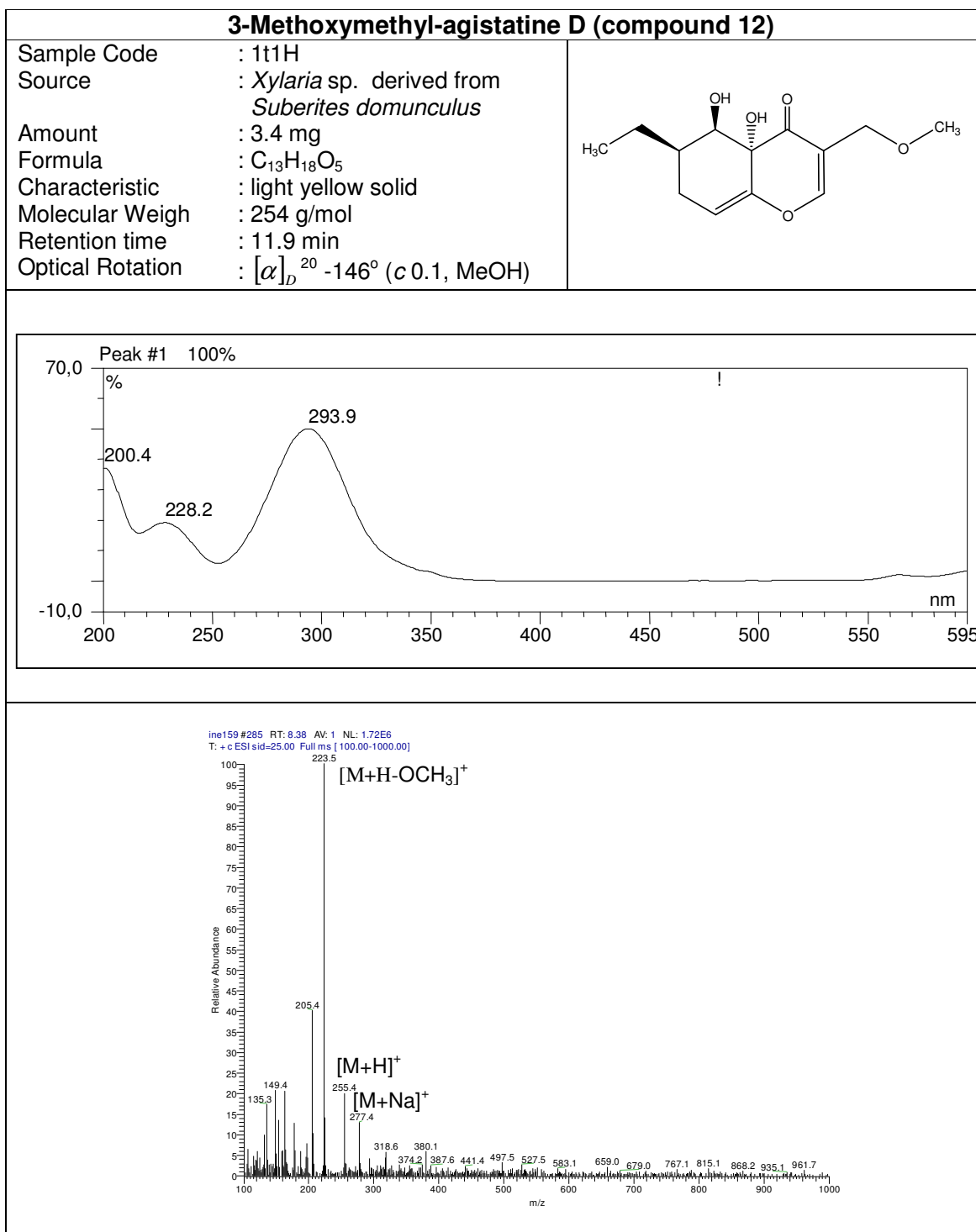


Figure 3.31 HPLC chromatogram of the ethyl acetate extract of *Xylaria* sp.

Table 3.13 Biological screening result of *Xylaria* sp. and its metabolites

Sample	Antimicrobial assay				L5178Y growth (%) Conc. 10 µg/mL	EC ₅₀ (µg/mL)
	BS	SC	CC	CH		
Ethyl acetate extract of <i>Xylaria</i> sp.	-	-	-	-	102.3	
3-methoxymethyl-agistatine D					41.4	
5-carboxymellein					37.3	

BS = *Bacillus subtilis*, SC = *Saccharomyces cerevisiae*, CC = *Cladosporium cucumerinum* and CH = *C. herbarum*

3.3.1 Compound 12 (3-methoxymethyl-agistatine D), new compound

Compound **12** (3-methoxymethyl-agistatine D) was a new compound isolated from *Xylaria* sp. through Sephadex LH-20 column chromatography with 100% methanol, followed by semi preparative HPLC. The UV spectrum exhibited maximum absorptions at 200.4, 228.2, and 293.9 nm. The UV spectrum indicated the location of this double bond in α position to a carbonyl group at λ_{max} 228.2 nm which was later confirmed by the presence of C-4 from HMBC spectrum [figure 3.34] at δ_{C} of 191.2 ppm.

The ESI-MS of this compound showed an intense peak at m/z 255 $[\text{M}+\text{H}]^+$, revealing a molecular weight of 254 g/mol and suggesting a molecular formula of $\text{C}_{13}\text{H}_{18}\text{O}_5$. This assumption was proved by careful analysis of ^1H NMR, COSY, HMBC and ROESY spectra. Characteristically, the ESI-MS gave a prominent fragment peaks at m/z 224 $[\text{M}+\text{H}-\text{OCH}_3]^+$, indicative of a methoxy group and at m/z 277 $[\text{M} + \text{Na}]^+$.

Structurally, this compound was found to be related to the known agistatines, notably agistatine A and agistatine D (Göhr *et al.*, 1995) as was evident from analysis of the COSY and HMBC spectra (see below), but differed from the latter in carrying a methoxymethyl side chain at C-3. In comparison to agistatine A, compound **12** had one more methylene group in the C-3 side chain and a double bond in position 2/3.

This compound is a 4a,5,6,7-tetrahydro-4H-chromen-4-one, substituted with an ethyl and two hydroxyl substituents. The ^1H NMR spectrum [CDCl_3 (500 MHz)] of this compound [figure 3.32] showed 16 proton signals, consisting of a methyl group attached to a methylene group (δ_{H} 0.99, $J=7.6$ Hz), a methoxy group (δ_{H} 3.36), three methylene groups (δ_{H} 1.50-1.59, 2.13-2.25, 4.04-4.13 ppm), an aromatic proton (δ_{H} 7.43), an aliphatic methine group (δ_{H} 1.95) as well as the signals of two additional olefinic protons at δ_{H} 5.98 and 4.26. Signals of hydroxyl groups were not detected in the ^1H NMR spectrum.

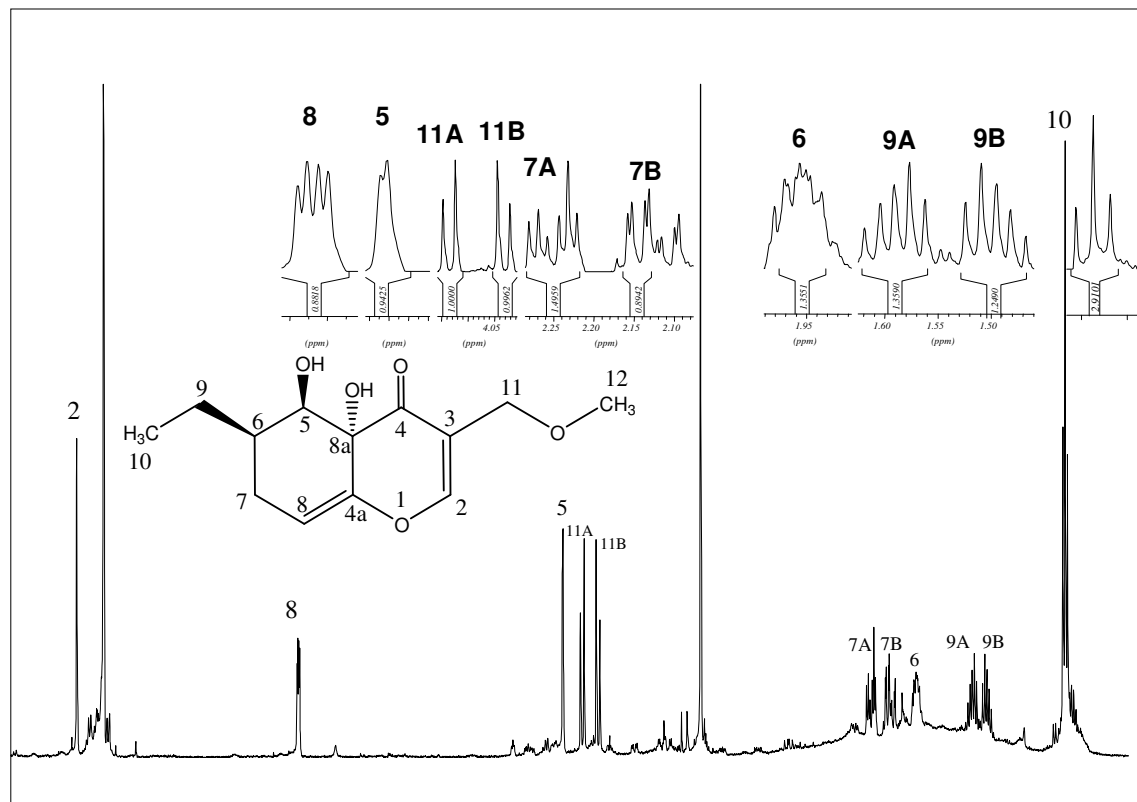
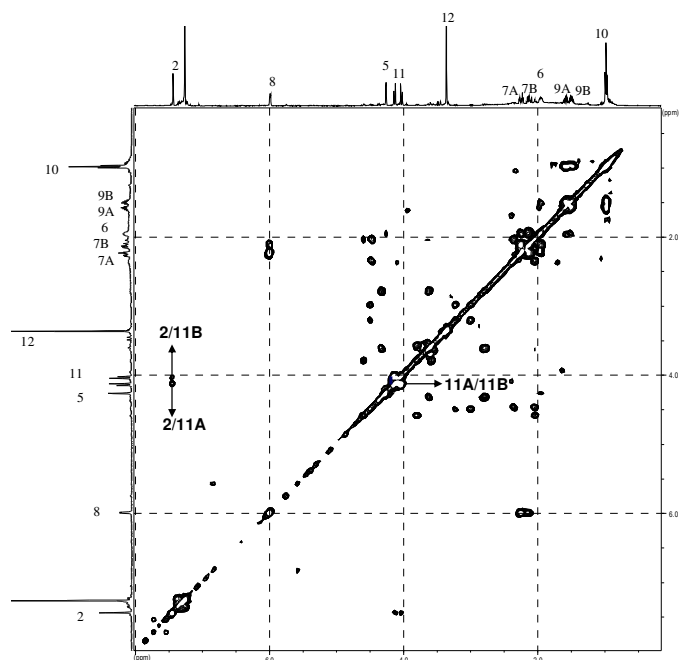
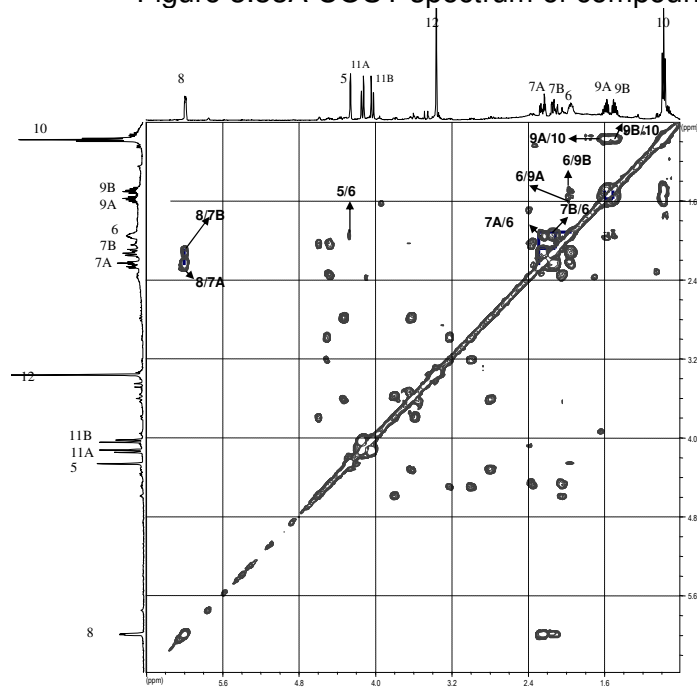


Figure 3.32 ^1H NMR spectrum of compound **12** (CDCl_3 , 500 MHz)

The methylene protons at position 7 (H-7A and H-7B) were observed at δ_{H} 2.25 ppm (dt, $J = 17.8$ and 6.6 Hz) and 2.13 ppm (ddd, $J = 17.8$, 10.7 and 2.7 Hz). H-7A and H-7B showed geminal coupling of 17.8 Hz. H-7A was observed coupling with H-2-9 with the coupling constant $J = 6.6$ Hz, whereas H-7B showed correlation with H-8 with $J = 2.7$ Hz. The methylene group H-11A and H-11B was detected at δ_{H} 4.14 and 4.03 ppm as doublets with coupling constants 11.7 Hz showing geminal coupling between those protons.

Figure 3.33A COSY spectrum of compound **12** (CDCl₃, 500 MHz)Figure 3.33B COSY spectrum of compound **12** (CDCl₃, 500 MHz)

The COSY spectrum revealed that there were two independent spin systems in this structure [figure 3.33 A, 3.33B and figure 3.35]. The first spin system comprised

the protons in the cyclohexene ring (H-5, H-6, H₂-7 and H-8) as well as the ethyl group attached to C-6 (H₂-9 and H₃-10), while the other one included the proton in the dihydropyranone ring (H-2) which was coupled to H₂-11.

The HMBC spectrum [figure 3.34] confirmed the attachment of the ethyl side chain at the cyclohexene ring (H₃-10 to C-6, and H₂-9 to C-5, C-6 and C-7) and also the connection between the methoxymethyl side chain and the dihydropyranone ring (H₂-11 to C-2, C-3 and C-4, H-2 to C-11) [figure 3.34 and 3.35].

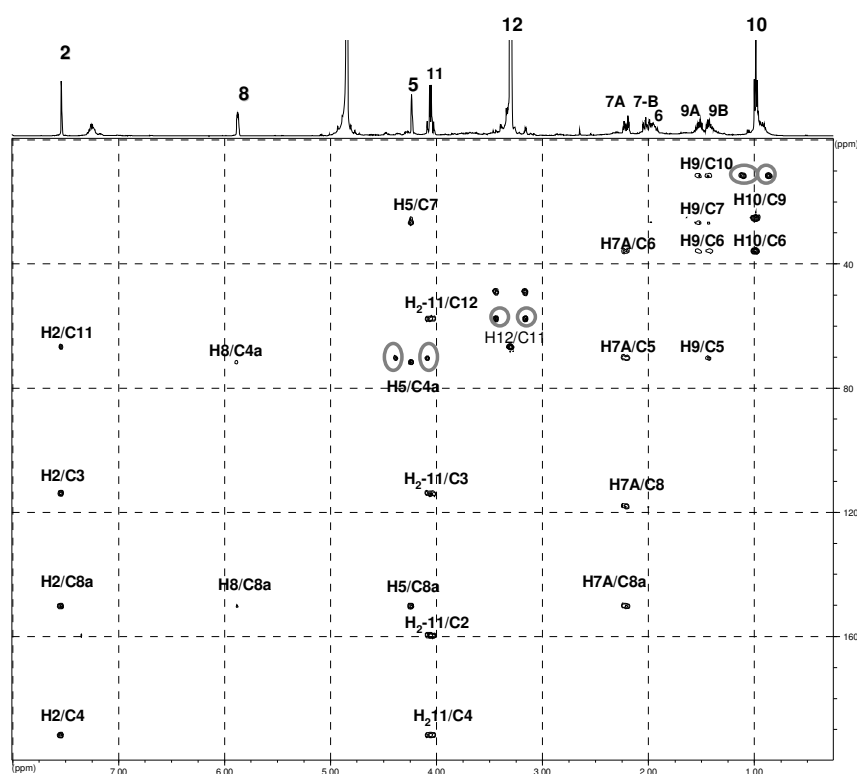


Figure 3.34 HMBC spectrum of compound **12** (CD₃OD, 500 MHz)

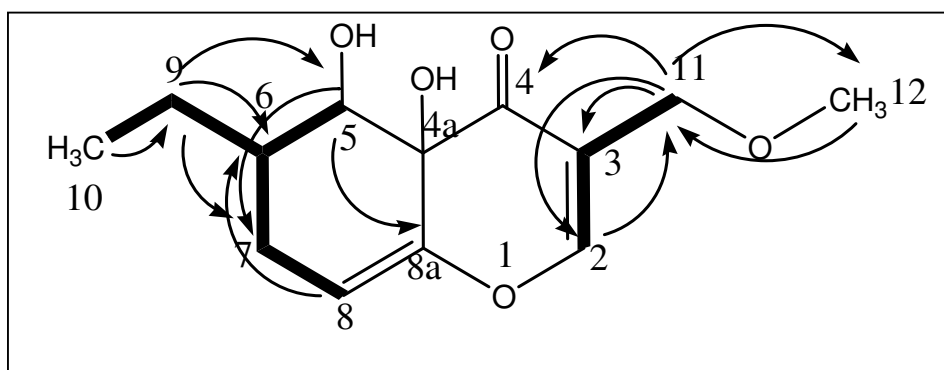


Figure 3.35 HMBC and COSY correlations of compound **12** (3-methoxymethyl-agistatine D)

The spectrum obtained from ROESY experiment could not be used to investigate relative stereochemistry of compound **12** since this experiment did not give any more information than the COSY spectrum. Analogue configuration of the centers of chirality in compound **12** was determined by the coupling constant extracted from ^1H NMR spectrum. The coupling constant of H-5 to H-6 was relatively small ($J = 1.9$ Hz) presuming that H-5 and H-6 had the same orientation.

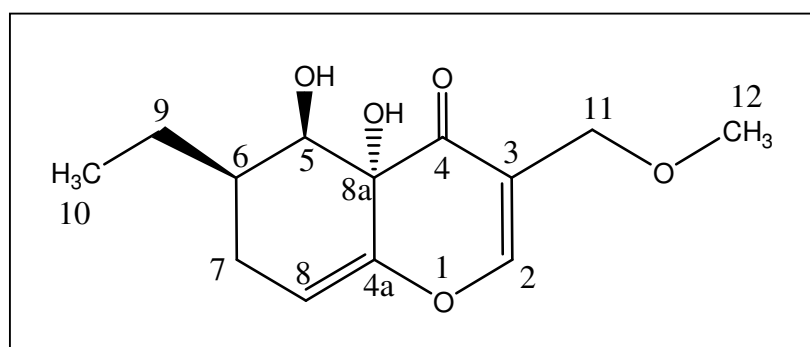


Figure 3.36 Stereochemistry of compound **12** (3-methoxymethyl-agistatine D)

The ^{13}C chemical shifts extracted from the HMBC spectrum [figure 3.34] were rather precise, except the difference of the chemical shift of C-3 at δ_{C} 113.7 ppm (δ_{C} 105.5 ppm) due to additional side chain sitting at position 3 which agistatine D did not possess. This fact confirmed that relative stereochemistry of 3-methoxymethyl-agistatine D was the same with agistatine D [figure 3.36]. Agistatine D, as well as agistatine A, B, C and E, was isolated from fungus FH-A-6239 *Fusarium* sp. by Göhrt *et al.* (1995).

Table 3.14 NMR data of compound **12** (3-methoxymethyl-agistatine D)

Position	multiplicity (<i>J</i> in Hz) (in CDCl_3)	δ_{C} (ppm) (in CD_3OD)	HMBC	multiplicity (<i>J</i> in Hz) of Agistatine D (Göhrt <i>et al.</i> , 1995)	
	δ_{H} (ppm)			δ_{H} (ppm)(in CDCl_3)	δ_{C} (ppm) (in acetone)
2	7.43 (1H,s)	159.4	3,4,8a,11	7.45 (1H, d, 6.0)	159.4
3	-	113.7		5.54 (1H,d, 6.0)	105.5
4		191.3			192.1
4a		71.3			72.1
4a-OH	-			2.82 (1H,s)	
5-OH	-			2.50 (1H,s)	
5-	4.26 (1H,d,1.9)	69.8	3,7,8a	4.25 (1H,s)	70,4
6	1.95 (1H,m)	35.8		1.95 (1H,m)	35.8
7	2.25 (1H,dt,17.8,6.6) 2.13 (1H,ddd17.8,10.7,2.7)	26.6	5,6,8,8a	2.04 – 2.32 (2H,m)	26.7
8	5.98 (1H,dd,5.4,2.7)	117.9	4a,8a	6.00 (1H,dd,5.0,2.5)	117.4
8a		150.1			150.2
9	1.59 (1H, m) 1.50 (1H, m)	25.1	5,6,7,10	1.36 – 1.72 (2H,m)	25.1
10	0.98 (3H,t,7.6)	11.5	6,9	0.98 (3H,t,7.0)	11.9
11	4.14 (1H,d,11.7) 4.03 (1H,d,11.7)	66.3	2,4,12		
12	3.36 (3H,s)	57.3			

3.4 Isolated secondary metabolites of the fungus *Fusarium equiseti*

Fusarium equiseti was isolated from the marine alga *Sargassum* sp. collected from the Java Sea. Two compounds have been isolated which were zearalenone (compound **13**) and tyramine (compound **14**).

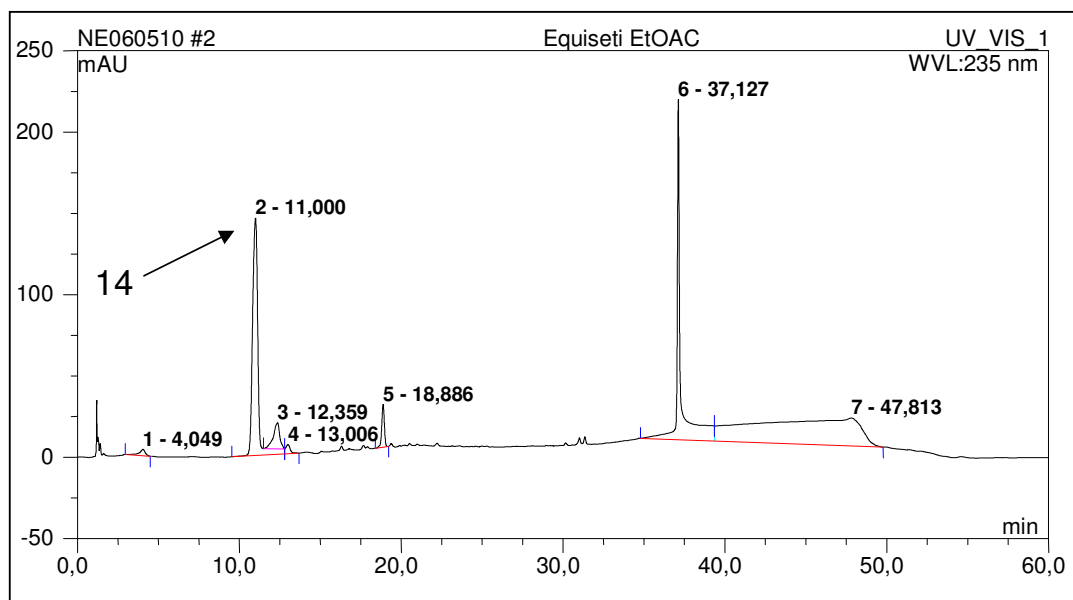


Figure 3.37 HPLC chromatogram of the ethyl acetate extract of *Fusarium equiseti*

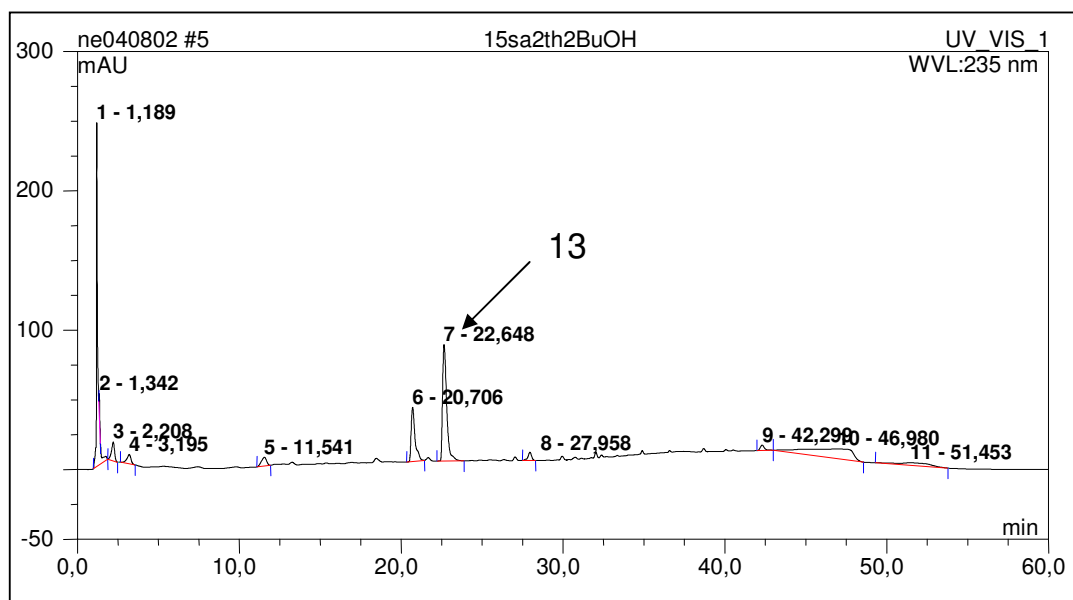


Figure 3.38 HPLC chromatogram of the butanol extract of *Fusarium equiseti*

Table 3.15 Biological test result of *Fusarium equiseti* and its metabolites

Sample	Antimicrobial assay				L5178Y growth (%)	EC ₅₀ (µg/mL)
	BS	SC	CC	CH	Conc. 10 µg/mL	
Ethyl acetate extract of <i>Fusarium equiseti</i>	-	-	-	-	101.2	
Zearalenone					53.4	
Tyramine					103.9	

BS = *Bacillus subtilis*, SC = *Saccharomyces cerevisiae*, CC = *Cladosporium cucumerinum* and CH = *C. herbarum*

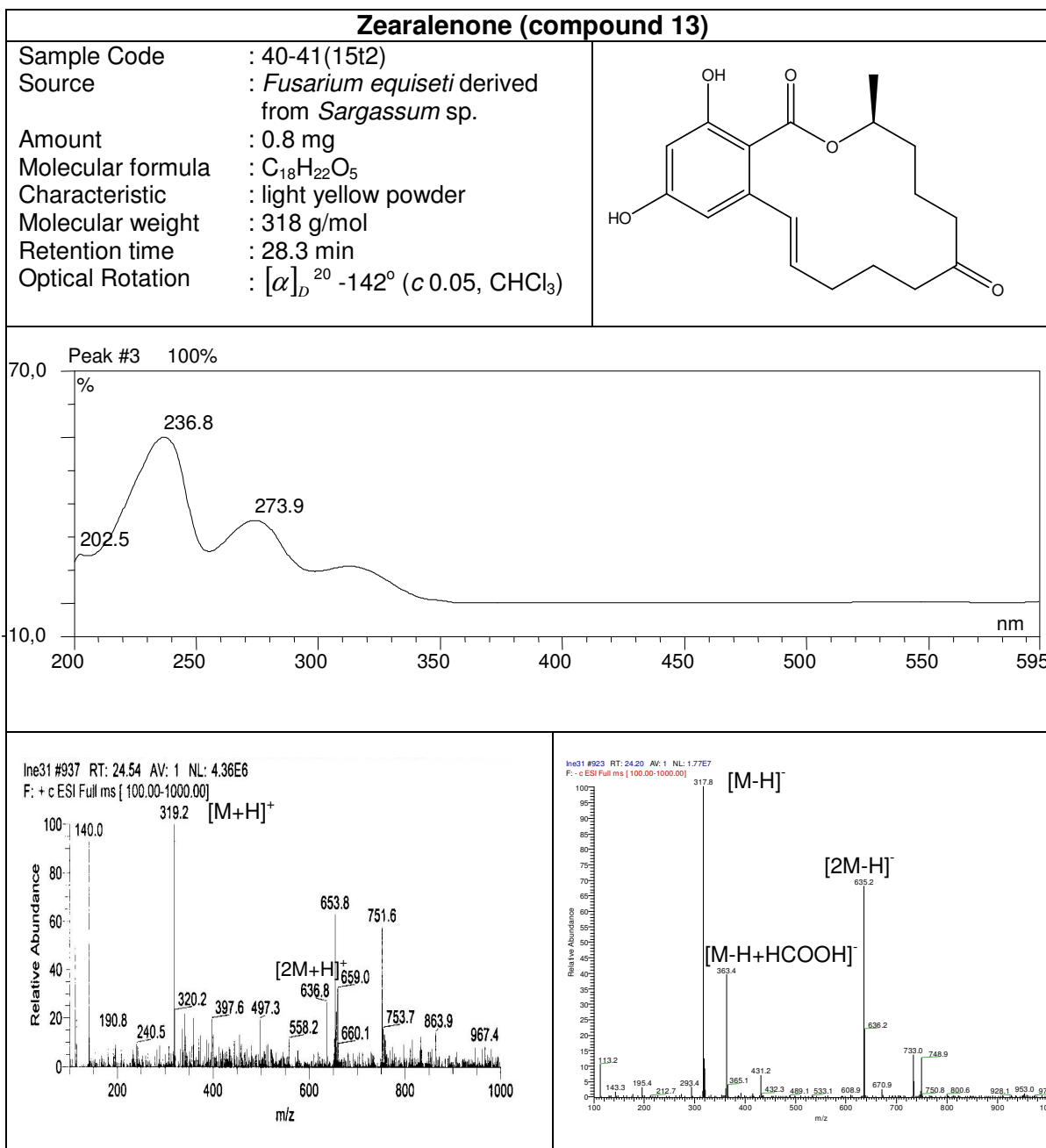
3.4.1 Compound 13 (zearalenone)

Compound **13** (zearalenone) was isolated from the *n*-butanol extract of *Fusarium equiseti* through Sephadex LH-20 column chromatography with 100% methanol. Its UV spectrum showed the maximum at 236.8 nm, with shoulders at 202.5 and 273.9 nm. In the ESI MS, a prominent [M+H]⁺ pseudomolecular ion was observed at *m/z* 319 upon positive ionization, together with an intense [M-H]⁻ at *m/z* 318 upon negative ionization which indicated a molecular weight of 318 g/mol. In addition with analysis of 1D and 2D NMR spectra, it was assumed that molecular formula of this compound is C₁₈H₂₂O₅.

Zearalenone was first isolated from the fungus *Fusarium graminearum* (Urry *et al.*, 1966). Structurally, the compound consisted of a 2,4-dihydroxybenzoic acid skeleton with a side chain in position 6, including one olefinic group and one keto function. The lactone ring was completed by an ester bond to the aromatic carboxylic acid group.

In the ¹H NMR spectrum [figure 3.39], two aromatic protons were detected at the chemical shifts δ 6.21 (H-3) and 6.37 (H-5). Investigation of coupling constants and the correlations in the COSY spectrum [figure 3.40B] allowed to concluding that those

two protons assembled an AB spin system in a 1,2,4,6 tetrasubstituted phenyl ring with a *meta*-coupling of 2.2 Hz.



Compound **13** has been observed to possess a methyl group appearing at 1.36 ppm (H₃-17) as a doublet due to methine group adjacent to this group. Two olefinic protons were detected at 6.98 (H-7) and 5.70 ppm (H-8) coupling with a coupling constant of 15.5 Hz, suggesting that they were part of a double bond in *trans*-configuration.

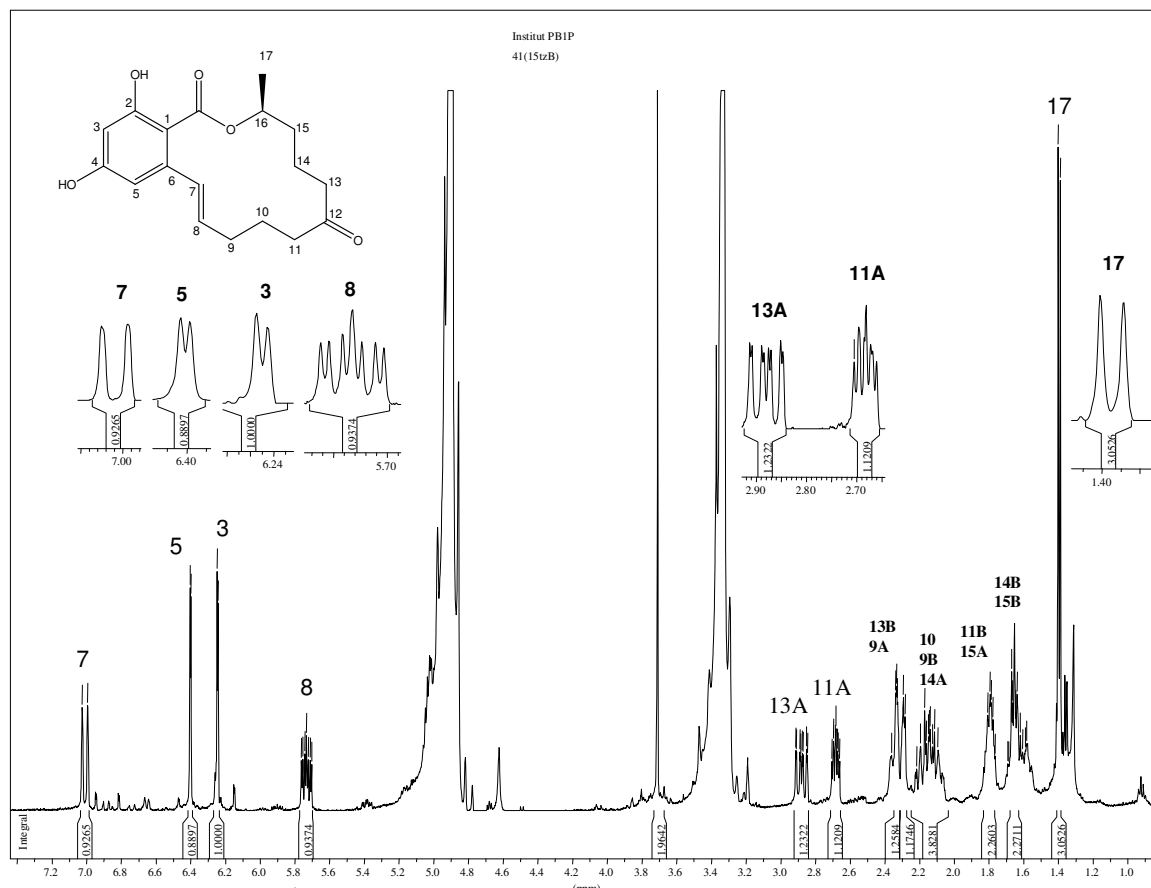
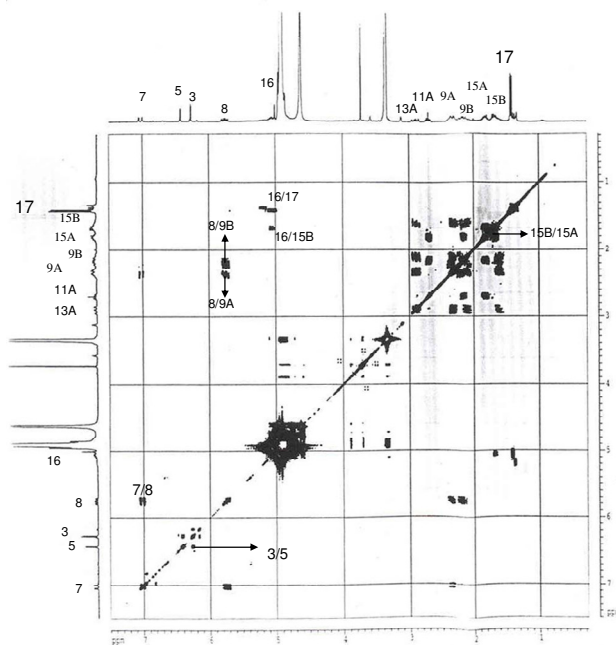
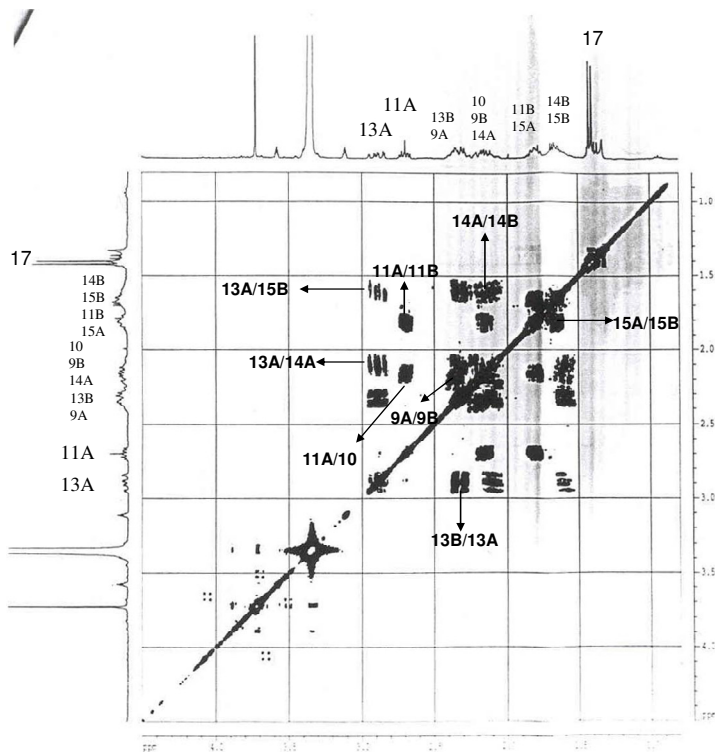
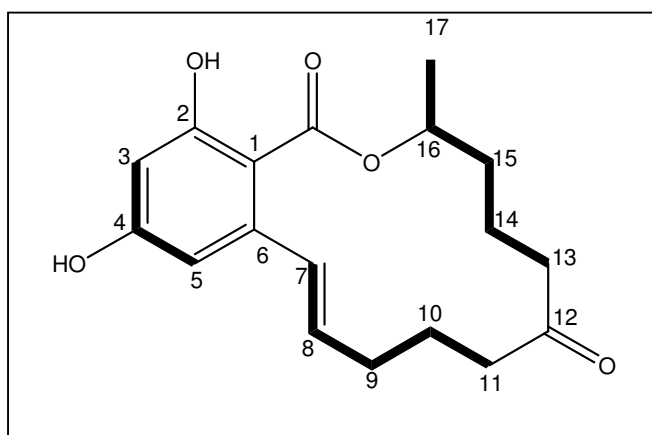


Figure 3.39 ¹H NMR spectrum of compound **13** (CD₃OD, 500 MHz)

The lactone ring in this compound contained a total of six methylene groups resonating between 1.62 and 2.85 ppm. Assignment of those overlapping signals of methylene groups was done by inspecting the correlations in the COSY spectrum [figure 3.40 and 3.41], which clearly showed that the methylene groups adjacent to the carbonyl group (H₂-11 and H₂-13) were shifted downfield.

Figure 3.40A COSY spectrum of compound **13** (CD₃OD, 300 MHz)Figure 3.40B COSY spectrum of compound **13** (CD₃OD, 300 MHz)

Figure 3.41 COSY correlations of compound **13** (zearalenone)Table 3.15 NMR data of compound **13** (zearalenone)

Position	δ H (ppm), multiplicity (J in Hz) (in CD ₃ OD)	δ H (ppm) multiplicity (J in Hz) of dimethyl ether zearalenone (Solladie <i>et al.</i> , 1992 in CD ₃ OD)	
2-OH	-		
2-OCH ₃		3.79 (3H,s)	
3	6.21 (1H,d,2.2)	6.30 (1H,d,2.1)	
4-OH	-		
4-OCH ₃		3.82 (3H,s)	
5	6.37 (1H,d,2.2)	6.39 (1H,d,2.1)	
7	6.98 (1H,d,15.5)	6.60 (1H,dd,15.5,1.9)	
8	5.70 (1H,ddd,15.5,10.1,3.8)	5.99 (1H,ddd,15.5,10.0,4.4)	
9	2.26 (1H,m) 2.09 (1H,m)	1.45 - 2.85 (12H)	
10	2.09 (2H,m)		
11	2.65 (1H,m) 1.76 (1H,m)		
13	2.85 (1H,m) 2.30 (1H,m)		
14	2.09 (1H,m) 1.62 (1H,m)		
15	1.76 (1H,m) 1.62 (1H,m)		
16	under water peak		5.32 (1H,m)
17	1.39 (3H,d,6.3)		

Compound **13** was identified as zearalenone which was substantiated by comparison with NMR data of zearalenone dimethyl ether isolated from *Fusarium graminearum* (Solladie *et al.*, 1992). The optical rotation of compound **13** ($[\alpha]_D^{20}$ -142°) allowed to conclude that this compound had the same absolute configuration as described in the literature ($[\alpha]_D^{20}$ -170.5°).

3.5 Secondary metabolites of fungus *Penicillium polonicum*

Penicillium polonicum was isolated from marine sponge *Tethya* sp. collected from Mediterranean Sea. There were six compounds successfully isolated from the ethyl acetate extract of *P. polonicum* after being grown in the Wickerham medium, which were fructigenin A (compound **15**), cyclophenol (compound **16**), cyclophenin (compound **17**), viridicatol (compound **18**), viridicatin (compound **19**) and *O*-methyl viridicatin (compound **20**).

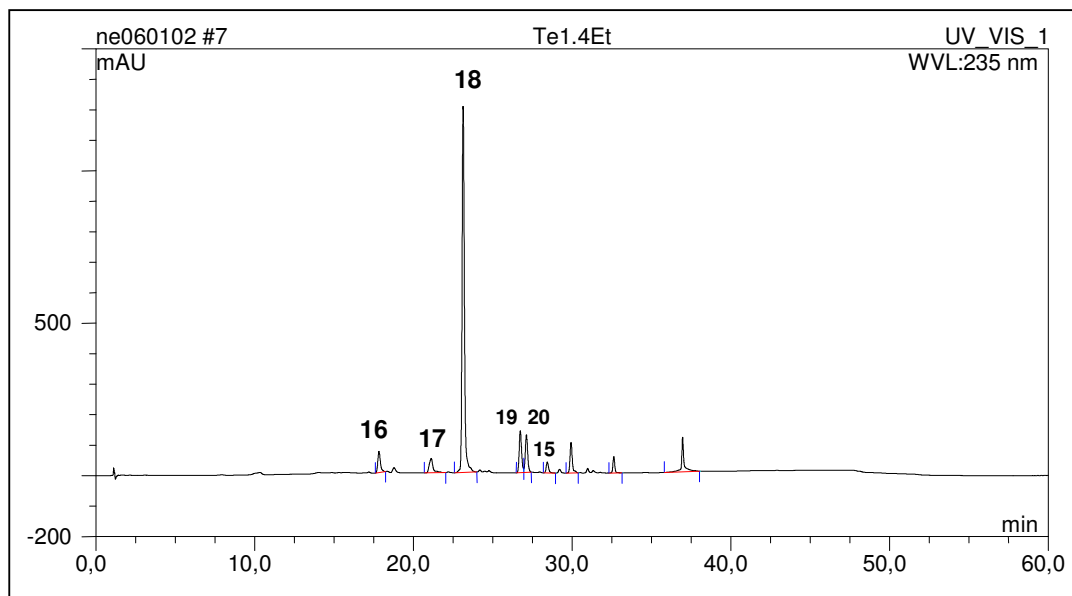
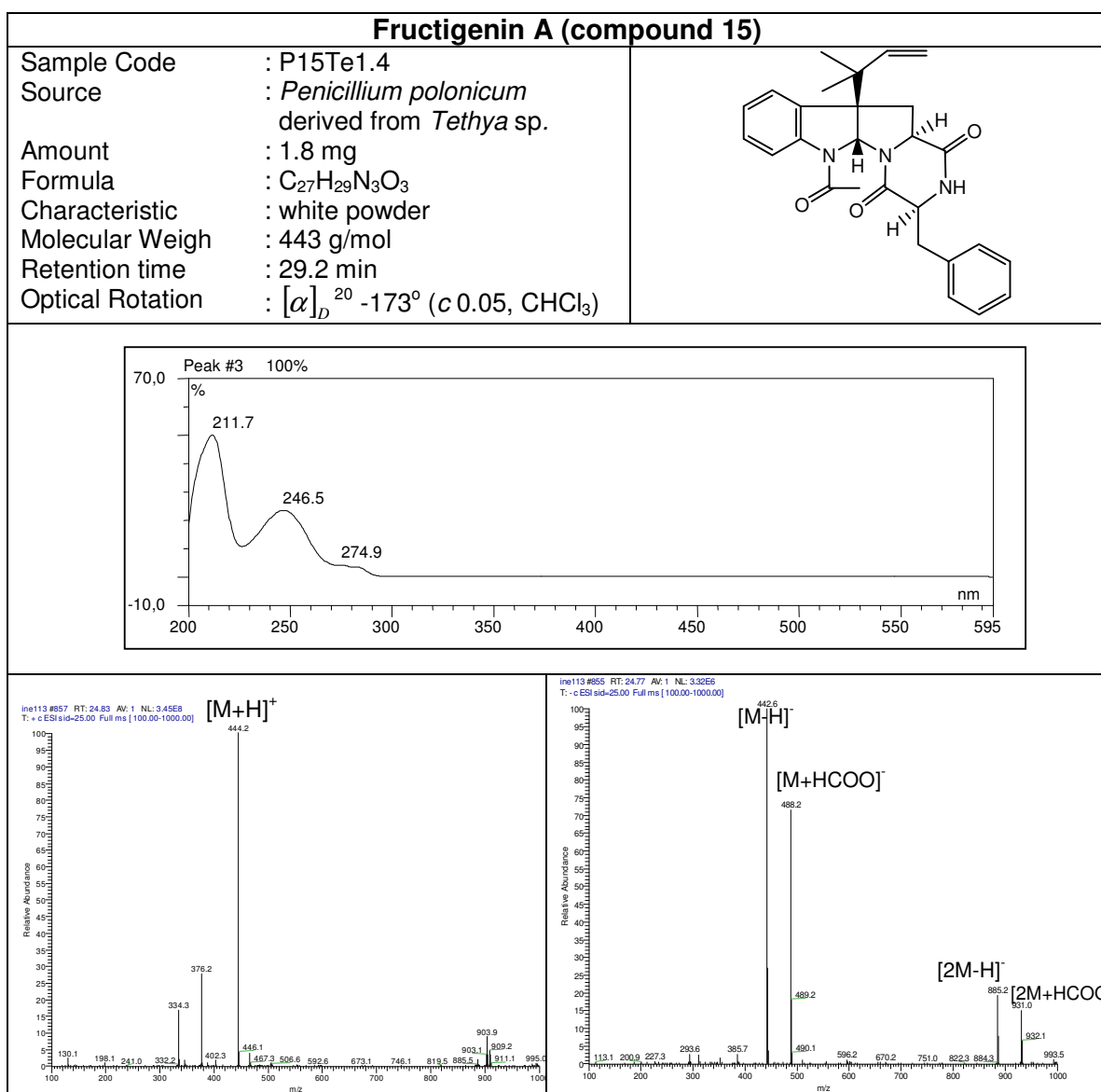


Figure 3.42 HPLC chromatogram of the ethyl acetate extract of *Penicillium polonicum*

Table 3.16 Biological test results of *P. polonicum* and its deriving compounds

Sample	L5178Y growth (%) Conc. 10 µg/mL	EC ₅₀ (µg/mL)
Ethyl acetate extract of <i>Penicillium polonicum</i>	- 3.5	
Fructigenin A	8.0	0.53
Cyclopenin	79.6	
Cyclopenol	110.9	
Viridicatol	79.1	
Viridicatin	82.2	
O-methyl viridicatin	93.0	

3.5.1 Compound 15 (fructigenin A)



Compound **15** (fructigenin A) was isolated from the ethyl acetate extract of *Penicillium polonicum* through Sephadex LH-20 column chromatography using 100% methanol. The ESI mass spectra showed the intense peaks at m/z 444 $[M+H]^+$ and m/z 442 $[M-H]^-$ in accordance with a molecular weight of 443 g/mol. Careful inspection of the ^1H and ^{13}C NMR data suggested the molecular formula to be $\text{C}_{27}\text{H}_{29}\text{N}_3\text{O}_3$. The UV spectrum exhibited maximum absorptions at 211.7, 246.5, and 274.9 nm.

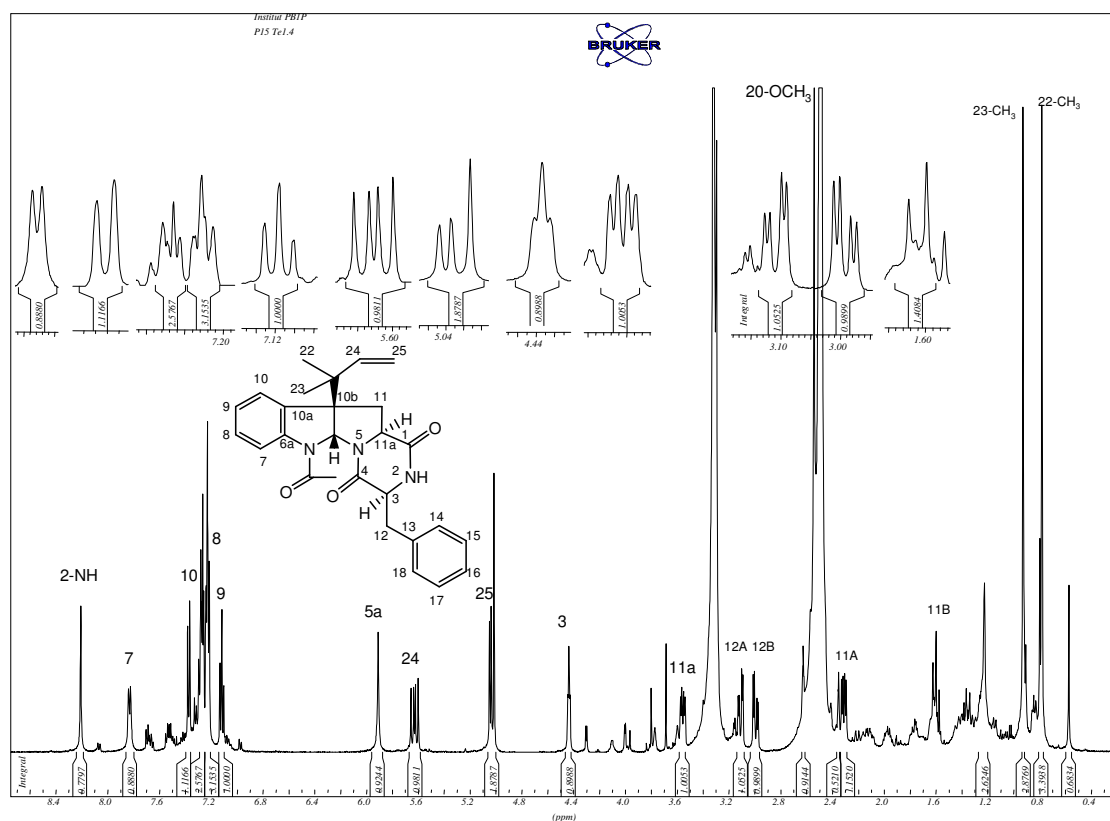


Figure 3.43 ^1H NMR of compound **15** (DMSO, 500 MHz)

In the ^1H NMR spectrum [figure 3.43], nine aromatic protons appeared at chemical shifts between δ 7.12 and 7.83, with some overlapping of these signals. With the help of the COSY spectrum [figure 3.44 and 3.45], it could be concluded that eight of those nine aromatic protons represented two aromatic spin systems, one ABCD

spin system for an *ortho*-disubstituted phenyl as well as a monosubstituted phenyl ring. The additional sharp singlet signal at δ 8.20 was assigned to an NH-group.

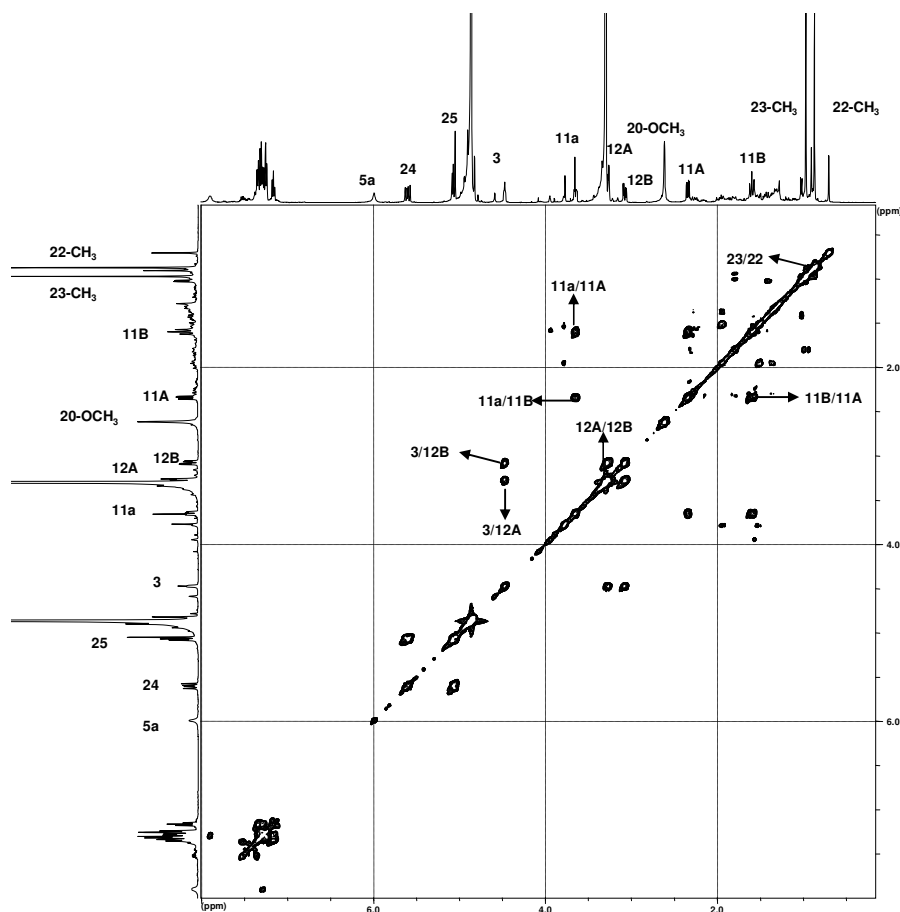


Figure 3.44 $^1\text{H},^1\text{H}$ -COSY spectrum of compound **15** (DMSO, 500 MHz)

The characteristic fragment resulting from loss of 42 amu at m/z 401 [$\text{M}+\text{H}-\text{COCH}_2$] $^+$ in the ESI mass spectrum showed the presence of an N-acetyl group in the molecule. This was corroborated by a signal at 2.62 ppm in the ^1H NMR spectrum attributed to the N-acetyl methyl group.

A 1,1-dimethyl-2-propenyl group was established on the basis of the two geminal methyl singlets at δ 0.87 ppm (H-22) and 1.04 ppm (H-23), the

exomethylene signals which resonated at δ 5.02 ppm (H₂-25, dd, 17.0,11.0) coupled with olefinic proton at the chemical shift δ 5.06 ppm (H₂₄,dd,17.0,11.0).

Furthermore, in the COSY spectrum two spin systems consisting each of a diastereotopic methylene group adjacent to an α -proton could be detected, which were assigned to H₂-11 and H-11a as well as H₂-12 and H-3, respectively.

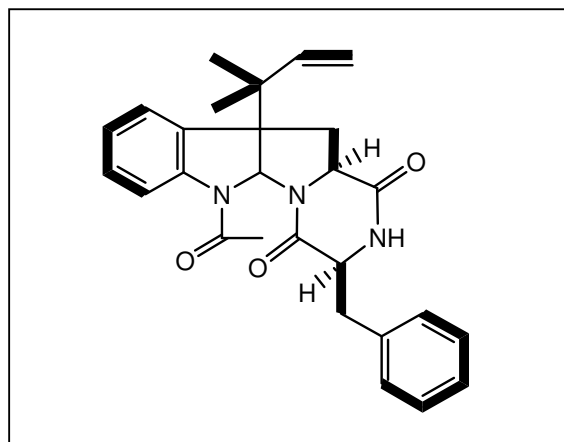


Figure 3.45 COSY correlation of compound **15** (fructigenin A)

Taken together, compound **15** was identified as fructigenin A which was substantiated by comparison with NMR data reported in the literature (Boyer-Korkis *et al.*, 1993). This alkaloid was first isolated from the fungus *Penicillium fructigenum*, but later also detected in further species of this genus such as *P. aurantiogriseum*, *P. rugulosum*, *P. puberulum* and *P. piscarium* (Arai *et al.*, 1989).

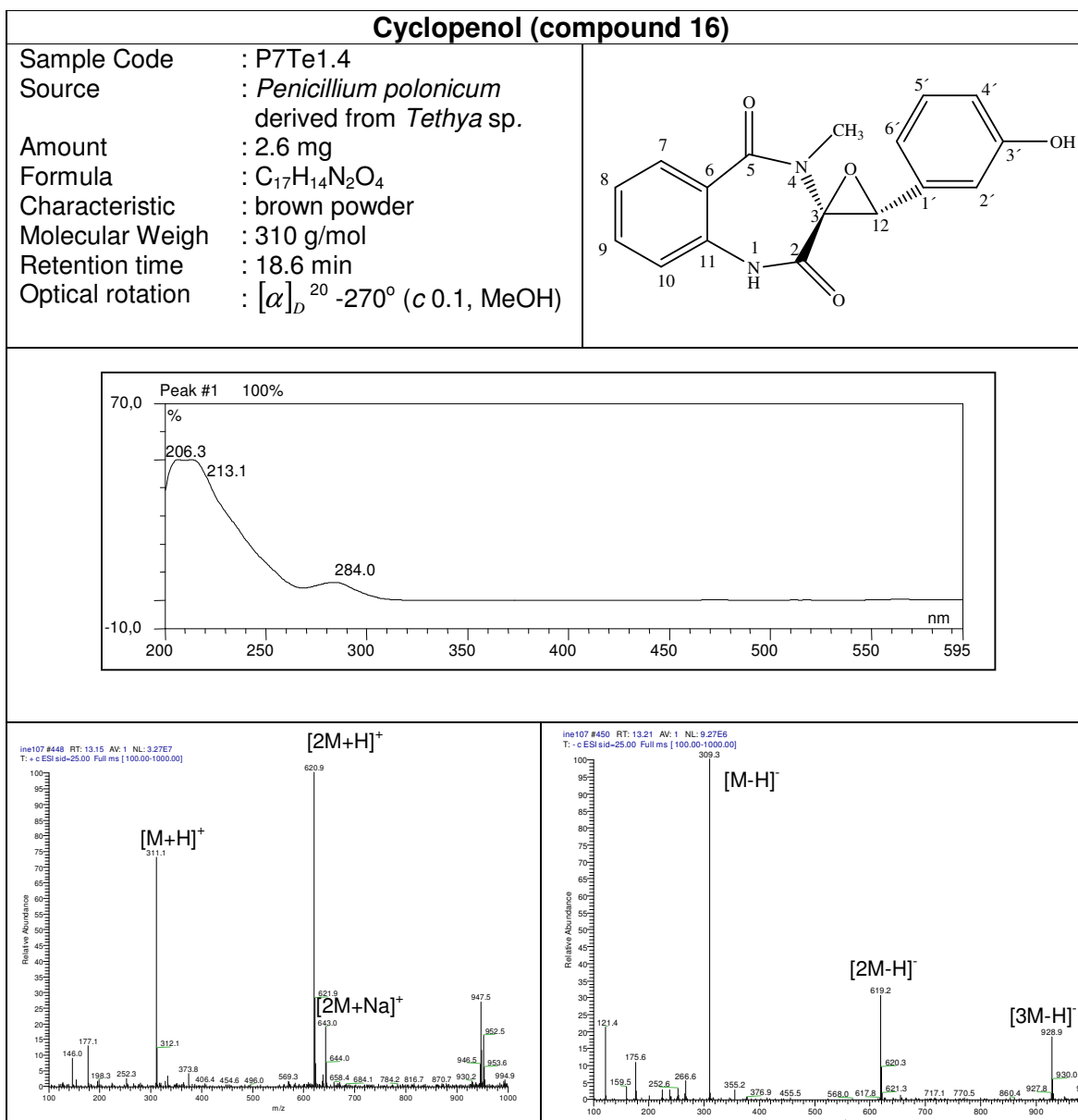
The measurement data of the optical rotation of compound **15** (-173°) allowed to conclude that this compound have the same stereochemistry with fructigenin A described in the literature which have optical rotation of -178° (Arai *et al.*, 1989).

Figure 3.17 NMR data of compound **15** (fructigenin A)

Position	δ H (ppm) multiplicity (<i>J</i> in Hz)(in DMSO)	δ H (ppm) multiplicity (Boyer-Korkis <i>et al.</i> , 1993) (<i>J</i> in Hz) in DMSO)
2-NH	8.20 (1H, s)	8.19 (1H, s)
3	4.43 (1H, bt, 4.1)	4.43 (1H, bt, 1.3, 4.3, 5.0)
5a	5.91 (1H, s)	5.92 (1H, s)
7	7.83 (1H, d, 7.6)	7.81 (1H, bd, 8.0)
8	7.23 (1H, dd, 7.6, 1.3)	7.24 (1H, dt, 7.7, 7.5, 1.1)
9	7.12 (1H, t, 7.6)	7.12 (1H, dt)
10	7.37 (1H, d, 7.6)	7.37 (1H, dd, 7.7, 0.9)
11	2.31 (1H, dd, 12.3, 5.4) 1.60 (1H, t, 12.0, 11.8)	2.31 (1H, dd, 12.2, 5.4) 1.60 (1H, t, 12.2, 11.8)
11a	3.55 (1H, dd, 11.4, 5.1)	3.55 (1H, ddd, 11.8, 5.4, 1.3)
12	3.11 (1H, dd, 14.2, 4.4) 2.99 (1H, dd, 14.2, 5.1)	3.11 (1H, dd, 14.0, 4.3) 2.99 (1H, dd, 14.0, 5.0)
14 – 18	7.20 – 7.30 (5H)	7.17 – 7.26 (5H)
20	2.53 (3H, s)	2.54 (3H, s)
22	0.78 (3H, s)	0.78 (3H, s)
23	0.93 (3H, s)	0.93 (3H, s)
24	5.63 (1H, dd, 17.3, 11.0)	5.63 (1H, dd, 17.3, 10.6)
25	5.02 (2H, dd, 17.3, 11.0)	5.02 (2H, dd, 17.3, 10.6)

3.5.2 Compound 16 (cyclophenol)

Compound **16** (cyclophenol) was isolated from the ethyl acetate extract of *Penicillium polonicum* through sephadex column chromatography with 100% methanol followed by preparative HPLC. It showed a UV maximum at 206.3, with shoulders at 213.1 and 284.0 nm. In the ESI mass spectrum, a prominent $[M+H]^+$ pseudomolecular ion was observed at m/z 311 upon positive ionization, together with an intense $[M-H]^-$ at m/z 309 upon negative ionization which indicated a molecular weight of 310 g/mol. In conjunction with the analysis of the ^1H NMR data, a molecular formula of $\text{C}_{17}\text{H}_{11}\text{N}_2\text{O}_4$ was derived.



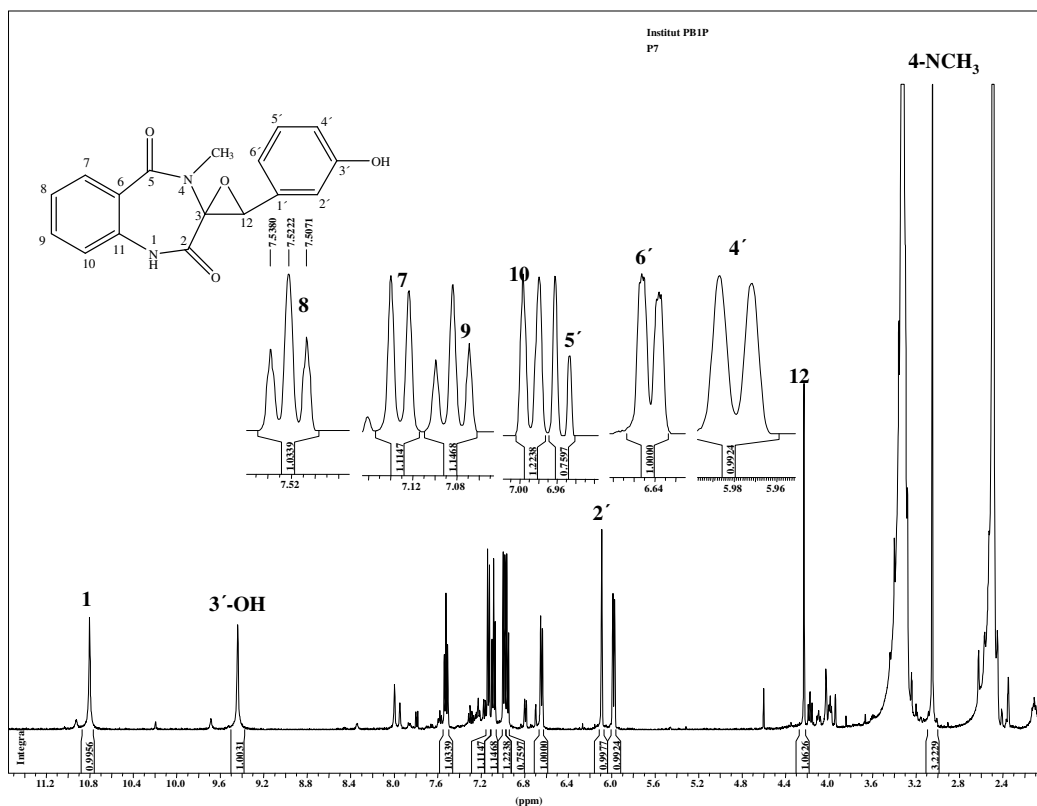


Figure 3.46 ^1H NMR spectrum of compound **16** (DMSO , 500 MHz)

In the ^1H NMR spectrum [figure 3.46], eight aromatic protons resonating between 6.70 and 7.33 ppm were detected. The COSY spectrum [figure 3.47 and 3.48] and inspection of the coupling constant allowed to conclude that those eight aromatic protons represented two individual ABCD spin systems characteristic of one 1,2 disubstituted and one 1,3 disubstituted aromatic system, respectively.

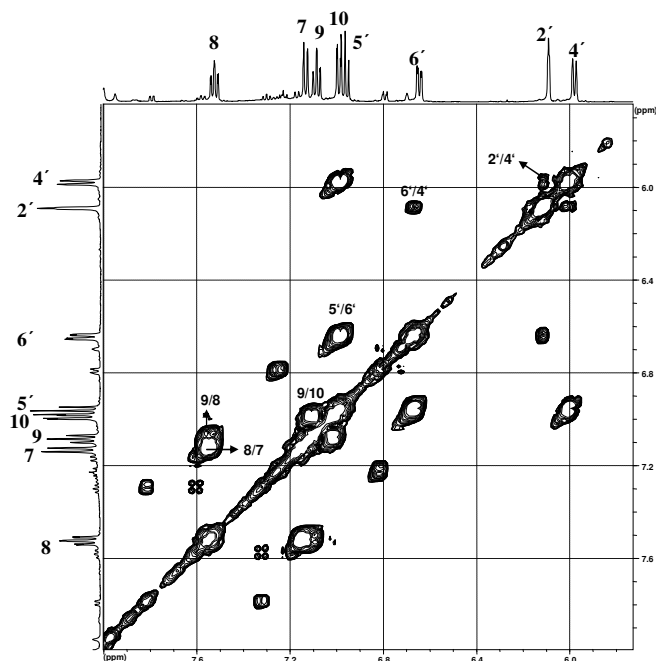


Figure 3.47 COSY spectrum of compound **16** (DMSO, 500 MHz)

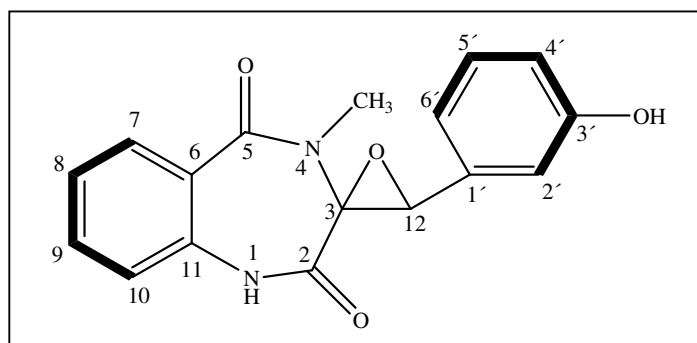


Figure 3.48 COSY correlation of compound **16** (cyclopropanol)

The first ring system consisted of protons H-2', H-4', H-5', and H-6', with H-2' and H-4' shifted upfield because of their position *ortho* to a phenolic hydroxyl substituent at C-3'. Their multiplicities confirmed the presence of 1,3-disubstituted aromatic system. The other spin system comprising H-7, H-8, H-9 and H-10 was identified as a 1,2-bisubstituted aromatic system based on the inspection of the coupling constants and splitting patterns. H-12 which had chemical shift of 4.07 ppm

was found to be situated at an oxiran ring. The sharp singlet signal at δ 10.81 ppm was assigned to the NH group of the indole ring, while the hydroxyl group at C-3' was observed at δ 9.49 ppm, and the *N*-methyl group at N-4 appeared at δ 3.20.

Compound **16** was substantially identified as cyclophenol based on comparison of its NMR data with that of cyclophenol isolated from *Penicillium verrucosum* Var. Cyclopium reported by Hodge *et al.* (1988). Measured optical rotation of compound 16 was -270° , whereas optical rotation previously reported in literature was -309° suggesting both compounds have the same stereochemistry, respectively.

Table 3.18 NMR data of compound **16** (cyclophenol)

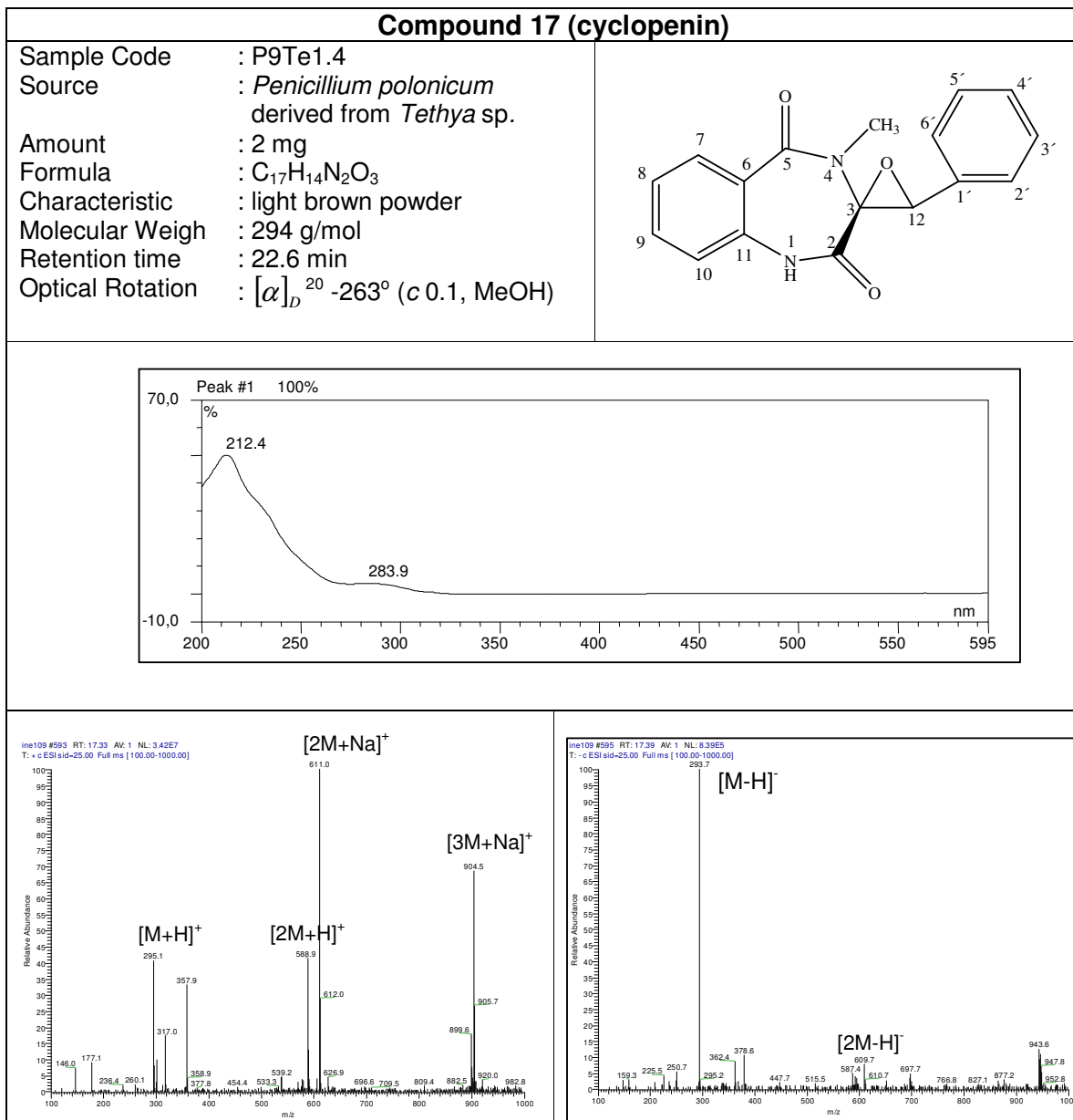
Position	δ H (ppm) multiplicity (<i>J</i> in Hz) (in DMSO)	δ H (ppm) multiplicity (<i>J</i> in Hz) (Hodge <i>et al.</i> , 1988 in d_6 acetone)
1-NH	10.81 (1H,s)	
3-OH	9.49 (1H,s)	
4-NCH ₃	3.05 (3H,s)	3.14 (3H,s)
7	7.13 (1H,d,7.9)	6.66–7.62 (1H,m)*
8	7.53 (1H,t,7.6)	6.66–7.62 (1H,m)*
9	7.09 (1H,t,7.9)	6.66–7.62 (1H,m)*
10	6.99 (1H,d,7.9)	6.66–7.62 (1H,m)*
12	4.23 (1H,s)	4.10 (1H,s)
2'	6.09 (1H,bt,1.8)	6.10–6.26 (1H,m)**
4'	5.98(1H,bd,7.6)	6.10-6.26 (1H,m)**
5'	6.97 (1H,t,8.0)	6.66–7.62 (1H,m)*
6'	6.65 (1H,dd,8.2,2.2)	6.66–7.62 (1H,m)*

*) or **) : overlapping signals

3.5.3 Compound 17 (cyclophenin)

Compound **17** (cyclophenin) was isolated from the ethyl acetate extract of *Penicillium polonicum* through sephadex LH-20 column chromatography and followed by preparative HPLC. UV spectra maxima of compound **17** were at 212.4 and 283.9 nm. ESI-MS spectrum showed molecular ion peaks at m/z 295 $[M+H]^+$ upon positive ionization and at m/z 293 $[M-H]^-$ upon negative ionization, revealing molecular weight

of 294 g/mol. Along with the analysis of the ^1H NMR spectrum, a molecular formula of $\text{C}_{17}\text{H}_{11}\text{N}_2\text{O}_4$ was derived.



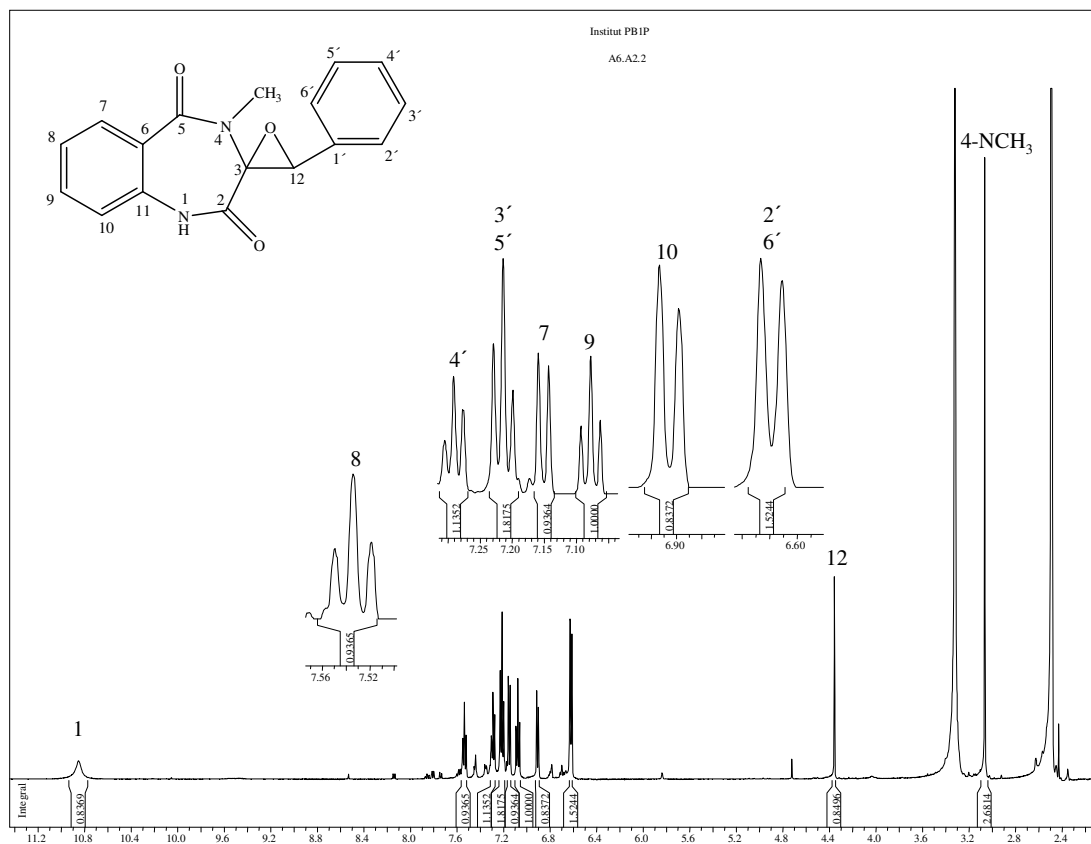


Figure 3.49 ^1H NMR spectrum of compound **17** (CDCl_3 ; 500 MHz)

In the ^1H NMR spectrum [figure 3.49], nine aromatic protons resonating between 6.62 and 7.53 ppm were detected. Some of those aromatic protons were overlapping. By the COSY experiment [figure 3.50] and inspection of coupling constant, it could be concluded that those protons represented two aromatic spin systems characteristic of one 1,2-disubstituted and one 1-monosubstituted aromatic spin system.

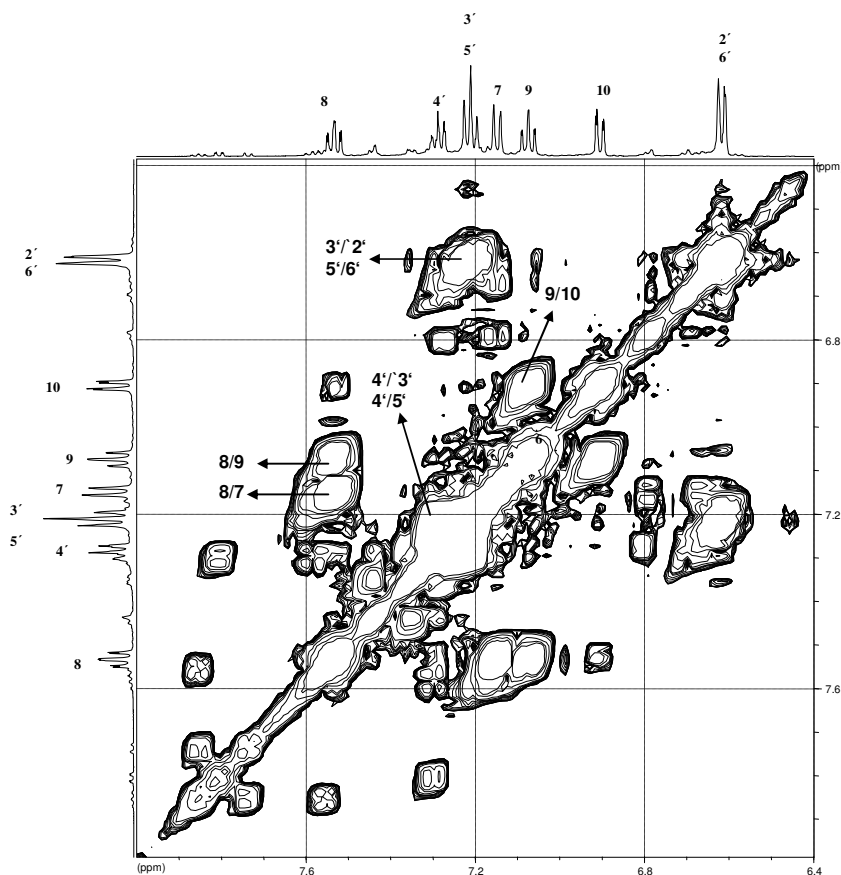
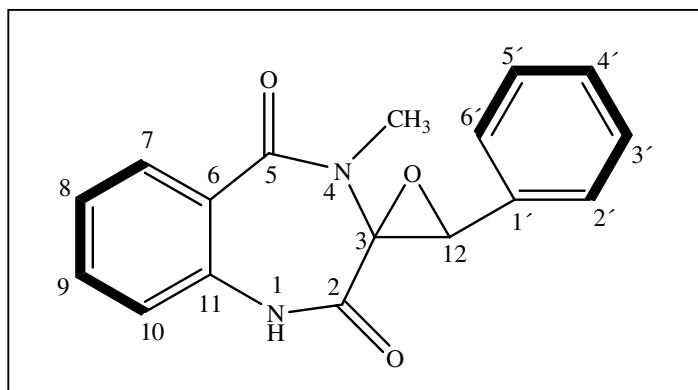


Figure 3.50 COSY spectrum of compound **17** (DMSO; 500 MHz)

The first aromatic spin system was assembled of protons H-2', H-3', H-4', H-5' and H-6'. Their multiplicities confirmed the characteristic of 1-monosubstituted phenyl ring,

The other spin system comprising of protons H-7, H-8, H-9 and H-10 which was identified as a 1,2-disubstituted aromatic system based on the inspection of the coupling constant and splitting patterns. H-12 was situated at an oxiran ring at the chemical shift δ 4.23 ppm. The sharp singlet signal at δ 10.81 ppm was assigned to the NH group of the indole ring and the *N*-methyl group at N-4 appeared at δ 3.06 ppm.

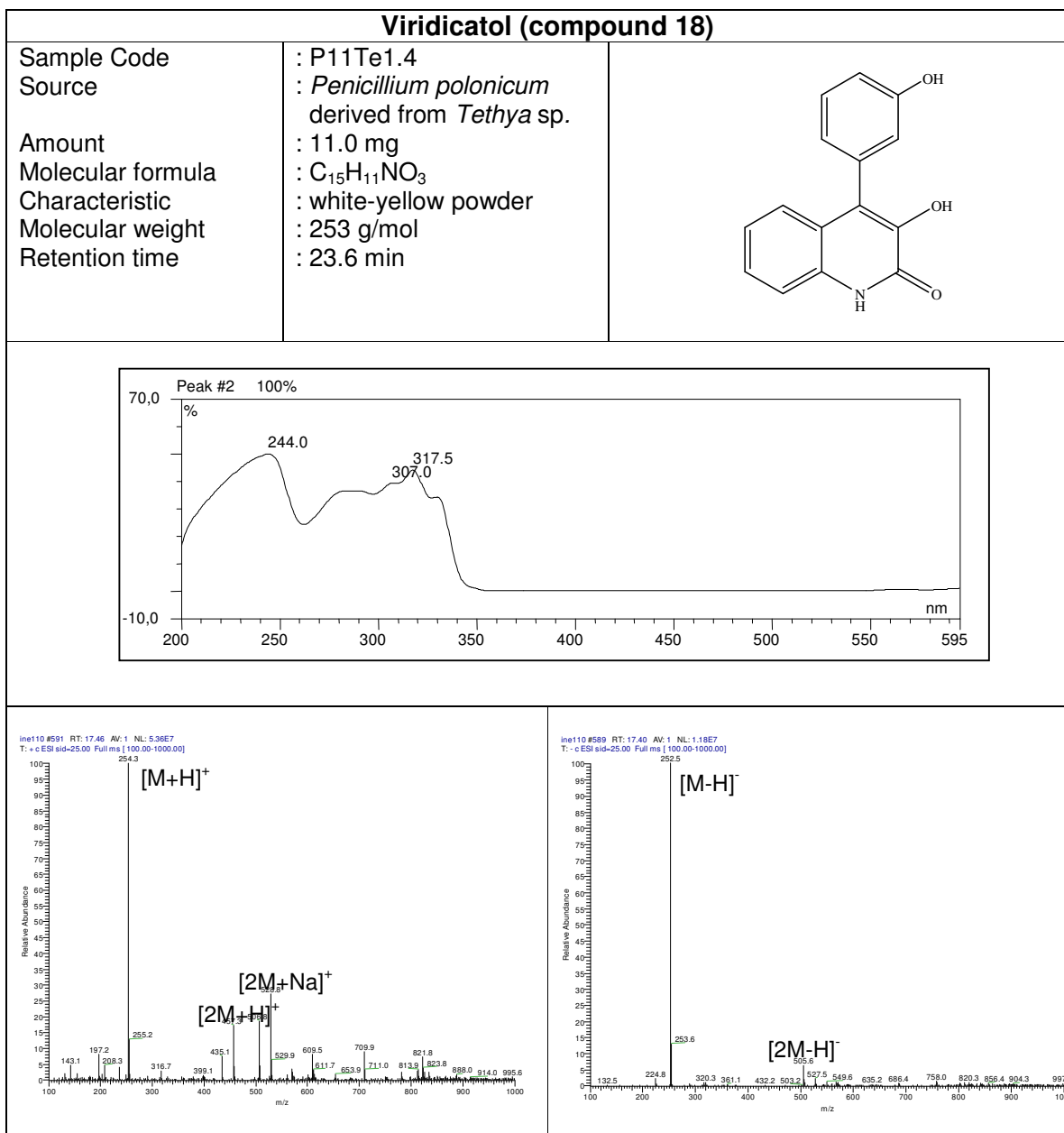
Figure 3.51 COSY correlation of compound **17**(cyclophenin)Table 3.19 NMR data of compound **17** (cyclophenin)

Position	δ H (ppm) multiplicity (<i>J</i> in Hz)(in DMSO)	δ H (ppm) multiplicity (<i>J</i> in Hz)(in CDCl ₃)	δ H (ppm) multiplicity (<i>J</i> in Hz) (Kusano <i>et al.</i> , 2000 in CDCl ₃)
1-NH	10.81(1H, s)	8.15 (1H, s)	8.95 (1H, s)
4-NCH ₃	3.06 (3H, s)	3.24 (3H, s)	3.24 (3H, s)
7	7.15 (1H,d,8.2)	7.18 -7.30 (1H,m)	7.09 – 7.39 (1H,m)
8	7.53 (1H, t, 7.6)	7.52 (1H,t,8.2)	7.09 – 7.39 (1H,m)
9	7.08 (1H,t,7.6)	7.15 (1H,t,7.6)	7.09 – 7.39 (1H,m)
10	6.91 (1H,d,7.6)	7.04 (1H,d,7.9)	7.09 – 7.39 (1H,m)
12	4.23 (1H, s)	4.00 (1H, s)	4.02 (1H, s)
2'	6.62 (1H, bd,7.9) ^a	6.65 (1H,d,7.6) ^b	6.66 (1H, d, 7.2) ^d
3'	7.23 (1H, t, 7.6)	7.18 -7.30 (1H,m) ^c	7.09 – 7.39 (1H,m)
4'	7.29 (1H, t, 6.9)	7.18 -7.30 (1H,m) ^c	7.09 – 7.39 (1H,m)
5'	7.23 (1H, t, 7.6)	7.18 -7.30 (1H,m) ^c	7.09 – 7.39 (1H,m)
6'	6.60 (1H, bd, 7.9) ^a	6.65 (1H,d,7.6) ^b	6.66 (1H, d, 7.2) ^d

a,b,c,d : overlapping signals

The splitting patterns and chemical shifts of compound **17** were found to be similar with published data for cyclophenin (Kusano *et al.*, 2000). Measured optical rotation of compound **16** was -263° , whereas optical rotation previously reported in literature was -317° suggesting both compounds have the same stereochemistry, respectively.

3.5.4 Compound 18 (viridicatol)



Compound **18** (viridicatol) was a major compound isolated from the ethyl acetate extract of *Penicillium polonicum* through Sephadex LH-20 column chromatography with 100% methanol and followed by preparative HPLC. Its UV spectrum displayed a maximum at 244.0 nm, with shoulders at 307.0 and 317.5 nm. Positive and negative ESI-MS showed prominent peaks at m/z 254 $[M+H]^+$ and m/z 252 $[M-H]^-$, revealing a molecular weight of 253 g/mol. Together with analysis of the ^1H NMR spectrum, the molecular formula of $\text{C}_{15}\text{H}_{11}\text{NO}_3$ was assumed.

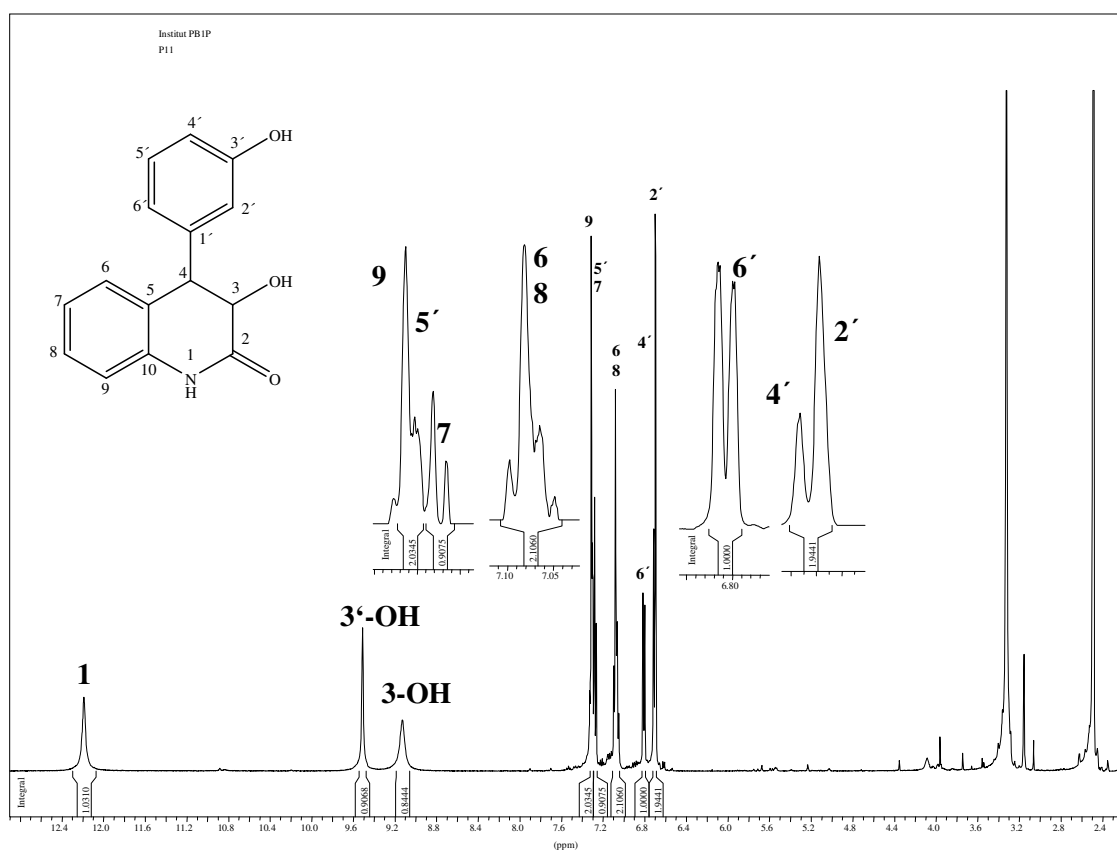


Figure 3.52 ^1H NMR spectrum of compound **18** (DMSO, 500 MHz)

In the ^1H NMR spectrum [figure 3.52], eight aromatic protons resonating between δ 6.80 and δ 7.32 ppm were observed. Some signals in the aromatic region were overlapping. The COSY spectrum [figure 3.53 and 3.54] and inspection of the coupling constants allowed to conclude that those eight protons resembled two individual

ABCD spin systems consisting of one 1,2-disubstituted and one 1,3-disubstituted phenyl ring, respectively.

The 1,3-disubstituted aromatic system was assembled of the protons H-2', H-4', H-5' and H-6'. H-2' and H-4' were shifted more upfield because of the shielding influence of the hydroxyl group in 3' position (broad singlet at δ 9.51 ppm). The other aromatic spin system (1,2 disubstituted phenyl ring) consisted of H-7, H-8, H-9 and H-10.

In the ^1H NMR spectrum [figure 3.52], a sharp singlet signal at the chemical shift of δ 12.19 ppm indicated a NH group. The hydroxyl group in position 3 appeared as another broad singlet at δ 9.13 ppm.

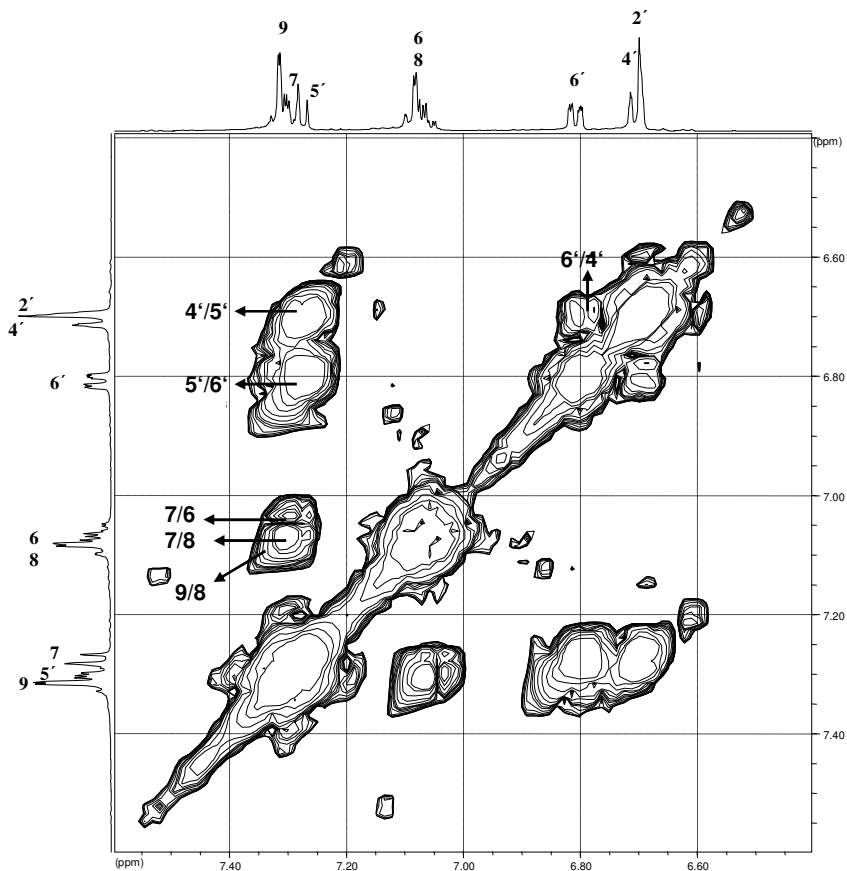
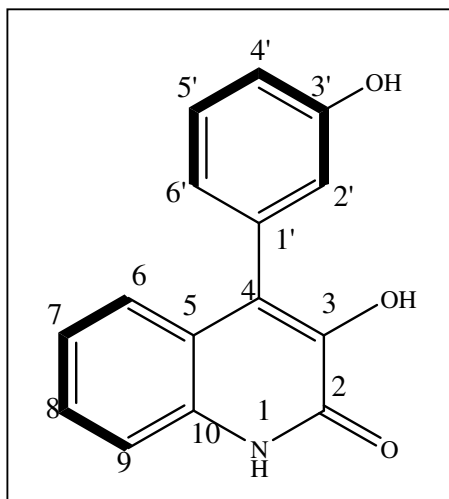


Figure 3.53 COSY spectrum of compound **18** (DMSO, 500 MHz)

Figure 3.54 COSY correlation of compound **18** (viridicatol)

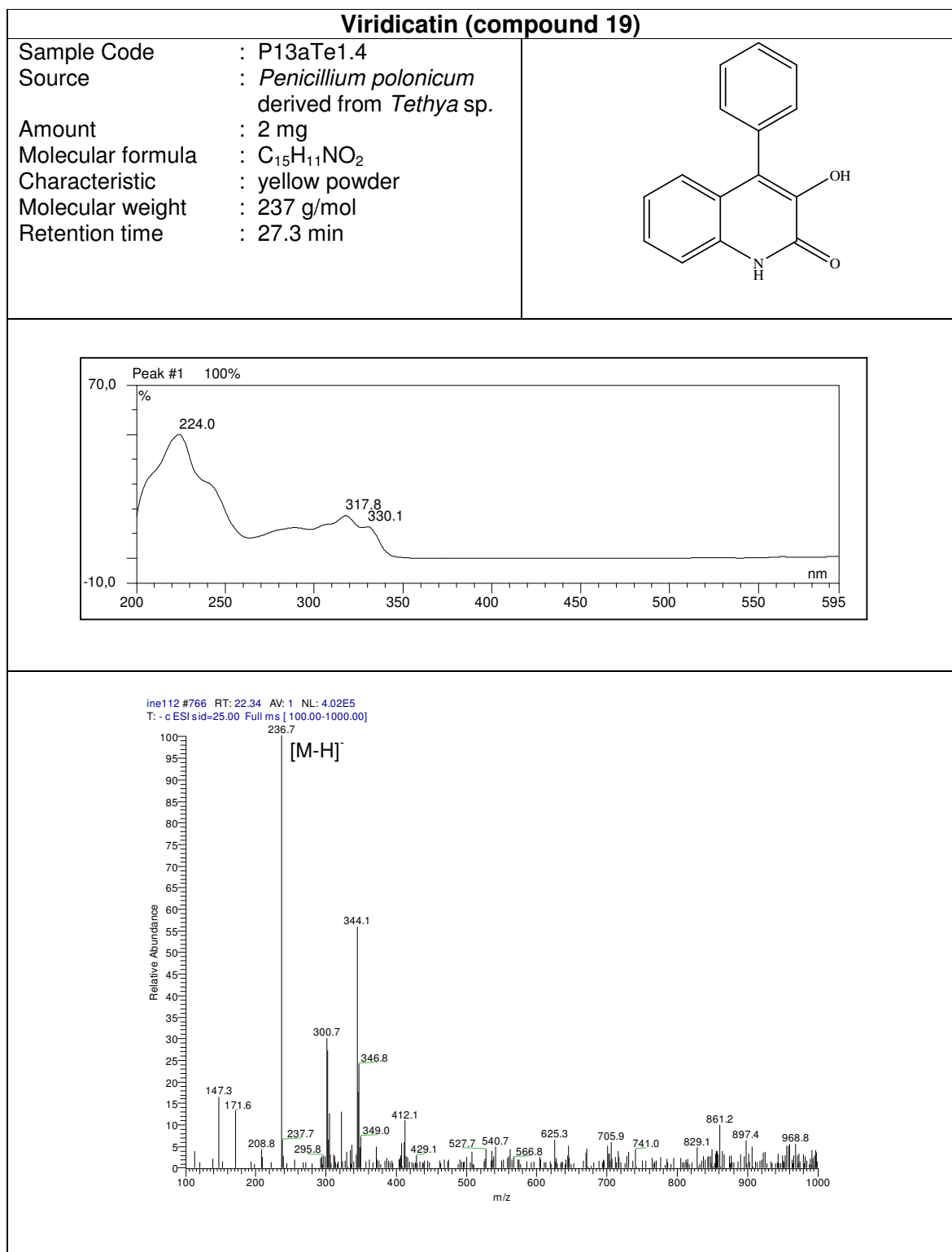
Compound **18** was identified as viridicatol fundamentally based on comparison of its NMR data [Table 3.20] with NMR data of viridicatol reported by Teuscher (2005).

Table 3.20 NMR data of compound **18** (viridicatol)

Position	δ H (ppm) multiplicity (<i>J</i> in Hz)(in DMSO)	δ H (ppm) multiplicity (<i>J</i> in Hz) (Teuscher, 2005 in CDCl ₃)
1-NH	12.19 (1H,bs)	12.19 (1H,bs)
3-OH	9.13 (1H,bs)	9.13 (1H,bs)
6	7.09(1H,m) ^a	7.09 (1H,m)
7	7.30 (1H,m) ^b	7.28 (1H,m)
8	7.08 (1H,m) ^a	7.07 (1H, m)
9	7.33 (1H,m) ^b	7.33 (1H,m)
2'	6.70 (1H,bs)	6.72 (1H,bs)
3'-OH	9.51 (1H,bs)	9.51 (1H,bs)
4'	6.71 (1H,d,7.6)	6.70 (1H,bs)
5'	7.28 (1H,t,7.6)	7.31 (1H,m)
6'	6.81 (1H,dq, 7.9,1.3)	6.81 (1H,dq,7,3,1.6)

^{a,b} : overlapping signals

3.5.5 Compound 19 (viridicatin)



Compound **19** (viridicatin) was isolated from the ethyl acetate extract of *Penicillium polonicum* through sephadex column LH-20 chromatography with 100% methanol and followed by preparative HPLC. Its UV spectrum shows λ_{max} at 224.0, 317.8 and 330.1 nm, and had similarity with λ_{max} of viridicatol. ESI-MS experiment of this compound showed the molecular ion peak at 236 [M-H]⁻ upon negative ionization, revealing the molecular weight of 237 g/mol.

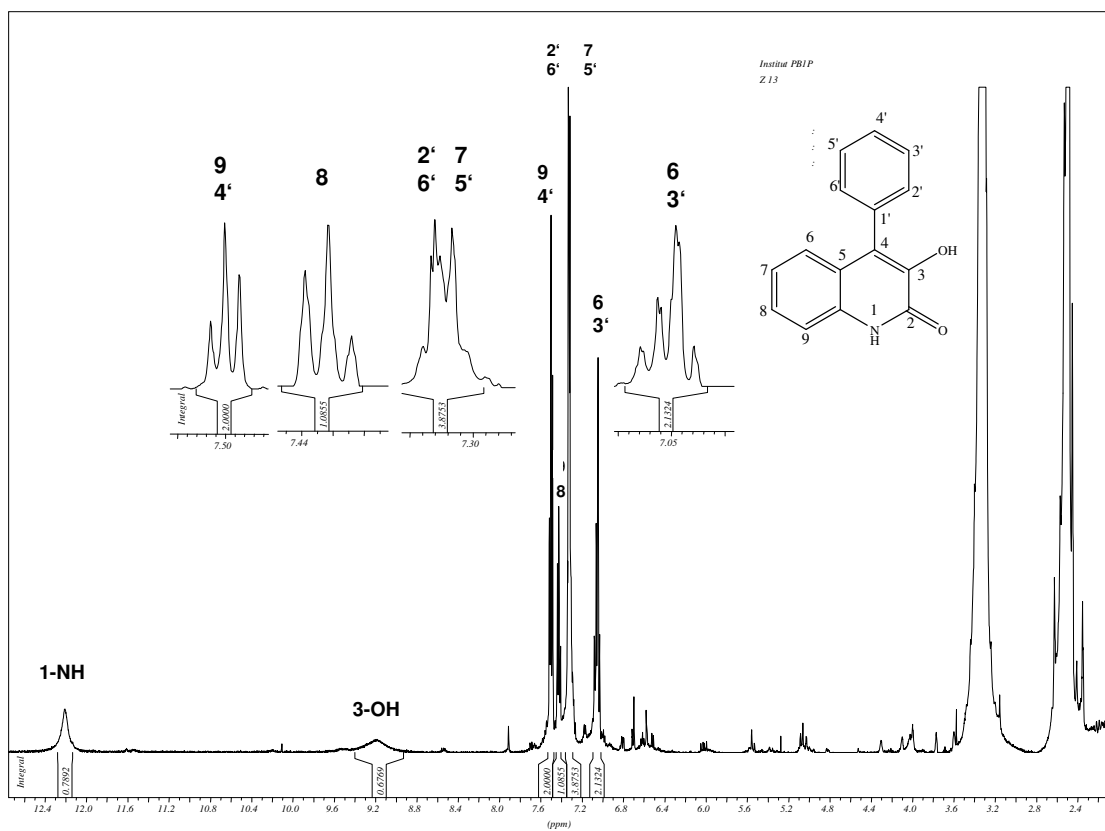


Figure 3.55 ¹H NMR spectrum of compound **19** (viridicatin)

The ¹H NMR spectrum [figure 3.55] showed nine aromatic protons resonating between the chemical shift δ 7.02 and 7.50 ppm, some partially overlapped. Inspection of the correlations in the COSY spectrum [figure 3.57] concluded that those aromatic

protons resembled two aromatic ring system characteristic of a monosubstituted phenyl ring and a 1,2-disubstituted phenyl ring.

The 1,2-disubstituted phenyl ring consisted of the protons H-6 at δ 7.05 ppm (1H,dd,8.5 and 1.6 Hz), H-7 at δ 7.32 ppm (1H,m), H8 at δ 7.42 ppm (1H,t,7.4Hz),and H-9 at δ .7.50 ppm (1H,d,7.4) as an ABCD spin system. The other phenyl ring was formed by H-4' at δ 7.50 ppm (1H,t,7.4), H-5' at δ 7.05 ppm (1H,t,8.5), H-2',H-3' and H-6' at δ between 7.30 and 7.35 ppm (3H,m), assembling an AA'BB'C spin system.

In the ^1H NMR spectrum [figure 3.55], there were two signals in downfield region were observed at δ 12.21 ppm revealing one NH group and at δ 9.19 ppm revealing one hydroxyl group at position 3'.

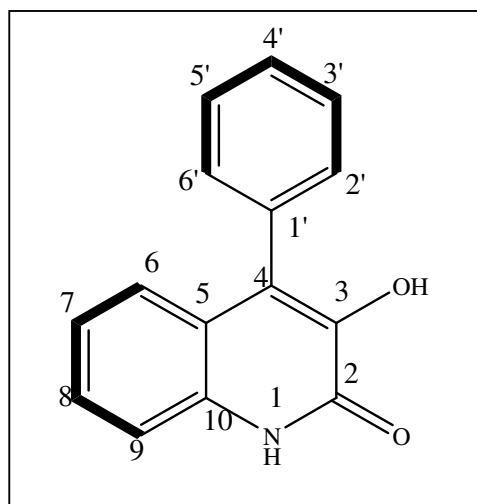


Figure 3.56 ^1H , ^1H -COSY spectrum of compound **19** (viridicatin)

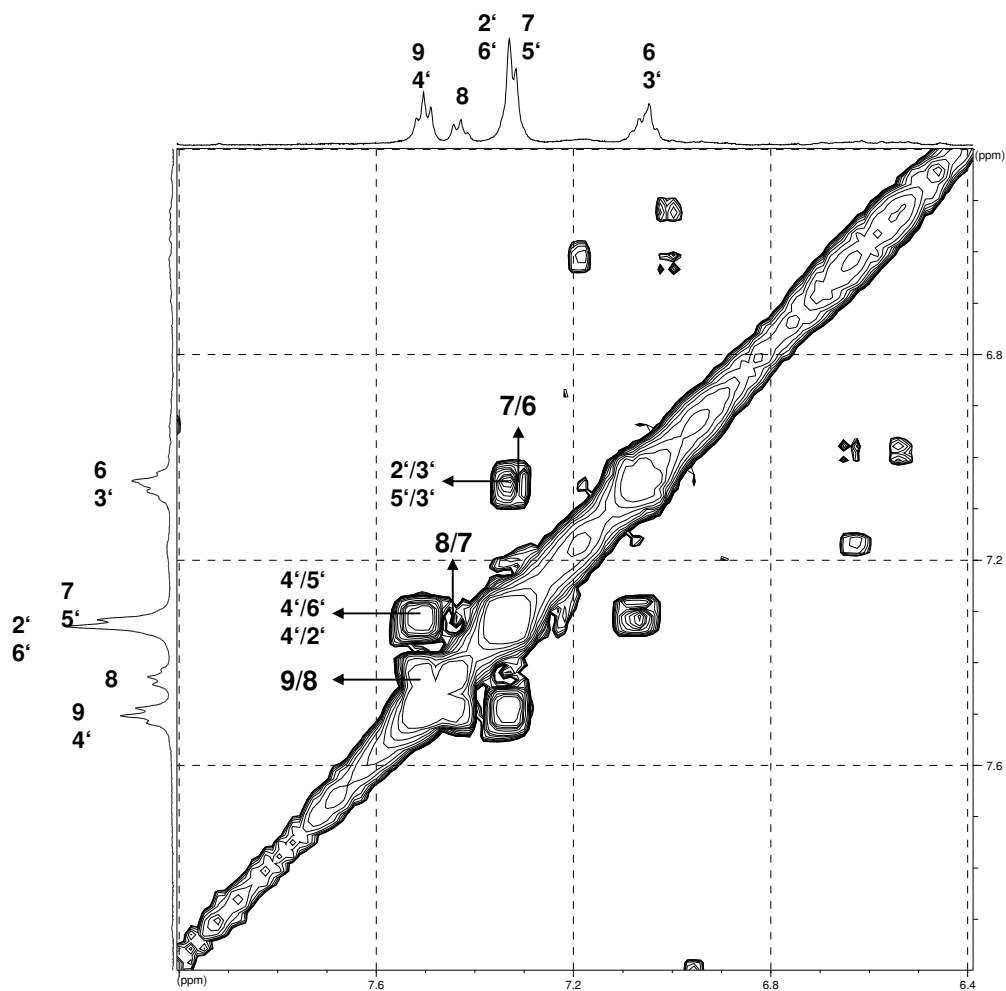


Figure 3.57 COSY correlation of compound **19** (viridicatin)

Compound **19** was substantially identified as viridicatin because the chemical shifts, splicing patterns and coupling constants of compound **19** and those of viridicatin described by Teuscher (2005) were almost identical [table.3.21]. Viridicatin was reported isolated from several species from genus *Penicillium* before such as *P. viridicatum*, *P. cyclopium*, *P. puberulum*, and *P. solitum* (Luckner *et al.*, 1964).

Table 3.21 NMR data of compound **19** (viridicatin)

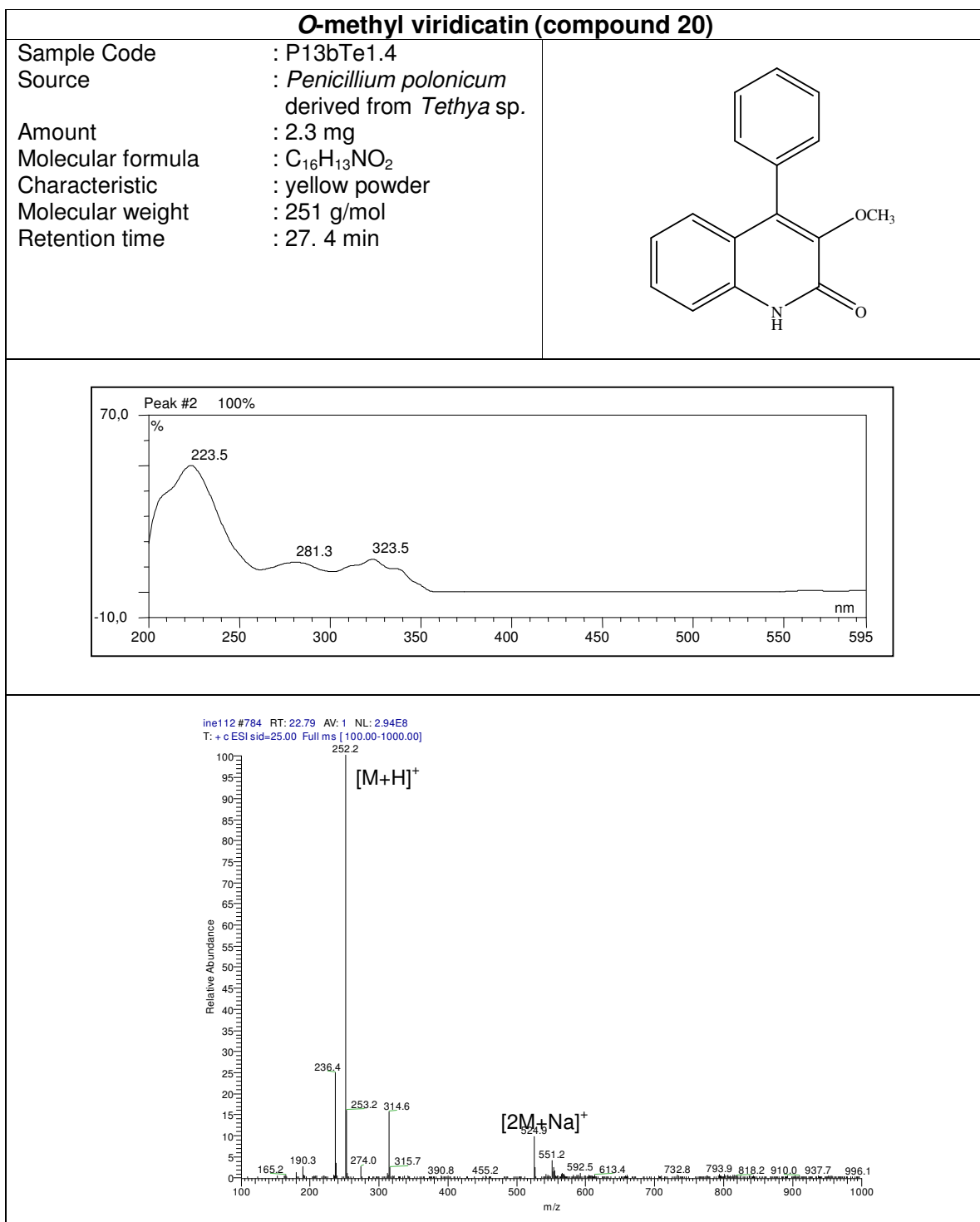
Position	δ H (ppm) multiplicity (J in Hz) (in DMSO)	δ H (ppm) multiplicity (J in Hz) of (Teuscher,2005 in DMSO)
1-NH	12.21 (1H,bs)	12.19 (1H,bs)
3-OH	9.19 (1H, bs)	9.18 (1H,bs)
6	7.02-7.08 (1H,dd,8.5,1.6) ^c	7.03-7.07 (1H,m)
7	7.30–7.35 (1H,m) ^a	7.32 (1H,ddd,6.9,1.3)
8	7.42 (1H,t,7.4)	7.41 (1H,m)
9	7.50 (1H,d,7.4) ^b	7.48-7.54 (1H,m)
2'	7.30 -7.35 (1H,m) ^a	7.03-7.07 (1H,m)
3'	7.30-7.35 (1H,m) ^a	7.28-7.31 (1H,m)
4'	7.50 (1H,t,7.4) ^b	7.48-7.54 (1H,m)
5'	7.02-7.08 (1H,t,8.5) ^c	7.03-7.07 (1H,m)
6'	7.30–7.35 (1H,m) ^a	7.28-7.31 (1H,m)

^{a,b,c} : overlapping Signals

3.5.4 Compound **20** (*O*-methyl viridicatin)

Compound **20** (*O*-methyl viridicatin) was a compound isolated as a mixture with viridicatin from the ethyl acetate extract of *Penicillium polonicum* through sephadex column LH-20 chromatography with 100% methanol and followed by preparative HPLC. UV maximum of this quinolinone compound was at 223.5 nm, with shoulders at 281.3 and 323.5 nm. Its ESI MS showed the molecular ion peak at m/z 252 upon positive ionization suggesting molecular weight of 251 g/mol.

The structure of *O*-methyl viridicatin was similar with viridicatin, except there was one methoxy group located in position 3' instead of the hydroxyl group in viridicatin. The ¹H NMR spectrum [figure 3.58] showed complete signals from viridicatin and *O*-methyl viridicatin. Furthermore signals of both quinoline compounds were very similar. The methoxy group of *O*-methyl viridicatin appeared as sharp singlet at the chemical shift of 3.06 ppm.



The COSY spectrum (figure 3.59 and 3.60) showed that nine protons which were belong to compound **20** (*O*-methyl viridicatin) assembled two aromatic spin systems which had character of one monosubstituted aromatic ring and one 1,2-disubstituted aromatic ring. The disubstituted aromatic ring was formed by protons H-6 at δ 6.97 ppm (1H,dd,7.9 and 1.0 Hz), H-7 at δ 7.06 ppm (1H,t,7.0 Hz), H-8 at δ 7.43 (1H,dt,7.0 and 1.3 Hz) and H-9 at δ between 7.43 and 7.56 ppm (1H,m). The monosubstituted ring consisted of the protons H-4' at δ between 7.45 and 7.54 ppm, H-2', H-3'; H-5' and H-6' resonating at δ between 7.30 and 7.37 ppm. .

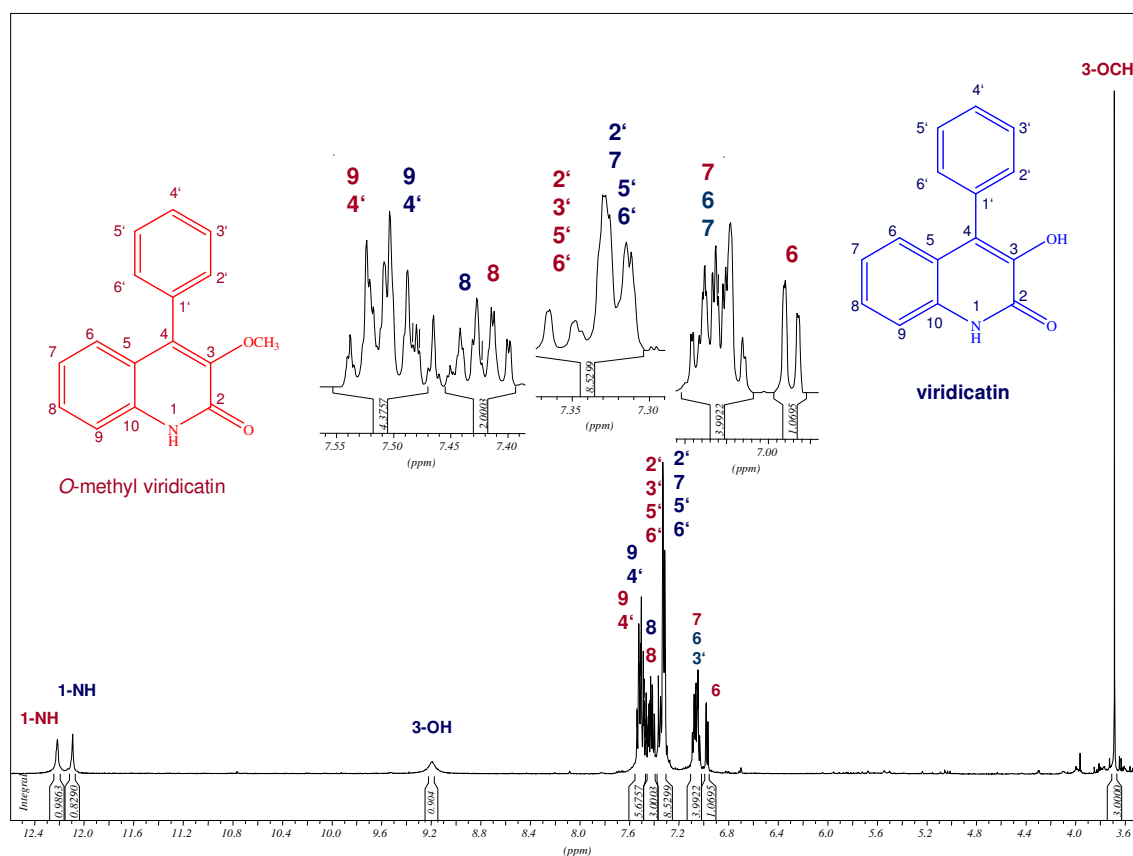


Figure 3.58 ¹H NMR spectrum of compound **20** (*O*-methyl viridicatin)

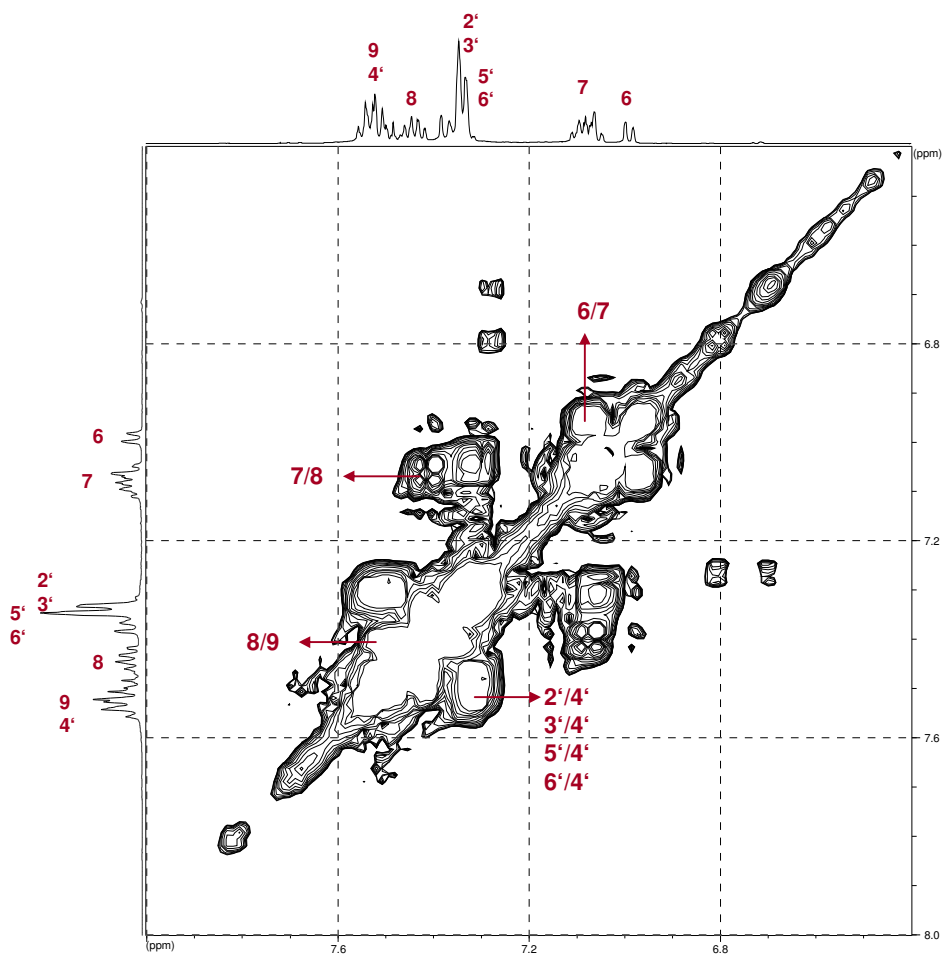


Figure 3.59 COSY spectrum of compound **20** (*O*-methyl viridicatin)

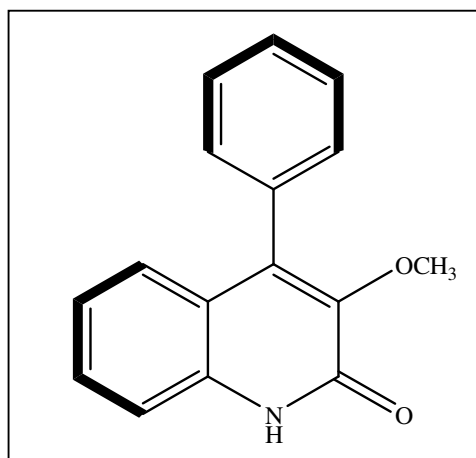


Figure 3.60 COSY correlation of compound **20** (*O*-methyl viridicatin)

O-methyl viridicatin was reported found from several species from genus *Penicillium* before such as *P. viridicatum*, *P. cyclopium*, *P. puberulum*, and *P. solitum* (Luckner *et al.*, 1976). NMR data of compound **20** in comparison with that of *O*-methyl viridicatin described by Hodge *et al.* (1988) indicated similar chemical shifts leading to a conclusion that both compounds were identical (table 3.20).

Table 3.22 NMR data of compound **20** (*O*-methyl viridicatin)

Position	δ H (ppm) multiplicity (<i>J</i> in Hz)(in DMSO)	δ H (ppm) multiplicity (<i>J</i> in Hz) (Hodge <i>et al.</i> , 1988 in CDCl ₃)
1-NH	10.85 (1H, bs)	11.07 (1H,bs)
3-OCH ₃	3.06 (3H,s)	3.84 (3H,s)
6	6.97 (1H,dd,7.9,1.0)	7.13 (1H,d,8.0)
7	7.06 (1H,t,7.0)	7.23 (1H,t,8.0)
8	7.43 (1H,dt,7.0,1.3)	7.43-7.56 (1H,m)
9	7.45-7.54 (1H,m) ^a	7.43-7.56 (1H,m)
2'	7.30-7.37(1H,m) ^b	7.43-7.56 (1H,m)
3'	7.30-7.37(1H,m) ^b	7.39 (1H,m)
4'	7.45-7.54 (1H,m) ^a	7.43-7.56 (1H,m)
5'	7.30-7.37(1H,m) ^b	7.39 (1H,m)
6'	7.30-7.37(1H,m) ^b	7.43-7.56 (1H,m)

^{a, b} : overlapping Signals

3.6 Secondary metabolites of fungus *Arthrinium* sp.

Arthrinium sp. was isolated from marine sponge *Tethya* collected from the Mediterranean Sea. Two metabolites were isolated from this fungus. They were indol-3-carboxylic acid (compound **21**) and myrocin A (compound **22**).

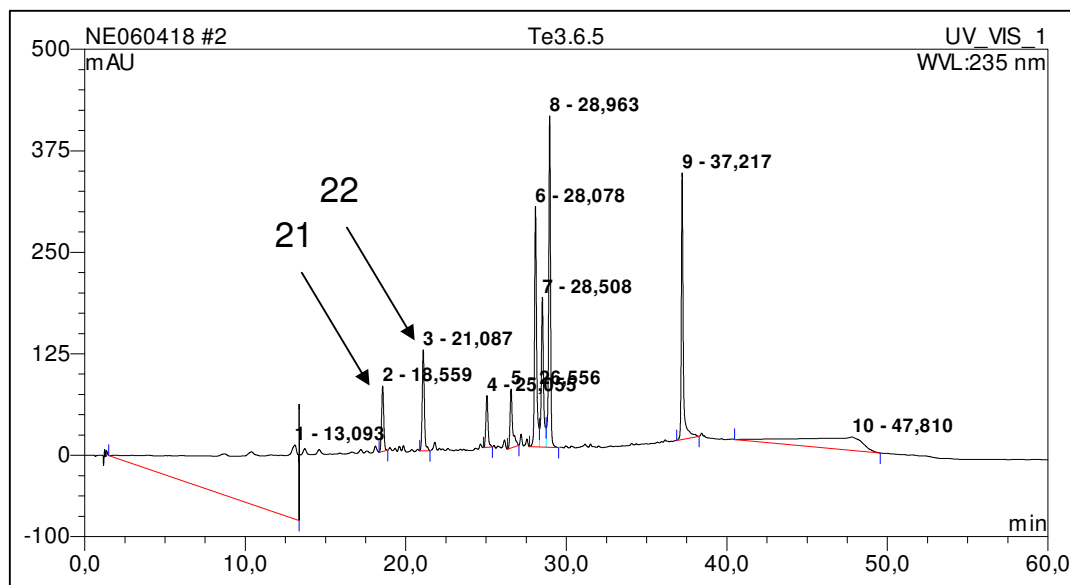
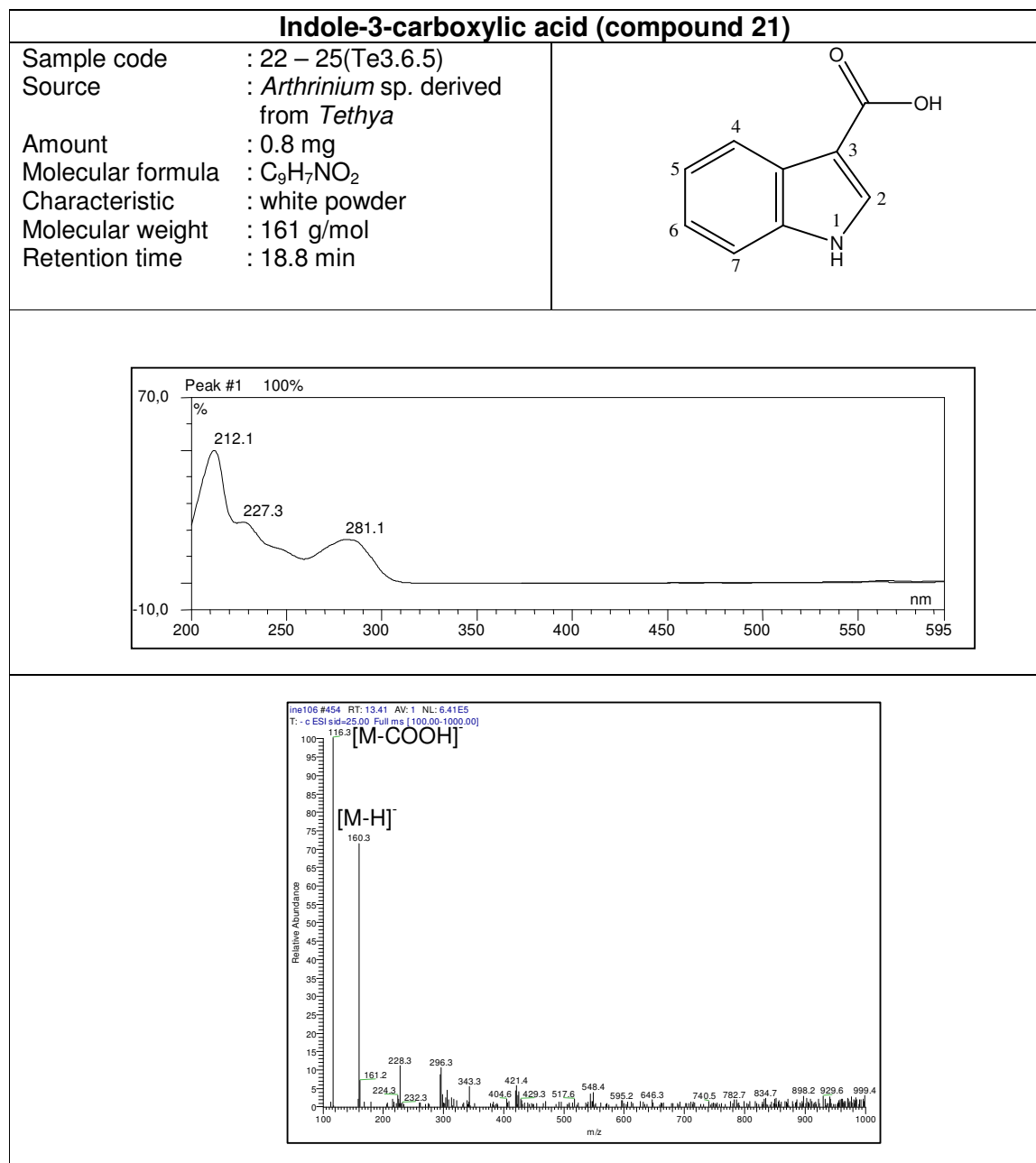


Figure 3.61 HPLC chromatogram of the ethyl acetate extract of *Arthrinium* sp.

Table 3.23 Biological screening of *Arthrinium* sp. and its metabolites

Sample	Antimicrobial assay				L5178Y growth (%) Conc. 10 µg/mL	EC ₅₀ (µg/mL)
	BS	SC	CC	CH		
Ethyl acetate extract of <i>Arthrinium</i> sp.	-	9	9	10	56.6	
Hexane extract of <i>Arthrinium</i> sp.	7	10	8	10		
<i>n</i> -butanol extract of <i>Arthrinium</i> sp.	-	6	-	-		
Indol-3-carboxylic acid					94.8	
Myrocin A					23.2	

BS = *Bacillus subtilis*, SC = *Saccharomyces cerevisiae*, CC = *Cladosporium cucumerinum* and CH = *C. herbarum*

3.6.1 Compound 21 (indole-3-carboxylic acid)

Compound **21** (indole-3-carboxylic acid) was isolated from the ethyl acetate extract of *Arthrinium* sp. through Sephadex LH-20 column chromatography with 100% methanol. It exhibited UV absorbances at λ_{max} (MeOH) 212.1, 227.3 and 281.1 nm. Its ESI MS showed the most intense peak at m/z 160 $[\text{M}-\text{H}]^-$ upon negative ionization revealing the molecular weight of 161 g/mol. Together with the analysis of the ^1H NMR spectrum, the molecular formula of $\text{C}_9\text{H}_7\text{NO}_2$ was suggested.

The characteristic fragment resulting from loss of 44 amu at m/z 116 in the ESI mass spectrum showed the presence of a carboxylic acid moiety in the molecule $[\text{M}-\text{COOH}]^-$.

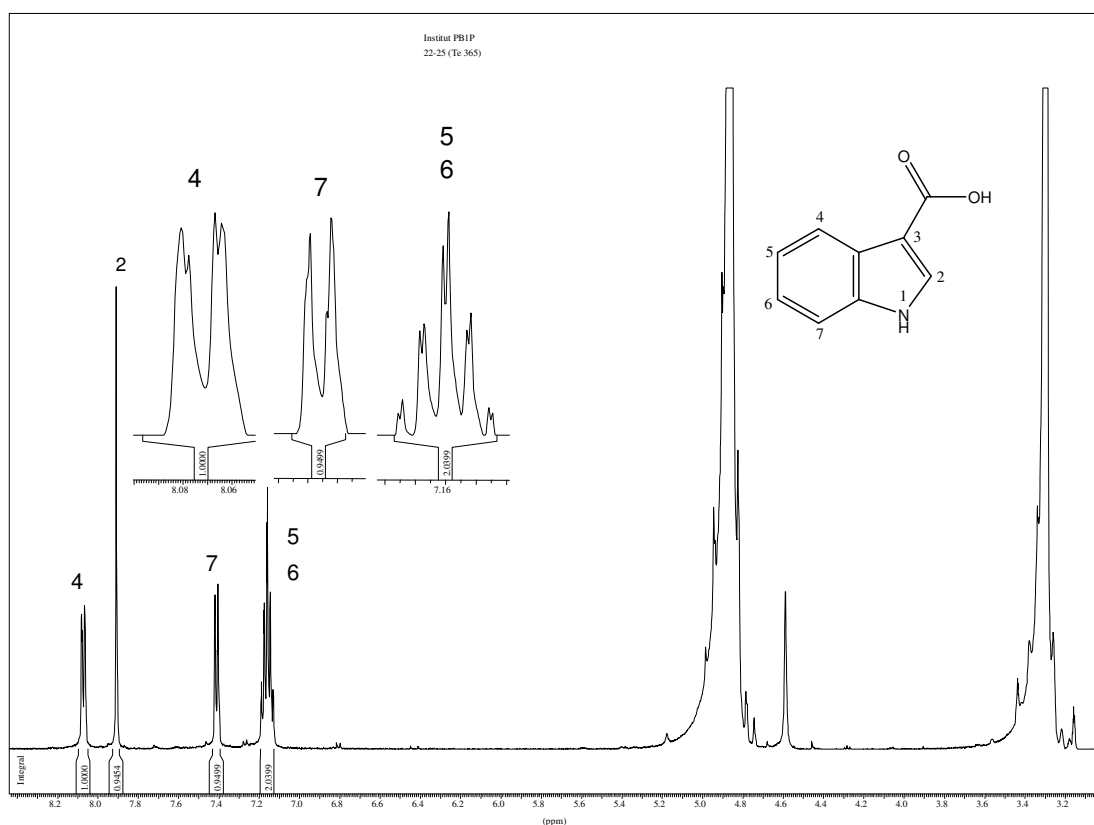


Figure 3.62 ^1H NMR spectrum of compound **21** (CD_3OD , 500 MHz)

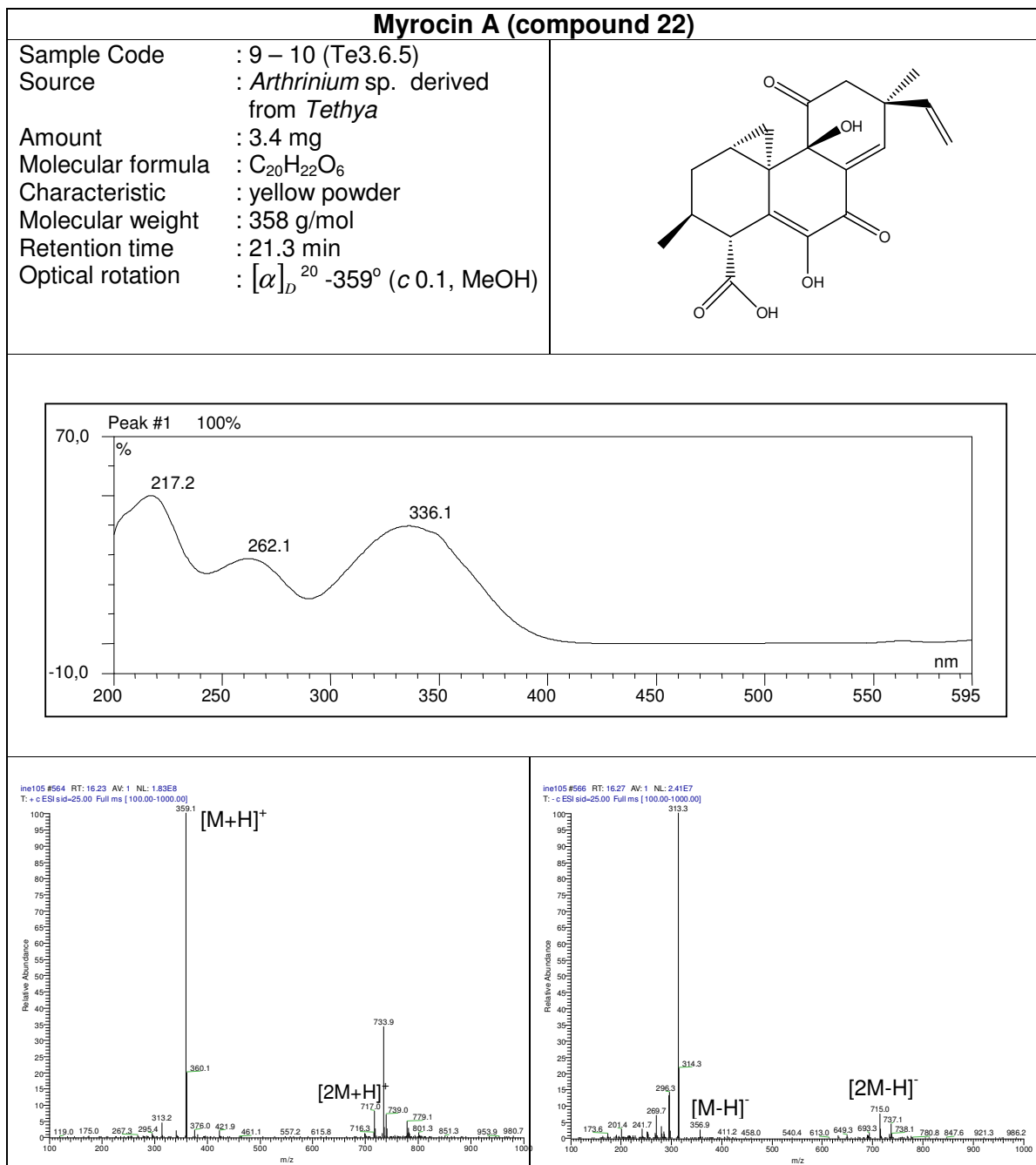
The ^1H NMR spectrum [figure 3.62] showed four aromatic protons assembling an ABCD aromatic spin system characteristic of an ortho disubstituted phenyl ring, which were resonating at chemical shifts of δ 8.08 (H-4) as doublet of doublet ($J = 7.0, 1.3$ Hz), δ 7.41 (H-7) as doublet of doublet ($J = 7.0, 1.3$ Hz) and δ 7.16 (H-5 and H-6). The proton H-4 was shifted downfield due to the influence of carboxyl group in β -position. An additional proton signal was present at the chemical shift of δ 7.91 appearing as singlet suggesting a 3-substituted indole ring.

Comparison of the NMR data with the literature (Aldrich library, 1992) led to the conclusion that compound **21** was indole-3-carboxylic acid.

Table 3.24 NMR data of compound **21** (indole-3-carboxylic acid)

Position	δH (ppm), multiplicity (J in Hz) (in MeOD)	δH (ppm) multiplicity (J in Hz) (Aldrich Library of NMR Spectra, 1992 in DMSO)
1-NH		
2	7.91 (1H,s)	8.05 (1H,s)
3-COOH		
4	8.07 (1H,dd,7.0,1.3)	8.05 (1H, d)
5	7.16 (1H, m)	7.20 (1H,m)
6	7.16 (1H, m)	7.20 (1H,m)
7	7.41 (1H, dd,7.0,1.3)	7.50 (1H,d)

3.6.2 Compound 22 (myrocin A)



Compound **22** (myrocin A) was isolated from the ethyl acetate extract of *Arthrinium* sp. through vacuum liquid chromatography (VLC) followed by sephadex LH-20 column chromatography with 100% methanol. It exhibited UV absorbances at λ_{max} 217.2, 262.1 and 336.1 nm. The ESI-MS of compound **22** showed the most intense peaks at m/z 359 $[M+H]^+$ upon positive ionization and at m/z 357 $[M-H]^-$ upon negative ionization, revealing the molecular weight of 358 g/mol. Together with the analysis of the ^1H NMR and ^{13}C NMR, a molecular formula of $\text{C}_{20}\text{H}_{22}\text{O}_6$ was derived.

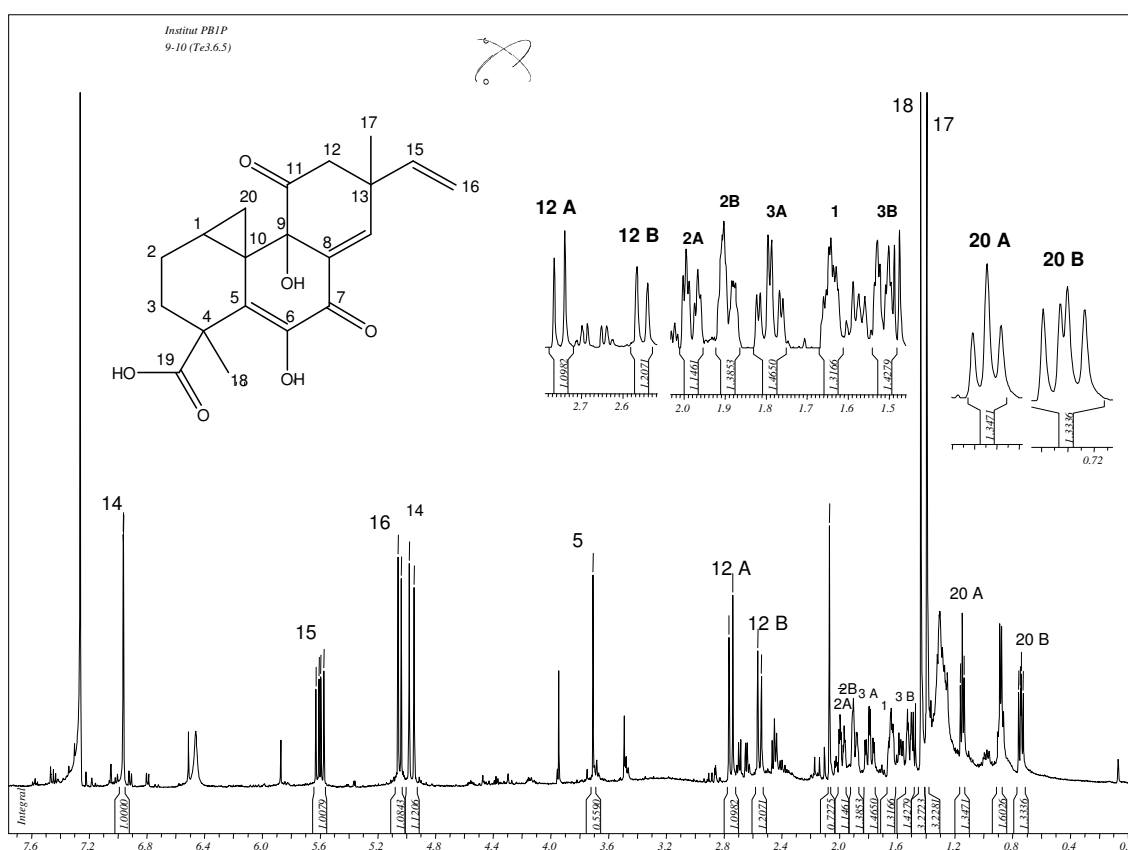


Figure 3.63 ^1H NMR spectrum of compound **22** (CDCl_3 , 500 MHz)

In the ^1H NMR spectrum [figure 3.63], 15 signals were detected. There were three upfield protons at 0.74 (H-20B), 1.15 (H-20A) and 1.64 ppm (H-1) showing correlations in the HMQC spectrum [figure 3.65] to carbons at 12.3 (C-20) and 15.6

ppm (C-1). The prominent upfield shift of these signals was indicative of a cyclopropane ring.

In the COSY spectrum [figure 3.64A and 3.64B], three spin systems were observed. The first comprised the olefinic proton (H-15) and two protons in position 16 (H-16A and H-16B), establishing a vinyl group, which was supported by coupling constants and splitting patterns displayed in the ^1H NMR spectrum. The second spin system observed in the COSY spectrum consisted of H-14 and H₂-12, while furthermore in the aliphatic region, the third system was composed of H₂-20, H-1, H₂-2, and H₂-3, although the correlation between H₂-3 and H₂-20 was difficult to be observed due to signal overlapping.

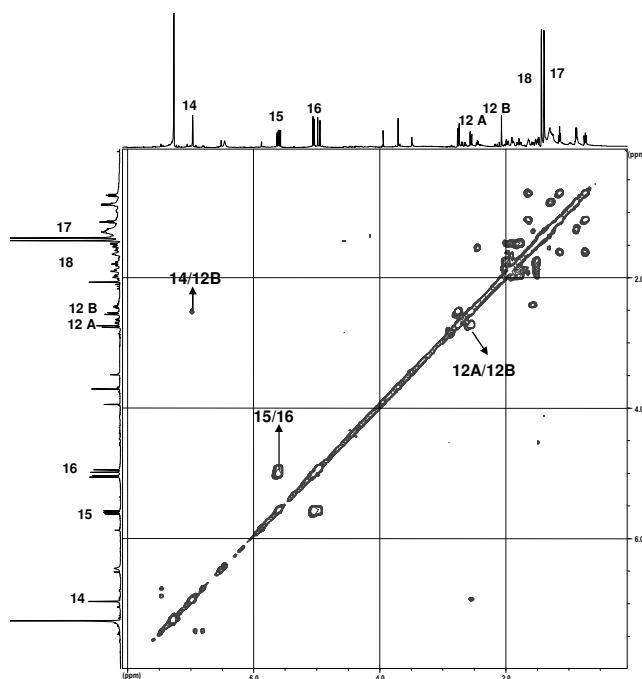


Figure 3.64A COSY spectrum of compound **22** (CDCl_3 , 500 MHz)

In the HMBC spectrum [figure 3.66] H-15, H-16A, H-16B, and also H₃-17, all correlated to C-13. Further HMBC correlations between H-12A, H-12B and H-14 to C-13 allowed to placing C-13 between C-12 and C-14. Further correlations included H-12A and H-12 B to C-11 which, due to its chemical shift, was attributed to a cyclic ketone (δ_C 208.0), and to C-9 which was an oxygenated quaternary carbon (δ_C 76.0). The latter also correlated to another olefinic proton, H-14, thus establishing the 2-hydroxy-cyclohexene-3-one ring system.

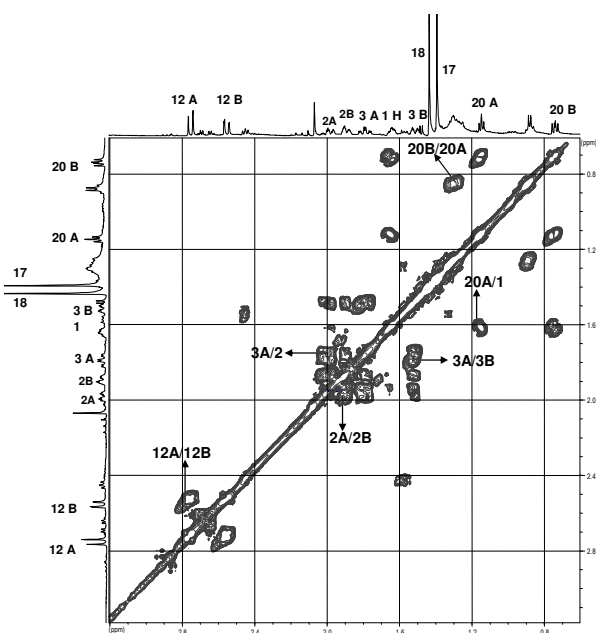


Figure 3.64B COSY spectrum of compound **22** (CDCl₃, 500 MHz)

Important HMBC correlations were observed for the methyl singlet H₃-18, which gave cross peaks to C-3, C-4, C-5, and C-18, out of which the latter two could be assigned to an sp²-hybridized carbon as well as a free carboxylic acid based on chemical shift arguments, leaving the quaternary C-4 as the only possible point of attachment for H₃-18. The correlations from H-20A and H-20B to C-5, C-8, C-9, and

C-10 completed the bicyclic heptane ring and placed it adjacent to the 2-hydroxy-cyclohexene-3-one ring described above.

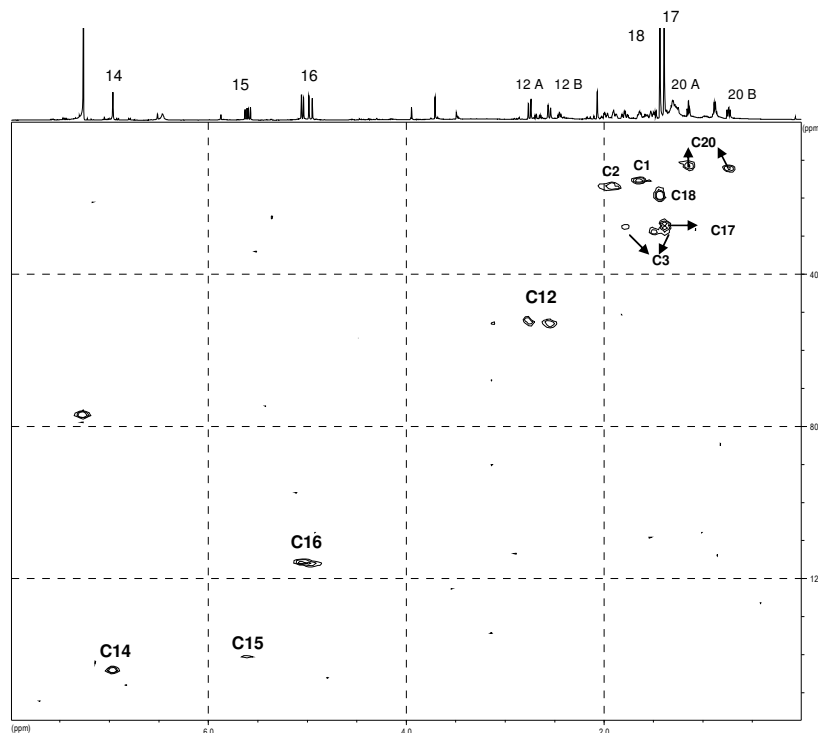


Figure 3.65 HMQC spectrum of compound **22** (CDCl_3 , 500 MHz)

Taken together, compound **22** was identified as myrocin A which was substantiated by comparison with published NMR data of myrocin A, a compound that was previously isolated from the fungus *Apiospora montagnei* derived from the marine alga *Polysiphonia violaceae* (Klemke *et al.*, 2003).

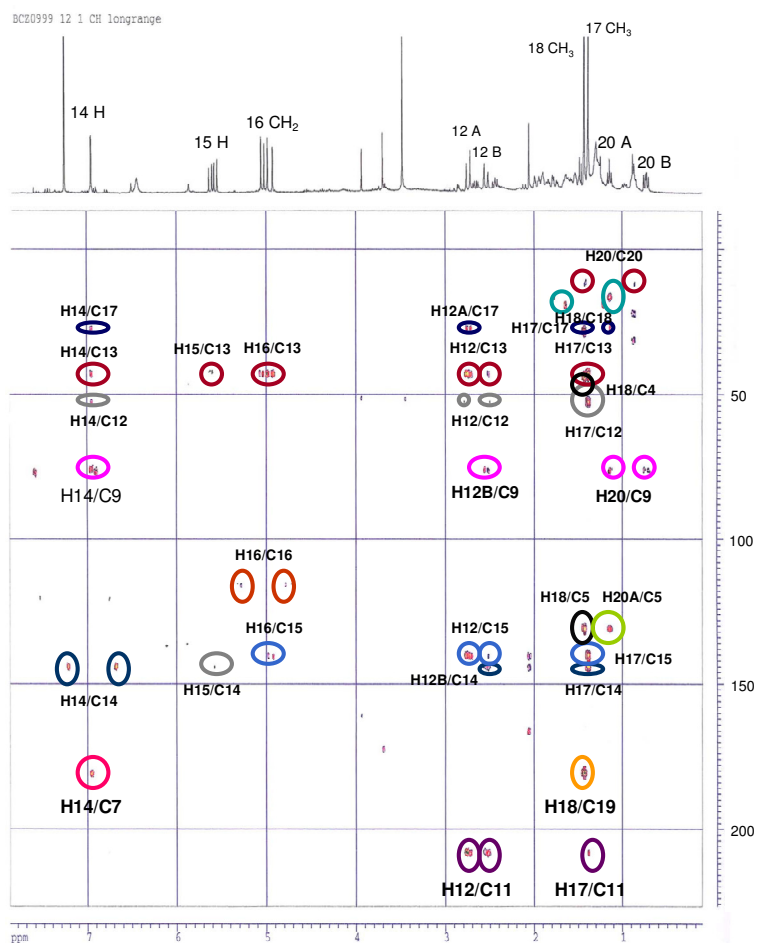
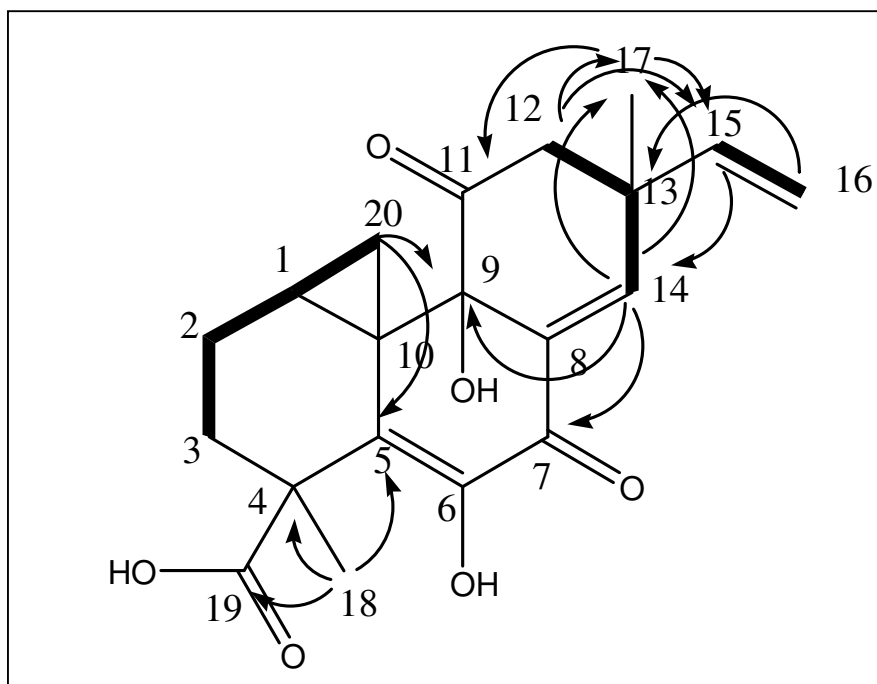


Figure 3.66 HMBC spectrum of compound **22** (CDCl_3 , 300 MHz)

The optical rotation of compound **22** was $[\alpha]_D^{20} -359^\circ$ whereas the reported value was $[\alpha]_D^{20} -418.6^\circ$ (Klemke *et al.*, 2003) suggesting both compounds to have the same absolute configuration.

Figure 3.67 HMBC and COSY correlations of compound **22** (myrocin A)Table 3.25 NMR data of compound **22** (myrocin A)

Position	δ H (ppm), multiplicity (<i>J</i> in Hz) (in CDCl ₃)	δ C (CDCl ₃)	δ H (ppm), multiplicity (<i>J</i> in Hz) (in CD ₃ OD)	HMBC (CD ₃ OD)
1	1.64 (1H,dd,8.8,6.3)	15.6	1.78 (1H,m)	
2	1.98 (1H,dt,3.8,3.2,14.2) 1.89 (1H,m)	17.2	2.04 (1H,m) 1.78 (1H,m)	
3	1.79 (1H,dt,14.2,13.9,4.4) 1.50 (2H,dd,6.3,13.9)	27.7	1.78 (2H,m)	
4		47.5		
5		135.0		
6				
6-OH	6.45 (1H, bs)		-	
7		183.0		
8		136.0		
9		76.0		
9-OH	3.82 (1H ,s)		-	
10				
11		208.0		
12	2.75 (1H,d , 12.9) 2.55 (1H,d, 12.9)	52.9	2.80 (1H,dd,13.6,1.6) 2.49 (1H,dd,13.6)	9,11,13,14,15,17
13		43.0		
14	6.96 (1H,s)	143.9	6.86 (1H,d,1.3)	7,9,12,13,17
15	5.60 (1H,dd,17.3,10.4)	140.3	5.69 (1H,dd,17.3,10.4)	13,14
16	5.05 (1H,d, 10.4) 4.96 (1H,d, 17.3)	115.8	5.01 (1H,m) 4.99 (1H,d,5.4)	13,15
17	1.40 (3H,s)	27.4	1.35 (3H,s)	11,12,13,14,15

18	1.44 (3H,s)	19.6	1.39 (3H,s)	4,5,19
19		181.0		
20	1.15 (1H,t,6.3) 0.74 (1H,dd,6.3,8.8)	12.3	1.08 (1H,m) 0.78 (1H,m)	5,9

3.7 Secondary metabolites of fungus *Botryosphaeria stevensii*

Botryosphaeria stevensii was isolated from the marine sponge *Tethya* sp. collected from the Mediterranean Sea. Griseofulvin (compound **23**) was isolated from this fungus.

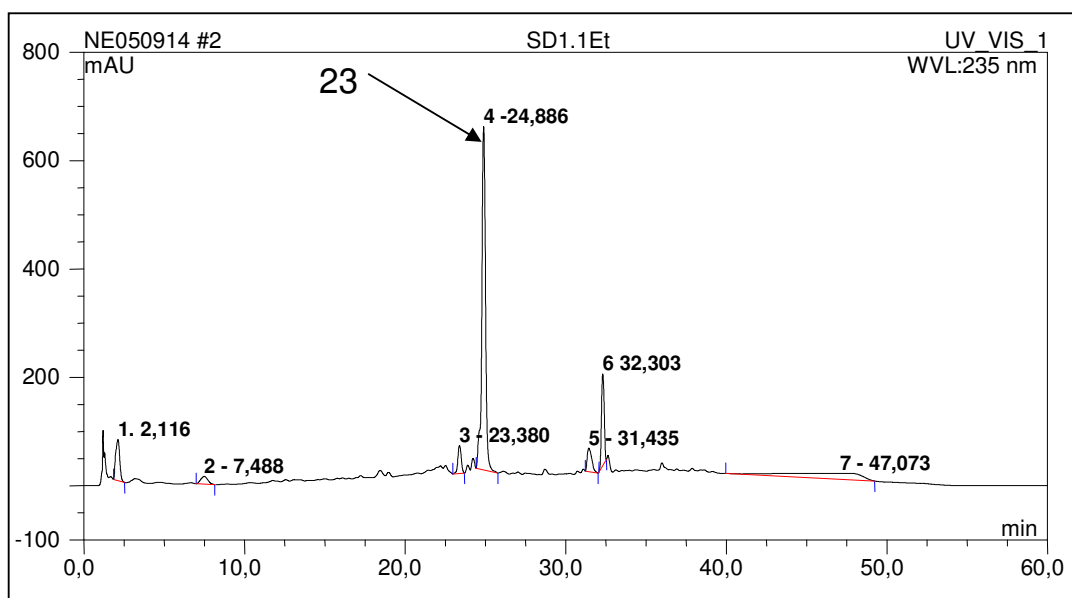
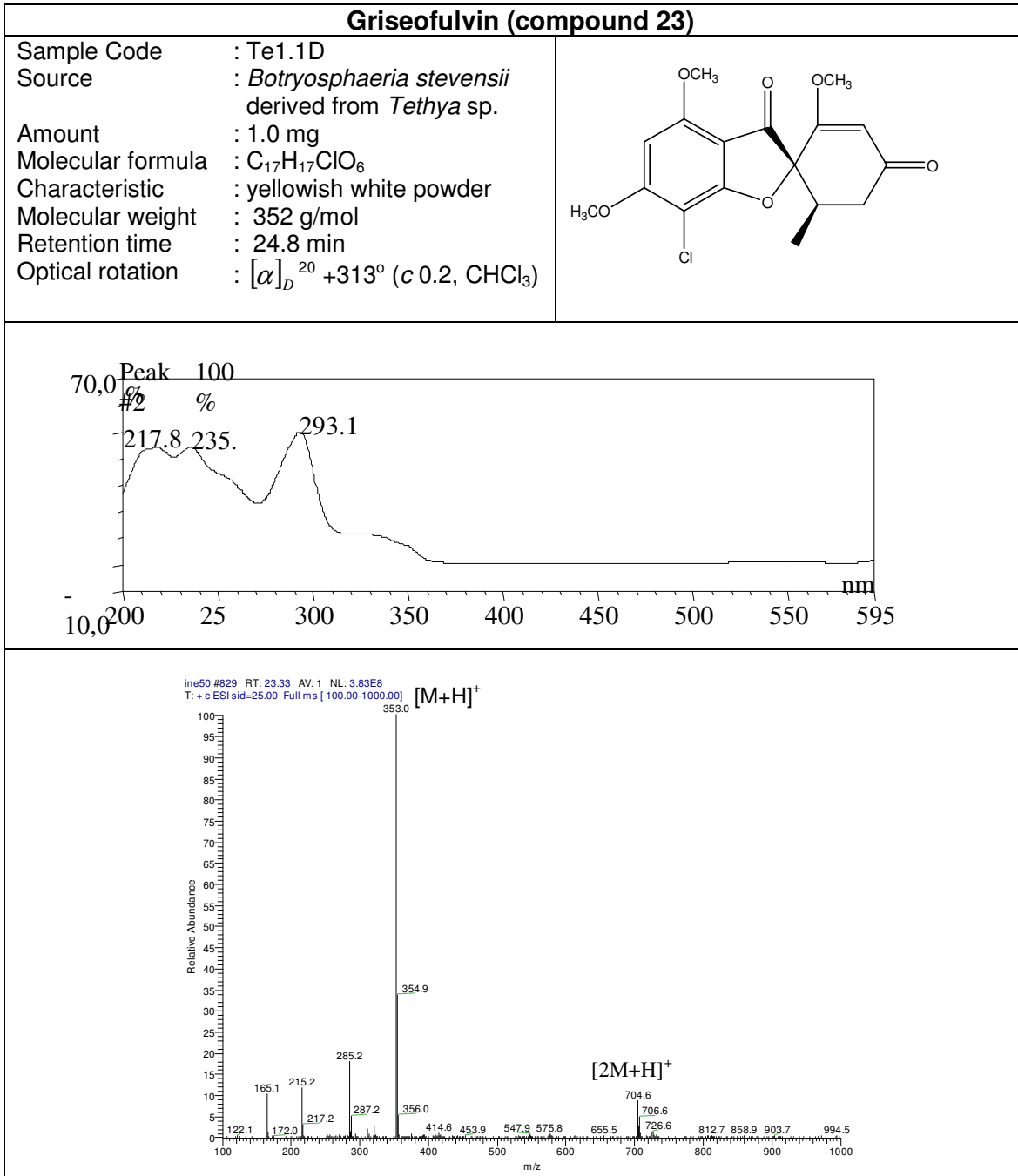


Figure 3.68 HPLC chromatogram of the ethyl acetate extract of *B. stevensii*

Table 3.26 Biological test result of *B. stevensii* and its metabolites

Sample	L5178Y growth (%) Conc. 10 µg/mL	EC ₅₀ (µg/mL)
Ethyl acetate extract of <i>Botryosphaeria stevensii</i>	3.2	
Griseofulvin	44.6	

3.7.1 Compound 23 (griseofulvin)



Compound **23** (griseofulvin) was isolated from the ethyl acetate extract of *Botryosphaeria stevensii* through Sephadex LH-20 column chromatography with 100% methanol followed by semi preparative HPLC. Its UV maximum was 293 nm with shoulders at 218 and 235 nm. Its ESI mass spectrum showed the most intense peak at m/z 353 $[M+H]^+$ upon positive ionization indicating a molecular weight of 352 g/mol. The presence of one chlorine atom could be observed by isotope cluster peaks separated by 2 mass units for the pseudomolecular and several fragment ions. Chlorine occurs in two stable isotopes ^{35}Cl (75%) and ^{37}Cl (25%) leading to a 3:1 ratio for the isotope cluster peaks in the mass spectrum.

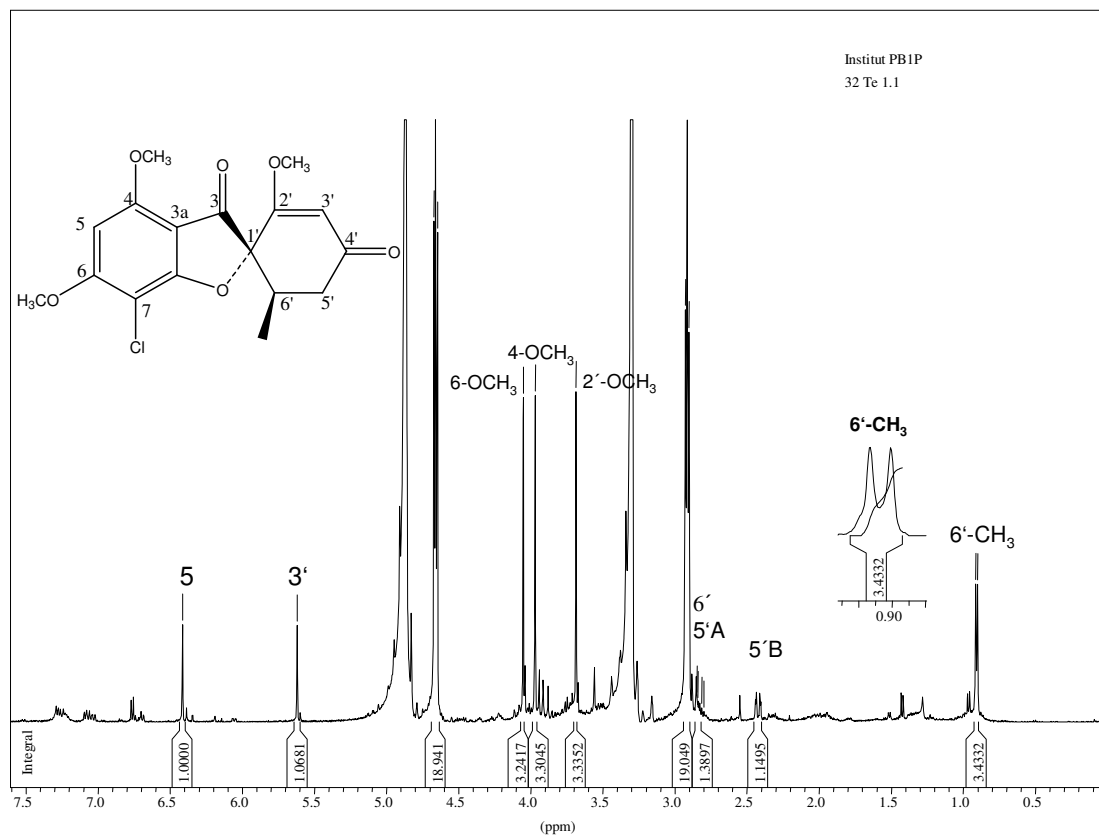


Figure 3.69 ^1H spectrum of compound **23** (CD_3OD , 500 MHz)

In the ^1H NMR spectrum [figure 3.69], one methyl group at δ 0.91 (d, $J = 6.0$) and three methoxy groups were observed as sharp singlets at δ 3.69, 3.96 and 4.05. One

isolated proton from the aromatic ring was observed at δ 6.41 as a sharp singlet. One proton from the cyclohexenone ring appeared at 5.62 ppm (H-3') as a sharp singlet. In the aliphatic region, three signals resonated at 2.83 (H-5'A), 2.42 ppm (H-5'B), and 2.85 ppm (H-6') forming a common spin system in the cyclohexenone ring, together with the methyl doublet at 0.91 ppm.

Table 3.27 NMR data of compound **23** (griseofulvin)

Position	δ H (ppm), multiplicity (<i>J</i> in Hz) (in CD ₃ OD)	δ H (ppm) multiplicity (<i>J</i> in Hz) (Aldrich Library of NMR Spectra, 1992 in MeOD)
2'-OCH ₃	3.69 (3H,s)	3.65 (3H,s)
3'	5.62 (1H,s)	5.55 (1H,s)
5'	2.83 (1H,m) 2.42 (1H,m)	2.85 (1H,m)* 2.35 (1H,m)
6'	2.85 (1H,m)	2.85 (1H,m)*
6'-CH ₃	0.91 (3H,d,6.0)	0.90 (3H,d)
4-OCH ₃	3.96 (3H,s)	3.95 (3H,s)
5	6.41 (1H,s)	6.40 (1H,s)
6-OCH ₃	4.05 (3H,s)	4.1 (3H,s)

* : overlapping signals

Compound **23** was identified as griseofulvin which was substantiated by comparison with NMR data of griseofulvin isolated from *Fusarium graminearum* reported in the literature (Solladie *et al.*, 1990).

The optical rotation of compound **23** $[\alpha]_D^{20} +313^\circ$ allowed to conclude that this compound had the same stereochemistry with griseofulvin described in the literature which showed an optical rotation of $[\alpha]_D^{20} +370.5^\circ$ (Solladie *et al.*, 1990).

3.8 Secondary metabolites of fungus PV1.1 (unidentified fungus)

PV 1.1 was isolated from the marine sponge *Petrosia ficiformis* collected from the Mediterranean Sea. 5-carboxy-mellein (compound **24**) was isolated from this fungus.

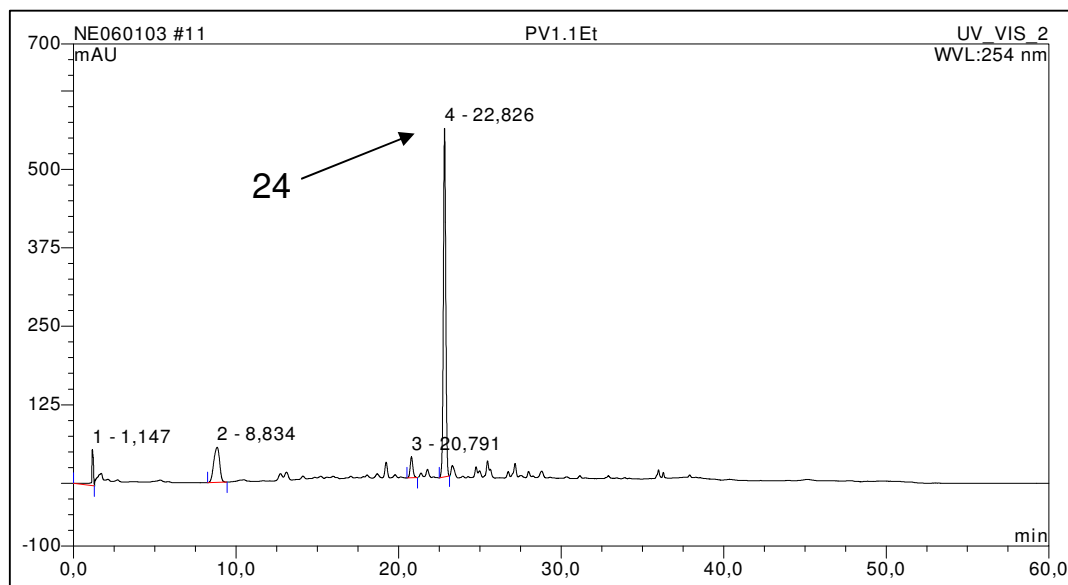


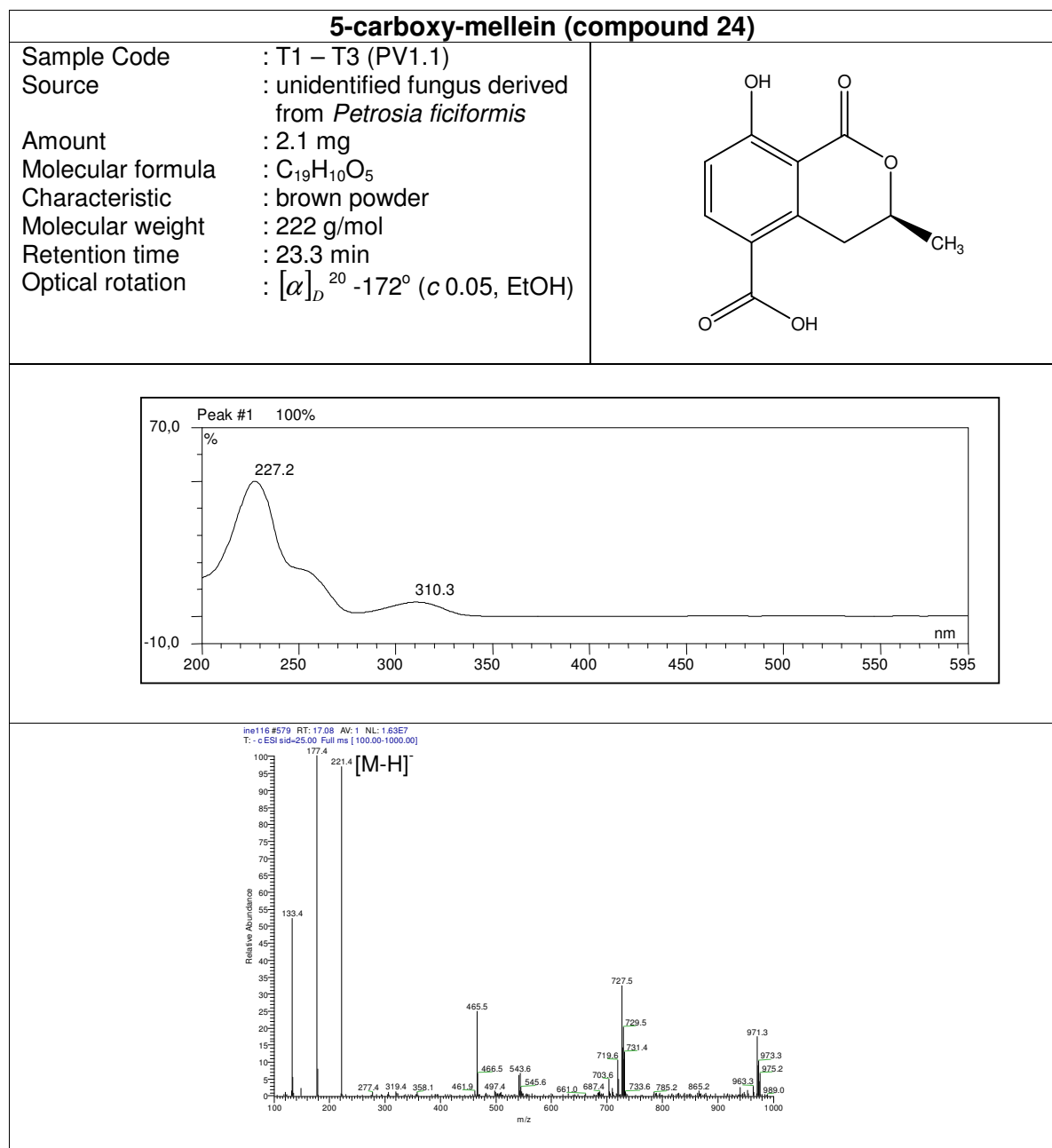
Figure 3.70 HPLC chromatogram of the ethyl acetate extract of fungus PV1.1

Table 3.28 Biological test result of fungus PV1.1 and its metabolite

Sample	Antimicrobial assay				L5178Y growth (%) Conc. 10 µg/mL	EC ₅₀ (µg/mL)
	BS	SC	CC	CH		
Ethyl acetate extract of PV1.1	-	-	-	-	58.2	
5-carboxy-mellein					37.3	

BS = *Bacillus subtilis*, SC = *Saccharomyces cerevisiae*, CC = *Cladosporium cucumerinum* and CH = *C. herbarum*

3.8.1 Compound 24 (5-carboxy-mellein)



Compound **24** (5-carboxy-mellein) was isolated from the ethyl acetate extract of the unidentified fungus PV1.1 through Sephadex LH-20 column chromatography using 100% methanol followed by semi preparative HPLC. The UV spectrum of compound **24** showed UV maxima at λ_{\max} (MeOH) 227 nm and 310 nm. Its ESI-MS showed the most intense peak at m/z 221 ($M-H$)⁻ revealing the molecular weight of 222 g/mol. Along with the ¹H NMR spectrum, a molecular formula of C₁₉H₁₀O₅ was assumed.

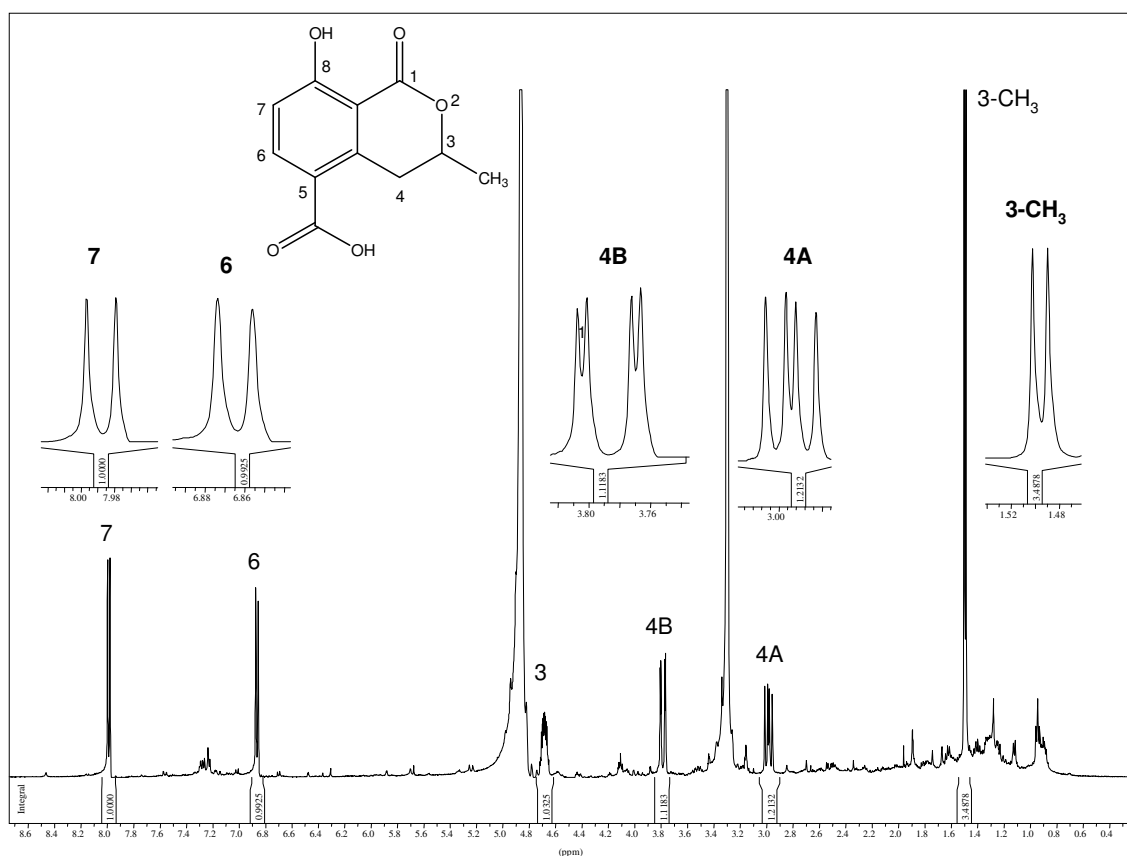


Figure 3.71 ¹H NMR spectrum of compound **24** (CD₃OD, 500 MHz)

The ¹H NMR spectrum [figure 3.71] showed two aromatic protons assembling an AB aromatic spin system proven by the COSY spectrum [figure 3.72] and their coupling constants. Those protons were detected at 6.82 (H-3) and 7.99 ppm (H-5) exhibiting an *ortho* coupling of 8.8 Hz. A methyl group appeared at 1.50 ppm as a

doublet, due to the presence of a methine group in α -position which appeared as a multiplet at 4.68 ppm. The chemical shift of the latter indicated that it was adjacent to an oxygen atom.

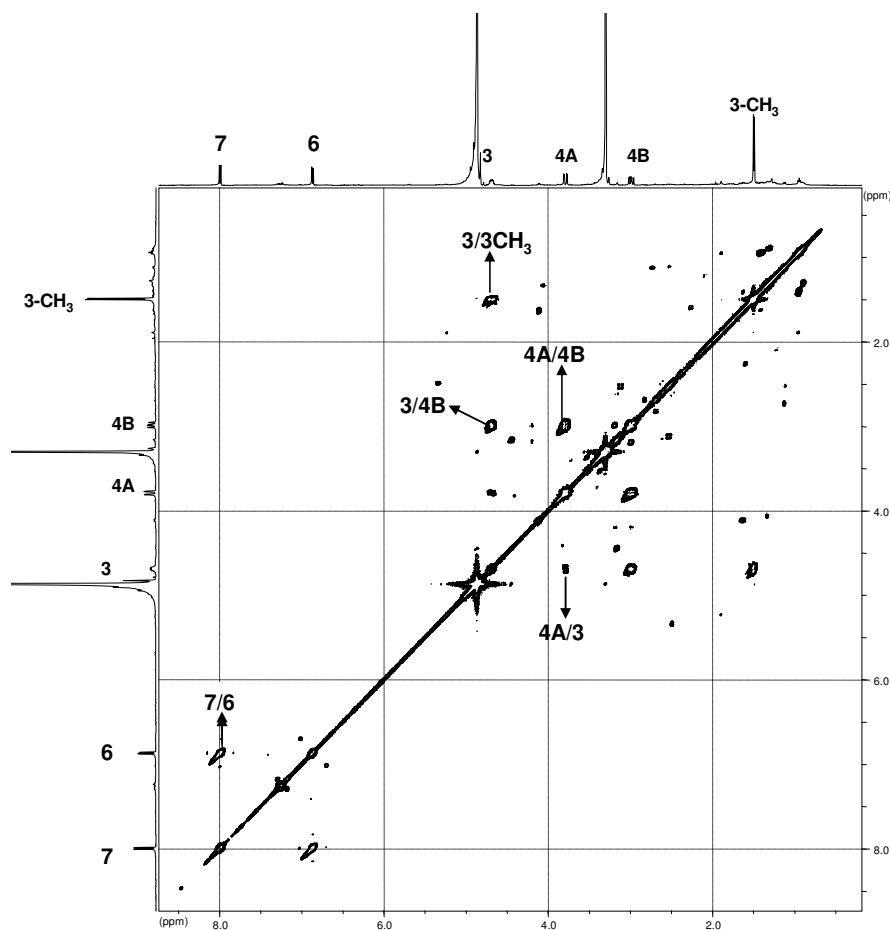


Figure 3.72 COSY spectrum of compound **24** (CD_3OD , 500 MHz)

The methylene protons (H-4A and H-4B) were observed at δ 2.99 ppm ($J = 17.3$ and 11.7 Hz) and 3.79 ppm ($J = 17.3$ and 3.0 Hz), appearing each as doublet of doublets. H-4A and H-4B showed geminal coupling of 17.3 Hz, as well as correlations to H-3, the coupling constant of 3.0 Hz can be explained by axial-equatorial positions, while the 11.7 Hz resembled axial-axial positions.

The COSY spectrum [figure 3.72 and 3.73] delivered another proof for the spin system formed by H₂-4 and H-3 in the tetrahydropyranone ring and its adjacent methyl group.

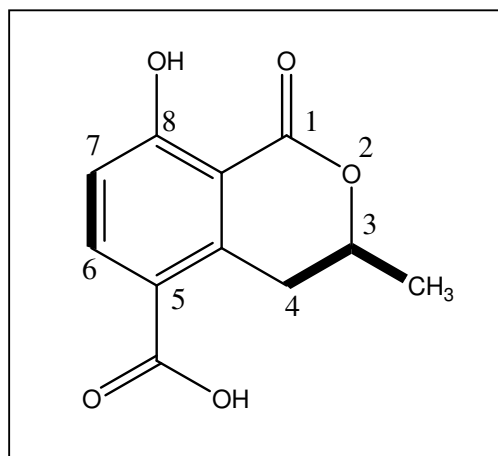


Figure 3.73 COSY correlation of compound **24** (5-carboxy-mellein)

Compound **24** was identified as 5-carboxy-mellein because the chemical shifts, splitting patterns and coupling constants of compound **24** and those of 5-carboxy-mellein described by Anderson *et al.* (1983) were very similar [table.3.27].

The measurement data of the optical rotation of compound **24** (-172°) allowed to conclude that this compound had the same stereochemistry with 5-carboxy-mellein described in the literature which had an optical rotation of -195° (Anderson *et al.*, 1983).

Table 3.29 NMR data of compound **24** (5-carboxy-mellein)

Position	δ H (ppm), multiplicity (<i>J</i> in Hz) (in CD ₃ OD)	δ H (ppm) multiplicity (<i>J</i> in Hz) (Anderson <i>et al.</i> , 1983 in acetone)
3	4.68 (1H,m)	4.60 (1H,m)
3-CH ₃	1.50 (3H,d,6.3)	1.46 (3H,d,6.0)
4	2.99 (1H,dd,17.3,11.7)	2.90 (1H,m)

	3.79 (1H,dd,17.3,3.0)	3.70 (1H,q)
5-COOH		11.60 (1H, bs)*
6	6.82 (1H,d,8.8)	6.86 (1H,d,8.0)
7	7.99 (1H,d,8.8)	7.96 (1H,d,8.0)
8-OH		11.60 (1H, bs)*

* : overlapping signals

3.9 Secondary metabolites of the fungus *Alternaria compacta*

Alternaria compacta was isolated from the marine sponge *Suberites domuncula* collected from Mediterranean Sea. Two metabolites were isolated from this fungus. They were tenuazonic acid (compound **25**) and alternariol (compound **26**).

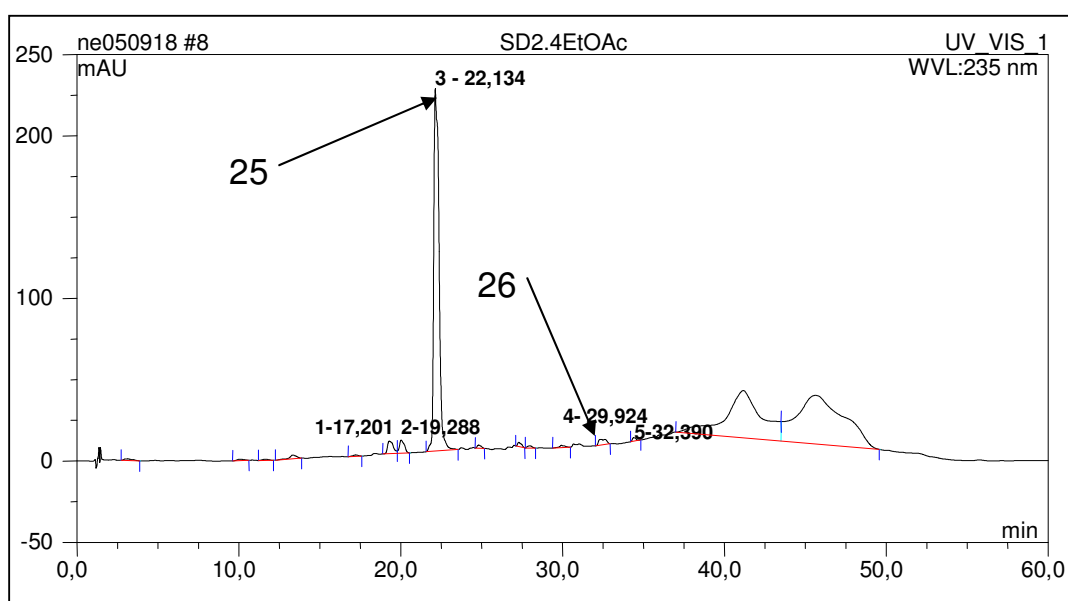


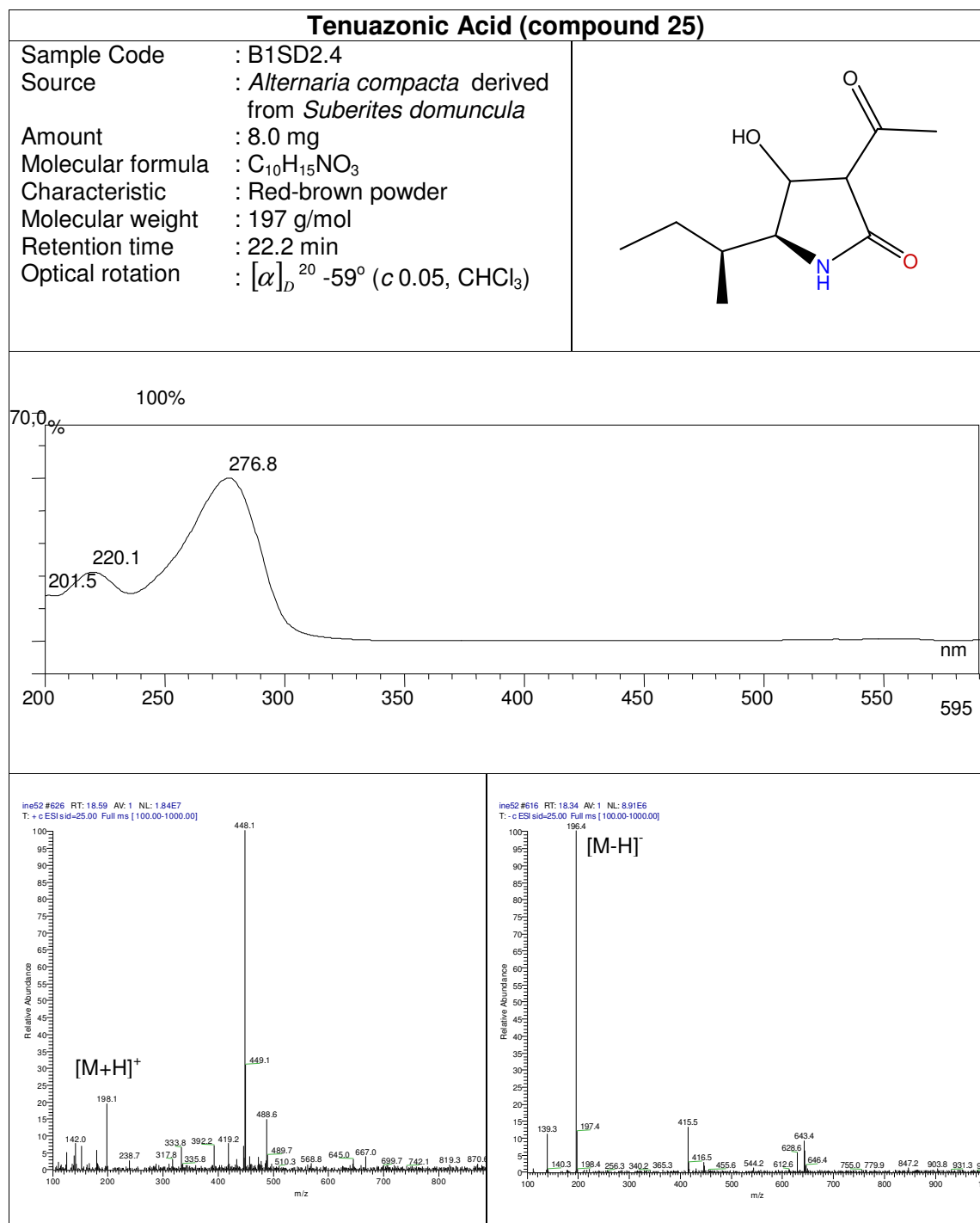
Figure 3.74 HPLC chromatogram of the ethyl acetate extract of *Alternaria compacta*

Table 3.30 Biological test result of *Alternaria compacta* and its metabolites

Sample	Antimicrobial assay				L5178Y growth (%) Conc. 10 µg/mL	EC ₅₀ (µg/mL)
	BS	SC	CC	CH		
Ethyl acetate extract of <i>Alternaria compacta</i> .	9	-	-	-	76.2	
Tenuazonic acid					101.8	
Alternariol					96.9	

BS = *Bacillus subtilis*, SC = *Saccharomyces cerevisiae*, CC = *Cladosporium cucumerinum* and CH = *C. herbarum*

3.9.1 Compound 25 (tenuazonic acid).



Compound **25** (tenuazonic acid) was isolated from the ethyl acetate extract of *Alternaria compacta* through semi preparative HPLC. It exhibited UV absorbances at λ_{max} (MeOH) 201.5, 220.1 and 276.8 nm. In the ESI-MS, a prominent $[M+H]^+$ pseudomolecular ion was observed at m/z 198 upon positive ionization, together with an intense $[M-H]^-$ at m/z 196 upon negative ionization which indicated a molecular weight of 197 g/mol. In conjunction with the analysis of the ^1H NMR data, a molecular formula of $\text{C}_9\text{H}_7\text{NO}_2$ was derived.

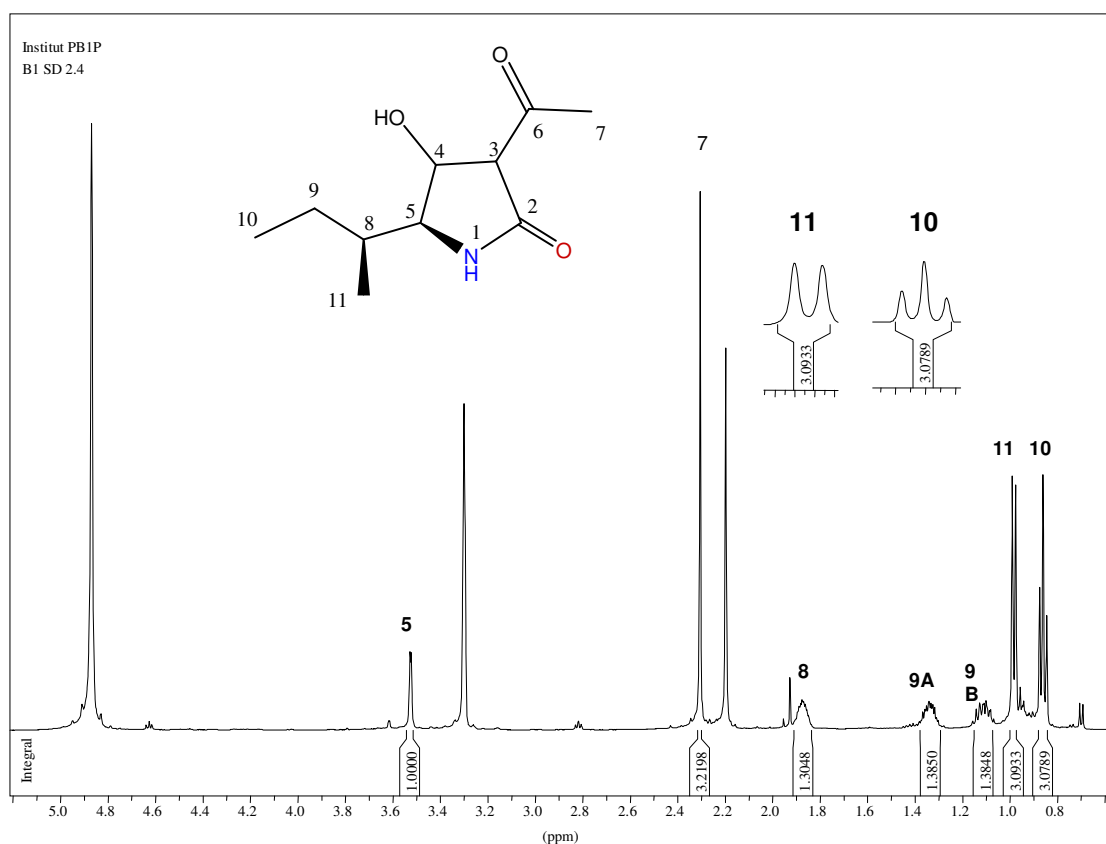


Figure 3.75 ^1H NMR spectrum of compound **25** (CD_3OD , 500 MHz).

In the ^1H NMR spectrum [figure 3.75], three methyl groups were observed. Two methyl signals were located at the chemical shifts δ 0.86 (H-10) as a triplet and 0.99 (H-11) as doublet. The third methyl signal was shifted downfield and appeared as a

sharp singlet at δ 2.30 (H-7), due to the influence of an adjacent carbonyl group. H-10 appeared as a triplet because of the presence of methylene group residing next to it. On the other hand, H-11 appeared as a doublet which can be explained by the presence of proton H-8.

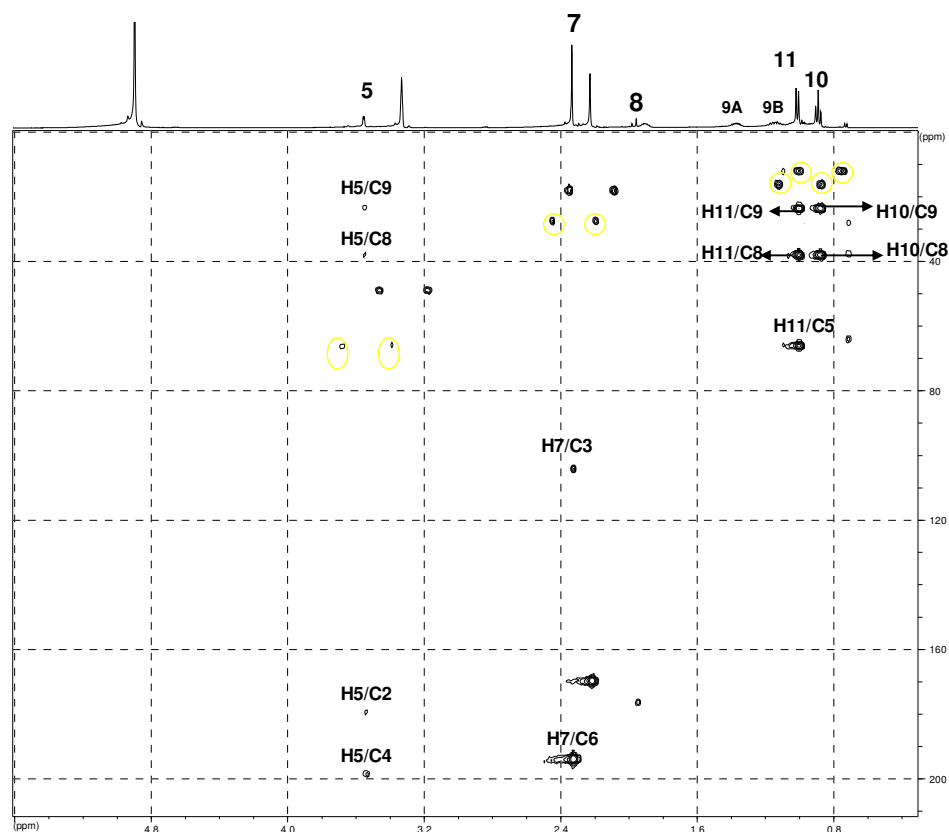


Figure 3.76 HMBC spectrum of compound **25** (CD₃OD, 500 MHz)

The structure of tenuazonic acid was also confirmed by its HMBC spectrum [figure 3.76]. In the pyrrolidine ring, H-5 showed a correlation with C-2 and also with C-8 which was located in the isobutyl side chain.

The methyl protons in position 11 had correlations with C-5, C-9, C-10 and C-11, while H₃-10 also showed cross peaks to these carbons, except for C-5. These

correlations confirmed the presence of the isobutyl side chain. On the other hand, the position of the acetyl side chain was evident from a correlation of H₃-7 to C-3.

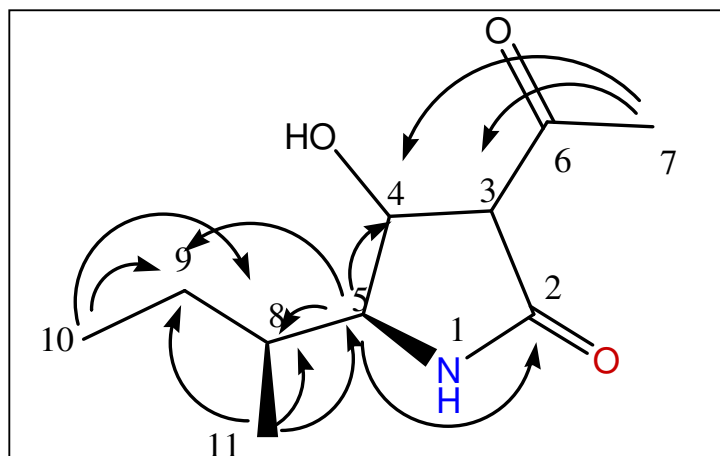


Figure 3.77 HMBC correlations of compound **25** (tenuazonic acid)

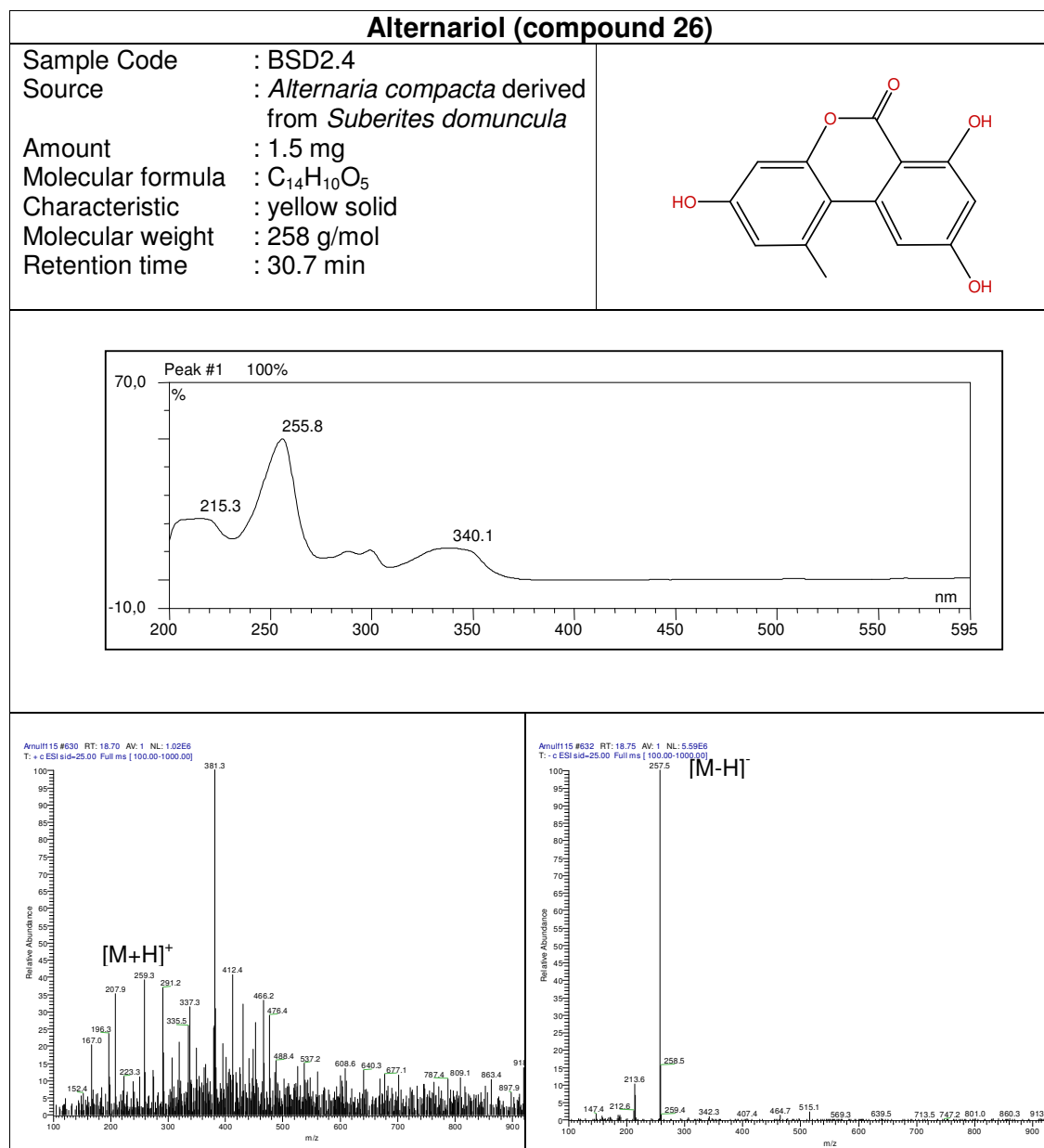
Table 3.31 NMR data of compound **25** (tenuazonic acid)

Position	δ H (ppm) multiplicity (<i>J</i> in Hz)(in CD ₃ OD)	δ H (ppm) multiplicity (<i>J</i> in Hz) (Steyn <i>et al.</i> , 1978 in CDCl ₃)	δ C (ppm) (in CD ₃ OD)	δ C (ppm) (Nolte <i>et al.</i> , 1980 in CDCl ₃)	HMBC (CD ₃ OD)
2			176.2	175.2	
3			104.2	103.9	
4			193.6	195.5	
5	3.52 (1H,d,2.2)	3.6 (1H, bs)	66.0	67.2	2,4,8,9
6				187.0	
7	2.30 (3H,s)	2.34 (3H,s)	27.7	20.3	3,4
8	1.87 (1H,m)	1.90 (1H,m)	38.0	38.2	
9	1.34 (1H,m) 1.12 (1H,m)	1.35 (1H,m) 1.14 (1H,m)	23.7	24.8	
10	0.86 (3H,t,7.3)	0.87 (3H,t,7.6)	12.3	12.2	5,8,9
11	0.98 (3H,t,7.3)	1.00 (3H,t,7.6)		15.9	8,9

Table 3.31 shows the NMR data comparison of compound **25** and tenuazonic acid reported by Steyn and Wessel (1978) and Nolte *et al.* (1980) which led to the conclusion that both compounds were identical. The optical rotation of compound **25** was $[\alpha]_D^{20} -59^\circ$ (c 0.05, CHCl₃), which proved the stereochemistry of this compound

comparing to optical rotation of tenuazonic acid from the literature (-136°) (Nolte *et al.*, 1980).

3.9.2 Compound 26 (alternariol)



Compound **26** (alternariol) was isolated from the ethyl acetate extract of *Alternaria compacta* through semi preparative HPLC. The UV maximum of this compound was at 255.8 nm, with shoulders at 215.3 and 340.1 nm. Positive and negative ESI-MS showed pseudomolecular peaks at m/z 259 $[M+H]^+$ and m/z 257 $[M-H]^-$, revealing the molecular weight of 258 g/mol.

In the ^1H NMR spectrum [figure 3.78], two AB spin systems for a total of four meta-coupled ($J = 2.2$ Hz in each case) aromatic protons were detected. The first one consisted of H-4 and H-6 (6.37 and 7.27 ppm, respectively) while the second one contained H-3' and H-5' (6.61 and 6.70 ppm), respectively. In addition, one methyl group adjacent to C-6' appeared as a singlet at 2.76 ppm.

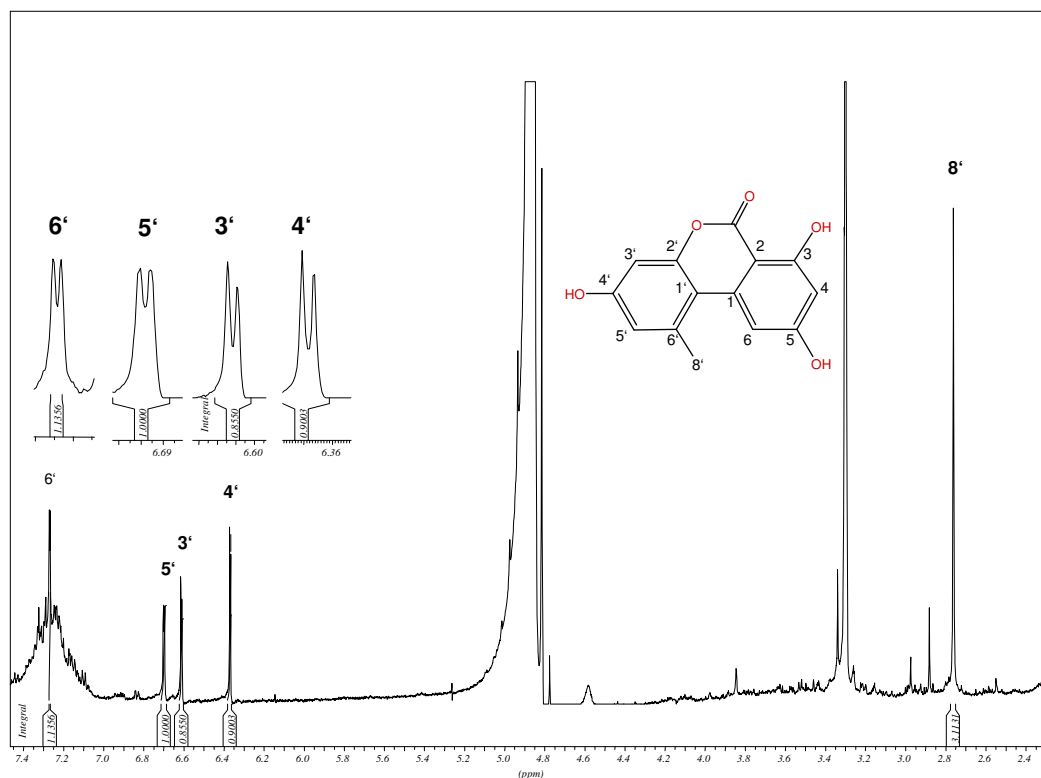


Figure 3.78 ^1H NMR spectrum of compound **26** (CD_3OD , 500 MHz)

Compound **26** was identified as alternariol because the splitting patterns, coupling constants and the chemical shifts were found to be similar with published data for alternariol (Onocha *et al.*, 1995).

Table 3.32 NMR data of compound **26** (alternariol)

Position	δ H (ppm) multiplicity (<i>J</i> in Hz) (in CD ₃ OD)	δ H (ppm) multiplicity (<i>J</i> in Hz) (Onocha <i>et al.</i> , 1995 in CDCl ₃)
4	6.37 (1H, d, 2.2)	6.41 (1H, d, 1.7)
6	7.27 (1H, d, 2.2)	7.30 (1H, d, 1.7)
3'	6.61 (1H, d, 2.2)	6.65 (1H, d, 2.2)
5'	6.70 (1H, d, 2.2)	6.74 (1H, d, 2.2)
8'-CH ₃	2.76 (3H, s)	2.66 (3H, s)

3.10 Secondary metabolites of the fungus *Paraphaeosphaeria michotii*

Paraphaeosphaeria michotii was isolated from the Mediterranean sponge *Petrosia ficiformis*. Five metabolites were isolated, including 3,4,8-trihydroxy 1-tetralone (compound **27**), cyclophenol (compound **16**), cyclophenin (compound **17**), viridicatol (compound **18**) and viridicatin (compound **19**).

Table 3.33 Biological test result of *P. michotii* and its metabolite

Sample	Antimicrobial assay				L5178Y growth (%) Conc. 10 μ g/mL	EC ₅₀ (μ g/mL)
	BS	SC	CC	CH		
Ethyl acetate extract of <i>Paraphaeosphaeria michotii</i>	-	-	-	-	21.8	
3,4,8-trihydroxy 1-tetralone						

BS = *Bacillus subtilis*, SC = *Saccharomyces cerevisiae*, CC = *Cladosporium cucumerinum* and CH = *C. herbarum*

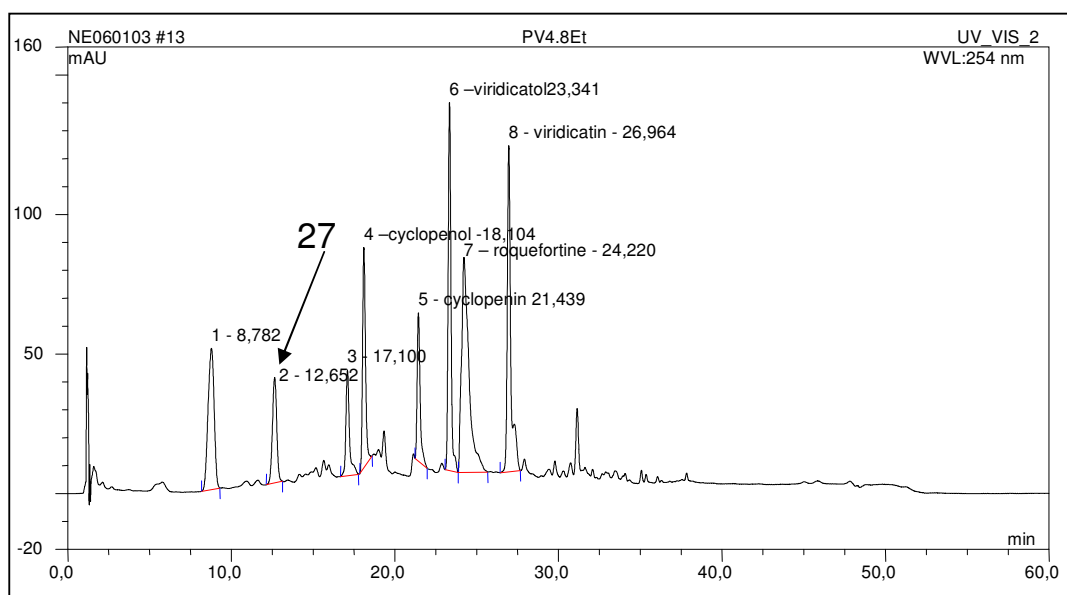
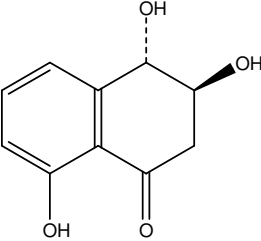
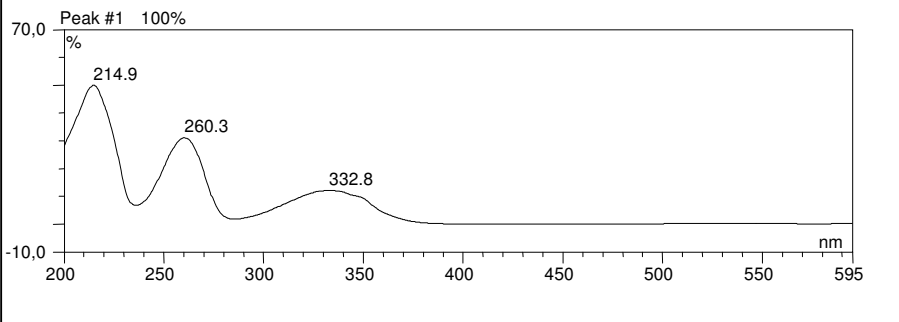
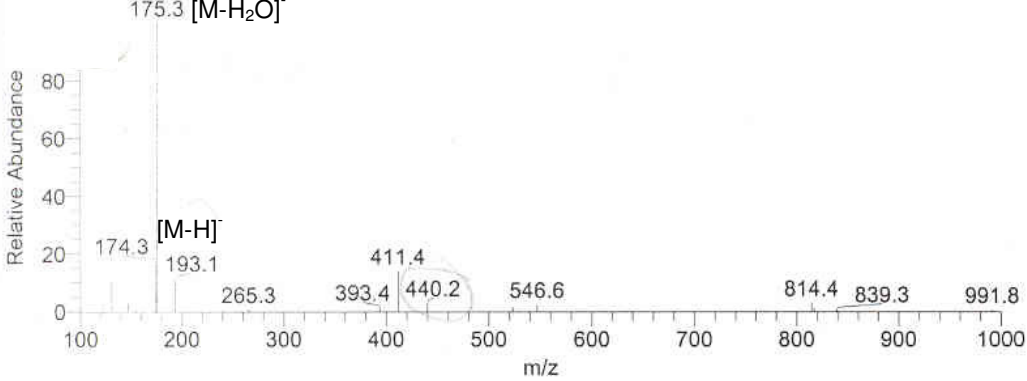


Figure 3.79 HPLC chromatogram of the ethyl acetate extract of *P. michotii*

3.10.1 Compound 27 (3,4,8-trihydroxy 1-tetralone)

Compound **27** (3,4,8-trihydroxy 1-tetralone) was isolated from the ethyl acetate extract of *Paraphaeosphaeria michotii* through semi preparative HPLC. Its UV spectrum exhibited maxima at $\lambda(\text{MeOH})$ 214.9, 260.3 and 332.8 nm. ESI-MS of compound **27** showed an intense peak at m/z 193 $[\text{M}-\text{H}]^-$ upon negative ionization revealing the molecular weight of 194 g/mol. Together with the inspection of ^1H and ^{13}C NMR spectra, a molecular formula of $\text{C}_{10}\text{H}_{10}\text{O}_4$ was suggested.

The ^1H and ^{13}C NMR spectra [figure 3.80 and 3.81] indicated the presence of a 1,2,3-trisubstituted aromatic ring, and one carbonyl carbon in the second ring to assemble a naphthalenone nucleus.

3,4,8-Trihydroxy 1-tetralone (compound 27)		
Sample Code Source Amount Molecular formula Characteristic Molecular weight Retention time Optical Rotation	: Z4PV4.8 : <i>Paraphaeosphaeria michotii</i> from <i>Petrosia ficiformis</i> : 2.0 mg : C ₁₀ H ₁₀ O ₄ : dark yellow powder : 194 g/mol : 12.9 min : $[\alpha]_D^{20} -5$ (c 0.1, CHCl ₃)	
		
<p>ine155 #212 RT: 6.28 AV: 1 NL: 3.74E5 T: -c ESI sid=25.00 Full ms [100.00-1000.00] 175.3 [M-H₂O]</p> 		

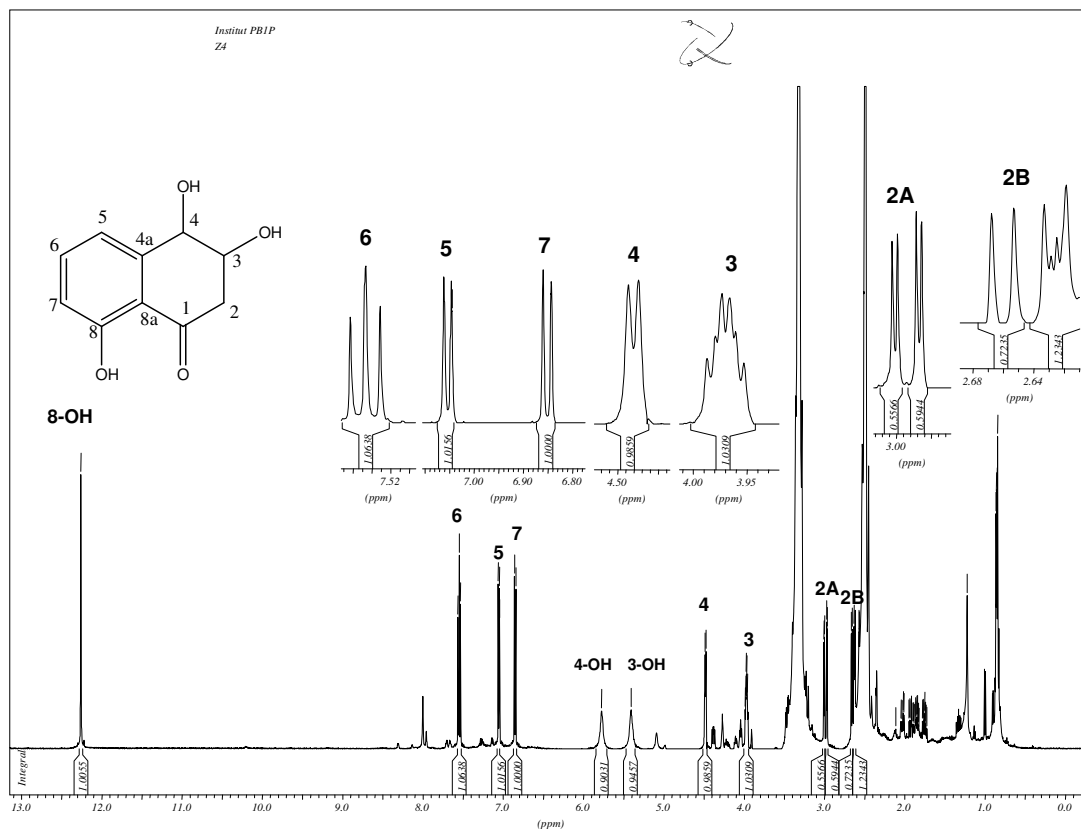


Figure 3.80 ^1H NMR spectrum of compound **27** (DMSO, 500 MHz)

In the ^1H NMR spectrum [figure 3.80], three aromatic protons were observed at 6.95 (H-7), 7.15 (H-5) and 7.65 ppm (H-6). In addition, three hydroxyl groups resonated as singlets at 5.51 (3-OH), 5.87 (4-OH) and 12.36 ppm (8-OH). The latter appeared as sharp singlet in the downfield region due chelating with the carbonyl group in β -position. Finally, a spin system consisting of a methylene group as well as two methine protons residing at oxygenated carbon atoms was detected, which was evident from signals at 2.64 and 2.99 ppm (H₂-2), exhibiting a large geminal coupling, and at 3.97 (H-3) and 4.58 ppm (H-4), respectively.

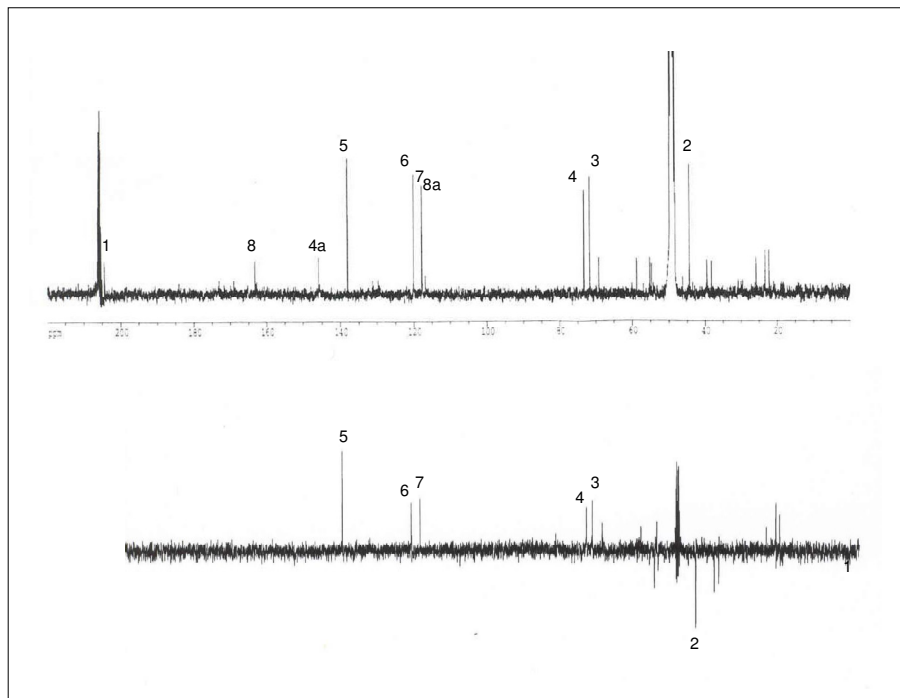


Figure 3.81 ^{13}C NMR and DEPT spectra of compound **27** (CD_3OD , 400 MHz)

The ^{13}C NMR and DEPT spectra [figure 3.81] showed that compound **27** possessed 10 carbon atoms, including one methylene group, five methine groups, and four quaternary carbon atoms. One carbonyl carbon (C-1) was detected at 204.3 ppm, while the remaining quaternary carbons were observed at the δ 163.2 (C-8), 145.8 (C-4a) and 117.8 (C-8a). C-8a was shifted more upfield due to the influence of both the carbonyl as well as the phenolic hydroxyl group in the two α -positions.

The methine carbons in the aromatic ring were observed at the typical chemical shifts δ 138.0 (C-5), 120.0 (C-6) and 117.8 (C-7), and the methylene carbon (C-2) was detected in the upfield region at δ 44.3 ppm.

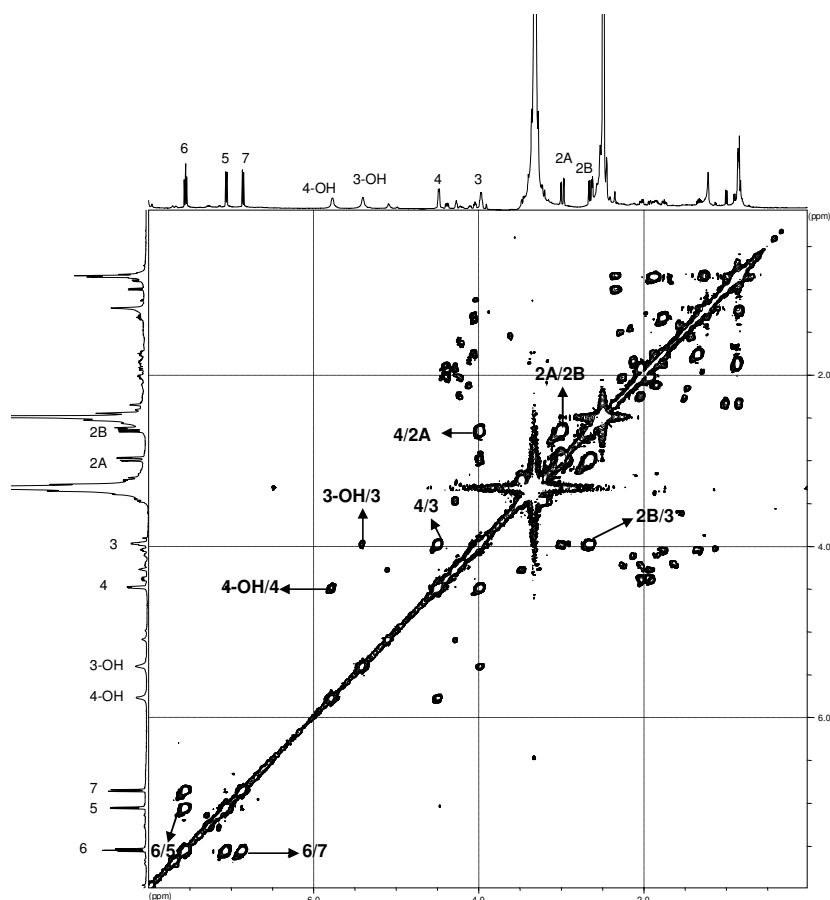


Figure 3.82 COSY spectrum of compound **27** (DMSO, 500 MHz)

In the HMBC spectrum [figure 3.83], there were two correlations between H-5 to C-4 and H-4 to C-6 which confirmed the linkage between the 1,2,3-trisubstituted phenyl ring and the 3,4-dihydroxycyclohexanone ring.

Compound **27** was identified as 3,4,8-trihydroxy 1-tetralone fundamentally based on comparison with NMR data [Table 3.32] of 3,4,8-trihydroxy 1-tetralone reported by Borgschulte *et al.* (1991). The measured optical rotation of compound **27** was -5° , whereas the optical rotation previously reported in the literature (Iwasaki *et al.*, 1971) was -36° suggesting both compounds to have the same absolute configuration.

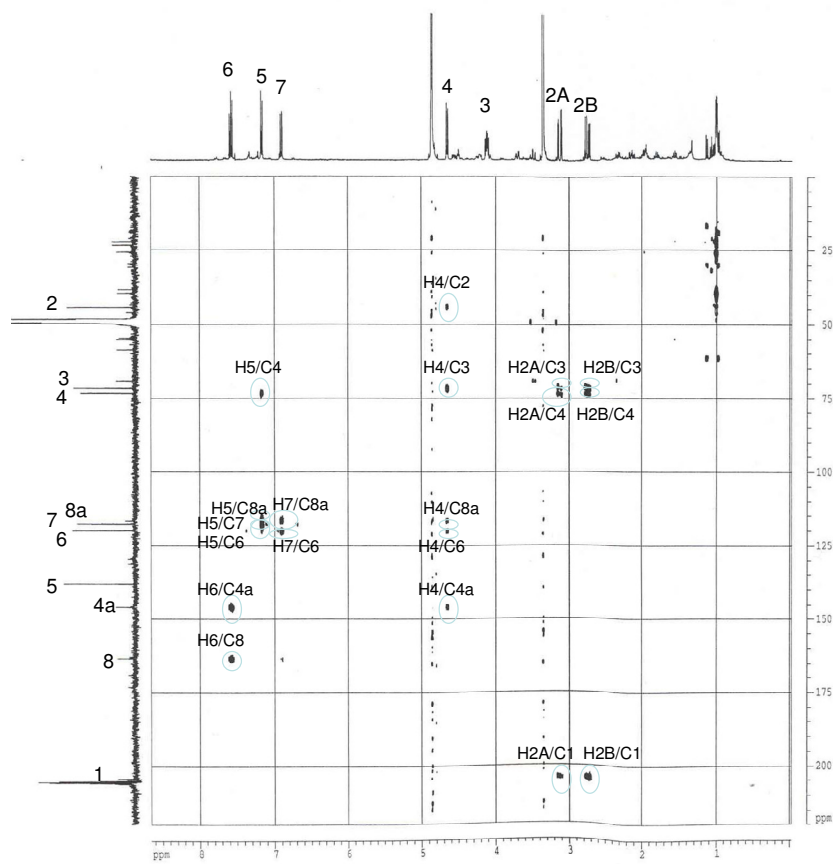


Figure 3.83 HMBC spectrum of compound **27** (CD₃OD, 400 MHz)

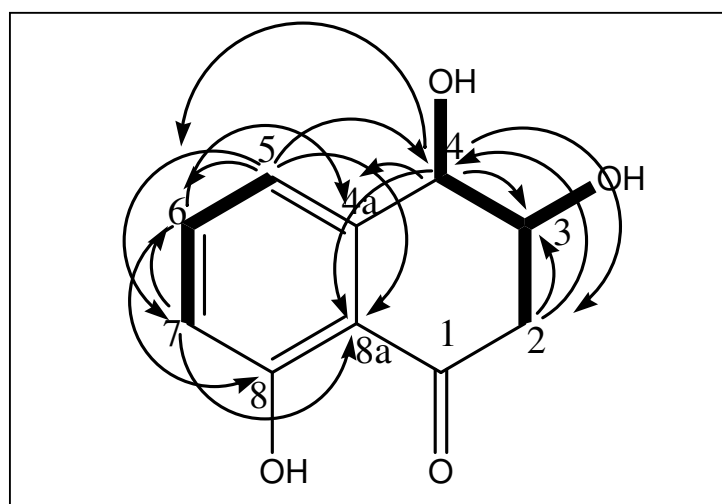


Figure 3.84 COSY and HMBC correlations of compound **27** (3,4,8-trihydroxy 1-tetralone)

Table 3.34 NMR data of compound **27** (3,4,8-trihydroxy 1-tetralone)

Position	δ H (ppm) multiplicity (<i>J</i> in Hz) (in DMSO)	δ C (ppm) (in DMSO)	δ H (ppm) (Borgschulte <i>et al.</i> , 1991 in CD ₃ OD)	δ C (Borgschulte <i>et al.</i> , 1991 in CD ₃ OD)	HMBC (CD ₃ OD)
1		204.3		204.3	
2	2.99 (1H,dd,17.0,3.8) 2.64 (1H,dd,17.3,7.3)	44.3	3.12 (1H,dd,17.2,4.0) 2.74(1H,dd,17.2,8.1)	44.4	1,3,4
3	3.97 (1H,dd,6.9,17.0)	71.7	4.12 (1H,ddd,8.1,6.8,4.0)	71.7	
3-OH	5.51 (1H,s)				
4	4.58 (1H, d, 6.0)	73.2	4.65 (1H,d,6.8)	73.3	2,3,4a,6,8a
4-OH	5.87 (1H,s)				
4a		145.8		140.0	
5	7.15 (1H,dd, 7.6,1.0)	138.0	7.17 (1H,d,7.6)	120	4,6,7,8a
6	7.65 (1H,t, 7.6)	120.0	7.58 (1H,dd,8.4,7.6)	117.7	4a,8
7	6.95 (1H,d, 8.2)	117.8	6.91 (1H,bd,8.4)	137.9	6,8a
8		163.2		163.2	
8-OH	12.36 (1H,s)				
8a		117.8		145.85	

3.11 Isolated secondary metabolites of the fungus *Nodulisporium* sp.

Nodulisporium sp. was isolated from the marine alga *Halimeda bornealis* collected from the Java Sea. Compound **28** (4,4',5,5'-tetrahydroxy-1,1'-binaphthyl) was major compound isolated from this fungus.

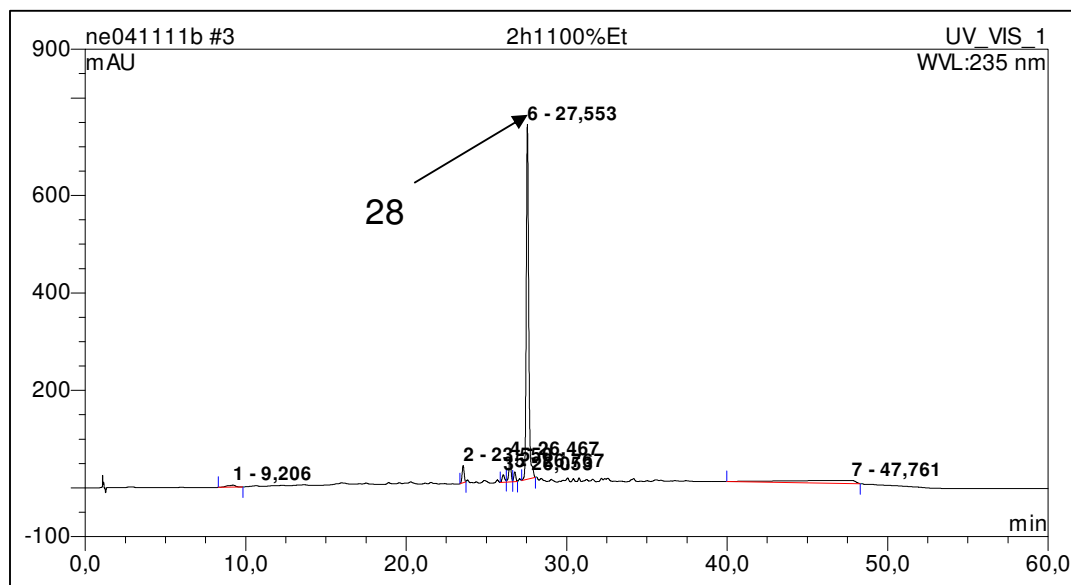


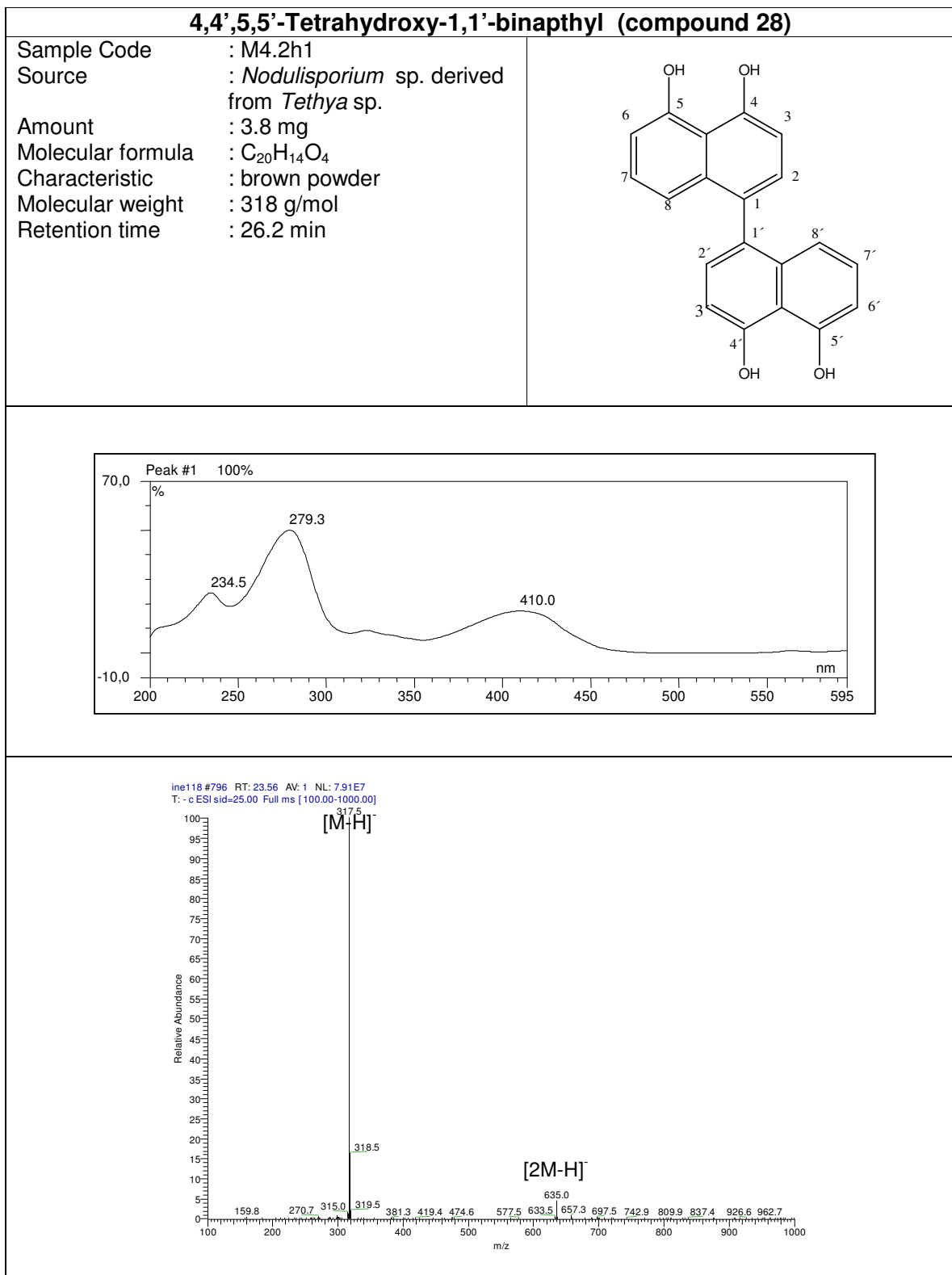
Figure 3.85 HPLC chromatogram of the ethyl acetate extract of *Nodulisporium* sp.

Table 3.35 Biological test result of *Nodulisporium* sp. and its metabolite

Sample	Antimicrobial assay				L5178Y growth (%) Conc. 10 µg/mL	EC ₅₀ (µg/mL)
	BS	SC	CC	CH		
Ethyl acetate extract of <i>Nodulisporium</i> sp.	-	-	-	-	0.2	
4,4',5,5'-tetrahydroxy-1,1'-binaphthyl					0.1	1.8

BS = *Bacillus subtilis*, SC = *Saccharomyces cerevisiae*, CC = *Cladosporium cucumerinum* and CH = *C. herbarum*

3.11.1 Compound 28 (4,4',5,5'-Tetrahydroxy-1,1'-binaphthyl)



Compound **28** (4,4',5,5'-tetrahydroxy-1,1'-binaphthyl) was isolated from the ethyl acetate extract of *Nodulisporium* sp. through Sephadex LH-20 column chromatography using 100% methanol, followed by semi preparative HPLC. UV maxima of compound **28** were at λ_{max} (MeOH) 226.4, 302.8 and 332.9 nm. Its ESI-MS showed a molecular ion peak at m/z 317 (M-H^-) upon negative ionization, suggesting a molecular weight of 318 g/mol.

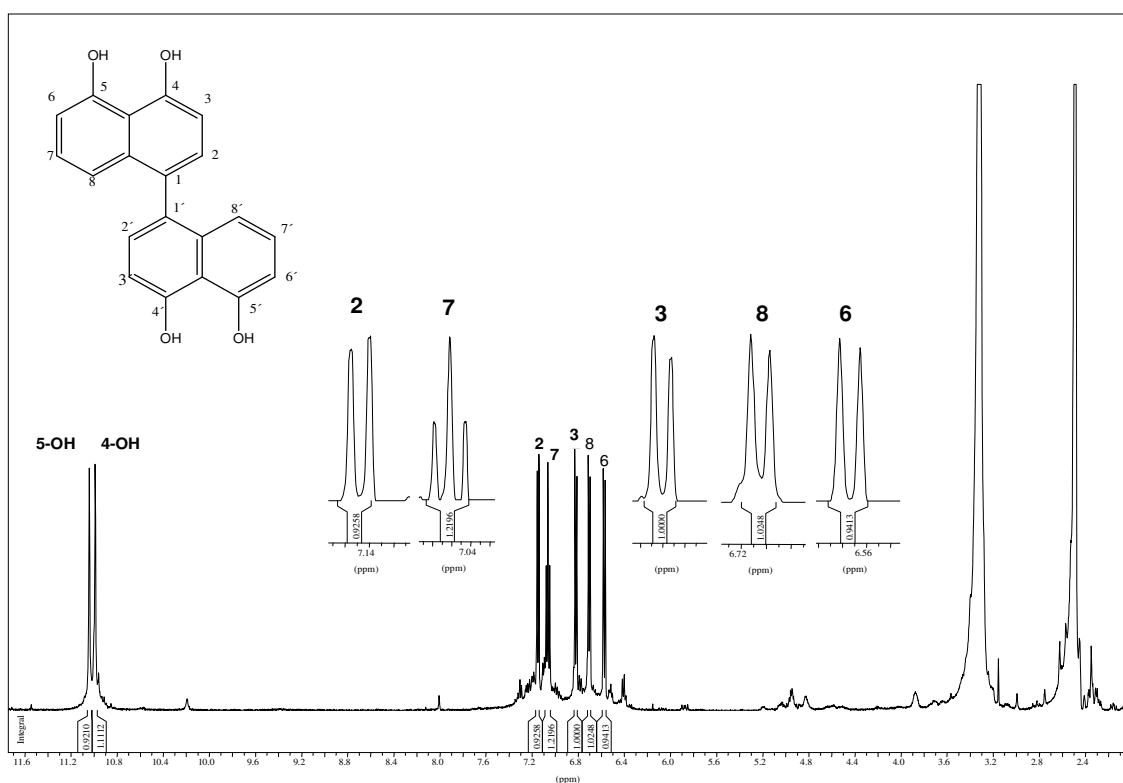


Figure 3.86 ^1H NMR spectrum of compound **28** (DMSO , 500 MHz)

In the ^1H NMR spectrum [figure 3.86] there were five signals of aromatic protons, and two singlets for hydroxyl groups in downfield region at δ 10.99 and 11.04. Based on a comparison with the molecular weight, the compound was thus identified as a symmetrical dimer.

In the COSY Spectrum [figure 3.87], two spin systems were observed, one ABC and one AB system. The AB aromatic spin system which belonged to a 1,2,3,4-substituted phenyl ring was constructed by protons H-2 at δ 7.15 (1H,dd,7.9 Hz) and H-3 at δ 6.82 (1H,d,7.9 Hz), whereas the ABC spin system was part of a 1,2,3-trisubstituted aromatic ring, and was assembled by protons H-6 at δ 6.57 (1H,d,8.5 Hz), H-7 at δ 7.06 (1H,t,8.5 Hz) and H-8 at δ 6.70 (1H,d,7.6 Hz).

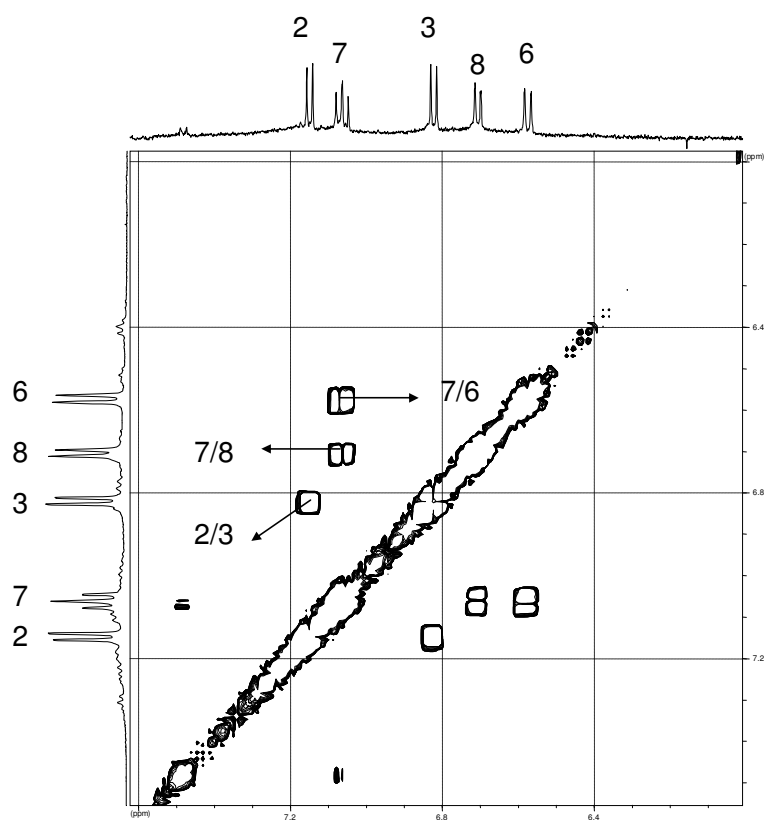


Figure 3.87 COSY spectrum of compound **28** (DMSO, 500 MHz)

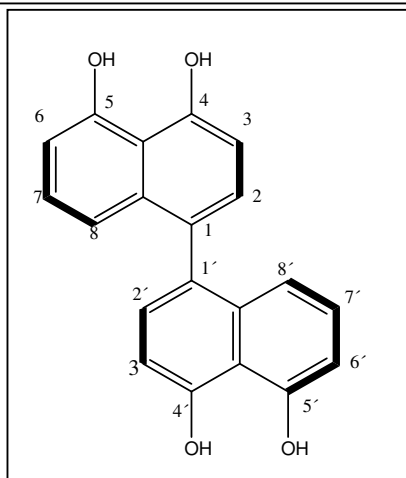


Figure 3.88 COSY correlations of compound **28** (4,4',5,5'-tetrahydroxy-1,1'-binaphthyl)

Compound **28** was identified as 4,4',5,5'-tetrahydroxy-1,1'-binaphthyl based on the comparison of its NMR data with NMR data of 5,5'-dimethoxy-1,1'-binaphthyl-4,4'-diol (Hashimoto *et al.*, 1994). The difference of the latter to **28** consisted in the presence of two methoxy groups at position 5 and 5' instead of hydroxy functions.

Table 3.36 NMR data of compound **28** (4,4',5,5'-tetrahydroxy-1,1'-binaphthyl)

Position	δ H (ppm) multiplicity (J in Hz) (in DMSO)
2, 2'	7.15 (2H, d, 7.9)
3, 3'	6.82 (2H, d, 7.9)
4-OH, 4'-OH	10.99 (1H, s)
5-OH, 5'-OH	11.04 (1H, s)
6, 6'	6.57 (1H, d, 8.5)
7, 7'	7.06 (1H, t, 8.5)
8, 8'	6.70 (1H, d, 7.6)

3.11 Isolated secondary metabolites of the fungus *Talaromyces wortmanii*.

The fungus *Talaromyces wortmanii* was isolated from the marine sponge *Aplysina aerophoba* collected from the Mediterranean Sea. Two metabolites were successfully isolated from this fungus. They were atrovirin B1 (compound **29**), atrovirin B2 (compound **30**) and skyrin (compound **31**).

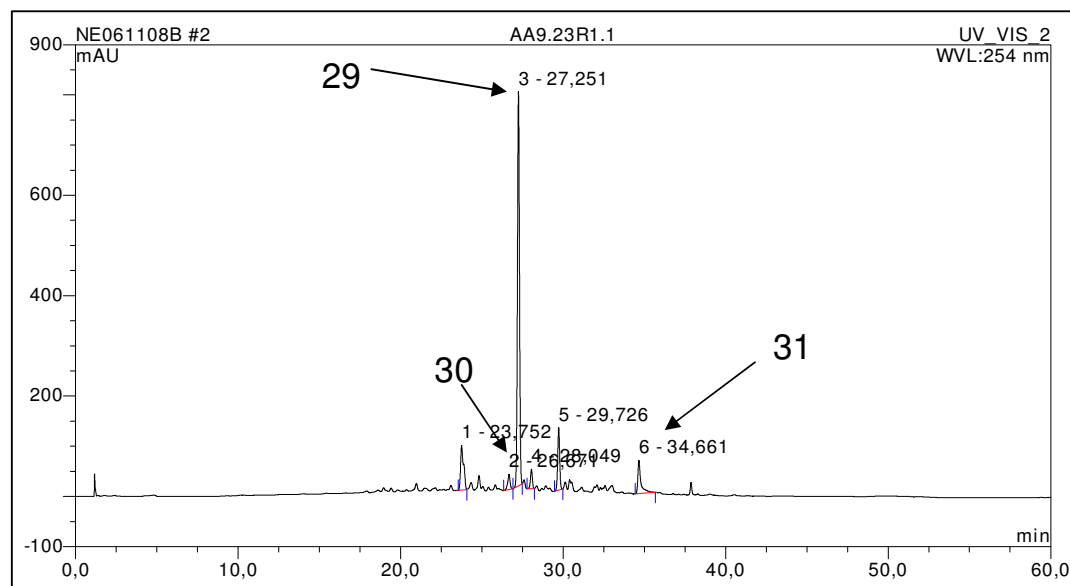


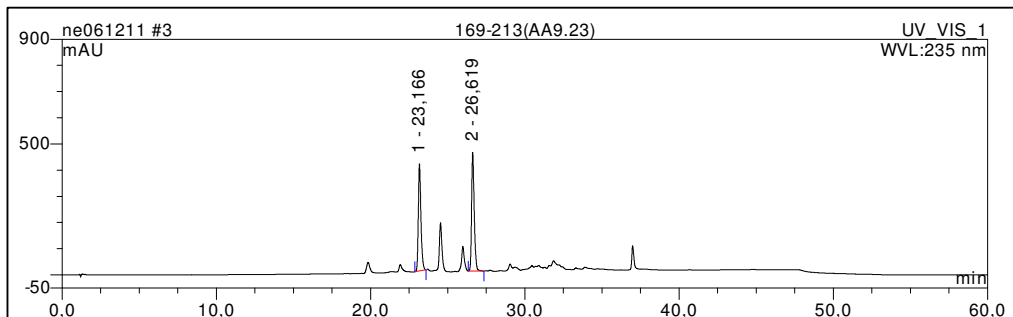
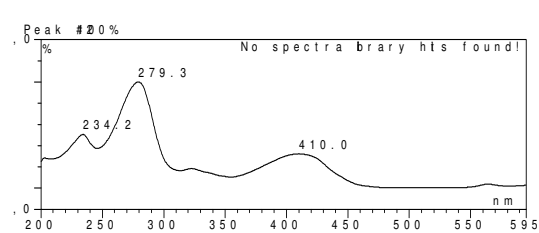
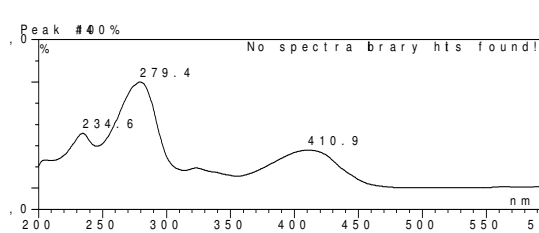
Figure 3.89 HPLC chromatogram of ethyl acetate extract of *Talaromyces wortmanii*

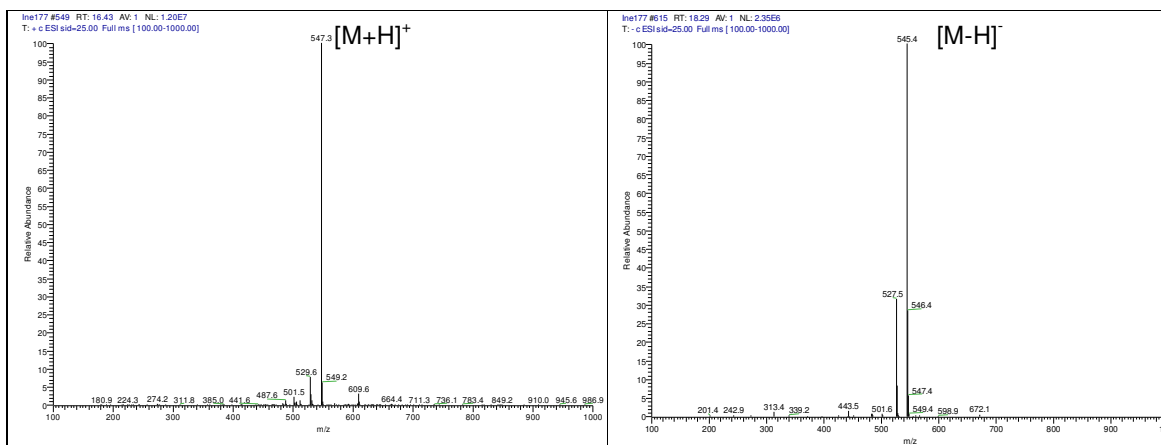
Table 3.37 Biological assays of *Talaromyces wortmanii* extract and its derived metabolites

Sample	Antimicrobial assay				L5178Y growth (%) Conc. 10 µg/mL	EC ₅₀ (µg/mL)
	BS	SC	CC	CH		
Ethyl acetate extract of <i>Talaromyces wortmanii</i>	-	-	-	-	85.7	
Atrovirin B					90.9	
Skyrin					98.7	

BS = *Bacillus subtilis*, SC = *Saccharomyces cerevisiae*, CC = *Cladosporium cucumerinum* and CH = *C. herbarum*

3.11.1 Compound 29 (atrovirin B1) and compound 30 (atrovirin B2)

Atrovirin B1 and B2 (compound 29 and 30)	
<p>Sample Code : AA9.23.2a and AA9.23.2b</p> <p>Source : <i>Talaromyces wortmanii</i> derived from <i>Aplysina aerophoba</i></p> <p>Amount : 3.8 mg</p> <p>Molecular formula : C₃₀H₂₆O₁₀</p> <p>Characteristic : brown powder</p> <p>Molecular weight : 546 g/mol</p> <p>Retention time : 26.6 min (atrovirin B2) 23.2 min (atrovirin B1)</p> <p>Optical rotation : $[\alpha]_D^{20} +5^\circ$ (c 0.02, CHCl₃)</p>	 <p>atrovirin B1</p> <p>atrovirin B2</p>
	
 <p>atrovirin B1</p>	 <p>atrovirin B2</p>



Compounds **29** (atrovirin B1) and **30** (atrovirin B2) were isolated as an inseparable mixture from the ethyl acetate extract of *Talaromyces wortmanii* through vacuum liquid chromatography (VLC), followed by Sephadex LH-20 column chromatography using methanol 100%. UV maxima of compound **29** were at λ_{\max} (MeOH) 234.5, 279.3 and 410.0 nm, whereas those of compound **30** were 234.7, 279.5 and 410.6 nm. Their ESI-MS showed molecular ion peaks at m/z 539 $[M+H]^+$ upon positive ionization and at m/z 537 $[M-H]^-$ upon negative ionization, indicating a molecular weight of 538 g/mol.

Based on the structure, atrovirin B1 was C-3 diastereomer of atrovirin B2. Both atrovirin B1 and B2 had molecular weight of 546 g/mol and showed atropisomerism. In the ^1H NMR spectrum [figure 3.90], the complete signals of both diastereomers were observed and proven by the integration. Most signals of both diastereomers were detected overlapping at the same chemical shifts, whereas the signal of the methyl groups at position C3 (3- H_3) had slightly different chemical shifts (δ_{H} 1.37 and 1.38 ppm).

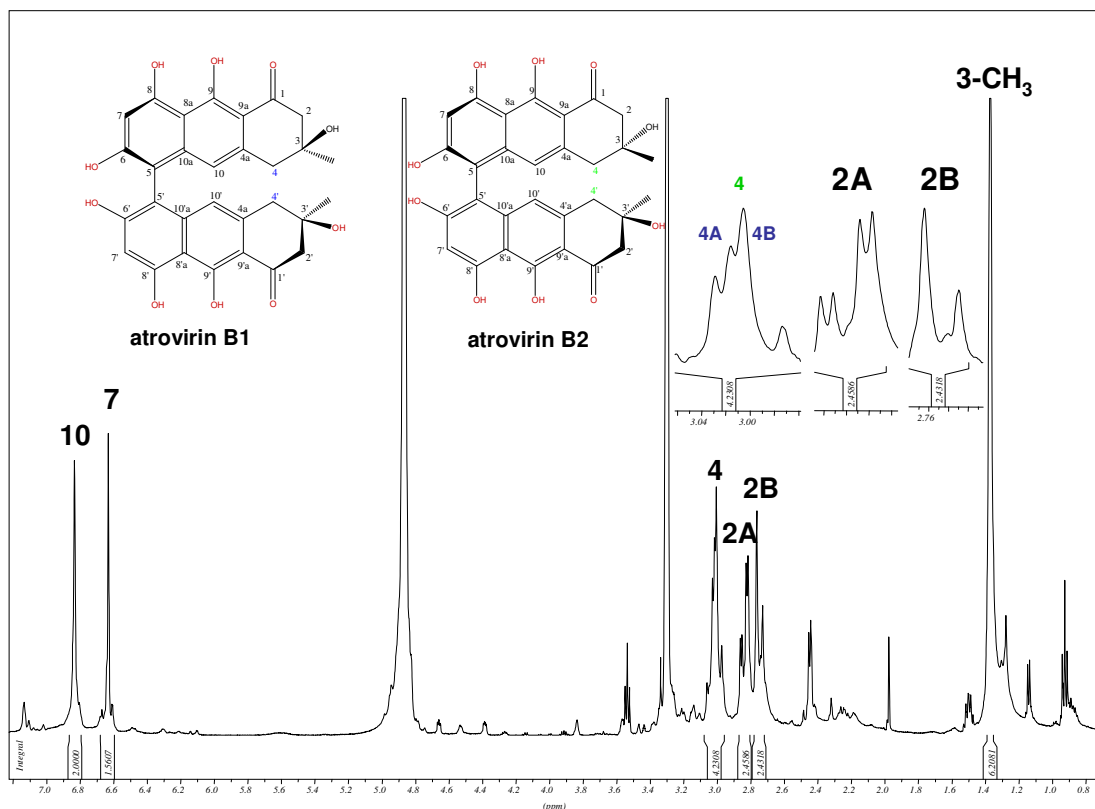
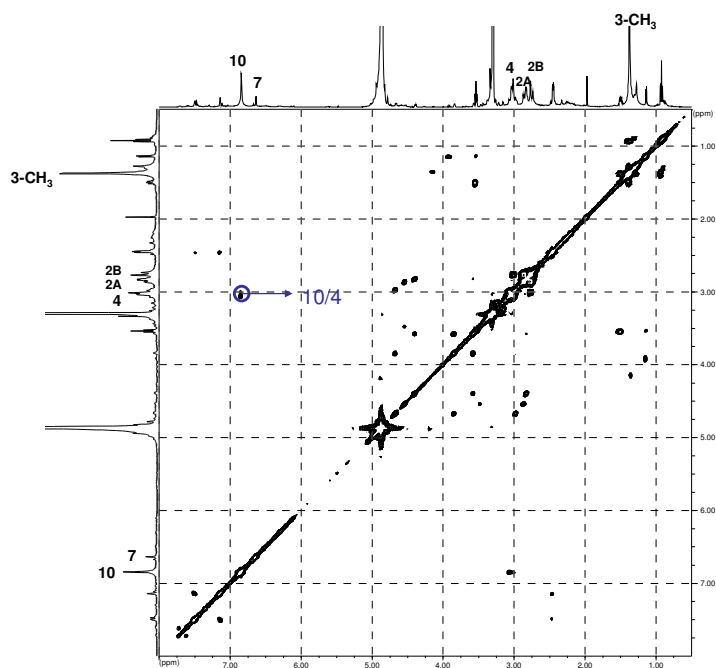
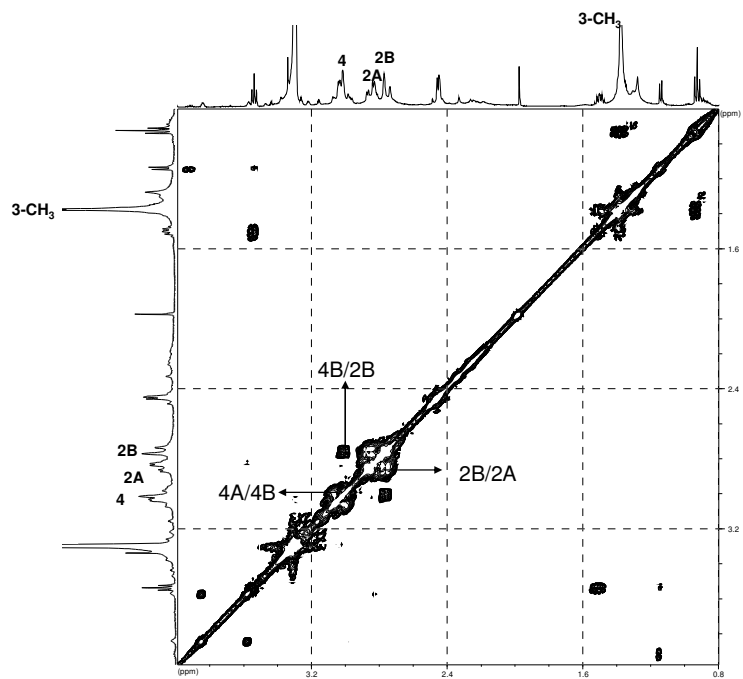


Figure 3.90 ^1H NMR spectrum of compound **29** and **30** (CD_3OD , 500 MHz)

In the ^1H NMR spectrum [figure 3.90], two aromatic protons from the different phenyl rings were detected as singlets at the chemical shifts δ 6.63 ppm (H-7,2H,s) and 6.83 ppm (H-10,2H,s). Compound **29** and **30** had two methylene groups H_2 -2 and H_2 -4. The methylene group H_2 -2 of both compounds appeared at the chemical shifts δ 2.84 ppm (1H, dd,17.4 and 5.4 Hz), and 2.78 ppm (d,17.4 Hz). The other methylene group H_2 -4 of atrovirin B1 was observed at δ 3.09 and 2.99 ppm, whereas H_2 -4 of atrovirin B2 appeared at the chemical shift of 3.01 ppm as singlet. The correlations between H-10, H_2 -4 and H_2 -2 were showed in the COSY spectrum [figure 3.91A and B].

Figure 3.91A COSY spectrum of compound **29** and **30** (CD₃OD, 500 MHz)Figure 3.91B COSY spectrum of compound **29** and **30** (CD₃OD, 500 MHz)

Gill and Morgan (2004) explained that H₂₋₄ of atrovirin B2 appeared as a broad two proton singlet at δ_{H} 2.87 ppm, whereas H₂₋₄ of atrovirin B1 was detected as an AB quartet and well separated at δ_{H} 2.95 and 2.73 ppm. Proton H4A and H4B of both atrovirins were unperturbed by the anisotropic influence of the adjacent aromatic rings resulting of anisotropic shielding depending on their stereochemistry to C-5 aromatic residue. In atrovirin B1, equatorial proton at methylene C-4 was more vulnerable to the shielding effects of the aromatic rings than its axial neighbour due to S chirality at C-3 stereogenic center. While in atrovirin B2, the shielding effect of both protons were equal due to R chirality at C-3 stereogenic center (Gill, 1999; Gill and Morgan, 2004).

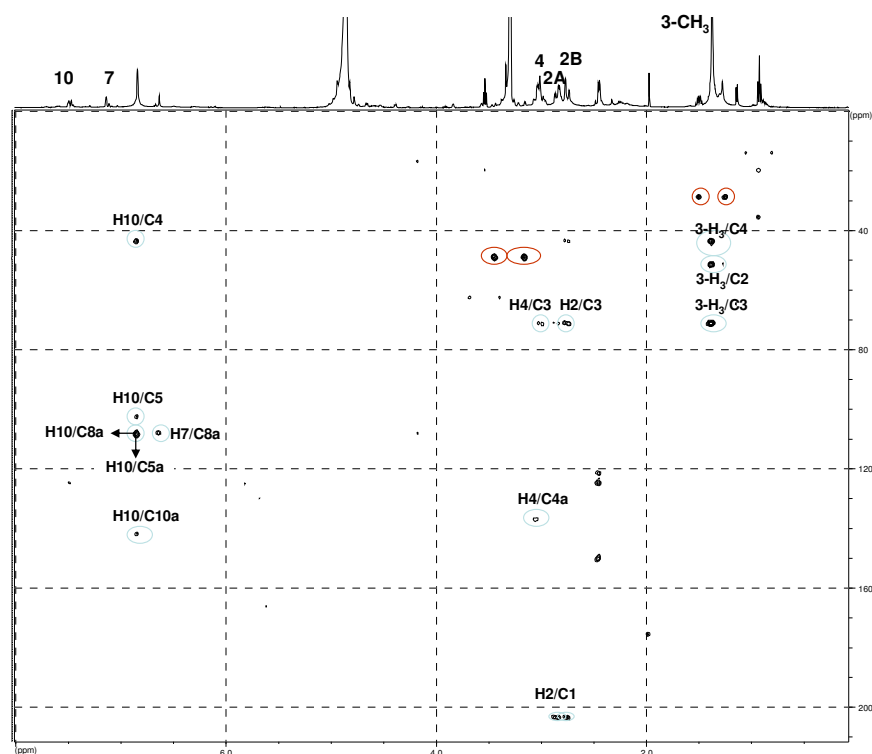


Figure 3.92 HMBC spectrum of compound **29** and **30** (CD₃OD, 500 MHz)

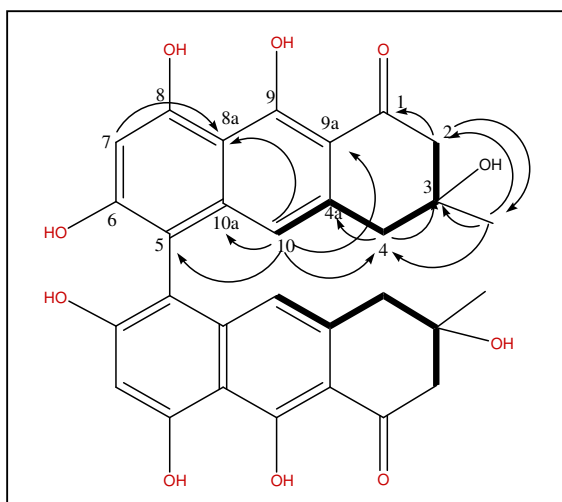


Figure 3.93 HMBC and COSY correlations of compound **29** (atrovirin B1) and **30** (atrovirin B2)

In the HMBC spectrum [figure 3.92], all correlations detected confirmed the proposed structure. The correlation between H-10 and C-5, H-10 and C-4 confirmed the position of C-10 in the second aromatic ring which was located in between the first phenyl ring represented by C-5 and cyclohexanone ring represented by C-4.

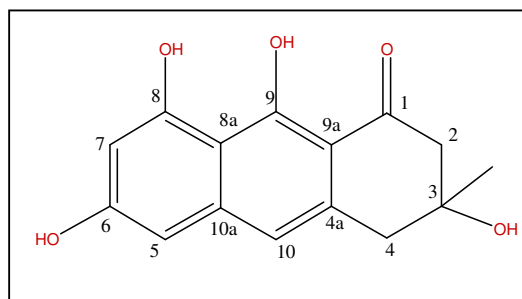
Table 3.38 NMR data of compound **29** (atrovirin B1) and compound **30** (atrovirin B2)

Position	δ H (ppm) multiplicity of compound 29 (J in Hz) (in CD ₃ OD)	δ H (ppm) multiplicity of compound 30 (J in Hz) (in CD ₃ OD)	δ C (ppm) of compound 29 and 30 (in CD ₃ OD)	HMBC
1, 1'			203.2	
2, 2'	2.84 (2H,dd,17.4,5.4) ^a 2.78 (2H,d,17.4) ^a	2.84 (2H,dd,17.4,5.4) ^a 2.78 (2H,d,17.4) ^a	51.4	1,3
3, 3'			71.1	
3-OH, 3'-OH				
3-Me 3'-Me	1.38 (6H,s)	1.37 (6H,s)	29.2	2,3,4
4, 4'	3.02 (2H,m) ^b 2.99 (2H,m) ^b	3.01 (4H,s)*	43.6	3,4a
4a, 4'a			137.2	
5, 5'	-	-	102.5	
6, 6'				
6-OH, 6'-OH				
7, 7'	6.63 (2H,s) ^c	6.63 (2H,s) ^c		8a
8, 8'				
8-OH, 8'-OH				
8a, 8'a			108.1	

9, 9'				
9-OH, 9'-OH				
9a, 9'a			108.5	
10, 10'	6.83 (2H,bs) ^d	6.83 (2H,bs) ^d		4,5,9a, 10a
10a, 10'a			143.2	

a,b,c,d : overlapping signals

Atrovirin B1 and B2 were dimers of dihydroanthracenone (Gill and Gimenez, 1991). Compound **29** and compound **30** were substantially identified as atrovirin B1 and atrovirin B2 based on the comparison of its NMR data with the chemical shifts, multiplicity and coupling constants of anthracenone (Gill and Gimenez, 1991). Other evidence came from the integration, mass spectra and comparison of UV spectra with atrovirin B1 and B2 published in the literature (Antonowitz *et al.*, 1994)

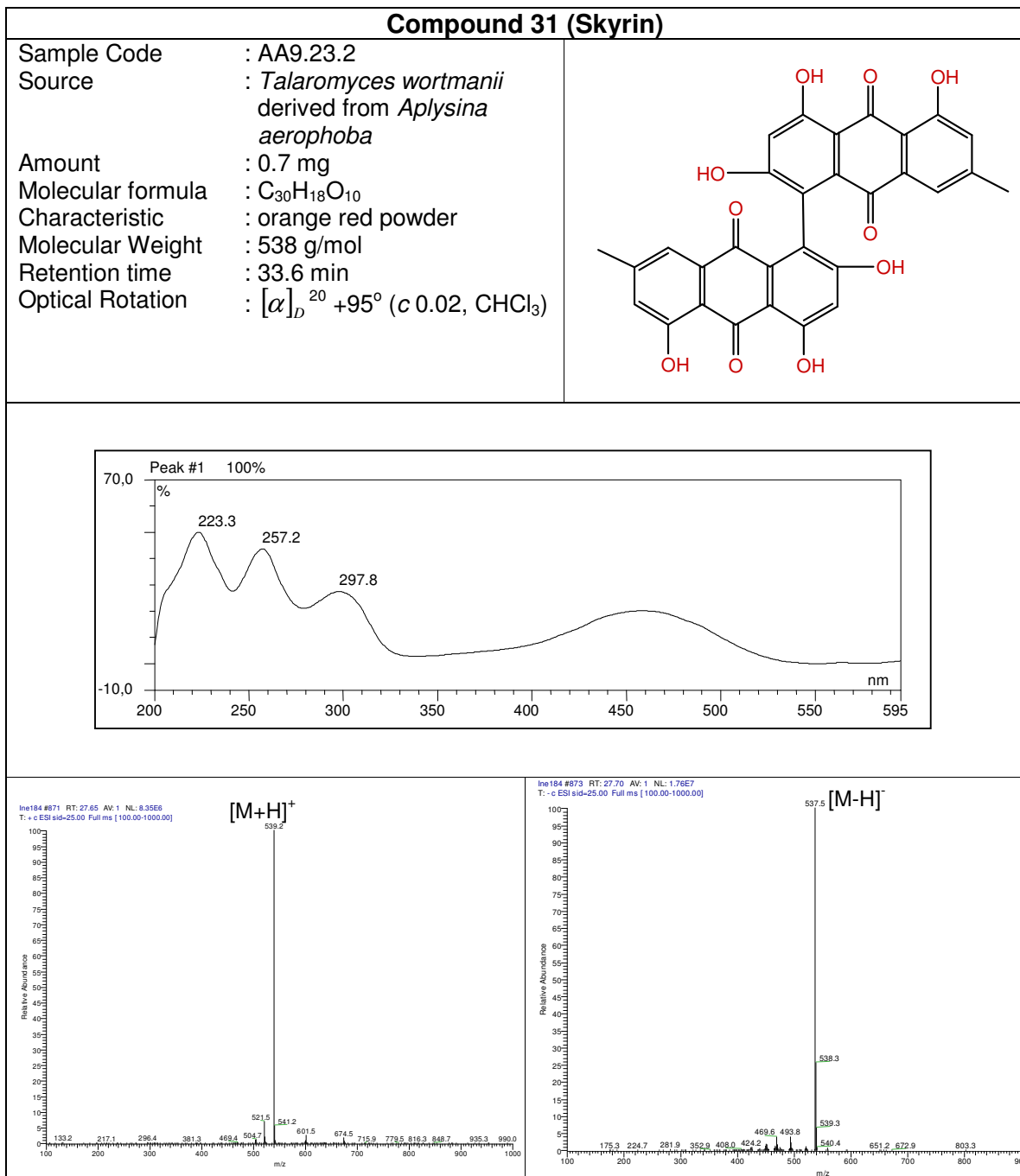


anthracenone

3.11.2 Compound 31 (Skyrin)

Compound **31** (skyrin) was a compound isolated from the ethyl acetate extract of the fungus *Talaromyces wortmanii* through vacuum liquid chromatography (VLC) and Sephadex LH-20 column chromatography. UV maxima of compound **31** were at λ_{\max} (MeOH) 223.3, 257.2 and 297.8 nm. In the ESI mass spectrum, a prominent $[M+H]^+$ pseudomolecular ion was observed at m/z 539 upon positive ionization, together with

an intense $[M-H]^-$ at m/z 537 upon negative ionization which indicated a molecular weight of 538 g/mol.



There were only seven proton signals observed in the ^1H NMR spectrum [figure 3.94], which did not account for the number of signals estimated for a molecular weight of 538 g/mol. Thus, it was concluded that compound **31** was a symmetrical dimer.

The ^1H NMR spectrum [figure 3.94] showed a pair of meta coupled protons which were at 7.14 ppm (H-2,H-2',1.0 Hz) and 7.27 (H-4,H-4',d,1.0 Hz) showing correlations in the HMQC spectrum [figure 3.96] to carbons at δ_{C} 123.4 and 120.3. Another aromatic proton was also observed at δ_{H} 6.71 ppm (H-7,H-7',s) and δ_{C} 106.9 based on the HMQC spectrum [figure 3.96].

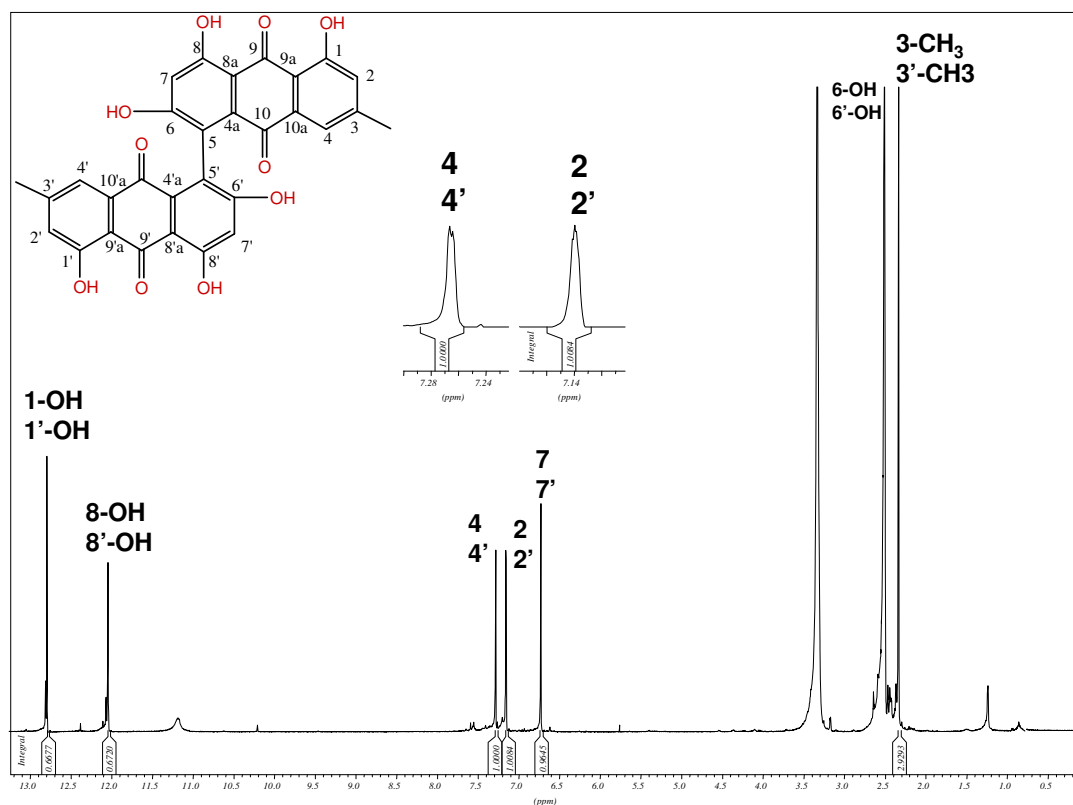


Figure 3.94 ^1H NMR spectrum of compound **31** (DMSO, 500 MHz)

Three hydroxyl groups were detected in the ^1H NMR spectrum [figure 3.94] at δ_{H} 12.77 (1-OH), 12.03 (8-OH) and 2.49 (6-OH). The hydroxyl groups at positions 1 and 8 appeared as sharp singlets and were located in the upfield region due to chelatisation with the keto group in β -position.

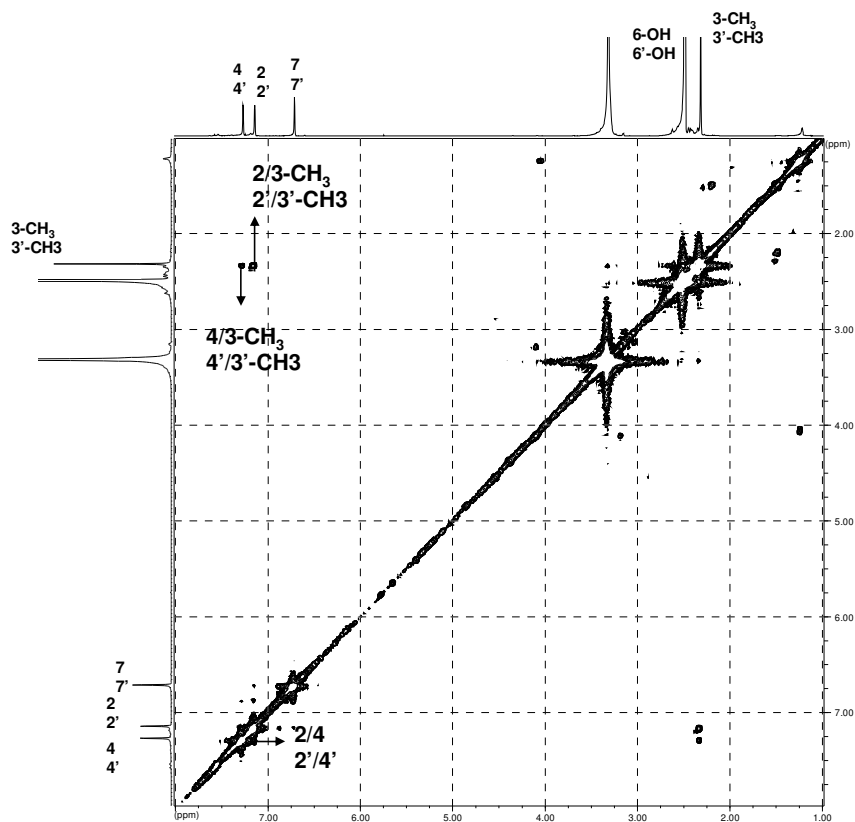
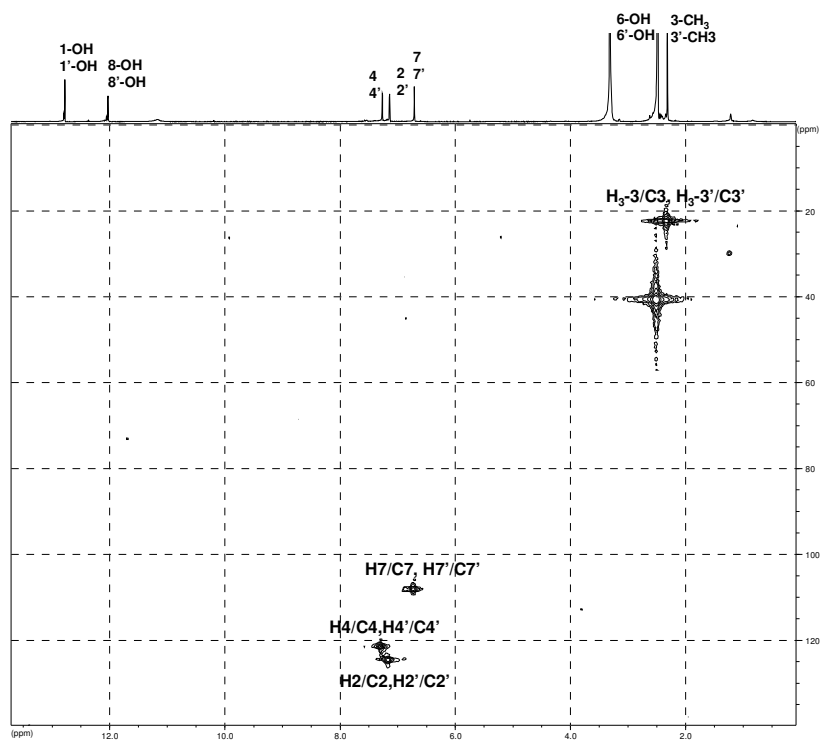
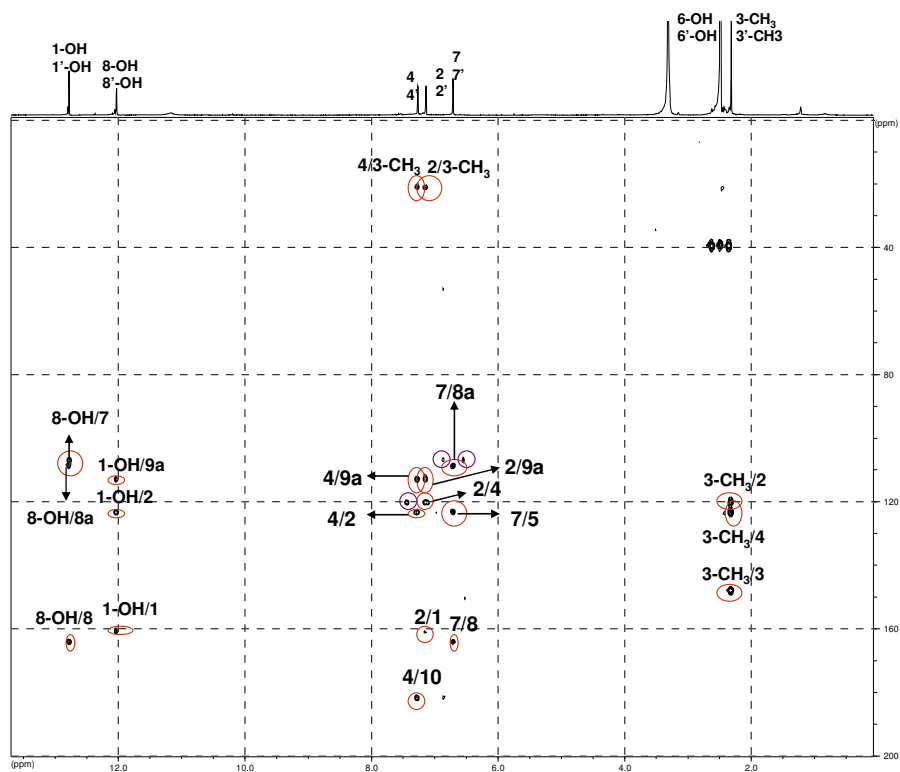
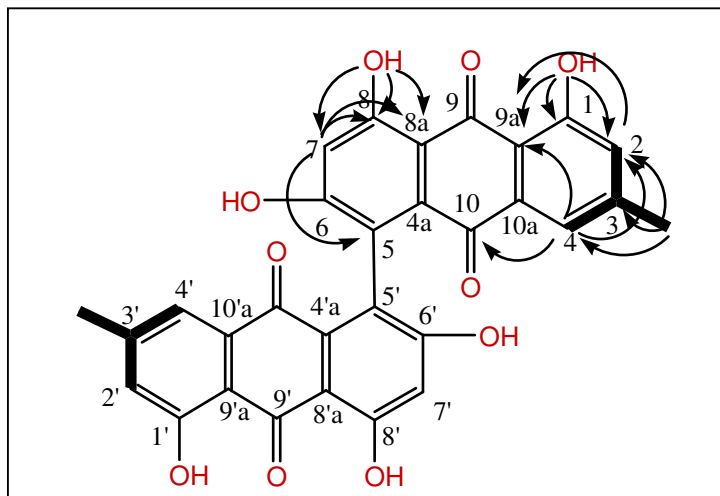


Figure 3.95 COSY spectrum of compound **31** (DMSO, 500 MHz)

A methyl group situated at an aromatic ring was detected at 2.32 ppm ($\text{H}_3\text{-3}, \text{H}_3\text{-3}'$) with the corresponding carbon resonating at 21.2 ppm, as evident from the HMQC spectrum [figure 3.96]. Long range correlations between $\text{H}_3\text{-3}$ and H-2 as well as H-4 were obvious from the COSY spectrum [figure 3.95]. In the HMBC spectrum [figure 3.97], correlations between H-7 and C-5 (and H-7' and C-5') were detected.

Figure 3.96 HMQC spectrum of compound **31** (DMSO, 500 MHz)Figure 3.97 HMBC spectrum of compound **31** (DMSO, 500 MHz)

Figure 3.98 HMBC and COSY correlation of compound **31** (skyrin)Table 3.39 NMR data of compound **31** (skyrin)

Position	δ H (ppm) multiplicity (J in Hz) (in CD ₃ OD)	δ H (ppm) multiplicity (J in Hz) (in DMSO)	δ C (ppm) (in DMSO)	HMBC
1-OH, 1'-OH		12.77 (2H,s)		1,2,9a
1			160.7	
2, 2'	7.02 (2H,d)	7.14 (2H,d,1.0)	123.4	1,3-CH ₃ ,4,9a
3, 3'			148.1	
3-CH ₃ , 3'-CH ₃	2.32 (6H,s)	2.32 (6H,s)	21.2	2,3,4
4, 4'	7.30 (2H,d)	7.27 (2H,d,1.0)	120.3	2, 3-CH ₃ ,9a,10
5,5'			122.9	
6-OH		2.49 (2H) ⁺		
7, 7'	6.65 (2H,s)	6.71 (2H,s)	106.9	5,8,8a
8,8'			164.2	
8a,8'a			109.0	
8-OH, 8'-OH		12.03 (2H,s)		7,8,8a
9a,9'a			113.2	
10,10'			181.6	

Compound **31** was identified as skyrin by comparison of its UV and NMR properties with data published in the literature (Cohen and Towers, 1995, and Fujitake *et al.*,1998).

Optical rotation of this compound was $[\alpha]_D^{20} +93^\circ$ (c 0.02, CHCl₃), whereas optical rotation of skyrin previously described in literature was $[\alpha]_D^{20} +105^\circ$ (c 0.4, dioxan) (Fujitake *et al.*,1997) suggesting both compounds have the same

stereochemistry. Even though the compound was totally symmetric and lacking any stereocenter, the optical rotation can be explained by the phenomenon of atropisomerism. In the case of skyrin, rotation around the axis between C-5 and C-5' was not possible because of the steric inhibition by the hydroxyl- and keto-groups in positions C-6, C-6', C-10 and C-10', resulting in the element of chirality to be located in this molecule axis.

4. RESULTS OF BIODIVERSITY DETERMINATION

4.1 Identification of fungi based on the DNA sequences of the ITS region

4.1.1 Optimization of fungal identification

Fungal identification was carried out based on the sequences amplified by primer pair ITS 1 and ITS 4 covering partial sequence of ITS 1, 5.8S rDNA, ITS2 and flanking region of 28S rDNA (“ITS region”). The optimization necessary for fungal identification method consisted of optimization in DNA isolation, evaluating of primers for amplification and optimization in PCR. Selecting annealing temperature, annealing time, concentration of primers and concentration of DNA template were included in the PCR optimization.

4.1.2 Optimization of fungal DNA isolation

Total DNA isolation of fungi was conducted using DNeasy plant mini kit (Qiagen, Hilden). Previously the isolation by phenol-chloroform was employed but replaced by the faster and environment friendly product as DNA isolation kit.

Before the lysis step, the mycelium had to be powderized in order to break the cell wall and cell membrane. The MixerMill showed good result compared to manual grinding using mortar and sea sand which often failed to yield DNA concentrations sufficient for downstream PCR.

4.1.3 Evaluating the primers

The forward and reverse primers used in fungal identification and assessing the fungal diversity were ITS 1 and ITS 4 which amplified partial sequence of ITS 1, 5.8S

rDNA, ITS2 and flanking region of 28S rDNA (“ITS region”). The primers had been known from several publications as reliable universal primers for fungal DNA.

Eventhough the primers have been successfully used for identifying the fungi, a deep research and evaluation had to be carried out to estimate whether the primer pair can be used from investigation of environmental complex sample.

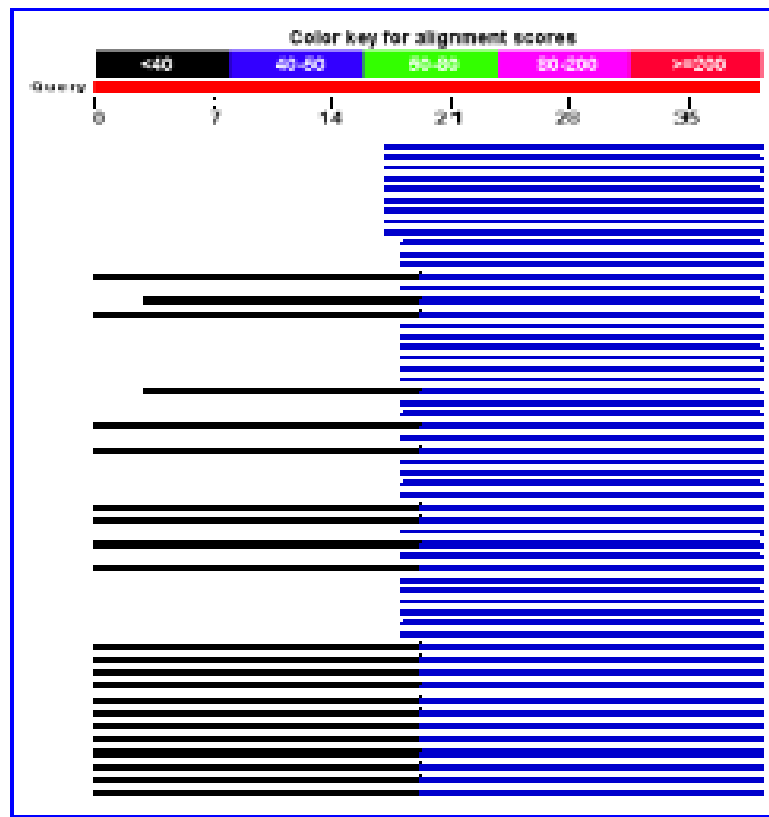


Figure 4.1 Distribution of 147 Blast Hits of ITS 1 and ITS 4 on the Query Sequence

Similarity between the sequences was analyzed with BLAST (basic local alignment search tool) search on the BLAST homepage, NCBI, Bethesda, USA in order to find regions of local similarity. BLAST search of primer sequences against GenBank provided information which could be interpreted about possible PCR product

of complex sample, especially whether the DNA of the host might be amplified with primer pair ITS 1 and ITS 4 and how long the products will be.

Table 4.1 showed organisms which had sequence accessible by ITS 1 and ITS 4, and E-value as match significance, the taxa where the organisms belong and the length of product possibly amplified by ITS 1 and ITS 4.

Most fungi yield products with the length of 530 bp until 600 basepairs when those were amplified with the primer pair ITS 1 and ITS 4. Organisms other than fungi which yielded products with ITS 1 and ITS 4 belonged to plants (viridiplantae), metazoa (class insecta) and alveolata (class protozoa and ciliata). Comparison of the length listed in the table 3.39 as well as experimental data allowed the conclusion that fungal and non-fungal PCR products can be distinguished easily by agarose gel electrophoretic separation.

Table 4.1 List of organisms accessible to be amplified with ITS 1 and ITS 4

(<http://www.ncbi.nlm.nih.gov/BLAST/Blast.cgi#92429611>)

Organism (Result of BLAST search)	E-value	Group	Nucleotide numbers
<i>Glomerella acutata</i>	0.022	Fungi	530-600 bp
<i>Physcia stellaris</i>	0.022	Fungi	530-600 bp
<i>Penicillium sp.</i>	0.022	Fungi	530-600 bp
<i>Fusarium sp.</i>	0.022	Fungi	530-600 bp
<i>Alternaria alternata</i>	0.022	Fungi	530-600 bp
<i>Cladosporium sp</i>	0.022	Fungi	530-600 bp
<i>Ampelomyces sp.</i>	0.022	Fungi	530-600 bp
<i>Mallada bonensis</i>	0.086	Metazoa (Insecta)	1122 bp
<i>Bracon hebetor</i>	0.086	Metazoa (Insecta)	1177 bp
<i>Cryptococcus humicola</i>	0.086	Fungi	530-600 bp
<i>Nectria sp.</i>	0.086	Fungi	530-600 bp
<i>Maxillaria aff. richii</i>	0.086	Viridiplantae	769 bp
<i>Lewia infectoria</i>	0.086	Fungi	530-600 bp
<i>Maxillaria rufescens</i>	0.086	Viridiplantae	707 bp
<i>Trichoderma sp</i>	0.086	Fungi	530-600 bp
<i>Jacobaea arnautorum</i>	0.086	Viridiplantae	706 bp
<i>Physcia stellaris</i>	0.086	Fungi	530-600 bp
<i>Stellilabium pogonostalix</i>	0.086	Viridiplantae	856 bp
<i>Peziza phyllogena</i>	0.086	Fungi	530-600 bp

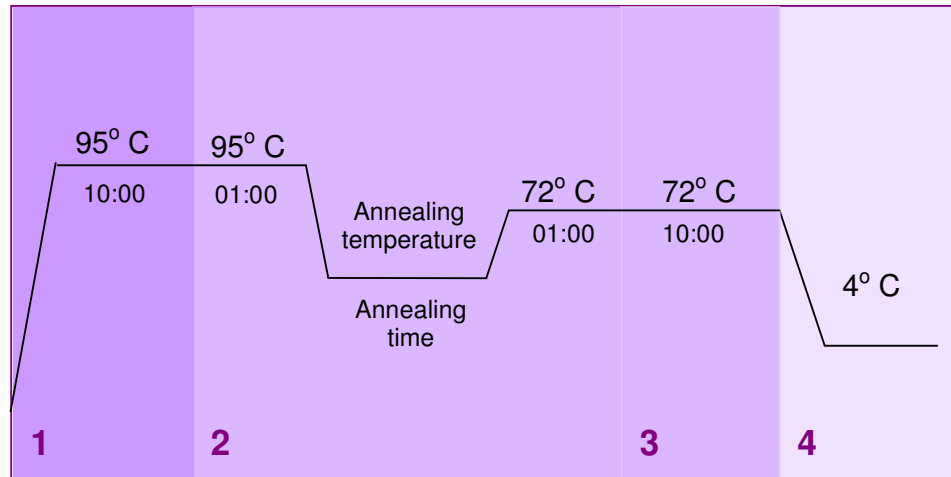
<i>Myrothecium cinctum</i>	0.086	Fungi	530-600 bp
<i>Colletotrichum orbiculare</i>	0.34	Fungi	530-600 bp
<i>Pyrenochaeta lycopersici</i>	0.34	Fungi	530-600 bp
<i>Orthoclada laxa</i>	0.34	Viridiplantae	835 bp
<i>Fusarium proliferatum</i>	0.34	Fungi	530-600 bp
<i>Gibberella moniliformis</i>	0.34	Fungi	530-600 bp
<i>Pythium ultimum</i>	0.34	Fungi	530-600 bp
<i>Colletotrichum gloeosporioides</i>	0.34	Fungi	530-600 bp
<i>Corynespora cassiicola</i>	0.34	Fungi	530-600 bp
<i>Erysiphe cruciferarum</i>	0.34	Fungi	530-600 bp
<i>Podosphaera fusca</i>	0.34	Fungi	530-600 bp
<i>Microsporum gallinae</i>	0.34	Fungi	530-600 bp
<i>Arthroderma obtusum</i>	0.34	Fungi	530-600 bp
<i>Paecilomyces sp.</i>	0.34	Fungi	530-600 bp
<i>Pestalotiopsis sp</i>	0.34	Fungi	530-600 bp
<i>Botryosphaeria rhodina</i>	0.34	Fungi	530-600 bp
<i>Nectria sp.</i>	0.34	Fungi	530-600 bp
<i>Cladosporium sp.</i>	0.34	Fungi	530-600 bp
<i>Paraphaeosphaeria sp</i>	0.34	Fungi	530-600 bp
<i>Aspergillus sp</i>	0.34	Fungi	530-600 bp
<i>Trichoderma sp</i>	0.34	Fungi	530-600 bp
<i>Myrothecium sp</i>	0.34	Fungi	530-600 bp
<i>Cladosporium oxysporum</i>	0.34	Fungi	530-600 bp
<i>Planchonella sp.</i>	0.34	Viridiplantae	730 bp
<i>Pouteria myrsinoides</i>	0.34	Viridiplantae	715 bp
<i>Niemeyera sp</i>	0.34	Viridiplantae	715 bp
<i>Curvularia sp</i>	0.34	Fungi	530-600 bp
<i>Bipolaris sp.</i>	0.34	Fungi	530-600 bp
<i>Hypocreaceae sp.</i>	0.34	Fungi	530-600 bp
<i>Stilbella sp</i>	0.34	Fungi	530-600 bp
<i>Hypocrea sp.</i>	0.34	Fungi	530-600 bp
<i>Plectosphaerella sp</i>	0.34	Fungi	530-600 bp
<i>Rhizopus oryzae</i>	0.34	Fungi	530-600 bp
<i>Debaryomyces hansenii</i>	0.34	Fungi	530-600 bp
<i>Gymnoascus reesii</i>	0.34	Fungi	530-600 bp
<i>Auxarthron reticulatum</i>	0.34	Fungi	530-600 bp
<i>Gymnoascoideus petalosporus</i>	0.34	Fungi	530-600 bp
<i>Malbranchea gypsea</i>	0.34	Fungi	530-600 bp
<i>Auxarthron alboluteum</i>	0.34	Fungi	530-600 bp
<i>Chrysosporium keratinophilum</i>	0.34	Fungi	530-600 bp
<i>Uncinocarpus reesii</i>	0.34	Fungi	530-600 bp
<i>Arthroderma multifidum</i>	0.34	Fungi	530-600 bp
<i>Phanerochaete chrysosporium</i>	0.34	Fungi	530-600 bp
<i>Cetrelia pseudolivetorum</i>	0.34	Fungi	530-600 bp
<i>Cordyceps sp</i>	0.34	Fungi	530-600 bp
<i>Gastrodia elata</i>	0.34	Viridiplantae	739 bp
<i>Botryotinia fuckeliana</i>	0.34	Fungi	530-600 bp
<i>Protoventuria alpina</i>	0.34	Fungi	530-600 bp
<i>Trichosporon sp</i>	0.34	Fungi	530-600 bp
<i>Trichosporon mycotoxinivorans</i>	0.34	Fungi	530-600 bp
<i>Symbiodinium sp.</i>	0.34	Alveolata	766 bp
<i>Sclerotinia homoeocarpa</i>	0.34	Fungi	530-600 bp

<i>Microstroma juglandis</i>	0.34	Fungi	530-600 bp
<i>Calonectria pauciramosa</i>	0.34	Fungi	530-600 bp
<i>Ruellia runyonii</i>	0.34	Viridiplantae	727 bp
<i>Gloeocantharellus sp.</i>	0.34	Fungi	530-600 bp
<i>Microcephalothrips abdominalis</i>	0.34	Metazoa (insecta)	755 bp
<i>Frankliniella intonsa</i>	0.34	Metazoa (insecta)	757 bp
<i>Amanita pantherina var. multisquamosa</i>	0.34	Fungi	530-600 bp
<i>Botrytis aclada</i>	0.34	Fungi	530-600 bp
<i>Cryptococcus flavescens</i>	0.34	Fungi	530-600 bp
<i>Chrysosporium keratinophilum</i>	0.34	Fungi	530-600 bp
<i>Uncinocarpus reesii</i>	0.34	Fungi	530-600 bp
<i>Arthroderma multifidum</i>	0.34	Fungi	530-600 bp
<i>Phanerochaete chrysosporium</i>	0.34	Fungi	530-600 bp
<i>Gymnoascus nodulosus</i>	0.34	Fungi	530-600 bp
<i>Gymnoascoideus petalosporus</i>	0.34	Fungi	530-600 bp
<i>Malbranchea pulchella</i>	0.34	Fungi	530-600 bp
<i>Auxarthron filamentosum</i>	0.34	Fungi	530-600 bp
<i>Phyllactinia fraxini</i>	0.34	Fungi	530-600 bp
<i>Melampyrum italicum</i>	0.34	Fungi	530-600 bp
<i>Lathraea squamaria</i>	0.34	Plant	306 bp
<i>Biscogniauxia arima</i>	0.34	Fungi	530-600 bp
<i>Xylaria venosula</i>	0.34	Fungi	530-600 bp
<i>Stilbohypoxylon elaeicola</i>	0.34	Fungi	530-600 bp
<i>Amphilogia gyrosa</i>	0.34	Fungi	530-600 bp
<i>Daldinia fissa</i>	0.34	Fungi	530-600 bp
<i>Hypoxylon rubiginosum</i>	0.34	Fungi	530-600 bp
<i>Annulohypoxylon bovei</i>	0.34	Fungi	530-600 bp
<i>Corynespora cassiicola</i>	0.34	Fungi	530-600 bp
<i>Colletotrichum capsici</i>	0.34	Fungi	530-600 bp
<i>Ceratobasidium</i>	0.34	Fungi	530-600 bp
<i>Didymella bryoniae</i>	0.34	Fungi	530-600 bp
<i>Hypocrea lixii</i>	0.34	Fungi	530-600 bp
<i>Laetisaria fuciformis</i>	21	Fungi	530-600 bp

4.1.4 Optimization of PCR conditions

Principally PCR was DNA replication which catalysed by enzyme DNA polymerase. The thermostable DNA polymerase from *Termus aquaticus* (*Taq*) was the most commonly and extensively used enzyme in PCR. Other thermostable DNA polymerases have been isolated from other organisms and were commercially available for performing PCR. The DNA polymerase used in this study was Hot start

master mix which contained hot start DNA polymerase, PCR buffer, and deoxynucleoside triphosphates (dNTPs).



Cycle 1 (1x) : Initial denaturation

Cycle 2 (35x): Amplification

Cycle 3 (1x) : Final extention

Hot start *Taq* polymerase was DNA polymerase mixed with an antibody which had ability to bind to the active or nucleotide-binding site of the polymerase and render the enzyme in inactive state. Upon heating, the protein would denature and dissociate from the polymerase, restoring enzyme activity. Because the reactant did not mix until the temperature was sufficiently high enough to denature the antibody, it minimized any nonspecific annealing of primers to nontarget DNA sequences and reduced the primer oligomerization incidence [Newton and Graham, 1997].

Annealing temperature and annealing time

Annealing temperature and time obtained from the literature was 54° C for 30 seconds (Abd-Elsalam *et al.*, 2003). The annealing temperature is the optimal

temperature which allows the primers to anneal to the single stranded template DNA. The temperature at this step depends on the melting temperature of the primers (T_m) and is usually between 50-60° C.

The melting temperature (T_m) can be calculated by the formula as below:

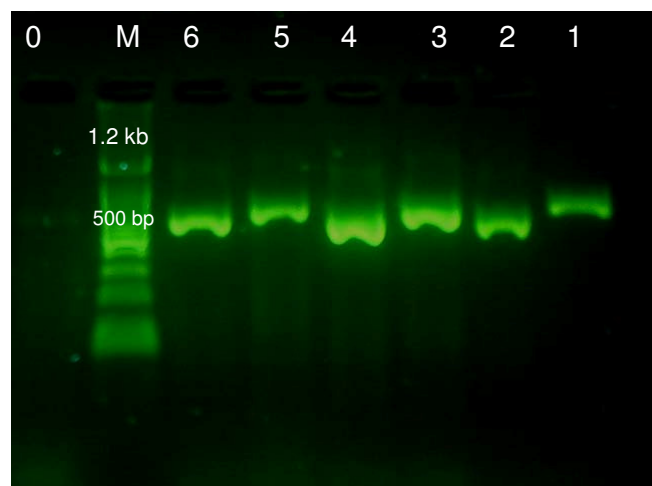
$$T_m = [(A + T) \times 2] + [(G + C) \times 4]$$

Based on this calculation, ITS 1 had a melting temperature of 62° C, whereas the melting temperature of ITS 4 was 58° C.

Annealing Temperature

Three experiments PCR using different annealing temperatures, 54° C, 56° C and 58° C, was conducted in order to define the optimal annealing temperature using fungal DNA of *Penicillium* sp. and *Chaetomium* sp.

Figure 4.2 Optimization of annealing temperature

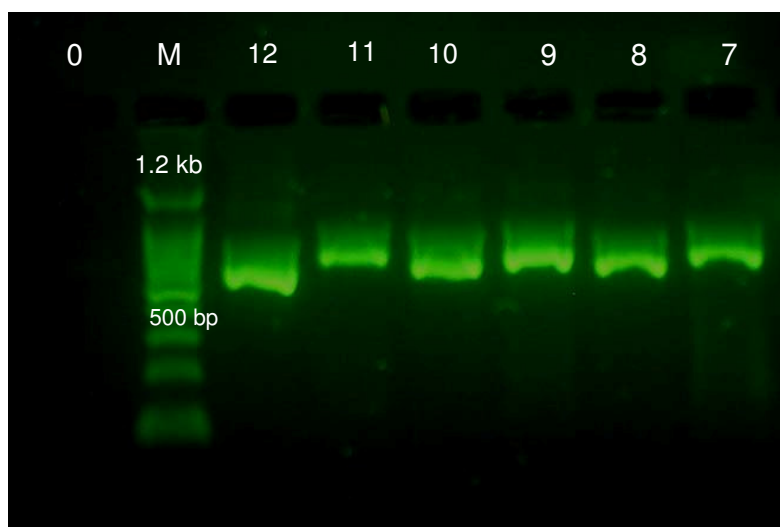


Code	Annealing temperature	Annealing Time (seconds)	DNA concentration	Primer concentration
M	DNA ladder			
1	54° C (<i>Penicillium</i> sp.)	45	2.5 mL	6 pmol
2	54° C (<i>Chaetomium</i> sp.)	45	2.5 mL	6 pmol
3	56° C (<i>Penicillium</i> sp.)	45	2.5 mL	6 pmol
4	56° C (<i>Chaetomium</i> sp.)	45	2.5 mL	6 pmol
5	60° C (<i>Penicillium</i> sp.)	45	2.5 mL	6 pmol
6	60° C (<i>Chaetomium</i> sp.)	45	2.5 mL	6 pmol
0	Negative control	45	0 mL	6 pmol

Agarose gel electrophoresis of the PCR products showed that the optimum annealing temperature was reached at 56° C.

Annealing time

Figure 4.3 Optimization of annealing time



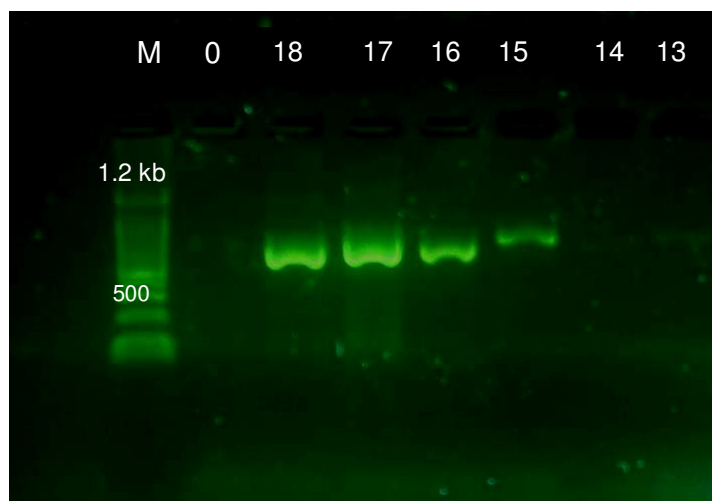
Code	Annealing time	Annealing temperature	DNA concentration	Primer concentration
M	DNA ladder			
7	45 seconds (<i>Penicillium</i> sp.)	56° C	2.5 µl	6 pmol
8	45 seconds (<i>Chaetomium</i> sp.)	56° C	2.5 µl	6 pmol
9	60 seconds (<i>Penicillium</i> sp.)	56° C	2.5 µl	6 pmol
10	60 seconds (<i>Chaetomium</i> sp.)	56° C	2.5 µl	6 pmol
11	90 seconds (<i>Penicillium</i> sp.)	56° C	2.5 µl	6 pmol
12	90 seconds (<i>Chaetomium</i> sp.)	56° C	2.5 µl	6 pmol
0	Negative control	56° C	0 µl	6 pmol

Three PCR experiments using different annealing times, 45, 60 and 90 seconds, were conducted with annealing temperature of 56° C. The best annealing time was 60 seconds based on agarose gel electrophoresis of the PCR products.

Concentration of primers

Optimization of primer concentration was conducted by performing PCR under previous optimal conditions with different primer concentrations, which were 2, 6, and 10 pmol of each primer ITS 1 and ITS 4. The optimal primer concentration based on the PCR result was 10 pmol.

Figure 4.4 Optimization of primer concentration



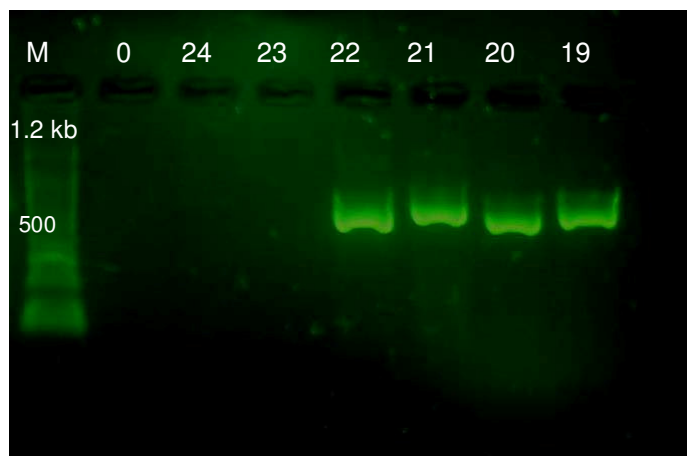
Code	Primer concentration
13	2 pmol (<i>Chaetomium</i> sp.)
14	2 pmol (<i>Penicillium</i> sp.)
15	6 pmol (<i>Chaetomium</i> sp.)
16	6 pmol (<i>Penicillium</i> sp.)
17	10 pmol (<i>Chaetomium</i> sp.)
18	10 pmol (<i>Penicillium</i> sp.)
0	Negative control
M	DNA ladder

Concentration of template DNA

In this PCR experiments using previous optimal conditions, template DNA concentration have been compared for the each fungus. DNA concentration of *Penicillium* sp. was 0.21 $\mu\text{g}/\mu\text{l}$, whereas that of *Chaetomium* sp. was 0.13 $\mu\text{g}/\mu\text{l}$. The DNA concentration was measured by spectrophotometer at the wavelength of 260 nm based on this formula.

$$[\text{DNA}] = A_{260} \times \text{dilution factor} \times 50 \mu\text{g/mL}$$

Figure 4.5 Optimization of template DNA concentration



Code	DNA concentration
19	2.5 μ l (<i>Chaetomium</i> sp.)
20	2.5 μ l (<i>Penicillium</i> sp.)
21	5 μ l (<i>Chaetomium</i> sp.)
22	5 μ l (<i>Penicillium</i> sp.)
23	10 μ l (<i>Chaetomium</i> sp.)
24	10 μ l (<i>Penicillium</i> sp.)
0	Negative control
M	DNA ladder

In this PCR experiment, three template DNA concentrations were compared for each fungus. The concentration of 5 μ l was found to be the best template DNA concentration for both fungi. PCR mixture:

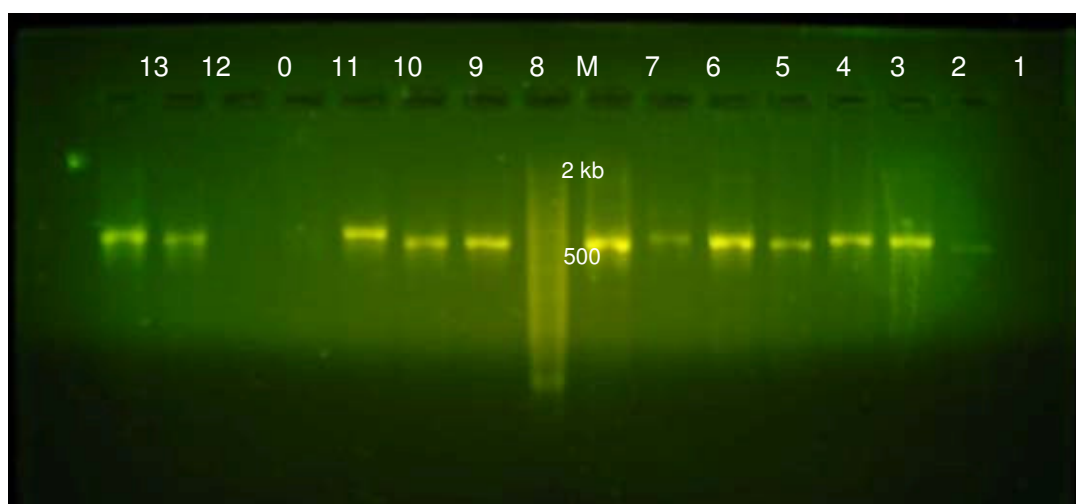
	Volume	Concentration
Hot start Master mix (Taq, dNTPs, buffer)	25 μ l	
Primers (ITS 1 + ITS 4)	3 μ l	10 pmol
Template DNA	5 μ l	0.1 – 0.5 μ g/mL
Water	17 μ l	
Total	50 μ l	

4.1.5 Identification of fungi

Identification of fungi derived from marine environment was carried out to 53 fungi. They were algae-derived fungi from Java Sea (11 strains), sponge-derived fungi from Mediterranean Sea (28 strains), anemone-derived fungi from Mediterranean Sea (7 strains), algae-derived fungi from Qingdao beach, China (6 strains) and mangrove plant-derived fungi from Hainan, China (17 fungi).

4.1.5.1 Fungal identification of algae derived- and mangrove derived fungi from China

Figure 4.6 PCR products of algae derived- and mangrove-derived fungi from China



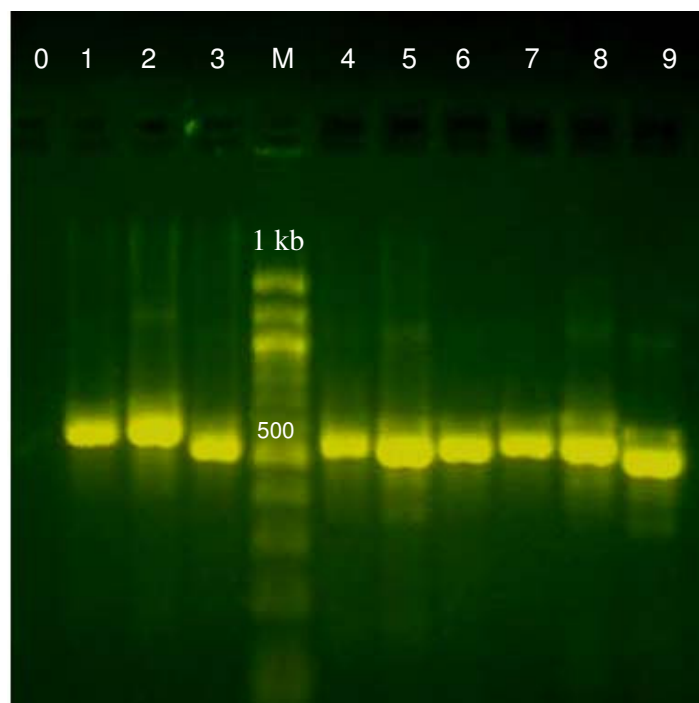
Nr.	Code	Fungi
0	Negative control	
1.	MGC1.3	<i>Fusarium incarnatum</i>
2.	MGC4.4	<i>Botryosphaeria lutea</i>
3.	MGC5.1	<i>Neurospora terricola</i>
4.	MGC5.6	<i>Botryosphaeria rhodina</i>
5.	MGC6.1	<i>Pestalotopsis microspora</i>
6.	MGC8.2	<i>Diaporthe</i> sp.
7.	MGC8.4	<i>Colletotrichum</i> sp.
8.	MGF12.3	<i>Xylaria</i> sp.

M	DNA ladder	
9.	QEN1	<i>Arthrinium sacchari</i>
10.	QEN4	<i>Alternaria tenuissima</i>
11.	QEN3	-
12.	QEN5	<i>Eurotium repens</i>
13.	QEN6	<i>Cladosporium sp.</i>

The samples of marine algae from Qingdao beach and mangrove plants were generously provided and isolated by Dr. Franka Teuscher in 2004 for phylogenetic analysis.

4.1.5.1 Fungal identification of algae-derived fungi from Java Sea

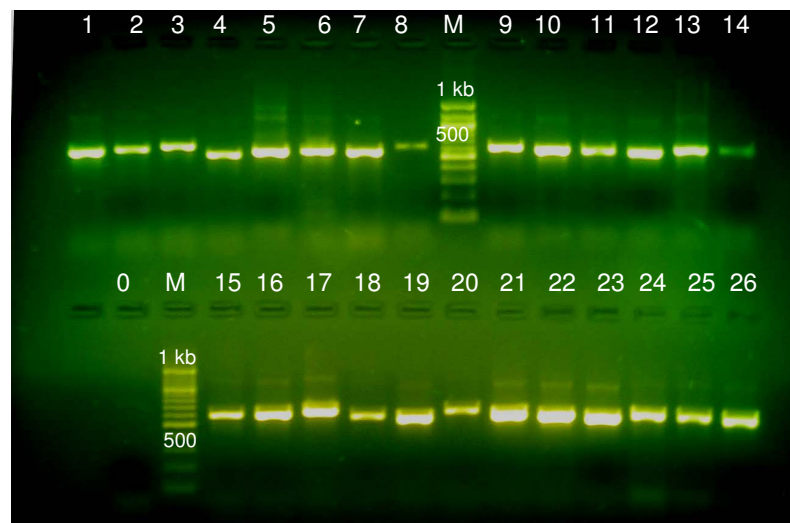
Figure 4.6 PCR products of algae-derived fungi from Java Sea



Nr.	Code	Fungi
0	Negative control	
1.	8 t	<i>Aspergillus</i> sp.
2.	18 TdBr	<i>Eutypella scoparia</i>
M	DNA ladder	
3.	15 t1	<i>Fusarium equiseti</i>
4.	4h2b	<i>Penicillium citrinum</i>
5.	1t1	<i>Xylaria</i> sp.
6.	15 Sa2th2l	<i>Nodulisporium</i> sp
7.	10hl	<i>Diaporthe phaseolorum</i>
8.	4h1	<i>Penicillium chrysogenum</i>
9.	2h1	<i>Nodulisporium</i> sp

4.5.3 Fungal identification of sponge-derived and anemone-derived fungi from Mediterranean Sea

Figure 4.7 PCR products of algae-derived fungi from Java Sea



Nr.	Code	Fungi
0	Negative control	
1.	PV6.6	<i>Paraphaeorosphaeria</i> sp.
2.	PV2.2	<i>Diatrype stigma</i>
3.	Te6.13	<i>Peniophora cinerea</i>
4.	Te 4.8	<i>Sclerotinia sclerotiorum</i>
5.	Te3.6	<i>Arthrinium</i> sp.
6.	Te1.4	<i>Penicillium polonicum</i>
7.	Te1.2	<i>Chaetomium</i> sp.
8.	Te1.1	<i>Arthrinium</i> sp.
9.	SD4.12	<i>Myrothecium</i> sp.
10.	SD4.10	not sequenced
11.	SD2.4	<i>Alternaria compacta</i>
12.	SD1.3	not sequenced
13.	SD1.2	not sequenced
14.	SD1.1	<i>Botryosphaeria stevensii</i>
15.	AA9.3	<i>Talaromyces wortmanii</i>
16.	AA9.2	<i>Talaromyces wortmanii</i>
17.	AA4.8	not sequenced
18.	AA4.7	<i>Nectria haematococca</i>
19.	AA3.5	<i>Didymella cucurbitacearum</i>
20.	AA2.2	<i>Trichoderma citrinoviride</i>
21.	CN9.1	<i>Paraphaeosporia michotii</i>
22.	CN5.5	not sequenced
23.	CN4.10	<i>Cladosporium cladosporioides</i>
24.	CN3.2	<i>Tritirachium</i> sp
25.	CN1.1	<i>Tritirachium</i> sp.

4.1.6 BLAST search for fungal identification

The sequences of PCR products amplified by primer pair ITS 1 and ITS 4 had to be aligned and BLAST (basic local alignment search tool) search could be conducted to find matching sequences in GenBank using our sequence product as query, using the BLAST homepage of the national centre of biotechnology information (NCBI), Bethesda USA. BLAST search was performed to define the identity of the fungal strain.

The BLAST search output consisted of a graphic visualizing similarity of the query with other sequences, a hit list showing the name of sequence similar to the query, the alignments describing every alignment between the query and the reported hits and the parameters which were total score, identity value, gap value and expectation value (E-value). Total score calculated the matching bases between query and the similar sequence in the hit lists considering also the base mismatch and the gap value, whereas identity value was the percentage value of query coverage (Claverie and Notredame, 2003).

Figure 4.8A, B and C described the example of the output of BLAST search conducted in fungus AA9.3. From BLAST result, it could be concluded that this fungus was *Talaromyces wortmanii* based on the high identity value (99%), small gap value (0%), high score which was 1009 bits and 0 E-value. E-value provided the most important measure of statistical significance. The lower E-value, the more similar the sequence and the more confidence the BLAST search result. The sequence identical to query had an E-value very close to 0. Matches above 0.001 were often close to the doubtful zone (Claverie and Notredame, 2003).

Figure 4.8A The BLAST search graphic display of fungus AA9.3

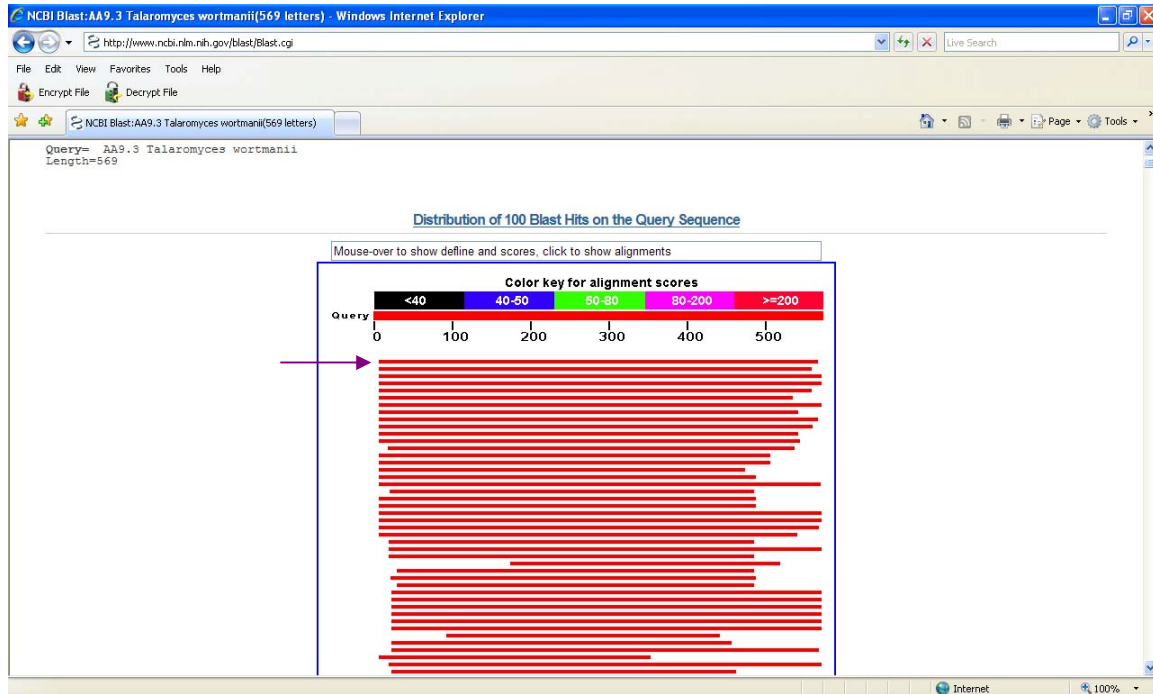


Figure 4.8B The BLAST search hit list of fungus AA9.3

Legend for links to other resources: [U](#) UniGene [E](#) GEO [G](#) Gene [S](#) Structure [M](#) Map Viewer

Sequences producing significant alignments:
(Click headers to sort columns)

Accession	Description	Max score	Total score	Query coverage	E value	Max ident	Links
AY533693.1	Talaromyces wortmannii isolate S17 internal transcribed spacer 1, pai	1009	1009	97%	0.0	99%	
AY699690.1	Fungal sp. R42 18S ribosomal RNA gene, partial sequence; internal tr	1005	1005	96%	0.0	97%	
AY373936.1	Penicillium variable strain FRR 1290 18S ribosomal RNA gene, partial	990	990	98%	0.0	98%	
L14507.1	Penicillium variable (FRR 1055) 5.8S rRNA and internal transcribed sc	981	981	98%	0.0	98%	
AB080725.1	Penicillium sp. Re011124 DNA, ITS1, 5.8S rRNA, ITS2, 2.8S rRNA reg	966	966	96%	0.0	98%	
L14532.1	Talaromyces wortmannii (FRR 1795) 5.8S rRNA and internal transcrib	922	922	91%	0.0	98%	
DQ981400.1	Penicillium radicum 18S ribosomal RNA gene, partial sequence; intern	881	881	98%	0.0	94%	
DQ778916.1	Penicillium sp. IBL 03126 18S ribosomal RNA gene, partial sequence;	869	869	93%	0.0	95%	
AF455543.1	Penicillium islandicum isolate wb156 small subunit ribosomal RNA gen	852	852	97%	0.0	94%	
L14504.1	Penicillium islandicum (FRR 1399) 5.8S rRNA and internal transcribed	850	850	96%	0.0	94%	
AF285115.1	Talaromyces rotundus internal transcribed spacer 1, partial sequence	845	845	93%	0.0	95%	
AY256855.1	Penicillium radicum 18S ribosomal RNA gene, partial sequence; intern	845	845	93%	0.0	95%	
AB176632.1	Talaromyces tardifaciens genes for ITS 1, 5.8S rRNA, ITS 2, partial a	813	813	90%	0.0	95%	
EU076949.1	Penicillium sp. 23-M-5 18S ribosomal RNA gene, partial sequence; int	802	802	86%	0.0	95%	
AY787845.1	Penicillium ruulosum strain DAOM 215361 internal transcribed spacer	791	791	86%	0.0	95%	
AB176638.1	Talaromyces wortmannii var. sublevisporus genes for ITS 1, 5.8S rRN	791	791	81%	0.0	97%	
AY787846.1	Penicillium strain 95M102 CT18 internal transcribed spacer 1,	741	741	83%	0.0	94%	
DQ666824.1	Penicillium piceum strain IMI 392509 18S ribosomal RNA gene, partial	739	739	98%	0.0	91%	
DQ093702.1	Saqenomella ariseoviridis isolate aurim1122 small subunit ribosomal f	736	736	81%	0.0	95%	
DQ666825.1	Penicillium piceum strain ATCC 5225 18S ribosomal RNA gene, partial	732	732	83%	0.0	94%	
DQ666826.1	Penicillium strain ATCC 10519 18S ribosomal RNA gene, partial	728	728	83%	0.0	94%	
AF033388.1	Talaromyces bacillisporus strain NRRL 1025 internal transcribed space	704	704	98%	0.0	89%	
AY373919.1	Penicillium islandicum strain FRR 2239 18S ribosomal RNA gene, parti	688	688	98%	0.0	89%	
AF033398.1	Penicillium resedanum strain NRRL 578 internal transcribed spacer 1,	662	662	97%	0.0	88%	
AY753343.1	Talaromyces bacillisporus strain BCC 14375 18S ribosomal RNA gene	658	658	92%	0.0	89%	
AB176608.1	Talaromyces bacillisporus genes for ITS 1, 5.8S rRNA, ITS 2, partial a	641	641	81%	0.0	91%	
L14526.1	Talaromyces mimosinus (FRR 1875) 5.8S rRNA and internal transcribe	640	640	96%	2e-180	87%	
AB176639.1	Talaromyces sp. IFM 53522 genes for ITS 1, 5.8S rRNA, ITS 2, partial	625	625	81%	7e-176	91%	
EU118826.1	Penicillium variable strain PVWN002 internal transcribed spacer 1, pai	608	608	59%	7e-171	98%	

The first file in the hit list would have the highest total score, the highest identity value and the smallest E-value. More to the end of the list, the value of total score would be lower, the identity value lower and E-value would be higher. The problem in fungal identification using blast search was choosing the right sequence which was the most similar with the query sequence of identifying fungus.

Figure 4.8C The BLAST search alignment of fungus AA9.3 with *Talaromyces wortmanii*

[gb|AY533693.1](#) *Talaromyces wortmanii* isolate S17 internal transcribed spacer 1, partial sequence; 5.8S ribosomal RNA gene and internal transcribed spacer 2, complete sequence; and 28S ribosomal RNA gene, partial sequence

Length = 559 bp

```

Score = 1009 bits (546), Expect = 0.0
Identities = 553/556 (99%), Gaps = 2/556 (0%)
Strand=Plus/Plus

Query 9      GTGCGGGTTCTAACGAGCCCAACCTCCCACCCGTGTTTACTGTTACCGCGTTGCCTcgggc 68
          |||
Sbjct 5      GTGCGGGTTCTAACGAGCCCAACCTCCCACCCGTGTTTACTGTTACCGCGTTGCCTCGGC 64

Query 69     gggcccaactggggcctggccccggctgcggggggggttctgccccgggccccgcgccccgc 128
          |||
Sbjct 65     GGGCCCACTGGGGCCTGGCCCCGGTGCGGGGGGCTTCTGCCCCCGGGCCCGCCCGC 124

Query 129    cgAAGCACCCCTAGAACCCTGCCTGAATAGTGAGTCTGAGTGAGAGATTAAATCATTAAAA 188
          |||
Sbjct 125    CGAAGCACCCCTAGAACCCTGCCTGAATAGTGAGTCTGAGTGAGAGATTAAATCATTAAAA 184

Query 189    CTTTCAACAACGGATCTCTTGGTTCGGCATCGATGAAGAACGCAGCGAAATGCGATAAG 248
          |||
Sbjct 185    CTTTCAACAACGGATCTCTTGGTTCGGCATCGATGAAGAACGCAGCGAAATGCGATAAG 244

Query 249    TAATGTGAATTGCAGAATTCCGTGAATCATCGAATCTTTGAACGCACATTGCGCCCCCTG 308
          |||
Sbjct 245    TAATGTGAATTGCAGAATTCCGTGAATCATCGAATCTTTGAACGCACATTGCGCCCCCTG 304

Query 309    GCATTCCGGGGGGCATGCCTGTCCGAGCGTCATTTCTGCCCTCCAGCACGGGCTGGGTG-T 367
          |||
Sbjct 305    GCATTCCGGGGGGCATGCCTGTCCGAGCGTCATTTCTGCCCTCCAGCACGGGCTGGGTGGT 364

Query 368    TGGGCGCTGTCCCCCGGGGACACGCCCAAAAGCAGTGGCGGCGCCGCGTCCGGTCCCTC 427
          |||
Sbjct 365    TGGGCGCTGTCCCCCGGGGACACGCCCAAAAGCAGTGGCGGCGCCGCGTCCGGTCCCTC 424

Query 428    GAGCGTATGGGGCTTTGTACCCCGCTCGGGAGGGACTCGGTTCGGCGCTGGTCTTCCITTT 487
          |||
Sbjct 425    GAGCGTATGGGGCTTTGTACCCCGCTCGGGAGGGACTCGGTTCGGCGCTGGTCTTCCITTT 484

Query 488    AGGCAGCCCTTCGGGGTGCCTCTTCCGGTIGACCTCGGATCAGGTAGGGCTACCCGCT 547
          |||
Sbjct 485    AGGCAGCCCTTCGGGGTGCCTCTTCCGGTIGACCTCGGATCAGGTAGGGCTACCCGCT 544

Query 548    GAACTTAAGCATATCA 563
          |||
Sbjct 545    GAACTTAAGCAT-TCA 559

```

In some cases, the BLAST search hit list could show the same parameters given in different species of the same genus, for example in many species from genus *Aspergillus* and *Alternaria* [figure 4.9]. In these cases, it could be concluded that several fungi in this genus had exactly the same sequence so that the identification only could identify the fungus until genus level.

Figure 4.9 The BLAST search hit list of fungus 8h2

Accession	Description	Max score	Total score	Query coverage	E value	Max ident	Links
AY373857.1	aspergillus oryzae strain SRRC 2103 18S ribosomal RNA gene, partial	1037	1037	99%	0.0	99%	
AY373848.1	aspergillus flavus strain SRRC 1000A 18S ribosomal RNA gene, partial	1037	1037	99%	0.0	99%	
AP007173.1	aspergillus oryzae RIB40 genomic DNA, rDNA tel3	1037	1037	99%	0.0	99%	
AP007172.1	aspergillus oryzae RIB40 genomic DNA, SC206	1037	1037	99%	0.0	99%	
AF459735.1	aspergillus oryzae NRRL 506 18S ribosomal RNA gene, partial sequen	1037	1037	99%	0.0	99%	
AF027863.1	aspergillus flavus strain NRRL 1957 internal transcribed spacer 1, 5.8:	1037	1037	99%	0.0	99%	
A1976522.1	aspergillus flavus 18S rRNA gene (partial), 5.8S rRNA gene, 20S rRNA	1037	1037	99%	0.0	99%	
A1971014.1	aspergillus flavus strain SK30 18S ribosomal RNA gene, partial sequen	1035	1035	99%	0.0	99%	
DQ467974.1	Aspergillus flavus strain SK20 18S ribosomal RNA gene, partial sequen	1035	1035	99%	0.0	99%	
DQ467973.1	Aspergillus flavus strain SK20 18S ribosomal RNA gene, partial sequen	1035	1035	99%	0.0	99%	
DQ467972.1	Aspergillus flavus strain SU9 18S ribosomal RNA gene, partial sequen	1035	1035	99%	0.0	99%	
DQ467971.1	Aspergillus flavus strain 13 18S ribosomal RNA gene, partial sequen	1035	1035	99%	0.0	99%	
DQ467969.1	Aspergillus sp. BN8 18S ribosomal RNA gene, partial sequence: intern	1035	1035	99%	0.0	99%	
DQ467968.1	Aspergillus flavus strain AF70 18S ribosomal RNA gene, partial sequen	1035	1035	99%	0.0	99%	
AY939782.1	Aspergillus flavus strain ATCC 20043 18S ribosomal RNA gene, partial	1035	1035	99%	0.0	99%	
AY214444.1	Aspergillus flavus strain UWFP 533 18S ribosomal RNA gene, partial si	1035	1035	99%	0.0	99%	
DQ467967.1	Aspergillus flavus strain UR3 18S ribosomal RNA gene, partial sequen	1033	1033	99%	0.0	99%	
DQ467977.1	Aspergillus flavus strain SA35 18S ribosomal RNA gene, partial sequen	1033	1033	99%	0.0	99%	
DQ467982.1	Aspergillus flavus strain UR24 18S ribosomal RNA gene, partial sequen	1029	1029	99%	0.0	99%	
DQ467976.1	Aspergillus nomius strain PT4 18S ribosomal RNA gene, partial sequen	1029	1029	99%	0.0	99%	
DQ467975.1	Aspergillus flavus strain SU19 18S ribosomal RNA gene, partial sequen	1029	1029	99%	0.0	99%	
AY939785.1	Aspergillus flavus isolate VA 103936-04 18S ribosomal RNA gene, par	1029	1029	99%	0.0	99%	
AY214445.1	Aspergillus flavus strain UWFP 570 18S ribosomal RNA gene, partial si	1029	1029	99%	0.0	99%	
DQ467980.1	Aspergillus flavus strain TK4 18S ribosomal RNA gene, partial sequen	1027	1027	99%	0.0	99%	
AF138287.1	Aspergillus flavus 18S ribosomal RNA gene, partial sequence: internal	1026	1026	99%	0.0	99%	
DQ767604.1	Uncultured Aspergillus clone ZN771 18S ribosomal RNA gene, partial r	1024	1024	99%	0.0	99%	
DQ467977.1	Aspergillus flavus strain PT18 18S ribosomal RNA gene, partial sequen	1024	1024	99%	0.0	99%	
DQ467979.1	Aspergillus flavus strain SU16 18S ribosomal RNA gene, partial sequen	1022	1022	99%	0.0	99%	
DQ467978.1	Aspergillus flavus strain SP9 18S ribosomal RNA gene, partial sequen	1022	1022	99%	0.0	99%	

Moreover, scientists all over the world could submit their sequences to Genbank via NCBI, so that the result is subjected to errors in submission. In rare case, it happened that the first several sequences in the hit list gave the same parameter values and most of them were the same fungus except the first one. Further literature search was performed to find out whether the fungus in the first file was their anamorph or teleomorph. When the first hit in the list was a fungus which neither had any relationship nor was closely related with the fungi of the next entries in the hit list, the second entry in the hit list had to be chosen instead of the first one.

4.2 Constructing of Phylogenetic Tree

4.2.1 Multiple sequence alignment

Phylogenetic analysis can be conducted to assess the sequences which have evolutionary origin such as sequence of ribosomal DNA. In general, the input set of query sequences are assumed to have an evolutionary relationship by which they share a lineage and are descended from a common ancestor. The multiple sequence alignment needs to be constructed to infer sequence homology and conduct phylogenetic analysis in the form of phylogenetic tree. Multiple sequence alignment is sequence alignment for three or more biological sequences, such as DNA, RNA or protein.

Aligning more than a pair of sequence is considerably more complex than aligning two sequences and it needs reliable software to compute some algorithm. The most common program for making multiple sequence alignment is *CLUSTALW* (Hall, 2005). This program in the beginning aligns each sequence to each of the other sequences in a series of pairwise alignment and these series help in creating multiple alignment. The software package used for computing multiple sequence alignment was Bioedit sequence alignment editor (Hall, 1999).

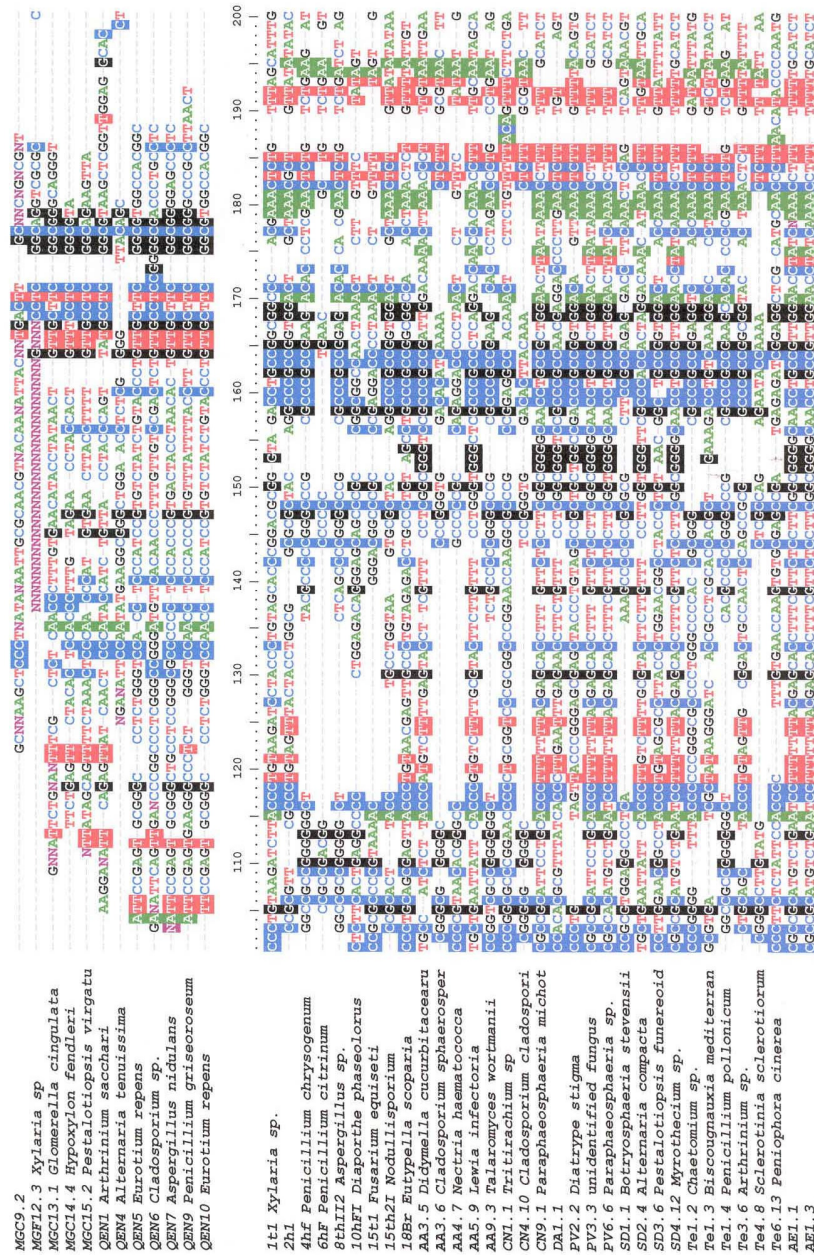
Figure 4.10 showed the multiple sequence alignment result of ITS 1 and ITS 4 amplified sequence of marine organism-derived fungi. The conservative and diverse regions could be detected [figure 4.10]. Less than 50% of the amplified sequence belonged to the conservative region which made it possible to perform phylogenetic analysis. Phylogenetic tree and multiple sequence alignment would not be possibly constructed by DNA region which had too much conservative region (more than 70%) (Hillis and Dixon, 1991; Claverie and Notredame, 2003).

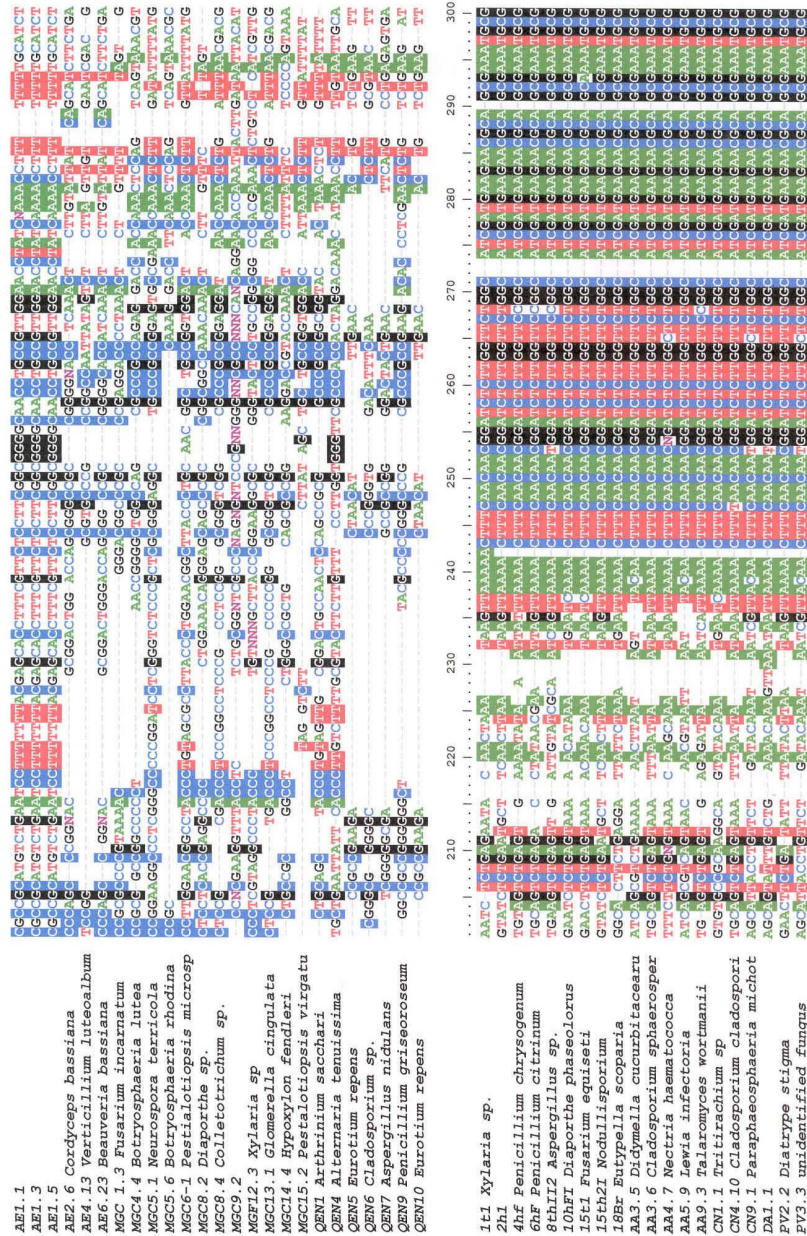
The sequences amplified by the primers ITS 1 and ITS 4 were covering partial sequence of ITS 1, complete sequence of 5.8S rDNA, complete sequence of ITS 2 and flanking region of 28S rDNA. ITS 1 and ITS 2 were internal transcribed region spacers which separated 18S, 5.8S and 28S genes (Hillis and Dixon, 1991). These spacer had diverse regions comparing to other ribosomal DNA region such as small subunit ribosomal DNA (18S rDNA), 5.8S rDNA and large sub unit ribosomal DNA (28S rDNA) which were more conservative (Hillis and Dixon, 1991).

The multiple sequence alignment of sequences amplified by ITS 1 and ITS 4 of marine-organism derived fungi [figure 4.10] showed that the conservative region of 5.8S rDNA was lying in the position number 230 until 460, preceded with partial sequence of ITS 1. The conservative region of 28S rDNA partial sequence could be detected in the position number 624 until 674, whereas the complete sequence of ITS 2 flanking in between 5.8S rDNA and partial sequence of 28S rDNA, which showed diverse region.

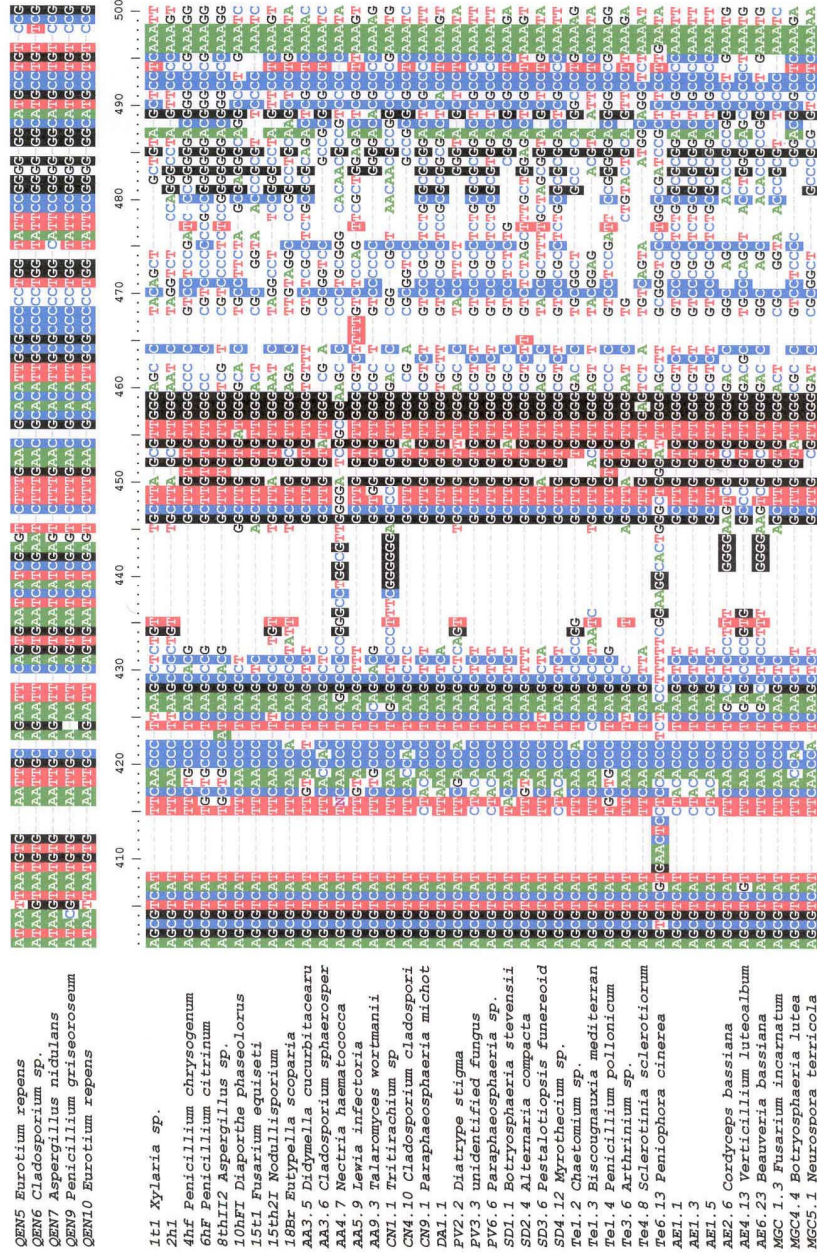
In figure 4.10, a lot of introducing gaps (spaces) are observed, which are biologically assumed to represent insertions or deletions that occurred as the sequenced diverged from a common ancestor. Permitting spaces was necessary to maximize the number of bases that match into one or other sequence. Nevertheless the number of gaps had to be constrained so that the resulting alignments still make biological sense (Hall, 2005).

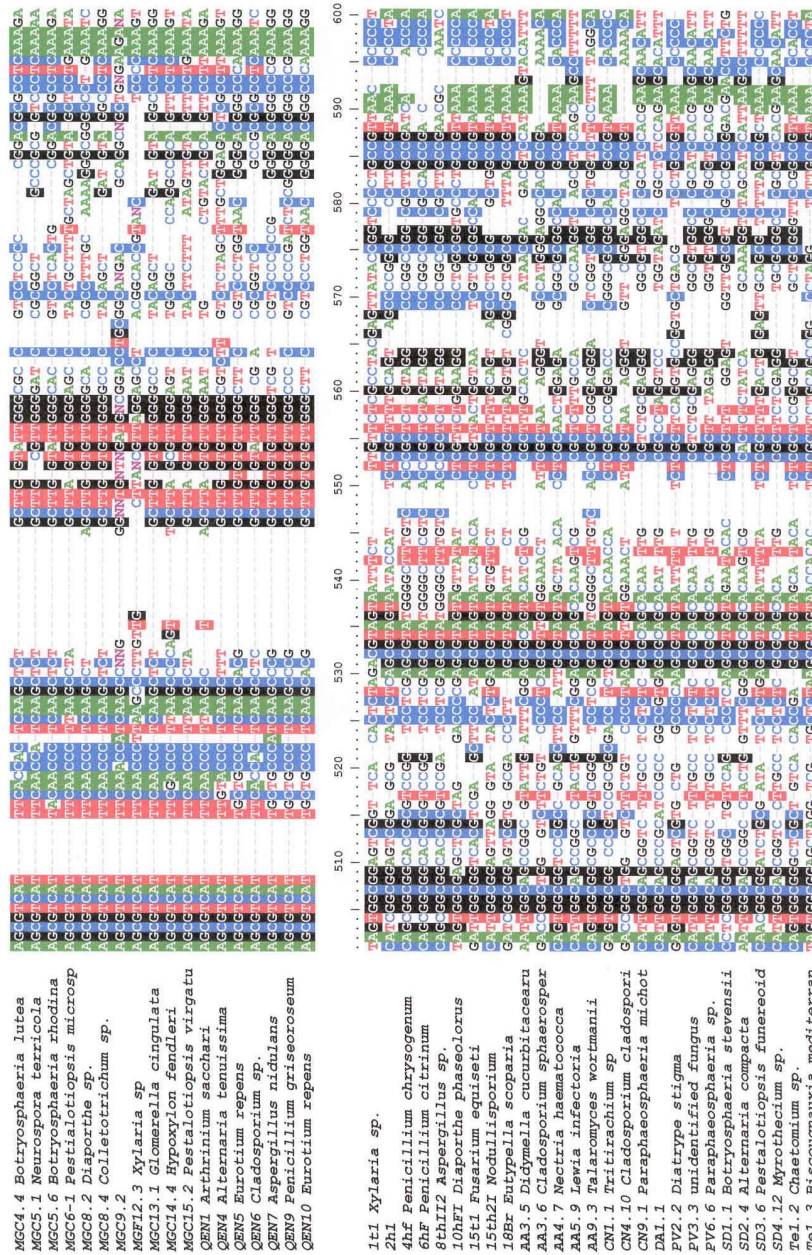
Scoring system was used to constrain the number of gaps so that matching residues got some sort of positive numerical score. The matching residues in nucleic acid got a score of 1, mismatches got a score for 0, and gaps got some sort of negative score or gap penalty. An alignment program seeks an arrangement that maximize the score (Hall, 2005).

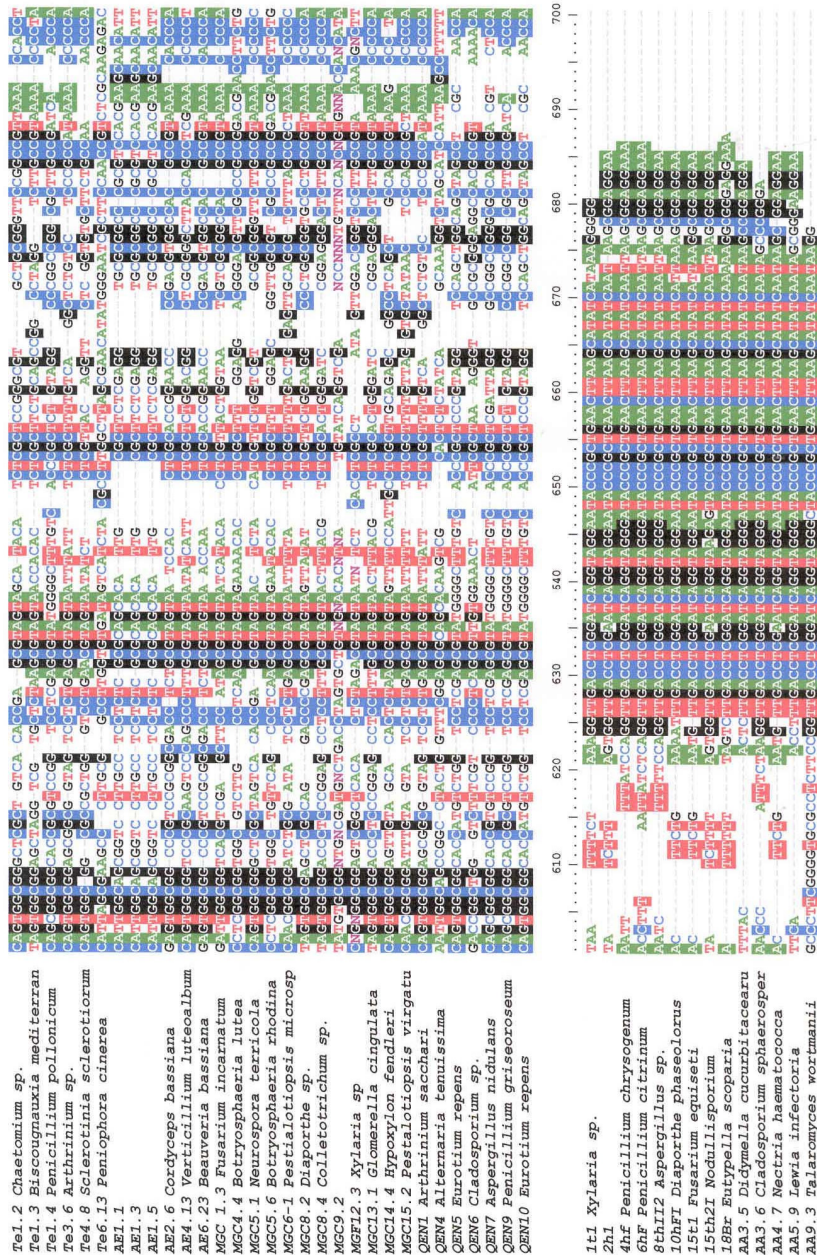


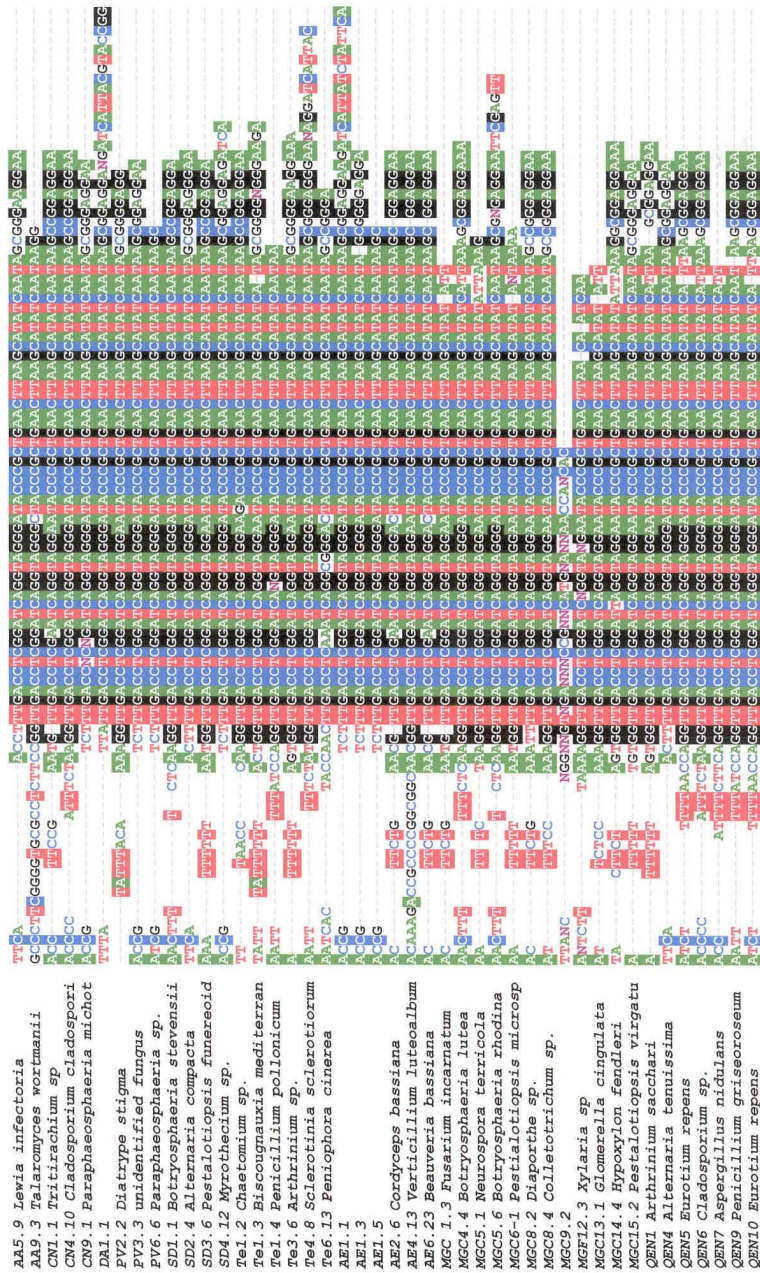


10HFI Diaporthe phaseolorus	ATAGCAATCG	CAATTC	CGCATC	CTTGG	GCATG	TATCC	GGG
15ti Fusarium equiseti	ATAGCAATCG	CAATTC	CGCATC	CTTGG	GCATG	TATCC	GGG
15thzi Nodulisporium	ATAGCAATCG	CAATTC	CGCATC	CTTGG	GCATG	TATCC	GGG
16Br Entyphella scoparia	ATAGCAATCG	CAATTC	CGCATC	CTTGG	GCATG	TATCC	GGG
AA3.6 Cladosporium curbitacearu	ATAGCAATCG	CAATTC	CGCATC	CTTGG	GCATG	TATCC	GGG
AA4.7 Nectria haematococca	ATAGCAATCG	CAATTC	CGCATC	CTTGG	GCATG	TATCC	GGG
AA5.9 Lewia infectoria	ATAGCAATCG	CAATTC	CGCATC	CTTGG	GCATG	TATCC	GGG
AA9.3 Talaromyces wortmanii	ATAGCAATCG	CAATTC	CGCATC	CTTGG	GCATG	TATCC	GGG
CNI.1 Tritirachium sp	ATAGCAATCG	CAATTC	CGCATC	CTTGG	GCATG	TATCC	GGG
CN4.10 Cladosporium cladospori	ATAGCAATCG	CAATTC	CGCATC	CTTGG	GCATG	TATCC	GGG
CN9.1 Paraphaeosphaeria michot	ATAGCAATCG	CAATTC	CGCATC	CTTGG	GCATG	TATCC	GGG
DA1.1	ATAGCAATCG	CAATTC	CGCATC	CTTGG	GCATG	TATCC	GGG
PV2.2 Diatype stigma	ATAGCAATCG	CAATTC	CGCATC	CTTGG	GCATG	TATCC	GGG
PV3.3 unidentified fungus	ATAGCAATCG	CAATTC	CGCATC	CTTGG	GCATG	TATCC	GGG
PV6.6 Paraphaeosphaeria sp.	ATAGCAATCG	CAATTC	CGCATC	CTTGG	GCATG	TATCC	GGG
SD1.1 Botryosphaeria stevensii	ATAGCAATCG	CAATTC	CGCATC	CTTGG	GCATG	TATCC	GGG
SD2.4 Alternaria compacta	ATAGCAATCG	CAATTC	CGCATC	CTTGG	GCATG	TATCC	GGG
SD3.6 Pestalotiopsis funereoid	ATAGCAATCG	CAATTC	CGCATC	CTTGG	GCATG	TATCC	GGG
SD4.12 Myrothecium sp.	ATAGCAATCG	CAATTC	CGCATC	CTTGG	GCATG	TATCC	GGG
Te1.2 Chaetomium sp.	ATAGCAATCG	CAATTC	CGCATC	CTTGG	GCATG	TATCC	GGG
Te1.3 Biscognuxia mediterran	ATAGCAATCG	CAATTC	CGCATC	CTTGG	GCATG	TATCC	GGG
Te1.4 Penicillium pollonicum	ATAGCAATCG	CAATTC	CGCATC	CTTGG	GCATG	TATCC	GGG
Te3.6 Arthrinium sp.	ATAGCAATCG	CAATTC	CGCATC	CTTGG	GCATG	TATCC	GGG
Te4.8 Sclerotinia sclerotiorum	ATAGCAATCG	CAATTC	CGCATC	CTTGG	GCATG	TATCC	GGG
Te6.13 Peniophora cinerea	ATAGCAATCG	CAATTC	CGCATC	CTTGG	GCATG	TATCC	GGG
AE1.1	ATAGCAATCG	CAATTC	CGCATC	CTTGG	GCATG	TATCC	GGG
AE1.3	ATAGCAATCG	CAATTC	CGCATC	CTTGG	GCATG	TATCC	GGG
AE1.5	ATAGCAATCG	CAATTC	CGCATC	CTTGG	GCATG	TATCC	GGG
AE2.6 Cordyceps bassiana	ATAGCAATCG	CAATTC	CGCATC	CTTGG	GCATG	TATCC	GGG
AE4.13 Verticillium luteoalbum	ATAGCAATCG	CAATTC	CGCATC	CTTGG	GCATG	TATCC	GGG
AE6.23 Beauveria bassiana	ATAGCAATCG	CAATTC	CGCATC	CTTGG	GCATG	TATCC	GGG
MGC 1.3 Fusarium incarnatum	ATAGCAATCG	CAATTC	CGCATC	CTTGG	GCATG	TATCC	GGG
MGC4.4 Botryosphaeria lutea	ATAGCAATCG	CAATTC	CGCATC	CTTGG	GCATG	TATCC	GGG
MGC5.1 Neurospora terricola	ATAGCAATCG	CAATTC	CGCATC	CTTGG	GCATG	TATCC	GGG
MGC5.6 Botryosphaeria rhodina	ATAGCAATCG	CAATTC	CGCATC	CTTGG	GCATG	TATCC	GGG
MGC6-1 Pestalotiopsis microsp	ATAGCAATCG	CAATTC	CGCATC	CTTGG	GCATG	TATCC	GGG
MGC8.2 Diaporthe sp.	ATAGCAATCG	CAATTC	CGCATC	CTTGG	GCATG	TATCC	GGG
MGC8.4 Colletotrichum sp.	ATAGCAATCG	CAATTC	CGCATC	CTTGG	GCATG	TATCC	GGG
MGC9.2	ATAGCAATCG	CAATTC	CGCATC	CTTGG	GCATG	TATCC	GGG
MGF12.3 Xylaria sp	ATAGCAATCG	CAATTC	CGCATC	CTTGG	GCATG	TATCC	GGG
MGC13.1 Glomerella cingulata	ATAGCAATCG	CAATTC	CGCATC	CTTGG	GCATG	TATCC	GGG
MGC14.4 Hypoxylon fendleri	ATAGCAATCG	CAATTC	CGCATC	CTTGG	GCATG	TATCC	GGG
MGC15.2 Pestalotiopsis virgatu	ATAGCAATCG	CAATTC	CGCATC	CTTGG	GCATG	TATCC	GGG
QEN1 Arthrinium sacchari	ATAGCAATCG	CAATTC	CGCATC	CTTGG	GCATG	TATCC	GGG
QEN4 Alternaria tenuissima	ATAGCAATCG	CAATTC	CGCATC	CTTGG	GCATG	TATCC	GGG
QEN5 Eurotium repens	ATAGCAATCG	CAATTC	CGCATC	CTTGG	GCATG	TATCC	GGG
QEN6 Cladosporium sp.	ATAGCAATCG	CAATTC	CGCATC	CTTGG	GCATG	TATCC	GGG









1t1 *Xylaria* sp.

4.2.2 Phylogenetic analysis

Phylogenetic analysis of fungal DNA [figure 3.76] was conducted using the software MEGA21 v 3.1 (Kumar, Tamura and Nei, 2004) with the bootstrapped neighbor join (NJ) method after multiple sequence alignment was performed using Bioedit sequence alignment editor (Hall, 1999). The neighbor joining (NJ) was employed because it was the favored implementation, relative accurate and provided a good trade-off between all the available methods such as unweighted pair group method with arithmetic mean (UPGMA), maximum parsimony (MP), maximum likelihood (ML), and bayesian (BAY) (Claverie and Notredame, 2003; Hall, 2005). The sequence divergence was computed by nucleotide kimura-2 program from Mega 21 version 3.1 software (Kumar, Tamura and Nei, 2004).

Even though in most cases the tree was globally correct, construction of phylogenetic tree could have some mistakes such as wrong data or incorrect alignment so that the tree would contain few of inaccurate branches. Tree bootstrapping was a method for checking the phylogenetic tree whether it was biologically correct and meaningful by assessing its robustness so that every portion of the alignment equally supported the tree (Hall, 2005).

Figure 4.11 Phylogenetic tree from the DNA sequences of ITS region of fungi derived from marine environment (original tree)

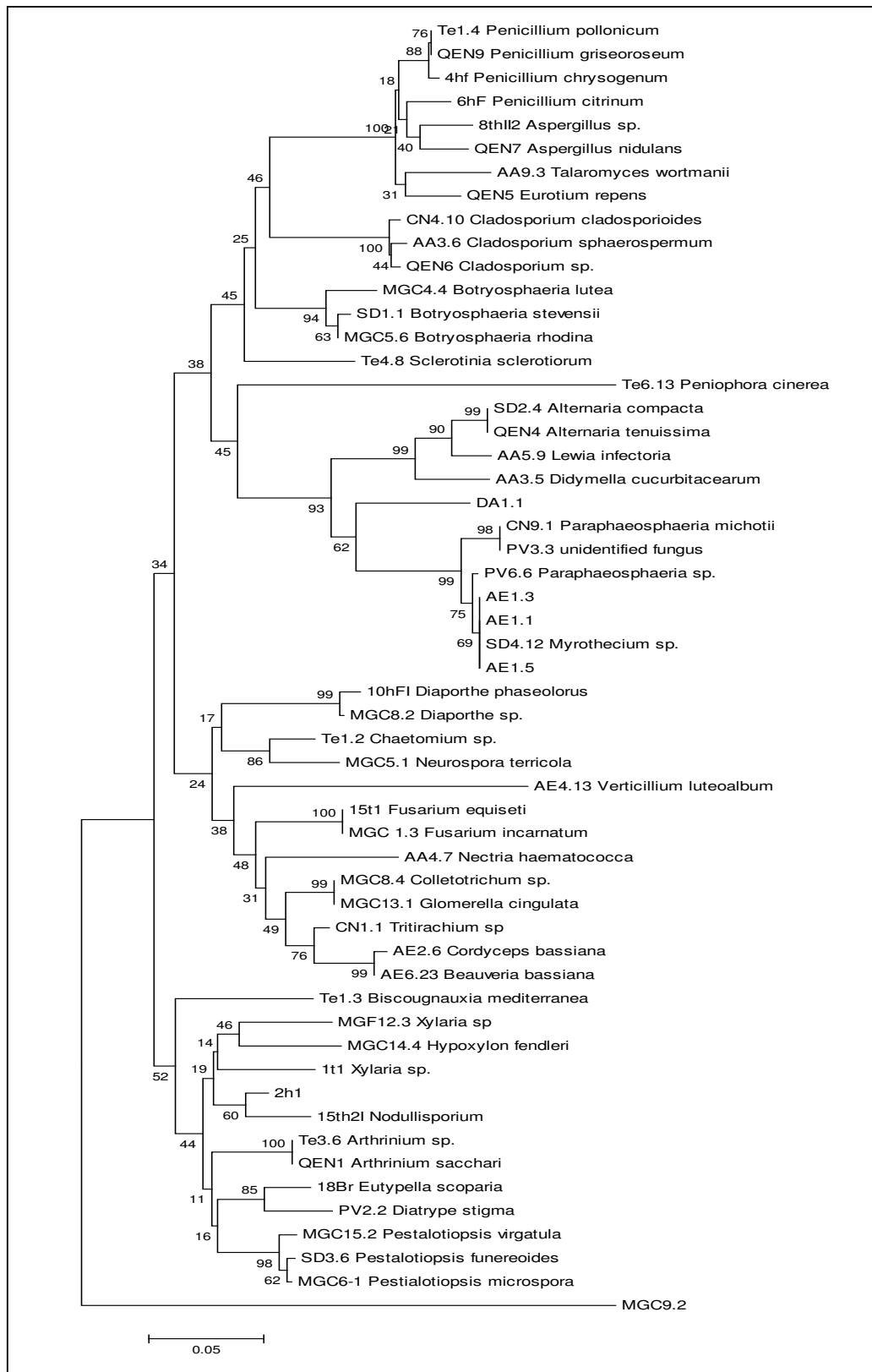
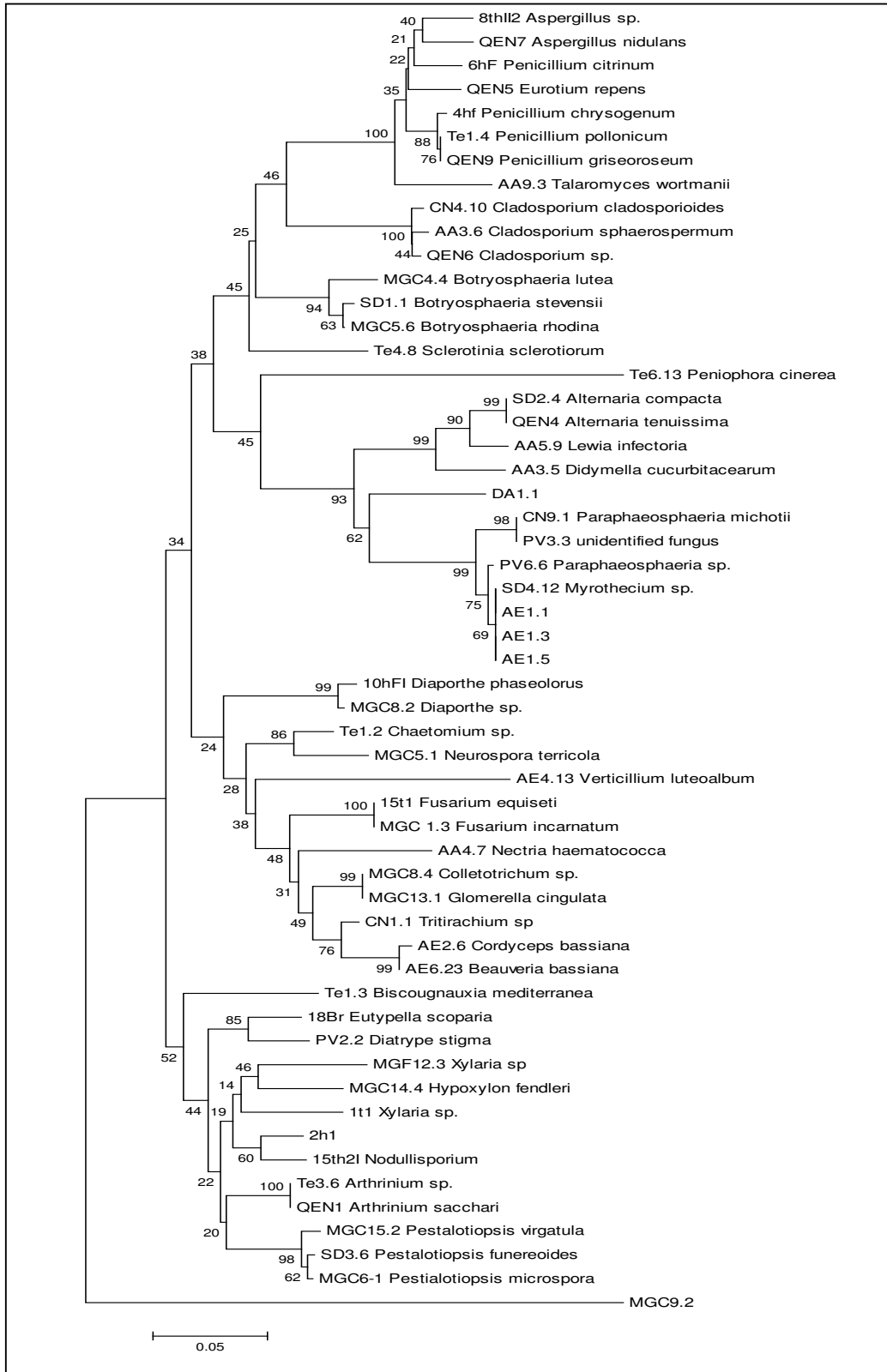


Figure 4.12 Phylogenetic tree from the DNA sequences of ITS region of fungi derived from marine environment (bootstrap consensus tree)



4.3 Assessing fungal diversity by DGGE methods using the DNA sequences of ITS region

4.3.1 Optimization of DGGE methods

PCR using ITS1-GC clamp and ITS 4 and DGGE electrophoresis were optimized using DNA templates of *Aspergillus niger*, *A. ochraceus*, *A. terreus*, and a mixed DNA of three *Aspergillus* species. Amplification was performed in two-stage PCR. The first PCR was conducted using primers ITS 1 and ITS 4. The second PCR was performed using the first PCR products as template with primers ITS1-GC clamp and ITS 4. Experimental data allowed the conclusion that the PCR protocol did not require modification due to GC clamp primer.

PCR using GC clamp in this experiment could be also directed and performed with only one direct PCR instead of two-stage amplification. The result of one direct PCR in this experiment showed weaker bands comparing to that of two stages amplification. PCR using GC clamp in complex environmental samples failed to yield any products, so that two-stage PCR was then routinely used. The reason was probably that abundance and presence of fungal organisms inside the host or environmental samples were so small.

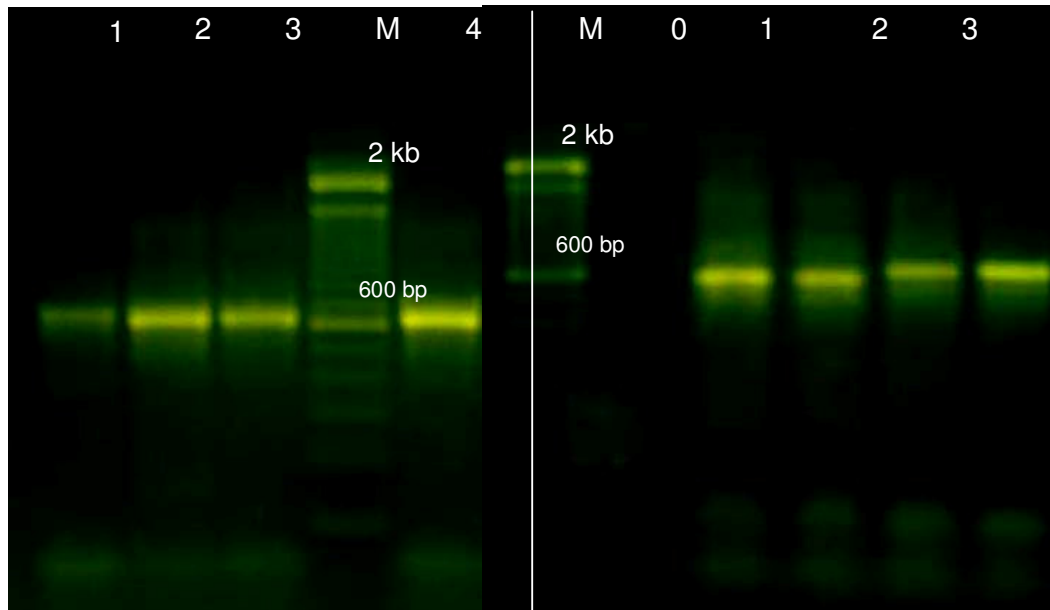
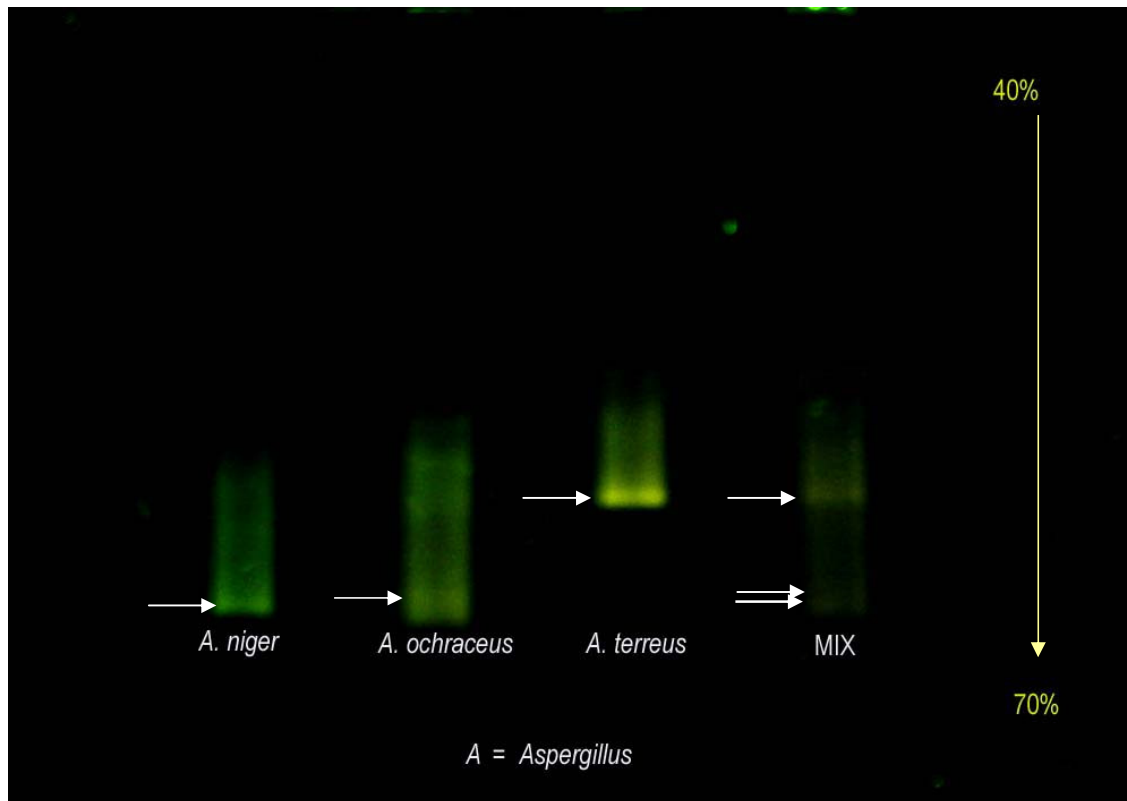


Figure 4.13 PCR products of *Aspergillus* species

A. First PCR using ITS 1 and ITS 4 **B.** Second PCR using ITS 1-GC clamp and ITS 4

M	DNA ladder
0	negative control
1	<i>Aspergillus niger</i>
2	<i>Aspergillus ochraceus</i>
3	<i>Aspergillus terreus</i>
4	DNA mixture of <i>A. niger</i> , <i>A. ochraceus</i> and <i>A. terreus</i>

Figure 4.14 DGGE of three species of *Aspergillus*

The electrophoretic separation was carried out using polyacrylamide gel with a gradient of 40% to 70% urea/ formamide at a field of 110 Volts for six hours. As expected, the sample of *A. niger*, *A. ochraceus* and *A. terreus* showed only one single band, whereas the mixture sample showed clearly distinguished three bands. The gel was stained with ethidium bromide 10 $\mu\text{g}/\text{mL}$. Due to the smear appearing in the lanes, the staining had to be improved.

The ability of primers ITS 1 and ITS 4 to amplify different or mixed templates was also proven by this experiment. Amplification of mixed DNA of *Aspergillus niger*, *A. ochraceus*, and *A. terreus* was successfully performed and checked after DGGE separation.

4.3.2 Estimating fungal diversity in marine sponges by DGGE

Optimization of Staining

Staining of DGGE gels was much more challenging than staining an agarose gel. In the case of a agarose gel – used to separate PCR products due to their length – it was sufficient to add 5 μL DNA stain per 100 mL of gel prior to casting, replacing a time-consuming submersion into a highly concentrated solution necessary due to the thickness of the gel. The risk of contamination by spilling DNA stain was minimized by introduction of the less hazardous Sybr Gold, an important benefit since ethidium bromide was used before.

This staining method provided very good detection without destaining and did not require any optimization. While sharing the same principle – separation of charged compound in electric field – the DGGE is very different in practice, requiring an optimization considering simplicity of handling, health and environmental concerns, quality of the result as well as the cost factor.

The agarose gel provided a big reservoir of DNA stain. its volume and the volume of the electrophoresis buffer were of the same order of magnitude. In the case of DGGE, the buffer volume was two orders of magnitude bigger. In the electric field the DNA stain migrated in the opposite direction of the DNA.

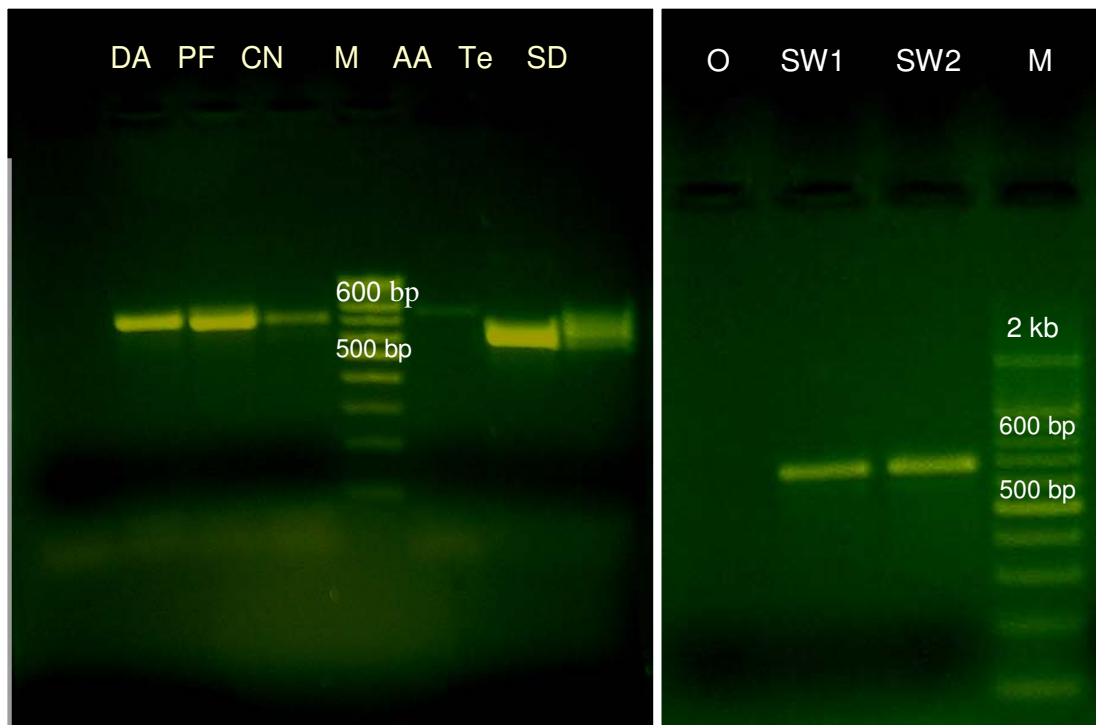
Considering a six times longer duration and the dilution factor, the whole stain would have been washed out from the gel. Compensation would have required high amounts of DNA stain, increasing cost and waste volume. Staining by submersion seemed to be the better alternative, but came along with disadvantages as well. The fragile gel had to be separated from the stabilizing glass sandwich, the handling increased the risk of spillage.

While the quality of staining increased with the duration of submersion the DNA migrated, decreasing the quality of separation. As a conclusion, staining by submersion was chosen due to costs for DNA stain, amount of waste and risk of spilling.

The choice of Sybr Gold over ethidium bromide reduced the health risk in case of contamination. Furthermore, Sybr Gold appeared to be the more sensitive stain, allowing shorter submersion. The final optimization step was the determination of the staining duration.

Total DNA extracts from Mediterranean sea sponges, *Dysidea avara* (DA), *Petrosia ficiformis* (PF), *Chondrilla nucula*, *Aplysina aerophoba* (AA), *Tethya sp.* (Te) and *Suberites domuncula* (SD), were subjected to two-stage PCR using ITS 1-GC clamp and ITS 4. Besides, total DNA obtained from the sea water sample enriched by a sterile filter was included.

Figure 4.15 Electropherogram of PCR products from Mediterranean sea sponges and sea water



Code	Samples
DA	<i>Dysidea avara</i>
PF	<i>Petrosia ficiformis</i>
CN	<i>Chondrila nucula</i>
M	DNA ladder
Te	<i>Tethya sp.</i>
SD	<i>Suberites domuncula</i>
0	Negative control
SW1	Seawater sample 1
SW2	Seawater sample 2

For electrophoretic separation, a polyacrylamide gel with a gradient of 40% to 70% urea/ formamide was used at 110 Volts for six hours. Optimization of staining was performed comparing the result of two staining protocols. The first staining protocol used 50 $\mu\text{g}/\text{mL}$ Sybr Gold in TAE buffer for 20 minutes and the second protocol for two hours. Both were destained using TAE buffer for 15 minutes.

Staining the gel for 20 minutes was giving better result and it allowed band cutting for amplification and identification by direct sequencing in the next step.

Figure 4.16 DGGE of Mediterranean Sea sponges and sea water

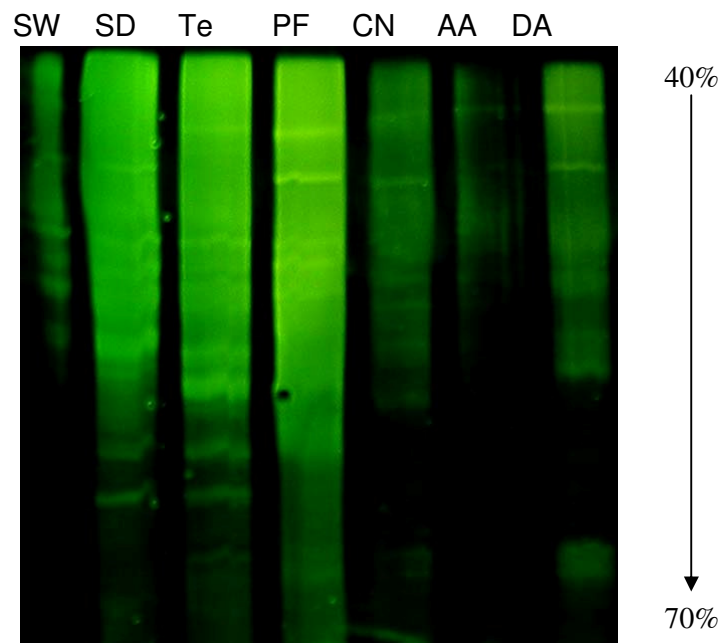
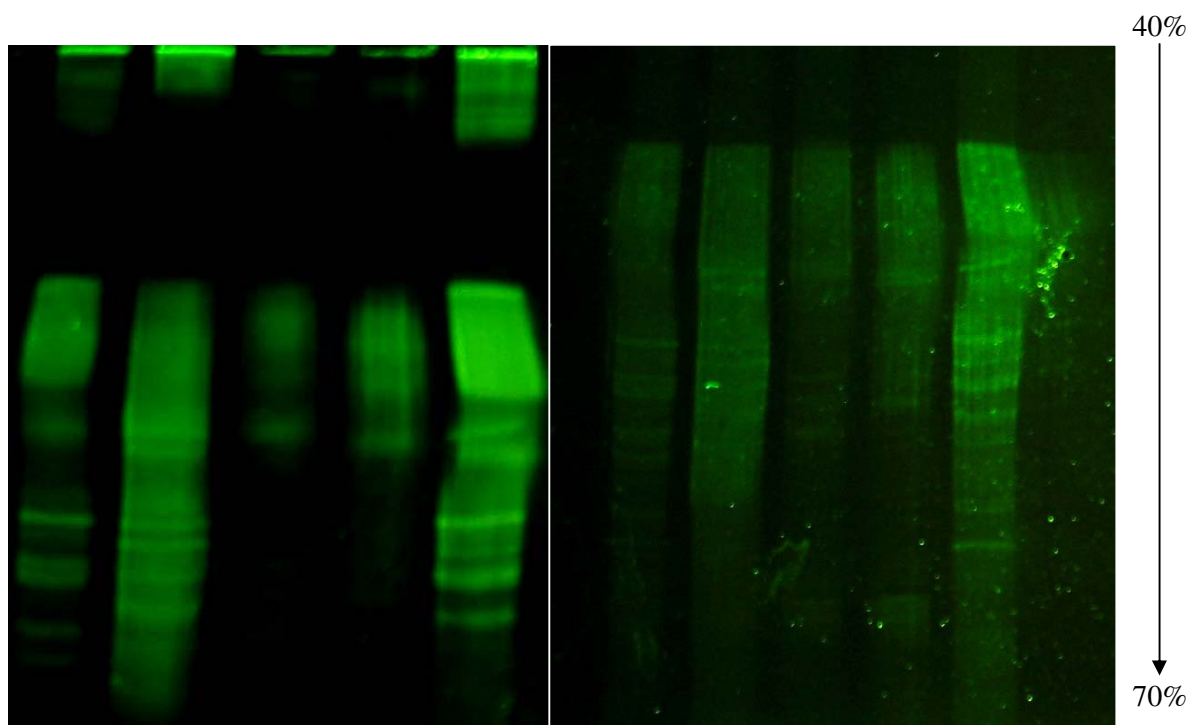
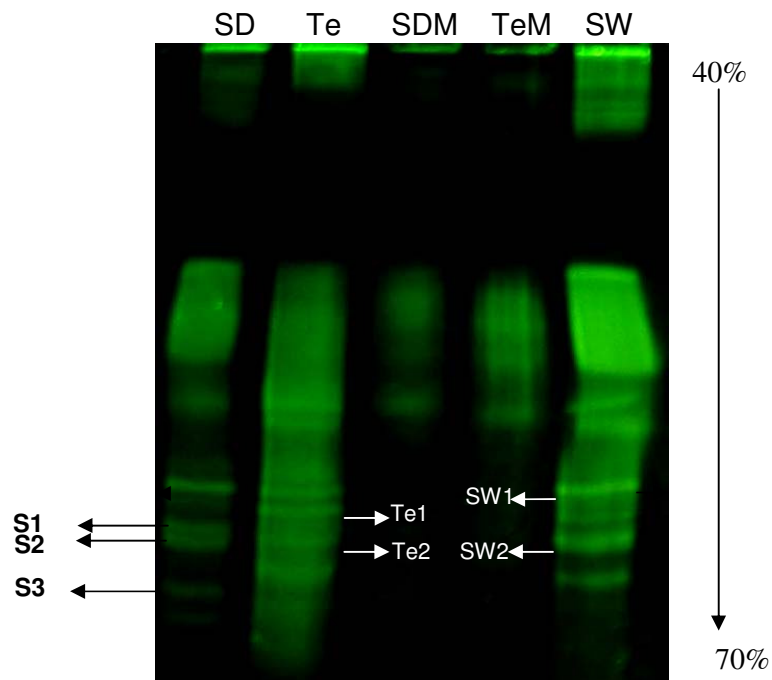


Figure 4.17 DGGE of sponges *Suberites domuncula*, *Tethya sp.* and sea water

Code	Samples
SD	<i>Suberites domuncula</i>
Te	<i>Tethya sp.</i>
SDM	DNA mixture of fungi isolated from <i>Suberites domuncula</i>
TeM	DNA mixture of fungi isolated from <i>Tethya sp.</i>
SW	Seawater

Seven bands were successfully cut from the DGGE gel under UV transillumination and targeted for amplification by PCR primers.



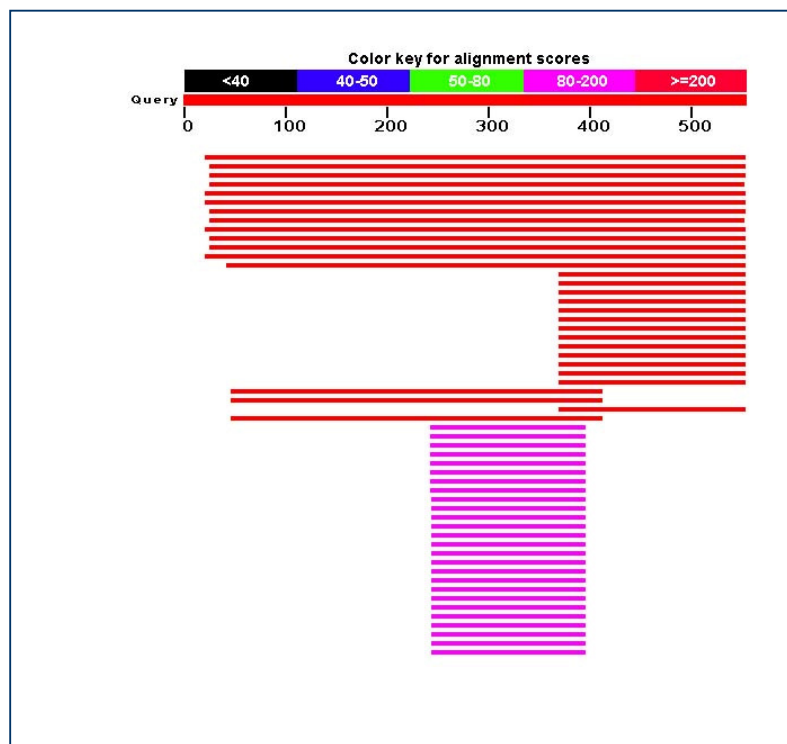
The bands were incubated in the elution buffer overnight and purified by PerfectPrep Gel Cleanup Kit due to the manufacturer's protocol and amplified by PCR using the primers ITS 1 and ITS 4. One band was recovered and gave positive result in the DNA electrophoresis. This single band then was subjected to direct sequencing using primer ITS 1.

Figure 4.18 Electropherogram of recovered bands from DGGE gel



The sequence obtained from the direct sequence was subjected to BLAST search in the GenBank (www.ncbi.nlm.nih.gov/blast) leading the sequence to be identified belonging to the marine sponge *Aplysina aerophoba*.

Figure 4.19 BLAST search from recovered DGGE band



Sequences producing significant alignments:
(Click headers to sort columns)

Accession	Description	Max score	Total score	Query coverage	E value	Max ident	Links
AY591786.1	<i>Aplysina aerophoba</i> 18S ribosomal RNA gene, partial sequence; intern	900	900	96%	0.0	93%	
AY591793.1	<i>Aplysina fulva</i> 18S ribosomal RNA gene, partial sequence; internal tra	822	822	95%	0.0	93%	
AJ621545.1	<i>Aplysina fistularis</i> 18S rRNA gene (partial), ITS1, 5.8S rRNA gene, ITS	822	822	95%	0.0	93%	
AJ705047.1	<i>Microciona prolifera</i> 18S rRNA gene (partial), 5.8S rRNA gene, 28S rR	821	821	94%	0.0	93%	
AY591795.1	<i>Aplysina lacunosa</i> 'hard' 18S ribosomal RNA gene, partial sequence; i	821	821	96%	0.0	93%	
AY591788.1	<i>Aplysina archeri</i> 18S ribosomal RNA gene, partial sequence; internal t	815	815	96%	0.0	93%	
AY591790.1	<i>Aplysina cauliformis</i> 'thick' 18S ribosomal RNA gene, partial sequence	813	813	95%	0.0	93%	
AY591792.1	<i>Aplysina fistularis</i> 18S ribosomal RNA gene, partial sequence; internal	811	811	94%	0.0	93%	
AY591789.1	<i>Aplysina cauliformis</i> 'thin' 18S ribosomal RNA gene, partial sequence;	809	809	96%	0.0	93%	
AY591791.1	<i>Aplysina fistularis</i> 18S ribosomal RNA gene, partial sequence; internal	808	808	95%	0.0	93%	
AY591794.1	<i>Aplysina insularis</i> 18S ribosomal RNA gene, partial sequence; internal	793	793	95%	0.0	92%	
AY591787.1	<i>Aplysina cavernicola</i> 18S ribosomal RNA gene, partial sequence; inter	582	582	96%	4e-163	86%	
AY591796.1	<i>Aplysina lacunosa</i> 'soft' 18S ribosomal RNA gene, partial sequence; in	407	407	92%	3e-110	80%	
DQ411443.1	<i>Aplysina aerophoba</i> voucher LT-S(1) MB03-1 5.8S ribosomal RNA gen	316	316	33%	5e-83	96%	
DQ411444.1	<i>Aplysina aerophoba</i> voucher LT-S(2) MB03-5 5.8S ribosomal RNA gen	305	305	33%	1e-79	95%	
DQ411442.1	<i>Aplysina cauliformis</i> voucher WM-B 604 5.8S ribosomal RNA gene, pa	300	300	33%	5e-78	95%	
DQ411440.1	<i>Aplysina cauliformis</i> voucher BW-B 618 5.8S ribosomal RNA gene, pai	300	300	33%	5e-78	95%	
DQ411439.1	<i>Aplysina fistularis</i> voucher WM-B(1) 607 5.8S ribosomal RNA gene, pa	300	300	33%	5e-78	95%	
DQ411433.1	<i>Aplysina fulva</i> voucher NN-B 609 5.8S ribosomal RNA gene, partial se	300	300	33%	5e-78	95%	
DQ411432.1	<i>Aplysina fulva</i> voucher WM-B 620 5.8S ribosomal RNA gene, partial si	300	300	33%	5e-78	95%	
DQ411431.1	<i>Aplysina fulva</i> voucher BP-B L03-25 5.8S ribosomal RNA gene, partial	300	300	33%	5e-78	95%	
DQ411436.1	<i>Aplysina fistularis</i> voucher WM-B(2) 619 5.8S ribosomal RNA gene, pa	298	298	33%	2e-77	94%	
DQ411435.1	<i>Aplysina fistularis</i> voucher RG-B 606 5.8S ribosomal RNA gene, partia	298	298	33%	2e-77	94%	
DQ411434.1	<i>Aplysina fulva</i> voucher SR-B 602 5.8S ribosomal RNA gene, partial se	298	298	33%	2e-77	94%	
DQ411441.1	<i>Aplysina cauliformis</i> voucher WH-B L03-15 5.8S ribosomal RNA gene,	294	294	33%	2e-76	94%	
DQ411438.1	<i>Aplysina cauliformis</i> voucher SR-B 603 5.8S ribosomal RNA gene, par	292	292	33%	8e-76	94%	
AY591798.1	<i>Aiolochroia crassa</i> 18S ribosomal RNA gene, partial sequence; interne	292	292	65%	8e-76	80%	
AJ621544.1	<i>Aiolochroia crassa</i> 18S rRNA gene (partial), ITS1, 5.8S rRNA gene, IT	292	292	65%	8e-76	80%	
DQ411437.1	<i>Aplysina fistularis</i> voucher BP-B L03-26 5.8S ribosomal RNA gene, pai	289	289	33%	1e-74	92%	
AY591797.1	<i>Veronula qiantea</i> 18S ribosomal RNA gene, partial sequence; interr	272	272	65%	1e-69	80%	

4.3.3 Estimating fungal diversity in mangrove plants by DGGE

Due to the fact that the primer pair ITS 1 and ITS 4 also will yield a PCR product as plant DNA, more than one band could be expected for the electrophoresis after the first PCR step in the case of mangrove plants. Only bands in the range of 500 to 600 basepairs, common length of fungi, have been selected for the second PCR using the ITS 1 GC and ITS 4 primers.

Experiment of DGGE of mangrove plants was carried out using a polyacrylamide gel with a gradient of 0% to 100% urea/ formamide at 110 Volts for six hours and stained by 10µg/mL ethidium bromide for 20 minutes. No band cutting was conducted in this experiment.

Figure 4.20 Electropherogram of PCR products from mangrove plants

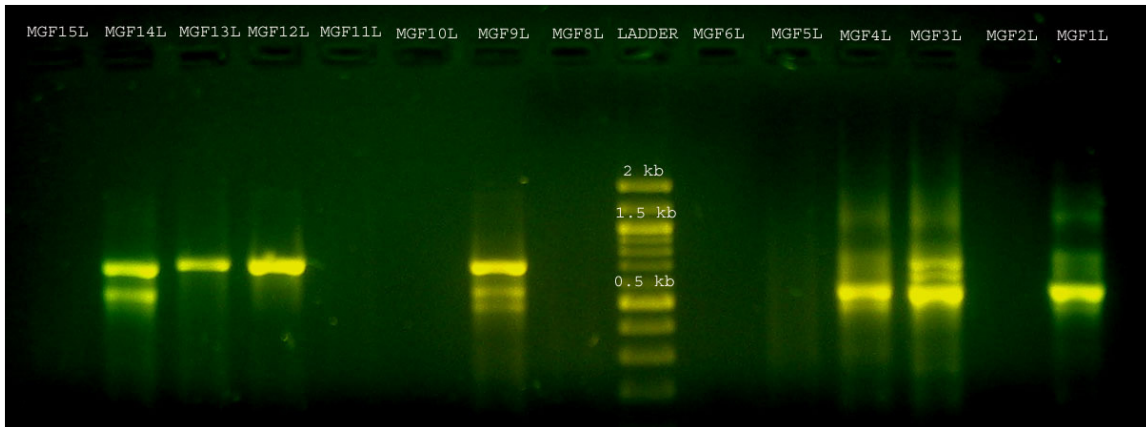
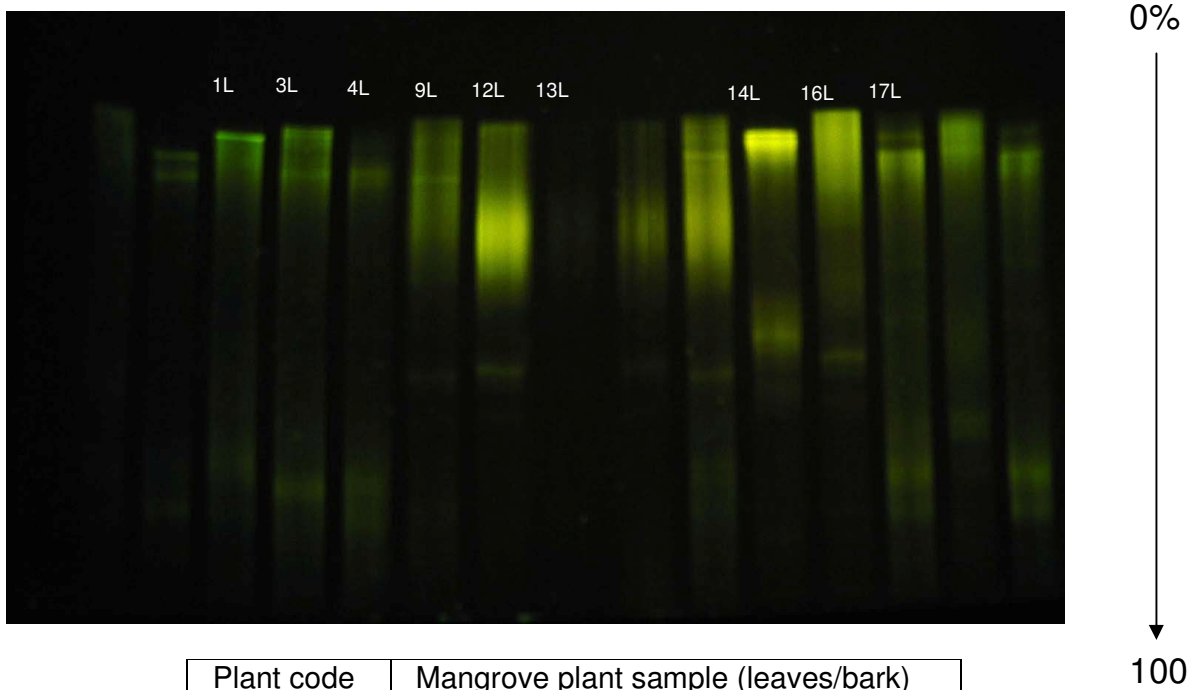


Figure 4.21 DGGE experiment of mangrove plants using a polyacrylamide gel with a gradient of 0% to 100% urea/ formamide



Plant code	Mangrove plant sample (leaves/bark)
MGF1	<i>Heritiera littoralis</i>
MGF 2	<i>Rhizophora mucronata</i>
MGF 4	<i>Bruguiera sexangula</i>
MGF 5	<i>Bruguiera gymnorrhiza</i>
MGF 6	<i>Sonneratia alba</i>
MGF 8	<i>Sonneratia</i> sp.

MGF 9	<i>Avicennia marina</i>
MGF 10	<i>Laguncularia racemosa</i>
MGF 12	<i>Aegiceras corniculatum</i> Blanco
MGF 13	<i>Sonneratia caseolaris</i>
MGF 14	<i>Kandelia candel</i>
MGF15	<i>Excoecaria agallocha</i>
MGF 16	<i>Xylocarpus granatum</i>

Seven samples showing positive results in PCR using ITS 1-GC clamp and ITS 4 were subjected to DGGE. The DGGE was then performed using polyacrylamide gel with a denaturing gradient from 40% to 70% urea/ formamide at 110 Volts for six hours using 50 µg/mL Sybr Gold.

Figure 4.22 Electropherogram of PCR products from mangrove plants

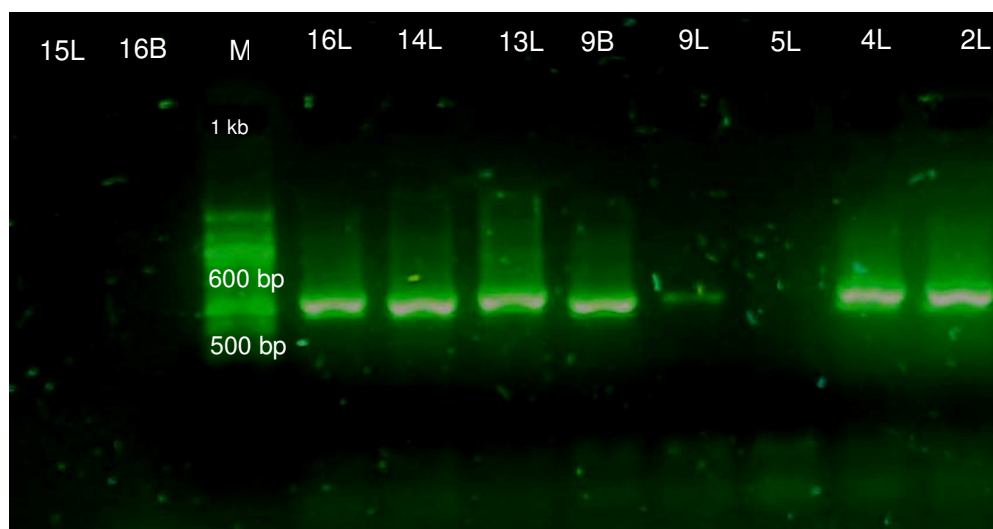
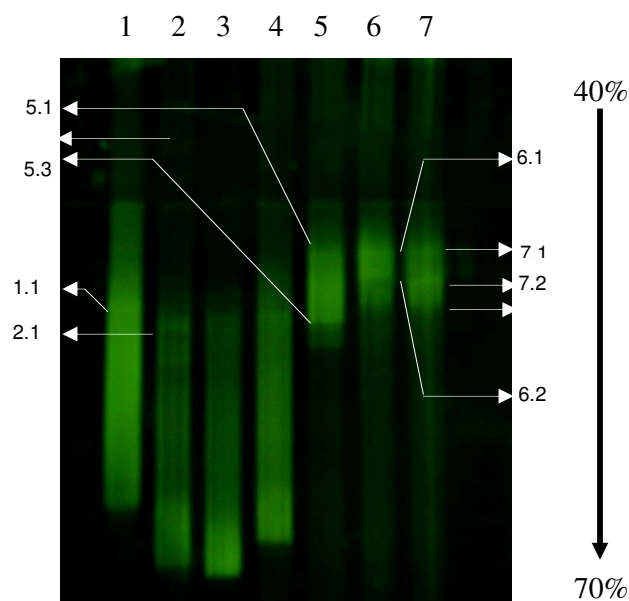


Figure 4.23 DGGE of mangrove plants using a polyacrylamide gel with a gradient of 0% to 70% urea/ formamide

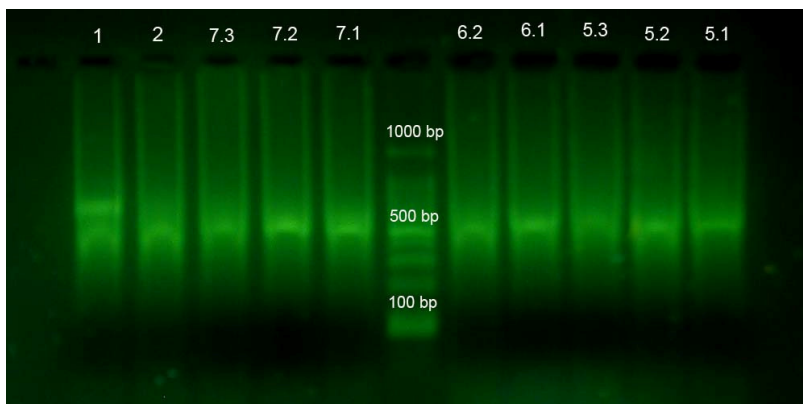


Code	Mangrove plant (environmental sample)
1.	MGF16L
2.	MGF14L
3.	MGF13L
4.	MGF4L
5.	MGF2L
6.	MGF9B
7.	MGF9L

Only sharp bands in the DGGE gel have been cut after staining with Sybr Gold for 20 minutes followed by destaining for 15 minutes. DNA was recovered by incubation of the polyacrylamide gel slices in water for 12 hours, followed by PCR using primer ITS 1 and ITS 4. The PCR products were then sequenced by direct

sequencing. Seven bands have been extracted and gave a positive result in PCR [figure 4.24]

Figure 4.24 PCR products recovered from DGGE separation



The PCR of recovered bands of DGGE gel yielded relatively thin bands in the agarose gel electrophoresis. Band 1 (MGF 16L) had two bands. Only one band with the length about 500-600 basepairs was purified and subjected for direct sequencing.

Nr.	PCR code	Plant code	Plant species	Source	Recovered Band(s)
1.	13	MGF16L	<i>Xylocarpus granatum</i>	leaves	1 band
2.	14	MGF14L	<i>Kandelia candel</i>	leaves	1 band
3.	15	MGF13L	<i>Sonneratia caseolaris</i>	leaves	-
4.	17	MGF4L	<i>Bruguiera sexangula</i>	leaves	-
5.	20	MGF2L	<i>Rhizophora mucronata</i>	leaves	3 bands (5.1,5.2,5.3)
6.	22	MGF9B	<i>Avicennia marina</i>	Bark	2 bands (6.1,6.2)
7.	27	MGF9L	<i>Avicennia marina</i>	leaves	3 bands (7.1,7.2,7.3)

Three of seven PCR products were successfully sequenced by direct sequencing using primer ITS 1 leading to a fungal organism:

Band code	Fungi species	Source	E-value	Gaps	Identities
6.1	<i>Alternaria</i> sp.	<i>Avicennia marina</i> (bark)	0.0	0%	97%
7.1	<i>Alternaria</i> sp.	<i>Avicennia marina</i> (leaves)	0.0	0%	95%
7.3	<i>Fusarium</i> sp.	<i>Avicennia marina</i> (leaves)	4e-115	0%	92%

5. DISCUSSION OF ISOLATED METABOLITES

In the course of this thesis, there were a total of 31 compounds isolated from twelve species of fungi including 14 alkaloids, 12 polyketides and 1 pimarane diterpene. In the polyketide group, the subgroups of macrolides, preanthraquinones and anthraquinones were present.

5.1 Alkaloids

Alkaloids comprise an enormous group of natural products, and are characterized by having a nitrogen atom in their molecules. In general, this nitrogen is biogenetically derived from amino acids, and usually incorporated into a heterocyclic ring and in most cases has basic properties (Seigler, 1998). Bick (1985) defined that an alkaloid is a cyclic compound containing a nitrogen atom in a negative oxidation state, which is of limited distributed among living organisms.

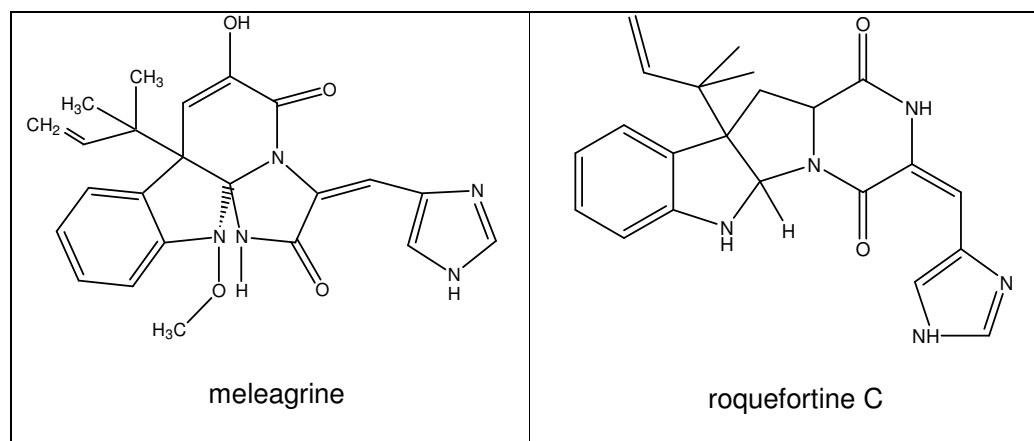
Alkaloids are derived from many biosynthetical pathways, including those of amino acids, but in some cases also including polyketide, shikimic acid, acetate and terpenoid-derived moieties. Most alkaloids are biosynthetically derived from amino acids such as lysine, phenylalanine, tyrosine, tryptophan, nicotinic acid, anthranilic acid and ornithine (Seigler, 1998).

5.1.1 Alkaloids from *Penicillium citrinum*

5.1.1.1 Meleagrins and Roquefortine

Meleagrins were first isolated and described by Hozawa and Nakajima in 1979 from the culture filtrate of *Penicillium meleagrinum*. Roquefortine C and meleagrins are biosynthetically closely related. Ohmomo *et al.* (1975) was the first group who isolated

roquefortine C from *Penicillium roquefortii*. Both compounds possess several unique structural features (see below).



In figure 5.1, a series of metabolites biosynthetically related and structurally similar to roquefortine and meleagrins are shown to be derived from a common biosynthetic pathway, the so-called roquefortine/oxaline pathway, as proposed by Reshetilova *et al.* in 1995. The initial steps include the formation of the diketopiperazine from tryptophan and histidine (Nozawa and Nakajima, 1979), which then is coupled to a (rearranged) dimethylallyl pyrophosphate unit to yield roquefortine D. The latter undergoes an intriguing skeletal re-arrangement to give roquefortine C. *N*-hydroxylation and subsequent *O*-methylation steps would then result in the formation of glandicoline A, meleagrins, and oxaline, respectively.

Roquefortine C still retains the original diketopiperazine-derived backbone. On the other hand, this backbone in meleagrins was rearranged and there is a single carbon atom carrying three nitrogen functionalities (Konda *et al.*, 1980).

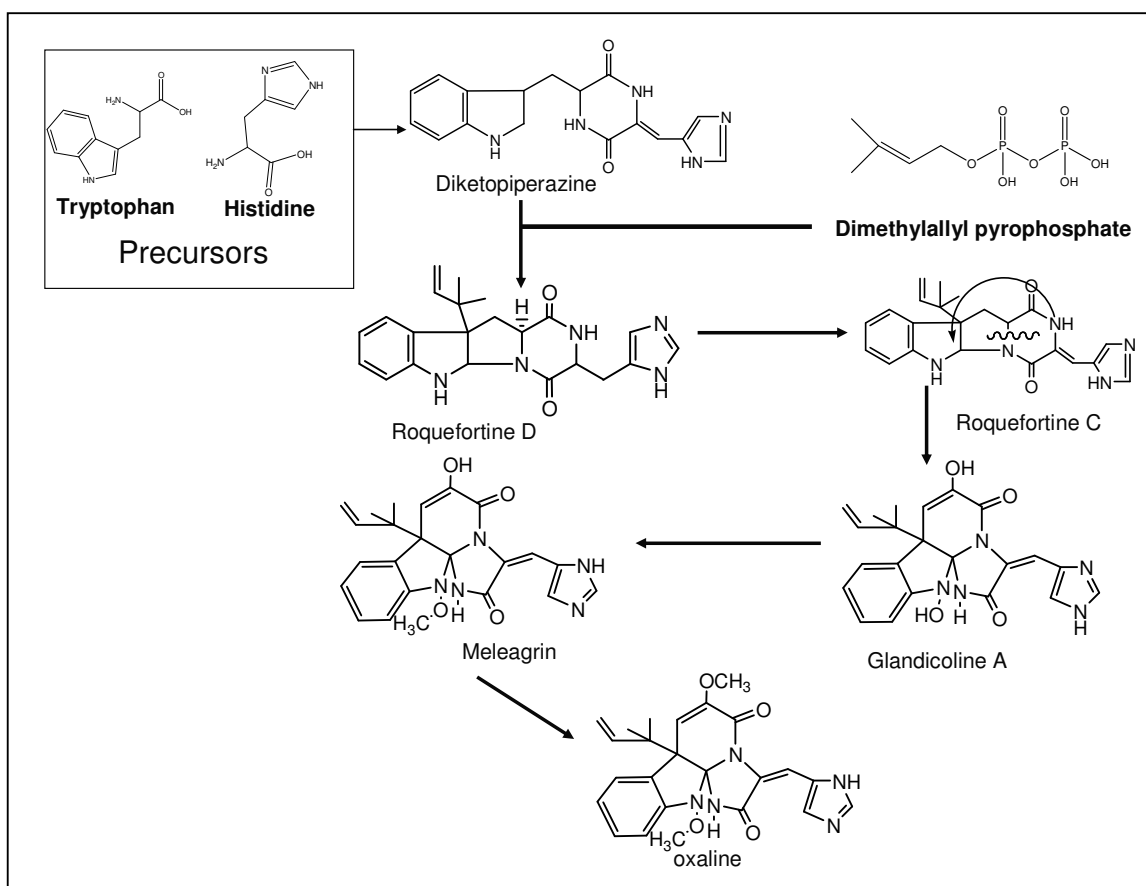


Figure 5.1 Roquefortine/oxaline biosynthetic pathway in *Penicillium ser. Corymbifera*
(Overy *et al.*, 2005)

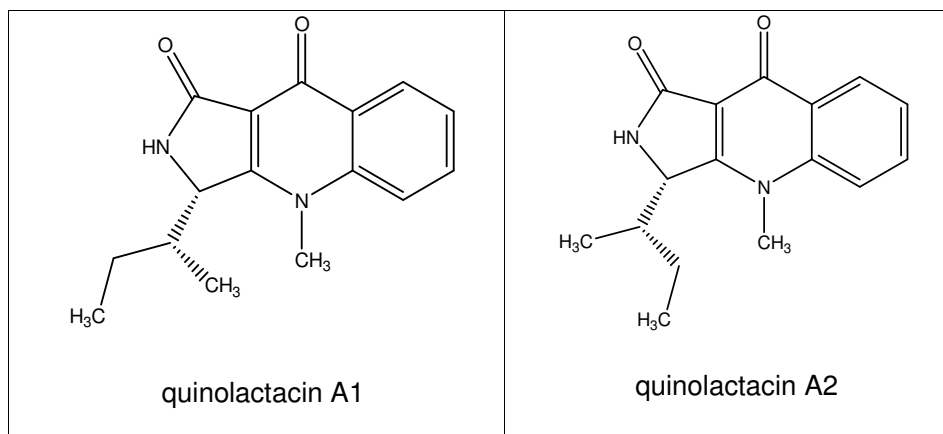
Penicillium citrinum and the other *Penicillium* spp. in the taxa of the *Penicillium ser. Corymbifera* are well known producing those alkaloids which were mentioned in the roquefortine/ oxaline pathway. All fungi need nitrogen for their biosynthesis of complex molecules such as amino acids, proteins and nucleic acids. For this reason, extracellular nitrogen sources such as proteins normally are broken down by proteases into smaller units in order to transport them into the cells. Most of the species belonging to the group *Penicillium ser Corymbifera* do not produce exogenous proteases and therefore they do not have ability to breakdown extracellular proteins into transportable amino acids (Overy *et al.*, 2005). Thus, there is speculation that roquefortine and other structural similar metabolites of the roquefortine/ oxaline

pathway may serve as exogenous nitrogen source. These compounds can enter and exit the cells through both energy-independent or succinate energy dependent mechanisms (Reshetilova *et al.*, 1995) so that nitrogen would not have to be actively pumped into the cells. Once these alkaloids accumulated in the colonized tissue, they could be transported subsequently into growing hyphae and germinating conidia, converted into primary metabolites to facilitate the growth. Additionally, the use of alkaloids as an exclusive and transportable nitrogen source has been previously proposed in plants (Wink *et al.*, 2003). Based on these findings, it was also hypothesized that this strategy is also employed by fungi.

Roquefortine C and meleagrins are reported to have also antimicrobial properties so that they prevent the utilization of accumulated reserves of amino acid resources by bacterial secondary infectors. Meleagrins, along with roquefortine C and D belong to the category of the tremorgenic mycotoxins. Tremorgenic mycotoxins are toxins produced by fungi which cause tremor (Walter, 2002). In this study, meleagrins showed cytotoxicity activity in MTT assay against L5178Y mouse T-cell lymphoma cells with EC₅₀ of 42 µg/ml.

5.1.1.2 Quinolactacin A1 and A2

Quinolactacin A1 and A2 were first discovered from the culture broth of *Penicillium* sp. EPF-6 which was isolated from the larvae of the mulberry pyralid, *Margarona pyloalis* Welker (Zhang *et al.*, 2002). Both quinolactacin A1 and A2 are proven to have anti-acetylcholinesterase activity. They also showed inhibitory activity against tumor necrosis factor (TNF) production by murine macrophages and macrophage-like J774.1 stimulated with lipopolysaccharide (Viegas *et al.*, 2005; Michael, 2002).

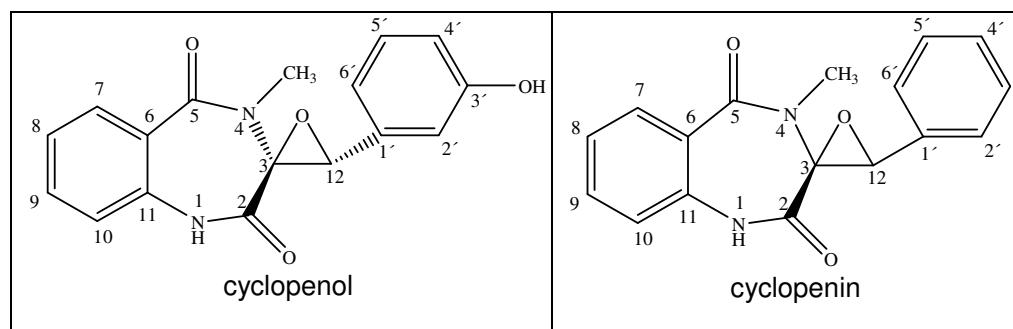


The pyrroloquinolone alkaloids quinolactacin A1 and A2 are diastereomers. Quinolactacin A1 is the C-1' diastereomer of quinolactacin A2. Uniquely, quinolactacin A2 showed 14 times higher activity in anti-acetylcholinesterase assays than its diastereomer, quinolactacin A1 (Kakinuma *et al.*, 2000).

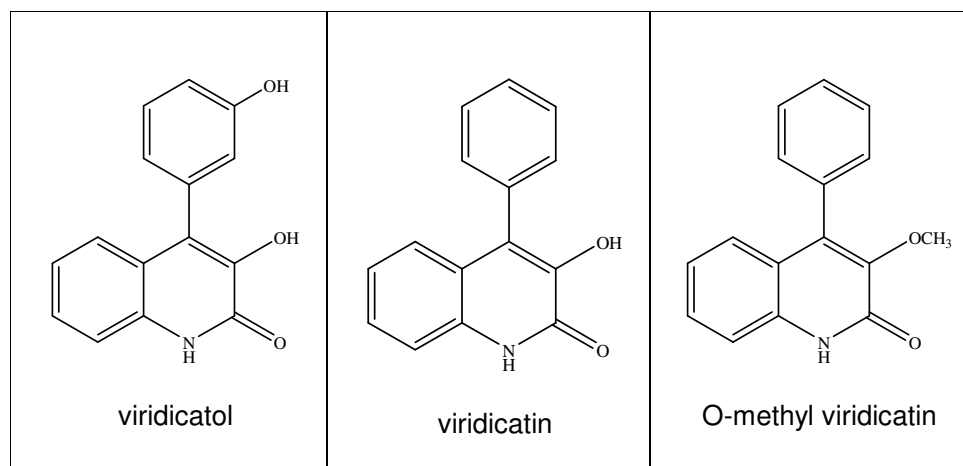
The quinolactacins are thought to be biologically synthesized from three components, i.e. isoleucine, anthranilic acid, and acetic acid. This hypothesis could actually represent a more general route to other analogues of quinolactacin-type antibiotics (Zhang *et al.*, 2002). Quinolactacin-type antibiotics such as quinolactacin B, C and the diastereomers quinolactacin A1 and A2, had a wide variety of antimicrobial activity since these compounds possessed a novel quinolone skeleton (Kakinuma *et al.*, 2000).

5.1.2 Alkaloids isolated from *Penicillium polonicum*

5.1.2.1 Cyclophenol, cyclophenin, viridicatol and viridicatin



The benzodiazepine alkaloids cyclophenin and cyclophenol were isolated by Bracker *et al.* (1954) from culture medium of *Penicillium cyclopium*. Besides chemical and physicochemical evidence, the proposal for the chemical structure of cyclophenin and cyclophenol had been influenced by biosynthetic considerations. Both alkaloids were regarded as derivatives of the cyclic dipeptide of anthranilic acid and phenyl alanine (Nover and Luckner, 1969).



This suggestion was corroborated by investigation on the biosynthesis of viridicatin and viridicatol which were first isolated by Luckner and Mothes in 1962 together from a strain of *Penicillium viridicatum* (Luckner and Mohammed, 1964). The

biosynthetic pathway for these quinoline alkaloids involves anthranilic acid and phenylalanine, with cyclophenin and cyclophenol representing intermediates [figure 5.2]. The rearrangement of the benzodiazepine ring system of the latter alkaloids to the quinoline nucleus of the former is catalyzed by a key enzyme called cyclophenase. Luckner and Winter (1969) reported that cyclophenase could be isolated from mycelium of *Penicillium viridicatum* and employed outside the fungal cell in converting cyclophenin to viridicatin.

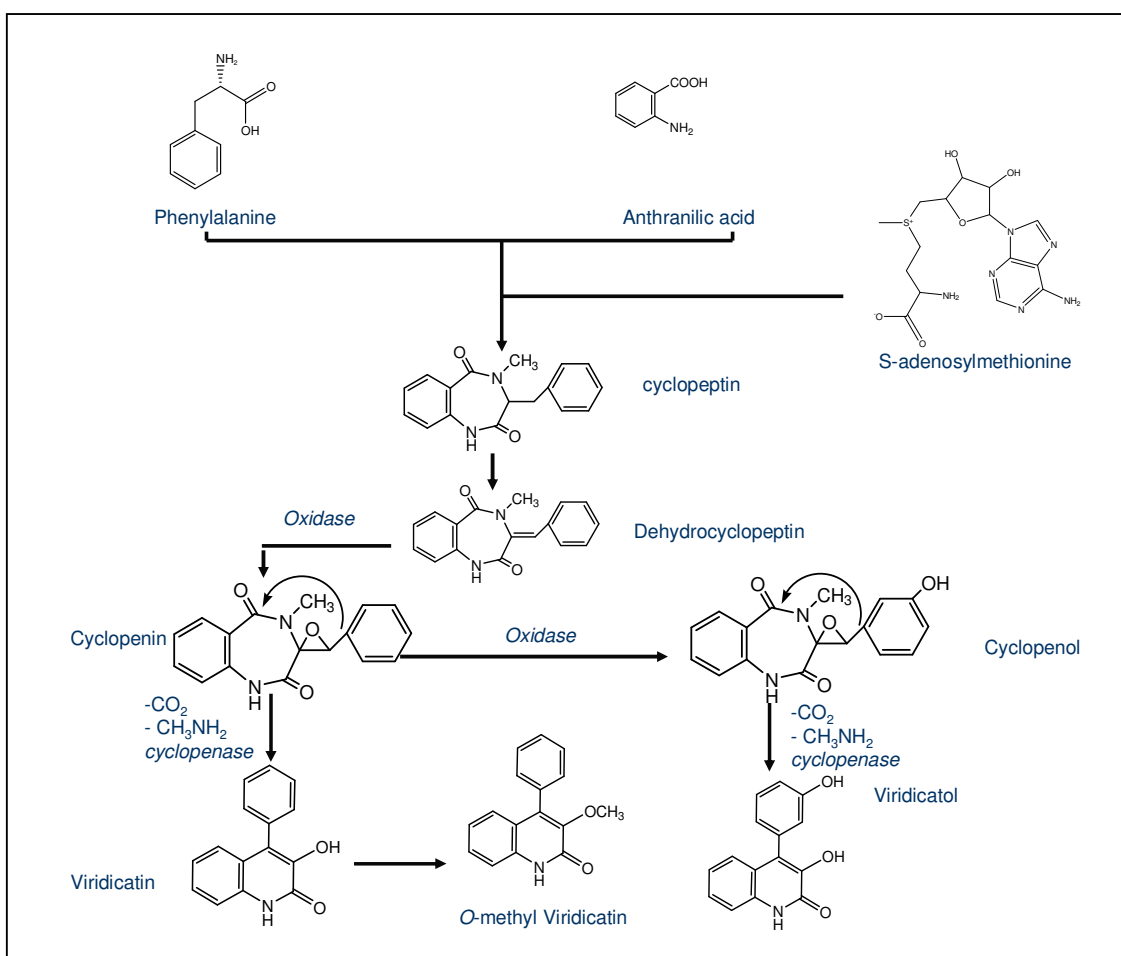


Figure 5.2 Cyclophenin/viridicatin biosynthesis pathway metabolites in *Penicillium* sp.

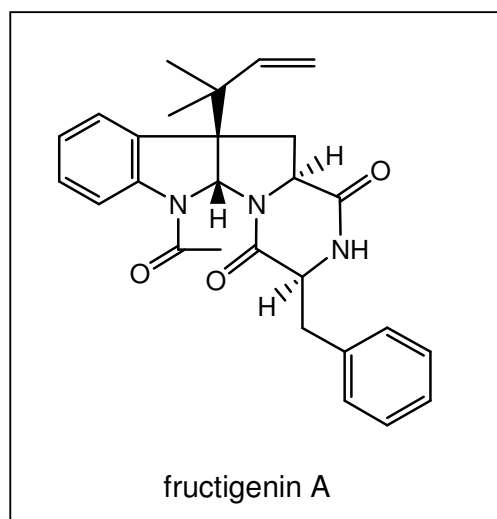
(Framm *et al.*, 1973).

Viridicatin has been described as a phytotoxin and has antimicrobial activity against *Bacillus subtilis*, *Mycobacterium tuberculosis*, *Staphylococcus aureus*, and *Saccharomyces cerevisiae* (Cunningham and Freeman, 1952). Cyclopenin and also cyclopenol are nematocidal agents and have antimicrobial activity against *S. aureus* and *Escherichia coli* (Kusano *et al.*, 2000).

5.1.1.2 Fructigenin A

Fructigenin A was first isolated by Arai *et al.* in 1989 from *Penicillium fructigenum* TAKEUCHI. Fructigenine A has a growth inhibitory activity against *Avena coleoptile* and L-5178Y cells (Arai *et al.*, 1989). The MTT assay in this study showed that EC₅₀ value of fructigenin was 0.53 µg/ml. However, this activity is probably not due to inhibition of protein kinases since it showed no activity in the protein kinase screening in this study.

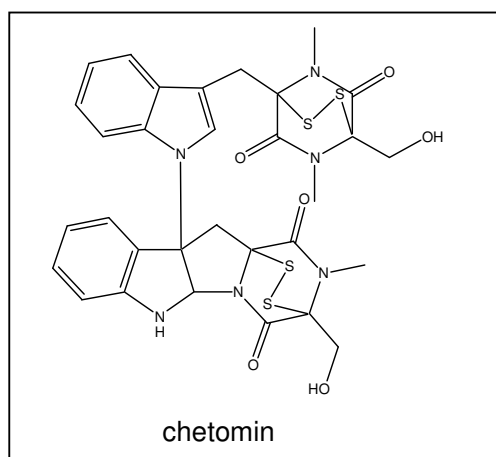
The precursors of fructigenin A based on the inspection of its structure were dimethylallyl pyrophosphate, amino acids triptophan and histidine. The structure similarity between fructigenin A and roquefortine C could be seen rather clearly.



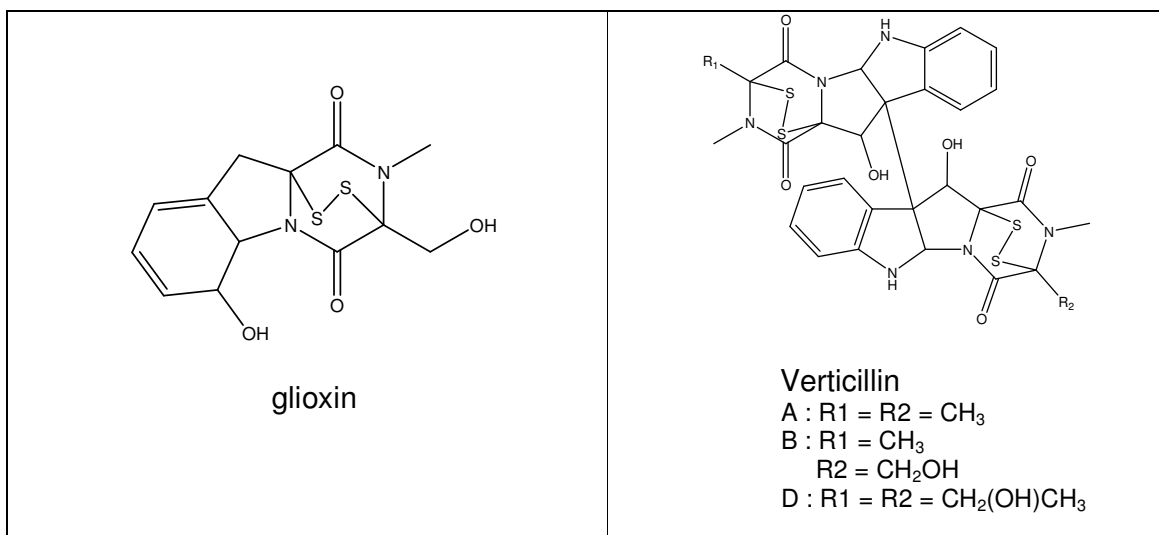
5.1.3 Alkaloids isolated from *Chaetomium* sp.

5.1.3.1 Chetomin

Chetomin is an alkaloid isolated previously from *Chaetomium cochliodes*, *C. globosum* and *C. subglobosum* which has antibiotic activity (Waksman and Bugie, 1944; Saito *et al.*, 1988). Brewer *et al.* (1972) and Taylor (1981) stated that the presence of sulphur atoms had influence to the antimicrobial activity.



Chaetomin, as well as gliotoxin and verticillin, is compound belonged to the class of epipolythiodioxopiperazines (ETP) which was characterized by the presence of internal disulphide bridge (Mullbacher *et al.*, 1986; Gardiner *et al.*, 2005).



The toxicity of this class of compounds made them attractive as potential therapeutic agents for disease such as cancer (Vigushi *et al.*, 2004). ETPs do not have exclusive protein targets. Pahl *et al.* (1996) stated that gliotoxin inhibited the transcription factor NF- κ B, probably via interaction with its essential thiol residues. Another cellular effect of ETPs is in the mitochondrion. Mitochondrial function in intact cells is inhibited by scabrosin ester of ETPs. Initially mitochondrial ATP is inhibited, then the membrane of mitochondria becomes hyperpolarized and followed by apoptosis of the cells (Moerman *et al.*, 2003).

ETP toxins can also conduct the reaction of oxidative-reductive of the cycle whereby the reduced ETP auto oxidized back to the disulphide form and produces deleterious reactive oxygen species (ROS) such as superoxide or hydrogen peroxide [figure 5.3] (Munday, 1982; Gardiner *et al.*, 2005).

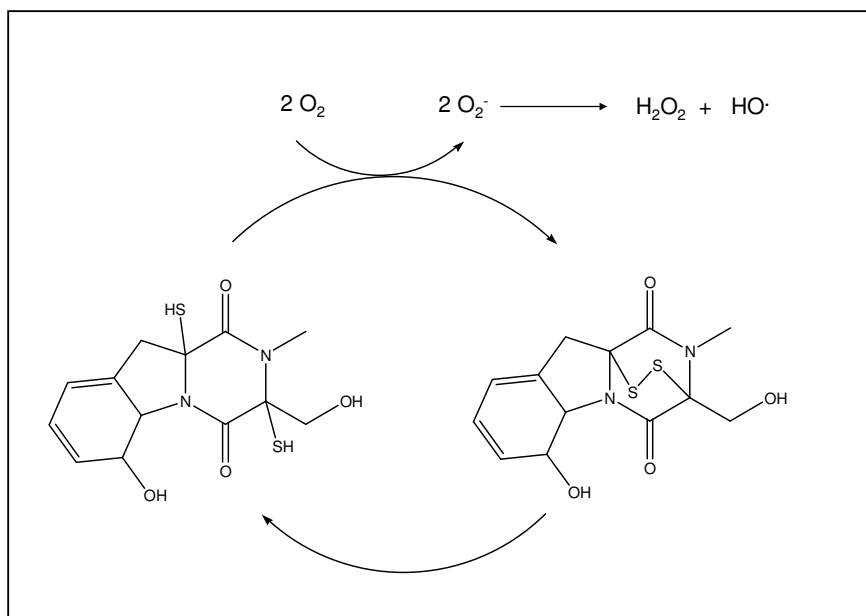


Figure 5.3 Redox cycling between the reduced (dithiol) and oxidized (disulphide) forms of gliotoxin (Gardiner *et al.*, 2005)

Amino acid precursors in chetomin biosynthesis are tryptophan, serine and sulphur containing amino acid, most probably cysteine [figure 5.4]. Introduction of the sulphur atoms into the core epipolythiodioxopiperazines is poorly understood. Labelling experiment conducted by Kirky and Robin (1980) showed that methionine, cysteine and sodium sulphate could act as source of sulphur, even though cysteine is thought to be the direct donor. The mechanism by which the sulphur was introduced is unknown and has no precedent in fungal secondary metabolism (Gardiner *et al.*, 2005).

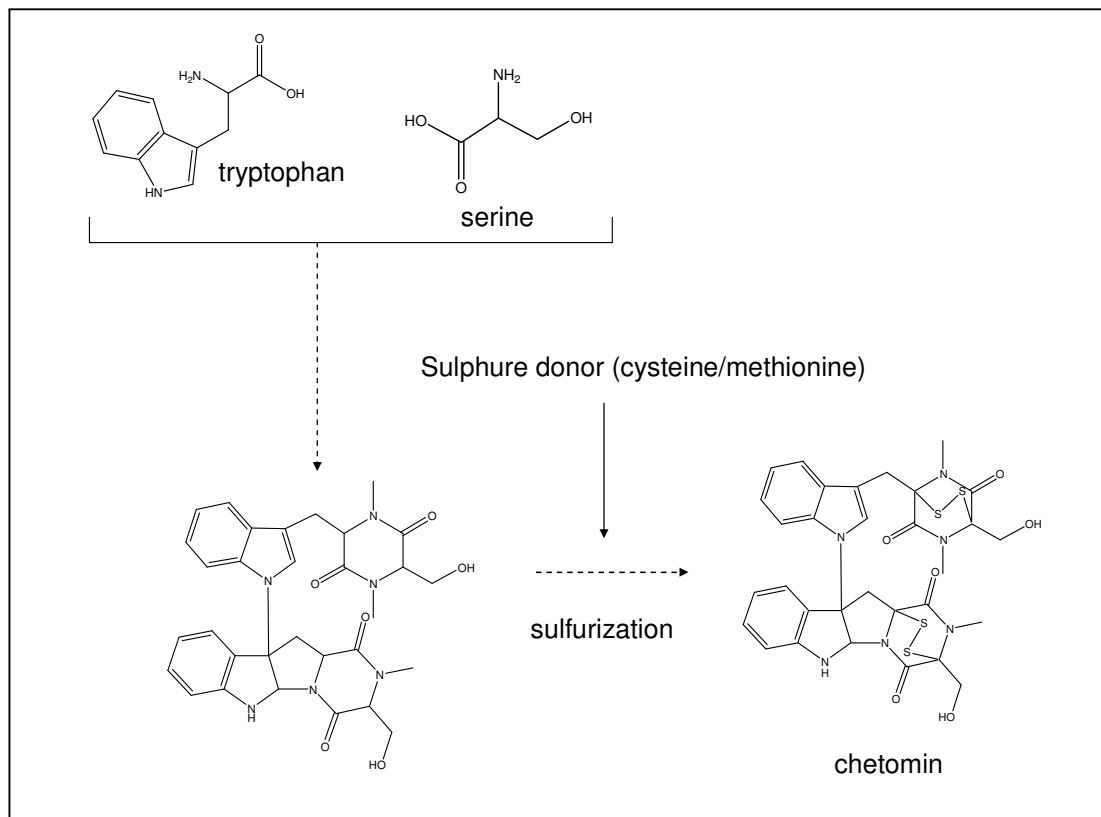


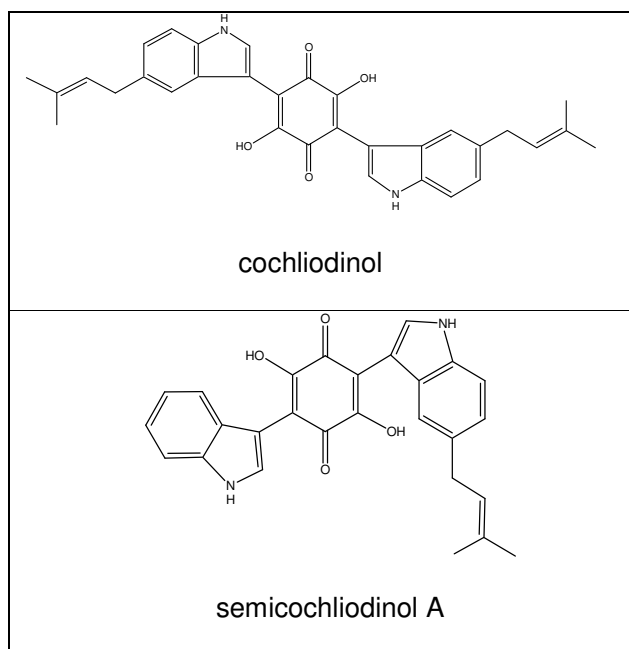
Figure 5.4 Predicted biosynthesis of chetomin (Gardiner *et al.*, 2005)

In MTT assay of this study, chetomin showed high cytotoxic activity against L5178Y mouse lymphoma cell with EC_{50} value of less than $0.1 \mu\text{g/ml}$. Protein kinase

inhibitory assay showed its inhibition activity toward ARK5, Aurora B, B-RAF-VE, CDK4/CycD1, EGF-R, ERB-B2, IGF-1R, SRC, VEGF-R2, VEGF-3, FLT3, INS-R, MET, and COT enzymes.

5.1.3.2 Cochliodinol and semicochliodinol A

Cochliodinol and isocochliodinol are biosynthesized from tryptophan and isopentenyl unit, such as dimethylallyl pyrophosphate derived from mevalonic acid. Confirmation of tryptophan and mevalonic acid as precursors of cochliodinol was proven by administration of ^{13}C - and ^{14}C - precursors. The result showed that tryptophan not only acted as precursors in indol rings of cochliodinol, but also incorporated into the oxygenated carbon atoms of its benzoquinone ring (Taylor and Walter, 1978).



Cochliodinol is mycotoxin isolated from *Chaetomium cochliodes* PALLISER and *C. globosum* and other species from genus *Chaetomium* (Sekita, 1983).

Semicochliodinol A, which first isolated from the fungus *Chrysosporium merdarium* and later also from species in genus *Chaetomium*, is known as an inhibitor of HIV-1 protease and epidermal growth receptor protein tyrosine kinase (EGF-R PTK) (Fredenhagen *et al.*, 1996). Protein tyrosine kinases are a family of enzymes catalyzing phosphorylation of tyrosine residues of protein substrates. The deregulation of these proteins activity in tumour cells is associated with malignant transformation.

In this study, cochliodinol and semicochliodinol A showed cytotoxic activity against L5178Y mouse T-cell lymphoma cells with EC₅₀ values of 0.33 µg/ml (cochliodinol) and 0.52 µg/ml (semicochliodinol A). Cochliodinol showed moderate inhibitory activity in the protein kinase assay toward EGF-R, IGHF1-R, SRC, VEGF-R2, COT and SAK enzymes, whereas semicochliodinol A showed a moderate activity toward IGHF-1R, SRC and VEGF-R2 kinases.

5.1.4 Alkaloid isolated from *Alternaria compacta*

5.1.4.1 Tenuazonic acid

Tenuazonic acid is known as a secondary metabolite found in the genera *Alternaria*, *Aspergillus* and *Sphaeropsidales* (Cole and Cox, 1981). This compound is notorious for causing several diseases in crops, especially in rice and tobacco such as sheath rot disease. In addition, tenuazonic acid also shows strong activity as insecticide, antineoplastic and antiviral agent, and in addition it is tremorgenic in mammals (Cole *et al.*, 1981). It has been found that this compound has strong cytotoxic effect against mouse lymphoma cells and human cervix cancer cell lines (Royles, 1995).

The biosynthesis of this tetramic acid proceeds through L-isoleucin and further via the intermediate, N-acetoacetyl-L-isoleucin [figure 5.5] (Royles *et al.*, 1995; Steyn

and Wessel, 1978). The substance shows keto-enol tautomerism, so that there are two more tautomers of tenuazonic acid (Royles *et al.*, 1995). Unsymmetrical cyclic β,β' -triketones can exist in solution as four different enolic forms, the external ($a,b \rightleftharpoons c,d$) and the internal ($a \rightleftharpoons b$; $c \rightleftharpoons d$) tautomers (Steyn and Wessels, 1978).

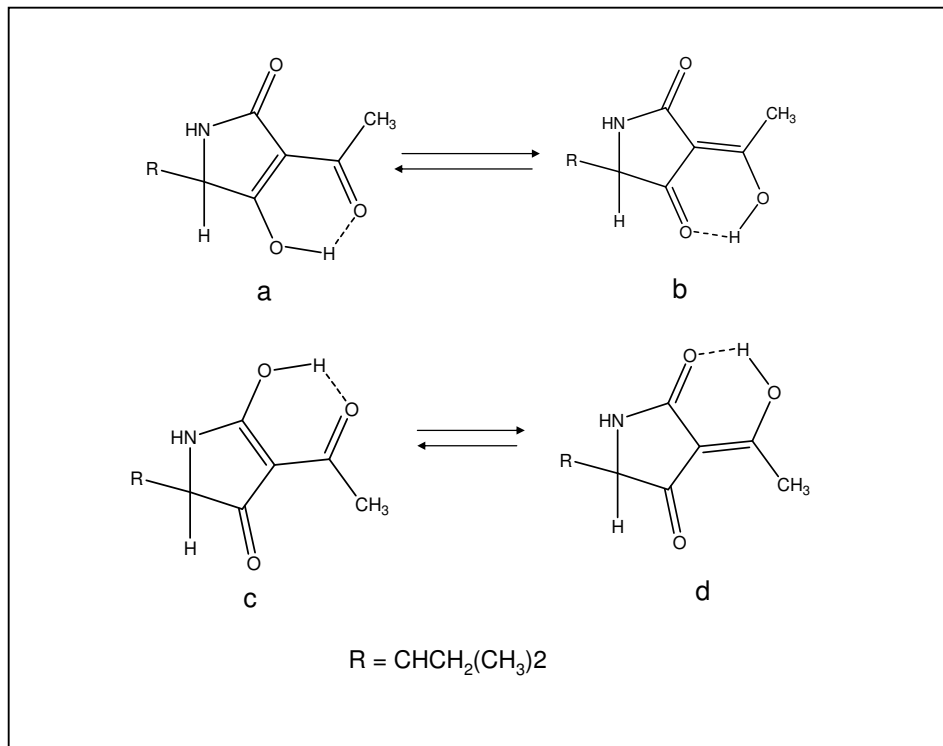


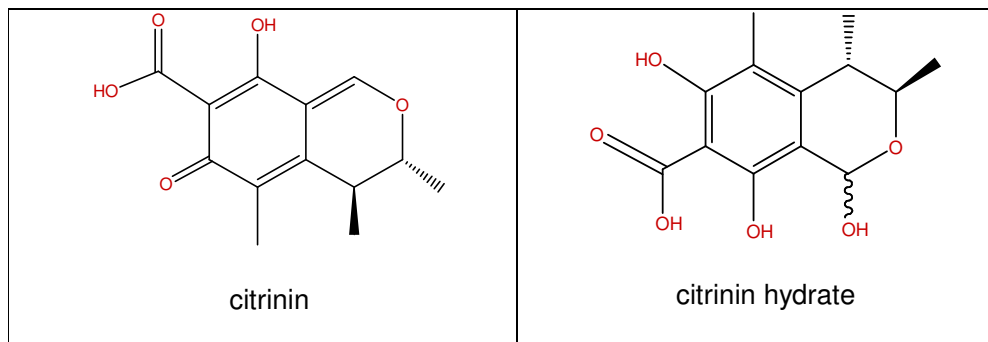
Figure 5.5 Tautomers of tenuazonic acid (Steyn and Wessels, 1978)

5.2 Polyketides

Polyketides are derived from the acetate-malonate pathway and in terms of biosynthesis are related to fatty acids. Polyketides are assembled by condensation of acetate and malonate units; however in contrast to fatty acid biosynthesis, the carbonyl group may not be reduced and intermediate compounds typically condense to produce aromatic ring systems, usually with phenolic substitution (Seigler, 1998).

5.2.1 Polyketides isolated from *Penicillium citrinum* (citrinin and citrinin hydrate)

5.2.1.1 Citrinin and citrinin hydrate



Citrinin is a mycotoxin of various species of the genera *Aspergillus* and *Penicillium* which produces effects similar to parasympathetic stimulants if given parenterally. Administration of this compound intravenous to rabbits resulted in clinical signs of meiosis, salivation, increased bronchial secretion and lacrimation. These effects were partially ameliorated by atropine (Hanika and Carlton, 1994). In addition, it also shows a broad-spectrum antibiotic activity (Barber *et al.*, 1981).

Biosynthetically, citrinin is a pentaketide, thus derived from five acetate/malonate units, and three C₁ units derived from S-adenosylmethionine (SAM) [figure 5.6]. There is substantial evidence that the biosynthesis proceeds via an enzyme-bound poly- β -ketone chain with the C-methylations occurring while the methylene groups are still acidified by the adjacent carbonyl functions, which would no longer be the case once the molecule is cyclized (Barber *et al.*, 1981; Colombo *et al.*, 1981).

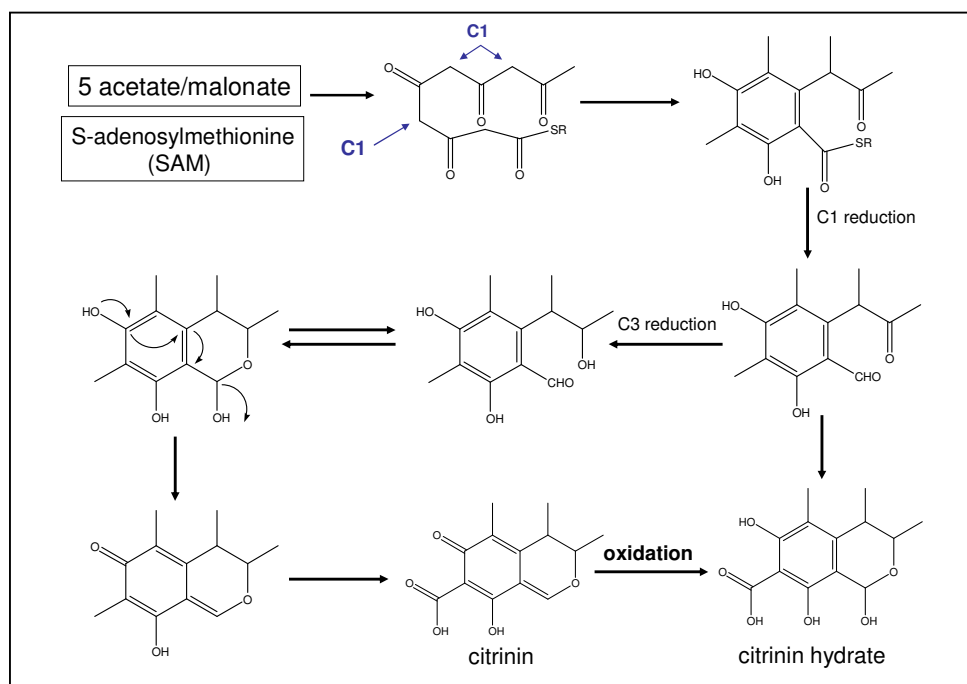


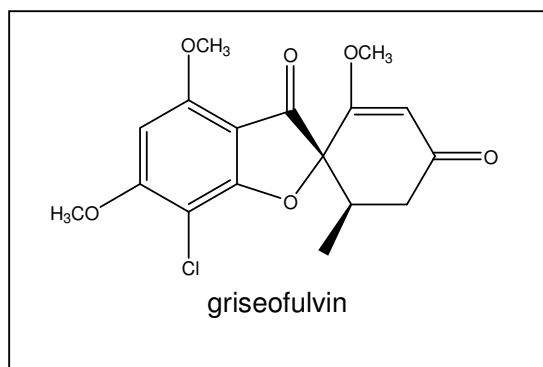
Figure 5.6 Biosynthetic pathway of citrinin and citrinin hydrate (Seigler, 1995 and Dewick, 2002)

5.2.2 Polyketide isolated from *Botryosphaeria stevensii*

5.2.2.1 Griseofulvin

Griseofulvin is a classical anti fungal agent which was first isolated in 1939 from *Penicillium griseofulvum* and also found in other *Penicillium* species. It acts via binding specifically to fungal tubulin (Pirrung *et al.*, 1991). Jarvis *et al.* (1996) reported a fungus outside the genus *Penicillium*, *Memnoniella echinata* produced griseofulvin.

Griseofulvin has two interesting structural features, on the one hand a unique spiro system formed by the two ketonic rings, and on the other hand an enol ether of an unsymmetrical β -diketone (Stork and Tomasz, 1964).



This compound is a heptaketide and known to be derived from acetate [figure 5.7]. Birch in 1967 have revealed the labelling pattern in the skeleton of griseofulvin after incorporation of (1-¹⁴C)-acetate using a strain of *Penicillium griseofulvum* and established the general validity of the acetic acid hypothesis (Sato and Oda, 1976). Formation of this substance involves both a Claisen and an aldol condensation (Seigler, 1995).

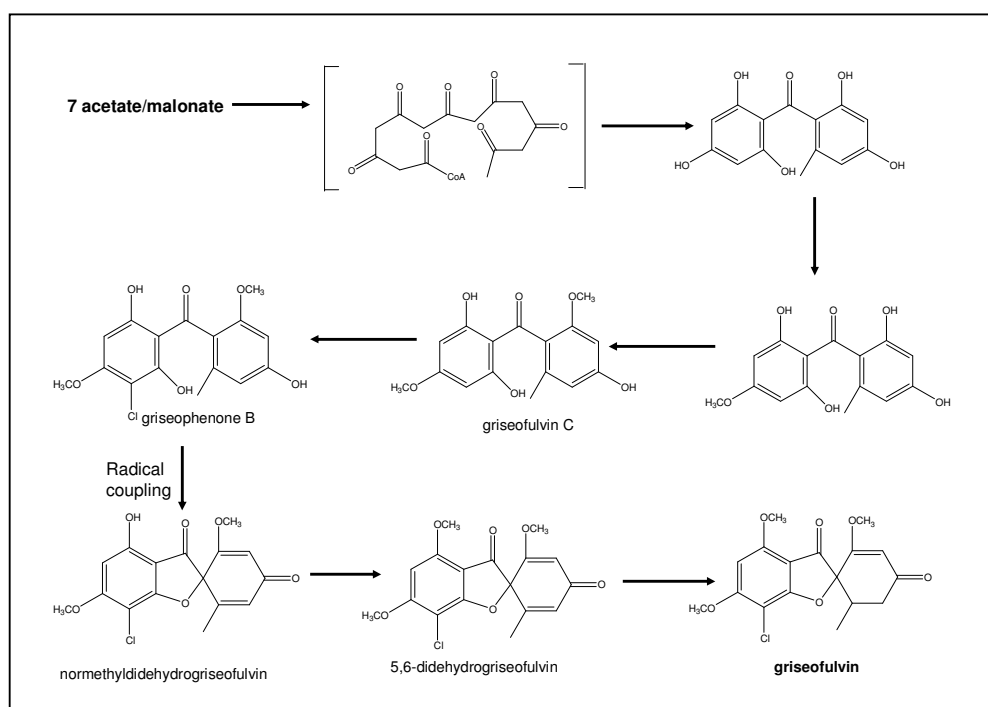


Figure 5.7 Biosynthetic pathway of griseofulvin (Seigler, 1995)

5.2.3 Polyketide isolated from *Alternaria alternata*

5.2.3.1 Alternariol

Alternariol is a dibenzopyrone derivative which was first described from *Alternaria tenuis* and suspected to cause several plant diseases in papaya, *Carica papaya* and passionfruit, *Passiflora incarnata* (Raistrick *et al.*, 1953). Later it was also isolated from the sponge-derived fungus *Penicillium citreonigrum* (Brauers, 2003) and shown to be a derivative of biphenic acid (Kanakam, *et al.*, 1990). This compound has phytotoxic properties and was described as a DNA intercalating mycotoxin (Onocha *et al.*, 1995).

Onocha *et al.* (1995) stated that djalonensone, 5-methoxylated derivative of alternariol, was found in *Anthocleista djalonensis*, a West African plant, which is used in the traditional medicine because of its antipyretic, analgetic and laxative effects. This may raise the question whether possibly an endophyte might be the actual origin of the compound. Considering the structure, this is almost certainly the case since structurally similar compounds are exclusively synthesized by fungi, but not by plants (Onocha *et al.*, 1995).

The biosynthesis of alternariol is rather complex, as it starts from a heptaketide chain via the unexpected linear norlichexanthon as intermediate [figure 5.8] (Stinson *et al.*, 1986), instead of the polyketide chain directly cyclizing to the angular framework of alternariol as believed previously (Dewick, 2002). In this context, there is an obvious analogy to the biosynthesis of the aflatoxins (Dewick, 2002; Townsend and Minto, 1999). So far, norlichexanthon was only found in lichen *Lecanora reuteri* and in the fungus *Penicillium patulum* but not in *Alternaria tenuis* or other *Alternaria* species, possibly because in the latter it is completely converted into alternariol (Stinson *et al.*, 1986).

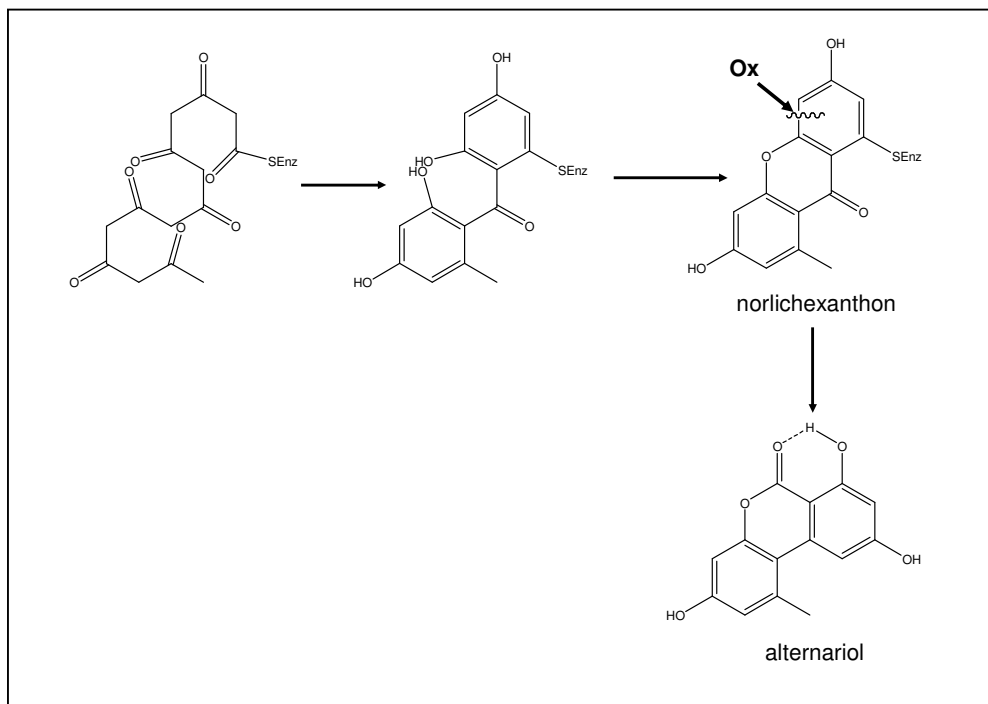
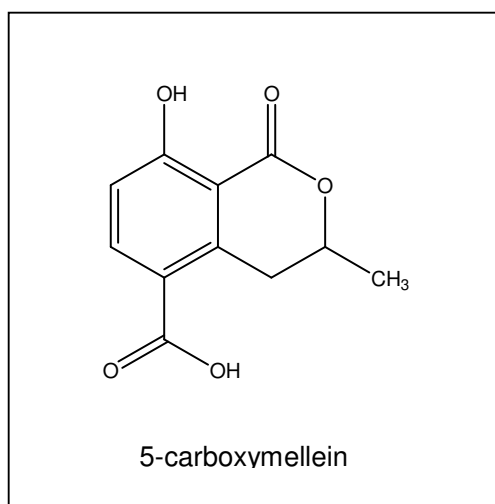


Figure 5.8 Biosynthetic pathway of alternariol (Stinson *et al.*, 1986)

5.2.4 Polyketide from unidentified fungus

5.2.4.1 5-carboxymellein

5-carboxymellein was reported as a typical metabolite of the xylariaceous fungi such as *Hypoxylon mammatum*, *H. illitum* and *Numularia discreta* (Anderson *et al.*, 1983). From a biosynthetic point of view, it is pentaketide-derived isocoumarin.

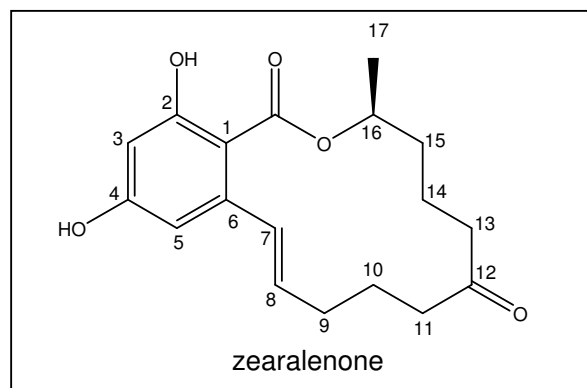


According to Krohn *et al.* (1997), the presence of mellein derivatives such as 5-carboxymellein, 5-methylmellein, 5-formylmellein, 5-methoxycarbonylmellein, 5-hydroxymethylmellein, 6-hydroxymellein, 6-methoxymellein, and 5-chloro-6-methoxymellein is a chemotaxonomic marker for the fungal family of Xylariaceae. Thus, it is tempting to speculate that the unidentified fungal strain which forms the basis of the current investigation should also be a member of the family Xylariaceae, even though it was not possible to identify the strain by molecular biological methods using the ITS1/ ITS4 primer pair.

5.2.5 Polyketide from *Fusarium equiseti*

5.2.5.1 Zearalenone

Zearalenone is a naturally occurring 14-membered orsellinic acid type macrolide lactone or macrolactone with anabolic and uterotropic activity (Solladie, *et al.*, 1990). Zearalenone is an estrogenic mycotoxin produced by various species of the genus *Fusarium* (Solladie *et al.*, 1990; Hitchcock and Pattenden, 1992). It is one of enantiomer of 6- β -resorcylic acid lactone I and a member of a rare class of natural products, the β -resorcylates (Urry *et al.*, 1966).



The hormonal activity of zearalenone and related naturally occurring derivatives has been linked to the close spatial similarity of these molecules to estradiol.

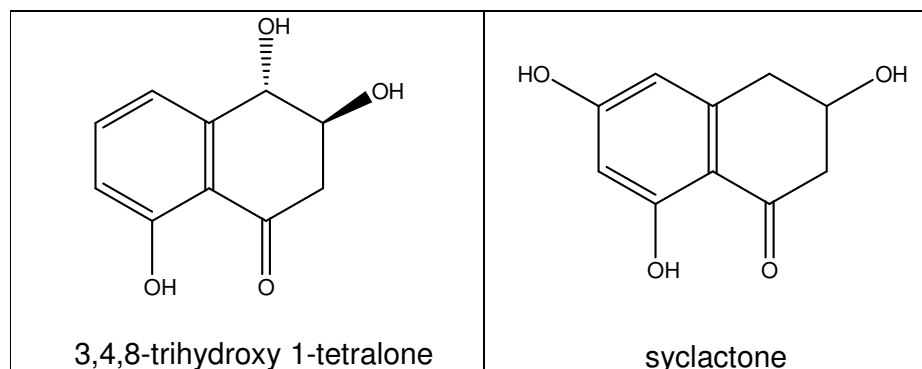
Nowadays, zearalenone is produced industrially by fermentation and is used in the manufacture of zearalanol 7 (also called zeranol). Zearalanol is employed as an anabolic cattle-growth stimulant and the compound was also subjected to clinical trials as a potential treatment for menopausal and post menopausal syndrome (Hitchcock and Pattenden, 1992).

5.2.6 Polyketide from the fungus *Paraphaeosphaeria michotii*

5.2.6.1 3,4,8-trihydroxy 1-tetralone

3,4,8-trihydroxy 1-tetralone is a phytotoxic substance, first isolated from fungus *Pyricularia oryzae* which was considered to be responsible for the symptoms of rice blast (Iwasaki *et al.*, 1972).

This compound is a simple polyketide and known to be derived from acetate. Syclactone, a compound structurally related to 3,4,8-trihydroxy 1-tetralone, is biosynthesized from one acetylCoA and four malonylCoA via a C-10 polyketo-intermediate. The biosynthesis of syclactone was known by tracing the fate of acetate hydrogen using [2-¹³C, 1-²H₃]-acetate (Sankawa *et al.*, 1981). Compound 3,4,8-trihydroxy 1-tetralone was probably biosynthesized using the same way since they were structurally related.



5.2.7 Pre-anthraquinones and anthraquinones from *Talaromyces wortmanii*

Anthraquinones and anthraquinone derivatives are the largest class of naturally occurring quinones which have widely been found in higher plants, mosses, lichens, fungi as well as in marine animals and algae (Seigler, 1995).

Natural anthraquinones are characterized by a large structural variety, wide range of biological activity and low toxicity. They possess purgative, antioxidant, anti-inflammatory, antitumor, bactericidal, antimutagenic, immunosuppressive, and enzyme-inhibitory effects. They are also involved in the process of metabolism, respiration, cell division, oxidative phosphorylation, complexation with RNA and DNA and in other physiological processes of vital importance. They are part of many medicines originally based on plants. Additionally, anthraquinones are also applied as dyes, pigments, luminophores, analytical reagents, or chemical means for plant protection (Choi *et al.*, 2000, Muzychkina, 1998).

Pure anthraquinones are usually not used in therapy, but most drugs consist of complex plant extracts. In many cases, at least in plants, they occur as glycosides, with the sugar moiety increasing solubility and facilitating transport to the site of action, but it is mainly the corresponding anthrone form that is effective. The use of anthraquinone drugs should be restricted to short-term treatment of constipation only, as frequent or long term use has been associated with increased risk of intestinal tumours (Samuelsson, 1999).

In general, anthraquinones are acetate-derived, however, selected representatives from plants such as alizarin are actually biosynthesized via the shikimic acid pathway. In most cases, inspection of the structure already allows to distinguish between both routes, since anthraquinones of polyketide origin usually show the distinctive pattern of alternating oxygenated and non-oxygenated carbon

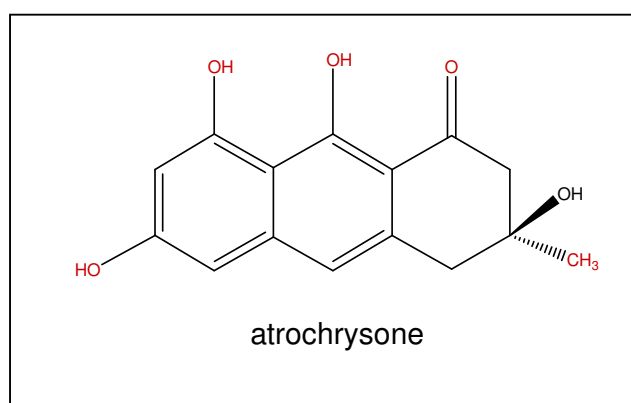
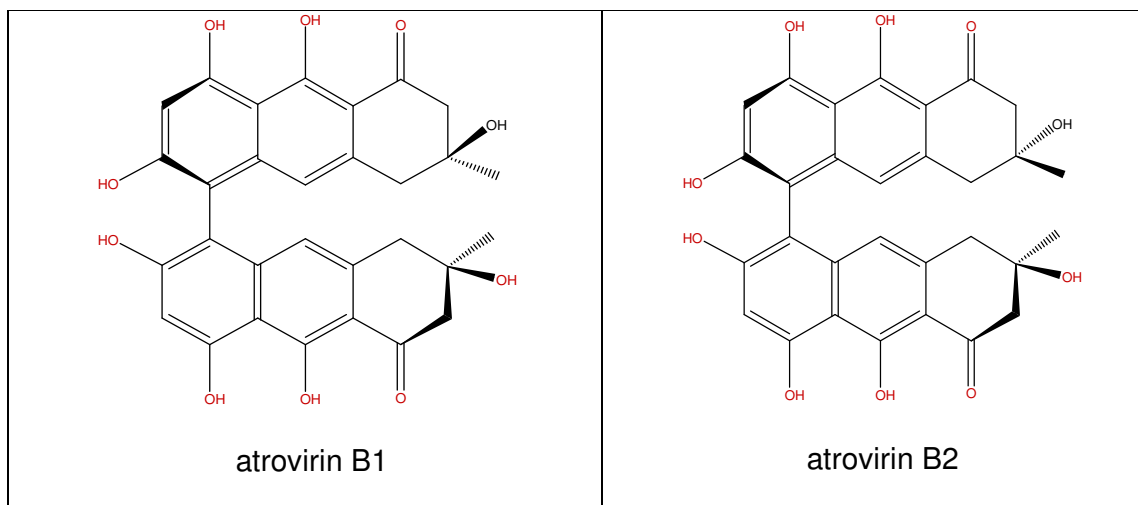
atoms, resulting in the presence of oxygen functions in both aromatic rings of the anthraquinone nucleus and additionally in many cases in *meta*-oriented protons. Emodine, an anthraquinone isolated from various fungi, particularly from the genera *Penicillium* and *Aspergillus* is a “classical” octaketide and thus generated through the acetate-malonate pathway. Emodin serves as an important intermediate in the biosynthesis of many other fungal metabolites (Sanakawa, 1980; Seigler, 1998)

The free anthraquinones have little therapeutic activity and need to be transformed into water-soluble glycoside to exert their action. Anthraquinones could be present as bianthraquinones which were assembled by phenolic oxidative coupling of two monomers or anthrone systems forming dianthrone systems or bianthraquinones (Dewick, 2002).

In the case that both monomers have a substitution in *ortho* position to the biaryl bond, the compound shows atropisomerism due to hindered rotation along the biaryl bond by the high steric strain barrier (Bringmann *et al.*, 2005).

5.2.7.1 Atrovirin B1 and B2

Atrovirin B was first isolated from the fruiting bodies of *Cortinarius atrovirens*, an European mushroom (Steglich and Oertel, 1984). Atrovirin B is a likely progenitor in a family of 5,5-coupled pre-anthraquinones that includes bidihydroantacenones, bianthrone and bianthraquinones such as austrovenetin, skyrin and hypericin (Antonowitz *et al.*, 1994). Atrovirin has been shown to be assembled by 5,5' coupling of atrochrysone (Gill and Gimenez, 1991).

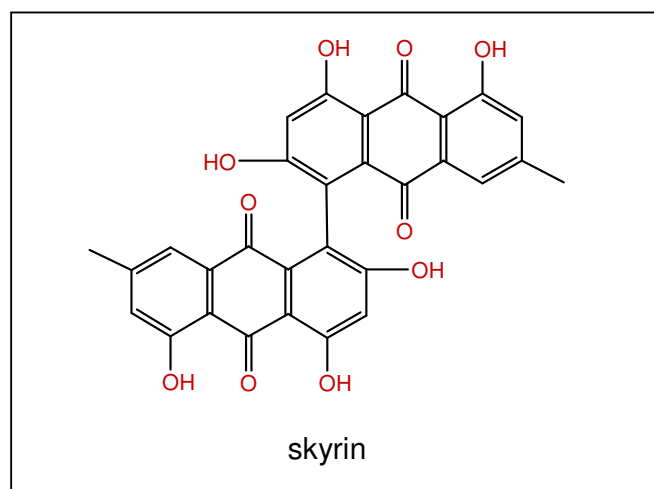


5.2.7.2 Skyrin

Skyrin is a bianthraquinone previously reported as orange pigment and has rather frequently been described as a fungal metabolite (Yosioka *et al.*, 1971). Skyrin was found widespread in molds or ascomycetes, but recently, it has also been identified as a typical metabolite from macromycetes belonging to the family Cortinariaceae. Gill and Steglich (1988) isolated this substance from yellow fruiting bodies of the indigenous Australian mushroom *Dermocybe austroveneta*. It had also been isolated from other species of the genus *Dermocybe* such as *D. alcalisensibilis*,

D. allienata, *D. luteostriatula*, *D. obscureolivea* var. *brunnea* and *D. olivipes* from South America, from the closely related *Cortinarius atrovirens*, *C. ionochlorus*, *C. odoratus*, and from the hypochraceous ascomycetes *Hypomyces aurantius*, *H. lactifluorum*, and *H. trichothecoides* (Gill and Gimenez, 1991).

Furthermore, as first recognized by Shibata *et al.* (1955), skyrin is quite often accompanied by related monomeric anthraquinone or protoanthraquinone derivatives which are the immediate biogenetic precursors.



In addition, several skyrin glycosides were reported from the plant *Hypericum perforatum* (Wirz *et al.*, 2000). This plant is widely used for the treatment of mild to moderate depression. The pharmacological activity of its extracts has been verified, even though its mode of action remains unclear (Linde and Mulrow, 1999). Wirz *et al.* (2000) isolated four skyrin glycosides, S-(+)-skyrin-6-O- β -glucopyranoside, R-(-)-skyrin-6-O- β -glucopyranoside, S-(+)-skyrin-6-O- β -xylopyranoside, and S-(+)-skyrin-6-O- β - α -arabinofuranoside from *H. perforatum*.

S-(+)-Skyrin-6-O- β -glucopyranoside and R-(-)-skyrin-6-O- β -glucopyranoside inhibited [125 I] sauvagine binding to the corticotrophin releasing hormone (CRH-1) receptor (Wirz *et al.*, 2000).

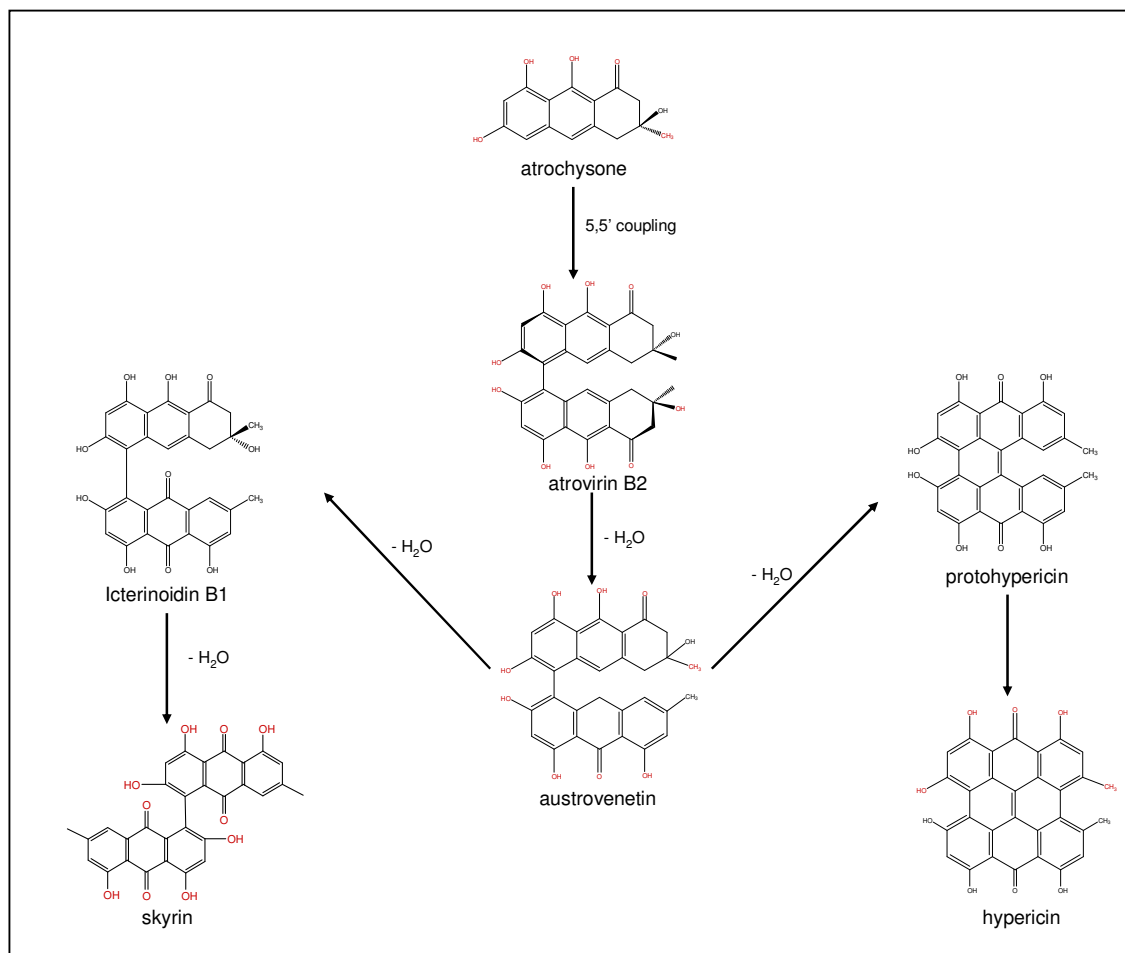


Figure 5.9 Possible origin of pigments in extract of fungus *Dermocybe austroveneta* (Gill and Gimenez, 1991)

Biosynthetically, skyrin is thought to originate from atrovirin B2, although the biosynthesis is not yet understood in full detail (Gill and Gimenez, 1991). Atrochysone and atrovirin B are involved in the early stages of the biosynthesis of austrovenetin [figure 5.9]. The latter represents an intermediate which could be rapidly oxidized *in vitro* to yield a complex mixture of skyrin and hypericin. A proposed biosynthetic

pathway relating those substances to the pigment is shown in figure 5.9. Although the biosynthesis of skyrin and atrovirin in microorganism, and hypericin in plants are not understood in detail, several molecules at the coupled pre-anthraquinone level have been invoked as prospective progenitors, often with *in vitro* chemical support (Gill and Gimenez, 1991). It had been proposed that emodine bianthrone may be involved in hypericin production in plants (Brockmann, 1957).

5.2.8 Pyranacetal compound isolated from *Xylaria* sp.

5.2.8.1 Methyl methoxy agistatine D (new compound)

This compound is a new representative of a family of pyranacetals which are characterized by a bicyclic cyclohexane/pyran ring system. The structurally related pyranacetals agistatin A, B, D and E, were first described from the fungus *Fusarium* sp. FH-A 6239 (Zeeck *et al.*, 1992). These agistatine compounds showed inhibitory activity in cholesterol biosynthesis (Göhrt *et al.*, 1996)

This compound belongs to its family of pyranacetals and bears a fundamental bicyclic cyclohexane/pyran ring system with ethyl, hydroxyl and oxo substituents. Göhrt *et al.* (1996) found and described four novel pyranacetal compounds, agistatines A, B, D and E, from fungus FH-A 6239 *Fusarium* sp, which were active as inhibitors of cholesterol biosynthesis (Zeeck, *et al.* 1992).

The chemical structure of methyl methoxy agistatine D is very similar with that of agistatin D. The difference is that methyl methoxy agistatine has one methyl methoxy moiety in position C-2. From the structural point of view as well, this type of secondary metabolites, especially tricyclic agistatine B and E, were novel and unique. Only diplosporin and 5-deoxydiplosporin, which were isolated from contaminant

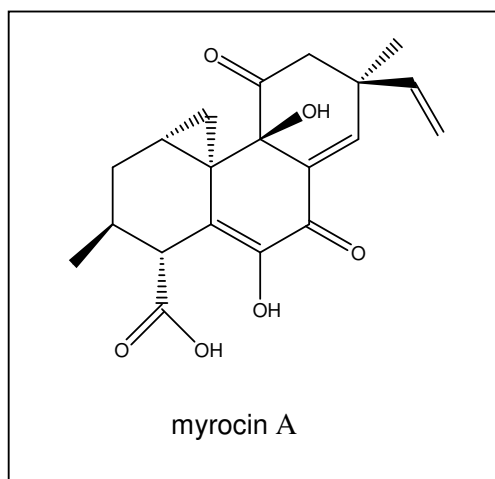
fungus *Diplodia macrospore Earle* of maize, showed some structural relationship to the bicyclic agistatine A and D (Göhrt *et al.*, 1996).

5.3 Diterpene

The diterpenes arise from geranylgeranyl diphosphate (GGPP) which is formed by addition of further a IPP molecule to farnesyl diphosphate. Cyclization reactions of GGPP is mediated by carbocation formation, and followed with Wagner-Meerwein rearrangement to form diterpenoids (Dewick, 2002).

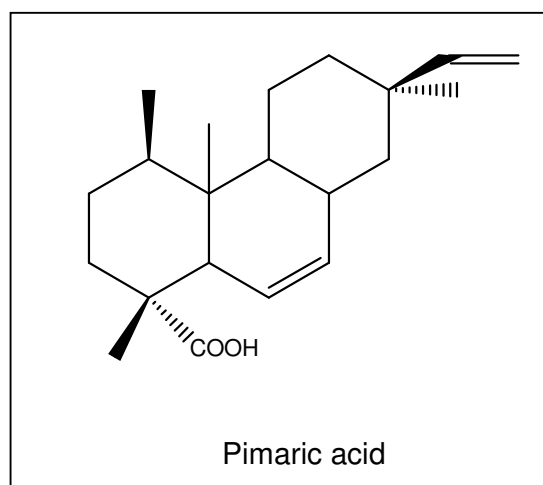
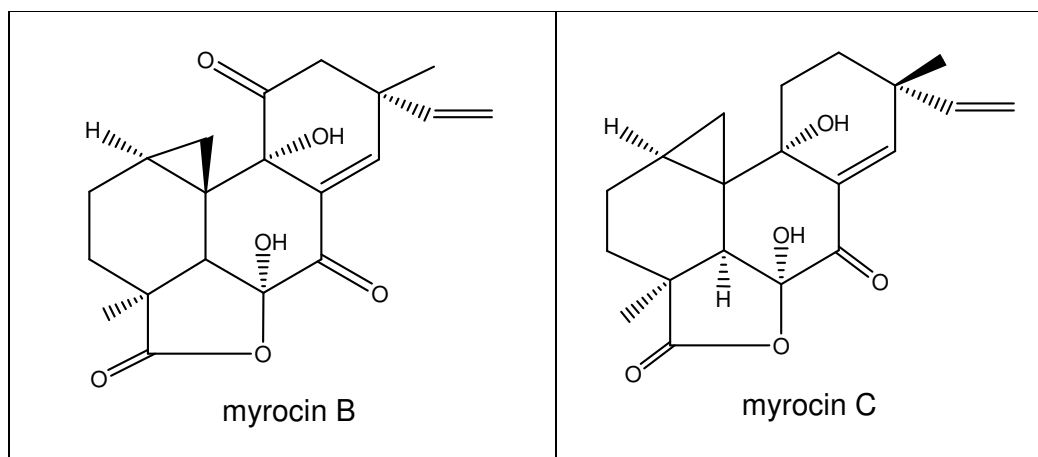
5.3.1 Diterpene isolated from *Arthrinium* sp. (myrocin A)

Myrocin A is a pimarane diterpene compound first isolated from the marine fungus *Apiospora montagnei* derived from the marine alga *Polysiphonia violacea* by Klemke *et al.* in 2003.



Myrocin A, as well as myrocin B and myrocin C, are pimaric acid derivatives. Myrocins, as well as pimaric acid, have pimarane C-20 basic skeleton. In contradiction to pimaric acid, which is a tricyclic diterpen, myrocin is tetracyclic due to a cyclopropane moiety. Pimaric acid type compounds as well as abeic acid type

compounds are tricyclic diterpen resin acids consisting of a tree-membered ring system, a carboxylic acid group and double bonds. Their empirical formula is $C_{19}H_{29}COOH$. Biologically, they act as protectants and wood preservatives produced by parenchymous epithelial cells surrounding resin ducts in trees, e.g. pines (Bardyshef *et al.*, 1962).



Both myrocin C and myrocin B was reported showing significant antimicrobial activity against gram-positive bacteria, fungi and yeast, and had theurapeutic effect on mouse Ehrlich ascites carcinoma (Hsu *et al.*, 1988), whereas myrocin A has weak

antimicrobial activity but shows cytotoxic effect against HM02, HepG2 and MCF7 human cancer cell lines (Abdel-Lateff *et al.*, 2002; Klemke *et al.*, 2003). Myrocin A has very weak cytotoxic activity against mouse lymphoma cell L5178Y in MTT assay of this study, nevertheless this compound has inhibitory activity in the protein kinase enzymes toward B-RAF-VE,EGF-R, IGF1-R, SRC, VEGF-R2 and SAK enzymes.

6. DISCUSSION OF BIODIVERSITY DETERMINATION

6.1 Fungal Identification

The primer pair ITS 1 and ITS 4 was successfully evaluated and used for identifying of fungal strains in this research effort on a routine basis.

ITS 1 and ITS 4 are known as universal primers which can be used to amplify the DNA of most fungi, from the phyla Oomycotina, Ascomycotina until Basidiomycotina. In this project, many fungi could be identified down to the species level, including members of the genera *Botryosphaeria*, *Cladosporium*, *Fusarium*, *Pestalotiopsis*, *Paraphaeosphaeria*, as well as some species from the genus *Penicillium* (*P. polonicum*, *P. citrinum*, *P. polonicum*, *P. griseoroseum*).

There are many reported primer pairs which amplify more specifically certain groups of fungi. The primers ITS1-F and ITS4 were used for amplifying the higher fungi from the phyla Ascomycotina and Basidiomycotina, whereas primers ITS1-F and ITS4-B were specific only for the phylum Basidiomycotina (Jasalavich, 2000). Those primers have effectively been used for detection of certain fungi in complex environmental samples or for diagnostic purposes of plant diseases caused by fungi [figure 6.1].

Primer sequences were designed for the purpose of amplifying the entire nuclear ribosomal DNA by use of the polymerase chain reaction. Primers pairs can be selected in conjunction with the analysis of divergence of the ribosomal RNA genes to address systematic problems throughout the hierarchy of life (White *et al.*, 1990; Hillis and Dixon, 1991).

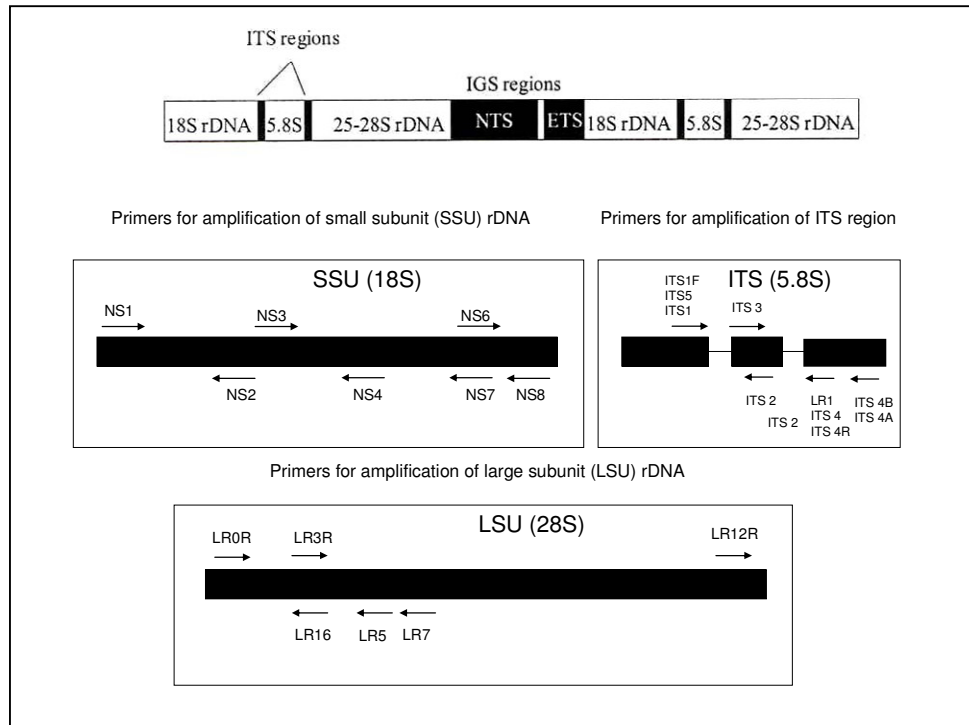


Figure 6.1 Conserved primer sequences for PCR amplification and sequencing from nuclear ribosomal RNA (White *et al.*, 1990)

Studies of ribosomal DNA sequences had been employed to infer phylogenetic history across a very broad spectrum, from studies among the basal lineages of life to relationships among closely related species and populations. The reasons for the systematic versatility of ribosomal DNA include the numerous rates of evolution among different regions of rDNA (both among and within genes), the presence of many copies of most rDNA sequences per genome and the pattern of concerted evolution that occurs among repeated copies. These features facilitate the analysis of ribosomal DNA by direct RNA sequencing, DNA sequencing, either by cloning or amplification, and restriction enzyme methodologies (Hillis and Dixon, 1991).

Many fungi from the genera *Aspergillus* and *Penicillium* can not be identified based on the DNA sequences of ITS region down to the species level, simply because the respective sequences are too similar for members of these genera. However,

based on ITS sequences, it is usually possible to assign a given strain to section or subgenus level (within the genus *Aspergillus*), especially in the sections *Flavi* and *Nigri* (Magnani *et al.*, 2005).

Aspergillus fungi from section *Nigri* could be identified until species level by employing RFLP (restriction fragment length polymorphism) and searching for the *RsaI* restriction site (GT/AC at positions 295 and 303 bp) following amplification of the ITS region using ITS 1 and ITS 4. By this method, it is possible to differentiate fungi in the section *Nigri*, for example *Aspergillus niger* and *A. tubingensis*. *A. niger* has a restriction site for the *RsaI* restriction endonuclease, whereas it is lacking in *A. tubingensis* (Jasalavich *et al.*, 2000).

A. flavus and *A. oryzae* belong to the section *Flavi*, as well as *A. tamari* and *A. parasiticus*. Identification down to the species level could not be achieved using the primer pair ITS 1 and ITS 4, so that new specific primers were designed for distinguishing fungal species in various *Aspergillus* sections (Jasalavich *et al.*, 2000; Peterson, 2000). The ITS 1-5.8S rDNA-ITS 2 region is extremely conservative between closely related species from the genera *Penicillium* (Skouboe *et al.*, 2005) or *Aspergillus* (Tamura *et al.*, 2005), so that another region of nuclear ribosomal DNA had to be amplified for distinguishing closely related species of *Penicillium* and *Aspergillus*. Primer ITS 1 and D2R were employed to yield sequences of about 1200 bp that included regions ITS 1 and ITS 2, and about 635 bases from 5' end of the large subunit rRNA. These sequences could be used specifically for distinguishing species in genera *Penicillium* and *Aspergillus*. The primer pair would amplify the ITS1-5.8S rDNA-ITS 2 region as well as the D1 and D2 regions of the large subunit rDNA [figure 6.2]. Regions D1 and D2 are considered highly variable (Peterson, 2000; Zuccaro *et al.*, 2003).

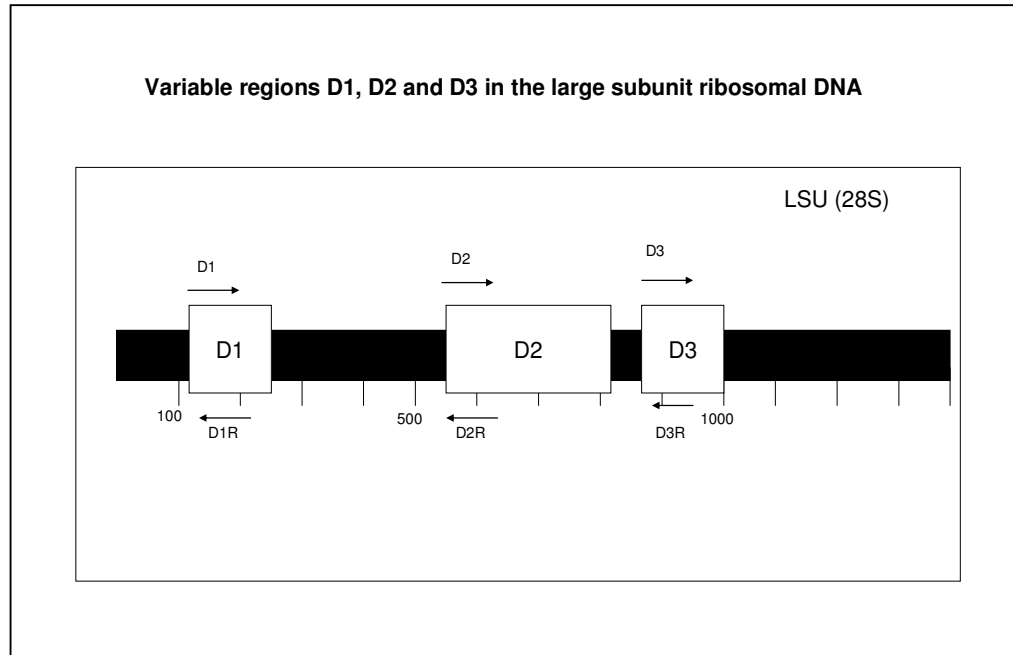


Figure 6.2 Map showing the primer-binding sites and the variable regions of D1, D2 and D3 in the 28S rDNA gene (Peterson, 2000; Zuccaro *et al.*, 2003)

A further approach described by Skouboe *et al.* (2005) to identify closely related *Penicillium* and *Aspergillus* species is based on amplifying and sequencing of the small subunit rDNA and ITS region using primer sets for amplifying 18S rDNA, such as the primers NS1 and NS2. The small subunit ribosomal RNA gene has been extensively used for phylogenetic analysis and identification purposes at the genus or species level in bacteria and eukaryotes.

6.2 Phylogenetic analysis based on ITS sequences

Traditionally, phylogenetic trees have been used to represent the evolutionary relationship of groups of organisms. A phylogenetic tree is a specific type of a cladogram where the branch lengths are proportional to the predicted or hypothetical evolutionary time between organisms or sequences (Hall, 2005).

There are three major reasons to construct phylogenetic trees:

1. Determining the closest relatives of the organism which is being identified.
2. Discovering the function of a gene
3. Retracing the origin of a gene which encodes products such as proteins. Most genes travel together through evolutionary time. However, from time to time there would be individual gene leaping from one species to another one (Hall, 2005; Berry and Bryant, 1999).

Phylogenetics trees using genes were used for reconstructing evolutionary history. Gene sequences are much easier to be interpreted and compared than the morphological data which were derived from characteristics of organism such as forms and structures (Herr *et al.*, 1999; Claverie and Notredame, 2002).

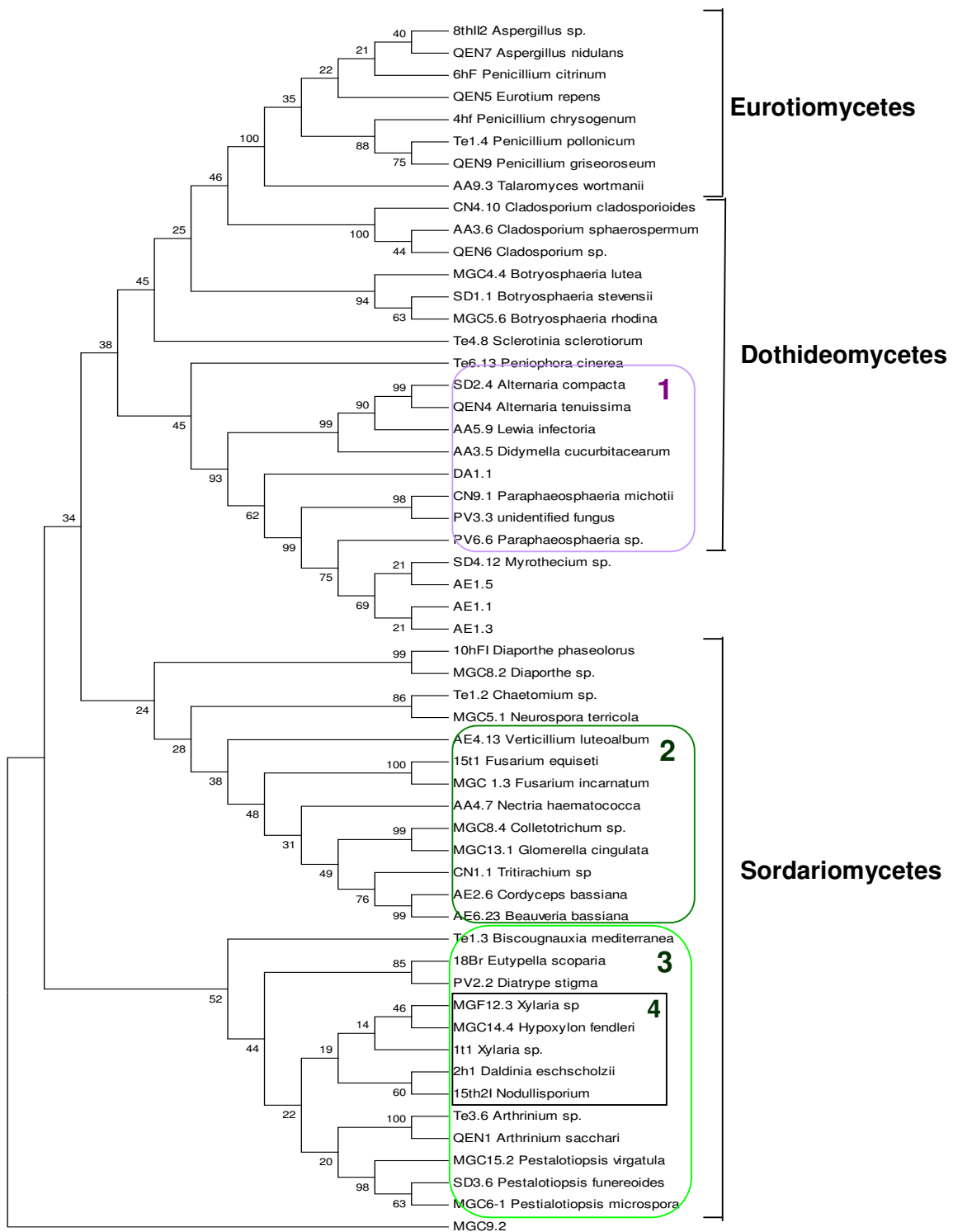


Figure 6.3 Phylogenetic tree based on ITS sequences of marine-derived fungi (bootstrapped NJ)

NOTE:

1. Order Pleosporales

2. Order Hypocreales

3. Order Xylariales

4. Family Xylariaceae

From the DNA sequences of the ITS/5.8S rDNA- regions of the marine-derived fungal strains investigated in the course of this thesis, a phylogenetic tree was constructed. The sequences of ITS region could be aligned, computed and analyzed to construct a solid phylogenetic tree which could explain the evolutionary relationship starting from the class, order until the genus levels. It was evident that there were three classes of fungi, Eurotiomycetes, Dothideomycetes and Sordariomycetes, clearly observed as separate entities in the phylogenetic tree [figure 6.3].

There is a growing interest in natural product researchers to investigate the relationship between secondary metabolite profiling and modern taxonomy based on molecular biological phylogenetic analysis. Fungal genome sizes range from 6000 genes in the yeast *Saccharomyces cerevisiae* to more than 10.000 genes in filamentous fungi (ascomycetes). Fungi are expected to share much of their primary metabolism; therefore a better understanding of the central metabolism and regulation in less-studied filamentous fungi can be learned from metabolite profiling and metabolomics of fungi (Smedsgaard and Nielsen, 2005).

Ascomycetes, to which most fungi investigated in this study belonged, have a very active and diverse secondary metabolism which may be the result of the additional genes present in this fungal taxon. Although the blueprint of a given organism is represented by its genome, its behavior expressed as its phenotype is very flexible, for example with regard to growth characteristics, cell differentiation, its

response to the environment or stress, the production of secondary metabolites and enzymes. Therefore chemodiversity, evident from secondary metabolite profiles, can be assessed through functional genomics, which is of great relevance for the search for new biotechnological applications. However, fungal chemodiversity is equally efficient for identification and classification of fungi and hence a powerful tool in fungal taxonomy or chemotaxonomy (Smedsgaard and Nielsen, 2005). Chemotaxonomy is based on the empirical observation that phylogenetically related organisms share common physiological and biochemical characteristics (Dreyfuss and Chapela, 1994).

Fungi, especially filamentous fungi and yeasts, show a lower degree of cellular differentiation compared to plants, but still they express a complex metabolism resulting in the production of a broad range of secondary metabolites and extracellular enzymes. This very high metabolic diversity has been actively explored and exploited for many decades, with many fungal natural products exhibiting bioactivity as antibiotics, cholesterol-lowering agents, antitumor agents, and immunosuppressants (Smedsgaard and Nielsen, 2005).

Chemotaxonomy could be also quite useful for investigations in the field of natural products. HPLC profiles had been generated for a number of *Penicillium* sp. and can provide information about the chemistry present. Incorporating chemotaxonomy into fungal natural products research should be useful for comparing strains and dereplication of known metabolites (Larsen *et al.*, 2005; Smedsgaard and Nielsen, 2005).

Some biologists stated that secondary metabolite production in fungi is strain-specific, others claimed that few secondary metabolites might be species specific, and yet others stated that most, if not all, secondary metabolites are species specific and even essential features of any species (Larsen *et al.*, 2005). Different species

represented different chemotypes, whereas the same species represent the same chemotype. Although in the recent knowledge, the same species of fungi derived from different habitat might show different chemotype, i.e. the same fungal species derived from terrestrial and marine environment might show different chemotype. This phenomenon will lead to the finding of new metabolite which had not been isolated from the same fungal species from different habitat (Rusman, 2006; Lin *et al.*, 2001). This might also not be the case for other organisms such as *Actinomycetes* where horizontal gene transfer could be a pronounced event leading to potential transferring of biosynthetic pathways (Larsen *et al.*, 2005).

Members of different fungal classes or subdivisions rarely produce the same secondary metabolites, for example beauvericin found in fungi imperfecti and basidiomycotina, oosporin in fungi imperfecti, ascomycotina and basidiomycotina. Higher plants could be demonstrated to contain known or suspected fungal origin compounds such as citrinin and tricothecenes (Dreyfuss and Chapela, 1994). The presence of these compounds in the plants could be explained by endophytic fungi residing in those plants.

Secondary metabolites in plants normally appear to be species specific, individual secondary metabolites yet often occur among widely different species that are not phylogenetic related. In very rare case, few plants was found to produce known fungal origin compounds, for example the plants morning glories from genus *Calystegia* spp. were proven producing ergot alkaloid related compounds such as d-lysergic acid amide (Dewick, 2002). This phenomenon could be explained by convergent evolution whereby organisms, which were not closely related or monophyletic can evolve independently similar traits as a result of adaptation to the same ecological niches (Tudzinsky, 2005). The convergent evolution could be

emerged by horizontal gene transfer between different organisms which was still far from our understanding.

Chemotaxonomy of fungi based on secondary metabolites was a controversial topic of researchers nowadays. It was thought to be proven limited in certain group of compounds, for example alkaloids which were produced by selected fungal genera such as *Penicillium*, *Aspergillus* and *Fusarium* and their perfect states. The application of chemotaxonomy based on secondary metabolites such as dihydroisocoumarine derivatives (5-methyl-mellein, 5-formyl-, 5-carboxy-, 5-methoxy-carbonyl-, 5-hydroxymethyl- and 6-methoxy-5-methyl-mellein) was also proposed by Anderson *et al.* (1983) in family Xylariaceae. Quang *et al.* in 2006 investigated carneic acid A and B as chemotaxonomically significant antimicrobial compounds in Xylariaceous ascomycetes based on HPLC profiling.

The genes coding for natural products, especially polyketide synthetase (PKS) genes are modular and encode multifunctional enzymes (Dewick, 2002). This phenomenon opens a new avenue to diversify natural microbial natural products, producing so-called non-natural products by shuffling genes around within these clusters. It is even possible to include genes from other pathways, thereby generating hybrid enzymes capable of synthesizing new molecules, which were difficult to produce by traditional chemical methods (Dewick, 2002).

Polyketides, such as the important antibiotic erythromycin or the cholesterol-lowering lovastatin, have been manipulated on a genetic level to explore the potential of genetic engineering for individual strain development by virtue of genomic microarrays, transcription profiles and metabolic profiling with the aim to guide yield improvement since they are biosynthesized by stepwise building of long carbon chains by multifunctional enzymes that was programmed by certain genes (Larsen *et al.*,

2005; Hopwood, 2007). These enzymes determine the chain length, oxidation state, and pattern of branching, cyclization and stereochemistry of the molecules in a combinatorial fashion to produce an enormous variety of structures (Dewick, 2002; Hopwood, 2007). The genetic engineering of polyketide genes opens new field of drug discovery based on rationally engineering the enzymes to produce 'unnatural natural product' with novel properties in a limited array (Hopwood, 2004).

Erythromycin was first produced by an actinomyce *Streptomyces erythraeus*. It was biosynthesized by type I Polyketidesynthase (PKS) which contains three subunits DEBS-1, 2 and 3. Each subunit was encoded by gene eryA-I, II and II consisted of six moduls needed for one cycle of polyketide-chain extension (Pieper *et al.*, 1996). The filamentous bacteria (actinomycetes) from genus *Streptomyces* were the best-known genus which produces polyketide antibiotics such as erythromycin, tetracycline, ansamycin, amphotericin, avermectin and doxorubicin (Dewick, 2002; Hopwood, 2007).

The very complex picture that arises when comparing the ability of fungal strains to produce a given secondary metabolite is well represented in the example of griseofulvin. This chlorinated polyketide antibiotic is produced by several Ascomycotina species. Some of them are closely related, while others are taxonomically distinct. All known species of *Khuskia* and *Nigrospora* (its anamorphic state) have been reported to produce griseofulvin, so it was concluded that griseofulvin production was apparently a monophyletic character of the genus (Frisvaad *et al.*, 2004). On the contrary, griseofulvin production is assumed to have been developed 9 independent times in the genus *Penicillium*, and thus this character was considered highly polyphyletic [table 6.1] (Larsen *et al.*, 2005). However, it is not known whether the four species in the series *Lanosa* and the four species in the series

Canescentia that produced griseofulvin, were those that were most closely related according to a single or multi-gene phylogeny.

In *Aspergillus*, griseofulvin production rarely appears and only reported in *A. lanosus*, but not in other species in the series *Flavi* of *Aspergillus*. The production of griseofulvin by *Memnoniella echinata* is also autapomorphic, *i.e.* not shared with phylogenetically closely related species, with no other species of *Memnoniella* or the closely related *Stachybotrys* are known to produce this polyketide (Frisvad *et al.*, 2004; Frisvad and Samson, 2000). In this context it is worth mentioning that many strains of the genus *Botryosphaeria* encountered in this study were found producing griseofulvin.

Table 6.1 Taxonomic placement of griseofulvin of 40 producers species

(Larsen *et al.*, 2005)

Species	Subgenus	Section	Series	Order
<i>Khuskia oryzae</i>	-	-	-	Trichosphaeriales ^a
<i>Khuskia sacchari</i>	-	-	-	Trichosphaeriales ^a
<i>Nigrospora musae</i>	-	-	-	Trichosphaeriales ^a
<i>Nigrospora sphaerica</i>	-	-	-	Trichosphaeriales ^a
<i>Memnoniella echinata</i>	-	-	-	Sordariales ^b
<i>Phomopsis</i> sp.	-	-	-	Diaporthales ^c
<i>Aspergillus lanosus</i>	<i>Circumdati</i>	<i>Flavi</i>	-	Eurotiales ^d
<i>P. nodulum</i>	<i>Aspergilloides</i>	<i>Aspergilloides</i>	<i>Implicata</i>	Eurotiales ^d
<i>P. aethiopicum</i>	<i>Penicillium</i>	<i>Chrysogena</i>	<i>Aethiopica</i>	Eurotiales ^d
<i>P. persicinum</i>	<i>Penicillium</i>	<i>Chrysogena</i>	<i>Persicina</i>	Eurotiales ^d
<i>P. coprophilum</i>	<i>Penicillium</i>	<i>Penicillium</i>	<i>Claviformia</i>	Eurotiales ^d
<i>P. dipodomycicola</i>	<i>Penicillium</i>	<i>Penicillium</i>	<i>Urticicolae</i>	Eurotiales ^d
<i>P. griseofulvum</i>	<i>Penicillium</i>	<i>Penicillium</i>	<i>Urticicolae</i>	Eurotiales ^d
<i>P. sclerotigenum</i>	<i>Penicillium</i>	<i>Penicillium</i>	<i>Expansa</i>	Eurotiales ^d
<i>P. jamesonlandense</i>	<i>Furcatum</i>	<i>Ramosum</i>	<i>Lanosa</i>	Eurotiales ^d
<i>P. lanosum</i>	<i>Furcatum</i>	<i>Ramosum</i>	<i>Lanosa</i>	Eurotiales ^d
<i>P. raistrickii</i>	<i>Furcatum</i>	<i>Ramosum</i>	<i>Lanosa</i>	Eurotiales ^d
<i>P. soppii</i>	<i>Furcatum</i>	<i>Ramosum</i>	<i>Lanosa</i>	Eurotiales ^d
<i>P. janczewskii</i>	<i>Furcatum</i>	<i>Eladia</i>	<i>Canescentia</i>	Eurotiales ^d
<i>P. murcianum</i>	<i>Furcatum</i>	<i>Eladia</i>	<i>Canescentia</i>	Eurotiales ^d
<i>P. nigricans</i>	<i>Furcatum</i>	<i>Eladia</i>	<i>Canescentia</i>	Eurotiales ^d
<i>P. nodusitatum</i>	<i>Furcatum</i>	<i>Eladia</i>	<i>Canescentia</i>	Eurotiales ^d
<i>P. yarmokense</i>	<i>Furcatum</i>	<i>Eladia</i>	<i>Canescentia</i>	Eurotiales ^d

^a Sordariaceae, Sordariomycetidae, Ascomycetes. ^b Chaetosphaeriaceae, Sordariomycetidae, Ascomycetes. ^c Valsaceae, Sordariomycetidae, Ascomycetes. ^d Trichocomaceae, Eurotiomycetidae, Ascomycetes.

It should be noted that an inherent problem associated with secondary metabolism in general is the focus of virtually all scientific journals on publication of new compounds, which renders the report of known secondary metabolites difficult, sometimes impossible. Thus, one should be very careful in inferring a species specific distribution for a given compound solely based on the deceptive seeming absence of additional reports in the literature apart from the original description.

For many industrial important microorganisms, it has been shown that the production of antibiotic substances is not a property characteristic of specific groups of organisms or even of given species within such groups, but only of a few selected strains within a given species (Waksman and Bugie, 1943).

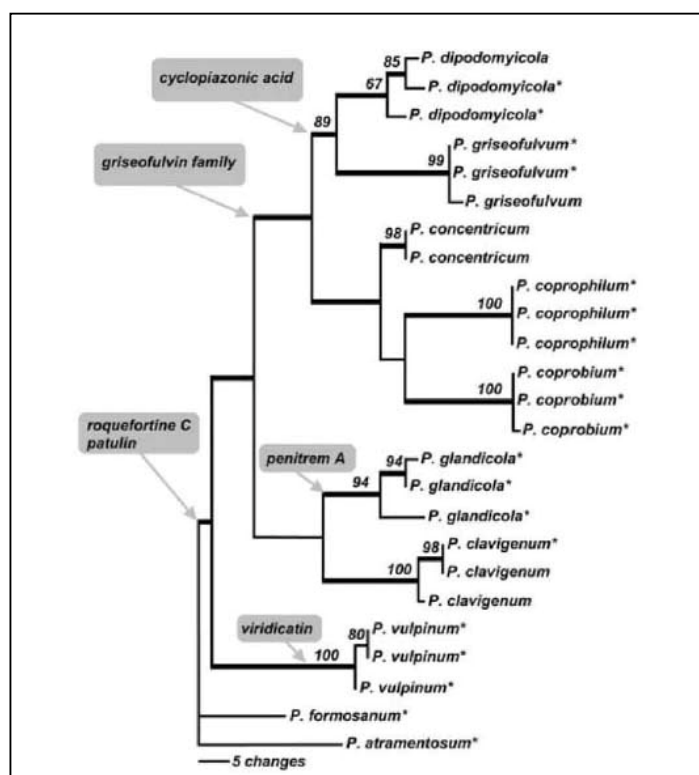


Figure 6.4 Classification of 7 species *Penicillium* series Claviformia based on cluster analysis of the raw mass profiles from ESI MS of crude extract (Smedsgaard *et al.*, 2004)

Smedsgaard *et al.* (2004) had investigated chemotaxonomic relationship between fungal specific metabolites such as roquefortine, viridicatin, griseofulvin, penitrem A and cyclopiazonic acid with many species from the genus *Penicillium* series Claviformia using two outgroups *P. formonasum* and *P. atramentosum* [figure 6.4]. They confirmed that secondary metabolites are closely linked to species based on their results (Smedsgaard *et al.*, 2004; Larsen *et al.*, 2005). Nevertheless, the species specificity of metabolites was limited in certain group of compound and in certain group of taxon.

A chemotaxonomic marker compound, 5-carboxymellein was found especially in the family of Xylariaceae (Anderson *et al.*, 1983). In the current study, 5-carboxymellein was observed based on the HPLC chromatograms as a major secondary metabolite in *Xylaria* sp. and *Daldinia eschotzii*; and also was present in small amounts in *Nodulisporium* sp. The fungal strain PV1.1 could not be identified based on the primers ITS 1 and ITS 4, but since it was found to produce 5-carboxymellein as a major compound, it is reasonable to assumed it belonged to the class Sordariomycetes, and most probably to the family Xylariaceae.

6.3 Assessment of fungal diversity in marine organisms and mangrove plants

In the course of the current study, assessment of fungal diversity in mangrove plants as well as in terrestrial plants such as *Taxus baccata* and *Alstonia scholaris* has already been established in the Düsseldorf laboratory, based on DGGE using fungal ITS sequences (Diesel, unpublished results). By sequencing, a single band obtained by DGGE was proven to represent a fungus living inside the tissue of the host plant (Diesel, unpublished results). Many publications described the molecular diversity of fungi relying primarily on identifying small subunit ribosomal RNA (SSU) or ITS

sequences after DGGE separation and cloning (Smit *et al.*, 1999, Vainio and Hantula, 2000, Landeweert *et al.*, 2003). However, the molecular identification of fungi can be a problem when using 18S ribosomal sequences, due to the limited availability of reference sequences, which is in part due to the much wider used identification based on ITS sequences (Kowalchuk, 1998).

In the DGGE gel, several bands with similar migration distances appeared for the total DNA extract of the host plants as well as for isolated fungal strains. For example, bands obtained for *Alternaria* sp. (band 6.1 and 7.1) also were present in the mangrove plants *Avicennia marina* (leaves) and *Rhizophora mucronata* (leaves and bark), having approximately 46% GC content. *Alternaria* sp. has frequently been described as a phytopathogen or endophyte in terrestrial plants (Raistrick *et al.*, 1953), but is obviously also present in mangrove plants as shown by these results. A band observed for *Avicennia marina* (leaves) with a longer migration distance (band 7.3) was identified as *Fusarium* sp. (about 50% GC content).

In the case of marine organisms such as marine sponges, marine anemones and marine algae, the assessment of fungal diversity proved far more difficult, even when identical experimental conditions were used. This could be due to the fact that the abundance of fungi living inside marine organisms was lower than that in plants. Most of the fungi were presumably in an inactive or dormant state inside the marine organisms and present only in very small, hardly detectable amounts such as single spores or fragments of hyphae that could not be accessed by amplifications using primers for ribosomal DNA (Proksch *et al.*, 2003; Zuccaro *et al.*, 2002).

Some techniques were employed to successfully amplify the small amount of the fungal DNA, for example adding Q solution to the PCR assay which increased sensitivity, but unfortunately the primers then also annealed to the ITS region of

sponge DNA. This was not happening in the case of mangrove plants. Furthermore, it was proven by phylogenetic analysis that fungi are taxonomically and evolutionary closer related to animals, notably even much closer related to lower animals such as sponges, than to plants [figure 6.5] (Hedges *et al.*, 2004). Thus, it came as no surprise that in the experiments conducted with sponge samples also sponge DNA was amplified, resulting in additional bands in the gel. Since sponge DNA, in comparison to fungal DNA, will occur in much higher concentrations in these samples, it will compete for primer binding and also be amplified by PCR. Accordingly, a far more complex set of PCR products resulted which proved difficult to resolve unambiguously, despite being well separated by DGGE.

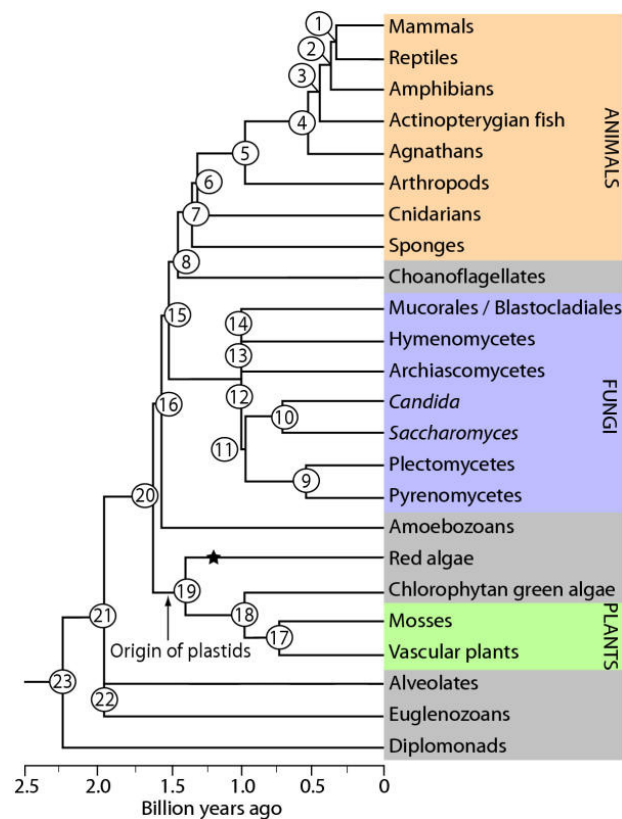


Figure 6.5 A time scale of eukaryote evolution (Hedges *et al.*, 2004).

Zuccaro *et al.* (2003) investigated a molecular detection of ascomycetes associated with the marine alga *Fucus serratus* using primers which amplified the small subunit and large subunit ribosomal DNA. PCR products from nested PCR reactions were separated using DGGE. Excised bands were re-amplified and sequenced directly or cloned before being sequenced. It was described in their publication that over half the recovered bands that were analysed in the DGGE gels represented animal sequences and some of these co-migrated with fungal products (Zuccaro *et al.*, 2003).

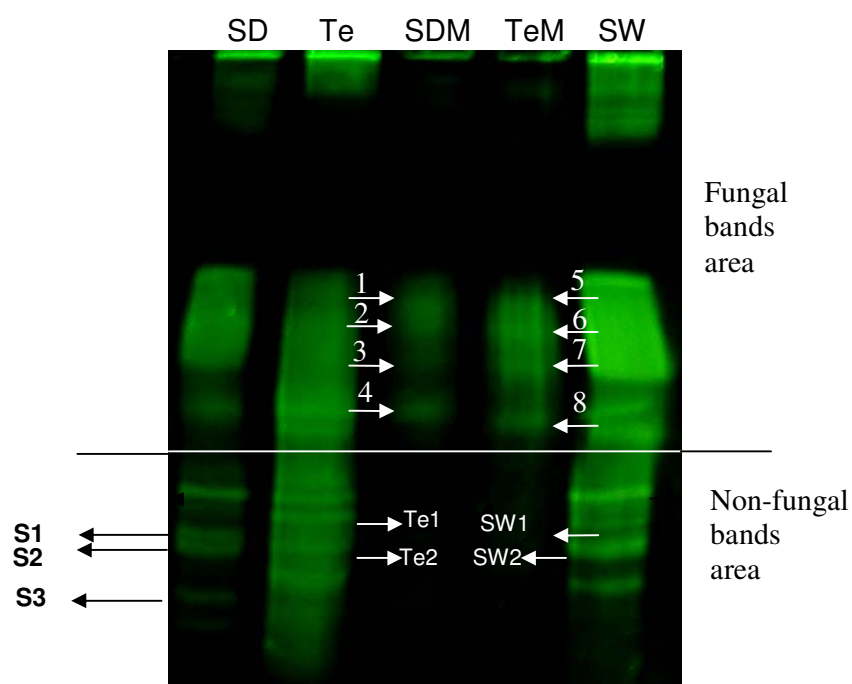
In the current study, it was found that the length of ITS PCR products of sponge DNA was relatively larger than the one of fungal sequences. Due to this fact, the absolute numbers of hydrogen bonds in sponge DNA sequences were normally higher, resulting in a longer migration distance. This is exemplified by sequencing band S1, which upon BLAST search showed a close homology to ITS sequence of the sponge *Aplysina aerophoba*.

Due to the difference in sizes, it was possible to clearly separate by DGGE bands in the upper area originating from fungi from bands in the lower area belonging to non fungal products [figure 6.6].

The mixture of ITS products from fungi isolated from *Suberites domuncula* (SDM) and *Tethya sp.* (TeM) have been used as a control and comparison tool for the DGGE separation of total DNA extract-derived amplification products from the marine sponges *Suberites domuncula*, *Tethya sp.* and total DNA obtained from enriched seawater. It could be observed in the DGGE gel that the lanes of *Suberites domuncula*, *Tethya* and sea water each showed a band of similar migration distance as band 4 in SDM (*Penicillium chrysogenum*) [figure 6.5]. As described above, each band represents one fungus and exhibits a specific migration distance depending on

its GC content (Muyzer *et al.*,1993). The same observation was made by Li *et al.* (2007) and confirmed by excising one band of similar migration distance in different lanes, giving identical results upon sequencing in each case.

Figure 6.6 Migration bands in the DGGE result of marine sponges



Band Code	Fungal code	Species	GC content (%)	Length (bp)	GC content (bp)
1.	SD2.4	<i>Alternaria compacta</i>	46.0	552	254
2.	SD1.1	<i>Botryosphaeria stevensii</i>	53.3	546	291
3.	SD4.12	<i>Myrothecium sp.</i>	52.6	583	307
4.	SD1.2	<i>Penicillium chrysogenum</i>	56.9	568	323
5.	Te4.8	<i>Sclerotinia sclerotiorum</i>	45.6	533	243
6.	Te1.2	<i>Chaetomium sp.</i>	54.7	556	304
7.	Te6.13	<i>Peniophora cinerea</i>	51.6	608	314
8.	Te1.3	<i>Penicillium polonicum</i>	57.5	565	325
	S1	<i>Aplysina aerophoba</i>	59.7	601	362

Lanes of *Tethya* sp. and sea water showed each bands of the same migration distance as band 8 in TeM (*Penicillium polonicum*), which, however, was lacking in *Suberites domuncula*. Hence, based on the band patterns observed by DGGE, it can be concluded that most of the fungi detected in the marine sponges *Suberites domuncula* and *Tethya* sp. were also present in the sea water sample [figure 6.5].

This phenomenon could be explained by the fact that sponges are filter feeders that pump large volumes of water through a unique and highly vascularized canal system, removing bacterial and small eukaryotes from seawater, translocating their food particles into their interior and leaving the expelled water essentially sterile (Hentschel *et al.*, 2002; Scheuermayer, 2006). As filter feeders, sponges are thus permanently exposed to microorganisms, including bacteria and fungi (Gernert *et al.*, 2005).

The assessment of microbial diversity in marine sponges by DGGE so far was successful in the field of the bacterial diversity (Fry *et al.*, 2006). Many investigations of sponge-associated bacteria and assessment of bacterial diversity within sponges were carried out by numerous research groups using DGGE method of small subunit rRNA sequences, for example in the sponge Mediterranean sponge *Aplysina cavernicola* (Thoms *et al.*, 2002), Mediterranean sponge *Chondrilla nucula* (Thiel *et al.*, 2007), Sponges *Stella tenuis*, *Halichondria rugosa*, *Dysidea avara* and *Craniella australiensis* from the South China sea (Li *et al.*, 2007) and in the freshwater sponge *Spongilla lacustris* (Gernert *et al.*, 2005).

Abundance of bacteria within the sponges is usually very high and can reach up to 40% of their total volume in the family Aplysinidae (Vacelet, 1975). In assessing sponge-associated bacterial diversity, successful amplification of total bacterial DNA could be enhanced by preceding cell separation and enrichment which separated

unicellular and filamentous bacteria from the sponge cells by repeated differential centrifugation in artificial seawater (Hentschel *et al.*, 2002; Fieseler *et al.*, 2004).

As a common result of all these studies cited above, there is an emerging picture that bacterial populations living inside sponges are highly specific for their hosts. In many cases, different bacterial strains obtained from sponges collected at geographically distinct sites are much more closely related to each other than to any other free-living bacteria encountered so far (Hentschel *et al.*, 2002; Thiel *et al.*, 2006). Interestingly, even an exclusively sponge-specific novel candidate phylum 'Poribacteria' was discovered by determination of sponge-associated bacterial diversity and phylogenetic analysis in the marine sponges *Aplysina aerophoba*, *A. fistularis*, *A. insularis*, *A. lacunosa*, *Verungula gigantea*, and *Smenospongia aurea* using 16S rRNA sequences (Fieseler *et al.*, 2004). At present, it is far too early to come to any conclusions whether the existence of sponge-specific associates would also hold true for fungal isolates. Not only are bacteria in marine sponges far more abundant than fungi, but furthermore the sequences of ITS regions from prokaryotes differ considerably and can thus easily be distinguished from potential host sequences, since the latter would be derived from eukaryotes such as algae or sponges. Hence, it is much easier to design bacteria-specific primers which would almost certainly not amplify eukaryotic ribosomal DNA.

Even though in this study the fungal universal primers ITS 1 and ITS 4 also amplified the sponge DNA, fungal DNA was successfully detected in the total DNA extract of marine sponge for the first time by employing PCR and DGGE technique. From all experiments, the obtained data were not robust enough to conclude that those fungi were specifically associated with sponges. Further studies with these

results as the basis are necessary to answer all questions which have been left about these chemically interesting organisms.

7. SUMMARY

A total number of 31 compounds was isolated comprising diverse structural groups including alkaloids, polyketides and terpenes, from 12 marine organism-derived fungi; one of which was a new pyranacetal derivative. The structures of the compounds were elucidated by performing mass spectrometry as well as one- and two-dimensional nuclear magnetic resonance (NMR) experiments.

1. Fungi from class Eurotiomycetes

Six nitrogen containing compounds were isolated from *Penicillium polonicum* derived from the marine sponge *Tethya* sp. Five of which, cyclophenin, cyclophenol, viridicatol, viridicatin and 3-methyl viridicatin, were biogenetically related.

Meleagrins, roquefortine, citrinin, citrinin hydrate and the diastereomers quinolactacin A1 and A2 were isolated from *Penicillium citrinum* derived from the marine alga *Sargassum* sp. Meleagrins, roquefortine and citrinin hydrate showed relatively high cytotoxic activity against the mouse lymphoma cell line L5178Y, whereas citrinin was inactive.

The anthraquinone skyrin and the preanthraquinones atrovirin B1 and atrovirin B2 were obtained from the extract of *Talaromyces wortmanii* derived from the marine sponge *Aplysina aerophoba*.

Two known compounds, tenuazonic acid and alternariol, were isolated from *Alternaria compacta* derived from the marine sponge *Suberites domuncula*.

2. Fungi from class Sordariomycetes

Three related alkaloids, chaetomin, cochliodinol and semicochliodinol, were isolated from *Chaetomium* sp. derived from the marine sponge *Tethya* sp. All of them

showed high cytotoxic activity against L5178Y cells and also displayed protein kinase inhibitory activity.

One new pyranacetal related to the family of cholesterol synthesis inhibitors agistatines was isolated from *Xylaria* sp. derived from the marine alga *Padina australis*. This compound was named 3-methyl methoxy agistatine D based on the methyl methoxy moiety at position C-3.

Daldinia escholzii derived from the marine alga *Halimeda borneoensis* was found to produce the known compound 4,4',5,5'-tetrahydroxy-1,1'-binaphthyl. This compound showed very high cytotoxic activity against L5178Y cells and also had protein kinase inhibitory activity, both of which had not been reported before.

The macrolide zearalenone was isolated from the fungus *Fusarium equiseti* derived from the alga *Sargassum* sp.

Indole-3-carboxylic acid and the diterpene myrocin A were obtained from *Arthrimum* sp. derived from *Tethya* sp. Myrocin A had cytotoxic activity and protein kinase inhibitory activity. A chemotaxonomic marker compound, 5-carboxymellein, was isolated from the fungus PV 1.1. Based on the results of the chemical analysis, it can be assumed that PV1.1 was a fungus that belonged to the family Xylariaceae.

3. Fungi from class Dothideomycetes

The antifungal compound griseofulvin was isolated from *Botryosphaeria stevensii* derived from the marine sponge *Suberites domuncula* and made this fungus one of the few griseofulvin producers outside the genus *Penicillium*. The fungus *Paraphaeosphaera michotii* derived from the marine sponge *Petrosia ficiformis* was found to produce cyclophenin, cyclophenol, viridicatol, viridicatin and 3,4,8-trihydroxy-1-tetralone.

Fungal diversity in marine organisms was assessed by performing polymerase chain reaction (PCR) using primers that target conserved, taxonomically significant genes, coupled with denaturing gradient gel electrophoresis (DGGE). The universal fungal primer pair ITS 1 and ITS 4 generated fungal DNA products which were suitable for DGGE analysis allowing broad-based molecular identification. DGGE using this primer pair was proven a trustworthy and reliable tool for determining fungal diversity in complex biological samples, most notably mangrove plants.

Fungal sequences could be recovered from the DGGE experiment involving mangrove plants, clearly demonstrating the each band represented one fungal strain. Two bands with similar migration distance in a bark sample of *Avicennia marina* and a leaf sample of the same plant were sequenced, and upon BLAST search were revealed to belong to the same fungus, *Alternaria* sp. Another band was recovered from a DGGE experiment of a leaf sample of *Avicennia marina*, and after sequencing, it was identified as *Fusarium* sp.

Detection of fungal DNA in the total DNA extract of marine sponge was carried out for the first time by employing PCR and DGGE techniques. The results showed that in this case there were also other bands representing sponge DNA sequences, besides bands representing fungal DNA. However, sponge-derived bands and fungi-derived bands can be distinguished in the DGGE gel based on their migration distances.

A phylogenetic analysis was performed using the DNA sequences of all fungal strains under investigation, amplified by the primer pair ITS 1 and ITS 4. The phylogenetic tree hence constructed was validated by bioinformatical methods and was shown to represent the evolutionary history and relationship within the kingdom fungi down to the genus level.

8. REFERENCES

- Abdel-Lateff, A., König, G.M., Fisch, K.M., Höller, U., Jones, P.G., and Wright, A.D. (2002). New antioxidant hydroquinone derivatives from the algicolous marine fungus *Acremonium* sp. *J. Nat. Prod.*, 65, 1605-1611.
- Abd-Elsalam, K.A., Aly, I.N., Abdel-Satar, M.A., Khalil, M.S., and Vereet. J.A. (2003). PCR identification of *Fusarium* genus based on nuclear ribosomal-DNA sequence data. *Africa J. Biotechnol.*, 2 (4), 82-85.
- Afdnal, A.F., and Welsch, R.L. (1991). The rise of modern jamu. The Context of Medicine in Developing Country, Ed. by Van der Geest, S., and White, S.R. Het Spinhuis, Amsterdam, 149-172.
- Aldrich Library of ¹³C and ¹H FT NMR Spectra.* (1992). Sigma-Aldrich 2, 1315B.
- Alexopoulos, C.J. Mims, C.W., and Blackwell, M. (2004). *Introductory mycology*, 4th ed., John Willey and Sons, Inc. New York, US. P. 182, 363.
- Anderson, J.R., Edwards, R.L., and Whalley, A.J.S. (1983). Metabolites of the higher fungi. Part 21. 3-methyl-3,4-dihydroisocoumarins and related compounds from the ascomycete family Xylariaceae. *J. Chem. Soc. Perkin Trans. I*, 2185-2192.
- Antonowitz, A., Gill, M., Morgan, P.M. and Yu, J. (1994). Coupled anthraquinones from the toadstool dermocybe Icterinoides. *Phytochemistry*, 37 (6), 1679-1683.
- Arai, K., Kimura, K., Mushiroda, T., and Yamamoto, M. (1989). Structures of fructigenines A and B, new alkaloids isolated from *Penicillium fructigenum* TAKEUCHI. *Chem. Pharm. Bull.*, 37, 2937-2939.
- Barber, J., Carter, R.H., Garson, M.J., and Staunton, J. (1981). The biosynthesis of citrinin by *Penicillium citrinum*. *J. Chem. Soc. Perkin Trans. I*, 2577-2583.

-
- Bardyshef, I.I., Tkachenko, O.T. and Cherches, Kh.A. (1962). Rosin acids. IV. Chemical composition of resin formed from the oleorosin of the common pine. *Zhurnal Obshchei Khimii*, 39, 999-1001.
- Bauer, A.W., Kirby, W.M.M., Sheriss, J.C., and Turck, M. (1966). Antibiotic susceptibility testing by a standardized single disc method. *Am. J. Clin. Pathol.*, 45 (4), 493-496.
- Berry, V., and Bryant, D. 1999. Faster reliable phylogenetic analysis. *Annual Conference on Research in Computational Molecular Biology*.
- Bick, I.R.C. (1985). Alkaloids. In *The Chemistry of Natural Products*, ed. by Thomson, R.H., Blackwell Scientific Publications, Oxford, 130-160.
- Birch, A.J. (1967). Biosynthesis of polyketides and related compounds. *Science*, 156, 202-206.
- Borgschulte, K., Rebuffat, S., Trowitzsch-Kienast, W., Schomburg, D, Pinon, J., and Bodo, B. (1991). Isolation and structure elucidation of Hymatoxins B – E and other phytotoxins from *Hypoxylon mammatum*, fungal pathogen of Leuce Poplars. *Tetrahedron*, 47(39), 8351-8360.
- Boyes-Korkis, J.M., et al. (1993). Anacine, a new benzodiazepine metabolite of *Penicillium aurantiogriseum* produced with other alkaloids in submerged fermentation. *J. Nat. Prod.*, 56, 1707-1717.
- Bracker, A., Pocker, A. and Raistrick, H. (1954). Studies in the biochemistry of micro-organisms. 93. Cyclophenin, a nitrogen-containing metabolic product of *Penicillium cyclopium* Westling. *Biochem. J.*, 57, 587-595.

- Brauers, G. (2003). Isolierung und Strukturaufklärung von neuen Naturstoffen aus schwamm-assoziierten Pilzen. *Dissertation*. Heinrich-Heine-Universität Düsseldorf.
- Brewer, D., Duncan, J.M., Jerram, W.A., Leach, C.K., Safe, S., Taylor, A. and Vining, L.C. (1972). Ovine ill-thrift in Nova Scotia. 5. The production and toxicology of chetomin, a metabolite of *Chaetomium* spp. *Can. J. Microbiol.*, 18, 1129.
- Brewer, D., McInnes, A.G., Smith, D.G., Taylor, A., Walter, J.A., Loosly, H.R., and Kis, Z.L. (1978). Sporidesmins. Part 16. The structure of chetomin, a toxic metabolites of *Chaetomium cochliodes*, by nitrogen-15 and carbon-13 nuclear magnetic resonance spectroscopy. *J. Chem. Soc. Perkin I*, 1248-1254.
- Bringmann, G., Lang, G., Mühlbacher, J., Schaumann, K. Steffens, S., Rytik, P.G., Hentschel, U. Morschhauser, J. and Müller, W.E.G. (2003). Sorbicillactone A: a structurally unprecedented bioactive novel-type alkaloid from a sponge derived fungus. *Progress in Molecular and Subcellular Biology*, 37, 231-253.
- Bringmann, G., Mortimer, A.J.P., Keller, P.A., Gresser, M.J., Garner, J. and Breuning, M. (2005). Atroposelective synthesis of axially chiral biaryl compounds. *Angewandte Chemie International Edition*, 44 (34), 5384-5427.
- Brockmann, H., Kluge, F., and Muxfeldt, H. (1957). Totalsynthese des Hypericins, *Chem. Ber.*, 2302-2318.
- Bugni, T.S and Ireland, C.M. (2004). Marine-derived fungi: a chemically and biologically diverse group of micro-organisms review. *Nat. Prod. Rep.*, 21.143-163.
- Butler, M.S. (2004). The role of natural products chemistry in drug discovery. *J. Nat. Prod.*, 67, 2141-2153.

-
- Choi, J.S., Chung, H.Y., Jung, H.A., and Yokozawa, T. (2000). Comparative evaluation of antioxidant potential of alternin (2-hydroxyemodin) and emodin. *J. Agric. Food Chem.*, 48, 6347-6351.
- Claverie, JM., and Notredame, C. (2003). *Bioinformatics for dummies*. Willey Publishing, Inc, NewYork, USA.
- Colombo, L., Gennari, C., Potenza, D., Scolastico, C., Aragozzini, F., and Merendi, C. (1981). Biosynthesis of citrinin and synthesis of its biogenetic precursors. *J. Chem. Soc. Perkin I*, 2594-2597.
- Cohen, P.A., and Towers, G.H.N. (1995). The Anthraquinones of *Heteroderma obscurata*. *Phytochemistry*, 40, 911-915.
- Cole, R.J., and Cox, R.H. (1981). Alternaria toxins. In: *Handbook of Toxic Fungal Metabolites*. Academic Press, New York, 615-45.
- Cunningham, K.G. and Freeman, G.G. (1952). The isolation and some chemical properties of viricatin, a metabolic product of *Penicillium viridicatum* Westling. *Biotechnol. J.*, 53, 328-332.
- Cushman, D.W., and Ondetti, M.A. (1999). Design of angiotensin converting enzyme inhibitors. *Nature Medicine*, 5(10), 1110-1112.
- DeAlvarenga, M.A., Fo, R.B., Gottlieb, O.R., Dias, J.P.P., Magalhaes, A.F., Magalhaes, E.G., de Magalhaes, G.C., Magalhaes, M.T., Maia, J.G.S., Marques, R., Marsaioli, A.J., Mesquita, A.A.L., de Moraes, A.A., de Oliveira, A.B., de Oliveira, G.G., Pedreira, G., Pereira, S.K., Pinho, S.L.V., Santana, A.E.G., and Santos, C.S. (1978). Dihydroisocoumarins and phthalides from wood samples infected by fungi. *Phytochemistry*, 17, 511-516.

-
- de Hoog, G.S., Guarro, J., Gene, Y., and Figuerres, M.J. (2000). *Atlas of Clinical Fungi*, 2nd edition, 14-18. CBS/ Universitat Rovira I Virgile.
- Demain, A.L., and Fang, A. (2000). The natural function of secondary metabolites. *Advances in Biochemical Engineering and Biotechnology*, 69, 1-39.
- Dewick, P.M. (2002). *Medicinal natural products. A biosynthetic approach..* John Willey and Sons, Ltd, Baffins Lane, Chichester, England
- Dreyfuss, M.M., and Chapela, I.H. (1994). Potential of fungi in the discovery of novel, low-molecular weight pharmaceuticals. *Biotechnology*, 26, 49-80.
- Ebel, R. (2006). Secondary metabolites from marine-derived fungi. In: *Frontiers in Marine Biotechnology*, ed. by Proksch, P., Müller, W. E.G. Horizon Scientific Press, Norwich, 73-143.
- Effendi, H. (2004). Isolation and structure elucidation of bioactive secondary metabolites of sponge-derived fungi collected from the Mediterranean sea (Italy) and Bali sea (Indonesia). *Dissertation*. Heinrich-Heine-Universität Düsseldorf.
- Endo, A. (1979). Monacolin K, a new hypercholesterolemic agent produced by *Monascus* species. *J. Antibiot.*, 32, 852-854.
- Elmi, A.A., and West, C.P. (1995). Endophyte infection effects on stomatal conductance, osmotic adjustment and drought recovery of tall fescue. *New Phytologist*, 131(1), 61-67.
- Faeth, S.H. (2002). Are endophytic fungi defensive plant mutualists? *Oikos* 98, 25-36.
- Fehler, M. and Schmidt, J.M. (2003). Property distributions: differences between drugs, natural products and molecules from combinatorial chemistry. *J. Chem. Inf. Comput. Sci.* 43, 218-227.

-
- Fieseler, L., Horn, M., Wagner, M., and Hentschel, U. (2004). Discovery of the novel candidate phylum Poribacteria in marine sponges. *Appl. Env. Microbiol.*, 3724-3732.
- Framm, J., Nover, L., El Azzouny, A., Richter, H., Winter, K., Wernert, S., and Luckner, M. (1973). Cyclopeptin und Dehydrocyclopeptin. Zwischenprodukte der Biosynthese von Alkaloiden der Cyclophenin-Viridicatin-Gruppe bei *Penicillium cyclopium* Westling. . *Eur. J. Biochem.*, 37, 78-85.
- Fredenhagen, A., Petersen, F., Tintelnot-Blomley, M., Rösel, J., Mett, H., and Hug, P. (1997). Semicochliodinol A and B: inhibitors of HIV-1 protease and EFG-R protein tyrosine kinase related to asterriquinones produced by the fungus *Chrysosporium merdarium*. *J. Antibiot.*, 50., 395-401.
- Frisvad, J.C., and Samson, R.A. (2000). Neopetromyces gen. nov. and an overview of teleomorph of *Aspergillus* subgenus *Circumdati*. *Studies in Mycology (Utrecht)*, 45, 201-207.
- Frisvad, J.C., Smedsgaard, J., Larsen, T.O. and Samson, R.A. (2004). Mycotoxins, drugs and other extrolites produced by species in the *Penicillium* subgenus *Penicillium*. *Studies in Mycology*, 49, 201–242.
- Fry, J.C., Webster, G., Cragg, B.A., Weightman, A.J. and Parkes, R.J. (2006). Analysis of DGGE profiles to explore the relationship between prokaryotic community composition and biogeochemical processes in deep subseafloor sediments from the Peru Margin. *Federation of European Microbiological Societies*, 58, 86-98.
- Fujimoto, H., Sumino, M., Okuyama, E and Ishibashi, M. (2003). Immunomodulatory constituents from an ascomycete, *Chaetomium seminudum*. *J. Nat. Prod.*, 67, 98-102.

-
- Fujitake, N., Suzuki, T., Fukumoto, M., and Oji, Y. (1998). Predomination of Dimers over Naturally Occurring Anthraquinones in Soil. *J. Nat. Prod.*, 61, 189-192.
- Gardiner, D.M., Waring, P. and Howlett, B.J. (2005). The Epipolythiodioxopiperazine (ETP) class of fungal toxins: distribution, mode of action, functions and biosynthesis. *Microbiology*, 151, 1021-1032.
- Geiser, D.M. (2004). Practical molecular taxonomy of fungi. In *Advances in Fungal biotechnology for industry, agriculture and medicine*, ed. by Tkacz and Lange.
- Gernert, C, Glöckner, F.O., Krohne, G., and Hentschel, U. (2005). Microbial diversity of the freshwater sponge *Spongilla lacustris*. *Microbial ecology*, 50, 206-212.
- Gill, M. and Morgan, P. (2004). Absolute stereochemistry of fungal metabolites icterinoidins A1 and B1, and atrovirin B1 and B2. *ARKIVOC*, 152-165.
- Gill, M. (1999). Pigments of fungi (macromycetes). *Nat. Prod. Rep.*, 16, 301-317.
- Gill, M. and Gimenez, A. (1991). Astrovenetin, the principal pigments of the toadstool *Dermocybe austroveneta*. *Phytochemistry*, 30 (3), 951-955.
- Gill, M. and Steglich, W. (1988). Pigments of fungi (Macromycetes). *Prog. Chem. Org. Nat. Prod.*, 51,67-90.
- Göhr, A. Grabley, S., Thiericke, R. and Zeeck, A. (1996). Agistatines, novel pyranacetals from the fungus FH-A 6239. *Liebigs Annalen*, 627-633.
- Grove, J.F., MacMilan, J., Mulholland, T.P.C., and Rogers, M. (1952). Griseofulvin. Part IV. The structures. *J. Chem. Soc.*, 3977-3987.
- Guarro, J., Gene, J. and Stchigel, A.M. (1999). Developments in fungal taxonomy. *Clin. Microbiol. Rev.*, 12(3). 454-500.

-
- Hall, T.A. (1999). BioEdit: a user friendly biological sequence alignment editor and analysis for Windows 95/98/NT. *Nucl. Acids Symp. Ser 41*, 95-98.
- Hall, B.G. (2005). *Phylogenetic trees made easy*. Sinauer Associated, Inc. Publisher Sunderland, Massachussets, USA.
- Hanika, C and Carlton, W.M. (1994). Toxicology and pathology of citrinin. *Biodeterioration Research*, 4, 41-63.
- Hashimoto, T., Tahara, S., Takaoka, S., Tori, M., and Asakawa, Y. (1994). Structures of a novel binaphthyl and three novel benzophenone derivatives with plant-growth inhibitory activity from the fungus *Daldinia concentrica*. *Chem. Pharm. Bull.*, 42(7), 1528-1530.
- Hedges, S.B., Blair, J.E., Venturi, M.L., and Shoe, J.L. (2004). a molecular timescale of eukaryote evolution and the rise of complex multicellular life. *BMC Evolutionary Biology*, 4(2), 1-9.
- Hentschel, U., Hopke, J., Horn, M., Friedrich, A.B., Wagner, M., Hacker, J. Moore, B.S. (2002). Molecular evidence for a uniform microbial community in sponges from different oceans. *Appl. Env. Microbiol.*, 68 (9), 4431-4440.
- Herr, R.A., Ajello, L., Taylor, J.W., Arseculeratne, S.N., and Mendoza, L. (1999). Phylogenetic analysis of *Rhinosporidium seeberi*'s 18S small subunit ribosomal DNA groups this pathogen among the member of the protoctistan mesomycetozoa clade. *J. Clin. Microbiol.* , 37, 2750-2754.
- Hibbet, D.S. (1992). Ribosomal RNA and fungal systematic. *Trans. Mycol. Soc*, 33, 533 – 556.
- Hillis, D.M., and Dixon, M.T. (1991). Ribosomal DNA: molecular evolution and phylogenetic interfere. *Q. Rev. Biol.*, 66, 411-453.

- Hitchcock, S.A. and Pattenden, G. (1992). Total synthesis of the mycotoxin (-)-zearalenone based on macrocyclisation using a cinnamyl radical intermediate. *J. Chem. Soc. Perkin Trans. I*, 1323-1328
- Hodge, R.P., and Harris, C.M. (1988). Verrucofortine, a major metabolites of *Penicillium verrucosum* Var. Cyclopium, the fungus that produces the mycotoxin verrucosidin. *J. Nat. Prod.*, 51, 66 -73.
- Hopwood, D.A. (2007). How do antibiotic-producing bacteria ensure their self-resistance before antibiotic biosynthesis incapacitates them? *Molecular Microbiology*, 63 (4), 937-940.
- Hsu, Y.H., Nakagawa, M., Hirota, A., Shima, S., and Nakayama, M. (1988). Structure of myrocin B, a new diterpene antibiotic produced by *Myrothecium verrucaria*. *Agric.Biol. Chem.*, 52, 1305-1307.
- Iwasaki, S., Muro, H., Nozoe, S., and Okuda, S. (1972). Isolation of 3,4-dihydro-3,4,8-trihydroxy-1(2H)-naphthalenone and tenuazonic acid from *Pyricularia oryzae* Cavara. *Tet. Lett.*, 1, 13-16.
- Jadulco, R., Proksch, P., Wray, V., Berg, A. and Grafe, U. (2001). New macrolides and furan carboxylic acid derivative from the sponge-derived fungus *Cladosporium herbarum* *J. Nat. Prod.*, 64, 527-530.
- Jasalavich, C.A., Ostrofsky, A. And Jellison, J. (2000). Detection and identification of decay fungi in spruce wood by restriction fragmen length polymorphism analysis of amplified genes encoding RNA. *Appl. Env.Microbiol.*, 66(11), 4725-4734.
- Jarvis, B.B., Zhou, Y., Jiang, J., Sorenson, W.G., Hintikka, E.L., Nikulin, M., Parikka, P., Etzel, R.A. and Dearborn, D.G. (1996). *Toxicogenic molds in water damaged*

-
- buildings: dechlorogriseofulvins from Memnoniella echinata. J. Nat. Prod.*, 59 (6), 553-554.
- Jerram, W.A., McInnes, A.G., Maass, W.S.G., Smith, D.G., Taylor, A., and Walter, J.A. (1975). The chemistry of cochliodinol, a metabolite of *Chaetomium* spp. *Can. J. Chem.*, 53(5), 727-737.
- Jobes, D.V and Thien, L.B. (1997). A conserved motif in the 5.8S ribosomal RNA (rRNA) gene is a useful diagnostic marker for plant internal transcribed spacer (ITS) sequences. *Plant Molecular Biology Reporter*, 15, 326 – 334.
- Kadam, S., Poddig, J., Humphrey, P., Karwowsky, J., Jackson, M., Tennent, S., Fung, L., Hochlowski, J., Rasmussen, R., and McAlpine, J. (1994). Citrinin hydrate and radinicin: human rhinovirus 3C-protease inhibitors discovered in a target-directed microbial screen. *J. Antibiot.*, 47, 836-839.
- Kakinuma, N. , Iwai, H., Takahashi, S., Hamano, K., Yanagisawa, T., Nagai, K., Tanaka, K., Suzuki, F., Kirikae, T. and Nakagawa, A. (2000). Quinolactacin A, B and C: novel quinolone compounds from *Penicillium* sp.EPF-6, taxonomy, production, isolation and biologicals properties. *J. Antibiot.*, 53, 1247-1251.
- Kanakam, C.C., Mani, N.S., and Subba Rao, G.S.R. (1990). Synthesis based on cyclohexadienes. Part 4. Novel synthesis of 6-aryl-2,4-dimethoxybenzoates . Alternariol and methyl trimethyl altenusin. *J. Chem. Soc. Perkin Trans. I*, 2233-2238.
- Karp, G. (1999). *Cell and Molecular Biology* 5th edition New York, John Willey and Sons.

-
- Kawai, K. , Koehei, N., Shoichi, N., and Yoichi, I. (1984). Studies on fungal products. VII. The structures of meleagrins and 9-*O*-*p*-bromobenzoylmeleagrins. *Chem. Pharm. Bull.*, 32, 94-98.
- Keil, G. (1989). *Das Lorsche Arzneibuch*. Wiss. Verl.-Ges., Stuttgart.
- Kelecom, A. (2002). Secondary metabolites from marine microorganisms. *Anais da Academia Brasileira de Ciencias*, 74 (1). 151-170.
- Kim, W.G., Song, N.K. and Yoo, I.D. (2001). Quinolactacins A1 and A2, new acetylcholinesterase inhibitors from *Penicillium citrinum*. *J. Antibiot.*, 54, 831-835.
- Klemke, C., Kehraus, S., Wright, A.D. and König, G.M. (2003). New secondary metabolites from the marine endophytic fungus *Apiospora montagnei*. *J. Nat. Prod.*, 67, 1058-1063.
- Kowalchuk, G.A. (1998). Fungal community analysis using denaturing gradient gel electrophoresis. *Molecular Microbial Ecology Manual 3.4.6*, ed. by Akkermans, A.D.L, van Elsas, J.D., and de Bruijn, F.J., Kluwer Academic Publishing, Dordrecht, 1–16.
- Kohlmeyer, J., and Kohlmeyer, E. (1979) *Marine Mycology – The Higher Fungi*. Academic Press, New York, 690.
- Konda, Y., Onda, M., Hirano, A., and Omura, S. (1980). Oxaline and neoxaline. *Chem. Pharm. Bull*, 28, 2987-2993.
- Koschinsky, S., Peters, S., Schwieger, F., and Tebbe, C.C. (1999). Applying molecular techniques to monitor microbial communities in composting process. *Eight International Symposium on Microbial Process during Composting*, The Society for Microbial Ecology. Halifax, Canada.

-
- Krohn, K., Bahramsari, R., Flörke, U., Ludewig, K., Kliche-Spory, C., Michel, A., Aust, HJ., Draeger, S., Schulz, B. and Antus, S. (1997). Dihydroisocoumarin from fungi: isolation, structure Elucidation, circular dichroism and biological activity. *Phytochemistry*, 45, 313–320.
- Kumar, S., Tamura, K., and Nei, M. (2004). MEGA3: Integrated software for molecular evolutionary genetics analysis and sequence alignment. *Briefings in Bioinformatics* 5, 150-163.
- Kusano, M., Koshino, H., Uzawa, J., Fujiola, S., Kawano, T. and Kimura, Y. (2000). Nematicidal alkaloids and related compounds produced by the fungus *Penicillium cf. simplicissimum*. *Biosci. Biotechnol. Biochem.*, 64, 2559-2568.
- Landeweert, R., Veenman, C., Kuyper, T.W., Fritze, H., Wernars, K., and Smit, E. (2003). Quantification of ectomycorrhizal mycelium in soil by real-time PCR compared to conventional quantification techniques. *FEMS Microbiol. Ecol.*, 45(3), 283-292.
- Larsen, T.O., Smedsgaard, J., Nielsen, K.F., Hansen, M.E. and Frisvad, J.C. (2005). Phenotypic taxonomic and metabolite profiling in microbial drug discovery. Review. *Nat. Prod. Rep.*, 22. 672-695.
- Li, J.Y., Sidhu, R.S., Ford, E., Hess, W.M., and Strobel, G.A. (1998). The induction of taxol production in endophytic fungus- *Periconia* sp. from *Torreya grandifolia*. *J. Ind. Microbiol. Biotechnol.*, 20, 259-264.
- Lin, W., Brauers, G., Ebel, R., Wray, V., Berg, A., Sudarsono, and Proksch, P. (2001). Novel Chromone Derivatives from the Fungus *Aspergillus versicolor* Isolated from the Marine Sponge *Xestospongia exigua*. *J. Nat. Prod.*, 66(1), 57-61.

-
- Liu, K., Wu, W.K., He, W., and Liu, C.L. (2007). *Ginkgo biloba* extract (EGb761) attenuates lung injury induced by intestinal ischemia/reperfusion in rats: roles of oxidative stress and nitric oxide. *World J. Gastroenterol.*, 13(2), 299-305.
- Linde, J., and Mulrow, C.D. (1999). St. John's wort for depression (Cochrane Review). In : The Cochrane Library, vol. 3, update software, Oxford.
- <http://ovid.sams.ch/ovidweb/ovidweb.cgi>
- Liu, K.X., Wu, W.K., He, W., and Liu, C.L. (2007). Ginkgo biloba extract (EGb 761) attenuates lung injury induced by intestinal ischemia/reperfusion in rats: Roles of oxidative stress and nitric oxide. *World J Gastroenterol* 3(2), 299-305.
- Long, L.M., and Troutman, H.D. (1949). Chloramphenicol (chloromycetin) Vii. Synthesis through p-nitroacetophenol. *J. Am. Chem. Soc.*, 71, 2473-2475.
- Luckner, M. and Mohammed, Y.S. (1964). Metabolic products of *Penicillium viridicatum* Westling and *Penicillium cyclopium* Westling; synthesis of viridicatol, 3'-methylviridicatol and N-methyl-3'-O-methylviridicatol. *Tet. Lett.*, 29, 1987-1989.
- Luckner, M. and Winter, K. (1969). Zur Bildung von Chinolinalkaloiden in Pflanzen 4. *Eur. J. Biochem.*, 7, 380-384.
- Magnani, M., Fernandes, T., Egidio, C., Prete, C., Homechim, M., Yurie, E., Ono, S., Vilas-Boas, A., Sartori, D., Furlaneto, M.C. and Fungaro, M.H.P. (2005). Molecular identification of *Aspergillus* spp. isolated from coffee beans. *Scientia Agricola (Piracicaba, Braz.)*, 62, 45-49.
- Malinowsky, D.P., and Belesky, D.P. (2000). Adaptation of endophyte-infected-cool-season grasses to environmental stresses: Mechanism of drought and mineral stress tolerance. *Crop. Sci.*, 40(4), 923-940.

-
- McInnes, A.G., Taylor, A., and Walter, J.A. (1976). The structure of chaetomin. *J. Am. Chem. Soc.*, 98(21), 6741.
- Michael, J.P. (2002). Quinoline, quinazoline and acridone Alkaloids. *Nat. Prod. Rep.*, 19, 742-760.
- Miller, J.D. (2000). Screening for secondary metabolites. *Marine Mycology: a practical approach*, ed. by Hyde, K.D and Pointing, S.B. Fungal Diversity Press, Hongkong. 158-172.
- Moerman, K.L., Chai, C.L.L. and Waring, P. (2003). Evidence that the Lichen-derived scabrosin esters target mitochondrial ATP synthase in P388D1 cells. *Toxicol. Appl. Pharmacol.*, 190, 232-240.
- Moore-Landecker. (1996). *Fundamental of the fungi*, 4th edition. Prentice-Hall, Inc. 501 – 504.
- Mullbacher, A., Waring, P., Tiwari-Palni, U. and Eichner, R.D. (1986). Structural relationship of epipolythiodioxopiperazines and their immunomodulatory activity *Molecular Immunology*, 23, 231-236.
- Munday, R. (1982). Studies on the mechanism of toxicity of the mycotoxin sporidesmin. I. Generation of superoxide radical by sporidesmin. *Chem Biol Interact*, 41, 361–374.
- Muyzer, G., de Waal and Uitterlinden, A.G. (1993). Profiling of complex microbial populations by denaturing gradient gel electrophoresis analysis of polymerase chain reaction-amplified genes coding for 16S rRNA. *Appl. Env. Microbiol.* 59(3): 695-700.

-
- Muzychkina, R.A. (1998). *Natural Anthraquinones, Biological and Physicochemical Properties*. Publishing House Phasis, Moscow, 864.
- Nakashima, R., and Slater, G.P. (1969). Configuration of echinulin II. Optical rotary dispersion of echinulin, hydroechinulin, and the stereoisomeric 3-methyl-6(indolyl-3-methyl)-piperazine-2,5-diones. *Can. J. Chem.*, 47, 2069-2074.
- Napryeyenko, O., and Borzenko, I. (2007). *Ginkgo biloba* special extract in dementia with neuropsychiatric features: a randomized, placebo-controlled. Double-blind clinical trial. *Arzneimittel Forschung*, 57(1), 4-11.
- Nemec, K., and Schubert-Zsilavec, M. (2003). Medizinische Chemie. From teprotide to captopril: Rational design of ACE inhibitors. *Pharmazie in Unserer Zeit*, 32 (1), 11-16.
- Newman, D.J., Cragg, G.M, and Snader, K.M. (2000). The influence of natural products upon drug discovery. *Nat. Prod. Rep.*, 17, 215-234.
- Newton, C. and Graham, A. (1997). *PCR*, second edition. Bios Scientific Publishers and Springer, Singapore.
- Newton, G.G.F, and Abraham, E.P. (1955). Cephalosporine C, a new antibiotic containing sulphur and D-a-aminoadipic acid. *Nature* (London) 175, 548.
- Nolte, M.J., Steyn, P.S. and Wessels, P.L. (1980). Structural investigation of 3-acylpyrrolidine-2,4-diones by nuclear magnetic resonance spectroscopy and X-ray crystallography. *J. Chem. Soc. Perkin I*, 1057-1065.
- Nover, L. and Luckner, M. (1969). On the biosynthesis of cyclophenin and cyclophenol, benzodiazepines alkaloids from *Penicillium cyclopium* Westling. *Eur. J. Biochem.*, 10, 268 -273.

-
- Nozawa, K., and Nakajima, S. (1979). Isolation of radicicol from *Penicillium luteoaurantium* and meleagrins, a new metabolite from *Penicillium meleagrinum*. *J. Nat. Prod.*, 42, 374-377.
- Numata, A., Takahashi, C., Ito, Y., Minoura, K., Yamada, T., Matsuda, C., and Nomoto, K. (1996). Penochalasin, a novel class of cytotoxic cytochalasins from a *Penicillium* species separated from a marine alga: structure determination and solution conformation. *J. Chem. Soc., Perkin Trans. 1*, 239 – 245.
- O'Callaghan, M., Gerard, E.M., Heilig, G.H.J., Zhang, H., Jackson, T.A. and Glare, T.R. (2003). Denaturing gradient gel electrophoresis—a tool for plant protection research. *New Zealand Plant Protection* 56, 143-150.
- Ohmomo, S., Sato, T., Utagawa, T., and Abe, M. (1975). Isolation of festuclavine and three new indol alkaloids roquefortine A, B, and C from the culture of *Penicillium roquefortii*. *Agric. Biol. Chem.*, 39, 1333-1334.
- Onocha, P., Okorie, D., Conolly, J., and Roycroft, D. (1995). Monoterpene diol iridioid glycoside and dibenzo-a-pyrone from *Anthocleista djalonensis*. *Phytochemistry*, 40, 1183-1189.
- Overy, D.P., Nielsen, K.F. and Smedsgaard, J. (2005). Roquefortine/oxaline biosynthesis pathway metabolites in *Penicillium Ser Corymbifera*: in plant production and implication for competitive fitness. *J. Chem. Ecol.*, 31, 2373-2390.
- Owen, N.L. and Hundley, N. (2004). Endophytes – the chemical synthesizers inside plants. *Science Progress*, 87(2), 79-99.
- Pahl, H.L., Krauss, B., Schulze-Osthoff, K and 9 other authors. (1996). The immunosuppressive fungal metabolite gliotoxin specifically inhibits transcription factor NF- κ B. *J. Exp. Med.*, 183, 1829-1840.

-
- Patwardhan, B., Vaidya, A.D.B., and Chorgade, M. (2004). Ayurveda and natural products drug discovery. *Current Science* 86 (6), 789-799.
- Peterson, S.W. (2000). Phylogenetic analysis of *Penicillium* sp. based on ITS and *lsu* rDNA nucleotide sequences. In *Integration of modern taxonomic methods for Penicillium and Aspergillus Classification*, ed. by Samson, R.A and Pitt, J.I. Harwood Academic Publisher, Amsterdam, The Netherlands, 163-178.
- Peterson, S.W. (2000). Phylogenetic relationships in *Aspergillus* based on rDNA sequence analysis. In *Integration of modern taxonomic methods for Penicillium and Aspergillus Classification*, ed. by Samson, R.A and Pitt, J.I. Harwood Academic Publisher, Amsterdam, The Netherlands, 323-356.
- Pieper, R., Ebert-Khosla, S., Cane, D.E. and Khosla, C. (1996). Erythromycin biosynthesis: Kinetic studies on a fully active modular polyketide synthase using natural and unnatural substrates., *Biochemistry*, 35, 2054-2060.
- Pirrung, M.C., Brown, W.L., Rege, S. and Laughton, P. (1991). Total synthesis of (+)-griseofulvin. *J. Am. Chem. Soc.*, 113, 8561-8562.
- Proksch, P. (1997). Jamu – traditionelle Heilkunde in Indonesiens. *Z. Phytoter.*, 18, 232-240.
- Proksch, P. , Edrada, R.A., and Ebel, R. (2002). Drugs from the seas – current status and microbiological implications. *Appl. Microbiol. Biotechnol.*, 59, 125-134.
- Proksch, P., Ebel, R., Edrada, R.A., Schupp, P. Lin, W.H., Sudarsono, Wray, V., Steube, K. (2003). Detection of pharmacologically active natural products using ecology. Selected example from Indopacific marine invertebrates and sponge-derived fungi. *Pure Appl. Chem.*, 75, 343 – 352.

-
- Proksch, P., Edrada, R. and Lin, W.H. (2006). Implications of marine biotechnology on drug discovery. In *Frontiers in Marine Biotechnology*, ed. by Proksch, P. and Müller, W.E.G. Horizon Bioscience, Wymondham, England.
- Quang, D.N., Stadler, M., Fournier, J., Asakawa, Y. (2006). Carneic acids A and B, chemotaxonomically significant antimicrobial agents from the xylariaceous ascomycete *Hypoxylon carneum*. *J. Nat. Prod.*, 69 (8), 1198-1202.
- Raistrick, H., Sticking, C., and Thomas, R. (1953). Alternariol, a new pyran from the fungus *Alternaria* sp. *Biochem. J.*, 55, 421-423.
- Reshetilova, T. A., Vinokurova, N. G., Khmelenina, V. N., and Kozlovsky, A. G. 1995. The role of roquefortine in the synthesis of alkaloids meleagrins, glandicolines A and B, and oxaline in fungi *Penicillium glandicola* and *P. atramentosum*. *Microbiology*, 64, 27-29.
- Rote Liste (2007). Arzneimittelinformationen für Deutschland. <http://www.roteliste.de>.
- Royles, B.J.L. (1995). Naturally occurring tetramic acids: structure, isolation and synthesis. *Chem. Rev.*, 95, 1981-2001.
- Rudgers, J.A., Koslow, J.M. and Clay, K. (2004). Endophytic fungi alter relationships between diversity and ecosystem properties. *Ecol. Lett.*, 7, 42-51.
- Saito, T., Yasushi, S., Kiyotaka, K., Shinsaku, N., Yoichi, I. and Takeshi, K. (1988). Chetracin A and chetracin B and C, three new epipolythiodioxopiperazines from *Chaetomium* spp. *Chem. Pharm. Bull.*, 36, 1942-1956.
- Samuelsson, G. (1999). *Drugs of Natural Origin*. A text book of pharmacognosy, 4th ed., Apotekarsocieteten, Stockholm, 551.

- Sanakawa, U. (1980). The biosynthesis of anthraquinonoid mycotoxins from *Penicillium islandicum* Sopp. and related fungi. *Biosynthesis of Mycotoxins*, ed. by Steyn, P., Academic Press, New York, 357-394.
- Sankawa, U., Shimada, H., Sato, T., Kinoshita, T., and Yamasaki, K. (1981). Biosynthesis of scytalone. *Chem. Pharm. Bull.*, 29(12), 3536-3542.
- Sato, Y and Oda, T. (1976). Griseofulvin biosynthesis: new evidence of two acetate-dispositions in the ring A from ^{13}C nuclear magnetic resonance studies. *Tet. Lett.*, 44, 3971-3974.
- Scheuermayer, M, Gulder, T.A.M, Bringmann, G. and Hentschel, U. (2006). *Rubritalea marina* gen.nov., sp.nov., a marine representative of the phylum 'Verrucomicrobia' isolated from a sponge (Porifera). *Int. J. Syst. Evol Microbiol*, 56, 2119-2124.
- Scott, P.M., Merrien, M.A., and Polonsky, J. (1976). Roquefortine and isofumiglacavine A, metabolites from *Penicillium Roqueforti*. *Experientia*, 32, 140-142.
- Scripnikov, A., Khomenko, A., and Napryeyenko, O (2007). Effects of Ginkgo biloba Extract EGb 761[®] on neuropsychiatric symptoms of dementia: findings from a randomised controlled trial. *WMW Wiener Medizinische Wochenschrift* 157, 295-300.
- Seigler, D.S. (1998). *Plant Secondary Metabolism*. Kluwer Academic Publisher, London, 759.
- Sekita, S. (1983). Isocochliodinol and Neocochliodinol, Bis(3-indolyl)-benzoquinones from *Chaetomium* sp. *Chem. Pharm. Bull.*, 31, 2998-3001.

-
- Sidik (1994). The current status of jamu and suggestions for further research and development. *Indigenous Knowledge and Development Monitor* (2), 13-15.
- Sipos, P., Gyory, H., Hagymasi, K., Ondrejka, P., and Blazovics, A. (2004). Special wound healing methods used in ancient Egypt and the mythological background. *World J. Surg.*, 28, 211-216.
- Smedsgaard, J. and Frisvad, J.C. (1996). Using direct electrospray mass spectrometry in taxonomy and secondary metabolite profiling of crude fungal extract. *J. Microbiol. Methods.*, 25(1), 5-17.
- Smedsgaard, J., and Nielsen, J. (2005). Metabolite profiling of fungi and yeast: from phenotype to metabolome by MS and informatics. *Journal of Experimental Botany*, 56(410), 273-286.
- Shibata, S., Tanaka, O., and Kitagawa, I. (1955). Metabolic products of fungi. V. The structure of skyrin. *Pharm. Bull.*, 3(4), 278-283.
- Skouboe, P., Taylor, J.W., Frisvad, D., Lauritsen, D., Larsen, L., Alboek, M.B. and Rossen, L. (2005). Molecular methods for differentiation of closely related *Penicillium* species. In *Integration of modern taxonomic methods for Penicillium and Aspergillus Classification*, ed. by Samson, R.A and Pitt, J.I. Harwood Academic Publisher, Amsterdam, The Netherlands, 179-188.
- Smit, P., Leeflang, P., Glandorf, B., van Elsas, J.D., and Wernars, K. 1999. Analysis of fungal community in the wheat rhizosphere by sequencing of cloned PCR-amplified genes encoding 18S rRNA and temperature gradient gel electrophoresis. *Appl. Env. Microbiol.*, 65, 2614-2621

- Soedigyo, M. (1990). Javanese traditional medicine. Paper presented at the *International Congress on Traditional Medicine and Medicinal Plants*. Denpasar, Bali, Indonesia
- Solladie, G., Maestro, M.C., Rubio, A., Pedrega, C., Carreio, M.C. and Ruana, J.L.G. (1990). Asymmetric synthesis of (S)-zearalenone dimethyl Ether, an orsellinic acid type macrolide. *J. Org. Chem.*, 56, 2317-2322.
- Steglich, W., and Oertel, B. (1984). Pigments of fungi. *Sydowia*, 37, 284.
- Steyn, P.S and Wessels, P.L. (1978). Tautomerism in Tetramic Acids: ^{13}C NMR determination of the structure and ratios of the tautomers in 3-Acetyl-5-isopropylpyrrolidine-2,4-dione. *Tet. Lett.*, 47, 4707-4710.
- Stinson, E., Wise, W., Moreau, R., Jurewicz, and Pfeffer, P. (1986). Alternariol: an evidence for biosynthesis via norlichexanthone. *Can. J. Chem.*, 64, 1590-1594.
- Stork G. and Tomasz, M. (1964). A new synthesis of cyclohexenones: the double michael addition of vinyl ethynyl ketones to active methylene compounds. application to the total synthesis of *dl*-griseofulvin. *J. Am. Chem. Soc.*, 86, 471-478.
- Strobel, G.A., Stierle, A., Stierle, D., and Hess, W.M. (1993). *Taxomyces andreanae* a proposed new taxon for bulbiferous hypomycete associated with pasific yew. *Mycotaxon*, 47, 71-78.
- Strobel, G.A., Yang, X. Sears, J. Kramer, R. Sidhu, R.S., and Hess, W.M. (1996).. Taxol from *Pestalotiopsis microspora*, an endophytic fungus of *Taxus wallichiana*. *Microbiology* 142, 435-440.
- Strobel, G.A. (2002). Rainforest endophytes and bioactive products. *Critical Reviews in Biotechnology*, 22 (4), 315-333.

-
- Strobel, G.A., Daisy, B. Castillo, U. and Harper, J. (2004). Natural products from endophytic microorganisms. *J. Nat. Prod.*, 67, 257-268.
- Takahashi, S., Kakinuma, N. Iwai, H., Yanagisawa, T., Nagai, K. Suzuki, K. Tokunaga, T., Nakagawa, A. (2000). Quinolactacin A,B and C: novel quinolone compounds from *Penicillium* sp.EPF-6, physico-chemical properties and structure elucidation. *J. Antibiot.*, 53, 1252-1256.
- Tamura, M., Kawahara, K., and Sugiyama, J. (2005). Molecular phylogeny of *Aspergillus* and associated teleomorphs in the Trichocomaceae (Eurotiales). In *Integration of modern taxonomic methods for Penicillium and Aspergillus Classification*, ed. by Samson, R.A and Pitt, J.I.
- Tan, R.X. and Zou, W.X. (2001). Endophytes: a rich source of functional metabolites. *Nat. Prod. Rep.*, 18, 448-459.
- Taylor, A., and Walter, J.A. (1978). Determination of low levels of incorporations of ¹³C-labelled precursors. Biosynthesis of the 2,5-dihydroxycyclohexadiene-1,4-dione system of cochliodinol. *Phytochemistry*, 17(6), 1045-1048.
- Taylor, A. (1981). *Microbial toxins, a comprehensive treatise*, Vol 7, Ed. By Rodick, J.V and Ciegler, A. Academic Press, NewYork, 337-376.
- Taylor, C.C.W. (2001). *Socrates: a Very Short Introduction*. Oxford University Press.
- Teuscher, F. (2005). Bioaktive Naturstoffe aus marinen endophytischen und schwammassoziierten Pilzen des Indischen und Pazifischen Ozeans. *Dissertation*. Heinrich-Heine-Universität Düsseldorf.
- Thiel, V., Leininger, S., Schmaljohann, R., Brümmer, F. , and Imhoff, J.F. (2007). Sponge-specific bacterial associations of the mediterranean sponge *Chondrilla nucula* (Demospongiae, Tetractinomorpha). *Microbial ecology*, 54, 101-111.

-
- Thoms, C., Horn, M., Wagner, M., Hentschel, U., and Proksch, P. (2003). Monitoring microbial diversity and natural products profiles of the sponge *Aplysina cavernicola* following transplantation. *Marine Biology*, 142, 685-692.
- Townsend, C.A. and Minto, R.E. (1999). Biosynthesis of aflatoxins. *Compr. Nat. Prod. Chem.*, vol. 1. Elsevier, Amsterdam, 443-471.
- Traber, R., Hofmann, H., Kuhn, M., and von Wartburg, A. (1982). Isolierung und strukturermittlung der neuen cyclosporin E, F, G, H und I. *Helv. Chim. Acta* 65, 1655-1677.
- Traber, R., Hofmann, H., Loosli, H.R., Ponelle, M., and von Wartburg, A. (1987). Neue cyclosporine aus *Tolypocladium inflatum*. Die cyclosporine K – Z. *Helv. Chim. Acta* 70, 13-36.
- Urry, W.H., Wehrmeister, H.L., Hodge, E.B. and Hidy, P.H. (1966). The structure of zearalenone. *Tet. Lett.*, 27, 3109-3114.
- Vacelet, J. (1975). Etude en microscopie electronique de l'association entre une cynophycee chroococcale et une eponge du genre *Verongia*. *J. Microsc.*, 12, 363-380.
- Vainio, E.J, and Hantula, J. (2000). Direct analysis of wood inhabiting fungi using denaturing gradient gel electrophoresis of amplified ribosomal DNA. *Mycol. Res.*, 104 (8), 927-930.
- Van Dorp, E.L.A., Yassen, A., and Albert, D. (2007). Naloxone treatment in opioid addiction: the risks and benefits. *Expert Opinion in Drug Safety*, 6(2), 125-132.
- Varoglu, M. and Crews, P. (2000) Biosynthetically diverse compounds from a saltwater culture of sponge-Derived *Aspergillus niger*. *J. Nat. Prod.*, 63, 41-43.

-
- Varoglu, M., Corberdt, T.H. and Valeriote, F.A. (1997). Asperazine, a selective cytotoxic alkaloid from a sponge-derived culture of *Aspergillus niger*. *J. Org. Chem.*, 62, 7078-7079.
- Viegas Jr., C., Bolzani, V.d.S., Eliezer, J., Fraga, M. and Carlos, A. (2005). New anti-alzheimer drug from biodiversity: The role of the natural scetylcholinesterase inhibitors. *Mini-Reviews in Medicinal Chemistry*, 5, 915-926.
- Vigushi, D.M., Mirsaidi, N., Brooke, G., Sun, C., Pace, P., Inman, L., Moody, C.J. and Coombes, R.C. (2004). Gliotoxin is a dual inhibitor of farnesyl transferase and geranylgeranyltransferase I with antitumor activity against breast cancer in vivo. *Med. Oncol.*, 21, 21-30.
- Waksman, S., and Bugie, E. (1944). Chaetomin, a new antibiotic substance produced by *Chaetomium cochliodes*: I. Formation and properties. *J. Bacteriol.*, 48, 527-530.
- Walter, S.L. (2002). Acute penitrem A and roquefortine poisoning in a dog. *Can. Veter. J.*, 43 (5), 372-374.
- Wani, M. C., Taylor, H. L., Wall, M. E., Goggon, P., McPhail, A. T. (1971). Plant antitumor agents. VI. Isolation and structure of taxol, a novel antileukemic and antitumor agent from *Taxus brevifolia*. *J. Am. Chem. Soc.*, 93, 2325-2327.
- White, T.J., Bruns, T., Lee, S. and Taylor, J.W. (1990). 38. Amplification and direct sequencing of fungal ribosomal RNA genes for phylogenetics. *PCR Protocols a guide for methods and application*, 315-322.
- William, D.H. and Fleming, I. (1995). *Spectroscopic methods in organic chemistry*, 5th Ed. McGraw-Hill Book Company.

-
- Wink, M. (2003). Evolution of secondary metabolites from an ecological and molecular phylogenetic perspective, *Phytochemistry*, 64, 3–19.
- Wirz, A., Simmen, J., Heilmann, J., Calis, I., Meier, B., and Sticher, O. (1995). Bisanthraquinone glycosides of *Hypericum perforatum* with binding inhibition to CRH-1. *Phytochemistry*, 55, 941-947.
- Woese, C.R., Balch, W.E., Magrum, L.J., Fox, G.E., and Wolfe, R.S. (1977). An ancient divergence among the bacteria. *J. Mol. Evol.*, 9, 305-311.
- Woese, C.R., and G.I Oelsen. (1986). Archaeobacteria physiology perspectives in the kingdoms. *System. Appl Microbiol.*, 7, 161-177.
- Wyllie, T.D. and Morehouse, L. G. (1946). Introduction. *Mycotoxic Fungi, Mycotoxins and Mycotoxicosis*, vol. 3, Marcel Dekker Inc., New York.
- Yosioka, I., Morimoto, K., Murata, K., Yamauchi, H., and Kitagawa, I. (1971). Skyrin from two lichen species. *Chem. Pharm. Bull.*, 19(11), 2420-2422.
- Zhang, X., Jiang, W. and Sui, Z. (2003). Concise enantioselective syntheses of quinolactacins A and B through alternative winterfeldt oxidation. *J. Org. Chem.*, 68, 4523-4526.
- Zhiyong, L., He, L., and Miao, X. (2007). Cultivable bacterial community from South China sea sponges as revealed by DGGE fingerprinting and 16S rDNA phylogenetic analysis. *Curr. Microbiol.* 55, 465-472.
- Zeeck, *et al.*, 1992. Agistatins, metabolites from *Fusarium* sp., process for their preparation and their use. *Eur. Pat. Appl.*
- Zuccaro, A., Schulz, B., and Mitchell, J.I. (2003). Molecular detection of ascomycetes associated with *Fucus serratus*. *Mycol. Res.*, 107, 1451-1466.

List of Abbreviations

[α]D	specific rotation at the sodium D-line
δ	chemical shift
1D	one dimension
2D	two dimension
^{13}C	carbon
^1H	hydrogen (proton)
Amu	Atomic Mass Unit
bp	base pairs
br	broad signal
BLAST	basic local alignment search tool
CDCl_3	deuterated chloroform
CHCl_3	chloroform
CI	chemical ionization
COSY	correlation spectroscopy
d	doublet
DCM	dichloromethane
dd	doublet of doublet
DEPT	distortionless enhancement by polarization transfer
DGGE	denaturing gradient gel electrophoresis
DMSO	dimethyl sulfoxide
DNA	Deoxyribonucleic acid
EI	electron impact ionization
ESI	electrospray ionization
<i>et al.</i>	<i>et altera</i> (and others)
EtOAc	ethyl acetate
eV	electronvolt
FAB	fast atom bombardment
g	gram
HMBC	heteronuclear multiple bond connectivity
HMQC	heteronuclear multiple quantum coherence
H_2O	water
HPLC	high performance liquid chromatography
H_3PO_4	phosphoric acid
HR-MS	high resolution mass spectrometry
Hz	Herz
ITS	Internal transcribed sequence
IZ	inhibition zone
L	liter
LC	liquid chromatography
LC/MS	liquid chromatography-mass spectrometry
LSU	large subunit
m	multiplet
M	molar
MeOD	deuterated methanol
MeOH	methanol
mg	milligram
MHz	mega Herz
min	minute

mL	milliliter
mm	millimeter
MS	mass spectrometry
MTT	microculture tetrazolium assay
<i>m/z</i>	mass per charge
µg	microgram
µL	microliter
µM	micromol
NaCl	sodium chloride
ng	nanogram
NMR	nuclear magnetic resonance
PBS	phosphate buffered saline
PCR	polymerase chain reaction
ppm	parts per million
q	quartet
rDNA	ribosomal DNA
rpm	rotation per minute
RP 18	reversed phase C 18
s	singlet
sp.	species
SSU	small subunit
T	triplet
TFA	trifluoroacetic acid
THF	tetrahydrofuran
TLC	thin layer chromatography
UV	ultra-violet
VLC	vacuum liquid chromatography

Attachment 1: Result of MTT cytotoxicity assays

	L5178Y growth (%) Conc.10 µg/mL	EC ₅₀ (µg/mL)
Chetomin	0.4	< 0.1
Cochliodinol	0.4	0.33
Semicochliodinol A	0.7	0.52
Meleagrín	1.6	4.2
Citrinin hydrate	5.5	5.1
Fructigenin A	8.0	0.53

Attachment 2: Result of prokinase protein assay

Compound concentration in the assay : 3E-10 g/mL to 1E-05 g/mL. semi-log step; n= 1

	AKT1	ARK5	Aurora-A	Aurora-B	B-RAF-VE	CDK2/CycA	CDK4/CycD1	CDK2-alpha1	EGF-R	EPHB4	ERBB2	FAK
Cochliodinol	5,2E-06	2,6E-06	2,0E-06	2,1E-06	2,2E-06	5,7E-06	2,5E-06	>1E-05	6,9E-07	1,0E-06	1,5E-06	3,6E-06
Chetomin	>1E-05	6,5E-06	>1E-05	6,4E-06	9,1E-06	>1E-05	3,2E-06	>1E-05	1,3E-06	>1E-05	8,6E-06	>1E-05
Semicochliodinol A	8,6E-06	1,7E-06	5,9E-06	5,5E-06	3,8E-06	8,9E-06	4,6E-06	>1E-05	1,6E-06	2,3E-06	3,2E-06	>1E-05
Tetrahydroxy binaphthyl	>1E-05	>1E-05	>1E-05	>1E-05	>1E-05	>1E-05	>1E-05	>1E-05	4,2E-06	9,0E-06	>1E-05	>1E-05
Myrocin A	>1E-05	>1E-05	>1E-05	>1E-05	9,4E-06	>1E-05	>1E-05	>1E-05	5,8E-06	>1E-05	>1E-05	>1E-05

	IGF1-R	SRC	VEGF-R2	VEGF-R3	FLT3	INS-R	MET	PDGFR-beta	COT	PLK1	SAK	TIE2
Cochliodinol	3,7E-07	3,0E-07	4,6E-07	1,5E-06	1,6E-06	2,1E-06	1,7E-06	5,5E-06	8,2E-07	6,7E-06	9,3E-07	1,6E-06
Chetomin	1,3E-06	2,7E-06	1,8E-06	6,1E-06	2,8E-06	3,5E-06	1,6E-06	>1E-05	6,3E-06	>1E-05	4,6E-07	3,8E-06
Semicochliodinol A	5,4E-07	6,9E-07	9,3E-07	2,6E-06	2,2E-06	2,7E-06	2,1E-06	7,8E-06	3,0E-06	>1E-05	1,9E-06	2,5E-06
Tetrahydroxy binaphthyl	2,6E-06	3,0E-06	3,1E-06	7,3E-06	5,1E-06	>1E-05	>1E-05	>1E-05	6,5E-06	>1E-05	5,0E-06	>1E-05
Myrocin A	3,8E-06	3,0E-06	5,1E-06	>1E-05	>1E-05	>1E-05	>1E-05	>1E-05	>1E-05	>1E-05	5,9E-06	>1E-05

Ranking of IC₅₀ values :

	IC 50 (g/mL) above 1E-05
	IC 50 (g/mL) between 1E-05 and 1E-06
	IC 50 (g/mL) between 1E-06 and 1E-07
	IC 50 (g/mL) below 1E-07

Curriculum Vitae

Name : Ine Dewi Indriani
Place/date of birth : Bandung, 17 February 1974
Nationality : Indonesian
Marital status : Married

EDUCATION

Dec 2003 – now : Doctoral study at the Institute für Pharmazeutische Biologie und Biotechnologie, Heinrich-Heine Universität Düsseldorf, Germany
Oct 1998 – Feb 2001 : Master program at the department of biology, Institut Teknologi Bandung, Indonesia
Oct 1992 – Oct 1997 : Bachelor program at the department of biology, Institut Teknologi Bandung, Indonesia

WORKING EXPERIENCE

Apr 2001 – Sept 2003 : Research assistant at Eijkman Institute for Molecular Biology
Apr 2002 – Sept 2003 : Lecturer at the Department of Biology, University As-Syafiiyah Jakarta
1998 - 2000 : Assistant lecturer of practical courses in Microbiology at the department of biology, Institut Teknologi Bandung, Indonesia
1995 - 1997 : Assistant lecturer of practical courses in Microbiology at the Department of Chemical Engineering Parahyangan University, Indonesia

PUBLICATION

Aly,A.H., Edrada-Ebel,R., **Indriani,I.D.**, Wray,V., Mueller,W.E.G., Totzke,F., Zirrgiebel,U., Schaechtele,C., Kubbutat,M.H.G., Lin,W., Proksch,P. and Ebel,R. Cytotoxic metabolites from the fungal endophyte *Alternaria* sp. and their subsequent detection in its host plant *Polygonum senegalense*. *The Journal of Natural Products* (in press).

SEMINAR

Oral presentation at the 1th Sino German Workshop, September 2007, Düsseldorf, Germany.